Cholesterol as a mediator of hepatic injury in non-alcoholic steatohepatitis

by

Derrick Michael Van Rooyen

BSc (Hons) MSc (Biochemistry)

A thesis submitted for the degree of Doctor of Philosophy of The Australian National University

April 2012

Preface

This thesis represents research carried out at the Australian National University Medical School (Liver Research Laboratory, The Canberra Hospital, Canberra, ACT), from November 2008 to April 2012, under the supervision of Professor Geoff C. Farrell.

The work presented in this thesis constitutes original work by the author and has not been submitted in any other form to another University or institution. Where use or reference was made of the work of others, it has been duly acknowledged in the text.

Derrick M. Van Rooyen

April 2012

Abstract

Non-alcoholic fatty liver disease (NAFLD), a highly prevalent disorder (15-45%) in modern societies, is related to over-nutrition and the obesity and T2D pandemics. About one quarter of patients with NAFLD develop a form of liver pathology characterised by steatosis (fatty liver cells), degenerative changes in hepatocytes (such as ballooning), and inflammation (lymphocytes, macrophages and polymorphonuclear lymphocytes), collectively termed non-alcoholic steatohepatitis (NASH). NASH usually precedes the development of hepatic fibrosis and hepatocellular carcinoma (HCC). While studies in humans affected by NAFLD have been informative as to risk factors and clinical outcomes, the reason why some develop NASH and others harbour only a benign form of NAFLD (simple steatosis) remains unclear. Studies into NASH pathogenesis have been hindered by lack of suitable pathophysiological animal models.

Foz/foz (*Alms1* mutant) mice develop hyperphagia and obesity-related NAFLD, in association with diabetes, hypoadiponectinemia and hypercholesterolemia. High fat (HF)-feeding to *foz/foz* mice induces NASH by 12 weeks, with liver fibrosis at 24 weeks. In this mouse model of NASH, hypercholesterolemia is associated with prodigious accumulation of cholesterol in the liver, and the latter correlates with the severity of liver injury. The aims of this research were to investigate the cause and effect of hepatic cholesterol dysregulation on NAFLD outcome in *foz/foz* mice, its pathogenic significance in NASH, and the potential of dietary and pharmacological approaches to reverse NASH.

By 24 weeks, hepatic free cholesterol (FC) and cholesteryl ester (CE) content were ~2 and ~200-fold higher, respectively, in HF-fed *foz/foz* than HF-fed WT mice. As a partial explanation for hepatic cholesterol accumulation, expression of low-density lipoprotein receptor (LDLR) was significantly elevated in HF-fed *foz/foz* mice, and expression was evident in both hepatocyte and endothelial cells. Cholesterol synthesis was not increased: HF-feeding actually suppressed HMG-CoA reductase (HMGR) activity, the rate limiting step in cholesterol biosynthesis, in both WT and *foz/foz* mice. Expression of acyl-CoA:cholesterol acyltransferase (ACAT)-2 was

significantly upregulated in HF-fed *foz/foz* mice, while cholesteryl ester hydrolase (CEH) was unchanged. Bile acid (BA) biosynthesis genes, including cholesterol 7-α-hydroxylase (Cyp7a1), were suppressed in HF-fed *foz/foz* mice, while hepatic expression of cholesterol and BA export proteins: ABCG5 and -8, and bile salt export protein (Bsep) (and also MRP-2 and MDR-2) were also decreased in HF-fed *foz/foz* mice. Transcriptional regulators of these metabolic pathways were differentially expressed in *foz/foz* mice with NASH: LXR-α and HNF-4α decreased, while SREBP-2, a nuclear regulator of LDLR and HMGR, increased significantly. An important novel observation was that expression of liver receptor homolog-1 (LRH-1), while significantly elevated in HF-fed WT mice, was unaltered in HF-fed *foz/foz* mice. To test whether concentrations of insulin that circulate in HF-fed *foz/foz* mice were responsible for some or all of these changes, experiments were conducted in primary murine hepatocyte cultures. Insulin activated both SREBP-2 and LDLR, while simultaneously decreasing Bsep and LRH-1 expression.

Reducing dietary cholesterol in HF-fed-*foz/foz* mice ameliorated liver injury as indicated by serum alanine transaminase (ALT), cytokeratin-18 fragmentation (M30; marker of hepatocellular cell death), and macrophage recruitment (F4/80 immunohistochemistry [IHC]); there were no significant differences in neutrophil recruitment (myeloperoxidase IHC). Conversely, high (2%) dietary cholesterol greatly accentuated liver injury. Further, the severity of liver injury in these dietary experiments correlated with hepatic FC and CE lipid profiles, and not with hepatic triglyceride (TG), diacylglycerides (DAG), monoacylglyceride (MAG) and free fatty acid lipids, levels of which were either unchanged or variably altered. Hepatic cholesterol loading was also found to activate nuclear factor (NF)-κB (shown by nuclear p65) and *c*-Jun *N*-terminal kinase (JNK), as well as serum levels of monocyte chemotactic protein (MCP)-1. Finally, quantitative analysis of sirius red staining in liver sections revealed a clear relationship between hepatic cholesterol and fibrosis severity of fatty liver disease.

To establish whether pharmacological modulation of cholesterol turnover could reduce hepatic cholesterol content and modulate disease severity of NASH, HF-fed *foz/foz* and WT mice were administered atorvastatin (20 mg/kg/day) and/or

ezetimibe (5 mg/kg/day) for 8 weeks, starting after NASH onset (at 16 weeks). Both atorvastatin and ezetimibe significantly lowered hepatic CE and FC but had no or inconsistent effects on other lipid fractions. Both agents, singularly and in combination, substantially lowered serum ALT ($P<0.05$) *versus* vehicle-treated *foz/foz* mice, in association with reduced serum total cholesterol and HDL. Likewise, hepatomegaly was reduced while peri-ovarian adipose weight and serum adiponectin levels increased in drug-treated *foz/foz* mice. Hepatocellular cell death and expression of nuclear NF-κB p65, JNK, vascular cell adhesion molecule-1 and inter-cellular adhesion molecule-1 were all suppressed in drug treated *foz/foz* mice, in addition to hepatic macrophage infiltration. Drug treatment had no effect on histological steatosis and ballooning scores, it conferred significant reduction in lobular inflammation score. Additionally, liver fibrosis was significantly reduced in HF-fed *foz/foz* drug treatment groups *versus* vehicle controls ($P<0.05$).

In HF-fed *foz/foz* mice, NASH is associated with profoundly disordered hepatic cholesterol turnover. Insulin-induced activation of SREBP-2 and suppression of LRH-1 likely result in increased LDLR expression and down-regulation of genes involved in cholesterol biotransformation (to BA) and export. Consequently, cholesterol accumulates within the livers of *foz/foz* mice with NASH. The evidence from both dietary and pharmacological intervention experiments is that hepatic cholesterol significantly mediates hepatocellular cell death, inflammatory cell recruitment and liver fibrosis in this model. Conversely, inhibition of intestinal/tissue cholesterol uptake/redistribution and biosynthesis and dietary cholesterol restriction reduces liver injury, inflammation, and fibrosis in *foz/foz* mice with NASH. These findings strongly support the hypothesis that hepatic cholesterol, accumulating as the consequence of insulin resistance, acts as a lipotoxic mediator of pro-fibrotic liver injury and inflammation in experimental NASH.

Acknowledgements

I wish to take this opportunity to thank the following people who have contributed to the research described in this thesis:

First and foremost, I wish to thank my principal supervisor, Professor Geoff Farrell, for his outstanding guidance and supervision throughout this project. The breadth and depth of Geoff's medical knowledge and enthusiasm for scientific research and writing have been inspirational. It has been a privilege to work in such an expertly staffed and well-funded laboratory.

My sincerest thanks go to my co-supervisor, Dr Claire Larter. This research would not have been completed without Claire's intellectual input, guidance and co-supervision. Her friendship, encouragement and willingness to proof-read my draft manuscripts have been indispensible throughout the course of this PhD.

I am also indebted to Associate-professor Narci Teoh, whose scientific insight and mentorship have contributed greatly to this project.

Special acknowledgements go to fellow members of the Liver Lab, namely Déborah Heydet, Sharon Pok, Betty Rooney, Lay Gan and Musa Drini for their friendship and support, which have made it a pleasure to come to work everyday.

I would also like to thank Leah Bala and Heng-Jian Wong for genotyping mice and assisting me with harvests. These simple tasks have saved me days, if not weeks of work. Additionally, special acknowledgements go to Vanessa Barn and Natalia Damiano for breeding mice, changing cages and managing general animal care and logistics. All of these less glamorous "behind the scenes" roles have made this research possible.

I am indebted to The Canberra Hospital Pathology Department for allowing me to use their microtomes and cryostat.

Without the assistance from collaborators, major aspects of this research would not have been possible. Special thanks go to Dr Geoff Haigh, who has spent many hours performing lipidomic analyses on the hundreds of liver samples and Associate-Professor Matthew Yeh for scoring the histopathology. I would also like to thank Drs Nick Shakel and Fiona Warner for kindly supplying CCl_4-treated mouse samples and Professor Richard Whitby (University of Southampton, Southampton, UK) for graciously providing the LRH-1 agonists, JS/5197/16C and JS/5197/74A.

I wish to thank The Australian National Health and Medical Research Council (NHMRC) for funding this research (Project grants 418101 and 585411) and providing me with a PhD scholarship (Dora Lush, 585539).

My sincerest gratitude goes to my parents, Sharon and Mike Van Rooyen, for their love, encouragement, and continual support of my academic career.

Finally, I wish to thank my wife, Claire Wright, for all her love and support. Thank you for being my pillar of strength, motivating me through the tough and frustrating times, and for always supporting my academic pursuits. Without you, I would not have completed this thesis. Thank you.

List of tables

List of figures

Presentations, publications, and awards

PRESENTATIONS:

Van Rooyen, D. M., Larter, C. Z., Teoh, N., Farrell, G. (2009). Abnormal hepatic cholesterol turnover in a metabolic syndrome murine model of NASH: relationship to hypercholesterolemia. *Australian Liver Association (ALA) workshop, Gastroenterological Society of Australia (GESA).* May 2009. Yarra Valley, Victoria.

Van Rooyen, D. M., Larter, C. Z., Teoh, N., Farrell, G. C. (2010). Role of hepatic SREBP-2 in hepatic cholesterol accumulation associated with non-alcoholic steatohepatitis. *Australian Society for Medical Research (ASMR).* June 2010. The Canberra Hospital.

Van Rooyen, D. M., Larter, C. Z., Teoh, N., Farrell, G. (2011). Fibrotic severity of NASH is increased in *foz/foz* mice by hepatic cholesterol loading, while ezetimibe and atorvastatin ameliorate liver injury. *ALA workshop, GESA.* May 2011. Kiama, New South Wales.

Van Rooyen, D. M., Larter, C. Z., Yeh, M. M., Haigh, W. G., Teoh, N., and Farrell, G. C. (2011). "Hepatic cholesterol loading worsens fibrotic severity of NASH in *foz/foz* mice, while ezetimibe and atorvastatin ameliorate liver injury" *Australian Society for Medical Research (ASMR).* June 2011. The Canberra Hospital.

PUBLISHED ABSTRACTS:

Van Rooyen, D. M., Larter, C. Z., Teoh, N., Farrell, G. C. (2009). "Disordered hepatic cholesterol turnover in mice with metabolic syndrome: relationship to NASH." *J. Gastroenterol. Hepatol.* 24(Suppl. 2): A280. Presented at *Australian Gastroenterology Week (AGW), GESA.* October 2009. Sydney, New South Wales.

Larter, C. Z., Yeh, M. M., Arsov, T., Van Rooyen, D. M., Brooling, J., Sheales, M., Nolan, C. J., Teoh, N., Farrell, G. C. (2009). "Steatohepatitis severity in high fat-fed *foz/foz* mice is dependent on genetic background" *J. Gastroenterol. Hepatol.* 24(Suppl. 2): A300.

Larter, C. Z., Yeh, M. M., Van Rooyen, D. M., Brooling, J., Teoh, N., Farrell, G. C. (2009). "Steatosis and hepatic injury are attenuated by WY 14,643 in a metabolic syndrome-related model of NASH" *J. Gastroenterol. Hepatol.* 24(Suppl. 2): A300.

* **Van Rooyen, D. M., Larter, C. Z., Yeh, M. M., Haigh, W. G., Teoh, N., and Farrell, G. C.** (2010). "Dietary cholesterol modulates severity of liver injury in mice with metabolic-syndrome related NASH." *J. Gastroenterol. Hepatol.* 25(Supp. 3): A5. Presented at *Australian Gastroenterology Week (AGW), GESA.* October 2010. Gold Coast, Queensland.

Van Rooyen, D. M., Larter, C. Z., Yeh, M. M., Haigh, W. G., Teoh, N., and Farrell, G. C. (2011). "Ezetimibe and atorvastatin ameliorate liver injury in *foz/foz* mice with NASH" *J. Gastroenterol. Hepatol.* 26(Supp. 4): pg 2. Paper of distinction. presented at *Australian Gastroenterology Week (AGW), GESA.* September 2011. Brisbane, Queensland.

PUBLICATIONS:

Larter, C. Z., Yeh, M. M., Van Rooyen, D. M., Teoh, N. C., Brooling, J., Hou, J. Y., Williams, J., Clyne, M., Nolan, C. J., Farrell, G. C. (2009). "Roles of adipose restriction and metabolic factors in progression of steatosis to steatohepatitis in obese, diabetic mice." *J. Gastroenterol. Hepatol.* 24(10): 1658-1668.

Van Rooyen, D. M., Farrell, G. C. (2011). "SREBP-2: a link between insulin resistance, hepatic cholesterol and inflammation in NASH" *J. Gastroenterol. Hepatol.* 26(5): 789-792.

Van Rooyen, D. M., Larter, C. Z., W. G. Haigh, Yeh, M. M., Ioannou, G., Kuver, R., Lee, S. P., Teoh, N., Farrell, G. C. (2011). "Hepatic free cholesterol accumulates in obese, diabetic mice and causes non-alcoholic steatohepatitis." *Gastroenterol.* 141:1393–1403.

Leclercq, I., Van Rooyen, D. M., Farrell, G. C. (2011). "Hepatic endoplasmic reticulum stress in obesity: deeper insights into processes, but are they relevant to NASH?" *Hepatol.* Accepted article.

Larter, C. Z., Yeh, M. M., Van Rooyen, D. M., Brooling, J., Ghatora, K., Farrell, G. C. (2011). "The PPAR-alpha agonist, Wy 14,643, improves metabolic indices, steatosis and ballooning in diabetic mice with NASH" *J. Gastroenterol. Hepatol.* Accepted article.

Farrell, G. C., Van Rooyen, D. M., Gan, L. T., Chitturi, S. (2011). "NASH is an inflammatory disorder: pathogenic, prognostic and therapeutic implications." *Gut Liver.* Manuscript in preparation.

Van Rooyen, D. M., Larter, C. Z., W. G. Haigh, Yeh, M. M., Ioannou, G., Kuver, R., Lee, S. P., Teoh, N., Farrell, G. C. (2011). "Pharmacological reduction of hepatic cholesterol abrogates JNK activation and reverses NASH in *foz/foz* mice." *Hepatol.* Manuscript in preparation.

Larter, C. Z., Yeh, M. M., Van Rooyen, D. M., Brooling, J., Heydet, D., Nolan, C., Teoh, N., Farrell, G. C. (2011). "Dietary restitution dampens liver injury, neutrophil inflammation and fibrosis in high fat-fed mice with fatty liver." *J Nutr.* Manuscript submitted.

AWARDS:

* Australian Gastroenterology Week (AGW) June Halliday Basic Science Young Investigators Award (2010).
- Dora Lush Australian National Health and Medical Research Council (NHMRC) PhD scholarship (585539).

List of abbreviations

24/25/4/7-OH	24/25/4/7-hydroxycholesterol
5,6-Epoxy	5,6-epoxy cholesterol
7-KD	7-ketocholesteryl docosahexaenoate
7-keto	7-keto-cholesterol
Å	ångström
AA	amino acid
ABC	ATP-binding cassette
ABCG1	ATP-binding cassette, sub-family G, member 1
ABCG5	ATP-binding cassette, sub-family G, member 5
ABCG8	ATP-binding cassette, sub-family G, member 8
ACAT	acyl-CoA : cholesterol acyltransferase
ALT	alanine aminotransferase
AMPK	AMP-dependent protein kinase
Apo	apolipoprotein
$ApoE^{-/-}$	apolipoprotein E knockout mouse
ATP	adenosine triphosphate
ATP	adenosine triphosphate
BA	bile acid
BAT	brown adipose tissue
BSEP	bile salt exporter protein
CA	cholic acid
cAMP	3'-5'-cyclic adenosine monophosphate
CD	cluster of differentiation
CD68	cluster of differentiation 68, also known as macrosialin
CDCA	chenodeoxycholic acid
cDNA	complementary DNA
CE	cholesteryl esters
CEH	cholesteryl ester hydrolase
Ck18	cytokeratin 18
CM	chylomicron

CR	chylomicron remnant
Cyp	cytochrome P450
Cyp27a1	sterol 27-hydroxylase
Cyp7a1	7α-hydroxylase
Cyp7b1	oxysterol 7α-hydroxylase
Cyp8b1	sterol 12α-hydroxylase
d.H_2O	deionised ultrapure water
DAG	diacylglycerol
DBD	DNA-binding domain
DEPC	diethylpyrocarbonate
DHCA	3α,7α-dihydroxycholestanoic acid
DNA	deoxyribonucleic acid
DPX	distyrene plasticiser xylene
DR	death receptor
ELISA	enzyme-linked immunosorbent assay
ER	endoplasmic reticulum
ERAD	ER-associated degradation
ERK	extracellular signal-regulated kinases
F4/80	epidermal growth factor-like module containing mucin-like hormone receptor like-1 antigen
FC	free cholesterol
FCT	forward cholesterol transport
FFA	free fatty acid
foz/foz	*Alms1* mutant mouse stain
FXR	farnesoid-X receptor
H&E	haematoxylin and eosin stain
HCC	hepatocellular carcinoma
HDL	high-density lipoprotein
HF	high fat
HMG-CoA	3-hydroxy-3-methylglutaryl-CoA
HMGR	HMG-CoA reductase
HNF	hepatocyte nuclear factor
HPLC	high-performance liquid chromatography
HSP90	heat shock protein 90

IDL	intermediate density lipoprotein
IHC	immunohistochemistry
IL	interleukin
IR	insulin resistance
JNK	*c*-Jun *N*-terminal kinases
kDa	kiloDalton (≡1.66 x 10^{-21} grams)
L	litre
LBD	ligand-binding domain
LCAT	lecithin:cholesterol acyltransferase
LDL	low-density lipoprotein
LDLR	LDL receptor
$LDLR^{-/-}$	LDL receptor knockout mouse
LPL	lipoprotein lipase
LRH-1	liver receptor homolog-1
LXR	liver-X receptor
M	molar ($mol.dm^{-3}$)
M30	cytokeratin-18 fragment epitope
MAG	monoacylglycerol
MCD	methionine and choline-deficient
MCP-1	monocyte chemotactic protein-1
MDR2	multidrug resistance protein-2
miR	micro RNA
mL	millilitre
MRP2	multidrug resistance-associated protein-2
MTTP	microsomal triglyceride transfer protein
MuFA	monounsaturated fatty acid
NADPH	nicotinamide adenine dinucleotide phosphate
NAFLD	non-alcoholic fatty liver disease
NASH	non-alcoholic steatohepatitis
nCEH	neutral cholesteryl ester hydrolase
NF-κB	nuclear factor-κB
NPC1L1	Niemann Pick C1-like-1 protein
NR	nuclear receptor
NS	not significant

Ø	diameter
PCSK9	proprotein convertase subtilisin/kexin type 9
PL	phospholipids
PM	plasma membrane
PPAR	peroxisome proliferator-activated receptor
PuFA	polyunsaturated fatty acid
PXR	pregnane-X receptor
qPCR	real-time polymerase chain reaction
RCT	reverse cholesterol transport
RNA	ribonucleic acid
RT	room temperature
RT-PCR	reverse transcription PCR
RXR	retinoic-X receptor
SaFA	saturated fatty acid
SCAP	SREBP cleavage activating protein
SCP	sterol carrier protein
Shp	short heterodimer partner
siRNA	small interfering RNA
SR-B1	scavenger receptor-B1
SREBP	sterol regulatory element binding protein
SS	simple steatosis
SSD	sterol-sensing domain
TBP	TATA box-binding protein
TG	triglyceride
THCA	3α,7α,12α-trihydroxycholestanoic acid
TLR	toll-like receptor
TMS	transmembrane segment
TNF	tumour necrosis factor
VLDL	very low-density lipoprotein
VTV	very low-density lipoprotein transport vesicle
WAT	white ovarian adipose tissue
WT	wild type
µL	microlitre

Table of contents

CHAPTER 1

Introduction

1.1 Historical background

Cholesterol is a 27-carbon essential sterol. It consists of a tetra-cyclic perhydrocyclopentanophenanthrene ring backbone, with an aliphatic side chain conjugated to C_{17}, two methyl groups at C_{10} and C_{13}, and a hydroxide group present on C_3 (Figure 1.1). Historically, cholesterol was first identified by Poulletier de la Salle in 1769, who, after studying the lipid composition of gallstones (McNamara *et al.* 2006), commented on the white lipid. Some time later, in 1816, the name 'cholesterine' was assigned to the lipid by Michel-Eugene Chevreul who utilised saponification to isolate several gallstone lipids. The name stems from the Greek words 'chole', for bile, and 'stereos,' for solid. Structurally, it was only in 1859 that the alcoholic properties of cholesterol were appreciated and attributed to the C_3 hydroxyl group (Figure 1.1) by Marcellin Berthelot. The name was therefore subsequently changed to 'cholesterol' (McNamara *et al.* 2006).

The first empirical formula ($C_{27}H_{46}O$) of cholesterol was proposed in 1888 by Friedrich Reinitzer (Vance and Van den Bosch 2000). An initial, albeit incorrect, structure was only proposed 40 years later (1928) by Adolf Windaus and Heinrich Wieland. The corrected structure was subsequently published in 1932 by Wieland and Dane, who used a combination of X-ray and chemical studies to validate the structure (Vance and Van den Bosch 2000). Windaus and Wieland later showed that bile acids share similar structures to cholesterol; both received Nobel Prizes, for their chemical studies in cholesterol (Windaus) and bile acids (Wieland) (Lunde 1930).

Almost 250 years after its discovery, cholesterol is now known to be crucial for numerous functions in mammals. These include: regulation of membrane fluidity and signalling, steroid hormone and vitamin synthesis, and (via bile acid formation) assisting intestinal lipid absorption (Yeagle 1991; Hornick 2002; Xu *et al.* 2005). Furthermore, most organisms other than plants are dependent on cholesterol for physiological cell growth. For example, 20-26% of mammalian bodily cholesterol

localises to plasma membranes (PM), which is responsible for regulating and maintaining membrane fluidity; specifically, cholesterol increases the viscosity of PMs (Mathews *et al.* 2000).

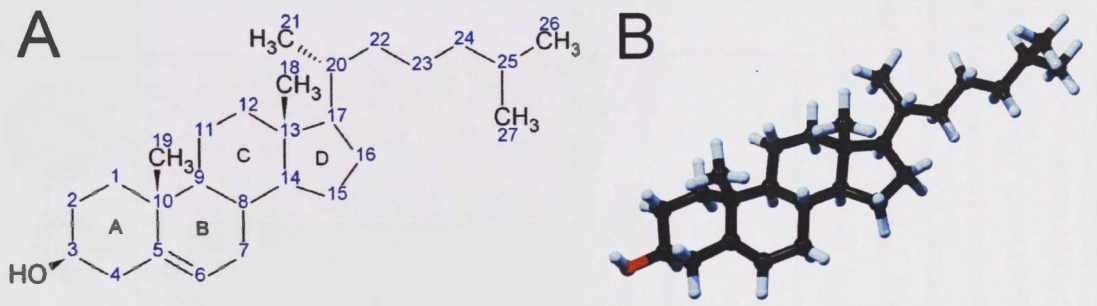

Figure 1.1 Schematic and spatial representations of cholesterol.

A) Schematic structure of cholesterol with carbon numbering (blue text) and ring identification (small letters A-D) shown. **B)** The optimised three-dimensional ball-and-stick model of cholesterol. Spatial optimisation was calculated in the absence of explicit hydrogens using Chemsketch v10.02 software (ACDLabs, Toronto, ON, Canada), and rendered using POVray software (Cason 2004).

While cholesterol is essential for life, once it is synthesised or absorbed into the body, it can only be catabolised by the liver. Overall, 99.8% of bodily cholesterol is catabolised or excreted by the liver, the remaining 0.2% is lost in urine (Siperstein and Murray 1955). It follows that strict control of cholesterol homeostasis is required. The various stages of cholesterol metabolism and regulation are discussed below.

1.2 Dietary cholesterol uptake and transport

Approximately 30% of all cholesterol present in the human body is acquired exogenously via absorption of dietary lipids (Hylemon *et al.* 2001). These include: triglycerides (TG), cholesteryl esters (CE), and phospholipids (PLs). In the intestine they are emulsified by bile acids (BAs) which facilitate lipid solubilisation and absorption into enterocytes (Tso and Balint 1986). Prior to absorption, intestinal and pancreatic lipases hydrolyse these lipids, yielding: long chain fatty acids (FA) and monoglycerides, free cholesterol and lysophospholipids, allowing most of these components to passively diffuse into enterocytes. Cholesterol uptake, however, is regulated by Niemann Pick C1-like-1 (NPC1L1) protein and cluster of differentiation (CD)-36 transporters found on the microvilli of enterocytes throughout the brush border of the proximal jejunum (Altmann *et al.* 2004; Ballantyne 2008) (Figure 1.2).

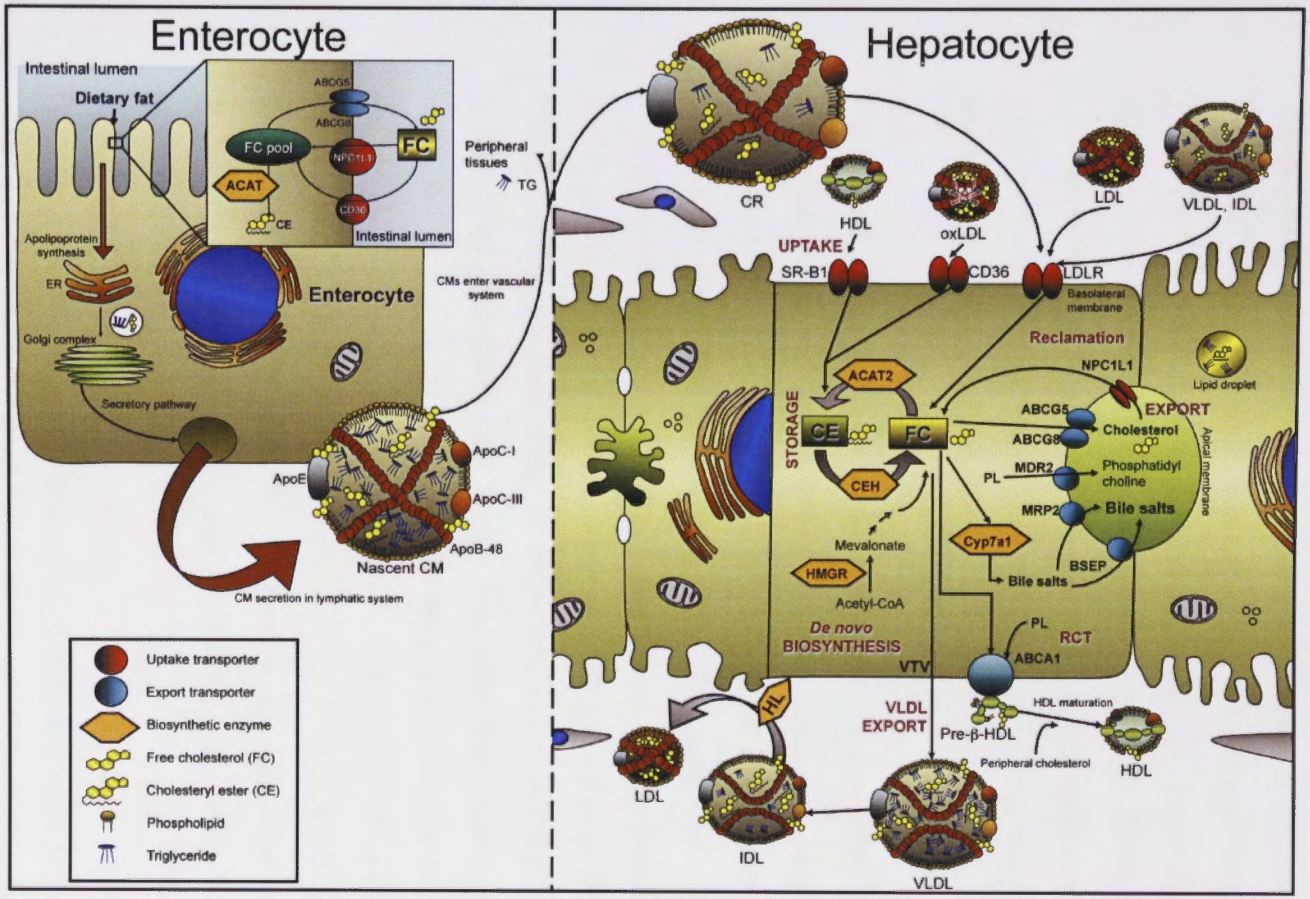

Figure 1.2 Schematic representation of dietary cholesterol absorption by enterocytes and hepatic regulation of serum cholesterol

Abbreviations: ABC, ATP binding cassette protein; ACAT, acyl-CoA:cholesterol acyltransferase; Apo, apolipoprotein; BSEP, bile salt export protein; CD36, cluster of differentiation-36; CE, cholesteryl esters; CEH, cholesteryl ester hydrolase; CM, chylomicron; CR, chylomicron remnant; Cyp7α1, 7α-hydroxylase; FC, free cholesterol; HDL, high-density lipoprotein; HL, hepatic lipase; HMGR, HMG-CoA reductase; IDL, intermediate-density lipoprotein; LDL, low-density lipoprotein; LDLR, LDL receptor; MDR2, multidrug resistance protein-2; MRP2, multidrug resistance associated protein-2; NPC1L1, Niemann Pick C1 like 1 protein, PL, phospholipid; RCT, reverse cholesterol transport; SR-B1, scavenger receptor-B1; TG, triglyceride; VLDL, very low density lipoprotein; VTV, VLDL transport vesicle.

NPC1L1 is an 140-160 kDa *N*-terminal glycosylated cholesterol-specific transporter (Sudhop *et al.* 2002; Altmann *et al.* 2004). CD36 is an 88 kDa glycosylated ortholog of rodent FA translocase (Zhang *et al.* 2003); it is able to transport both long-chain FAs and cholesterol (Endemann *et al.* 1993; Nassir *et al.* 2007). Within enterocytes, intracellular cholesterol concentrations are tightly regulated by plasma membrane-bound ATP-binding cassette, sub-family G, members (ABCG)-5 and -8, transporters. These form a heterodimeric shunt responsible for controlling the *efflux* of excess cholesterol back into the intestinal lumen (Berge *et al.* 2000; Lee *et al.* 2001) (Figure 1.2). However, the majority of the cholesterol is transported *into* the body where it is used for membrane formation and stabilisation, steroid biosynthesis and biliary lipid absorption via bile acid formation (Voet and Voet 1999).

Cholesterol is insoluble in water. In order to transport hydrophobic cholesterol molecules within the body, enterocytes form chylomicron (CM) micelles (Clement 1976). However, before CMs can be synthesised and secreted, TG reassembly takes place in the endoplasmic reticulum (ER) from long chain FAs (>12 carbons) and monoglyceride precursors (Sabesin and Frase 1977). Simultaneously, cytoplasmic cholesterol is chaperoned by sterol carrier protein (SCP)-2 to enter the ER (Gavey *et al.* 1981), where acyl-coenzyme A:cholesterol-acyltransferase (ACAT) catalyses the formation of cholesteryl ester from a long-chain fatty acyl-CoA and a free cholesterol molecule (Pape *et al.* 1995; Yu *et al.* 1999). Two ACAT isotypes, -1 and -2 have been identified in mammals (Meiner *et al.* 1996). ACAT1 is ubiquitously expressed throughout the human body. However, in the liver it is predominantly expressed by Kupffer cells (Parini *et al.* 2004). Conversely, ACAT2 is the predominant cholesterol-acyltransferase expressed by hepatocytes (Chang *et al.* 2000), where it is responsible for hepatocellular esterification of FC.

Once lipid esterification has taken place, CM formation is initiated by the synthesis of apoB, an apolipoprotein responsible for plasma TG transport (Manchekar *et al.* 2004). Enterocytes perform a 52% *N*-terminal truncation of apoB-100 mRNA, synthesising a 241 kDa apoB-48 (Table 1.1) protein, which is often used as a CM marker (Fisher and Ginsberg 2002). ApoC-II and apoA-I (Table 1.1) are also synthesised; these facilitate CM formation by creating an amphipathic environment where hydrophobic neutral cholesteryl esters and TGs form the CM core. The nascent CM complex is relatively

large, having a diameter (Ø) of 5000 Å and total cholesterol concentration of 0-2 mg/dL (Fredrickson *et al.* 1967) (Figure 1.3A,B). These CM colloids are secreted into the mesenteric lymph via the villus lacteals, and are then transported via the thoracic duct which gains entry into the venous circulation via the left subclavian vein (van Greevenbroek and de Bruin 1998).

Circulating CM release FFA from TGs upon proximal contact with lipoprotein lipases (LPL; 1,3-triacylglycerol esterase) present on the endothelial lining of extrahepatic capillary vessels (Cryer 1981). FFAs are thereby transferred to adipose and peripheral tissues for use as an energy source; this involves β-oxidation of FFAs to form acetyl CoA, which subsequently enter the Krebs cycle (Voet and Voet 1999). Meanwhile, reduction of the TG content from CMs results in the formation of chylomicron remnants (CR) which are removed from circulation by the liver (Figures 1.2 and 1.6) (Ontko and Zilversmit 1967; Cooper and Yu 1978).

Table 1.1 Summary of apolipoprotein properties.

Table adapted from Voet and Voet (1999) and Brody (1998).

Apolipoprotein	AA residues	kDa	Characteristics	Function
A-I	243	29	Major HDL protein	Activates LCAT
A-II	77	17	Major HDL constituent	Inhibits LCAT, activates HDL
B-48	2152	241	Found exclusively in CMs	Cholesterol clearance
B-100	4536	550	Major LDL constituent, present in VLDL	Cholesterol clearance
C-I	56	6.6	Found in CMs	Activates LCAT
C-II	79	8.9	Present in VLDL	Activates LPL
C-III	79	8.8	Present in CMs, VLDL, HDL	Inhibits LPL, activates LCAT
D	19	19	HDL protein	CE transfer
E	299	34	Present in CM, VLDL, LDL, HDL	Cholesterol clearance

Abbreviations: AA, amino acid, CE, cholesteryl ester; CM, chylomicron; HDL, high-density lipoprotein; kDa, kiloDalton; LCAT, lecithin:cholesterol acyltransferase; LDL, low-density lipoprotein; LPL, lipoprotein lipase; VLDL, very low-density lipoprotein.

1.3 Hepatic uptake of dietary cholesterol

When venous blood enters the liver via the portal vein, CRs are removed from circulation by low-density lipoprotein receptor (LDLR)-mediated endocytosis (Havel 1998) (Figures 1.2 and 1.6). LDLR is a cell surface-bound protein synthesised in the rough endoplasmic reticulum (ER) as an 860 amino acid, 120 kDa precursor holoprotein. Post-translational modification results in a mature 140-160 kDa glycosylated LDLR protein (Davis *et al.* 1986), which binds apoB and apoE lipoproteins present on CRs, intermediate-density lipoproteins (IDL), low-density lipoproteins (LDL) and very low-density lipoproteins (VLDL) (Table 1.1, Figures 1.2 and 1.6) (Mathews *et al.* 2000). LDLR localises to the plasma membrane of hepatocyte sinusoidal microvilli in the space of Disse, just below the hepatic sieve plate (Wisse *et al.* 1985; Havel and Hamilton 2004).

Once CR or LDL colloids complex with LDLR, receptor-mediated endocytosis takes place. The endocytosed complex is acidified via a membrane-bound ATPase proton pump (Zatta *et al.* 2000), with vesicles exhibiting a pH of ~4.0, sufficient to activate acid lipase/cholesteryl lipase (cholesteryl ester hydrolase [CEH]). CEH is a 49 kDa lysosomal protein responsible for the hydrolysis of CEs to FC. Acid lipase protein differs from neutral cholesteryl ester hydrolase (nCEH), in that a low pH is required for enzyme activity (Hui 1996). FC molecules subsequently translocate into the cytoplasm. From here they are sequestered to the various membranes within the cell, or esterified by ACAT-1 or -2 to CE and stored in lipid droplets. Liberated LDLR is recycled back to the basolateral surface of the hepatocyte (Brown *et al.* 1983).

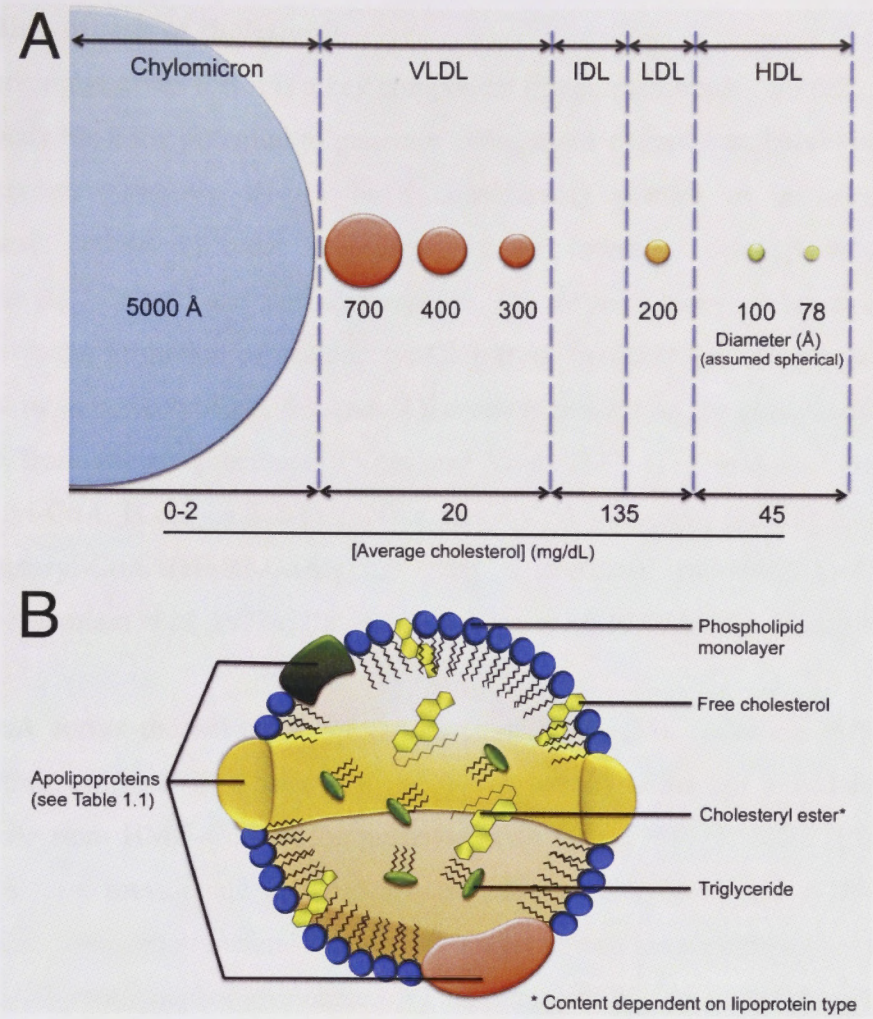

Figure 1.3 Physical and structural characteristics of mammalian lipoproteins

(**A**) Comparison of apolipoprotein size and cholesterol content of chylomicrons, very low density (VLDL), intermediate density (IDL), low-density (LDL) and high density (HDL) lipoproteins. (**B**) Generalised structural composition of lipoprotein colloids, showing phospholipid and free cholesterol monolayer, apolipoproteins (see Table 1.1 for apolipoprotein characteristics and functions), and cholesteryl ester and triglyceride-rich interior.

Cytoplasmic FC is esterified by microsomal ACAT2 to form cholesteryl esters (most commonly cholesteryl oleate), which are the primary storage form of cholesterol in the liver (Figure 1.2). Conversely, cholesteryl ester hydrolase (CEH) is responsible for catalysing the hydrolysis of the ester bond, resulting in the generation of FC from CE. The dynamic flux between ACAT2 and CEH in the liver is responsible for ensuring that FC is only present when required; excess FC is esterified immediately upon uptake. Together, FC and CE constitute the total cholesterol pool within the liver (Figure 1.2).

1.4 Biosynthesis of cholesterol

Not surprisingly, given that it is a key component of cell membranes, all cells within the human body have the potential to generate endogenous cholesterol. However, the liver and other steroidogenic tissues have considerably greater *de novo* cholesterol biosynthesis activity in order to provide for the increased demands of the sterol precursors for bile acid and steroid synthesis. The *de novo* biosynthesis of cholesterol begins with the formation of acetoacetyl-CoA from two acetyl-CoA molecules, a step catalysed by acetoacetyl-CoA thiolase. All carbons present on the cholesterol molecule originate from acetate precursors (Voet and Voet 1999) (Figure 1.4). Once formed, acetoacetyl-CoA, is conjugated to another acetyl-CoA molecule, yielding 3-hydroxy-3-methylglutaryl-CoA (HMG-CoA); this step is mediated by HMG-CoA synthase (Balasubramaniam *et al.* 1977a; Balasubramaniam *et al.* 1977b; Celis *et al.* 1994).

HMG-CoA forms the substrate for cytoplasmic HMG-CoA reductase (HMGR), the rate-limiting enzyme in cholesterol synthesis, which catalyses the formation of mevalonate from HMG-CoA in the presence of two NADPH molecules (Brown *et al.* 1973). In turn, mevalonate undergoes two-step phosphorylation via ATP-dependent mevalonate-5-phosphotransferase and phosphomevalonate kinase enzymes respectively, forming 5-pyrophosphomevalonate. This molecule is decarboxylated by pyrophosphomevalonate decarboxylase in the presence of ATP, forming isopentenyl pyrophosphate. The latter isomerises (via isopentyl pyrophosphate isomerase) in a reversible reaction, yielding dimethylallyl pyrophosphate. An isopentenyl pyrophosphate is conjugated to this molecule by phenyl transferase to form geranyl pyrophosphate, which is bound to isopentenyl pyrophosphate also via phenyl transferase (Figure 1.4). This forms farnesyl pyrophosphate, the precursor for farnesylated and geranylgeranylated proteins that include ubiquinone, dolichol, isopentenyl adenosine (tRNA base) and cholesterol (Ness 1983; Roitelman and Shechter 1984; Goldstein and Brown 1990; Sato *et al.* 1993). In the case of cholesterol biosynthesis, farnesyl pyrophosphate is converted to squalene by squalene synthase, a NADPH-dependent enzyme. Oxidation of squalene by squalene epoxidase to form 2,3-oxidosqualene is catalysed before cyclisation occurs. Cyclisation is a two step enzyme-mediated protonation and deprotonation reaction, which results in a neutral lanosterol molecule (Bloch 1965) (Figure 1.4).

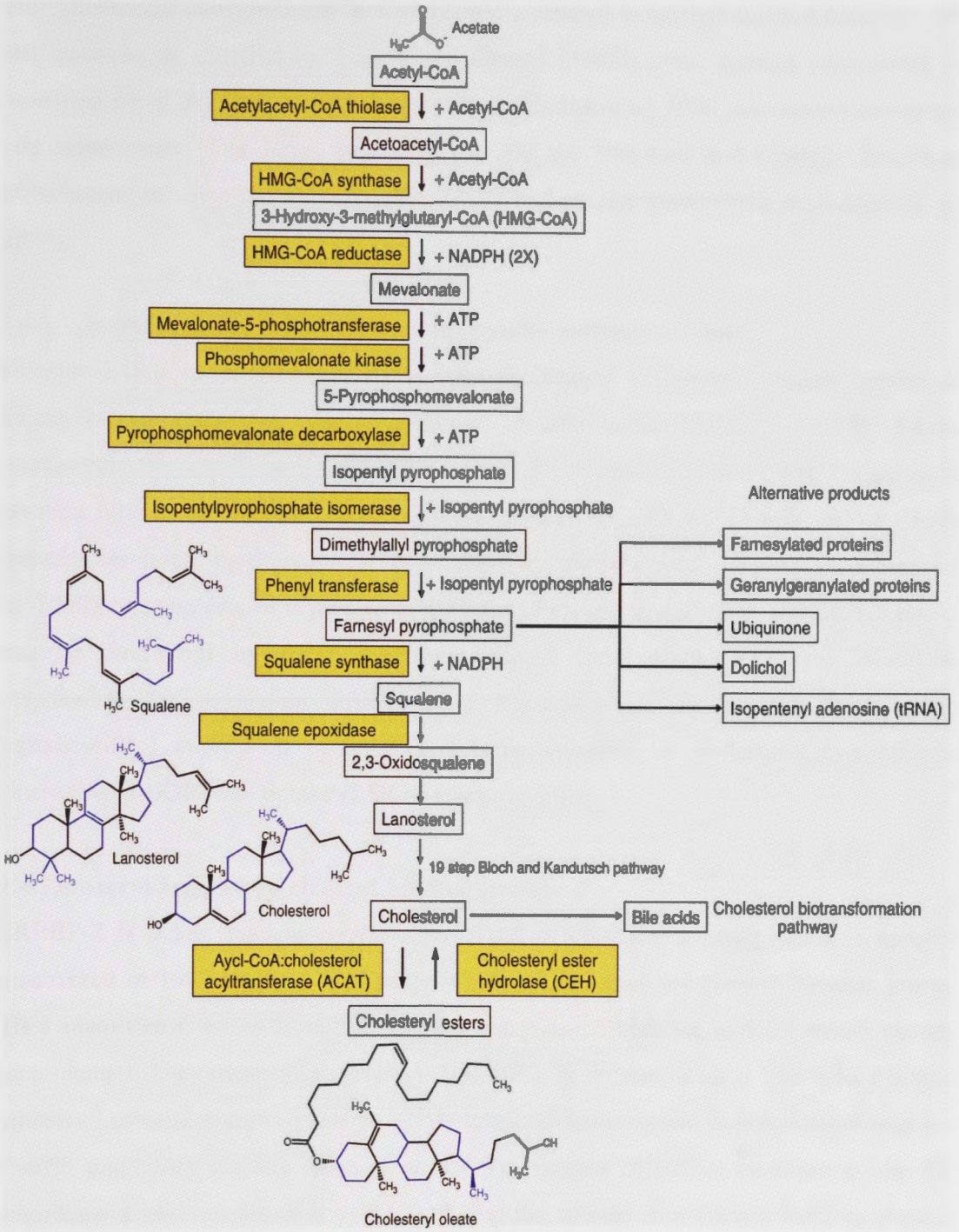

Figure 1.4 Biosynthetic pathway responsible for *de novo* cholesterol biosynthesis in mammals

Schematic representation of the enzymes and substrates involved in the *de novo* biosynthesis of nascent cholesterol. The structures of key products, substrates, or intermediates are shown. Abbreviations: ATP, adenosine-5'-triphosphate; HMG-CoA, 3-hydroxy-3-methyl-glutaryl-CoA; NADPH, nicotinamide adenine dinucleotide phosphate.

The subsequent conversion of lanosterol to cholesterol is carried out in a complex 19-step cascade, as detailed by Rilling and Chayet (1985). Once formed, cholesterol is esterified by ACAT2, as previously described (Meiner *et al.* 1996), or sequestered to the cell membranes. The latter primarily include the PM and endoplasmic reticulum membranes, but also the mitochondria, Golgi and nuclear membranes (Goldstein *et al.* 2008).

1.4.1 Regulation of hepatic cholesterol uptake and biosynthesis

Oxysterols are monohydroxylated or keto-cholesterol derivatives, usually produced during auto-oxidation or biotransformation of cholesterol (Gill *et al.* 2008). These compounds are sensed within the liver by sterol-responsive proteins, sterol-regulatory element binding protein (SREBP), cleavage protein (SCAP) and HMGR, all of which possess sterol-sensing domains (SSD) within their transmembrane regions (Goldstein *et al.* 2008). As cholesterol is present in the ER and plasma membranes, cholesterol levels can be monitored by these membrane-located sterol-sensing proteins. SCAP is responsible for regulating SREBP-2, a transcriptional factor that controls the transcriptional expression of several proteins involved in cholesterol biosynthesis (including HMGR) and uptake (LDLR) (Ness 1983).

1.4.1.1 Sterol-regulatory element binding protein-2

SREBP-2 is a key nuclear regulator involved in cholesterol homeostasis, originally discovered in 1993 by the Nobel prize winning Goldstein and Brown research group. They identified it as the third SREBP; the others are SREBP1a, and -1c which govern long-chain FA synthesis (lipogenesis). SREBP-2 is expressed as a 125 kDa inactive precursor protein, comprised of an $-NH_2$ terminal transcription factor domain and a –COOH regulatory domain (Hua *et al.* 1993). Nascent SREBP-2 localises to the ER membrane with both terminal domains facing the cytosol in a hairpin fashion; there it binds SCAP via the –COOH terminal regulatory region. Under conditions of low intracellular cholesterol, SCAP acts as a chaperone protein responsible for translocating SREBP-2 to the Golgi apparatus (Figure 1.5) (Edwards *et al.* 2000). Translocation of SREBP-2/SCAP to the Golgi apparatus is dependent on the interaction of Sar1/Sec23/24 coat protein (COP)-II complex proteins (McPherson and Gauthier 2004). Within the Golgi, two proteases, site-1 serine protease and site-2 metalloproteinase,

cleave off a 68 kDa SREBP-2 transcription-regulatory fragment. This is capable of further increasing the expression of SREBP-2, thereby resulting in a feed-forward mechanism of regulatory control. Conversely, in response to heightened cellular cholesterol levels, the sterol-sensing domain of SCAP changes conformation and binds to insulin-induced genes (Insig)-1 and -2. This retains the SREBP-2/SCAP complex within the ER (Radhakrishnan *et al.* 2008), impairing its translocation to Golgi. This inhibits SREBP-2 cleavage, leaving the parent protein intact and inactive (Figure 1.5). In these ways, SREBP-2 functions as a cholesterol-sensitive critical regulatory checkpoint responsible for controlling intracellular cholesterol homeostasis.

Active (nuclear) SREBP-2 fragments are responsible for transcriptional regulation of most proteins involved in cholesterol biosynthesis, uptake, and hydrolysis of cholesteryl esters (Table 1.2) (Jackson *et al.* 1995; Ericsson *et al.* 1996; Guan *et al.* 1997; Pai *et al.* 1998; Natarajan *et al.* 1999; Kim *et al.* 2001; Sakakura *et al.* 2001; Horton *et al.* 2002; Nagai *et al.* 2002). The most important of these are HMGR (the rate limiting step in biosynthesis) and LDLR, the plasma membrane transporter responsible for receptor-mediated endocytosis of serum LDL cholesterol. Nuclear SREBP-2 (active) is also responsible for negative regulation of several genes involved in intracellular cholesterol efflux (Table 1.2) (Misawa *et al.* 2003; Zeng *et al.* 2004; Jeong *et al.* 2008). Studies by Norlin and Chiang (2004) found that SREBP-2 inhibits Cyp7b1, an enzyme involved in the biotransformation of cholesterol to bile acids (discussed later). Indirectly, SREBP-2 is also responsible for negative regulation of LDLR, through transcriptional promotion of proprotein convertase subtilisin/kexin type 9 (PCSK9), a protein which binds to LDLR so as to prevent LDLR recycling following its receptor-mediated endocytosis; this results in lysosomal degradation of LDLR (Abifadel *et al.*, 2003).

Table 1.2 SREBP-2 responsive genes involved in cholesterol homeostasis.

This list is by no means exhaustive. It simply refers to those SREBP-2 target genes principally involved in cholesterol homeostasis. Regulation denotes whether positive (+) or negative (–) transcriptional regulation takes place.

Gene	Regulation	Function	References
7-Dehydrocholesterol reductase	+	Cholesterol biosynthesis	(Kim *et al.* 2001)
ABCA1	–	HDL assembly and cholesterol export	(Zeng *et al.* 2004)
Acetoacetyl CoA thiolase	+	Cholesterol biosynthesis	(Horton *et al.* 2002)
Cholesteryl ester hydrolase	+	Hydrolysis of cholesteryl esters	(Natarajan *et al.* 1999)
CYP51	+	Cholesterol biosynthesis	(Pai *et al.* 1998)
Geranyl pyrophosphate synthase	+	Cholesterol biosynthesis	(Horton *et al.* 2002)
HMG-CoA reductase	+	Cholesterol biosynthesis	(Jackson *et al.* 1995, Ness, 1983)
HMG-CoA synthase	+	Cholesterol biosynthesis	(Jackson et al. 1995)
HNF-4α	–	Nuclear transcription factor	(Misawa *et al.* 2003)
Isopentyl pyrophosphate isomerase	+	Cholesterol biosynthesis	(Horton *et al.* 2002)
Lanosterol synthase	+	Cholesterol biosynthesis	(Pai *et al.* 1998)
Lathosterol oxidase	+	Cholesterol biosynthesis	(Pai *et al.* 1998)
LDL receptor	+	Cellular cholesterol uptake	(Horton *et al.* 2002)
Mevalonate kinase	+	Cholesterol biosynthesis	(Sakakura *et al.* 2001)
Mevalonate pyrophosphate decarboxylase	+	Cholesterol biosynthesis	(Sakakura *et al.* 2001)
MTTP	–	VLDL export	(Sato *et al.* 1999)
PCSK9	+	Inhibition of LDLR	(Jeong *et al.* 2008)
Phenyl transferase (farnesyl diphosphate synthase)	+	Cholesterol biosynthesis	(Ericsson *et al.* 1996, Jackson *et al.* 1995)
Phosphomevalonate kinase	+	Cholesterol biosynthesis	(Sakakura *et al.* 2001)
Squalene epoxidase	+	Cholesterol biosynthesis	(Nagai *et al.* 2002)
Squalene synthase	+	Cholesterol biosynthesis	(Guan *et al.* 1997, Pai *et al.* 1998)

Abbreviations: ABCA1, ATP-binding cassette, sub-family A, member 1; CYP51, lanosterol 14α-demethylase; HMG-CoA, 3-hydroxy-3-methylglutaryl-CoA; HNF-4α, hepatocyte nuclear factor-4α; LDLR, low-density lipoprotein receptor; MTTP, microsomal triglyceride transfer protein; PCSK9, pro-protein convertase subtilisin/kexin type-9.

1.4.1.2 HMG-CoA reductase-specific regulation

As HMGR is critical for the control of intracellular cholesterol levels, regulation of the activity of this enzyme is strictly controlled at several stages including: transcriptional, translational, and post-translational levels. Such complex interactions result in either long- or short-term feedback regulation. Long-term regulation is achieved by controlling enzyme expression within the cell, by modulating both the expression and degradation of proteins. HMGR transcription is regulated by SREBP-2 (Table 1.2), which, as previously described, increases under conditions of low-cholesterol concentrations. Once synthesised, HMGR localises to the ER membrane in a similar manner to SREBP-2, where it is post-transcriptionally regulated by oxysterols. These include lanosterol, which is sensed by the sterol-sensing domain (SSD) located between transmembrane segments, (TMS)-2 and -6 (Gil *et al.* 1985) (Figure 1.5). When

oxysterols are sensed within the ER membrane, HMGR binds to Insig-1 and gp78 (Sever *et al.* 2003b; Song *et al.* 2005). Gp78 is a ubiquitin-ligating enzyme which ubiquitinates Lys^{89} and Lys^{248} residues (Sever *et al.* 2003a). In doing so, this results in entry of HMGR into the ER-associated degradation (ERAD) pathway, which in turn is assisted by valosin-containing protein (VCP) which binds to Insig-1 and gp78 to result in HMGR degradation by the 26S proteasome (Song *et al.* 2005) (Figure 1.5).

Short-term regulation of HMGR is temporarily achieved by phosphorylation at Ser^{872} in humans and Ser^{871} in rodents (Omkumar *et al.* 1994; Istvan *et al.* 2000); these phosphorylations inactivate the enzyme (Gillespie and Hardie 1992; Sato *et al.* 1993). Serine phosphorylation at these residues is carried out by AMP-dependent protein kinase (AMPK) (also known as HMG-CoA reductase kinase), in a process that is thought to be related to cell stress (Corton *et al.* 1994). In contrast, the activity of HMGR can be enhanced by increased levels of cellular thiols such as reduced glutathione (GSH) (Roitelman and Shechter 1984). Cholesterol-related sterols, such as lanosterol (product of cholesterol biosynthesis; see Figure 1.4), also promote the inhibitory phosphorylation of HMGR (Miller *et al.* 1989).

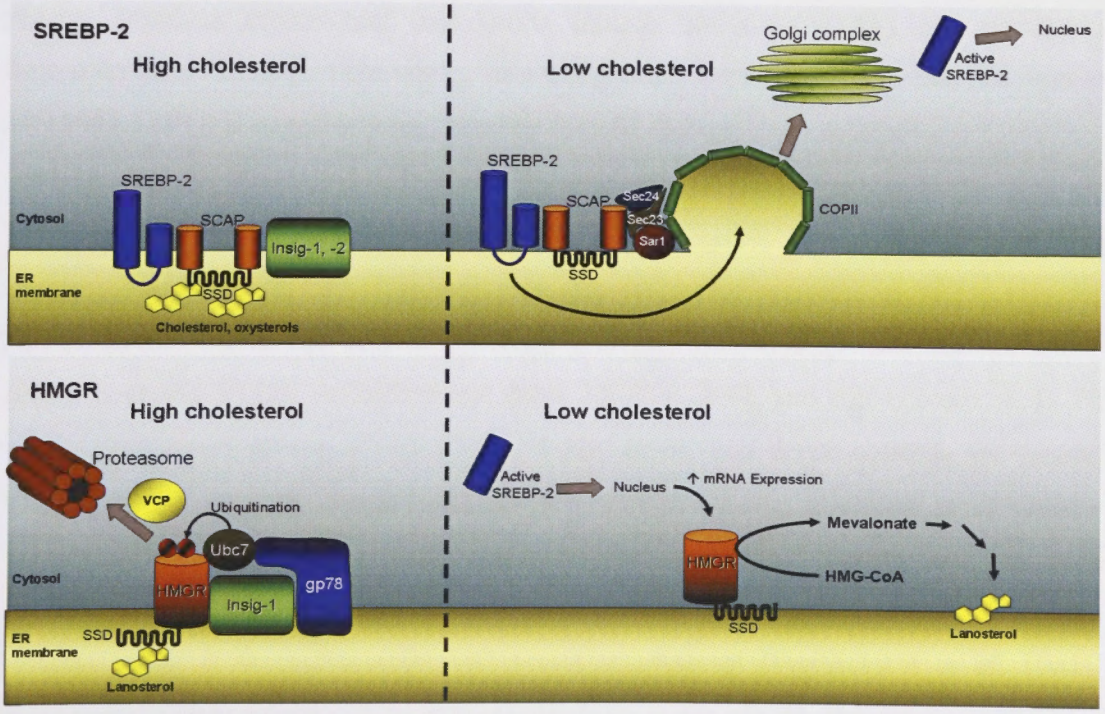

Figure 1.5 Sterol-responsive regulation of SREBP-2 and HMGR.

Abbreviations for Figure 1.5: COPII, coat-protein-II; Insig, insulin-sensitive gene protein -1, -2; HMGR, 3-hydroxy-3-methylglutaryl-CoA reductase; SCAP, SREBP cleavage protein; SREBP-2, sterol regulatory element binding protein-2; SSD, sterol sensing domain; VCP, valosin-containing protein. Image adapted from Goldstein *et al.*, 2008.

1.5 Forward cholesterol transport

Following esterification of FC by ACAT, CE can be stored in the hepatocyte as droplets or secreted into the blood stream as very low-density lipoprotein (VLDL) colloids. This process is also known as *forward cholesterol transport*, and is required for transporting high energy TGs and fat-soluble vitamins to peripheral tissues (Fielding and Fielding 1995) (Figure 1.6). It is important to note that forward cholesterol transport is dependent on ACAT activity, the inhibition of which decreases VLDL secretion (Musanti *et al.* 1996; Brown and Gibbons 1997; Brown *et al.* 1999; Burnett *et al.* 1999). Assembly of VLDL particles begins with the elaboration of a non-truncated, 550 kDa apoB-100 protein in the ER (Table 1.1) that folds in such a fashion as to assist in the transport of hydrophobic lipid molecules (Johs *et al.* 2006). Once expressed, apoB-100, along with nascent apoC-II and apoE lipoproteins, leaves the ER and fuses with the Golgi complex. Within the Golgi, apolipoproteins merge with a large TG-rich droplet containing CEs and minor fat soluble vitamins (Bamberger and Lane 1988; German *et al.* 2006); this process involves microsomal triglyceride transfer protein (MTTP) and results in formation of a VLDL particle which, in a Golgi-dependent step, is secreted (Gordon *et al.* 1994). MTTP is negatively regulated by SREBP-2 (Sato *et al.* 1999).

The VLDL secretory vesicle is referred to as the VLDL transport vesicle (VTV) (Siddiqi 2008) (Figure 1.2). This vesicle is responsible for secretion of VLDL into the blood stream, where the colloid becomes biologically active (Fisher and Ginsberg 2002). Secreted VLDL colloids range from 300-700 Å Ø, and can contain up to 20 mg/dL cholesterol (Olson 1998) (Figure 1.3). Larger, less dense colloids are termed $VLDL_1$, while smaller, denser particles are termed $VLDL_2$ (German *et al.* 2006). Empirical findings have identified a correlation between type 2 diabetes and increased VLDL secretion. It should also be noted that CRs structurally resemble VLDL; they have an ~700 Å Ø, and contain ~20 mg/dL cholesterol (Fredrickson *et al.* 1967). However, CR only contain ~10% the original TG content of CM. Due to the similarities in size, density and composition of lipoprotein colloids, apolipoproteins are able to freely exchange between different colloids (Figure 1.6).

In the circulation, VLDL colloids are acted upon by extrahepatic LPLs in a similar fashion to CRs (Cryer 1981). In the process, TG, FFAs, and fat-soluble vitamins are transferred to peripheral tissues (Figure 1.6). TG-depleted VLDL remnant colloids are commonly termed intermediate density lipoproteins (IDLs) (German *et al.* 2006) (Figure 1.3A). IDL colloids are returned to the liver, where they are either taken up by LDLR or remodelled by hepatic lipases which remove the remaining TG content, so resulting in the formation of high-cholesterol LDL particles (Figure 1.6). LDL particles contain the highest amount of cholesterol of all four lipoprotein classes, and account for roughly two-thirds of all plasma-transported cholesterol (Oram and Heinecke 2005) (Figure 1.3). They are responsible for transporting cholesterol (predominantly in the form of cholesteryl esters) to peripheral tissues for utilisation in steroidogenesis and as a component of plasma membranes. Excess bodily LDL is re-circulated to the liver and reclaimed via LDLR (Figure 1.6).

Due to their atherogenic nature, however, an accumulation of LDL particles in the vascular system can lead to atherosclerosis (Havel 1998; Kellner-Weibel *et al.* 1999b; Vine *et al.* 2008). In this respect, it should also be noted that LDL can undergo oxidation reactions in the periphery, the products of which are not recognised by LDLR, but instead is taken up by scavenger receptor-B1 (SR-B1) and CD36 (these transporters will be discussed later).

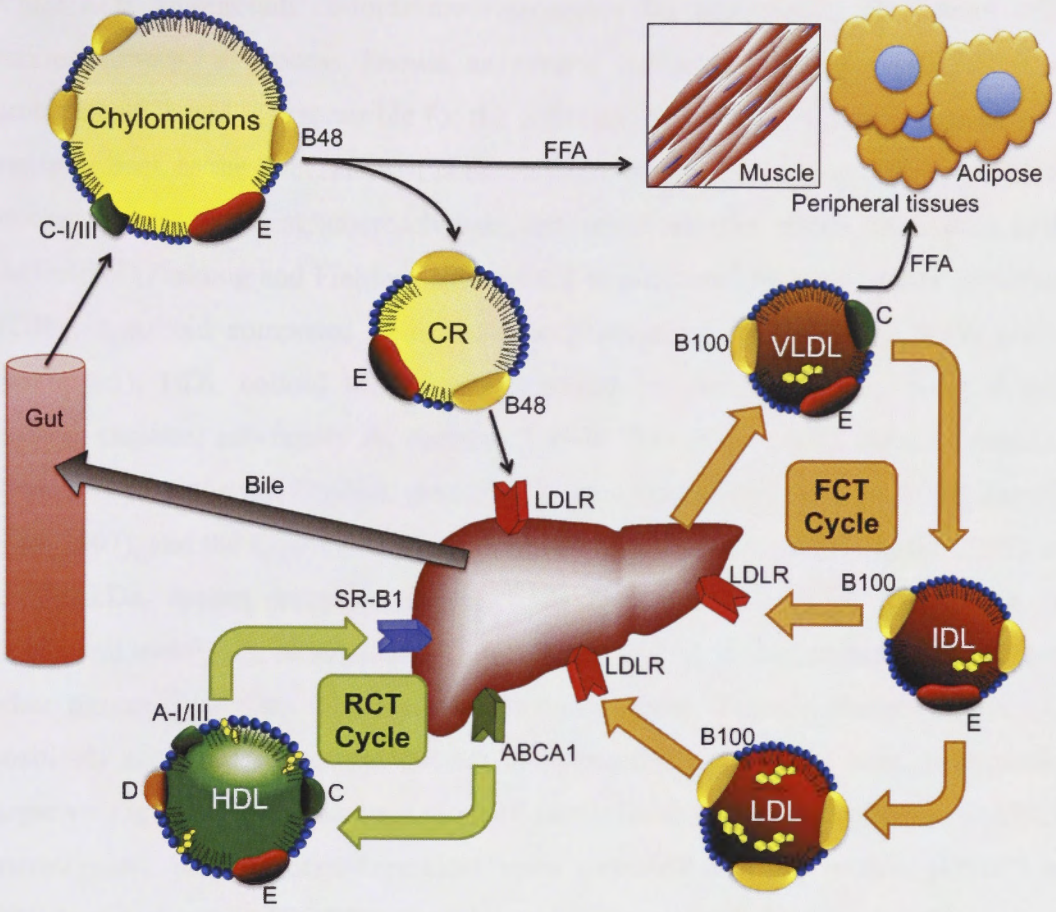

Figure 1.6 Schematic diagram depicting lipoprotein metabolism and involvement in forward and reverse cholesterol transport

Lipids absorbed by the gut are packaged into chylomicrons, which circulate within the vascular system and deliver FFAs (liberated from TG by cell surface lipases) to peripheral tissues. The TG-depleted chylomicron remnants (CR) are taken up into the liver by low density lipoprotein receptor (LDLR). The liver is also responsible for forward cholesterol transport (FCT), in which very low density lipoprotein (VLDL) is assembled and secreted (see Figure 1.3 for cholesterol content). VLDL also circulates and distributes cholesterol and FFAs to the peripheral tissues. This process, in turn, results in intermediate density (IDL) and low density (LDL) lipoprotein colloid products, which are taken up into the liver via LDLR. Separately, reverse cholesterol transport (RCT) is a liver-dependent mechanism responsible for collecting excess peripheral cholesterol. ATP-binding cassette, sub-family A, member 1 (ABCA1) expressed by the liver and other peripheral tissues is responsible for the formation of high density lipoproteins (HDL) and cellular efflux of cholesterol. HDL absorbs peripheral cholesterol for delivery back to the liver, where these colloids are taken up by scavenger receptor-B1 (SR-B1). Letters refer to apolipoprotein type: A-I/III, Apolipoprotein A-I/III;; B48, ApoB-48; B100, ApoB-100; C-I/III, ApoC-I/III; E, ApoE.

1.6 Reverse cholesterol transport

While LDL lipoprotein colloids are responsible for transporting cholesterol to the various tissues, a process known as *reverse-cholesterol transport* (RCT) occurs simultaneously and is responsible for the collection of excess peripheral cholesterol for transport back to the liver. Here, it is biotransformed and excreted in bile. In effect, this process protects against atherosclerosis and other adverse effects of excess bodily cholesterol (Fielding and Fielding 1995). RCT is facilitated by high-density lipoprotein (HDL), a colloid composed of helical apolipoproteins: apoA-I, A-II, A-IV, and –E (Table 1.1). HDL colloid formation is initiated by plasma membrane-bound ATP-binding cassette, sub-family A, member 1 (ABCA1) (Figure 1.2). ABCA1 assists in apoA-I folding, the rate-limiting step of HDL biosynthesis (Sahoo *et al.* 2004; Zarubica *et al.* 2007), and the export of FC and PLs (Oram 2003; Oram and Heinecke 2005). It is a 254 kDa, 6-pass transmembrane, glycosylated protein, which localises to the basolateral membrane of hepatocytes. However, ABCA1 is also expressed in numerous other tissues, including intestine, muscle and adipose. Transcriptionally, ABCA1 is positively regulated by several nuclear receptors (NR), described later. In regards to negative regulation, the accumulation of intracellular oxysterols suppresses ABCA1 transcription, in a process dependent upon oxysterol binding protein (OSBP) and OSBP-related protein 8 (ORP8) (Bowden and Ridgway 2008; Yan *et al.* 2008).

ABCA1 forms a homo-tetramer which binds apoA-I and possesses cholesterol and PL translocase activities (Denis *et al.* 2004b; Vedhachalam *et al.* 2007). The protein has two large extracellular loops, located between transmembrane segments (TMS)-1 and -2. These are responsible for stabilising apoA-I and initiating a lipidation cascade whereby peripheral cholesterol and phospholipids bind to the helical structure of apoA-I. In turn this results in pre-β1-HDL colloid formation (Denis *et al.* 2004a) (Figure 1.2).

Pre-β1-HDL is a "lipid-poor" HDL particle 60-70 kDa in size, composed of ~40% lipid and apoA-I only (Table 1.1). These nascent HDL particles contain small amounts of PL and FC; the latter is subject to FA esterification catalysed by LCAT to form CEs. The accumulation of lecithin leads to pre-β2-HDL or "discoidal-HDL" development, where apoA-I forms a perimeter around the hydrophobic lipid content of the particle. Further accumulation of cholesterol and PL drives the formation of mature, spherical, HDL. HDL returns to the liver where it binds to SR-B1. SR-B1 selectively transports HDL-

bound CEs into hepatocytes, where they are biotransformed to bile acids (described below) and excreted (Fielding and Fielding 1995) (Figure 1.2 and 1.6). Increased ABCA1 expression also lowers hepatocyte biosynthesis and secretion of VLDL particles (Sahoo *et al.* 2004).

1.7 Biotransformation of cholesterol to form bile salts

Biotransformation of cholesterol into bile acids is the major pathway for cholesterol catabolism in mammals. It is essential, because excess cholesterol within the body can precipitate, and in the process generate cholesterol crystals that result in cell death (Brown and Goldstein 1997). Cholesterol biotransformation is achieved by the addition of several hydrophilic hydroxyl groups to cholesterol ring structure and side chain, culminating in the formation of bile acids, which are soluble detergent-like molecules. Conversion of cholesterol into bile acids accounts for ~90% of cholesterol turnover (the remainder is utilised in steroidogenesis), with production of bile acids in humans averaging 300-500 mg/day (Hofmann 2001). Once synthesised, BAs are secreted across the canalicular (or apical) pole of hepatocytes where they emulsify with PLs and cholesterol to form bile (Nemchausky *et al.* 1977). The bile canaliculi eventually join to form bile ductules, which network and culminate in larger bile ducts that eventually form the common hepatic duct, which receives the cystic duct emanating from the gallbladder where bile is stored before use during digestion of meals. Bile enters the duodenum via the common bile duct and the sphincter of Oddi.

The detergent properties of BAs are responsible for the emulsification of dietary lipids, cholesterol and fat-soluble vitamins (Whiteside *et al.* 1965). This process, termed micellisation, precedes lipid absorption by enterocytes and recycling of BAs back to the liver in a process known as the enterohepatic circulation (Irvin 1952). On average, the body is able to recycle ~95% of the BA pool, the remaining fraction is excreted (Galatola *et al.* 1991).

The biosynthesis of BAs is catalysed by a specialised group of cytochromes P450 (CYP*) mono-oxidases or mono-oxygenases, which catalyse the hydroxylation of cholesterol, as well as modification of the cholesterol side chain (Ferdinandusse and Houten 2006). BA biosynthesis can be subdivided into four separate pathways: initiation, ring structure modification, side chain oxidation and amino acid conjugation.

A total of 17 different enzymes are responsible for the biosynthesis from cholesterol to cholic (CA) and chenodeoxycholic acid (CDCA), the primary BAs in humans, and cholic and β-muricholic acid in mice.

*Footnote: The international nomenclature for this large family of proteins uses all capital notation (eg: CYP7A1) for humans, and lower case letters for murine homologs (eg: Cyp7a1). Since the discussion in this part of the thesis refers principally to humans, the upper case (CYP) notation will be used, but in the data Chapters (3-7) describing results in mice, the style will revert to lower case (Cyp).

1.7.1 Initiation of cholesterol biotransformation

Initiation of BA synthesis is started by the 7α-hydroxylation of cholesterol. This step is predominantly catalysed by microsomal 7α-hydroxylase (CYP7A1) (*classical pathway*), which supplies ~75% of all hepatic 7α-hydroxycholesterol in mice, and ~90% in humans (Russell 2003) (Figure 1.7). The remainder of 7α-hydroxycholesterol is formed by three minor *alternative pathways,* involving the hydroxylation of cholesterol at either: C_{24}, C_{25}, or C_{27} positions; the corresponding reactions are catalysed by cholesterol 24-hydroxylase (CYP46A1), cholesterol 25-hydroxylase (CH25H) or mitochondrial sterol 27-hydroxylase (CYP27A1). It should be noted that CYP27A1 is also able of hydroxylating C_{24} and C_{25} on the cholesterol molecule (Ferdinandusse and Houten 2006) (Figure 1.7). Following side chain hydroxylation, 7α-hydroxylation takes place via one of two pathways depending on the side chain hydroxylated. 24-Hydroxycholesterol is catalysed by oxysterol 7α-hydroxylase (CYP39A1) yielding: 7α,24-hydroxylcholesterol, while 25- and 27-hydroxycholesterol are catalysed by a separate oxysterol 7α-hydroxylase (CYP8B1) to form 7α,25-hydroxycholesterol and 7α,27-hydroxycholesterol, respectively (Figure 1.7).

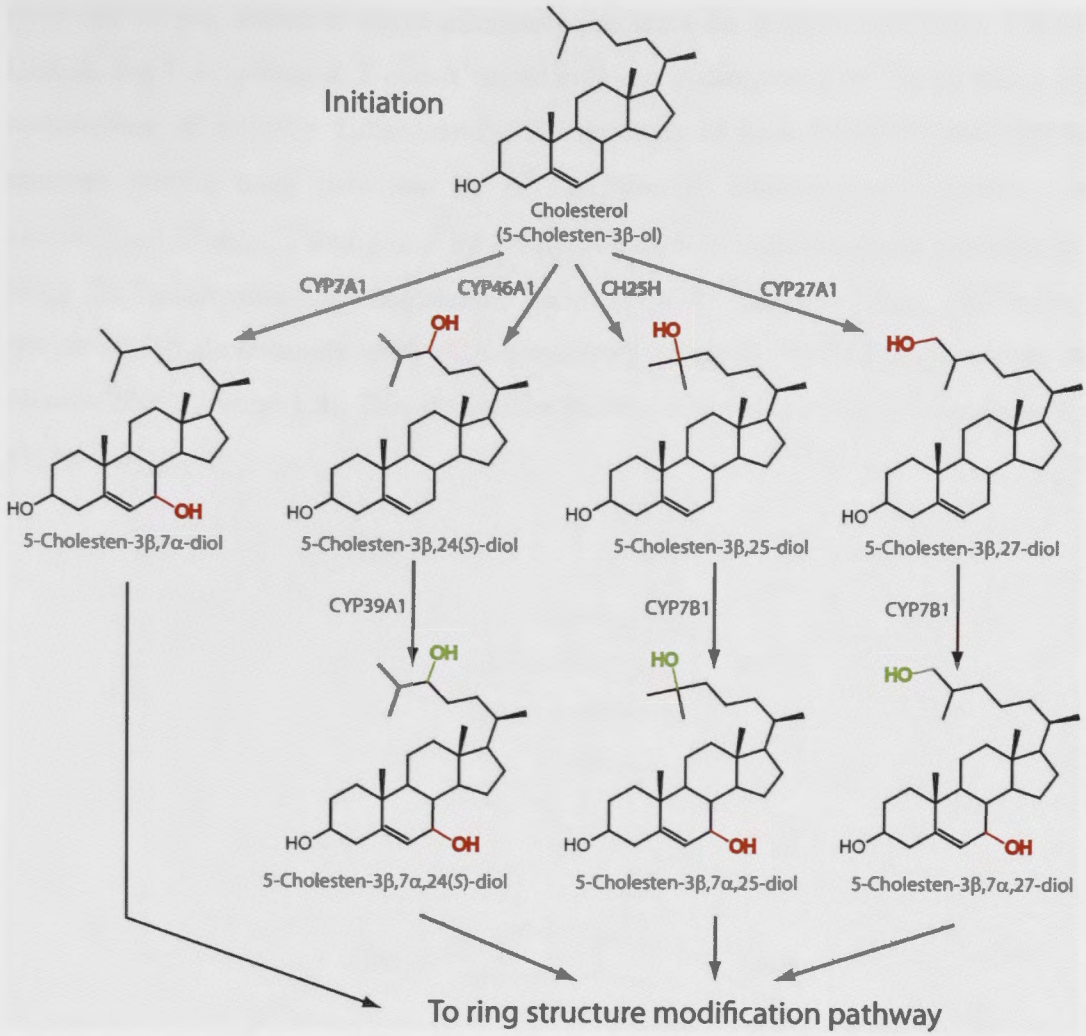

Figure 1.7 Pathways responsible for the initial stages of cholesterol bioconversion to bile acids

Enzymes responsible for the various reactions are named adjacent to reaction arrows, with added moieties highlighted in red. This particular pathway is detailed in Section 1.7.1. Green highlighted moieties denote cumulative changes made to the original cholesterol backbone. Image adapted from Russell (2003). Abbreviations: CH5H, cholesterol 25-hydroxylase; CYP7A1, cholesterol 7α-hydroxylase; CYP7B1, 25-hydroxycholesterol 7-α-hydroxylase; CYP27A1, mitochondrial sterol 27-hydroxylase; CYP39A1, oxysterol 7α-hydroxylase; CYP46A1, cholesterol 24-hydroxylase.

1.7.2 Ring structure modification

The 7α-hydroxylated products enter the ring structure modification pathway where they are acted upon by 3β-hydroxy-Δ^5-C_{27}-steroid oxidoreductase (HSD3B7). This enzyme catalyses the simultaneous isomerisation of the double carbon-bond from C_5 to C_4 and conversion of the 3β-hydroxyl-group to a 3-oxo-Δ^4 oxysterol (Russell 2003; Ferdinandusse and Houten 2006) (Figure 1.8). The products from this reaction can then

enter one of two reactions which ultimately predicate the formation of either CA or CDCA. For CA synthesis, 3-oxo-Δ^4 oxysterols are hydroxylated at C_{12} by sterol 12α-hydroxylase (CYP8B1). Subsequently, the products of both HSD3B7 and CYP8B1 undergo double bond reduction by Δ^4-3-oxosteroid, 5β-reductase (AKR1D1) and alcoholation of the C_3 oxo-group by 3α-hydroxysteroid dehydrogenase (AKR1C4) to yield 3α,7α-dihydroxy-5β-cholestanoic acid (CDCA precursor) and 3α,7α,12α - trihydroxy-5β-cholestanoic acid (CA precursor) (Russell 2003; Ferdinandusse and Houten 2006) (Figure 1.8). This step marks the end of the ring structure modification of cholesterol.

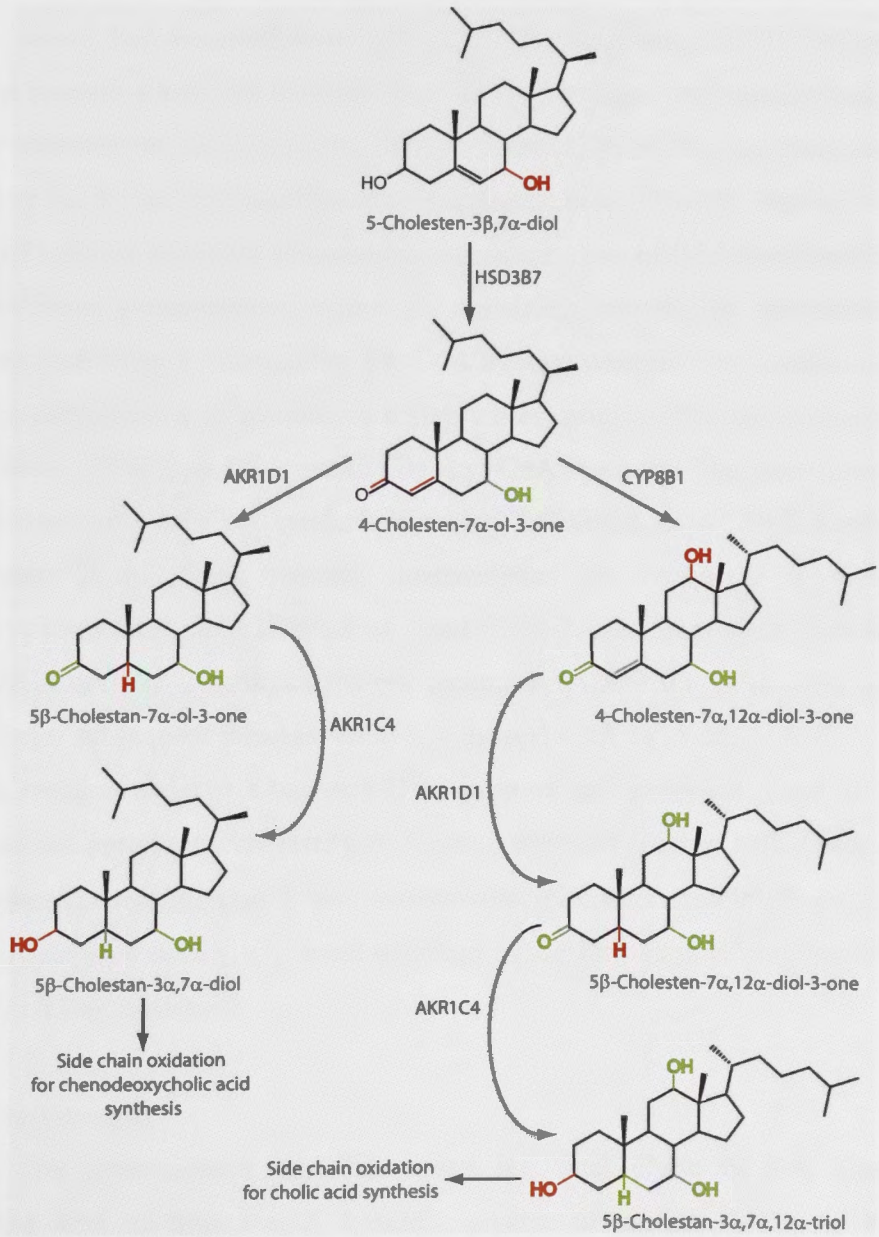

Figure 1.8 Ring structure modification pathway involved in the biotransformation of cholesterol to bile acids

Legend for Figure 1.8.

Enzymes responsible for the various reactions are named adjacent to reaction arrows, with added moieties highlighted in red. This particular pathway is detailed in Section 1.7.2. Green highlighted moieties denote cumulative changes made to the original cholesterol backbone. Image adapted from Russell (2003).

Abbreviations: AKR1C4, 3α-hydroxysteroid dehydrogenase; AKR1D1, Δ^4-3-oxosteroid,5β-reductase; CYP8B1, sterol 12α-hydroxylase ; HSD3B7, 3β-hydroxy-Δ^5-C27-steroid oxidoreductase.

1.7.3 Side chain oxidation

Products from the ring-structure modification steps enter a side chain oxidation pathway, where they are acted upon by CYP27A1. At this stage, CYP27A1 catalyses a three step process where the C_{27} side chain is hydroxylated, converted to an aldehyde and then a carboxylic acid (Russell 2003) to form (25*R*)-3α,7α-dihydroxycholestanoic (DHCA) or (25*R*)-3α,7α,12α-trihydroxycholestanoic acid (THCA) (Shefer *et al.* 1978) (Figure 1.9). These products subsequently translocate out of the mitochondria into ER and peroxisomal compartments, where the remaining steps in BA biosynthesis occur. These intermediates are activated by BA-CoA ligation whereby CoA ester is conjugated to the C_{27} carboxylic acid residue, in a step either catalysed by very long-chain acyl-CoA synthase (VLCS) or ER-specific bile acyl-CoA synthase. The latter is also known as very long-chain acyl-CoA synthase homolog 2 (Mihalik *et al.* 2002; Ferdinandusse and Houten 2006). Once formed, intermediates are racemised to (25*S*)-3α,7α-dihydroxycholestanoic acid (DHC-CoA) and (25*S*)-3α,7α,12α-trihydroxycholestanoyl-CoA (THC-CoA) by 2-methylacyl-CoA racemase (AMACR). DHC-CoA and THC-CoA undergo subsequent β-oxidation of C_{24} by acyl-CoA oxidase (ACOX)-2. Products from this reaction undergo a two-step C_{24} hydration and oxidation phase catalysed by *D*-bifunctional protein, which results in C_{24}-oxo products (Figure 1.9). These are acted upon by peroxisomal thiolase-2, also known as sterol carrier protein-chi or SCPχ. This enzyme hydrolyses the C_{24}-C_{25} bond resulting in the formation of propionyl-CoA and C_{24}-CoA BA intermediates.

1.7.4 Conjugation

C_{24}-CoA BA intermediates can then enter the final phase of BA biosynthesis, conjugation with an amino acid, typically glycine or taurine to C_{24}, in a reaction catalysed by bile acid coenzyme A:amino acid N-acyltransferase (BAAT). BAAT is a peroxisomal enzyme expressed within hepatocytes. Amino acid conjugation results in

the formation of glycocholic, taurocholic, glycochenodeoxycholic and taurochenodeoxycholic acids (Figure 1.10). Within the intestine, glycine and taurine residues are hydrolysed to liberate cholic and chenodeoxycholic bile salts, which can then either be reabsorbed or excreted. In addition to amino acid liberation, cholic and chenodeoxycholic primary BAs can be acted upon by intestinal bacteria and converted to secondary BAs, such as deoxycholate and lithocholate (Russell 2003; Ferdinandusse and Houten 2006).

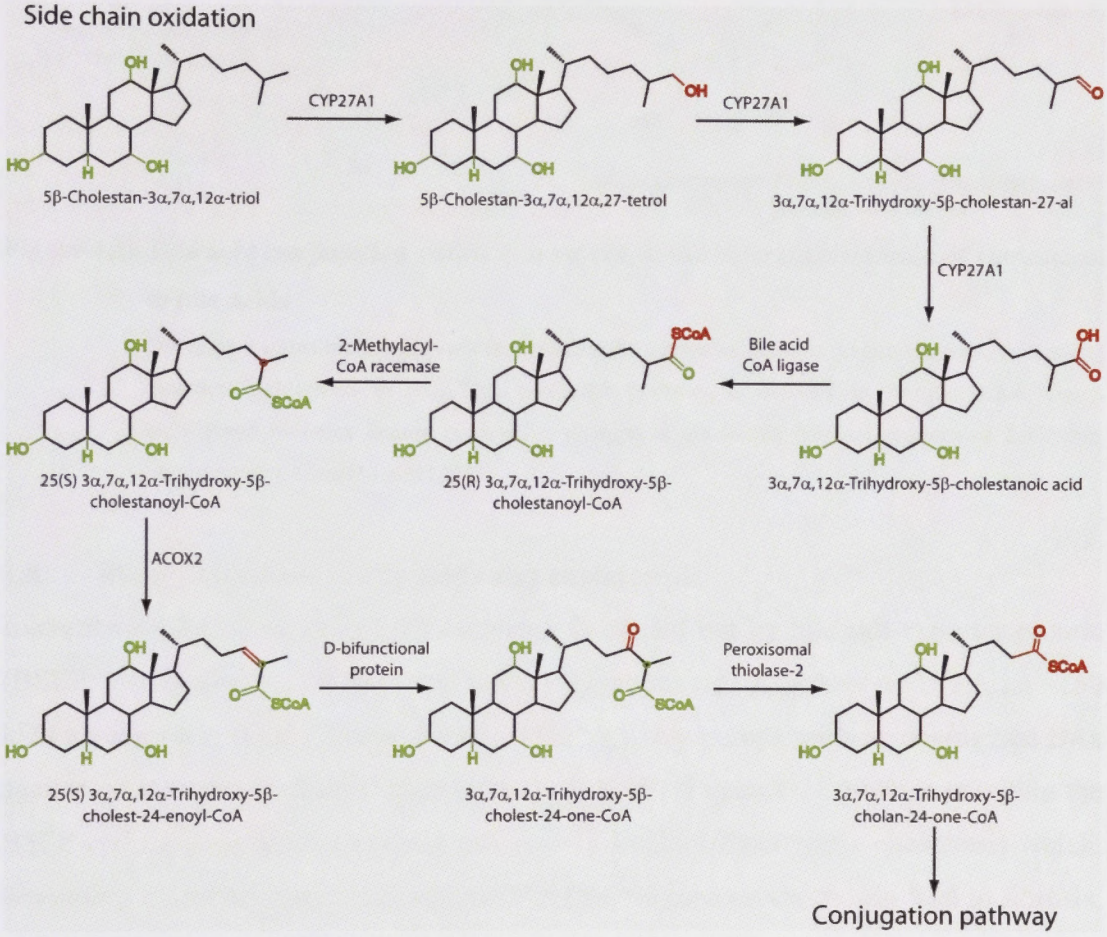

Figure 1.9 Side chain oxidation pathways involved in the biotransformation of cholesterol to bile acids

Enzymes responsible for the various reactions are named adjacent to reaction arrows, with added moieties highlighted in red. This particular pathway is detailed in Section 1.7.3. Green highlighted moieties denote cumulative changes made to the original cholesterol backbone. Image adapted from Russell (2003).

Abbreviations: CYP27A1, mitochondrial sterol 27-hydroxylase.

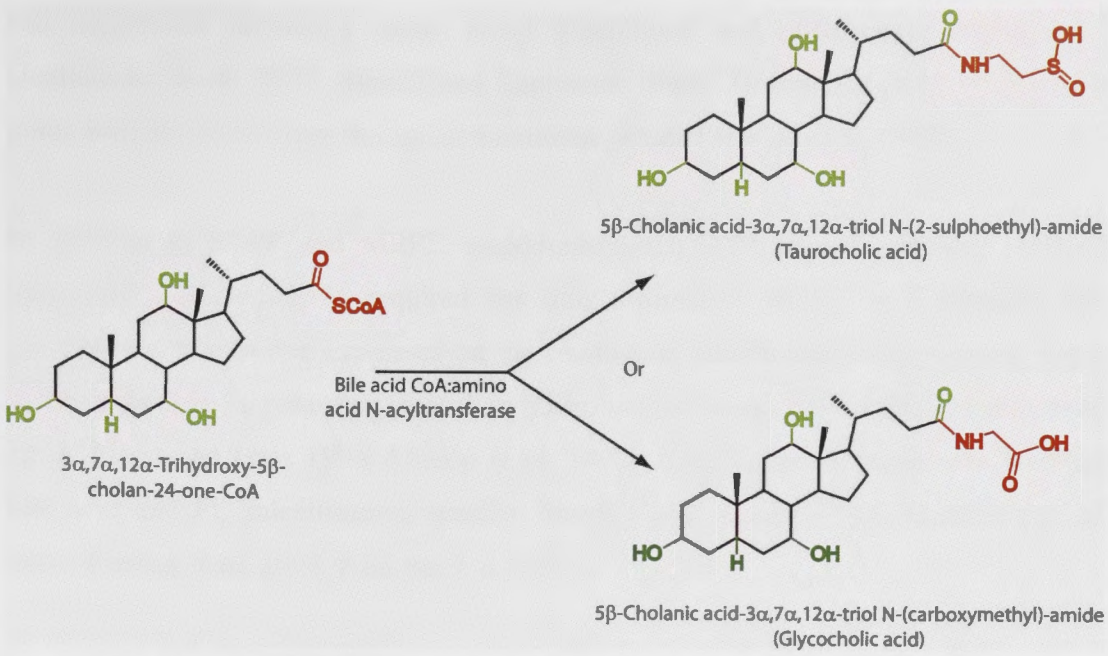

Figure 1.10 Bile acid conjugation pathway involved in the biotransformation of cholesterol to bile acids

Enzymes responsible for the various reactions are named adjacent to reaction arrows, with added moieties highlighted in red. This particular pathway is detailed in Section 1.7.4. Green highlighted moieties denote cumulative changes made to the original cholesterol backbone. Image adapted from Russell (2003).

1.8 Biliary secretion of bile acids and cholesterol

Excretion of BAs into the biliary canaliculi is carried out by bile salt exporter protein (BSEP; also known as ABCB11 and sister-*P*-glycoprotein) (Childs *et al.* 1995), an ~160 kDa glycoprotein (Gerloff *et al.* 1998). BSEP actively pumps primary conjugated BAs against an extreme gradient (Strautnieks *et al.* 2008) (Figure 1.2). Mutations within the BSEP-coding gene result in type-2 progressive familial intrahepatic cholestasis which, depending on the severity, as determined by type of gene mutation, can lead to fibrosis, cirrhosis and end-stage liver disease (Strautnieks *et al.* 2008).

The biliary export of BAs by BSEP is complemented by multidrug resistance-associated protein-2 (MRP2; also known as ABCC2 or multispecific organic anion transporter [MOAT]) (Figure 1.2). MRP2 is a 190 kDa transmembrane protein which colocalises with BSEP on the canalicular (apical) membrane of hepatocytes (Keppler *et al.* 1997; Tanaka *et al.* 1999; Zinchuk *et al.* 2002). It is an organic anion transporter responsible for export of conjugated BAs, leukotrienes, glutathione, several steroids and bilirubin glucuronides. In addition, MRP2 is responsible for excretion of numerous endogenous

and xenobiotic (including many drug) glutathione and glucuronide conjugates (Jedlitschky *et al.* 1997; Suzuki and Sugiyama 1998). However, MRP2 is unable to pump primary BAs across the apical membrane (Oude Elferink *et al.* 1995).

In addition to BSEP and MRP2, multidrug-resistance-associated protein-2 (MDR2) transporter functioning is required for bile formation. MDR2 is a 140-150 kDa glycoprotein transporter expressed on the canalicular membrane of hepatocytes, where it is responsible for secreting phosphatidylcholine (PC) into the canaliculi (Smit *et al.* 1993; Ruetz and Gros 1994; Madon *et al.* 1997). Canalicular PC molecules facilitate bile acid and FC micellisation, thereby forming bile (Cohen 1999; Yasumiba *et al.* 2001; Ehehalt *et al.* 2004; Kimura *et al.* 2007).

In a similar process to that observed in enterocytes (Section 1.1), an ABCG-5 and -8 heterodimer is also present on the hepatocyte apical membrane. Here ABCG5/8 is responsible for pumping FC into the bile canaliculi (Figure 1.2). While ABCG-5 and -8 have been found to dimerise, localisation studies have observed solitary ABCG-8 expression throughout the bile ducts, suggesting that ABCG-8 may possess individual protein functions (Klett *et al.* 2004). The FC is subsequently emulsified by BAs and phospholipids to form mixed micelles, which results in the formation of bile.

A physiological pathway that is not so well appreciated is the reclamation of cholesterol from bile. This is regulated by hepatocellular, canalicular-bound NPC1L1 protein, which effectively regulates the concentration of cholesterol in bile by returning some of it back into hepatocytes (Temel *et al.* 2007) (Figure 1.2). The potential significance of NPC1L1 on the canalicular membrane for pharmacological reduction of hepatic FC stores will be addressed in Chapter 6.

1.8.1 Regulation of bile acid biosynthesis and cholesterol/bile acid export

BA biosynthesis is critical for disposal of accumulated cholesterol. Conversely, however, excess BA biosynthesis and/or failure to efficiently secrete BAs results in cytotoxicity as reported in various cell lines (Benedetti *et al.* 1997; Lu *et al.* 2000; Hino *et al.* 2001; Chen *et al.* 2009; Barrasa *et al.* 2011). This is largely because detergent properties of BAs are capable of disrupting lipid, protein and nucleic acid components, interfering with plasma membrane physiology, and generation of ER and mitochondrial

stress, all of which lead to liver injury and cellular apoptosis or necrosis (Gauthier *et al.* 2007; Perez and Briz 2009). Excess intracellular cholesterol, on the other hand, can undergo crystallisation to form cholesterol monohydrate crystals (Phillips 1990; Huang *et al.* 1999), leading to cell damage and liver injury. In *in vitro* foam cell models, intracellular cholesterol accumulation results in macrophage injury and apoptosis (Kellner-Weibel *et al.* 1998; Kellner-Weibel *et al.* 1999a; Kellner-Weibel *et al.* 2003), suggesting that excess intracellular cholesterol is lipotoxic. Within the liver, intracellular cholesterol and BA concentrations are precisely regulated, with intracellular cholesterol content controlled through uptake, biotransformation to BAs and export (See above). Co-ordinately, hepatic BA content is regulated through careful control of Cyp expression and activity. Collectively, several nuclear receptors (NR) are responsible for the regulation of the above mentioned genes involved in cholesterol and BA regulation.

1.8.1.1 Nuclear receptors

NRs constitute the largest mammalian family of transcription factors responsible for regulating gene expression in response to extra-/intracellular stimuli (McKenna and O'Malley 2001; Wang *et al.* 2011a). These stimuli include small hydrophobic steroid, retinoid, and/or thyroid hormone molecules (see review by Hilser and Thompson [2011]). According to function and structural aspects, NRs are divided into three major categories: (i) steroid hormone receptors and vitamin D/thyroid/retinoid receptors, ii) peroxisome proliferator activated receptors, and iii) orphan receptors [these receptors have no known ligands]), and seven subfamilies termed NR0-NR6 (Wang *et al.* 2011a). In total, humans and mice have 48 and 49 NRs, respectively (Zhang *et al.* 2004; Hilser and Thompson 2011). Structurally, NRs generally possess five domains, namely (from –N to –C terminus), a variable region (A/B domain) which typically contains a ligand-independent domain, a DNA binding domain (DBD) containing two zinc fingers which recognise *cis*-regulatory element DNA sequences referred to as *hormone response elements* (HREs), a ligand-binding domain (LBD), and a variable C-terminal region. NR-dependent gene regulation is complex and involves DNA and/or protein interactions, which are induced by several ligands. For purposes of clarity, only NR related to cholesterol homeostasis are discussed here.

Cholesterol and BA homeostasis are predominately regulated by liver receptor homolog-1 (LRH-1), liver X receptors (LXR), hepatocyte nuclear factors (HNF), farnesoid X-receptor (FXR), and small heterodimeric partner (Shp) NRs. The functions of these specific NRs are briefly discussed below.

1.8.1.2 Liver receptor homologue-1

LRH-1, also known as α-fetoprotein transcription factor, is an enterohepatic (confined to tissues of endodermal origin) transcription factor expressed in the liver, pancreas, and small intestine; lower LRH-1 expression is also observed in the ovaries, placenta and adipose tissues (Fayard *et al.* 2004). LRH-1 is the second member of nuclear receptor family 5A (NR5A2) (Becker-Andre *et al.* 1993). Transcriptionally, LRH-1 is regulated by GATA transcriptional elements (Pare *et al.* 2001), and HNF-1/HNF-3β in humans (Zhang *et al.* 2001b); TNF-α also capable of inducing LRH-1 expression (Bohan *et al.* 2003). Interestingly, HNF factors (-1, -3β, and -4α) are transcriptionally controlled by LRH-1 (Pare *et al.* 2001), suggesting that LRH-1 may constitute one of the principle NR responsible for maintaining the hepatic phenotype.

LRH-1 shares a large degree (~95%) of sequence conservation with steroidogenic factor-1 (SF-1; NR5A1), a nuclear receptor responsible for the differentiation of steroidogenic tissues and subsequent development of sexual traits in mammals. Physiologically, LRH-1 is responsible for the positive transcriptional regulation of most of the genes involved in reverse cholesterol transport, these include: HDL cholesterol uptake and assembly (SR-B1 and ABCA1), BA biosynthesis (Cyp7a1, etc...), and cholesterol and bile acid export (ABCG5/-8, Bsep, MRP2) (del Castillo-Olivares and Gil 2000a; Schoonjans *et al.* 2002; Bohan *et al.* 2003; Freeman *et al.* 2004; Lee *et al.* 2006; Song *et al.* 2008) (a summary of these genes is presented in Table 1.3) (Figure 1.11). Phosphorylation of LRH-1 occurs at Ser^{238} and Ser^{243}, which increases activation of down-stream LRH-1 responsive genes (Lee *et al.* 2006). In contrast, transcriptional activity of LRH-1 is antagonised by another nuclear receptor, Shp (Figure 1.11), which will be discussed later in Section 1.8.1.5.

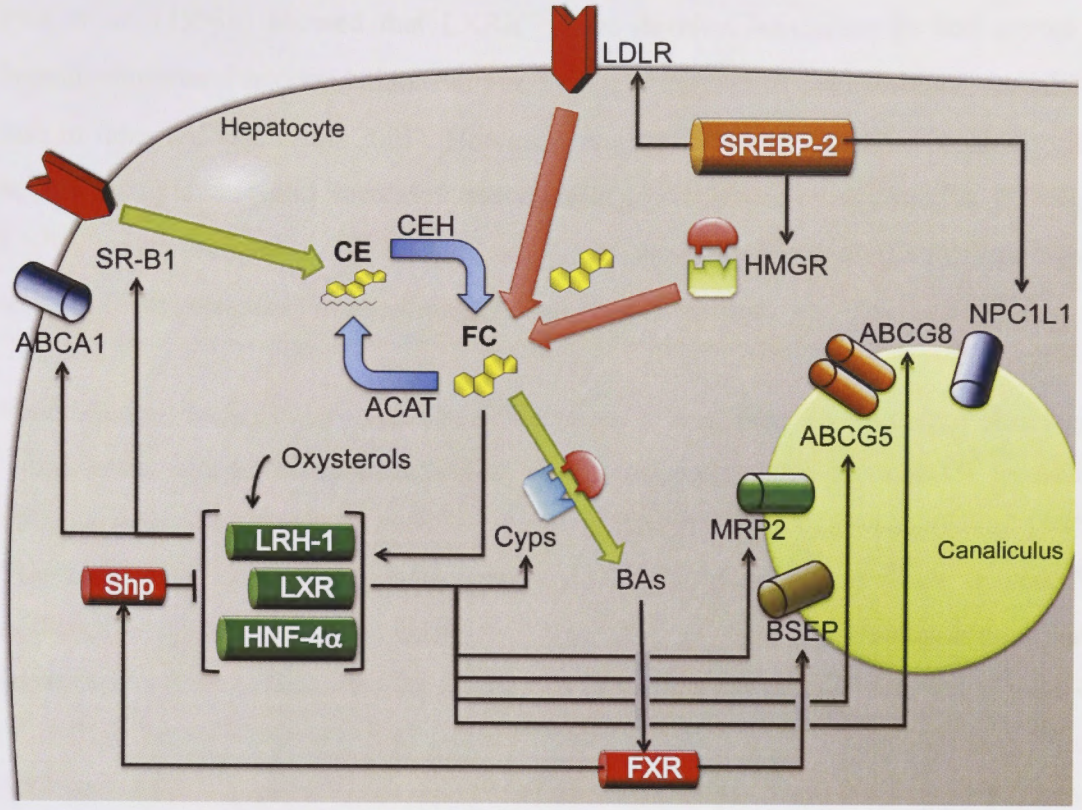

Figure 1.11 Nuclear receptors involved in positive and negative transcriptional regulation of pathways involved in cholesterol homeostasis

Low intracellular cholesterol levels activate SREBP-2 (as described in Section 1.4.1.1), which subsequently increases low density lipoprotein receptor (LDLR) and HMG-CoA reductase expression, thereby increasing intrahepatic cholesterol levels. Conversely, increased intracellular cholesterol and oxysterol levels activate liver receptor homolog-1 (LRH-1), liver X receptor (LXR), and hepatocyte nuclear factor-4α (HNF-4α) which positively regulate: scavenger receptor-B1 (SR-B1), ATP-binding cassette, sub-family A, member 1 (ABCA1), cytochrome P450s (Cyps) involved in the biotransformation of cholesterol to bile acids (BA), and canalicular transporters responsible for bile acid and cholesterol efflux. Raised intrahepatic BAs activate farnesoid X-receptor (FXR), which in turn activates bile salt export protein (BSEP) and small heterodimeric partner (Shp). Once activated, Shp inhibits LRH-1 and HNF-4α, thereby reducing pathways of reverse cholesterol transport.

1.8.1.3 Liver X receptors

LXR nuclear receptors are members of the first nuclear receptor family (NR1). Mammals express two LXR isoforms, namely LXRα (NR1H3), which is expressed in liver and macrophages and LXRβ (NR1H2), which is ubiquitously expressed by most tissue types (Lund *et al.* 2003). LXRα and –β share a 77% sequence homology (Zelcer and Tontonoz 2006). Functional studies, using knockouts, identified that LXRα is the dominant isoform involved in cholesterol homeostasis (Bischoff *et al.* 2010). Studies by

Peet *et al.* (1998b) showed that LXRα$^{-/-}$ mice develop hepatomegaly and severe hepatic cholesterol accumulation. Further, LXRα is capable of compensating for LXRβ loss in mice (Alberti *et al.* 2001). However, double LXRα/–β knockout mice develop severe dyslipidemia and increased susceptibility to atherosclerosis, similar to single LXRα$^{-/-}$ mice (Schuster *et al.* 2002). Collectively, these studies highlight the importance of LXR (α in particular) in regulating cholesterol homeostasis.

Functionally, intracellular cholesterol, oxysterols, and retinoids (vitamin A-related compounds) trigger the upregulation of the heterodimeric LXR form (LXR forms an obligate heterodimer with retinoid X-receptors [RXR]) (Willy and Mangelsdorf 1997). The LXR/RXR heterodimer subsequently enters the nucleus and binds to specific LXR/RXR-responsive DNA elements consisting of two hexanucleotide repeats separated by four nucleotides; this is referred to as a canonical DR4 element (Quack *et al.* 2002) (this should not be confused with death receptors [DR], discussed later). Thus, LXR activation augments the expression of a plethora of pathways involving cholesterol uptake, efflux, and reverse cholesterol transport (Willy *et al.* 1995; Lehmann *et al.* 1997; Willy and Mangelsdorf 1997; Zelcer and Tontonoz 2006; Shen *et al.* 2011) (LXR-responsive genes directly related to cholesterol homeostasis are summarised in Table 1.3). Briefly, LXR is required for ABCA1, ABCG5/8, Cyp7a1, and SR-B1 expression (Malerod *et al.* 2002; Murthy *et al.* 2002; Repa *et al.* 2002; Repa and Mangelsdorf 2002; Sparrow *et al.* 2002; Wong *et al.* 2006; Hozoji-Inada *et al.* 2011). It is important to note that LXR, like most NRs, may function differently between species. For example, in mice, LXRα has also been shown to positively regulate Cyp7a1 (Chiang *et al.* 2001), whereas LXR suppresses CYP7A1 gene expression in human cells (Goodwin *et al.* 2003). Nevertheless, LXR is an important NR involved in positive regulation of RCT pathways.

1.8.1.4 Hepatocyte nuclear factors

HNF NRs are expressed in numerous tissues, but are concentrated in the liver. Importantly, HNF factors are largely responsible for regulating the gene expression of several metabolic pathways, thereby maintaining components of the hepatic phenotype (Chaya *et al.* 1997; Ktistaki and Talianidis 1997; Hayhurst *et al.* 2001). As previously mentioned, these NRs are transcriptional governed by LRH-1 (see Section 1.8.1.2) (Rausa *et al.* 1999; Pare *et al.* 2001). Although HNF factor involvement in cholesterol

homeostasis is secondary to LRH-1 and LXR, several cholesterol-related genes are co-regulated by HNF NRs, in particular HNF-1, -3β and 4α.

HNF-4α (NP2A1) is a 53 kDa NR involved in the regulation of Cyp7a1, Cyp8b1, and Cyp27a1 expression (Zhang and Chiang 2001; Chen and Chiang 2003; Abrahamsson *et al.* 2005) (Table 1.3). Furthermore, studies by Pramfalk *et al.* (2005; 2007; 2009) of Paolo Parini's laboratory have found that ACAT2 is transcriptionally regulated by HNF-4α, in addition to HNF-1 (Table 1.3). These same workers also demonstrated that NPC1L1 is transcriptionally regulated by HNF-1α, in addition to SREBP-2 (Pramfalk *et al.* 2010). In regards to BA efflux, studies have demonstrated that MRP2 transcription is subject to HNF-1 and -3β regulation (Stöckel *et al.* 2000) (Table 1.3).

1.8.1.5 Farnesoid X-receptor (FXR)

To ensure that intrahepatic cholesterol and BA levels remain constant, pathways of RCT and cholesterol/BA biosynthesis are subject to negative regulation through FXR. FXR is the fourth member of the first NR family (NR1H4) (Parks *et al.* 1999) and is activated by BA ligands (Bramlett *et al.* 2000). Interestingly, FXR is inhibited by insulin stimulation (Duran-Sandoval *et al.* 2004).

Physiologically, FXR is responsible for feedback inhibition of BA biosynthesis (via Cyp inhibition), and simultaneously promotes pathways of hepatic BA efflux (Liu *et al.* 2003; Deng *et al.* 2006). These changes are achieved via two pathways. Firstly, FXR is able to effect positive transcriptional regulation of BSEP and MDR2 expression (Liu *et al.* 2003; Deng *et al.* 2006). Secondly, activated FXR is responsible for down-stream activation of Shp (Goodwin *et al.* 2000) (Table 1.3 and Section 1.8.1.6). It should be noted that in addition to FXR activation, intracellular BA accumulation may also activate fibroblast growth factor (FGF)-15 in mice and FGF19 in humans, which subsequently inhibit Cyp7a1 gene expression independently of Shp (Song *et al.* 2009).

Table 1.3 Positive and negative transcriptional regulation of genes involved in cholesterol homeostasis

It should be noted that this list is by no means exhaustive.

Gene	Function	Positive regulation		Negative regulation	
		Regulation	References	Regulation	References
ABCA1	HDL formation and cholesterol efflux in RTC	**LXR, SREBP-2**	Hozoji-Inada *et al.* 2011; Murthy *et al.* 2002; Sparrow *et al.* 2002; Wong *et al.* 2006	**ORP8, OSBP**	Bowden *et al.* 2008; Yan et al. 2008
ABCG5/-8	Hepatic cholesterol export	**LRH-1, LXR**	Freeman *et al.* 2004; Repa *et al.* 2002	**Shp (FXR)**	Freeman *et al.* 2004
ACAT2	Acyl-coenzyme A:cholesterol acyltransferase	**Intracellular cholesterol, HNF-1, HNF-4α**	Pramfalk *et al.* 2005, 2007, 2009	*Unknown*	
BSEP	Hepatic BA efflux	**LRH-1, FXR**	Song *et al.* 2008; Deng *et al.* 2006	*Unknown*	
CEH	Hydrolysis of cholesteryl esters	**SREBP-2**	Natarajan *et al.* 1999	*Unknown*	
Cyp27a1	Mitochondrial sterol 27-hydroxylase (see Figure 1.7)	**HNF-4α**	Chen *et al.* 2003	**Shp (FXR)**	Chen *et al.* 2003
Cyp7a1	Microsomal 7α-hydroxylase (see Figure 1.7)	**HNF-4α, LRH-1, LXRα***	Abrahamsson *et al.* 2005, del Castillo-Olivares *et al.* 2000a	**FGF15/-19, Shp (FXR), LXR#**	Goodwin *et al.* 2003, Song *et al*. 2009
Cyp7b1	25-hydroxycholesterol 7-α-hydroxylase (see Figure 1.7)	*Unknown*		**LXR, SREBP-2**	Norlin and Chiang 2004
Cyp8b1	Sterol 12-α-hydroxylase; determines ratio of cholic acid and chenodeoxycholic acid	**LRH-1, HNF-4α**	del Castillo-Olivares et al. 2000b, Zhang *et al.* 2001	**Shp (FXR)**	Miao *et al.* 2011; Zhang *et al.* 2001
FXR	Bile acid receptor	**Bile acids, *D*-glucose**	Bramlett *et al.* 2000; Duran-Sandoval *et al.* 2004	**Insulin, hypoglycemia**	Duran-Sandoval *et al.* 2004
HMGR	Rate limiting step involved in cholesterol biosynthesis	**SREBP-2**	Jackson *et al.* 1995; Ness, 1983		
HNF-1	Hepatocyte differentiation factor	**LRH-1**	Paré *et al.* 2001		
HNF-3β	Hepatocyte differentiation factor	**LRH-1**	Paré *et al.* 2001		
HNF-4α	Hepatocyte differentiation factor	**LRH-1**	Paré *et al.* 2001	**Shp**	Lee *et al.* 2000
LDLR	LDL cholesterol uptake	**SREBP-2**	Horton *et al.* 2002		
LRH-1	Principle NR involved in hepatic development and RCT	**GATA elements**	Paré *et al.* 2001	**Shp (FXR)**	Lee *et al.* 2002
LXR	Nuclear receptor involved in mediating RCT	**Intracellular cholesterol, oxysterols, retinoids**	Lehmann *et al.* 1997; Zelcer *et al.* 2006; Shen *et al.* 2011		
MDR2	Canalicular phospholipid flippase	**FXR**	Liu *et al.* 2003		
MRP2	Hepatic efflux of conjugated BAs	**HNF-1, HNF-3, LRH-1**	Bohan *et al.* 2003, Stöckel *et al.* 2000	**IL-1β**	Hisaeda *et al*. 2004
NPC1L1	Intestinal and canalicular cholesterol uptake	**HNF-1α, SREBP-2**	Pramfalk *et al.* 2010		
Shp	Inhibitory nuclear receptor	**FXR**	Goodwin *et al.* 2000		
SR-B1	Hepatic HDL colloid uptake	**LRH-1, LXRα**	Malerod *et al.* 2002; Schoojans *et al.* 2002	**Shp (FXR)**	Malerod *et al.* 2005
SREBP-2	Nuclear receptor responsible for increasing intracellular cholesterol levels	**Decreased intracellular cholesterol**	Edwards *et al.* 2000		

Abbreviations for Table 1.3.

ABC, ATP-binding cassette; ACAT, acyl-CoA : cholesterol acyltransferase; BSEP, bile salt exporter protein; CEH, cholesteryl ester hydrolase; Cyp, cytochrome P450; FGF, fibroblast growth factor; FXR, farnesoid X receptor; HMGR; HMG-CoA reductase; HNF, hepatocyte nuclear factor; IL, interleukin; LDLR, low density lipoprotein receptor; LRH-1, liver receptor homolog-1; LXR, liver X receptor; MDR2, multidrug resistance protein-2; MRP2, multidrug resistance-associated protein-2; NPC1L1, Niemann Pick C1-like-1 protein; ORP8, oxysterol-binding protein-related protein-8; OSBP, oxysterol-binding protein; Shp, short heterodimer partner; SR-B1, scavenger receptor-B1; SREBP-2, sterol regulatory element binding protein-2.

1.8.1.6 Small heterodimeric partner

Shp, as mentioned above, is an FXR-responsive NR responsible for inhibiting several NRs. Shp is the second member of the zero nuclear receptor subfamily (NR0B2), and is expressed as a small 28 kDa protein (Goodwin *et al.* 2000). Unlike most nuclear receptors, Shp lacks the capacity to bind DNA, but instead interacts with other nuclear receptors, in particular LRH-1, RXR, and HNF-4α (Lee *et al.* 2000; Lee and Moore 2002). These interactions prevent nuclear receptor DNA-binding and thereby alter transcriptional functions of the genes involved (Goodwin *et al.* 2000; Lee *et al.* 2000). As a result, FXR-dependent Shp activation suppresses several bile acid biosynthesis and export genes, including Cyp7a1, Cyp8b1, SR-B1 (Malerod *et al.* 2005; Miao *et al.* 2011) (see Section 1.8.1.1, Table 1.3 and Figure 1.11).

1.9 Non-alcoholic fatty liver disease

Non-alcoholic fatty liver disease (NAFLD) is a condition in which steatosis (accumulation of fat within hepatocytes) is attributable to overnutrition and its metabolic complications, and not to excessive alcohol intake, viruses, or toxic causes. Epidemiologically, NAFLD constitutes the most common chronic liver disease in the Western and developing world, the latter includes rates of 15-30% in many parts of Asia (Chitturi *et al.* 2007; Bellentani and Marino 2009; Bellentani *et al.* 2010; Chitturi *et al.* 2011; Wong *et al.* 2011). The high prevalence of NAFLD parallels the global obesity pandemic, with 80-90% of obese adults and 40-70% of obese children showing evidence of NAFLD (Bellentani *et al.* 2010). In Australia, it is anticipated that the next 15 years will see normal-weight individuals constituting <40% of the population, while the prevalence of overweight/obese individuals will increase to >60% (Walls *et al.* 2011). Accordingly, rates of NAFLD are also set to rise further, presently being ~30% of the population (Browning *et al.* 2004; Thorburn 2005).

While NAFLD is relatively benign in most individuals (the pathology is referred to as simple steatosis [SS]), approximately 5-25% of affected individuals will develop non-alcoholic steatohepatitis (NASH), the most severe form of NAFLD (Farrell and Larter 2006; Lazo and Clark 2008; Williams *et al.* 2011; Wong *et al.* 2011). NASH is characterised by hepatocellular injury (ballooning, Mallory hyaline), cell death, inflammation and development of liver fibrosis. These pathologies, if untreated, can lead to cirrhosis, hepatic decompensation, and hepatocellular carcinoma (Zen *et al.* 2001; Brunt 2004; Mori *et al.* 2004; Yoshioka *et al.* 2004; Hashizume *et al.* 2007; Hashimoto *et al.* 2009; Tokushige *et al.* 2010; Yasui *et al.* 2011). Furthermore, up to 30% of cirrhotic NASH patients will die from liver-related causes in the next 10 years (McCullough 2006). Bellentani and colleagues (2008; 2009; 2010) have estimated that 2-3% of the current global population currently has NASH. Further, this portion is predicted to increase as the availability of healthy foods decreases and transition to sedentary lifestyles (lack of exercise in proportion to energy intake) continues to become more prevalent. Assuming that the 2-3% value proposed by Bellentani *et al.* (2009; 2010) is correct, between 140 and 210 million people have or will soon develop NASH, of whom 40-70 million could die from NASH-related complications, and far more from cardiovascular disease (Sanyal *et al.* 2006) and common cancers for which insulin resistance (and NAFLD) is a risk factor (breast, colon). NASH is therefore set to stretch global health care services and resources. Accordingly, the prevention of transition of SS to NASH constitutes an important target in managing fatty liver disease and preventing further complications (Hedley *et al.* 2004; Kouris-Blazos and Wahlqvist 2007).

The exact mechanisms responsible for transition to NASH remain unclear. Day and James (1998) first proposed the widely accepted two "hit" hypothesis of NASH pathogenesis, which states that NASH occurs as the cumulative result of two events (physiological assaults). Firstly, development of hepatic steatosis (first "hit"), sensitises the liver to secondary "hits", which are hypothesised to include lipid peroxidation, oxidative stress and/or cytokine-mediated injury (Day and James 1998). More recently, this two "hit" model of NASH pathogenesis has been challenged by many observations and has been replaced by a model of lipotoxicity, which envisages multiple interactive

connections between the metabolic and inflammatory determinants of NASH (Tessari *et al.* 2009; Larter *et al.* 2010; Neuschwander-Tetri 2010a).

Injury mechanisms are clearly operative in NASH; they include oxidant stress and immuno-modulation via cytokines and innate immunity, such as Kupffer cell and other macrophage activation. These processes culminate in hepatocellular injury/cell death (particularly by apoptosis) and liver fibrosis (Day 2002). The more embracing lipotoxicity hypothesis, however, is based on the premise that metabolic and injury domains of steatohepatitis are interactive, not separate. Specifically, one or more "toxic/pro-inflammatory" lipid species accumulate in the liver in some cases of steatosis, and these molecules are what subsequently lead to hepatic inflammation, cell death ("hepatitis") and fibrosis (Neuschwander-Tetri 2010a). While genetic polymorphisms that are associated with both steatosis and liver injury in NAFLD have been described (especially PNPLA3), the mechanisms by which lipotoxicity occurs in NASH remain unclear, as does the identity of which among several candidate lipid molecules is/are the lipotoxic culprits.

1.10 Translational animal models of NAFLD

NAFLD can be studied experimentally by using several animal models. These include dietary (e.g.: high fat, high sucrose; intragastric hyperalimentation; American Lifestyle-induced obesity syndrome [ALIOS] model; methionine and choline-deficient [MCD] diet-fed mice; defined amino acid choline deficient diet-fed mice) and genetic (*ob/ob*, *db/db*, LDLR deficient [$LDLR^{-/-}$], ApoE knockout [$ApoE^{-/-}$], *foz/foz*) models of obesity and liver injury.

1.10.1 Methionine and choline-deficient (MCD) model

Feeding a MCD diet is a non-pathophysiological (nutritional depletion) model of NAFLD in rodents. MCD-diet-fed mice rapidly develop fatty livers as a result of choline deficiency which inhibits phosphatidylcholine (PC) biosynthesis, while methionine deficiency causes rather extreme oxidant stress (as in the methionine adenosyltransferase-1A knockout mouse [MATO] (Lu *et al.* 2001; Lu *et al.* 2002)). Since VLDL colloids are encapsulated in a PC monolayer, MCD-feeding ultimately results in suppressed hepatic VLDL export (Rinella *et al.* 2008), leading to hepatic lipid peroxidation and oxidative stress (Leclercq *et al.* 2000). The resultant hepatic steatosis,

lobular inflammation, hepatocellular cell death and liver fibrosis are similar to human NASH. However, despite developing this severe NASH phenotype, MCD-fed mice lose weight, have lower serum leptin levels, and exhibit both insulin sensitivity (low serum insulin) and normal or increased serum adiponectin levels (Rinella and Green 2004; Larter *et al.* 2008b). Accordingly, these mice do not develop NASH in the context of metabolic syndrome.

1.10.2 LDLR ($LDLR^{-/-}$) and ApoE knockout ($ApoE^{-/-}$) mice

$LDLR^{-/-}$ and $ApoE^{-/-}$ gene-deleted mice were first described by Ishibashi and colleagues (1994) from the Goldstein and Brown laboratory. These knockout mice were created to delineate the role of ApoE in hepatic LDL and chylomicron uptake. Subsequent studies reported severe atherosclerosis, in addition to hepatic steatosis with raised serum ALT and hepatic necroinflammation in both the knockout lines (Paszty *et al.* 1994; Coenen and Hasty 2007; Ma *et al.* 2008; Alger *et al.* 2010; Lalloyer *et al.* 2011).

While the MCD diet-fed and $LDLR^{-/-}$/$ApoE^{-/-}$ knockout mouse models have furthered our understanding of injury processes, inflammatory cell recruitment and fibrogenesis in NASH, their non-pathophysiological (toxic) nature restricts the direct translation of experimental data into the context of human NASH. Some of these limitations can be overcome by use of over-nutrition models, such as the forced hyperalimentation Tsukamoto-French model (Deng *et al.* 2005), the American Lifestyle-Induced Obesity Syndrome (ALIOS) model and *foz/foz* mice. The last is arguably the most convenient and most striking model of metabolic syndrome-related NASH.

1.10.3 *Foz/foz* mouse model of NAFLD

The Fat Aussie (*Alms1* mutant or *foz/foz*) mouse model was established following the observation of a single obese, diabetic mouse amongst a colony of non-obese diabetic (NOD, more specifically NOD/SHiL) mice maintained at The Canberra Hospital Animal Facility in 2003. The mouse was approximately 50% heavier than its littermates. It were subsequently characterised, with gene identification and phenotype characterisation undertaken by Todor Arsov (PhD project), under the supervision of Prof. Nikolai Petrovsky (Australian National University, The Canberra Hospital). An early finding was that *foz/foz* mice developed obesity and hyperglycaemia from age 90 days (Arsov 2006). The *foz/foz* NOD mice was subsequently outbred to a C57BL/10

mouse strain in order to characterise the autosomal recessive (~1:4 offspring were found to be obese and diabetic) mutation responsible for the observed obese/diabetic phenotype.

Gene mapping of *foz/foz* mice identified an 11-base pair (bp) deletion within the *Alms1* exon 8 on chromosome 6. This mutation was found to induce a reading frame-shift and premature TAG stop codon, resulting in truncation of the Alms1 protein (Arsov 2006). Truncation of Alms1 is hypothesised to result in loss-of-function, and the human homolog (ALMS) results in obesity, diabetes, and fatty liver disease (Collin *et al.* 2002; Collin *et al.* 2005). While the exact function of Alms1 is unknown, research carried out by the host laboratory indicates that Alms1 may be involved in intracellular signalling, and more specifically regulation of food intake through defects in hypothalamic leptin signalling (Heydet *et al.* 2010). The *Alms1* mutation present in *foz/foz* mice appears to cause loss of satiety, resulting in overnutrition. Thus, Arsov *et al.* (2006a) reported an ~1.3-fold increase in food intake in female *foz/foz* mice compared with WT NOD.B10 littermates.

In addition to obesity and type-2 diabetes (T2D), studies of NOD.B10 *foz/foz* mice (subsequently referred to as *foz/foz* mice in this thesis) in the host laboratory identified that high fat (HF)-feeding (47% carbohydrate, 23% fat, 0.2% cholesterol) is accompanied by development of hypercholesterolemia, hypertriglyceridemia, hypoadiponectinemia, hepatomegaly and severe NASH (Arsov 2006; Arsov *et al.* 2006a; Arsov *et al.* 2006b). The fact that NASH pathogenesis occurs within the context of metabolic syndrome (obesity, diabetes, dyslipidemia, hypoadiponectinemia) contributes to the importance of this model as reflecting both the metabolite context and pathological spectrum (SS, NASH, fibrosis) of NAFLD. Accordingly, this model was chosen to explore pathways pertaining to NASH etiopathogenesis.

1.11 Lipotoxic mediators of NASH

The concept of lipotoxicity was first proposed in rodent β-cells, where palmitate/oleate long chain FA stimulation deregulated glucose-stimulated insulin secretion (Lee *et al.* 1994). Since then, the term lipotoxicity has been modified to describe tissue injury resulting from the presence of FAs, FA metabolites (including ceramides [sphingosine conjugated to a fatty acid]) and TG in excess of those required for oxidative

metabolism, which enter non-oxidative pathways that subsequently results in cellular damage (Shimabukuro *et al.* 1998; Unger and Zhou 2001).

In regards to NAFLD, excess hepatic glucose, a consequence of insulin-resistance-related hyperglycemia, is converted to pyruvate (Oakes *et al.* 1997). Intracellular pyruvate then enters the Krebs cycle, resulting in the formation of citrate, which is subsequently converted to acetyl-CoA, in a reaction catalysed by ATP citrate lyase (Hardwick 1966; Spencer and Lowenstein 1966). Two subsequent steps, carried out by acetyl-CoA carboxylase 1 and fatty acid synthase, convert acetyl-CoA into palmitic acid, which is eventually converted to oleic acid (Spencer and Lowenstein 1966). Oleic acid is the end-product of nascent FA synthesis (Browning and Horton 2004). Accordingly, hepatic FFA levels increase in both humans and animal models of insulin-resistance (Browning and Horton 2004; Avramoglu *et al.* 2006; Meshkani and Adeli 2009). Numerous studies and reviews have documented the mechanisms of FFA-induced injury (Kusminski *et al.* 2009; Neuschwander-Tetri 2010a; Schrauwen *et al.* 2010; Trauner *et al.* 2010). Briefly, three major mechanisms are thought to be responsible, namely: oxidative stress, mitochondrial dysfunction and lipid peroxidation (Browning and Horton 2004). These mechanisms culminate in the generation of pro-oxidant (free radical oxygen, hydrogen peroxide and other reactive oxygen species [ROS]) molecules. Importantly, ROS generation may be augmented by FA oxidation within peroxisomes, mitochondria and ER (Browning and Horton 2004).

In a recent article, Neuschwander-Tetri (2010b) reviewed the evidence against TG lipotoxicity. He argued a role for FFA and/or FFA metabolites, but in this review any potential of cholesterol was overlooked. An expanding body of work now indicates that cholesterol may constitute one of the lipotoxic species that could cause NASH.

1.11.1 Cholesterol: a potential lipotoxic mediator?

In 2007 and 2009, two human studies identified increased hepatic FC in NASH patients compared with lean individuals and patients with simple steatosis (Puri *et al.* 2007; Caballero *et al.* 2009). Although, the predominant hepatic lipid in NASH is TG, this lipid species has been excluded as lipotoxic in NASH, and FFAs (saturated FFAs in particular) are considered to be important lipotoxic candidate species (Gentile and Pagliassotti 2008; Neuschwander-Tetri 2010a, 2010b). However, several recent animal

studies have implicated a clearer involvement of cholesterol in NASH progression (Mari *et al.* 2006; Wouters *et al.* 2008; Wouters *et al.* 2010; Subramanian *et al.* 2011).

Dysregulation of cholesterol metabolism has been extensively characterised in such pathological disorders as type 2 diabetes, gallstones development, and atherosclerosis. The latter may lead to myocardial infarction and potentially fatal cardiac failure and/or cerebrovascular accident (Keber and Keber 1992; Blann *et al.* 1997; Namazi 2002). The role of cholesterol in human NASH remains largely unexplored. Although no definitive evidence has linked cholesterol to NASH pathogenesis, the aforementioned human studies identified increased hepatic cholesterol content and augmented SREBP-2 expression in human NASH livers (Puri *et al.* 2007; Caballero *et al.* 2009). In addition, a retrospective study conducted by Ioannou *et al.* (2009), found that dietary cholesterol consumption correlates with risk of liver cirrhosis in humans. Dietary cholesterol intake has also been found to be "superabundant" in non-obese patients with NAFLD (Yasutake *et al.* 2009).

In regards to animal studies, mitochondrial cholesterol loading increases the susceptibility of hepatocytes to FasL- and TNF-α-mediated cell death (Mari *et al.* 2006); Fas and TNF have both been implicated in the pathogenesis of NASH (Feldstein *et al.* 2003; Nan *et al.* 2007; Ruiz *et al.* 2007; Koca *et al.* 2008; Tamimi *et al.* 2011). Further, studies by Wouters and colleagues (2008), using humanised ApoE2 knock-in ($ApoE2^{ki}$) and $LDLR^{-/-}$ mice found that dietary cholesterol correlated with hepatic inflammation and foam cell development. Omitting dietary cholesterol resolved liver injury and lowered serum VLDL levels (Wouters *et al.* 2008). In subsequent studies using the same mouse models ($ApoE2^{ki}$ and $LDLR^{-/-}$), these authors showed that hepatic cholesterol accumulation and liver injury were resolved by treating mice with an LXR agonist, T0901317 (Wouters *et al.* 2010).

In the *foz/foz* mouse model, a key observation informing the research conducted towards this thesis is that development of NASH is accompanied by a ~200-fold increase in total hepatic cholesteryl ester content and ~5 fold increase in FC *versus* chow-fed *foz/foz* and HF-fed WT mice with simple steatosis, or lean livers (chow-fed WT mice). These findings were interpreted as indicating a perturbation in hepatic cholesterol homeostasis, either preceding or during NASH development. Together with the limited data of

cholesterol lipotoxicity (Section 1.11), the finding led to development of the key hypothesis underlying this research.

Hypothesis: that *free cholesterol initiates and/or augments the pathogenesis of NASH.*

1.12 Summary and aims of this research

1.12.1 Aims

The principle aims of this research are outlined below, with the Chapters in which these aims are addressed shown in parentheses.

1. Characterise the pattern and causation of hepatic cholesterol dysregulation in *foz/foz* mice with NASH (Chapter 3).
2. Identify the key factors responsible for inducing cholesterol dysregulation (Chapter 4).
3. Use dietary manipulations to establish whether cholesterol is directly involved in the pathogenesis of NASH in *foz/foz* mice (Chapter 5).
4. Use pharmacological interventions to clarify whether inhibition of cholesterol uptake and/or inhibition affects NASH outcome in *foz/foz* mice (Chapter 6).
5. Identify the signalling pathways whereby cholesterol could mediate liver injury and/or cell death in this model of NASH (Chapter 7).

CHAPTER 2

General materials and methods

A number of commonly used biochemical techniques used throughout this study are described here for convenience. Detailed procedures for more specialised techniques and methods are included in the relevant Chapters. Chemicals and reagents used in these studies are listed below.

2.1 Reagents

Most reagents were purchased from Sigma Aldrich (St. Louis, MO) and were of the highest purity available. The following were purchased from Sigma Aldrich (St. Louis, MO): ammonium persulfate (APS), bovine pancreas insulin, bovine serum albumin (BSA), $CaCl_2$, 3-[3-[*N*-(2-chloro-3-trifluoromethylbenzyl)-(2,2-diphenylethyl)amino]propyloxy]phenylacetic acid hydrochloride (GW3965), coomassie-G250, 3-(2,6-dichlorophenyl)-4-(3'-carboxy-2-chlorostilben-4-yl) oxymethyl-5-isopropylisoxazole (GW4064), diethylpyrocarbonate (DEPC), direct red-80, ethylenediaminetetraacetic acid (EDTA), ethylene glycol tetraacetic acid (EGTA), fast green-FCF, filipin, geranylgeraniol, glycerol, glucose-6-phosphate, glucose-6-phosphate dehydrogenase, *N*-[4-(1,1,1,3,3,3-hexafluoro-2-hydroxypropan-2-yl)phenyl]-*N*-(2, 2, 2-trifluoroethyl) benzenesulfonamide (T0901317), hydrogen peroxide (H_2O_2), 4-(2-hydroxyethyl)-1-piperazineethanesulfonic acid (HEPES), hydroxy-3-methylglutaryl coenzyme-A (HMG-CoA), Igepal CA-630, KCl, KH_2PO_4, K_2HPO_4, and lactate dehydrogenase (LDH) *in vitro* toxicity assay, mevalonic acid lactone, $MgCl_2$, NaCl, $NaH_2PO_4.H_2O$, NaN_3, nicotinamide adenine dinucleotide phosphate (NADP), nicotinamide, nile red, (17*Z*)-pregna-4,17(20)-diene-3,16-dione (guggulsterone), picric acid, phosphatase inhibitor cocktail 1 & 2, ponceau S, protease inhibitor cocktail, saponin, sodium bicarbonate, sodium citrate dehydrate tribasic, sodium deoxycholate, sodium dodecyl sulphate (SDS), sucrose, TRI-reagent, triton X-100, trypan blue, and tween-20.

Hank's balanced salt solution (HBSS), rat-tail type-1 collagen, and William's E media were purchased from Gibco-Invitrogen (Paisley, UK). Dithiothreitol (DTT), Superscript

III, and ProLong® Gold antifade reagent were from Invitrogen (Carlsbad, CA). Arylamide/bis-acrylamide (30% 29:1 ratio), iQ SYBR Green Supermix, Precision Plus™ Prestained Protein standards, and qPCR reaction tubes and plate sealers were all purchased from Bio-Rad (Hercules, CA). Random and oligo $(dT)_{15}$ primers were from Promega (Madison, WI). Tetramethylethylenediamine (TEMED) was from GE Healthcare Biosciences (Buckinghamshire, UK). Ethanol, glycine, HCl, methanol, and Tris (tris-(hydroxymethyl)aminomethane) were purchased from Astral Scientific (Caringbah, NSW, Australia). Chemicon immunohistochemistry reagents, polyvinylidene fluoride (PVDF), and serum insulin assay kits were from Millipore (Billerica, MA). Mouse serum adiponectin, interleukin (IL)-1β, monocyte chemotactic protein (MCP)-1, and tumour necrosis factor (TNF)-α ELISA kits were purchased from R&D Systems (Minneapolis, MN), while murine serum IL-18 ELISA kits were purchased from Medical & Biological Laboratories Co., Ltd. (Nagoya, Japan). Formalin and paraformaldehyde were obtained from Electron Microscopy Sciences (Hatfield, PA). Aquasol scintillation liquid, scintillation tubes, *DL*-3-(Glutaryl-3-^{14}C)-HMG-CoA, and *RS*-(5-^{3}H)-mevalonolactone were purchased from Perkin Elmer (Waltham, MA). Atorvastatin calcium (Lipitor®) and Ezetimibe (Ezetrol®) were purchased from Pfizer (West Ryde, NSW, Australia) and Schering-Plough (Whitehouse Station, NJ) respectively. Nuclear/cytoplasmic protein extraction kits, and SuperSignal West Femto enhanced chemiluminescence (ECL) substrate solution were bought from Thermo Scientific (Rockford, IL).

LRH-1 agonists JS/5197/16C and JS/5197/74A were a kind gift from Professor Richard Whitby (University of Southampton, Southampton, UK).

Preabsorbant glass-backed thin layer chromatography (TLC) plates were purchased from Whatman (Clifton, NJ). Type-2 collagenase was bought from Worthington Biochemical Corporation (Lakewood, NJ). Annexin-V FITC was purchased from BD Pharmingen (San Jose, CA). Phosphate buffered saline (PBS) tablets were bought from Amresco (Solon, OH). LDH enzyme standards were from Cayman Chemicals (Ann Arbor, MI). Gill's haematoxylin was purchased from ProSciTech (Thuringowa, Qld, Australia). Ultra-pure water was obtained from Baxter Healthcare (Toongabbie, NSW, Australia). Ketamine hydrochloride and xylazil were from Troy Laboratories

(Glendenning, NSW, Australia). Skim milk powder (Diploma, Fonterra Foodservices, North Ryde, NSW, Australia) was purchased from a local food retailer.

Cell culture flasks (T_i 75) and dished (T_i 55), sterile freezing vials (2.0 mL), 24- and 96-well plates were from Iwaki Sterilin (Staffordshire, UK). Sterile 15 mL and 50 mL plastic screw top tubes used in cell culture were purchased from Sterilin Bibby (Staffordshire, UK) and Nunc (Roskilde, Denmark), respectively. Cell strainers (100 μm) were purchased from BD Biosciences (Franklin Lakes, NJ). Deionised ultrapure water ($d.H_2O$) was obtained from a Milli-RO® water purification system (Millipore, Billerica, MA), and had a minimum resistance of 18 $M\Omega.cm^{-1}$.

2.2 Antibodies

Antibodies were purchased from Abcam (Oxford, UK), Affinity bioreagents (Rockford, IL, USA), BD Pharmingen (Franlin Lakes, NJ), Cayman Chemicals (Ann Arbor, MI), Cell Signaling Technology (Danvers, MA), Invitrogen (Carlsbad, CA), Lifespan Biosciences (Seattle, WA), Millipore (Billerica, MA), Molecular Probes (Eugene, OR) Proteintech Group Inc. (Chicago, IL), R&D Systems, Roche Applied Science (Mannheim, Germany), Santa Cruz (Santa Cruz, CA), Sigma-Aldrich (St. Louis, MO), and Thermo Scientific (Rockford, IL). Primary and secondary antibody supplier details, catalogue numbers, and application details are shown in Tables 2.1 and 2.2, respectively.

2.3 Animals and diets

All animal experimentation was approved by the ANU Animal Experimentation Ethics Committee (protocols F.MS.07.05 and F.MS.16.08). Female wild-type (WT) and *foz/foz* (*Alms1* mutant) mice were bred in The Canberra Hospital animal facility. Mice were fed chow (5% fat, 67% carbohydrate, 19% protein, 0% cholesterol) from weaning until 6 weeks of age, thereafter they were fed either chow or high-fat (HF) diet (23% fat, 45% carbohydrate, 20% protein, 0.2% cholesterol) (SF03-020, Specialty Feeds, Glen Forrest, WA, Australia). All mice were fed food and water *ad-libitum* and maintained in a sterile animal facility under constant 12/12 h light/dark cycle at 22°C, with a relative humidity greater than 40%. Mice were housed (3-5/cage) in individually ventilated cages (IVC) (Tecniplast, Philadelphia, PA). Cages were lined with sterile aspen shavings and Enviro-dri® nesting material (Eco Animal Bedding, Condell Park, NSW, Australia).

Each cage received approximately 70 air changes/h. Special diets and/or feeding conditions are described in relevant Chapters.

2.4 Mouse harvesting and tissue collection

At experimental endpoints, mice were fasted for 4 h from 6 AM, after which serum glucose readings were taken (Accu-Check, Roche Diagnostics, Castle Hill, NSW, Australia), and mice anaesthetised by intraperitoneal injection of ketamine hydrochloride and xylazil (100 and 20 mg/kg body weight, respectively). Blood was collected by cardiac puncture, as described by Hoff (2000), centrifuged (3,500 x g, 10 min, 4°C), and serum collected. Following cardiac puncture, livers were excised, weighed, sectioned, and samples taken for storage (frozen) and formalin-fixation. Tissue and serum samples were stored at -80°C.

2.5 Serum and hepatic analyses

Serum alanine transaminase (ALT), cholesterol (total and HDL), glucose, and triglycerides levels were assessed using automated techniques (Clinical Chemistry Department, The Canberra Hospital). Hepatic cholesteryl esters (CE), diacylglycerides (DAG), free cholesterol (FC), free fatty acids (FFA), monoacylglycerides (MAG), and triglycerides (TG) were quantitated using high-performance liquid chromatography (HPLC) by Dr Geoff Haigh (University of Washington, Seattle, WA) using the methodology described by Silversand and Haux (1997). Hepatic lipid values were normalised to liver weight, while individual FFAs were calculated as percentages of total FFA.

2.6 Histological stains and analyses

Formalin-fixed (10% [m/v] neutral-buffered formalin, 24 h, 4°C), paraffin-embedded, liver sections (4 μm) were deparaffinised, stained with haematoxylin and eosin (H&E) (John Curtin School of Medical Research, ANU, Canberra), or sirius red (liver fibrosis stain, described below), and scored blinded by an expert liver pathologist (Associate-Professor Matthew Yeh, Department of Pathology, University of Washington Medical Centre, Seattle, WA) using the NAFLD activity scoring (NAS) system (Kleiner *et al.* 2005). This score combines individual scores for steatosis, inflammation, and ballooning, while a fibrosis score is estimated separately (Kleiner *et al.* 2005). Immunohistochemistry (IHC), using specific antibodies, was used to identify cellular or subcellular localisation of proteins of interest, as well as to stain populations of

inflammatory cells (macrophages and neutrophils), and to quantify cell death. Methodologies relating to fibrosis staining and IHC are described below.

Table 2.1 Primary antibodies used in this research

Antibody	Host	Supplier	Catalog number	Application	Dilution	Band detection (kDa)
ABCA1 (H10)	Mouse	Abcam	ab18180	IHC	1:200	254
ABCA1 (HJ1)	Mouse	Abcam	ab66217	WB	1:2000	254
ABCB4 (MDR)	Rabbit	Lifespan	LS-C2974	WB	1:200	150
ABCG5 (H-300)	Rabbit	Santa Cruz	sc-25796	WB	1:500	75
ABCG8 (H-300)	Rabbit	Santa Cruz	sc-30111	WB	1:500	140
ACAT2	Rabbit	Cayman	100027	WB	1:180	60
α-SMA	Rabbit	Abcam	ab32575	WB	1:1000	42
α–Tubulin	Mouse	Abcam	ab7291	WB	1:5000	50
β–Actin	Mouse	Sigma-Aldrich	A5441	WB	1:5000	42
BSEP (F-6)	Mouse	Santa Cruz	sc-74500	WB	1:180	160-190
BSEP (H-180)	Rabbit	Santa Cruz	sc-25571	IHC	1:200	160-190
Caspase 3A	Rabbit	Abcam	ab2302	IHC, WB	1:20, 1:1000	17-20
CD36	Mouse	R&D Systems	MAB2519	WB	1:250	89
Chop	Mouse	Cell Signaling	2895	WB	1:1000	27
CPS1	Rabbit	Abcam	ab3682	ICC	1:100	165
F4/80	Rat	Abcam	MCA497R	IHC	1:135	160
FXR	Rabbit	Abcam	ab28676	WB	1:1800	55
GRP78	Rabbit	Abcam	ab21685	ICC, WB	1:1400	75
HMGR (pan)	Mouse	Abcam	ab70087	WB	1:500	97
pHMGR (Ser872)	Rabbit	Millipore	09-356	WB	1:1000	98
HNF-4α	Mouse	Abcam	ab41898	IHC, WB	1:200, 1:500	52
HSP90	Goat	R&D Systems	AF3775	WB	1:2000	90
ICAM-1	Goat	R&D Systems	AF796	WB	1:500	80
IKBα	Rabbit	Santa Cruz	Sc-371	WB	1:200	36
IKBβ	Rabbit	Santa Cruz	Sc-945	WB	1:200	45
JNK	Rabbit	Cell Signaling	9258	WB	1:1000	46,54
Lamin B1	Rabbit	Abcam	ab16048	ICC	1:1000	68
LDLR	Rabbit	Abcam	ab52818	IHC, WB	1:200; 1:1700	140
LRH-1	Mouse	Abcam	ab41901	WB	1:500	61
LXRα	Rabbit	Abcam	ab28478	WB	1:500	50
LXRβ	Rabbit	Abcam	ab28479	WB	1:500	51
M30	Mouse	Roche	12 140 322 001	IHC	1:100	13
MCP-1	Rabbit	Abcam	ab7202	WB	1:2000	18
MPO	Rabbit	Abcam	ab15484	IHC	1:150	59
MRP2	Rabbit	Abcam	ab58709	IHC	1:200	150
Na/K-ATPase	Mouse	Abcam	ab7671	ICC	1:5000	112
NFkB p65	Rabbit	Cell Signaling	4764	WB	1:2000	65
NPC1	Rabbit	Abcam	ab36983	IHC, WB	1:100; 1:1500	140
NPC1L1	Rabbit	Thermo Scientific	PA1-16801	IHC, WB	1:250; 1:1800	140-190
PCSK9	Rabbit	Abcam	ab31762	IHC, WB	1:200; 1:500	62
pJNK	Rabbit	Cell Signaling	4668	WB	1:750	46,54
PPARγ	Rabbit	Abcam	ab27649	WB	1:500	50
Shp	Goat	Santa Cruz	sc-23057	WB	1:200	26
SR-B1	Rabbit	Abcam	ab52629	IHC, WB	1:200, 1:1800	80
SREBP-2	Rabbit	Abcam	ab28482	WB	1:500	120, 68
TBP	Mouse	Abcam	ab818	WB	1:2000	38
VCAM-1	Goat	R&D Systems	AF643	WB	1:500	85-110

Abbreviations for preceding Table (2.1): ABC, ATP-binding cassette protein; ACAT, acyl-CoA:cholesterol acyltransferase; α-SMA, α-smooth muscle actin; BSEP, bile salt exporter protein; CD36, macrophage type B scavenger receptor; caspase-3a, active caspase 3; Chop, C/EBP- homologous protein; CPS1, carbamoyl phosphate synthetase-1; F4/80, EGF-like module containing mucin-like hormone receptor like-1 antigen; FXR, farnesoid X receptor; GRP78, glucose regulated protein-78; HMGR, HMG-CoA reductase; Hnf, hepatocyte nuclear factor; HSP90, heat shock protein-90; ICAM-1, inter-cellular adhesion molecule-1; ICC, immunocytochemistry; IHC, immunohistochemistry; IkBα, nuclear factor κ B inhibitor-α; IkBβ, nuclear factor κ B inhibitor-β; JNK, c-Jun N-terminal Kinase; LDLR, LDL-receptor; LRH-1, liver receptor homolog-1; LXR, liver X receptor; M30, cytokertain-18 fragment; MCP-1, monocyte chemotactic protein-1; MPO, myeloperoxidase; MRP2, multidrug resistance associated protein-2; Na/K-ATPase, sodium-potassium ATPase; NFkB p65, nuclear factor κ-B protein 65; NPC1, Niemann Pick C1; NPC1L1, Niemann Pick C1-like 1 protein; PCSK9, proprotein convertase subtilisin/kexin type-9; pHMGR (Ser^{871}), phosphorylated HMGR Ser^{871}; pJNK, phospho-JNK; PPARγ, peroxisome proliferator-activated receptor-γ; Rab7, small GTP binding protein Rab7; Shp, small heterodimer partner; SR-B1, scavenger receptor B-1; SREBP-2, sterol response element binding protein-2; TBP, TATA box-binding protein; VCAM, vascular cell adhesion protein 1; WB, western blot. Antibodies were purchased from Abcam (Cambridge, UK), AbD Serotec (Oxford, UK), Cayman Chemicals (Ann Arbor, MI), Cell Signaling (Danvers, MA); Lifespan Biosciences (Seattle, WA), Millipore (Billerica, MA), R&D Systems (Minneapolis, MN), and Santa Cruz Biotechnology, Inc (Santa Cruz, CA).

Table 2.2 Secondary antibodies used in this research

Antibody	Host	Supplier	Catalog number	Conjugate	Application	Dilution
Goat	Rabbit	Santa Cruz	Sc-2768	HRP	WB	1:10,000
Mouse	Goat	Santa Cruz	Sc-2005	HRP	WB	1:10,000
Rabbit	Goat	Santa Cruz	Sc-2004	HRP	WB	1:10,000
Rat	Goat	Santa Cruz	Sc-2006	HRP	WB	1:10,000
Goat	Donkey	Santa Cruz	Sc-2042	Biotin	IHC	1:250
Mouse	Goat	Santa Cruz	Sc-2039	Biotin	IHC	1:250
Rabbit	Goat	Santa Cruz	Sc-2040	Biotin	IHC	1:250
Rat	Goat	Santa Cruz	Sc-2041	Biotin	IHC	1:250
Goat	Chicken	Molecular probes	A-21467	Alexa 488	ICC	1:1000
Mouse	Goat	Invitrogen	A-11001	Alexa 488	ICC	1:1000
Rabbit	Chicken	Molecular probes	A-21441	Alexa 488	ICC	1:1000
Rat	Chicken	Molecular probes	A-21470	Alexa 488	ICC	1:1000

Abbreviations: HRP, horseradish peroxidase; ICC, immunocytochemistry; IHC, immunohistochemistry; WB, western blot. Antibodies were purchased from Invitrogen (Carlsbad, CA), Molecular Probes (Eugene, OR), and Santa Cruz Biotechnology, Inc (Santa Cruz, CA).

2.6.1 Sirius red fibrosis stain

Sirius red, a collagen-specific stain originally developed by Sweat *et al.* (1964), was employed in this study to stain for liver fibrosis in formalin-fixed liver samples.

2.6.1.1 Reagents

Sirius red staining solution (0.1% [m/v] Direct Red-80, 0.1% [m/v] Fast Green-FCF in saturated picric acid). Direct Red-80 (0.2 g) and Fast Green-FCF (0.2 g) were dissolved in saturated picric acid (200 mL). The solution was stored in an opaque, sealed container at room temperature (RT).

2.6.1.2 Procedure

Deparaffinised liver sections (4 μm) were rinsed in d.H_2O, and incubated with Sirius red staining solution (1 h, RT, in dark, orbital shaker). Sections were rinsed briefly (3-5 sec, d.H_2O), dehydrated (70-100% ethanol gradient), washed in xylene, and mounted in distyrene plasticiser xylene (DPX) prior to viewing. Sirius red-stained sections were quantified using ImageJ (National Institutes of Health, USA) as previously described (Liu *et al.* 2010). Briefly, six random high-powered field colour images were captured from each Sirius-red stained liver section using an Olympus IX70 microscope fitted with a high-resolution CCD camera (Olympus, Wendenstrasse, Hamburg, Germany). Images underwent colour deconvolution (ImageJ) to separate red, green and blue (RGB) components. The area of red staining was subsequently calculated as a percentage of green staining (total area). Detection threshold was standardised for all sections. Calculated areas were averaged for each liver section.

2.6.2 Immunohistochemistry (IHC)

Proteins were localised on liver sections using IHC. The streptavidin-biotin IHC method was used to increase the signal to background ratio (Gould *et al.* 1985). The methodology is described below:

2.6.2.1 Reagents

Antigen retrieval buffer (10 mM sodium-citrate, 0.05% [v/v] tween-20, pH 6.0). Sodium citrate dehydrate tribasic (2.94 g) was dissolved in d.H_2O (950 mL). Tween-20 (0.5 mL) was added, and pH adjusted to 6.0. Final volume was adjusted to 1 L. Solution was prepared fresh prior to use.

Endogenous peroxidase quench solution (3% [v/v] H_2O_2 in d.H_2O). Hydrogen peroxide (600 μL of 50% [v/v] stock solution) was diluted in d.H_2O (9.4 mL) just prior to use.

Antibody diluent, blocking, streptavidin-conjugated horseradish peroxidase (HRP), 3,3'-diaminobenzidine (DAB), and IHC wash solutions were all purchased from Chemicon

(Millipore, Billerica, MA) as a single kit, and required no additional preparation. Primary and secondary antibodies were diluted in antibody diluent (Millipore, Billerica, MA), as described in Tables 2.1 and 2.2, respectively.

2.6.2.2 Procedure

Formalin-fixed, paraffin-embedded, liver sections (4 μm) were deparaffinised before antigen retrieval (antigen retrieval buffer, pH 6.0, 125°C, 10 min). Sections were cooled under running tap water (2 min), washed in Chemicon wash buffer (4 x 10 sec), and blocked using Chemicon IHC blocking solution (5 min, RT, moisture tray). Sections were then incubated with primary antibodies (60 min, RT, moisture tray) (antibody dilutions shown in Table 2.1), after which, sections were washed (4 x 10 sec), and endogenous peroxidase activity was quenched using 3% (v/v) H_2O_2 quench solution (10 min, RT). Quench solution was aspirated, sections washed (4 x 10 sec), incubated with secondary antibody (Table 2.2) (1:250 dilution, 30 min, RT, moisture tray), washed again (4 x 10 sec), and incubated with streptavidin-HRP (Chemicon) (10 min, RT, moisture tray). Sections were thoroughly washed (6 x 10 sec), developed with DAB solution (10 min, RT, moisture tray), rinsed under running tap water (2 min), counterstained with Gill's haematoxylin (45 sec), and DPX mounted prior to viewing. For IHC quantitation, a minimum of 6 random high-power fields were quantitated for each section. Positively stained cells were counted and normalised to hepatocyte cell number (quantified by counting hepatocyte nuclei). Quantitative IHC sections were blinded prior to scoring.

2.7 Semi-quantitative analysis of gene expression

Transcriptional mRNA expression was assessed through the use of real-time reverse transcriptase (RT)-PCR amplification of desired genes, using designed primers (Table 2.3). In order to assess mRNA gene expression, total hepatic RNA was first isolated, after which cDNA was synthesised, and finally real-time PCR performed. The methodology relating to these various steps is outlined below:

2.7.1 Ribonucleic acid (RNA) isolation

Total ribonucleic acid (RNA) was isolated using the guanidinium thiocyanate-phenol-chloroform extraction method originally developed by Chomczynski and Sacchi (2006).

2.7.1.1 Reagents

Diethylpyrocarbonate (DEPC)-treated water. DEPC (0.4 mL) was added to qPCR-grade d.H_2O (200 mL). The solution was thoroughly mixed and incubated overnight (RT, fume hood), prior to liquid-cycle autoclaving.

Salt solution (5 M NaCl in DEPC-treated d.H_2O). NaCl (11.68 g) was dissolved in DEPC-treated d.H_2O (final volume 40 mL).

75% (v/v) Ethanol-DEPC. Ethanol (150 mL of >99% [v/v] solution) was diluted with DEPC-treated d.H_2O (50 mL).

TRI reagent, chloroform, and isopropanol were all purchased commercially, and required no additional preparation prior to use.

2.7.1.2 Procedure

Frozen (-80°C) liver samples (30-40 mg) were homogenised in TRI reagent (1 mL) using an electric homogeniser (Polytron, Kinematica, Lucerne, Switzerland), incubated (10 min, RT), and centrifuged (16,000 x g, 10 min, 4°C). Pelleted cell debris was discarded and supernatants were transferred to sterile Eppendorf tubes. Choloroform (200 µL of 100% [v/v] stock) was added, samples vortexed (15 sec), and incubated (15 min, RT) prior to centrifugation (16,000 x g, 15 min, 4°C). Clear upper phases containing total RNA were transferred to sterile Eppendorf tubes, after which isopropanol (500 µL, 100% [v/v]) and salt solution (20 µL of 5 M NaCl DEPC-treated stock) were added, samples incubated (5 min, 4°C), and centrifuged (16,000 x g, 15 min, 4°C) to pellet RNA. Supernatants were discarded and pellets washed with 75% (v/v) DEPC-treated ethanol (1 mL) prior to centrifugation (16,000 x g, 10 min, 4°C). Ethanol was aspirated from tubes, and pellets resuspended in DEPC water (50 µL) before drying out.

RNA samples were stored at -80°C. RNA samples were quantified using spectrophotometry (Nanodrop, Thermo Scientific, Wilmington, DE). For cDNA synthesis, RNA samples were standardised to 1 µg/µL concentrations in DEPC-treated d.H_2O. All working surfaces were cleaned thoroughly with RNAse decontamination solution (RNAse*Zap*®, Ambion, Applied BioSciences, Carlsbad, CA) prior to use, and pyrogen-free consumables were used throughout the procedure.

2.7.2 Complementary deoxyribonucleic acid (cDNA) synthesis

Once isolated, total RNA was subjected to reverse transcription using a commercial reverse-transcription PCR (RT-PCR) kit (Invitrogen, Carlsbad, CA).

2.7.2.1 Reagents

10 mM deoxynucleosides (dNTPs), 1 μg/μL random hexamers, 0.1 M dithiothreitol (DTT), 5 x first strand buffer, and Superscript® III reverse transcription (RT) enzyme (200 U/μL) were all commercially purchased (Invitrogen, Carlsbad, CA) and required no preparation prior to use.

DEPC-treated d.H_2O and RNA samples were prepared as described in Sections 2.6.1.1 and 2.6.1.2, respectively.

Mastermix #1 (1.11 nM dNTPs, 0.11 μg/μL random hexamers in DEPC-treated d.H_2O). 10 mM dNTPs (1 μL), 1 μg/μL random hexamers (1 μL) and DEPC-treated d.H_2O (7 μL) were added together for each RT-PCR reaction.

Mastermix #2 (17 nM DTT, 0.8 x first strand buffer, 200 U Superscript® III). 0.1 M DTT (1 μL), 5 x first strand buffer (4 μL), and Superscript® III (1 μL) were all added together for each RT-PCR reaction.

2.7.2.2 Procedure

RNA samples (5 μg prepared in Section 2.6.1.2) were aliquoted into sterile 0.5 mL PCR tubes. Master mix #1 (9 μL) was added to each tube, incubated (65°C, 10 min, heat block), after which tubes were chilled on ice (1 min). Separately, PCR tubes containing master mix #2 were prepared (6 μL each). Tubes were all heated (50°C, 2 min), after which master mix #2 (6 μL) was added. Tubes were then incubated (50°C, 1 h), heated (70°C, 15 min) to inactivate Superscript® III, chilled on ice (5 min), and diluted by adding DEPC-treated PCR grade water (30 μL) to give an approximate stock cDNA concentration of 0.1 μg/μL. cDNA stocks were further diluted 1:50 (PCR-grade d.H_2O) prior to qPCR analysis. Samples within individual studies were all underwent RT-PCR concurrently to negate inter-assay variation, commonly observed between separate cDNA synthesis reactions (Stahlberg *et al.* 2004).

Table 2.3 Primer sets for semi-quantitative real-time PCR

Target gene	Primer sense (5' to 3')	Primer antisense (5' to 3')
Acat1	CGT AAT GAG CAG AGG AGC AAC AC	GCA GTA TTC TCA GCA CAG TTA CCC
Acat2	GAG ACC AGA GCG ACA AGA TGA ATG	GGA CAG GCA CGG TGG ACA G
Atf6	TGC CTT GGG AGT CAG ACC TAT G	GGA GAT GGA GCA ACT GGA GGA A
Asc	CCA TCC TGG ACG CTC TTG AAA AC	GCC CAT AGC CTT CTC GCA GTT
B2M	TCC AGA AAA CCC CTC AAA TTC A	AGT ATG TTC GGC TTC CCA TTC TC
Bssl	CAA CAC CTA TGG GCA AGA AGA CTG	CAT AGA TCC AGA CCA TCA CAG GCA
Caspase-1	TGC CTG CCC AGA GCA CAA G	TGG TCC CAC ATA TTC CCT CCT G
Cd68	GCA GCA CAG TGG ACA TTC AT	CAA GGT GAA CAG CTG GAG AA
Ceh	ACG CTT GCC AGA CCC TCT TC	CTC AGC CAC TTC AGC ATC GC
Chop	ATG AAG GAG AAG GAG CAG GAG AAC	GAT CAG AGC CCG CCG TGT G
Cyp27a1	TCA TCG CAC AAG GAG AGC AAT G	CGT TTA AGG CAT CCG TGT AGA GC
Cyp7a1	TTG TTC AAG ACC GCA CAT AAA GCC	CGT AGA CGG ATC AGT TCA GAG ACC
Cyp7b1	TTT CAG TCC ACT TCA CCA GAG AAC	GCA CAG CCT CAG AAC CTC AAG A
Cyp8b1	CCC TGA GCC CAC AGC CTT C	GGA TCT TCT TGC CCG ACT TGT AG
Eif2	AGC CAC ATC CAG GAA GTG ACA AG	ACA GGA GTA GGA GCC GCA TCA
Fxr	TGC GAT TAC CAC CAC CAC CTG	CCG AAC TTT AGC CAG CCA CCA
Hmgr	GCT GGA GAT CAT GTG CTG CTT C	ACG ACC CTC ACG GCT TTC AC
Hnf-1α	TGG CTC TGA AGA TGA CAC GGA TG	TGA CTC CAC CAC GGC TTT CTG
Hnf-3β	CCA GCG AGT TAA AGG GTC GTT TG	CTT CCA TCT TCA CGG CTC CCA
Hnf-4α	GCA ATG GAC AGA TGT GTG AGT GG	TTG GTG GTG ATG GCT GTG GAG
Hsl	ATC CCA GGC TCA CAG TTA CCA TC	CCA GGC TGT TGA GTA CCT TGC T
Icam-1	TCG GAA GGG AGC CAA GTA ACT	GAT CCT CCG AGC TGG CAT T
Insig	GGG AAA CAT AGG ACG ACA GTT AGC	TCT TCA TCA CAC CCA GGA CCA G
Ire1	AGG CAC CTC CAA GTT ACT GAT AGC	CAT CTT CCA GAC CCA CAG CAC A
Lrh1	GGC TCC GTT CCC TTC AGT TCG	TTC ACC TGC TCT TGG ACA CCT TC
Lxr-α	GAG AGG AAG GAG AGA GAT GGA A	AGC CCT GGA CAT TAC CAA GA
Mcp-1	GTG GGG CGT TAA CTG CAT	CAG GTC CCT GTC ATG CTT CT
Mln64	GCC CAT CAT TTC ATT CAT CCT TGC	TCT TCT GCC TCT TGA GGT AAC ACT
Mkiller	GGA GCA TGG AGG CAA TGG TTG CT	ATG CAC ACG AGT TCG CAC TT CG
Mttp	ATG ATC CTC TTG GCA GTG CTT	TGA GAG GCC AGT TGT GTG AC
Myd88	CCG CAT GGT GGT GGT TGT TTC	AGG AAT CAG TCG CTT CTG TTG GA
Nalp3	CAG GTT CAG TGT GTT TTC CCA GAC	TTG AGA AGA GAC CAC GGC AGA AG
Npc1	TCA GTC TGA ATG CGG TCT CCT TG	TGG TAC TCA TGG TGA ATG CTC TCG
Npc2	TTT ACC AGC GGC ACT CAG TCC	CCA CTC TTA CAA CCG TCA GGC T
Pannexin-1	GCC CAC CGA GCC CAA GTT C	CAG AGG TAG ACC CAC GGC AAT AC
Perk	CTC AGC GGA CGC AGC CTA C	GCT TCG GAC GGA CAA AGT TCA AA
Pxr	CCC TAA TGG TGG CTT CCA GAA AC	GCA TCA GCA CAT ACT CCT CCT TAT
Rpl13a	CCT GCT GCT CTC AAG GTT GT	GGC TGT CAC TGC CTG GTA CT
Rxra	TGC CTG CGA GCC ATT GTC C	CTT CTC CCT CAA CGC CTC CAC
Scap	ACA CCA GAA GCC CAT CAC AGC	AGG CAA CAC GAG TCA TCC AGT C
Shp	AAG GGC ACG ATC CTC TTC AAC C	CAG GGC TCC AAG ACT TCA CAC A
StAR	CTC ACT TGG CTG CTC AGT ATT GAC	CAG GTG GTT GGC GAA CTC TAT CT
TLR2	CAC TGG TGT CTG GAG TCT GCT G	CAC GCC CAC ATC ATT CTC AGG TA
TLR3	TCT GGG CTG AAG TGG ACA AAT CTC	AAG GAA CCG TTG CCG ACA TCA
TLR4	CTG GGG AGG CAC ATC TTC TGG	CTC TGC TGT TTG CTC AGG ATT CG
TLR5	AGA CTG CGA TGA AGA GGA AGC C	GAC TAC AAG GGT GAT GAC GAG GAA
TLR6/1	GGC TGT CAC TGG GGC TTT CC	CCT GTG CCT GGT CTG TGT CC
TLR7	GTG ATG CTG TGT GGT TTG TCT GG	TTT GAC CTT TGT GTG CTC CTG GA
TLR8	GTG CTT TTG TCT GCT GTC CTC TG	GGG AGT TGT GCC TTA TCT CGT CA
TLR9	GCA CCC TCC TCC AGA AAC TCG	GAG AAT GTT GTG GCT GAG GTT GAC
Tnfα	CAC GTC GTA GCA AAC CAC CAA	CCC ATT CCC TTC ACA GAG CAA
TnfR1	CTC AGG TAC TGC GGT GCT GTT	TCG GCA CAT TAA ACT GAT GAA GAT
TnfR2	CAA TTG GTC TGA TTG TTGGAGTGA	TTTCCTCTGCACCAGGATGAA
TRAIL	CTG GGA TCA CTC GGA GAA GA AC	CAA TCT TCT GGC CTA AGG TCT TTC
Vcam-1	CTA CAA GTC TAC ATC TCT CCC AGG AA	CCT CGC TGG AAC AGG TCA TT

Abbreviations for preceding Table (2.3): Acat, acyl-CoA:cholesterol acyltransferase; Asc, apoptosis-associated speck-like protein containing a caspase recruitment domain; Atf6, activating transcription factor-6; B2M, β2-microglobulin; Bssl, bile salt-stimulated lipase; Cd68, cluster of differentiation 68; Ceh, cholesteryl ester hydrolase; Chop, C/EBP homologous protein; Cyp27a1, sterol 27-hydroxylase; Cyp7a1, 7α–hydroxylase; Cyp7b1, oxysterol 7α-hydroxylase; Cyp8b1, sterol 12-α-hydroxylase ; Eif2, eukaryotic initiation factor 2a; eNOS, endothelial nitric oxide synthase; Fxr1, farnesoid X receptor-1; Hmgr, 3-hydroxy-3-methyl-glutaryl-CoA reductase; Hnf, hepatocyte nuclear factor; Hsl, hormone-sensitive lipase; Icam-1, inter-cellular adhesion molecule-1; iNOS, inductible nitric oxide synthase; Insig1, insulin-sensitive gene-1; Ire1, inositol-requiring protein-1; Lrh1, liver-receptor homolog-1 (Nr5a2); Lxr-α, liver X receptor-α; Mcp-1, monocyte chemotactic protein-1; MKiller, mouse killer (death receptor 5); Mln64, metastatic lymph node 64 protein; Mttp, microsomal triglyceride transfer protein; Myd88, myeloid differentiation primary response gene-88; Nalp3, (nacht domain-, leucine-rich repeat-, and PYD)-containing protein 3; Npc½, Niemann Pick C½ protein; Perk, protein kinase RNA-like ER kinase; Pxr, pregnane X receptor (Nr1l2); Rpl13a, 60S ribosomal protein L13a; Rxrα, retinoid X receptor-α; Scap, sterol regulatory element–binding protein (SREBP) cleavage-activating protein; Shp, small heterodimer partner; Star, steroidogenic acute regulatory protein; TLR, toll-like receptor; Tnfα, tumor necrosis factor-α; TRAIL, TNF-related apoptosis-inducing ligand; Vcam-1, vascular cell adhesion protein-1.

2.7.3 Real-time PCR

2.7.3.1 Reagents

PCR-grade d.H_2O (ultra-pure Baxter Healthcare irrigation water), and iQ SYBR Green Supermix were purchased commercially and required no additional preparation before use.

Primers were all designed using Beacon Designer™ V7.0 (PREMIER Biosoft, Palo Alto, CA), ensuring amplicon products crossed at least 1 exon boundary; the sequences are summarised in Table 2.3. Designed primers were ordered from Geneworks (Thebarton, SA, Australia).

250 μM primer stocks. Lyophilised primers were prepared to 250 μM stock concentrations by adding qPCR grade (calculated from primer nmol weights).

Primer working solution (7.5 μmol primer in qPCR-grade d.H_2O). Primer stocks (6 μL of 250 μM) were diluted in qPCR-grade water (194 μL), yielding 7.5 μmol working stock solutions.

cDNA standard solutions. Standard cDNA samples were constructed by pooling cDNA, and serially diluting with PCR-grade d.H_2O to create 1:10, 1:40, 1:160, 1:640, and

1:2560 dilutions of pooled cDNA. Standards were included in each qPCR reaction, allowing relative gene expression to be calculated in relation to global gene expression.

Master-mix solution (0.4 units of iQ SYBR Green Supermix, 150 nM sense and anti-sense primer, 32.5% [v/v] PCR-grade d.H_2O). iQ SYBR Green Supermix (10 µL), sense and anti-sense primer (0.4 µL each), and ultra-pure sterile water (5.2 µL) were added together for each template DNA amplification. Solution was mixed thoroughly by vortexing for 15 sec. Master mixes were used immediately.

2.7.3.2 Procedure

Master-mix solution (16 µL) containing the forward and reverse primers (Table 2.3) were pipetted into Bio-Rad 96-well PCR plates. cDNA samples, standards, and no template controls (PCR-grade d.H_2O) were added (4 µL) to wells, after which plates were sealed (Bio-Rad clear Microseal® 'B' adhesive seals), vortexed and qPCR reactions carried out in a Bio-Rad iQ5 Thermocycler (Hercules, CA) under the following conditions: polymerase activation at 95°C (3 min), followed by 45 cycles consisting of 95°C (10 sec), 65°C (20 sec), and 72°C (20 sec). SYBR green I fluorescence emission was reported after each successive cycle, and iQ5 Optical Systems software (Bio-Rad, Hercules, CA) was used to establish sample starting quantity. Gene expression was expressed as relative gene expression, typically normalised to levels in chow-fed WT animals (the controls for most experiments in this thesis). Melt curves were run after each PCR reaction to assess amplicon product quality and to check for primer-dimer product formation.

2.8 Hepatic protein isolation

Different methods were used to isolate the following protein fractions: whole liver, nuclear, cytoplasmic, and microsomal fractions. As described later in the thesis, these various compartments were used to establish the expression and enzyme activity of various proteins of interest. The methods used to isolate each protein fraction are described below:

2.8.1 Total hepatic protein isolation

2.8.1.1 Reagents

Protease and phosphatase inhibitors were purchased commercially and required no additional preparation before use.

Cell lysis buffer (50 mM HEPES, 150 mM NaCl, 1.5 mM $MgCl_2$, 1 mM EGTA, 10% [v/v] glycerol, 0.1% [v/v] triton X-100). HEPES (5.96 g), NaCl (4.84 g), $MgCl_2$ (71.5 mg), EGTA (190 mg), glycerol (50 mL), and triton X-100 (500 µL) were mixed together and made up to 500 mL with d.H_2O. Solution was aliquoted (10 mL) and stored at -20°C. Protease and phosphatase inhibitors (100 µL ea/10 mL) were added to cell lysis buffer before use.

2.8.1.2 Procedure

Frozen liver (-80°C) samples (~80 mg) were homogenised in cell lysis buffer (9 x volume/liver weight) to produce 10% (m/v) homogenates. Cell debris was pelleted (12,000 x g, 4°C, 5 min), supernatants aliquoted, and snap frozen in liquid nitrogen prior to storage (-80°C).

2.8.2 Hepatic nuclear/cytoplasmic sub-cellular protein isolation

Nuclear and cytoplasmic proteins were extracted from frozen (-80°C) liver tissue using the NE-PER nuclear/cytoplasmic extraction kit (Thermo, Rockford, IL), as per the Manufacturer's instructions. Protease and phosphatase inhibitors (Sigma-Aldrich) were added to buffers to inhibit protein degradation. Isolated protein fractions were aliquoted and frozen (-80°C).

2.8.3 Microsomal protein isolation

Hepatic microsomal proteins were isolated in order to assess HMG-CoA reductase enzyme activity, and were prepared as originally described by von Jagow *et al.* (1965), as detailed below:

2.8.3.1 Reagents

Potassium phosphate buffer #1 (0.2 M KH_2PO_4). KH_2PO_4 (27.2 g) was dissolved in d.H_2O (500 mL), with the final volume adjusted to 1 L.

Potassium phosphate buffer #2 (0.2 M K_2HPO_4). K_2HPO_4 (34.8 g) was dissolved in d.H_2O (500 mL). The final volume was adjusted to 1 L.

Microsome preparation buffer (0.01 M potassium-phosphate, pH 7.4, 1 mM EDTA, 0.25 M sucrose, 153 mM KCl). Potassium phosphate buffer #1 (9.5 mL) was added to potassium phosphate buffer #2 (40.5 mL). Solution pH was adjusted to 7.4 using buffer #2. EDTA (0.37 g), sucrose (85.57 g) and KCl (11.4 g) were dissolved in the solution, and final volume adjusted to 1 L using d.H_2O.

Microsome storage buffer (50 mM potassium-phosphate, 20% [v/v] glycerol, pH 7.4). Potassium phosphate buffer #1 (9.5 mL) was added to potassium phosphate buffer #2 (40.5 mL). The pH of the solution was adjusted to 7.4 using buffer #2. Glycerol (40 mL) was dissolved, and final volume adjusted to 200 mL using d.H_2O.

2.8.3.2 Procedure

Using Potter-Elvehjem glass homogenisers, frozen liver tissue (~200 mg) was homogenised in microsome preparation buffer (13 mL/sample). Homogenates were centrifuged (9,000 x g, 20 min, 4°C) to pellet cell debris, after which supernatants were transferred to ultra-centrifuge tubes and ultracentrifugated (100,000 x g, 60 min, 4°C). Supernatants were discarded and the pelleted microsomes were redissolved in microsome storage buffer (0.3 mL), prior to storage (-80°C). All steps were carried out on ice. For enzyme activity assays, samples were generally analysed within 4 days following isolation.

2.9 Protein determination

In order to determine the total protein content of isolated protein fractions, protein determination was carried out on samples using a commercial kit (DC™ Protein Assay, Bio-Rad, Hercules, CA), as per the Manufacturer's instructions.

2.10 Sodium dodecyl sulfate polyacrylamide gel electrophoresis (SDS-PAGE)

Protein samples were separated by size using sodium dodecyl sulfate polyacrylamide gel electrophoresis (SDS-PAGE). The Bio-Rad Mini-PROTEAN® electrophoresis system (0.75 mm thickness) was used, according to the Manufacturer's instructions. The methodology is briefly outlined below:

2.10.1 Reagents

Tetramethylethylenediamine (TEMED), 30% (m/v) acrylamide, and molecular weight markers (Bio-Rad Precision Plus Protein Prestained Standards) were all purchased commercially and required no preparation.

3 M Tris-HCl, pH 8.8 stock. Tris (363.42 g) was dissolved in d.H_2O (0.8 L), pH adjusted to 8.8 with HCl, and the final volume made up to 1 L with d.H_2O.

1 M Tris-HCl, pH 6.8 stock. Tris (121.14 g) was dissolved in d.H_2O (0.8 L), pH adjusted to 6.8 with HCl, and the final volume made up to 1 L with d.H_2O.

10% (m/v) SDS stock. SDS (50 g) was dissolved in d.H_2O (450 mL), pH adjusted to 7.2 with HCl, and the final volume made up to 0.5 L with d.H_2O.

10% (m/v) APS stock (100 mg/mL APS in d.H_2O). APS (1 g) was dissolved in d.H_2O (10 mL), aliquoted and stored at -20°C.

10 M DTT in d.H_2O. DTT (1.54 g) was dissolved in d.H_2O (1 mL), aliquoted, and stored at -20°C.

5X Reducing treatment buffer (300 mM Tris-HCl, pH 6.8, 10% [m/v] SDS, 50% [v/v] glycerol, 0.04% [m/v] bromophenol blue, 0.5 M DTT). Tris (1.81 g) was dissolved in d.H_2O (15 mL), pH adjusted to 6.8. SDS (5 g), glycerol (25 mL), bromophenol blue (20 mg) added, pH rechecked and final volume made up to 47.5 mL with d.H_2O. Buffer was aliquoted (0.95 mL) and stored at -20°C. Just before use, 10 M DTT (50 µL) was added.

Running buffer (100 mM Tris, 76 mM glycine, 0.1% [m/v] SDS, pH 8.3). Tris (27 g), glycine (129 g), and SDS (2.25 g) were dissolved in d.H_2O (2.25 L).

2.10.2 Procedure

The Bio-Rad Mini-Protean® electrophoresis gel casting apparatus was assembled as per the Manufacturer's specifications. Gels were prepared as described in Table 2.4, with resolving and loading gels poured and set sequentially, before being transferred into Bio-Rad Mini-Protean® electrophoresis modules containing running buffer. Protein

samples were standardised to concentrations of either 3.0 mg/mL (for total hepatic protein) or 5.0 mg/mL (for isolated nuclear and cytoplasmic protein). Samples were standardised by diluting protein in d.H_2O. Standardised protein samples were subsequently reduced in 5X reducing treatment buffer, heated (100°C, 5 min) and loaded (30 µg/well for total hepatic and 50 µg/well for nuclear and cytoplasmic protein), along with commercial BioRad protein molecular weight markers (10 µL/well) prior to electrophoresis (120 V, 2 h, RT).

Table 2.4 Volumes of SDS-PAGE reagent used for preparation of four Bio-Rad mini-Protean® 0.75 mm thick gels of varying running gel pore-size

Solution	Running gel (2.7% C)				Stacking gel
	15% T	12.5% T	10% T	7.5% T	(4% T, 2.7% C)
30% (m/v) Acrylamide	7.00 mL	5.30 mL	4.40 mL	3.30 mL	1.04 mL
3 M Tris-HCl, pH 8.8	3.30 mL	3.30 mL	3.30 mL	3.30 mL	-
1 M Tris-HCl, pH 6.8	-	-	-	-	2.00 mL
10% (w/v) SDS	250 µL	250 µL	250 µL	250 µL	160 µL
d.H_2O	2.72 mL	4.42 mL	5.32 mL	6.42 mL	4.88 mL
10% (w/v) APS	100 µL	100 µL	100 µL	100 µL	50 µL
TEMED	10 µL	10 µL	10 µL	10 µL	10 µL
Final volume	13.38 mL	13.38 mL	13.38 mL	13.38 mL	8.14 mL

Abbreviations: % C, cross-linker percentage concentration; % T, total percent concentration; APS, ammonium persulfate; SDS, sodium dodecyl sulphate; TEMED, tetramethylethylenediamine.

2.11 Western blotting

Western blotting (immunoblotting) was employed to quantify specific proteins through the use of protein-antibody interactions (Renart *et al.* 1979; Celis *et al.* 1994). The methodology incorporates two major steps, the first involves the immobilisation of SDS-PAGE separated proteins onto a PVDF membrane via electrophoretic elution, the second is a "probing" step using specific commercially purchased antibodies (Towbin *et al.* 1979). The SDS-PAGE protocol is described in Section 2.5.2, and the subsequent steps for protein immobilisation and probing are outlined below:

2.11.1 Reagents

Transfer buffer (25 mM Tris-HCl, 192 mM glycine, 20% [v/v] methanol, 0.01% [m/v] SDS, pH 8.3). Tris (9 g) and glycine (43.2 g) were dissolved in d.H_2O (2.4 L). SDS (2

mL of 10% [m/v] stock solution, Section 2.10.1), methanol (600 mL) was added, and buffer was stored at 4°C without pH adjustment.

Tris-buffered saline, containing Tween-20 (TBST) (20 mM Tris-HCl, 200 mM NaCl, pH 7.4, 0.05% [v/v] tween-20). Tris (2.42 g) and NaCl (11.7 g) were dissolved in d.H_2O (950 mL). The pH was adjusted to 7.4 with 5N HCl. Tween-20 (2 mL of 25% [v/v] stock) was added and the final volume adjusted to 1 L.

Blocking solution (5% [m/v] skim milk powder in TBST, pH 7.4). Skim milk powder (5 g) was dissolved in TBST (100 mL). The solution was prepared just prior to use.

Antibody diluent (0.5% [m/v] BSA in TBST). BSA (0.5 g) was dissolved in TBST (100 mL). The solution was prepared just before use.

2.11.2 Procedure

The western blotting procedure outlined in this section is identical to the methodology described by Furuyama and Fujisawa (2000). Following SDS-PAGE electrophoresis (Section 2.9.2), gels, along with blotting paper (2 sheet/gel), and 85 x 55 mm pieces of PVDF membrane (0.45 μm pore) (1 sheet/gel) were equilibrated in cold transfer buffer. Protein transfer sandwiches were assembled using Bio-Rad Mini-Protein® Tetra Cell electrophoresis cassettes according to the Manufacturer's instructions. Briefly, resolved SDS-PAGE gels (Section 2.9.2) were placed against PVDF membranes and encapsulated by blotting paper (1 sheet/side), ensuring that no air bubbles were trapped between layers (Towbin *et al.* 1979). Sandwiches were then placed in Bio-Rad transfer tanks (containing ice-cold transfer buffer), with PVDF membranes orientated towards the apparatus anode. Magnetic stirrers ensured constant mixing of buffer throughout the transfer. Transfer tanks were covered with ice, and electrophoresis performed (125 V, 2 h, voltage limiting), after which PVDF membranes were stained using Ponceau S to determine transfer efficiency. Ponceau S stain was removed with d.H_2O, and the drop-wise addition of 1 M NaOH solution. PVDF membranes were stored in TBST buffer prior to probing.

For "probing", PVDF membranes were blocked against non-specific protein-protein interactions with 5% (m/v) skim milk powder blocking solution (1 h, RT, orbital

shaker). Membranes were then incubated with primary antibodies (see Table 2.1) diluted in 0.5% (m/v) BSA-TBST antibody diluent (16 h, 4°C, orbital shaker), and washed (TBST, 2 x 5 min). Immunoreactivity was subsequently detected by incubating membranes with HRP-conjugated secondary antibodies diluted in 0.5% BSA-TBST (see Table 2.2). A final washing step was carried out (TBST, 3 x 5 min), after which membranes were immersed in SuperSignal West Femto Substrate solution (5 min, RT) and proteins detected using a digital enhanced chemiluminescence image capture system (LAS-4000, FujiFilm, Tokyo, Japan). Densitometry was quantified (MultiGauge V3.0, FujiFilm, Tokyo, Japan), and values normalised to house keeping gene expression (heat shock protein-90 [HSP90] and TATA box-binding protein [TBP] densitometry). Protein expression was subsequently normalised to WT chow levels. Western blots were run in triplicate or quadruplicate and groups compared on multiple combination gels.

2.12 HMG-CoA reductase (HMGR) activity assay

HMG-CoA reductase activity was assessed using the method described by Stone *et al.* (1989), as briefly outlined below:

2.12.1 Reagents

Potassium phosphate buffer #1 and potassium phosphate buffer #2 were prepared as per Section 2.8.3.1.

HMG-CoA reductase assay buffer #1 (50 mM potassium phosphate, 5 mM DTT, 1 mM EDTA, pH 7.4). Potassium phosphate buffer #1 (9.5 mL) was added to potassium phosphate buffer #2 (40.5 mL). EDTA (74 mg) was dissolved, and pH was adjusted to 7.4 using buffer #2. The final volume adjusted to 200 mL using d.H_2O, solution aliquoted (9.95 mL), and stored at -20°C.

HMG-CoA reductase assay buffer #2 (200 mM potassium phosphate, pH 7.4). Potassium phosphate buffer #1 (19 mL) was added to potassium phosphate buffer #2 (81 mL). The pH was adjusted to 7.4 using buffer #2, and stored at -20°C.

NADP/G-6-P solution (25 mM NADP, 200 mM glucose 6-phosphate). NADP (74 mg) and glucose 6-phosphate (225 mg) were dissolved in d.H_2O (4 mL), aliquoted and stored at -20°C.

Substrate solution (DL-3-[glutaryl-3-^{14}C]-hydroxy-3-methylglutaryl coenzyme A [10 μCi/500 μL], containing 0.5 μM cold HMG-CoA). HMG-CoA (10 mg) was dissolved in d.H_2O (1 mL), and added (46 μL) to (^{14}C)-HMG-CoA (10 μCi). Solution was stored at -20°C.

Glucose 6-phosphate dehydrogenase (1 U/μL glucose 6-phosphate dehydrogenase). Glucose 6-phosphate dehydrogenase (100 units) was dissolved in HMG-CoA reductase assay buffer (100 μL). Solution was aliquoted and stored at -20°C.

Mevalonic acid lactone (1 mg/μL mevalonic acid lactone). Mevalonic acid lactone (1 g) was dissolved in d.H_2O (1 mL), aliquoted and stored at -20°C.

Thin layer chromatography (TLC) resolving solvent (chloroform:acetone 1:1). Chloroform (100 mL) and acetone (100 mL) were added together and stored in the dark.

Aquasol-2 liquid scintillation counting cocktail, *DL*-3-(glutaryl-3-^{14}C)-hydroxy-3-methylglutaryl coenzyme A, and *RS*-(5-^{3}H)-mevalonolactone were purchased commercially and required no preparation before use.

2.12.2 Procedure

Microsomal protein samples (Section 2.7.3) were standardised to 100 μg protein/40 μL (diluted in 50 mM potassium phosphate assay buffer #1, pH 7.4). Reaction master mixes were prepared for each enzyme reaction as follows: NADP/G-6-P solution (10 μL), glucose 6-phosphate dehydrogenase (1 μL), and HMG-CoA reductase assay buffer #2 (40 μL) were added together, along with microsomal protein samples (40 μL). Samples were incubated (37°C, 15 min), after which substrate solution (10 μL) was added and tubes reincubated (37°C, 90 min). Reactions were arrested with concentrated HCl (10 μL). Mevalonic acid lactone solution (1 μL) was then added to each sample and proteins were precipitated by centrifugation (16,000 x g, 5 min, 4°C). Supernatants (75 μL) were transferred to fresh Eppendorf tubes and spiked with RS-(5-^{3}H)-

mevalonolactone (4.5 nCi). Samples were then loaded (75 µL) onto preabsorbant, glass-backed TLC plates, allowed to dry, and separated via TLC using 1:1 chloroform:acetone (60 min, RT, TLC tank). TLC plates were air-dried, and stained using iodine vapour. The area of iodine staining corresponding to the mevalonolacetone (retention factor [*Rf*] of 0.76-1.0) was marked, and an area of 20 x 30 mm was scraped into scintillation vials. Scrapings were resuspended in Aquasol-2 liquid scintillation cocktail (7 mL), rested (1 h, RT), after which radioactivity was analysed by liquid scintillation counting (TriCarb 2100TR, Packard, CT). Recovery of product was calculated from (5-^{3}H)-mevalonolactone activity present, with final HMGR activity expressed as nmol of (^{14}C)-mevalonolactone formed/min/mg protein.

2.13 Primary hepatocyte cell culture

Primary hepatocytes were isolated from mice as previously described (Clayton and Darnell 1983). The procedure is briefly outlined below:

2.13.1 Reagent

William's E and Hank's buffered salt solution (HBSS) were purchased commercially and required no additional preparation.

0.5 M EDTA stock solution. EDTA (18.612 g) was dissolved in d.H_2O (80 mL), pH adjusted to 8.0 with NaOH, and final volume adjusted to 100 mL. Solution was aliquoted and sterilised by autoclaving.

1 M $CaCl_2$ stock solution. $CaCl_2$ (11.1 g) was dissolved in d.H_2O (100 mL) and filter sterilised.

Perfusion buffer solution (20 mM HEPES, 404 µM $NaHCO_3$ in HBSS, pH 7.4). HEPES (2.38 g) and $NaHCO_3$ (17 mg) were dissolved in HBSS (0.5 L), pH adjusted to 7.4, and solution filter sterilised. Solution was heated (39°C) before use.

Perfusion buffer #2 (20 mM HEPES, 404 µM $NaHCO_3$, 0.5 mM EDTA in HBSS, pH 7.4). EDTA (25 µL of 0.5 M stock) was added to perfusion buffer solution (25 mL). Solution was heated (39°C) before use.

Perfusion buffer #4 (20 mM HEPES, 404 μM $NaHCO_3$, 5 mM $CaCl_2$, 100 U/mL type-2 collagenase in HBSS, pH 7.4). $CaCl_2$ (250 μL of 1 M stock) and type-2 collagenase (20 mg of 248 U/mg stock) were added to perfusion buffer solution (50 mL). Solution was heated (39°C) before use.

Hepatocyte culture media (10 mM HEPES, 1% (m/v) BSA, 10 mM nicotinamide in William's E, pH 7.4). HEPES (2.38 g), BSA (10 g), and nicotinamide (1.21 g) were dissolved in William's E buffer (950 mL), and pH adjusted to 7.4. Final volume was made up to 1 L with William's E buffer, before solution was filter sterilised.

2.13.2 Procedure

Once anaesthetised (Section 2.4), mice underwent midline laparotomy. Intestines were displaced to expose the portal vein (PV). Adipose tissue was carefully blunt-dissected away from the PV. A 22 G intravenous catheter was used to cannulate the PV, and secured using silk sutures. A peristaltic pump was subsequently used to perfuse buffer solutions at a constant rate (8 mL/min). Care was taken to ensure no air entered the circulatory loop. Perfusion buffer solution (50 mL) was used to initially flush out blood from the liver. At the onset of perfusion, the hepatic artery and vein were both severed to prevent hydrostatic pressure build-up, and, following an initial "wash-out", livers were perfused with EDTA-containing buffer # 2 (25 mL); this chelates Ca^{2+}, thereby facilitating desmosome-cytoskeleton dissociation (Mattey and Garrod 1986; Berry *et al.* 1997). EDTA solution was flushed from liver by inflow of perfusion buffer solution (25 mL), after which perfusion buffer #4 (50 mL) containing 100 U/mL collagenase was perfused until the liver was appreciably softened, typically 7 min.

Following collagenase digestion, livers were excised, and cells suspended in ice cold culture media. Suspensions were passed through 100 μm cell sieves, then centrifuged (100 x g, 2 min, 4°C) to pellet hepatocytes. Non-parenchymal cell fractions (supernatant) were discarded. This step was repeated twice to purify parenchymal cell fractions. Hepatocytes were then seeded onto rat-tail collagen-coated 55 cm^2 plates (5 $\mu g/cm^2$), and cultured at a cell density of ~6.5 x 10^4 viable cells/cm^2. Specific experimental details are described in relevant Chapters.

2.14 Fluorescent cholesterol localisation

Methodologies for lipid staining and subcellular organelle colocalisation are identical to those described by Mari *et al.* (2006), and are described below.

2.14.1 Reagents

Phosphate-buffered saline (PBS) tablets were purchased commercially and prepared according to the Manufacturer's instructions.

3.7% (m/v) Paraformaldehyde working solution buffered in PBS, pH 7.4. Paraformaldehyde (6 mL of 16% [m/v] stock) was added to PBS, pH 7.4 (20 mL). Solution was prepared just before use.

0.1% (m/v) Saponin buffered in PBS, pH 7.4. Saponin (0.1 g) was gently dissolved in PBS, pH 7.4 (100 mL). Solution was prepared just before use.

Block/permeabilisation solution (1% [m/v] BSA, 0.1% [m/v] saponin buffered in PBS, pH 7.4). BSA (1.0 g) was gently dissolved in PBS, pH 7.4 (100 mL). Solution was prepared just before use.

Antibody diluent (0.5% [m/v] BSA in PBS). BSA (0.25 g) was dissolved in PBS (50 mL). Solution was prepared just before use.

Filipin working solution (5 μg/mL filipin in DMF). Filipin (1 mg) was dissolved in dimethyl sulfoxide (DMSO) (200 μL) and diluted in PBS (20 mL). Solution was shielded from light.

Nile red stock solution (1 mg/mL nile red in DMSO). Nile red (10 mg) was dissolved in DMSO (100 μL), and made up to with 10 mL with DMSO. Solution was stored at 4°C.

Nile red working solution (1.5 μg/mL [v/v] nile red in PBS). Nile red (1.5 μL of 1 mg/mL stock solution) was diluted in PBS (1 mL). Solution was prepared just before use.

2.14.2 Procedure

Frozen liver sections (5 μm) were mounted on clean slides, air dried (1 h, RT), and fixed in 3.7% (m/v) paraformaldehyde (15 min, RT). Sections were washed (3 x 10 sec, PBS), and incubated with filipin working solution (4-16 h, 4°C, moisture chamber, in dark). Filipin staining solution was removed and sections were washed (3 x 10 sec, PBS, dark), and permeabilised with block/permeabilisation solution (5 min, RT, dark). Sections were rinsed (3 x 10 sec, PBS, dark) and incubated with primary antibodies diluted in antibody diluent (Table 2.1) (5 h, RT, dark). Slides were washed (3 x 10 sec, PBS, dark), and incubated with fluorescent secondary antibodies (Table 2.2) (45 min, RT, dark), washed (3 x 10 sec, PBS, dark). Sections were desalted (2 x 10 sec, d.H_2O, dark) and air-dried in the dark. Slides were mounted using ProLong® Gold antifade reagent, and sealed using nail varnish.

For esterified lipid localisation, frozen liver sections (5 μm) were fixed in 3.7% (m/v) paraformaldehyde (15 min, RT), washed (3 x 10 sec, PBS), and incubated with Nile red working solution (30 min, RT, in dark). Sections were washed (3 x 10 sec, PBS, dark), mounted using ProLong® Gold antifade reagent, and sealed using nail varnish. All fluorescent images were captured using a Zeiss Axioplan2 microscope with Apotome (Zeiss, GmbH, Germany). Images were analysed with AxioVision V4.8 (Zeiss, GmbH, Germany).

2.15 Statistical analyses

All data were analysed by analysis of variance (ANOVA), with Tukey post-hoc testing (SPSS V17.0, Chicago, IL, USA). Histological assessments (categorical) were analysed using Kruskal-Wallis' test, and group comparisons (continuous variables) made using Mann-Whitney *U*-test. Cell culture data was assessed for statistical significance using Student's t-test. Statistical significance was defined as $P<0.05$. All data are presented as mean ± standard error of the mean (SEM).

CHAPTER 3

Characterisation of hepatic cholesterol turnover in *foz/foz* mouse model of non-alcoholic steatohepatitis

3.1 Introduction

As discussed in Chapter 1 (Sections 1.2-1.9), cholesterol homeostasis within the body is subject to strict regulation: hepatic uptake, storage, trafficking, biotransformation, and excretion are all tightly controlled processes. These are effected by nuclear transcriptional regulators which are largely responsible for regulating the expression of the various enzymes and transporters tasked with facilitating cholesterol equilibrium. The accumulation of cholesterol has been shown to have numerous pathological effects in mammals, including atherosclerosis, foam cell death (Kellner-Weibel *et al.* 1998; Kellner-Weibel *et al.* 1999b), nephrotoxicity (Ruan *et al.* 2009), gallstone formation (Uppal *et al.* 2008), and neurotoxicity (Fernandez *et al.* 2009). However, to date cholesterol has not been directly implicated in mediating liver injury, although several human NASH studies have shown correlative elevations in both serum and hepatic cholesterol levels in NAFLD compared to lean controls (Puri *et al.* 2007; Caballero *et al.* 2009).

In rodents hepatocyte free cholesterol (FC) accumulation has been shown to increase cell stress and sensitise hepatocytes to TNF-α- and FasL-mediated cell death (Mari *et al.* 2006). Further, in at least one experimental model, FC was thought to contribute to hepatic inflammation and progression of NAFLD to NASH (Wouters *et al.* 2008; Wouters *et al.* 2010; Subramanian *et al.* 2011). However, due to ethical and logistical limitations, including sample availability and lack of appropriate control tissue, no studies have comprehensively addressed the cause and implications of cholesterol accumulation in humans with NASH, or in an animal model that faithfully reflects both the metabolic setting and tissue pathology of NASH.

Previous studies in the *foz/foz* model of NASH undertaken in the host laboratory have found that NASH develops between 6 and 12 weeks of dietary intake in mice fed a HF-diet that contains 0.2% (w/w) cholesterol; fibrogenesis is observed between 12 and 24

weeks. Total serum cholesterol levels increase significantly in *foz/foz* mice with NASH (Figure 3.1A), in a pattern which correlates with the extent of liver injury, as assessed both histologically and by raised serum alanine transaminase (ALT) levels (Larter *et al.* 2009).

3.2 Purpose of study: hypotheses and aims

The underlying hypothesis of this research is that hepatic cholesterol levels correlate with the onset and extent of liver injury in the obese, diabetic *foz/foz* mouse model of NASH.

The specific aims of the studies described in this Chapter were to:

1. Determine hepatic cholesterol levels in *foz/foz* mice with NASH compared with simple steatosis and lean liver.
2. Measure relative proportions of free and esterified cholesterol, as well as characterise subcellular localisation of hepatic cholesterol pools.
3. Assess pathways responsible for cholesterol uptake, trafficking, storage, biotransformation, and excretion.
4. Analyse the expression levels of nuclear regulators of cholesterol homeostasis.

3.3 Methods

3.3.1 Mice and diets

Female WT and *foz/foz* NOD.B10 mice (n=5-10/group) were fed either chow (containing 0% cholesterol) or HF-diet (containing 0.2% cholesterol) for 12- or 24 weeks (see Table 5.1 for more detail on HF diets used). Mice were maintained as described in Section 2.3, and at experimental time points harvested as described in Section 2.4.

3.3.2 Procedures

Serum and hepatic cholesterol fractions were quantified as described in Section 2.5, while FC and CE/TG lipids were localised in frozen liver sections as described in Section 2.14.

Subcellular localisation of FC was carried out as described in Section 2.14, using subcellular marker antibodies listed in Table 2.1.

SDS-PAGE, western blotting, semi-quantitative qPCR and IHC were carried out as described in Sections 2.10, 2.11, 2.7, and 2.6.2.1, respectively. The antibodies and primers used for western blotting and qPCR are shown in Tables 2.1 and 2.3, respectively.

Microsomal protein was isolated as described in Section 2.8.3. HMGR activity was quantified using a radiometric assay, as described in Section 2.12.

All statistical analyses were conducted as described in Section 2.15.

3.4 Results

3.4.1 Increases in serum and hepatic cholesterol fractions correspond with NASH severity in *foz/foz* mice

By 24 weeks of dietary intake, serum total cholesterol increased to 6.86 ± 0.26 mmol/L in HF-fed *foz/foz* mice compared to dietary and genotype controls (P<0.0001, Figure 3.1A) (chow-fed WT: 2.31 ± 0.26; chow-fed *foz/foz*: 3.27 ± 0.13; HF-fed WT: 2.95 ± 0.26 mmol/L). Similarly, serum HDL cholesterol was also increased ~2.5-fold (P=0.001, Figure 3.1B) in *foz/foz* mice with NASH at this time point. However, when expressed as a ratio of total serum cholesterol, serum HDL cholesterol was relatively lower in both chow and HF-fed *foz/foz* mice compared with corresponding WT controls (P<0.05, Figure 3.1C).

HF-feeding profoundly increased hepatic total cholesterol content with corresponding increases in both the cholesteryl ester (CE) and FC fractions in both *foz/foz* and WT mice compared to respective chow-fed controls (both P<0.05, Figure 3.1D,E). Compared to diet-matched WT controls, hepatic CE profiles were ~200-fold greater in HF-fed *foz/foz* mice at 12 weeks, and values increased a further ~4-fold by 24 weeks (P<0.0001, Figure 3.1D). FC was found to increase in both *foz/foz* and WT mice at 12 weeks compared to dietary controls (P<0.05, Figure 3.1E). However, the increase in hepatic FC in HF-fed WT mice at 12 weeks was evanescent, with values returning to those of chow-fed controls by 24 weeks. At this later time (when T2D and NASH are established), hepatic FC was significantly higher in HF-fed *foz/foz* versus HF-fed WT mice (P<0.05, Figure 3.1E).

To localise FC and esterified lipids, frozen liver sections were stained with filipin and Nile Red, respectively. Esterified lipids, which include TG and CE, were predominantly found within the cytoplasm of hepatocytes, while FC appeared to accumulate around macrosteatotic vesicles containing TG and CE lipid species (Figure 3.1F). No cholesterol crystals were evident in this analysis; however, electron microscopy (EM) would be required to completely rule out their presence.

FC localisation has been found to play an important role in the generation of cell stress (Mari *et al.* 2006) and macrophage cell death (Senokuchi *et al.* 2008). We therefore conducted colocalisation studies between FC and subcellular markers (Figure 3.2). In frozen liver sections from 24 week HF-fed *foz/foz* mice with NASH, FC colocalised with the endoplasmic reticulum (ER) marker, glucose-regulated protein-78 (GRP78) (Figure 3.2A), with the mitochondrial marker, carbamoyl phosphate synthetase-1 (CPS1) (Figure 3.2B), the hepatocyte nuclei marker, hepatocyte nuclear factor-4α (HNF-4α) (Figure 3.2C), the nuclear plasma membrane marker, lamin B1 (Figure 3.2D), and with the plasma membrane marker, Na/K-ATPase (Figure 3.2E). ImageJ (NIH, USA) image analysis of FC colocalisation demonstrated (see highlighted green in far right panels) that the major portion of FC localised to the hepatocyte plasma membrane (Figure 3.2E), while a lesser extent of mitochondrial (Figure 3.2B) and ER localisation (Figure 3.2A) was also observed. No colocalisation was observed between FC and hepatocyte nuclei (Figure 3.2C), or with the nuclear membrane (Figure 3.2D).

The temporal relationship between hepatic cholesterol accumulation, onset of NASH at 12 weeks and its progression to fibrosis at 24 weeks, together with localisation of FC to plasma membrane, mitochondria and ER, is consistent with a pathogenic role of cholesterol in NASH. This aspect is explored in Chapter 4. To further elucidate the mechanisms responsible for the profound increases in hepatic and serum cholesterol fractions in *foz/foz* mice with NASH, the various pathways responsible for cholesterol homeostasis were assessed as the central topic of this Chapter.

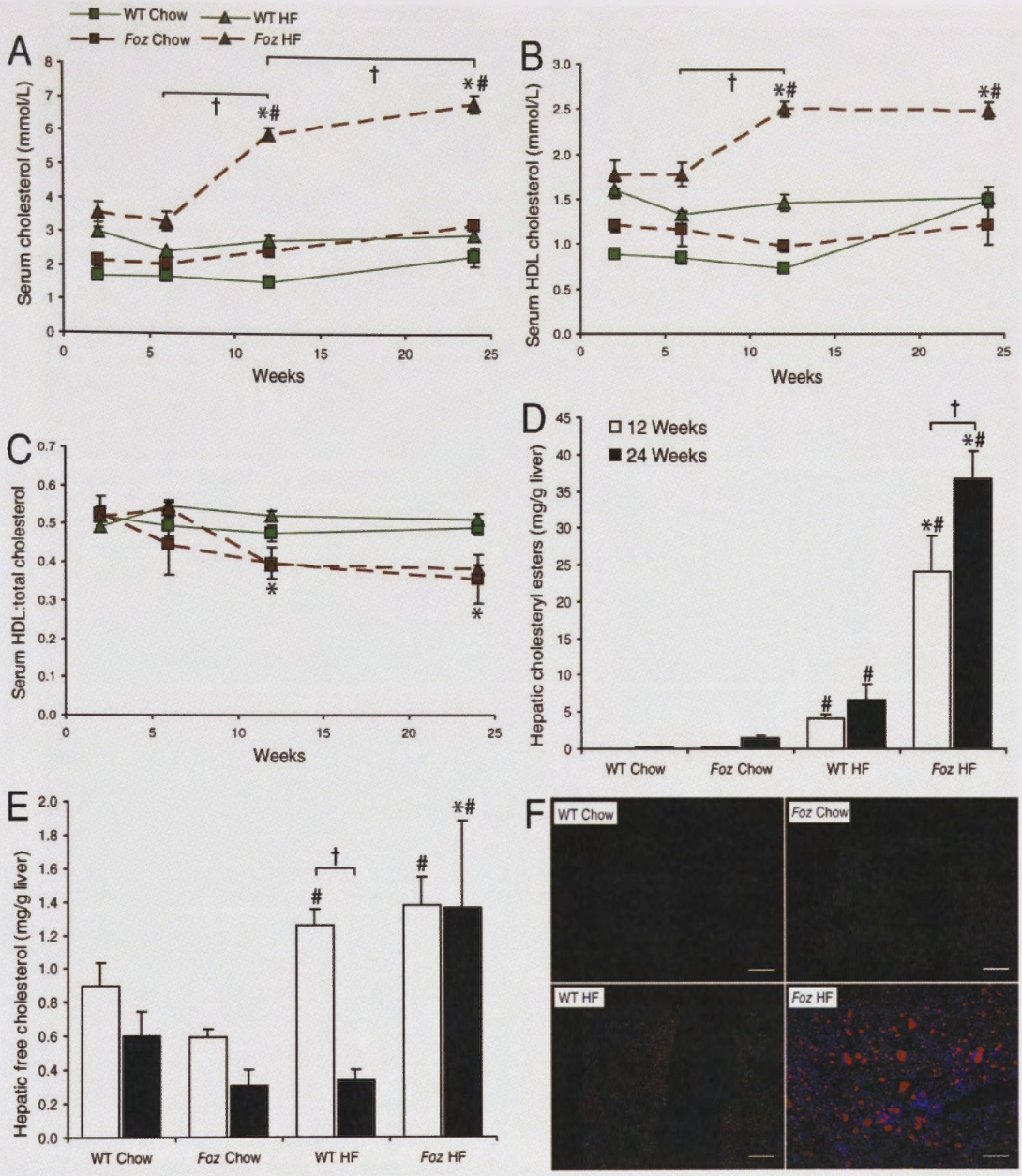

Figure 3.1 Serum and hepatic cholesterol levels increase in *foz/foz* and wildtype mice

(**A**) Serum total cholesterol and (**B**) high-density lipoprotein (HDL) cholesterol in normal chow (0% [w/w] cholesterol) and HF (0.2% [w/w] cholesterol)-fed WT and *foz/foz* mice over 24 weeks (n=5-14/grp). (**C**) HDL cholesterol expressed as a ratio to total cholesterol in mice over 24 weeks. (**D**) Hepatic cholesteryl esters (CE) and (**E**) free cholesterol (FC) content in mice at 12- (□) and 24- (■) weeks (n=5-10/grp) as determined by HPLC. (**F**) Representative low magnification (10X objective) images obtained from frozen HF-fed *foz/foz* liver sections (24-weeks on diet) stained for cholesterol (blue filipin staining) and cholesteryl esters (Nile red staining). Scale bars represent 200 μm. Data are mean ± SEM. *P<0.05, vs. diet-matched control. $^{\#}P$<0.05, vs. genotype-matched control. $^{\dagger}P$<0.05, vs. genotype and diet-matched group.

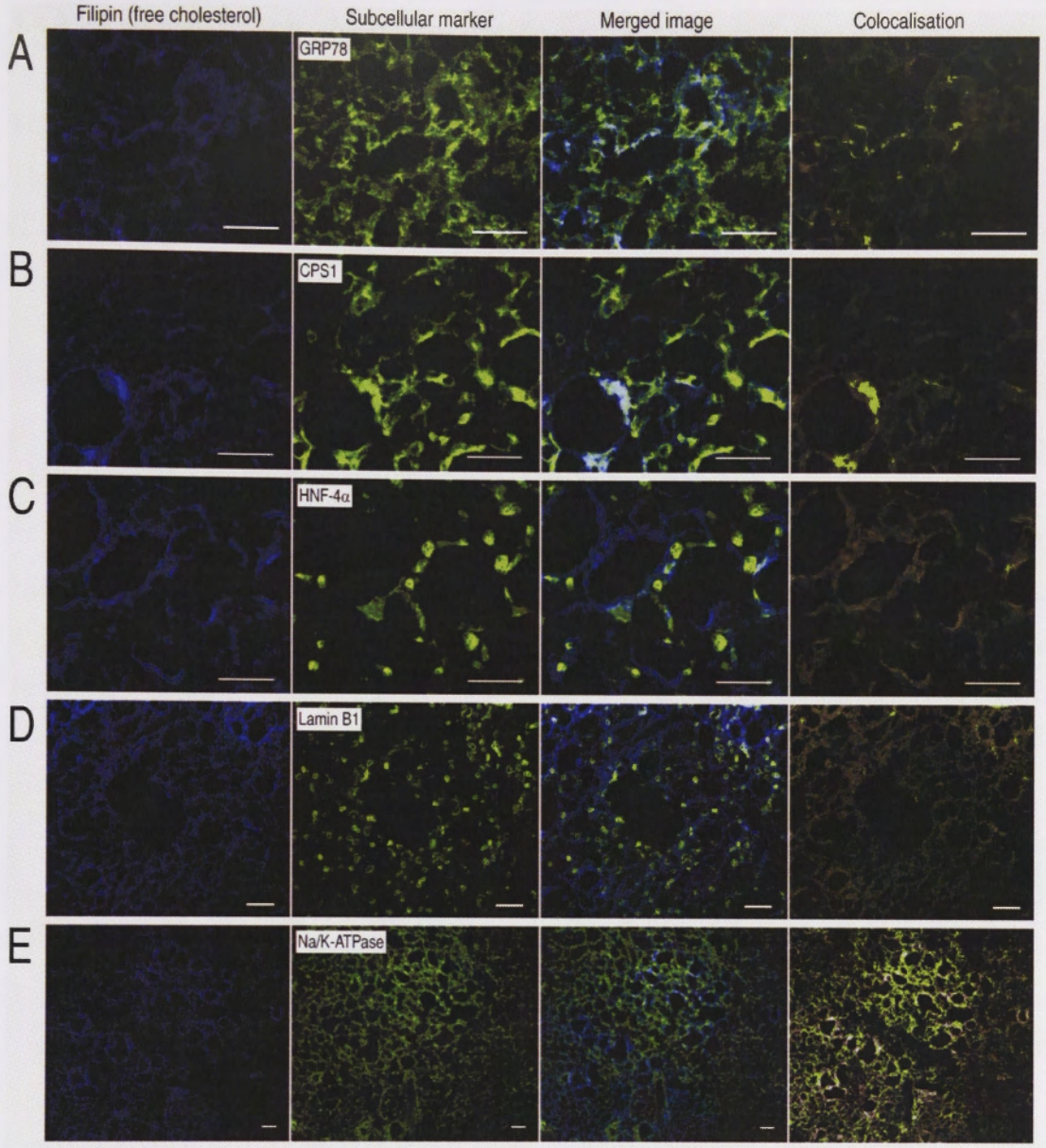

Figure 3.2 Subcellular free cholesterol localisation in HF-fed *foz/foz* mice with NASH

Frozen liver sections from 24 week HF-fed *foz/foz* mice were co-stained for free cholesterol (blue) and various subcellular markers. (**A**) Glucose regulated protein-78 (GRP-78), (**B**) carbamoyl phosphate synthetase-1 (CPS1), (**C**) hepatocyte nuclear factor-4α (HNF-4α), (**D**) lamin B1, and (**E**) Na/K-ATPase subcellular markers (green) were labelled using specific antibodies (Table 2.1) and detected using FITC conjugated secondary antibodies (Invitrogen, Carlsbad, CA). Images were captured using a Zeiss Axioplan2 (Zeiss, GmbH, Germany) microscope and merged using AxioVision V4.8 (Zeiss, GmbH, Germany) software. Colocalisation (far right panels) was calculated using ImageJ (NIH, USA) and highlighted in green. Scale bars represent 50 μm.

3.4.2 The hepatic free cholesterol uptake pathways are differentially regulated in HF-fed *foz/foz* mice

There are at least three pathways for hepatic cholesterol uptake from sinusoidal blood. They include the scavenger receptor-B1 (SR-B1), the low density lipoprotein receptor (LDLR) and cluster differentiation protein-36 (CD-36). The up-regulation of CD-36 expression in the *foz/foz* model of NASH has been previously reported in HF-fed *foz/foz* mice over 24 weeks (Larter *et al.* 2009). In the present studies, SR-B1 protein expression was found to be down regulated in *foz/foz* mice compared with WT controls ($P<0.05$, Figure 3.3A), although immunostaining of this transporter showed no change in its sinusoidal localisation (Figure 3.3B). Conversely, LDLR, the major transporter responsible for FC uptake, was significantly increased at both 12- and 24 weeks in HF-fed *foz/foz* mice ($P<0.05$, Figure 3.3C). Further, over-expression of LDLR was accompanied by an extension from physiological vascular endothelial expression to hepatocyte localisation, as shown by IHC (Figure 3.3D). The differential regulation of LDLR and SR-B1 is consistent with the proposal that an increase in LDLR FC uptake contributes to increased hepatic cholesterol in *foz/foz* mice with NASH. Interestingly, pro-protein convertase subtilisin/kexin type-9 (PCSK9), the endogenous inhibitor of LDLR, was also found to be upregulated in HF-fed *foz/foz* mice with NASH, as well as in HF-fed WT mice by 24 weeks (Figure 3.3E). However, in contrast to LDLR, there was no significant change to the restricted non-parenchymal cell localisation pattern observed in dietary and genotype controls (Figure 3.3F), a finding which implies that hepatocellular LDLR can act unopposed to transport FC in diabetic mice with NASH.

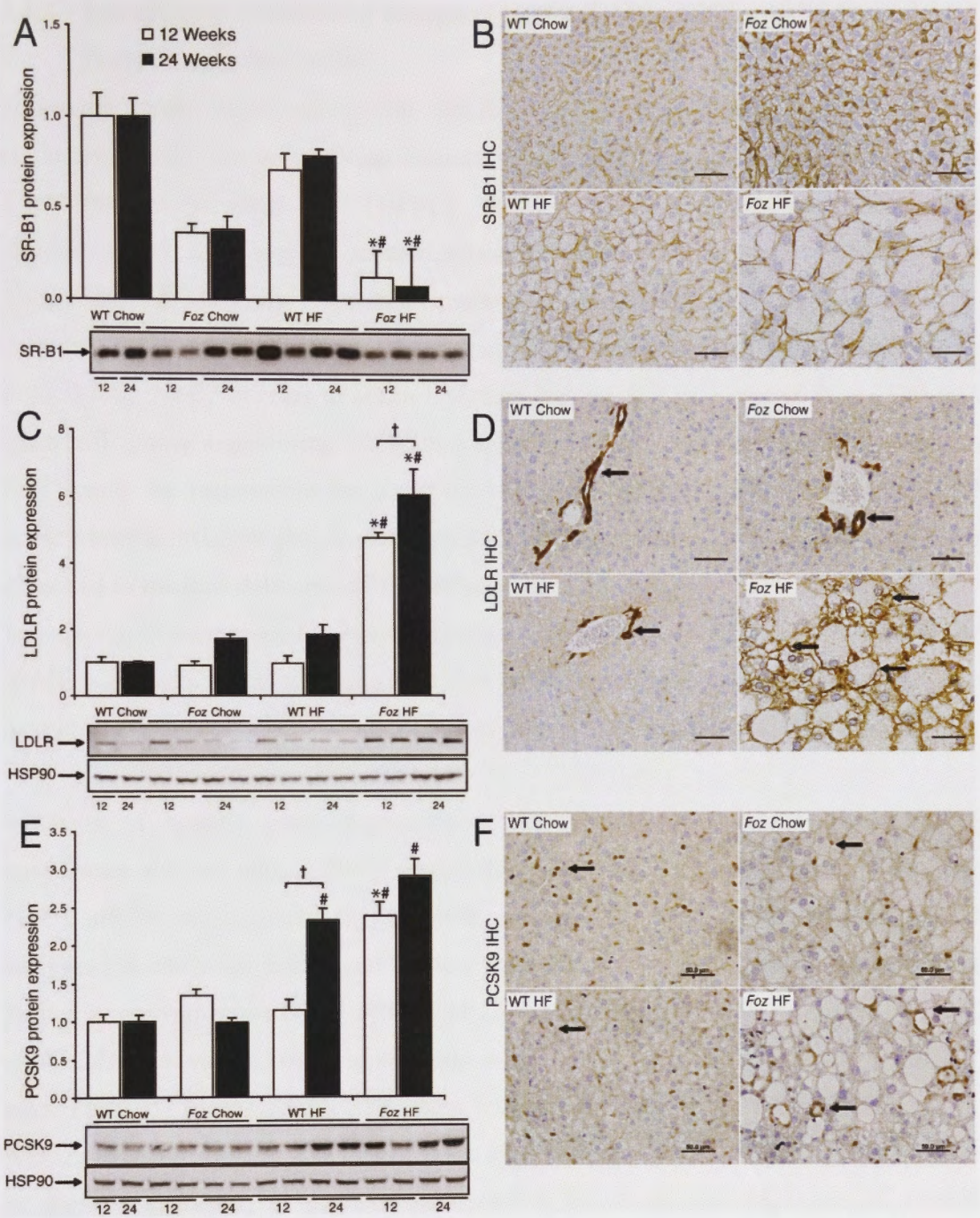

Figure 3.3 Cholesterol uptake pathways are differentially regulation in *foz/foz* mice with NASH

Whole liver homogenates from 12- (□) and 24- (■) week mice (n=5-9/grp) were probed for (**A**) scavenger receptor-B1 (SR-B1), (**C**) LDL receptor (LDLR), and (**E**) proprotein convertase subtilisin/kexin type-9 (PCSK9) expression. Western blot quantitation was normalised to heat-shock protein 90 (HSP90) expression. The HSP90 blot is shared for both LDLR and SR-B1. Representative (**B**) SR-B1, (**D**) LDLR, and (**F**) PCSK9 IHC from 24-week liver sections. Scale bars represent 50 μm. Arrows indicate positive staining. Data are mean ± SEM. *P<0.05, vs. diet-matched control. $^{\#}P$<0.05, vs. genotype-matched control. $^{\dagger}P$<0.05, vs. genotype- and diet-matched group.

3.4.3 Intracellular cholesterol transport pathways are differentially altered in *foz/foz* mice with NASH

Following uptake of cholesterol via LDLR-dependent receptor-mediated endocytosis, cholesterol undergoes intracellular cholesterol transport via several chaperone proteins. These include Niemann Pick (NP)-C1, NPC2, metastatic lymph node 64 protein (MLN64), and steroidogenic acute regulatory protein (StAR). NPC1 is tasked with trafficking of FC from the lysosomal compartment to various subcellular compartments, including the plasma membrane (Watari *et al.* 1999) and endoplasmic reticulum (Watari *et al.* 2000). NPC2 appears to act in a similar fashion to NPC1, except it is ~100-fold more efficient at transferring FC to and from lysosomal compartments. Furthermore, NPC2 may be responsible for assisting NPC1 in trafficking FC to non-lysosomal compartments. MLN64 chaperones cholesterol from the late endosome, and it has been proposed to mediate delivery of FC to mitochondrial membranes (Charman *et al.* 2010). Mitochondrial membrane FC is subsequently pumped into the mitochondrial matrix by StAR, which acts as the rate limiting step in steroidogenesis. Likewise, StAR expression also influences rates of bile biosynthesis and export in rodents (Ren *et al.* 2004).

Analysis of hepatic gene expression of the intracellular cholesterol trafficking chaperones showed altered NPC1 expression as the only major change. Specifically, NPC1 mRNA levels increased with both genotype and diet at week 12, with values increased in chow-fed *foz/foz* and HF-fed WT mice (Figure 3.4A). However, in HF-fed *foz/foz* mice, values for NPC1 mRNA at 12 weeks were similar to chow-fed controls, while 24 week values were significantly lower than control values from HF-fed WT mice ($P<0.05$, Figure 3.4A). The other intracellular cholesterol transporters, namely NPC2, MLN64, and StAR did not change significantly (Figure 3.4B,C,D), irrespective of diet or genotype. If the observed mRNA levels are representative of protein expression, it can be assumed that intracellular cholesterol transport is largely unchanged between *foz/foz* and WT mice, irrespective of diet or genotype. However, this conclusion would require verification through analysis of protein expression (western blotting) and intracellular protein localisation. Since intracellular cholesterol transport was not a major focus of the present aims, these studies have not been performed.

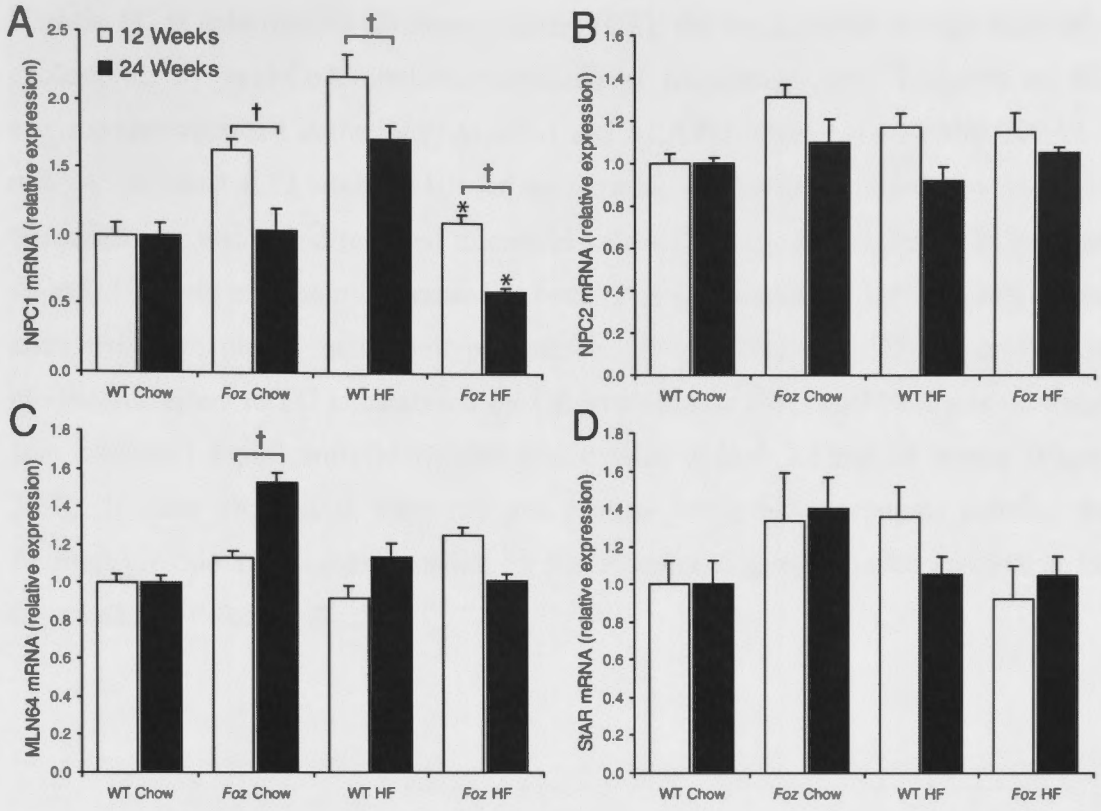

Figure 3.4 Intracellular cholesterol transporter gene expression in *foz/foz* and wildtype mice

(**A**) Niemann Pick (NP)-C1 and (**B**) NPC2, (**C**) metastatic lymph node 64 protein (MLN64), and (**D**) steroidogenic acute regulatory protein (StAR) mRNA expression at 12- (□) and 24-weeks (■).Data are mean ± SEM. **P*<0.05, vs. diet-matched control. $^{\#}P$<0.05, vs. genotype-matched control. $^{\dagger}P$<0.05, vs. genotype- and diet-matched group.

3.4.4 Cholesterol esterification and hydrolysis are up-regulated in HF-fed *foz/foz* mice with NASH, but *de novo* cholesterol biosynthesis is not

In light of the hepatic accumulation of FC in obese, diabetic *foz/foz* mice, we investigated pathways responsible for the *de novo* synthesis of cholesterol and for the dynamic relationship between CE and FC. By 12 weeks of HF feeding, HMG-CoA reductase (HMGR) activity appeared (NS) to increase in *foz/foz* mice, but by 24 weeks enzyme activity was reduced ~10-fold in both HF-fed *foz/foz* and WT mice compared to respective chow-fed controls (*P*<0.05, Figure 3.5A). These findings are consistent with reported effects of cholesterol feeding on suppression of hepatic cholesterol synthesis (Liscum *et al.* 1983). Interestingly, HMGR mRNA expression appeared to decrease in HF-fed *foz/foz* mice with NASH at 12 weeks (NS) and subsequently to increase by 24 weeks (NS) compared with dietary and genotype controls (Figure 3.5B), suggesting an inappropriate adaptive response to HF, cholesterol feeding.

Hepatic FC is esterified to cholesteryl esters (CE), the intracellular storage form of cholesterol, by acyl-CoA cholesterol:cholesteryl transferase. Two isoforms of this enzyme are expressed in the liver, ACAT-1 and ACAT-2 (Chang *et al.* 2000). ACAT-1 mRNA increased at 12 weeks in HF-fed *foz/foz* mice compared to controls, by 24 weeks transcript expression had returned to control values ($P<0.05$, Figure 3.5C). In contrast, ACAT-2 protein expression increased at both 12- and 24-weeks in HF-fed *foz/foz* mice compared with dietary and genotype controls ($P<0.05$, Figure 3.5D). Hydrolysis of cholesterol esters to FC is catalyzed by CE hydrolase (CEH), mRNA levels of which also increased significantly in HF-fed *foz/foz* mice at both 12 and 24 weeks (Figure 3.5E). If these changes in transcript and protein levels reflect enzyme activity, the findings provide a partial explanation for the observed disproportionate increase in FC observed in HF-fed *foz/foz* mice.

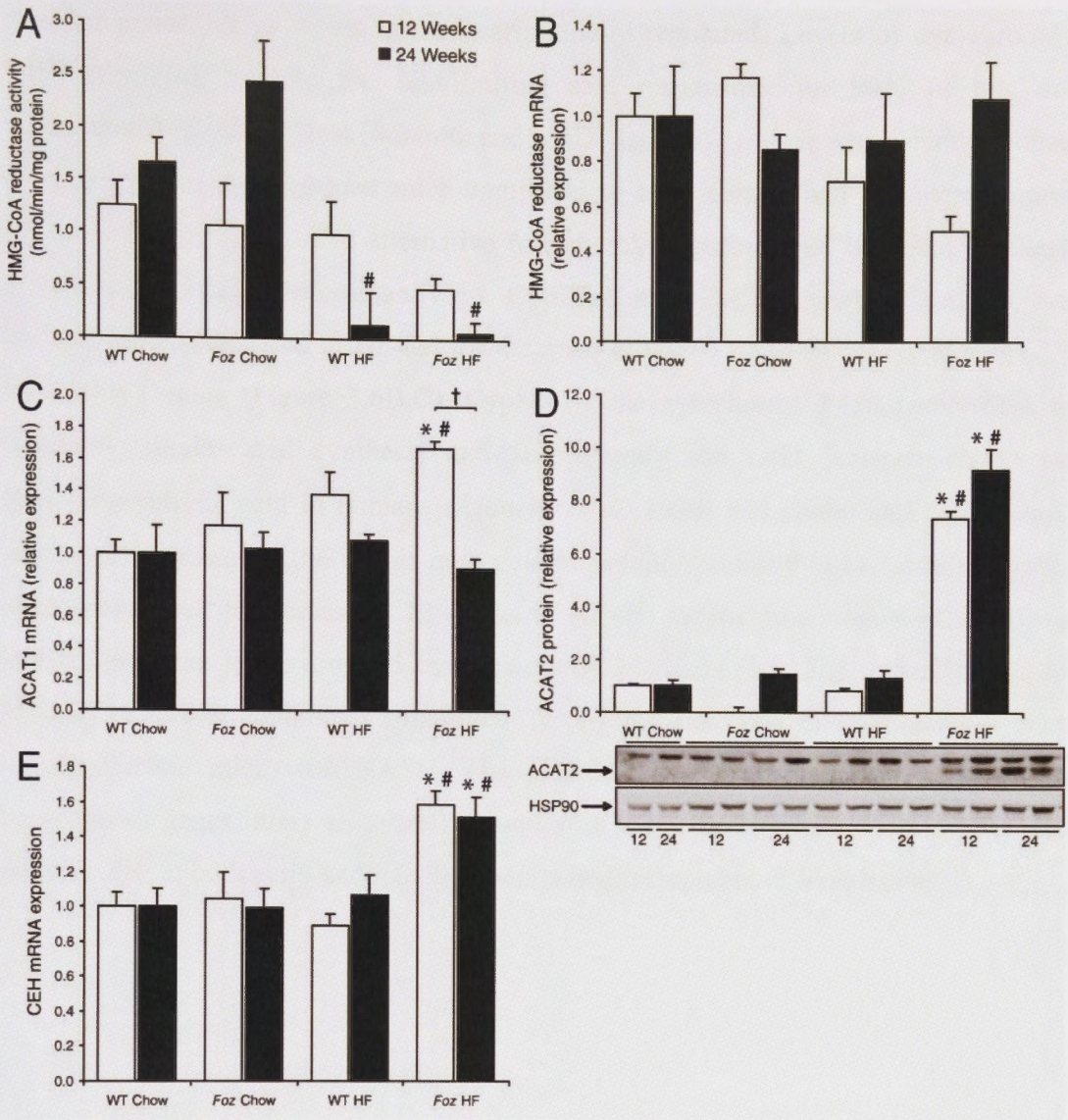

Figure 3.5 Hepatic cholesterol biosynthesis and storage pathways in *foz/foz* and wildtype mice.

(**A**) Microsomal HMG-CoA reductase activity and (**B**) mRNA expression at 12- (□) and 24-weeks (■) in *foz/foz* and WT (n=5-8/grp) mice according to diet. Hepatic (**C**) acyl-CoA:cholesterol acyltransferase (ACAT)-1 mRNA, (**D**) ACAT2 protein and (**E**) lysosomal cholesteryl ester hydrolase (CEH) mRNA expression. Western blot quantitation was normalised to heat-shock protein 90 (HSP90) expression. Data are mean ± SEM. $^{*}P<0.05$, vs. diet-matched control. $^{\#}P<0.05$, vs. genotype-matched control. $^{\dagger}P<0.05$, vs. genotype- and diet-matched group.

3.4.5 Pathways of bile acid synthesis are down-regulated in *foz/foz* mice with NASH

In mammals, the liver is the sole site of cholesterol biotransformation into bile acids, a major pathway of cholesterol catabolism (Kuipers *et al.* 1989). Pathways for bile acid synthesis were quantified using RT-PCR to detect and semiquantify transcripts for

relevant genes, all of which are transcriptionally regulated. Levels of cytochrome P450 (Cyp)7a1 mRNA, the rate-limiting step responsible for 90% of bile acid production from cholesterol (Schmitz and McDonald 1974), were significantly reduced (~3.5 fold) in HF-fed *foz/foz* mice compared to both dietary and genotype controls ($P<0.05$, Figure 3.6A). The alternative mitochondrial pathway of bile acid synthesis, which is mediated predominantly by Cyp27a1 and Cyp7b1 enzyme activity, was likewise down-regulated in HF-fed *foz/foz* mice at both 12 and 24 weeks compared to HF-fed WT mice (Figure 3.6B,C). Cyp8b1 is the cytochrome P450 responsible for regulating cholic acid synthesis and subsequently the ratio between cholic and chenodeoxycholic acid in humans (Ahlberg *et al.* 1979) and cholic and β-muricholic acid in mice (Russell 2003). This ratio determines the solubility of FC in bile. Cyp8b1 mRNA appeared to increase at 12 weeks in HF-fed *foz/foz* mice compared to HF-fed WT controls, but levels dropped significantly by 24 weeks (NS, Figure 3.6D). This fall is likely to further compound impairment of physiological bile acid formation in these obese, diabetic mice with NASH. The global decrease in expression of bile acid biosynthesis genes infers an overall reduction in bile acid biosynthesis in *foz/foz* mice with NASH, at both early and late time points in development of liver lesions.

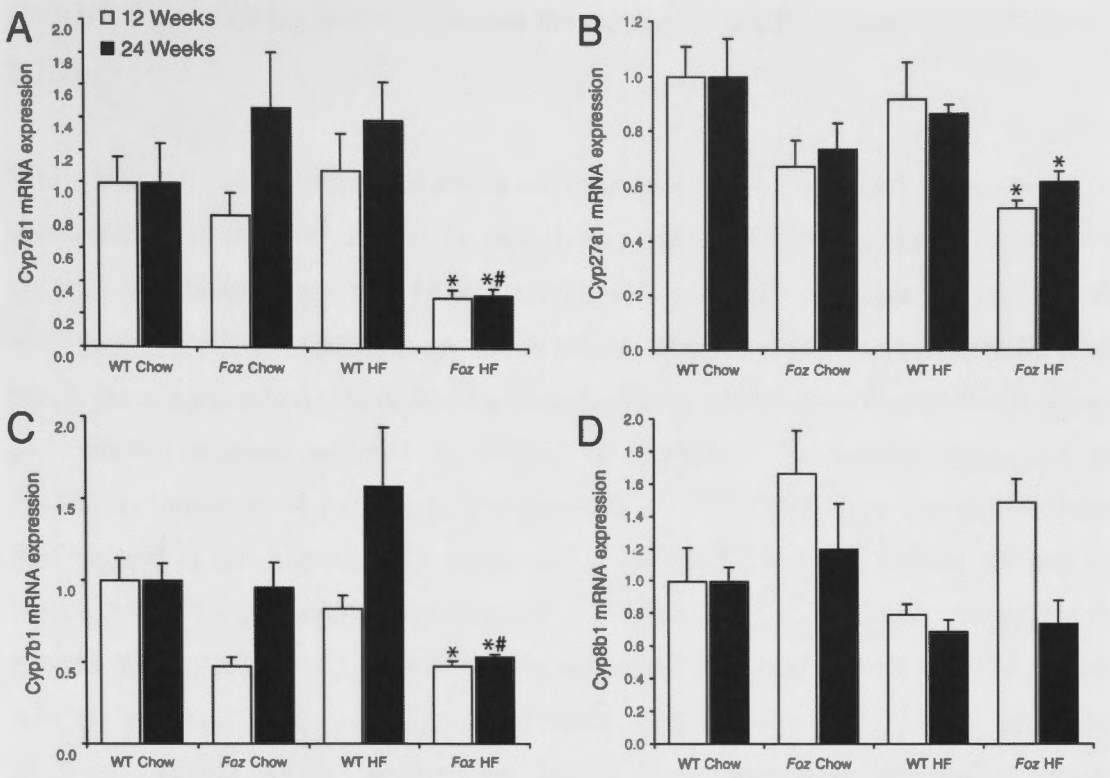

Figure 3.6 Decreased bile acid biosynthesis gene expression in HF-fed *foz/foz* versus wildtype mice

(**A**) Cytochrome P450 (Cyp)-7a1, (**B**) Cyp7b1, (**C**) Cyp27a1, and (**D**) Cyp8b1 mRNA expression at 12- (□) and 24-weeks (■) in *foz/foz* and WT (n=5-8/grp) mice according to diet and genotype. Data are mean ± SEM. *P<0.05, vs. diet-matched control. $^{\#}P$<0.05, vs. genotype-matched control. $^{\dagger}P$<0.05, vs. genotype- and diet-matched group.

3.4.6 Canalicular transporters for cholesterol, bile acids and phospholipid are down-regulated in HF-fed *foz/foz* mice with NASH

In addition to biotransformation of cholesterol to bile acids, hepatocytes are responsible for the efflux of both cholesterol and bile acids across the canalicular membrane. The protein transporters responsible for this physiological function were therefore analysed. Bile acids are exported across the hepatic canalicular membrane by bile acid export protein (Bsep) and multi-drug resistance-associated protein-2 (MRP2), a canalicular multi-specific organic anion transporter (Keppler and Konig 1997). Both of these transporter proteins were significantly suppressed in *foz/foz* mice following HF feeding. Bsep protein was reduced ~54-fold (P<0.05, Figure 3.7A) compared with HF-fed WT mice. Furthermore, IHC confirmed a distinct reduction in hepatocyte canalicular Bsep staining (Figure 3.7B). Analysis of MRP2 protein expression and IHC localisation showed similar changes in HF-fed *foz/foz* mice. Thus, protein expression decreased

($P<0.05$, Figure 3.7 C), while so too did the number of MRP2-positive cells (Figure 3.7D).

While bile acid biosynthesis and efflux are important in the catabolism and removal of cholesterol from the liver, FC can be directly exported across the canalicular membrane by the ATP-binding cassette (ABC) protein-G5 and –G8 heterodimer. Multi-drug resistance protein-2 (MDR2) is an additional canalicular-bound phospholipid flippase which pumps phospholipids across the canalicular membrane; together with bile acids, phosphotidyl choline secreted by MDR2 is important for micelle formation to "solubilise" cholesterol passage in bile (Smit *et al.* 1993). Protein expression of both ABCG5 and -8 was significantly suppressed in HF-fed *foz/foz* mice at both 12- and 24 weeks. ABCG5 expression decreased in HF-fed *foz/foz* mice at 12 weeks compared with HF-fed WT mice ($P<0.05$, Figure 3.8A), with more profound reduction at 24 weeks. ABCG8 expression was even more profoundly suppressed at both 12- and 24 weeks ($P<0.005$, Figure 3.8B). Analysis of MDR2 gene expression showed a similar suppression in HF-fed *foz/foz* mice, with a ~6-fold reduction observed at both 12- and 24-weeks (Figure 3.8C). Collectively, these results suggest that biliary cholesterol efflux is impaired in *foz/foz* mice with NASH. Unfortunately, the purchased antibodies against ABCG5/8 and MDR2 were found to be unsuitable for IHC and immunofluorescent staining. As a result, validation of the canalicular localisation of these proteins in the present experiments could not be confirmed.

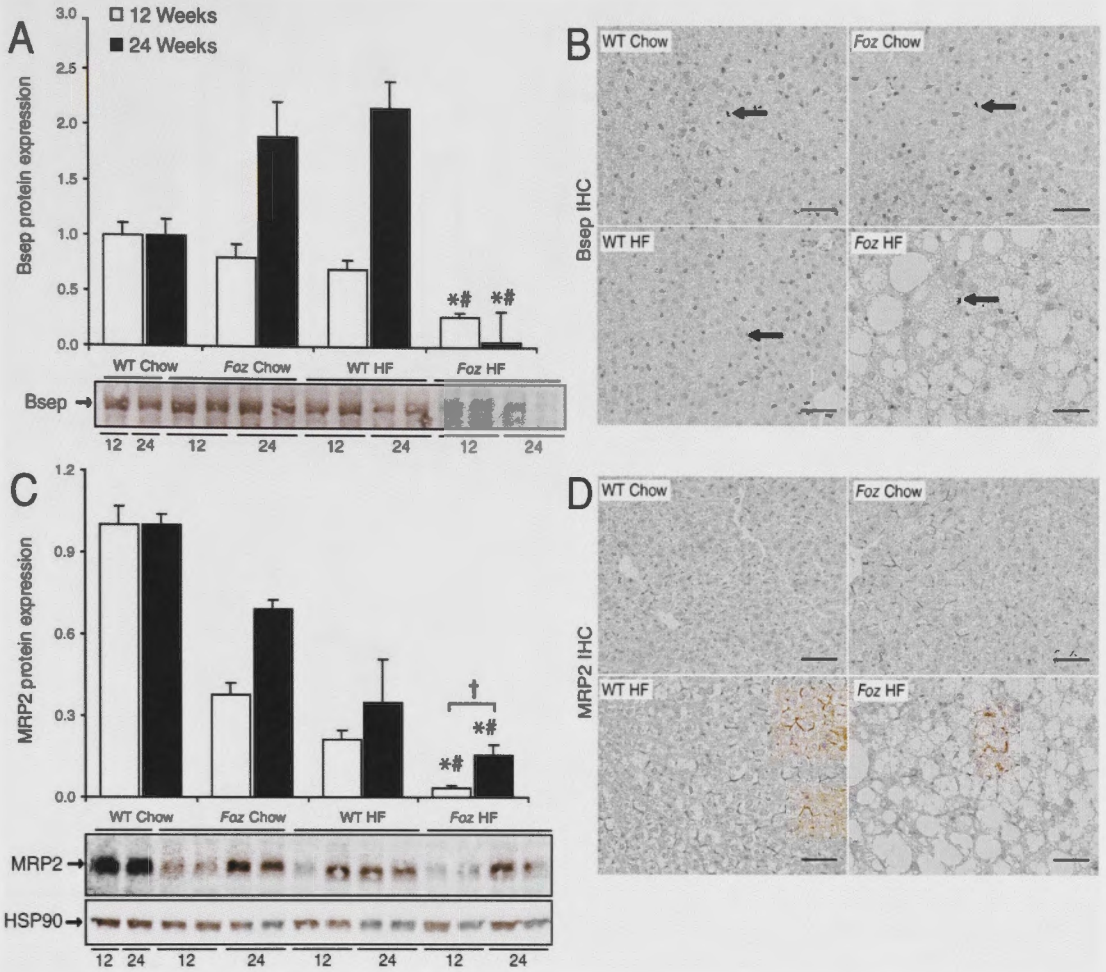

Figure 3.7 Decreased bile salt and organic ion canalicular transporter gene expression in HF-fed *foz/foz* versus wildtype mice

(**A**) Bile salt exporter protein (Bsep) and (**C**) multi-drug resistance-associated protein-2 (MRP2) expression at 12- (□) and 24-weeks (■) in chow and HF-fed WT and *foz/foz* mice. (**B**) Bsep and (**D**) MRP2 IHC localisation in 24-week liver sections. Western blot quantitation was normalised to heat-shock protein 90 (HSP90) expression (not shown in panel A for clarity, but similar to panel C). Scale bars represent 50 μm. Arrows indicate positive staining. Data are mean ± SEM. $^{*}P<0.05$, vs. diet-matched control. $^{\#}P<0.05$, vs. genotype-matched control. $^{\dagger}P<0.05$, vs. genotype- and dietary-matched group.

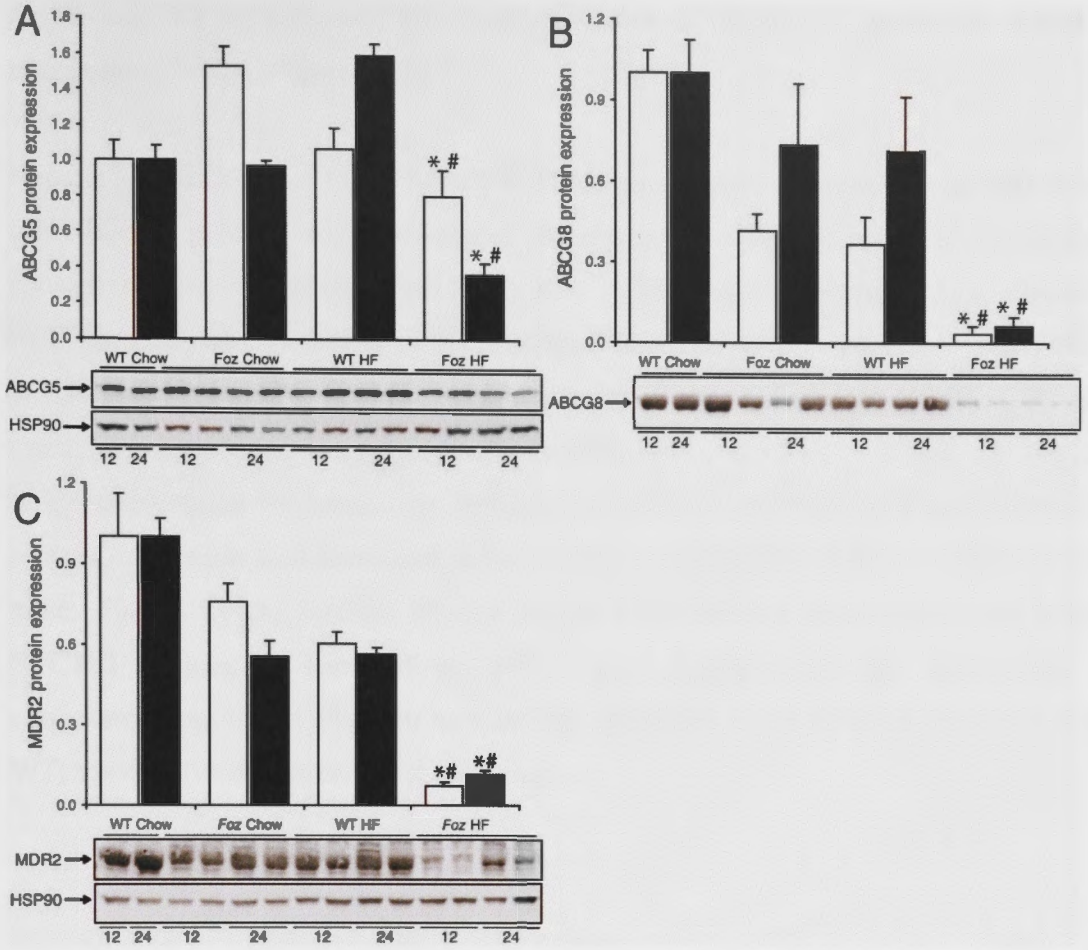

Figure 3.8 Decreased cholesterol export and phospholipid canalicular transporter gene expression in HF-fed *foz/foz* versus wildtype mice

(**A**) ATP-binding cassette protein-G5 (ABCG5), (**B**) –G8 (ABCG8), and (**C**) multi-drug resistance protein-2 (MDR2) protein expression at 12- (□) and 24-weeks (■). Western blot quantitation was normalised to heat-shock protein 90 (HSP90) expression. The ABCG8 HSP90 panel is shown in panel A (membranes were cut and probed for ABCG5/8 and HSP90 simultaneously). Scale bars represent 50 μm. Data are mean ± SEM. $^{*}P<0.05$, vs. diet-matched control. $^{\#}P<0.05$, vs. genotype-matched control. $^{\dagger}P<0.05$, vs. genotype- and dietary-matched group.

3.4.7 Reverse cholesterol transport and reclamation in *foz/foz* mice

One of the principle functions of the liver is to take up peripheral cholesterol deposits, via HDL collection colloids. These transport cholesterol back to the liver, where it is taken up via SR-B1, and ultimately excreted either directly via ABCG5/8, or indirectly in the form of bile acids. This process is referred to as reverse cholesterol transport (RCT). HDL assembly is mediated by ABCA1. Hepatic ABCA1 protein was unchanged in HF-fed *foz/foz* mice at 12-weeks (Figure 3.9A). By 24-weeks, however, both HF-fed

foz/foz and WT mice showed increased expression of this plasma membrane bound transporter ($P<0.05$, Figure 3.9B).

Hepatic Niemann Pick C1-like 1 (NPC1L1) protein, serves to reclaim excess cholesterol from bile, a process which decreases the energy expenditure required for hepatic cholesterol biosynthesis (Jia *et al.* 2011). NPC1L1 shares 42% amino acid identity with NPC1 protein, and was subsequently assigned the name NPC1L1 (Davies *et al.* 2000). When intracellular cholesterol levels decrease, NPC1L1 protein localises to the canalicular membrane. In the process, it can contribute, along with HMGR and LDLR, to increase cellular FC levels (Yu 2008). Compared with chow-fed WT mice, NPC1L1 protein expression was decreased in *foz/foz* mice, irrespective of diet ($P<0.05$ vs. WT mice, Figure 3.9C). Further, HF-fed *foz/foz* mice showed little canalicular bound NPC1L1 protein, as assessed by IHC (Figure 3.9D). Thus, the reclamation of cholesterol from bile is likely to be relatively decreased in *foz/foz* mice compared with WT, irrespective of diet and liver pathology.

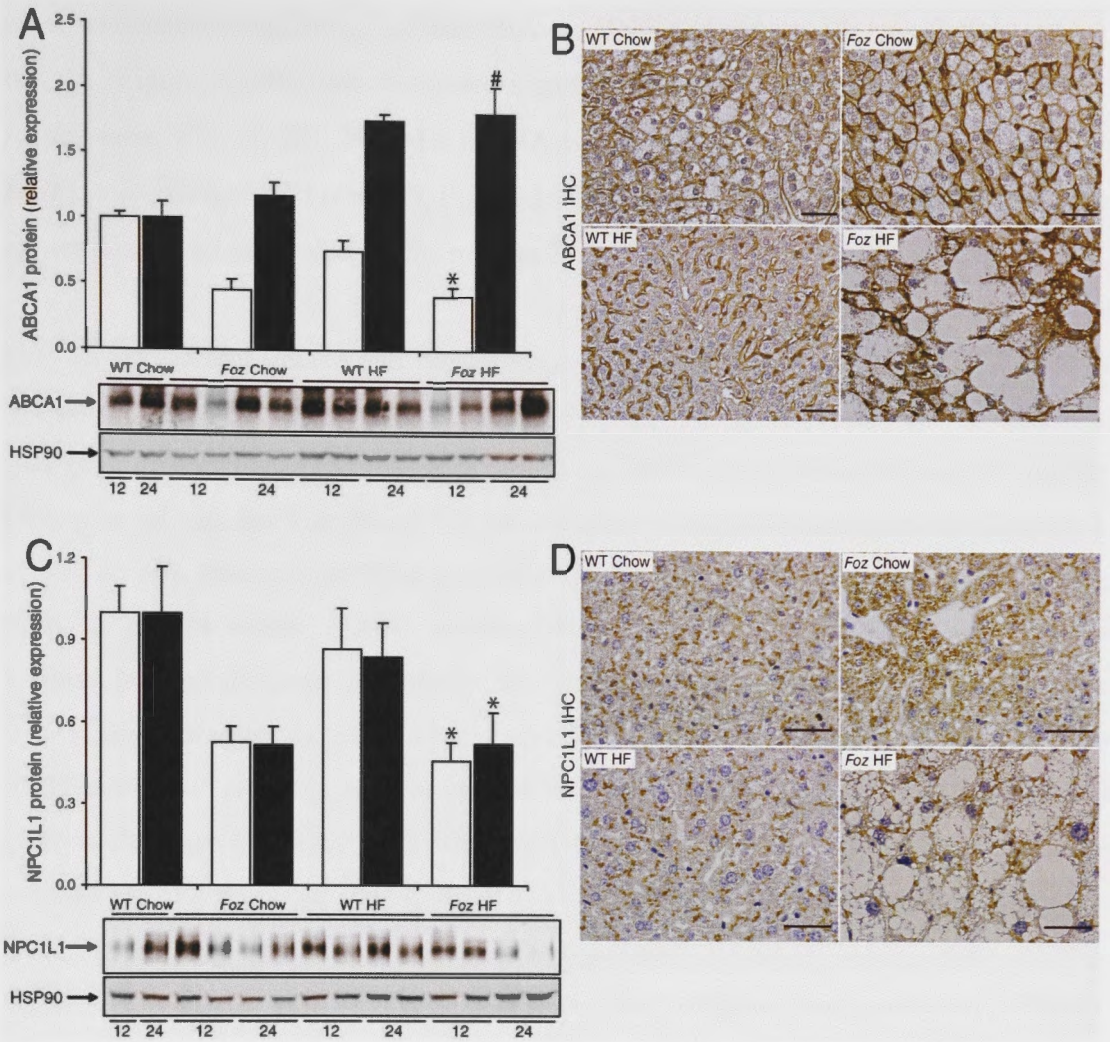

Figure 3.9 ATP-binding cassette protein-A1 and Niemann Pick-C1 like-1 proteins are differentially expressed in HF-fed *foz/foz* versus wildtype mice

(**A**) ATP-binding cassette protein-A1 (ABCA1) and (**C**) Niemann Pick C1-like 1 (NPC1L1) protein expression at 12- (□) and 24-weeks (■) in WT and *foz/foz* mice. IHC localisation of (**C**) ABCA1 and (**D**) NPC1L1 in 24-week liver sections. Western blot quantitation was normalised to heat-shock protein 90 (HSP90) expression. Scale bars represent 50 μm (panel B) and 200 μm (panel D). Data are mean ± SEM. *$P<0.05$, vs. diet-matched control. $^{\#}P<0.05$, vs. genotype-matched control. $^{\dagger}P<0.05$, vs. genotype and dietary-matched group.

3.4.8 Expression of nuclear regulators of cholesterol and bile acid homeostasis is perturbed in HF-fed *foz/foz* mice with NASH

Nuclear receptors involved in regulation of hepatic cholesterol homeostasis include, amongst others, hepatocyte nuclear factors (HNF), sterol-regulatory element binding protein-2 (SREBP-2), liver receptor homolog-1 (LRH-1), liver X receptors (LXR)-α and -β, farnesoid-X receptor (FXR), small heterodimeric partner (Shp) and retinoid X-receptor (RXR). Several HNFs are responsible for controlling the expression of several

other cholesterol-regulating nuclear factors. HNF-4α protein (Figure 3.10A) and mRNA (Figure 3.10B) both decreased significantly ($P<0.05$) by 24 weeks in diabetic *foz/foz* mice with NASH. HNF-1α mRNA was also found to decrease significantly in *foz/foz* mice with NASH ($P<0.05$, Figure 3.10C), but the trend for HNF-3β mRNA gene expression to fall in HF-fed *foz/foz* mice at 24 weeks was not significant (Figure 3.10D).

Hepatic cholesterol uptake and biosynthesis is largely controlled by SREBP-2, which transcriptionally upregulates both LDLR and HMGR gene expression. In addition, SREBP-2 also regulates PCSK9, an endogenous inhibitor of LDLR-mediated FC uptake (Jeong *et al.* 2008). The SREBP-2 activation pathway was discussed in Chapter 1 (Introduction). Nuclear SREBP-2 protein expression increased in HF-fed *foz/foz* mice at both 12- and 24 weeks ($P<0.05$, Figure 3.11A). Interestingly, SREBP-2 was found to localise in predominantly macrosteatotic regions in *foz/foz* mice with NASH (Figure 3.11B), compared to its acinar zone 1 and 2 distribution in HF-fed WT mice (Figure 3.11B). SREBP cleavage activating protein (SCAP) mRNA (Figure 3.11E) appeared (NS) to decrease in *foz/foz* mice with NASH, which could be a response to increased hepatic FC (Eberle *et al.* 2004; Radhakrishnan *et al.* 2008). Insulin-induced gene 1 (Insig-1) mRNA, was increased in *foz/foz* mice with NASH ($P<0.05$, Figure 3.11D), which is consistent with the hyperinsulinemic state of these insulin-resistant, diabetic mice.

LRH-1, the principle regulator of SR-B1, Cyp7a1, Cyp8b1, ABCG5 and -8, MRP2 and Bsep, all strongly down-regulated in obese, diabetic *foz/foz* mice with NASH (Figures 3.3A, 3.6, 3.7, and 3.8), increased significantly ($P<0.05$) in HF-fed WT mice compared with chow-fed WT mice. Conversely, in HF-fed *foz/foz* mice there was no up-regulation of this nuclear receptor (Figure 3.12A), consistent with failure of LRH-1 to maintain appropriate expression of SR-B1, Cyp7a, Cyp8b1, ABCG5, -8, MRP2 and Bsep. The three isomeric forms of LRH-1 detected (Figure 3.12A) correspond to the native and phosphorylated forms of LRH-1 (Lee *et al.* 2006). The mRNA expression profile (Figure 3.12B) matched nuclear protein levels.

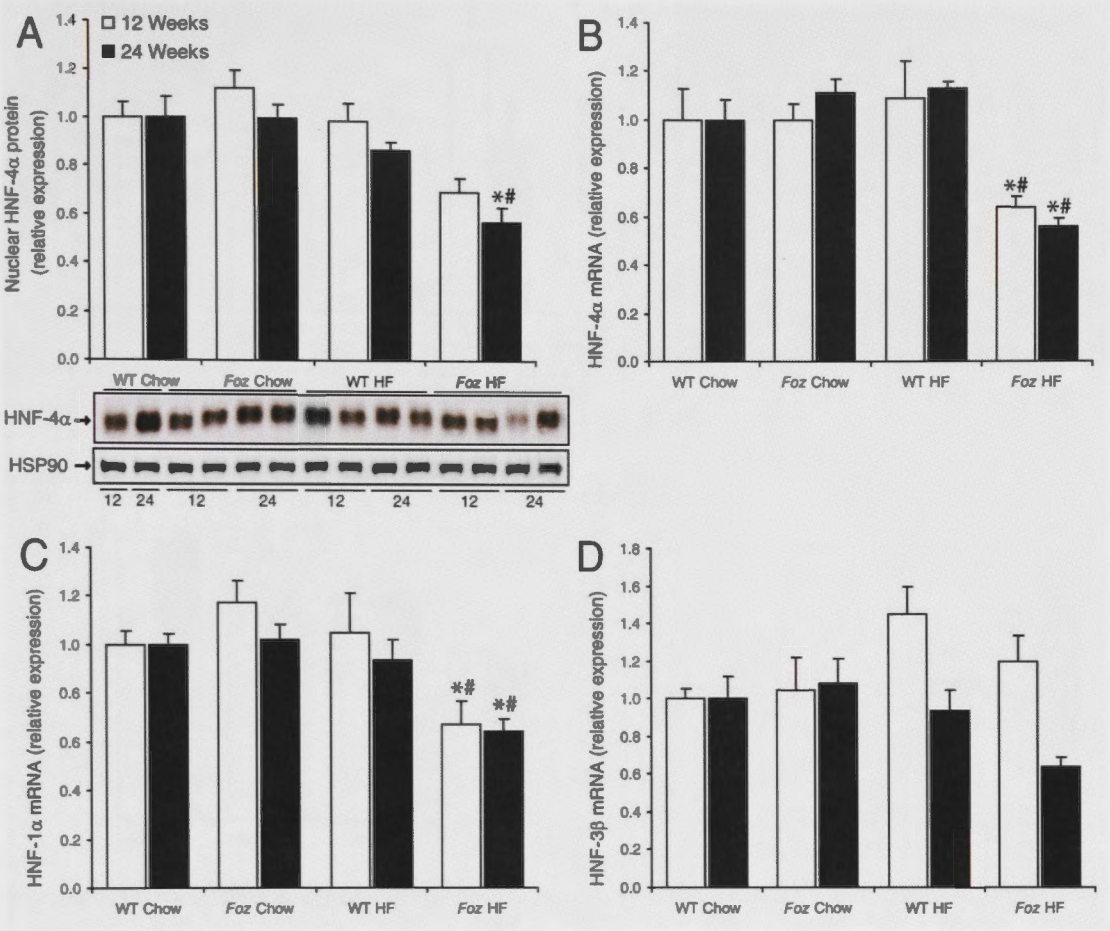

Figure 3.10 Hepatocyte nuclear factor expression is decreased in HF-fed *foz/foz* versus wildtype mice

(**A**) Nuclear hepatocyte nuclear factor (HNF)-4α protein, and (**B**) HNF-4α mRNA, (**C**) HNF-1α, and (**D**) HNF-3β mRNA expression at 12- (□) and 24-weeks (■) in WT and *foz/foz* mice. Western blot quantitation was normalised to nuclear heat-shock protein 90 (HSP90) expression (panel A). Data are mean ± SEM. **P*<0.05, vs. diet-matched control. #*P*<0.05, vs. genotype-matched control.

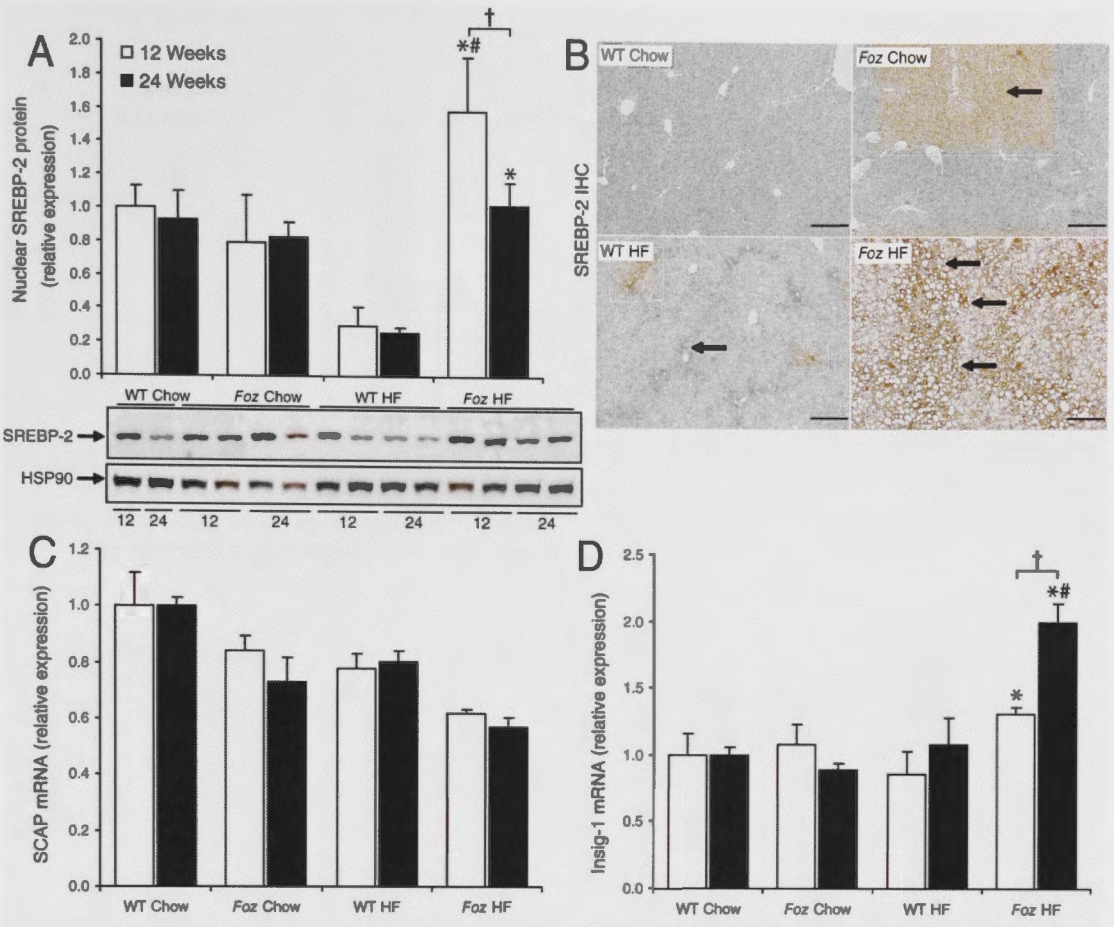

Figure 3.11 SREBP-2 pathway gene expression in HF-fed *foz/foz* versus wildtype mice

(**A**) Nuclear sterol response element binding protein (SREBP)-2 protein expression at 12- (□) and 24-weeks (■) in WT and *foz/foz* mice. (**B**) SREBP-2 protein IHC demonstrating localisation to macrosteatotic regions in 24-week liver sections of HF-fed *foz/foz* mice. (**C**) SREBP cleavage activating protein (SCAP) mRNA, and (**D**) insulin-induced gene 1 (Insig-1) mRNA gene expression are differentially regulated in HF-fed *foz/foz* mice. Western blot quantitation was normalised to nuclear heat-shock protein 90 (HSP90) expression (panel A). Scale bars represent 50 μm. Arrows represent SREBP-2 positive stained regions (Note: colocalisation of SREBP-2 to macrosteatotic regions in HF-fed *foz/foz* mice). Data are mean ± SEM. $^{*}P<0.05$, vs. diet-matched control. $^{\#}P<0.05$, vs. genotype-matched control. $^{\dagger}P<0.05$, vs. genotype- and dietary-matched group.

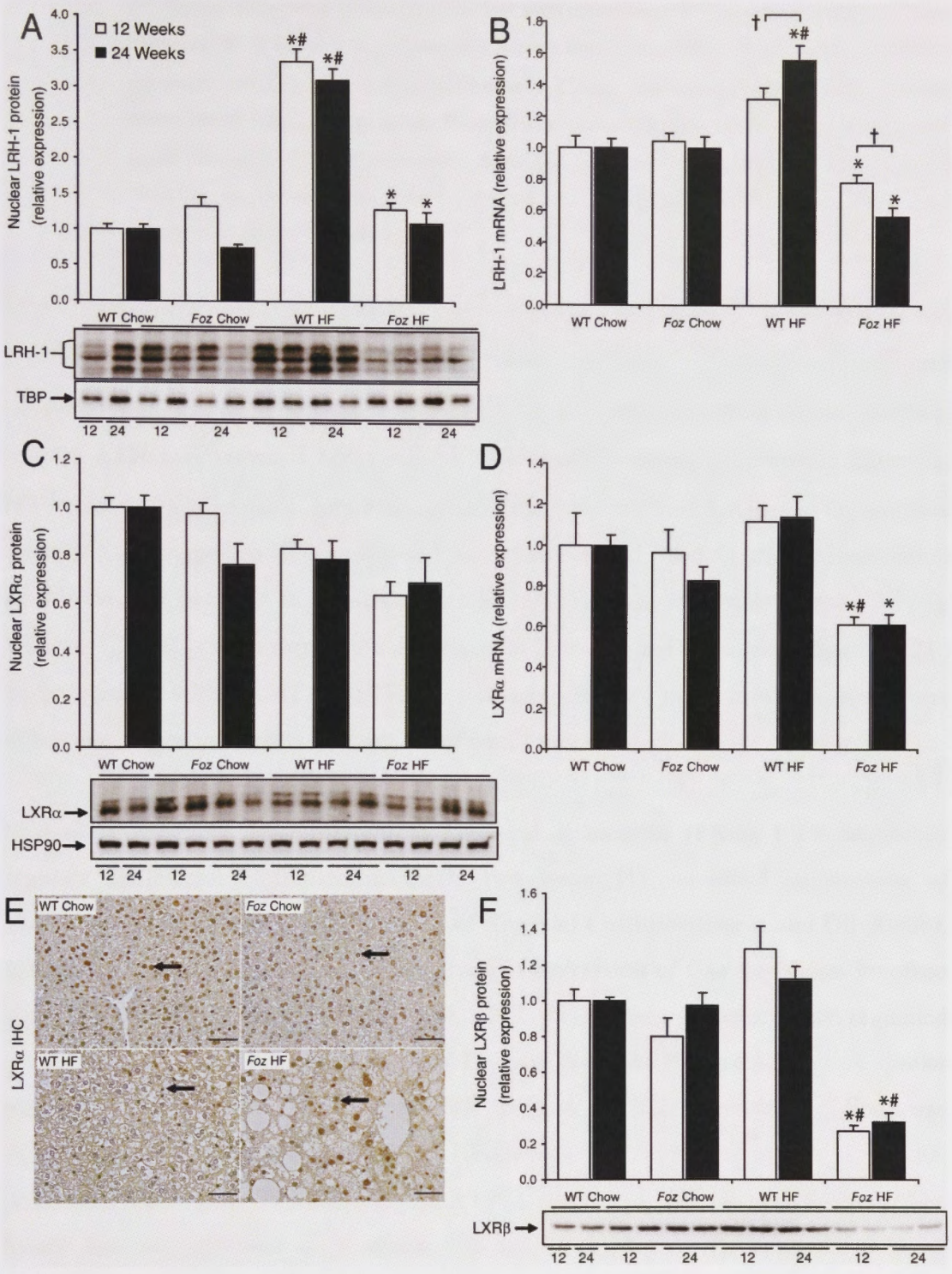

Figure 3.12 Analysis of cholesterol biotransformation and excretion promoter pathways in HF-fed *foz/foz* versus wildtype mice

Legend for Figure 3.12.

(**A**) Nuclear liver receptor homolog (LRH)-1 protein and (**B**) mRNA expression at 12- (□) and 24-weeks (■) in WT and *foz/foz* mice. (**C**) Nuclear liver X-receptor (LXR)-α protein, (**D**) mRNA expression, and (**E**) IHC localisation in mice at 12- and 24-weeks. (**F**) Nuclear LXRβ protein expression at identical time points. Western blot quantitation was normalised to nuclear heat-shock protein 90 (HSP90) expression. Scale bars represent 50 μm. Data are mean ± SEM. $^{*}P<0.05$, vs. diet-matched control. $^{\#}P<0.05$, vs. genotype-matched control. $^{\dagger}P<0.05$, vs. genotype- and dietary-matched group.

LRH-1 cooperates with regulation of Cyp7a1, Cyp8b1, ABCG-5 and -8 expression, and LXR-β may function in a similar manner (Quinet *et al.* 2006). There were no significant changes in nuclear LXR-α protein expression for any dietary group at 12- or 24 weeks (Figure 3.12C). However, LXR-α mRNA expression decreased significantly following HF-feeding in *foz/foz* mice. Interestingly, nuclear localisation of LXR-α in hepatocytes remained unchanged in HF-fed *foz/foz* mice. However, HF-feeding shifted localisation of this nuclear receptor to non-parenchymal cell nuclei in WT mice (Figure 3.12E). Nuclear LXR-β protein expression decreased at both 12- and 24 weeks (Figure 3.12F) in *foz/foz* mice with NASH ($P<0.05$), but not in HF-fed WT mice, in which levels were either unchanged or slightly (but not significantly) elevated.

Bile acids stimulate the formation of farnesoid X receptor (FXR). FXR negatively regulate cholesterol biotransformation in two ways: (1) via direct suppression of Cyp7a1, and (2) indirectly by activation of Shp (del Castillo-Olivares and Gil 2000b). Consistent with the impairment we observed in expression of four key genes involved with bile acid biosynthesis (Figure 3.6), FXR protein was likewise down-regulated ($P<0.05$) in HF-fed *foz/foz* mice at both 12- and 24-weeks (Figure 3.13A). A similar pattern was observed for FXR mRNA (Figure 3.13B). Conversely, Shp was significantly increased ($P<0.001$) by HF-feeding in *foz/foz* mice at 12 weeks, profoundly more so at 24 weeks (Figure 3.13C), whereas in WT mice induction of Shp by HF diet only occurred at 24 weeks. Shp mRNA displayed what appeared to be an inverse pattern of expression, with mRNA seemingly less (NS) in HF-fed *foz/foz* mice (Figure 3.13D).

Expression levels of retinoid X receptor (RXR), an obligate heterodimer required for functional activity of LXR-α/β, FXR, PXR and other nuclear transcriptional regulators,

were assessed at protein and mRNA levels. Protein expression decreased in *foz/foz* mice ($P<0.05$), irrespective of diet (Figure 3.14A). While there was not a significant change in RXR mRNA in HF-fed WT mice, decreased expression was observed in HF-fed *foz/foz* mice (Figure 3.14B). Pregnane X-receptor (PXR) is also partially involved in cholesterol homeostasis, with PXR activation found to influence rates of hypercholesterolemia and atherosclerosis (Zhou *et al.* 2009). PXR mRNA levels were not significantly different between groups (Figure 3.14C), suggesting that this pathways is not important in the development of hypercholesterolemia in *foz/foz* mice.

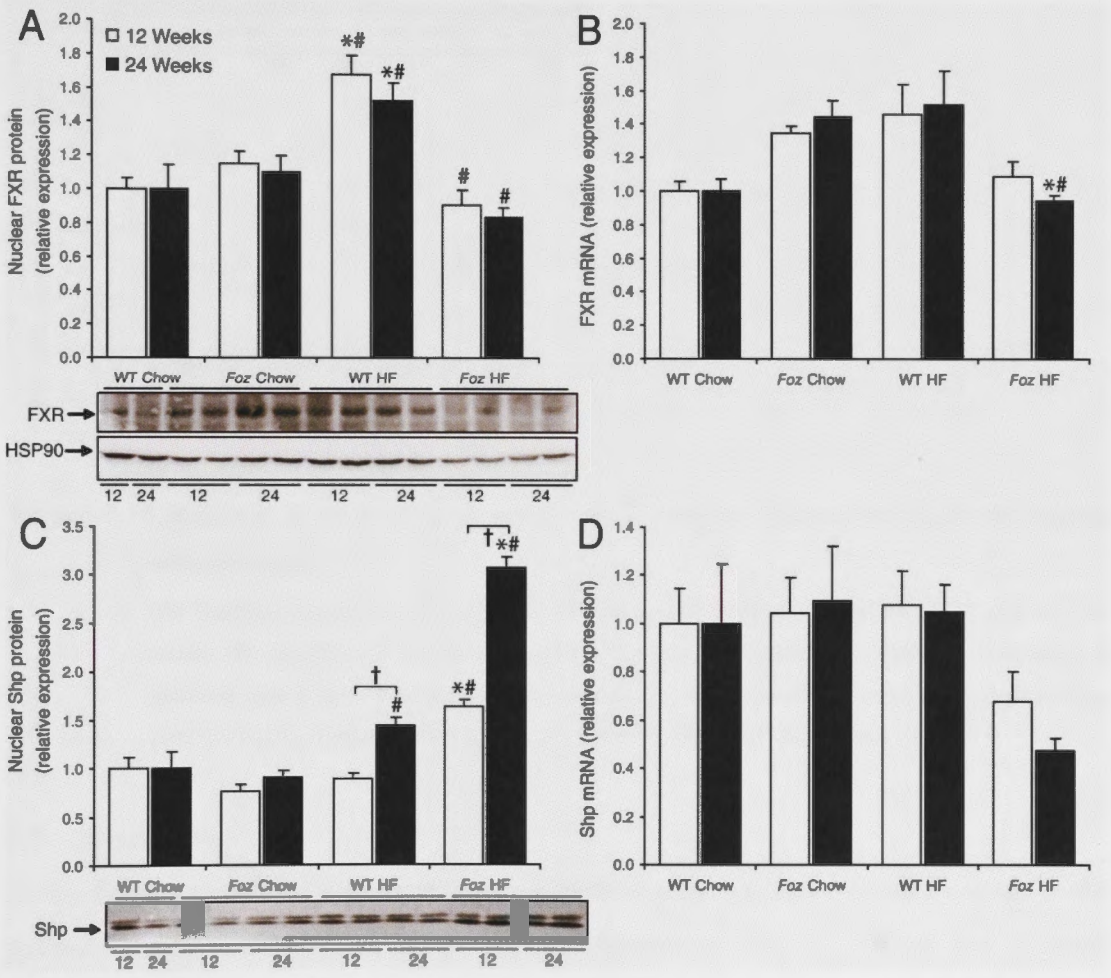

Figure 3.13 FXR and Shp are differentially expressed in HF-fed *foz/foz* versus wildtype mice.

(**A**) Nuclear farnesoid X-receptor (FXR) protein and (**B**) mRNA expression at 12- (□) and 24-weeks (■) in WT and *foz/foz* mice. (**C**) Nuclear small heterodimer partner (Shp) protein and (**D**) mRNA expression at identical time points. Western blot quantitation was normalised to nuclear heat-shock protein 90 (HSP90) expression (shown in panel A). Data are mean ± SEM. *$P<0.05$, vs. diet-matched control. $^{\#}P<0.05$, vs. genotype-matched control. $^{\dagger}P<0.05$, vs. time-matched control.

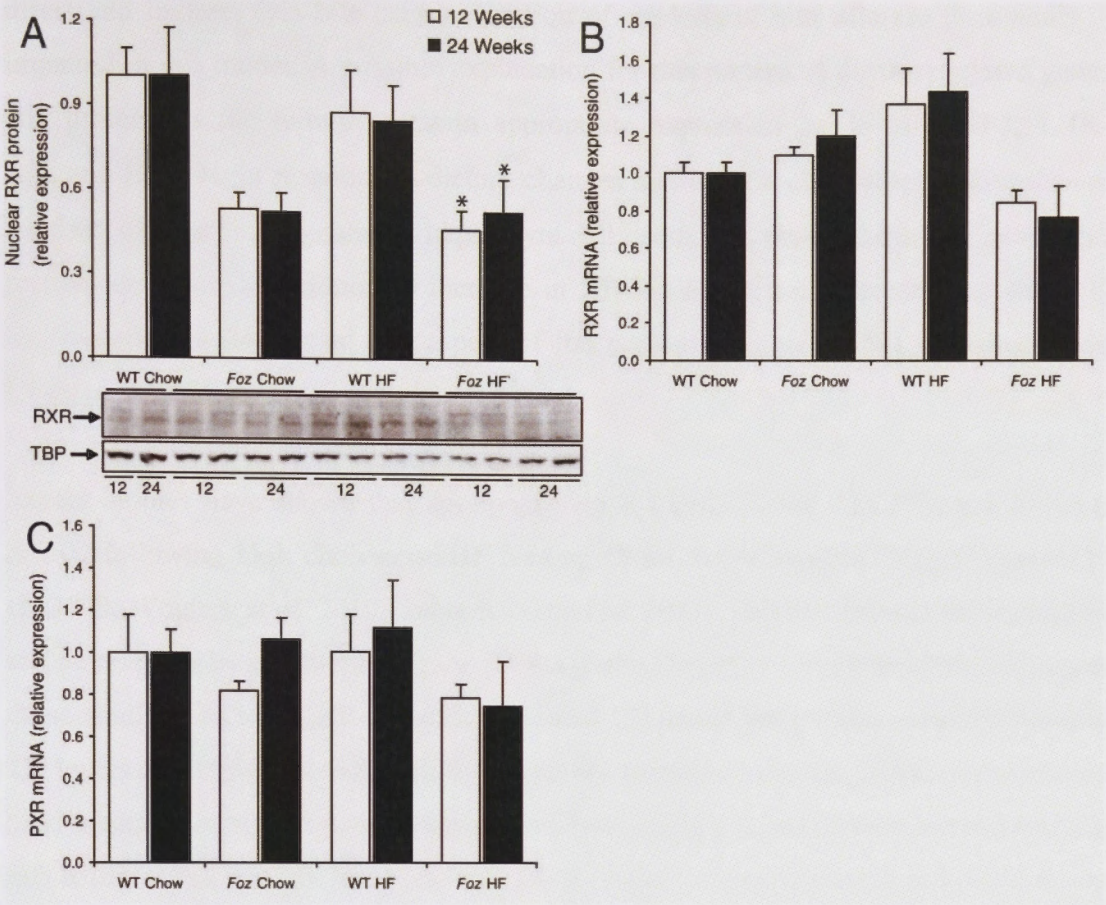

Figure 3.14 Retinoid X-receptor and pregnane X receptor expression in *foz/foz* versus wildtype mice.

(**A**) Nuclear retinoid X-receptor (RXR) protein and (**B**) mRNA expression at 12- (□) and 24-weeks (■) in WT and *foz/foz* mice. (**C**) Pregnane X receptor (PXR) mRNA expression at identical time points. Western blot quantitation was normalised to nuclear TATA-box binding protein (TBP) expression. Data are mean ± SEM. **P*<0.05, vs. diet-matched control.

3.5 Discussion

In the first part of these studies, it was demonstrated that hepatic FC accumulates in the *foz/foz* dietary and genetic model of obesity-related NASH. Given the putative importance of hepatic free cholesterol in NASH pathogenesis, as explored in later Chapters, several approaches were used here to resolve how this cholesterol accumulation might be related to known pathways that regulate cholesterol homeostasis. First it was shown that, while hepatic cholesterol biosynthesis is suppressed (or normal) during pathogenesis of diabetes and hypercholesterolemia in these mice, expression of the hepatic cholesterol uptake transporter, LDLR, is increased. Further, LDLR becomes over-expressed on hepatocytes as well as vascular endothelium. Importantly, the pathways responsible for cholesterol biotransformation to form bile acids, and both the

direct and indirect (via bile acids) secretion of cholesterol into bile are profoundly impaired in this model. A possible explanation for this pattern of down-regulated genes and proteins is the failure to attain appropriate expression levels of LRH-1, LXR-α/β, and HNF-4α in response to dietary changes and hepatic cholesterol accumulation. Markers of liver injury, namely, hepatocyte cell death, and macrophage and neutrophil recruitment, were also found to increase in HF-fed *foz/foz* mice, correlating with FC accumulation at 24 weeks: this aspect of the pathogenesis of NASH is addressed in Chapters 5 and 6.

Recent studies have shown that apolipoprotein E $(ApoE)^{-/-}$ and $LDLR^{-/-}$ mice develop NASH following high cholesterol/HF feeding (Shiri-Sverdlov *et al.* 2006; Wouters *et al.* 2008; Wouters *et al.* 2010; Subramanian *et al.* 2011), and that hepatic inflammation can be reversed by treatment with the LXR agonist, T0901317. An interesting finding in those studies was that LXR activation reduced FC levels but simultaneously increased TG levels (steatosis), providing further evidence to support the role of FC as the critical lipid mediator of NASH pathogenesis. Mari *et al.* (2006) found that cholesterol loading rats using a choline-deficient diet was able to increase hepatic cholesterol profiles and increased hepatic sensitivity towards TNF-α and Fas ligand. Further investigation using $LDLR^{-/-}$ mice (which do not develop obesity, hyperinsulinemia, or T2D) has shown that SR-B1 and CD36-mediated uptake of *modified* (oxidized) LDL activates Kupffer cells during high-cholesterol feeding, and that such activated Kupffer cells are likely to mediate liver injury (Bieghs *et al.*). Our observation of down-regulated SR-B1 in HF-fed *foz/foz* mice makes a role for oxidized LDL (transported by this route) less likely in the present obesity and diabetes-related NASH model, although direct studies of oxidised LDL would be required to confirm this.

In human NAFLD, two limited lipidomic studies of liver biopsies have found increased hepatic cholesterol content, but data have been too restricted to establish the pathogenic basis for such cholesterol accumulation (Puri *et al.* 2007; Caballero *et al.* 2009). The multifaceted regulation of cholesterol turnover in liver includes tightly regulated control of uptake, biosynthesis and storage, biotransformation (to primary bile acids), and export pathways, particularly into bile (Figure 1.2). Circulating serum cholesterol levels are physiologically controlled by a strict balance between *forward-cholesterol transport* (FCT), involving active transport of LDL cholesterol to peripheral tissues, and reverse

cholesterol transport (RCT), which involves HDL-associated collection of peripheral cholesterol for removal/return transport back to the liver. RCT is facilitated by ABCA1-associated assembly of HDL colloids (Oram and Vaughan 2000). Increased hepatic ABCA1 expression in HF-fed *foz/foz* mice (Figure 3.9A), together with reduced expression of SR-B1, the HDL uptake transporter, may contribute to impaired RCT function in the obese, diabetic and hypercholesterolemic mice with NASH. In particular, these changes are likely to account for the observed increases in HDL cholesterol in these mice (Figure 3.1B). It is important to note that SR-B1 regulation is largely controlled by LRH-1 (Schoonjans *et al.* 2002; Lee *et al.* 2006), the significance of which will be discussed later. With impaired RCT in obese, diabetic *foz/foz* mice accelerated atherogenesis would be expected, and further studies to investigate this aspect are in train.

Uptake of *FCT cholesterol* is also subject to regulation by PCSK9, which binds LDLR and, following receptor-mediated endocytosis, induces its lysosomal degradation (Abifadel *et al.* 2003). Insulin upregulates PCSK9 expression (Costet *et al.* 2006). High levels of circulating insulin are observed in our diabetic *foz/foz* mice with NASH (Larter *et al.* 2009), which may explain the observed increases in PCSK9 expression in these mice. However, an important detail in the present studies is that PCSK9 localised only to hepatic non-parenchymal cells; little to no staining of hepatocytes was observed (Figure 3.3F). These findings are consistent with the proposal that PCSK9, despite its up-regulation by insulin in livers with NASH, fails to inhibit the function of LDLR expressed on hepatocytes in response to increased nuclear SREBP-2 levels (Figures 3.2, 3.11). Loss-of-function PCSK9 mutations provide protection against atherosclerosis by increasing hepatic LDLR expression (Cohen *et al.* 2005; Zhang *et al.* 2007; Burnett and Hooper 2008). However, in the *foz/foz* model, despite increased LDLR expression, hepatic and serum cholesterol levels are increased. Furthermore, in earlier studies conducted by the host lab, an alternative cholesterol and fatty acid uptake pathway, CD36, was also upregulated in a dietary and temporal pattern consistent with this pathway also contributing to CE uptake (Larter *et al.* 2009). Further studies are required to establish the extent to which this less well-studied transporter also contributes to hepatic cholesterol accumulation in the presence of hyperinsulinemia.

While HF-fed *foz/foz* and WT mice both exhibit apparently lower HMGR activity after 24 weeks of dietary intake, chow-fed *foz/foz* mice appeared to show increased HMGR activity at this time. Together, these data suggest that *de novo* biosynthesis of cholesterol could contribute to NASH pathogenesis at the earlier stages, but it does not appear to be the major pathway to continued hepatic cholesterol accumulation during the later stages. Once synthesised or taken up, FC can be stored in the form of CEs, a process catalysed by ACAT1/2; ACAT2 protein increased in HF-fed *foz/foz* mice. Conversely, CEs can be hydrolysed to FC by neutral or lysosomal CEH. The increased expression of CEH transcripts (if they reflect enhanced enzyme activity) may partially explain the disproportionate increase in FC in HF-fed *foz/foz* mice by 24 weeks. Under physiological conditions, however, most hepatic cholesterol is biotransformed to bile acids. The two key pathways are Cyp7a1-dependent, which accounts for ~90% of hepatic BA production, and the mitochondrial Cyp27a1/7b1-dependent pathway, which forms the remainder. In turn, residual FC and bile acids are pumped across the canalicular membrane in energy (ATP)-dependent processes effected by a set of ABC transporters: the latter include ABCG5/8, Bsep, and MRP2 (Figure 1.2). The most profound changes in pathways of hepatic cholesterol turnover in the *foz/foz* model of NASH were suppression of the above genes and proteins that mediate biotransformation and direct or indirect biliary excretion of cholesterol. In summation, this indicates a comprehensive failure of appropriate nuclear regulatory responses to the profound accumulation of cholesterol.

As mentioned, cholesterol flux is ultimately regulated by the interplay between several sterol-responsive nuclear receptors. Reduced expression of HNF-4α and 1α, the two principle hepatocyte nuclear factors, was observed in *foz/foz* mice with NASH, and could account for the subsequent changes in SREBP-2, LXR-α/β, and LRH-1 nuclear expression, although other effectors could also be involved (as discussed later in Chapter 4). HNF-4α has been shown to interact with LRH-1, which in turn acts in concert with LXR-α/β to regulate expression of several genes involved with cholesterol homeostasis (Repa *et al.* 2002; Freeman *et al.* 2004). It is therefore plausible that altered HNF expression may have far-reaching pleiotropic effects. Interestingly, despite being under positive regulatory control by HNF-4α (Misawa *et al.* 2003), nuclear SREBP-2 expression was elevated while HNF-4α decreased in HF-fed *foz/foz* mice with NASH.

One possible mechanism responsible for this seemingly paradoxical observation will be explored in Chapter 4.

SREBP-2 is physiologically activated in response to lowered intracellular cholesterol, as are its target genes; these include LDLR and HMGR (Field *et al.* 2001b, 2001a). The increase in SREBP-2 observed in this study is consistent with the reported increases in SREBP-2 and FC in human NASH (Caballero *et al.* 2009), therefore indicating an *inappropriate* SREBP-2 response to FC accumulation during pathogenesis of NASH in both humans and the present murine model. Interestingly, parenchymal SREBP-2 expression appeared greatest in regions of hepatic macrosteatosis (Figure 3.11B). Given the reductions in SCAP mRNA, it can be assumed that an over-expression of SCAP is not responsible for the observed increases in nuclear SREBP-2. Studies have demonstrated a relationship between cell stress and SREBP-2 activation. This may constitute another possible activation pathway in *foz/foz* mice, although in related studies described in Chapter 7, it was demonstrated that ER stress markers are significantly suppressed in mice with NASH. Another highly likely explanation for up-regulation of SREBP-2 in diabetic *foz/foz* mice is hyperinsulinemia; studies to test this attractive proposal are described in Chapter 4. Studies with human monocyte-derived macrophages have shown that triglyceride but not cholesterol loading induces IL-1β secretion (Persson *et al.* 2006). Zhang *et al.* (2011) and Zhao *et al.* (2011) have both demonstrated the ability of IL-1β to induce nuclear SREBP-2 activation and subsequent LDLR expression in hepatocytes. Although IL-1β was not measured in this study, inflammatory stress may contribute to increased LDLR expression in *foz/foz* mice.

Although altered, SREBP-2 is mainly responsible for controlling cholesterol uptake and biosynthetic gene responses (the activity of the latter was found to be decreased in *foz/foz* mice with NASH); it has no regulatory control over expression of Cyps and efflux transporters. The latter functions are largely regulated by LRH-1 and LXR-α/β nuclear factors. While LXR-α and -β share a high degree of sequence homology, studies have demonstrated that they can function independently (Alberti *et al.* 2001). LXR-α deficiency lowers hepatic Cyp7a1 mRNA expression (Peet *et al.* 1998a), and LXR-α acts similarly to LRH-1 by activating ABCG5/8 (Freeman *et al.* 2004). This indicates possible co-operativity between the LXRs and LRH-1. In the present studies, no significant changes in LXR-α protein expression were observed, but HF-fed *foz/foz*

mice exhibited profoundly reduced expression of LXR-β. This could contribute to the profound impairment in expression of cholesterol biotransformation and excretion genes observed in mice with NASH.

The most interesting change in nuclear regulator expression, however, was the failure of HF-fed *foz/foz* mice to increase LRH-1 expression, as reflected by both LRH-1 mRNA and protein levels (Figures 3.12A,B). Such an increase was clearly evident in WT mice fed the HF diet at both 12- and 24 weeks. LRH-1 is a well documented transcriptional regulator of Cyp7a1, 7b1, 27a1, ABCG5/8, Bsep, MRP2, and MDR2. Failed up-regulation of this nuclear receptor would therefore result in decreased expression of Cyp7a1, 7b1, and 27a1 enzymes, each of which is transcriptionally regulated. This would result in lowered BA biosynthesis. In turn, the lower levels of hepatic BAs would decrease activation of FXR (Figure 3.13A). FXR positively regulates Bsep expression, so that decreased FXR activation would compound the reductions in LRH-1-dependent Bsep and MRP2 expression as observed in diabetic *foz/foz* mice with NASH (Figure 3.7A,B). Candidate effectors responsible for down-regulating LRH-1 are discussed in the next Chapter.

FXR is able to directly down-regulate Cyp7a1 expression, but it also activates Shp, an LRH-1 inhibitor (Li *et al.* 2005; Shibata *et al.* 2007), which therefore acts indirectly to suppress expression of genes involved with BA synthesis and secretion. Interestingly, the present studies showed up-regulation of Shp by both diet and genotype (12 and 24 weeks in HF-fed *foz/foz* mice). However, such Shp up-regulation was apparently independent of FXR, which was not increased in HF-fed *foz/foz* mice compared to HF-fed WT mice (the latter showed appropriate FXR activation). The activation of Shp during NASH pathogenesis has not been documented (to the best of the authors knowledge). It could pose a novel pathway of LRH-1 inhibition, but further studies are required to establish whether this is indeed the case, and how a Shp increase that is apparently independent of FXR could be mediated in the context of metabolic syndrome and NASH.

Foz/foz mice possess an 11 base-pair deletion in *Alms1*. This results in what is likely to be a loss-of-function, truncated Alms1 protein. It seems unlikely that this mutation has any direct effects on hepatic lipid homeostasis. As previously mentioned (Section

1.10.3), Alms1 protein localizes to the basal body of primary cilia, including those on hypothalamic neurons that are critical for appetite regulation. However, hepatocytes are one of few cell types that do not bear a primary cilium, so it is hard to envisage how an *Alms1* mutation could be directly involved in cholesterol turnover and NASH pathogenesis. In Chapter 6, it will be demonstrated that changes in cholesterol homeostasis observed in these studies correlate strongly with increases in circulating insulin levels, and this increase is not observed in chow-fed *foz/foz* mice with SS. To further support the argument that the *Alms1* mutation is irrelevant to cholesterol homeostasis, chow-fed *foz/foz* mice show similar hepatic cholesterol homeostasis compared with genotype controls (Figures 3.1 and 3.3-3.11). In particular, levels of FC and CE are not altered, while uptake, biotransformation, storage, and excretion pathways did not change. In light of these findings, it seems evident that the *foz/foz* genotype alone does not play an important role in mediating cholesterol dysregulation. On the other hand, an interaction between genotype and diet is clearly evident in this study. We contend that the role of genotype (*Alms1* mutation) is likely mediated via appetite dysregulation, that facilitates rapid weight gain and hyperinsulinemia (particularly with HF diet), but that dietary composition is an additional factor in NASH pathogenesis, and will be discussed in Chapter 5.

The HF diet used in this study contains large amounts of carbohydrate (predominantly sucrose, which has a high glycemic index) (see the 0.2% cholesterol diet composition in Table 4.1). High-sucrose feeding has been shown to increase serum LDL levels in Sprague-Dawley rats (Ryu and Cha 2003), and to increase cholesterol biosynthesis directly in diabetic fatty rats (Ohta *et al.* 2007). Although HMG-CoA reductase acts as the rate-limiting step, cholesterol biosynthesis is also largely dependent upon the availability of simple acetate precursor molecules, which can be derived from sugar precursors (Leung 2004). Therefore, the high carbohydrate content of this study may contribute to the early (before 12 weeks on diet, noting that HMGR activity decreased between 12- and 24 weeks) cholesterol biosynthesis in HF fed *foz/foz* mice. Furthermore, seminal studies of cholesterol homeostasis demonstrated that cholesterol biosynthesis is proportional to caloric intake in rats (Tomkins and Chaikoff 1952). The long chain fatty acids found in the HF diet (Table 5.1), particularly saturates, are an additional source of acetate precursor, and may therefore also contribute to the formation of CE in HF-fed *foz/foz* mice during the esterification of FC.

Notwithstanding the extensive studies undertaken in this section to characterise disordered hepatic cholesterol turnover in NASH, there are some limitations that need to be acknowledged. First, cytochrome P450, ACAT and CEH enzyme activity were not assessed, and it remains possible that these (less likely with Cyps involved in BA synthesis) could differ from observed gene or protein expression levels. Secondly, rates of lipoprotein and cholesterol uptake, VLDL formation and biliary efflux of cholesterol and BAs were not measured, nor were faecal sterol content or bile composition. These elements would be required for a complete physiological picture of bodily cholesterol deposition. Not withstanding these limitations, this section of work has led to the major findings, again summarised below.

3.6 Summary of findings

1. FC as well as CE accumulates in *foz/foz* mice with NASH.
2. Hepatic, including hepatocellular, LDL cholesterol uptake pathways are upregulated; this change correlates with (and is likely due to) increased nuclear SREBP-2, and failed hepatocyte-PCSK9 regulation.
3. Cholesterol synthesis (HMGR activity) is either unchanged (early) or suppressed in HF-fed *foz/foz* mice during evolution of NASH, and cannot explain the hepatic accumulation of cholesterol in these mice with diabetes and NASH.
4. Pathways responsible for cholesterol biotransformation (Cyps 7a1, 7b1, 27a1) and canalicular export of cholesterol (ABCG5/8) and bile acids (BSEP, MRP2) are all profoundly suppressed in *foz/foz* mice; by substantially reducing cholesterol disposal, such changes are likely to exacerbate cholesterol accumulation.
5. HNF nuclear regulators and LXR-α/β are down-regulated in mice with NASH, while LRH-1 fails to increase in response to HF diet, as is observed as an adaptive response in WT mice.
6. Conversely, Shp expression is increased, but in an FXR-independent fashion.

Collectively, these data indicate a correlation between hepatic FC accumulation and liver injury in NASH, and offer at least a partial explanation for the cholesterol turnover pathways responsible for profound accumulation of FC and CE lipids in metabolic syndrome. However, the outstanding issue remains the ultimate root cause of

cholesterol dysregulation in *foz/foz* mice with NASH. Among several outstanding questions remaining, the following will be address in later Chapters:

1. What regulates the metabolic regulators?
2. Is hepatic cholesterol accumulation truly pathogenic for NASH?

In the subsequent Chapter question 1, will be addressed. Question 2 will be addressed in Chapters 5 and 6.

CHAPTER 4

Insulin upregulates hepatic SREBP-2 and de-regulates cholesterol homeostasis in primary murine hepatocytes

4.1 Introduction

In the previous Chapter, HF-fed *foz/foz* mice with NASH were demonstrated to have increased hepatocellular LDLR expression, which is likely to be a key uptake pathway for hepatic FC in obese, diabetic mice. Augmented LDLR expression was attributable to increased nuclear SREBP-2 expression at both 12- and 24 week time points. Concurrently, nuclear LRH-1 protein levels fail to increase in these mice despite profound increases in hepatic FC and CE lipid species. Failure to upregulate LRH-1, as well as decreased HNF-4α and LXR-α, results in suppression of the genes responsible for biotransformation of cholesterol to bile acids, and for canalicular efflux of both bile acids and FC out of the liver; impairment of these "disposal" processes could be expected o exacerbate the hepatic accumulation of cholesterol. As described in Section 1.4.1.1, SREBP-2 is regulated by intracellular cholesterol levels. Briefly, low intracellular cholesterol conditions result in the activation and nuclear translocation of SREBP-2, which subsequently binds an endogenous sterol regulatory element (*sre-1;* ATCACCCCAC) present within the coding genes of such SREBP-2-responsive genes as LDLR and HMGR (Osborne 1991; Pak 1996; Kotzka *et al.* 2000).

Apart from regulating genes associated with cholesterol uptake and biosynthesis, SREBP-2 has been shown to directly interact with other nuclear factors involved in cholesterol homeostasis. Importantly for the context of this research, Kanayama *et al.* (2007) identified a reciprocal inhibitory relationship between SREBP-2 and LRH-1, in which these two nuclear factors act as transcriptional inhibitors of each other. Thus, increased SREBP-2 expression negatively regulated LRH-1 transcription, with simultaneous reductions in *Shp* and *Cyp7a1* gene transcription. Conversely, LRH-1 over expression, using recombinant plasmid transfections in HepG2 and human hepatoma Huh7 cell lines, suppressed SREBP-2, and subsequently LDLR and HMGR, in dose-dependent fashion. In separate experiments, the same group knocked down LRH-1 in

Huh7 cells using small interfering RNA (siRNA); this resulted in increased SREBP-2, LDLR, and HMGR promoter activity. Comparative binding interactions were then carried out between various permutations of truncated SREBP-2 and LRH-1 protein constructs. The SREBP-2 basic helix-loop-helix leucine zipper present between amino acids 331 and 381 of SREBP-2 was found to interact with the DNA-binding region of LRH-1.

Collectively, these data indicate the existence of a delicate balance between SREBP-2 and LRH-1 within the liver. During periods of low intracellular cholesterol, SREBP-2 levels and activity increase, and subsequently this inhibits LRH-1-responsive gene transcription. A bias towards increased cholesterol uptake and biosynthesis results from the simultaneous activation of LDLR and HMGR, respectively, while cholesterol biotransformation and efflux pathways are suppressed. On the other hand, during periods of raised intracellular cholesterol levels, activated SREBP-2 levels dissipate, thereby allowing LRH-1 gene expression and associated transcription to dominate. The biochemical effects are increased biotransformation of cholesterol to form bile acids (via Cyp7a1 and Cyp27a1), and induction of cholesterol and bile acid canalicular transporters to effect removal of cholesterol and bile acids from liver cells. With regards to the dysregulation in cholesterol homeostasis observed in HF-fed *foz/foz* mice with NASH, an inappropriate increase in nuclear SREBP-2 is observed despite profound increases in intracellular FC and CE levels. We interpret this "disconnect" as indicating either a failure of SREBP-2 to sense intracellular cholesterol levels, or a stimulation of SREBP-2 expression (by other factors) in spite of high intracellular cholesterol levels, or a possible combination of the two.

With regards to possible "peripheral" (non-cholesterol responsive) pathways of SREBP-2 upregulation, Xie *et al.* (2009) demonstrated that T2D, insulin-resistant *db/db* mice manifest low hepatocellular HNF-4α protein expression, while streptozotocin-treated mice, which develop type 1 diabetes as the result of drug-induced destruction of insulin-producing pancreatic β-cells, display elevations of HNF-4α protein; HNF-4α is hypothesised to interact with and be negatively regulated by SREBP-2 (Misawa *et al.* 2003). Further *in vivo* and *in vitro* investigations have indicated that insulin positively regulates SREBP-2 expression within hepatocytes. In turn, this suppresses hepatic HNF-4α expression, thereby accounting for the observed suppression of HNF-4α in

db/db mice, which develop hyperinsulinemia as a result of β-cell compensation during the development of insulin resistance.

These findings are of particular relevance to human NASH. Thus, SREBP-2 mRNA has been found to be significantly raised in human NASH patients versus those with simple steatosis and lean controls (Caballero *et al.* 2009). Furthermore, the data provided by Kanayama *et al.* and Xie *et al.* may provide an indication why hyperinsulinemia and hypercholesterolemia share a strong association in human patients with metabolic syndrome (Paolisso *et al.* 1992; Jia *et al.* 2005), and why patients with T2D are at a significantly higher risk of developing atherosclerosis and resultant cardiovascular disease (La Montagna *et al.* 2007; Chien *et al.* 2008; Park *et al.* 2008; Caccamo *et al.* 2010; DeFronzo 2010; Mihalcea and Pandele 2010; Yu *et al.* 2011).

In addition to regulation by insulin and intracellular cholesterol levels, there is now emerging evidence that hepatic SREBP-2 may be up-regulated directly by liver inflammation and injury. Zhao *et al.* (2011) recently demonstrated that hepatic inflammation influences SREBP-2 expression, and subsequent LDL receptor (LDLR) and HMG-CoA reductase (HMGR) expression, both *in vivo* and in *in vitro* model systems. Chronic low grade inflammation, and IL-1β and IL-6 cytokine stimulation triggered SREBP-2 activation and increased hepatic LDLR receptor expression, in addition to enhancing HMG-CoA reductase activity. Moreover, inflammation-dependent modulation of these pathways increased hepatic levels of both free and esterified cholesterol. Interestingly, chronic low grade inflammation was found to interfere with the feedback mechanism responsible for decreasing nuclear SREBP-2 in the presence of heightened intracellular FC levels, thereby deregulating cholesterol homeostasis. In C57Bl/6J mice, subcutaneous casein injections induced the expression of both IL-6 and serum amyloid A protein (similar to human C-reactive protein), simultaneously increasing nuclear SREBP-2 and downstream LDLR and HMGR expression. Similar results have been obtained in human HepG2 cells (an HCC cell line), whereby IL-1β and IL-6 exposure augmented the expression of LDLR and HMGR. Both *in vivo* and *in vitro* experimental approaches were found to increase hepatic intracellular cholesterol and lipid, confirming that the cholesterol uptake and biosynthesis pathways expressed molecularly did lead to biological changes in cholesterol accumulation.

As mentioned in Section 1.4.1.1, the SREBP-2 encoding region contains a highly conserved micro-RNA, miR-33, which is responsible for inhibition of cellular cholesterol export via ABCA1, and mitochondrial free fatty acid (FFA) β-oxidation through suppression of several enzymes. In turn, this increases hepatic FFA accumulation (Horie *et al.* 2010) (Figure 4.1); FFA are candidate lipotoxins within the liver in NASH (Neuschwander-Tetri 2010a, 2010b) (Figure 4.1). In addition to miR-33, miR-122 may also play an important role in hepatic SREBP-2 regulation. Physiologically, miR-122 is the most abundant miRNA in the liver, and it is strongly down-regulated in NASH patients (Cheung *et al.* 2008). Suppression of miR-122 in mice, significantly increases in SREBP-2 and HMGR expression, both *in vivo* and in *in vitro* systems (Gerin *et al.* 2010). It has subsequently been hypothesised that miR-122 acts, effectively, as a negative post-transcriptional regulator of SREBP-2 activation; it could stabilise the inactive SREBP-2 protein, the absence of which results in increased SREBP-2 activation. This constitutes an additional pathway that may increase SREBP-2 activation in human NASH (Figure 4.1).

Collectively, contemporary research suggests that appropriate SREBP-2 regulation is paramount to maintaining physiological bodily cholesterol homeostasis within mammals. In the HF-fed *foz/foz* model, mice with NASH display raised serum insulin levels after 2 weeks HF-feeding ($P<0.05$, Figure 4.2A), with further profound (>30 fold) increase at 12- and 24 weeks (Larter *et al.* 2009). Corresponding with increased serum insulin, these mice also display significantly higher expression of total hepatic LDLR, the pattern of which strongly correlates with serum insulin levels in these hyperinsulinemic HF-fed *foz/foz* mice ($P<0.05$, Figure 4.2B) (note: the data in Figure 4.2B partially replicates those in Figure 3.4; they are shown here to appreciate the relationship to circulating insulin levels). WT and chow-fed *foz/foz* mice, however, show unaltered LDLR expression over time (full time course results not shown; 12- and 24-week data presented in Chapter 3). Given the data put forward by Kanayama *et al.* and Xie *et al.*, and in light of the fact that hepatic SREBP-2 expression is higher in human NASH, the present study was designed to test the effects of insulin stimulation on regulatory pathways of cholesterol metabolism in primary hepatocytes.

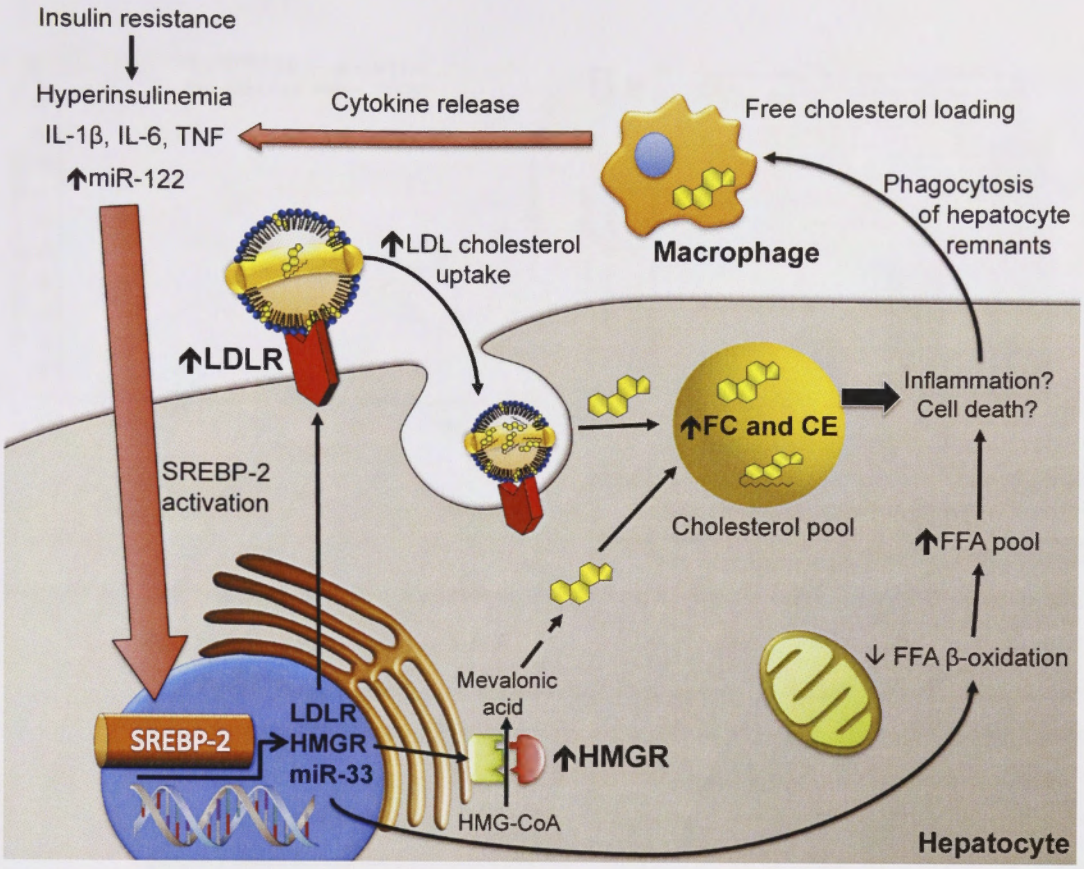

Figure 4.1 Activation of hepatocellular SREBP-2 by cholesterol, insulin, inflammatory responsive pathways and miRNAs: implications for cholesterol homeostasis

Nuclear SREBP-2 is up-regulated by inflammatory cytokines (IL-1β, IL-6, TNF), in addition to hyperinsulinemia, and decreased miR-122. Increased nuclear SREBP-2 induces expression of LDLR, which increases LDL cholesterol uptake, HMGR, which induces nascent cholesterol biosynthesis, and miR-33, which results in suppression of mitochondrial β-oxidation of FFA, and cholesterol efflux. Collectively, these pathways culminate in increased hepatic cholesterol accumulation, which may affect hepatocellular cell death and hepatic inflammation, resulting in macrophage and neutrophil recruitment. The combined effect is increased cytokine release, which exacerbates SREBP-2 activation.

Abbreviations: CE, cholesteryl esters; FC, free cholesterol; FFA, free fatty acids; HMG-CoA, 3-hydroxy-3-methyl-glutaryl-CoA; HMGR, HMG-CoA reductase; IL, interleukin; LDLR, low-density lipoprotein receptor; miR, micro RNA; SREBP-2, sterol response element binding protein-2; TNF, tumour necrosis factor.

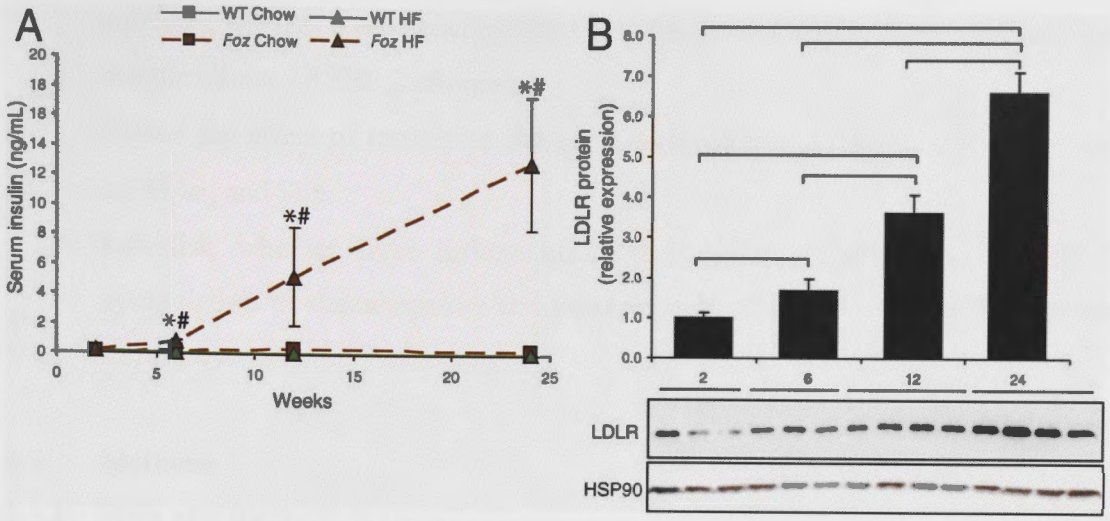

Figure 4.2 Correlation between hyperinsulinemia and hepatic LDL receptor expression in HF-fed *foz/foz* mice over time

(**A**) Serum insulin levels in normal chow (0% [w/w] cholesterol) and HF (0.2% [w/w] cholesterol)-fed WT and *foz/foz* mice over 24 weeks (n=5-14/grp). (**B**) Hepatic LDL receptor (LDLR) protein expression in HF-fed *foz/foz* mice over 24 weeks. Same mice as Chapter 3. Western blot quantitation was normalised to heat-shock protein 90 (HSP90) expression. NB: Serum insulin levels were measured by Dr. Claire Z. Larter. $^{*}P<0.05$, vs. diet-matched control. $^{\#}P<0.05$, vs. genotype-matched control. Bars represent $P<0.05$, between groups.

Because NASH is an inflammatory and fibrotic condition, as well as a metabolic disorder, archival liver samples from two other models were used to allow any separate effect of inflammation on LDLR expression to be discerned. Liver samples were from mice fed a methionine and choline-deficient (MCD) diet and chronic CCl_4-treated mice. In the first, MCD diet-fed mice develop severe, fibrosing steatohepatitis (i.e. have liver inflammation) but have normal or low serum insulin levels (Rinella and Green 2004; Leclercq *et al.* 2007; Larter *et al.* 2008b). These tissues were generated in the host laboratory. CCl_4-treated mice are another (toxic) model of chronic liver injury with inflammation and fibrosis (Gaynes and Watkins 1989). These tissues were generated in the laboratory of Drs Nicholas Shackel and Fiona Warner.

4.2 Purpose of study: hypotheses and aims

The underlying hypothesis of this study is that insulin is primarily responsible for upregulating hepatocellular nuclear SREBP-2 levels in NASH. The effects of insulin on hepatic cholesterol homeostasis have not been fully investigated, especially in the context of NASH. The specific aims of the studies described in this Chapter were to:

1. Using primary murine hepatocytes, establish an insulin "dose-response" to elucidate whether a relationship exists between media insulin concentrations and hepatocellular SREBP-2 expression.
2. Assess the effect of insulin on the gene expression of LRH-1, LXR-α and -β, HNF-4α, and Shp.
3. Establish whether liver inflammation has any direct effect on SREBP-2 upregulation in steatohepatitis and other models of chronic liver inflammation and injury.

4.3 Methods

4.3.1 Mice and diets

Female chow-fed WT NOD.B10 mice (6-10 weeks of age) were used for lean primary hepatocyte isolation.

4.3.2 Hepatocyte culture

4.3.2.1 Reagents

Sterile rat-tail collagen (5 mg/mL) and trypan blue were purchased commercially and required no additional preparation.

Perfusion buffer solutions, HBSS and William's E media were all prepared as described in Section 2.13.1.

Bovine pancreatic insulin (I5500) was purchased commercially (Sigma-Aldrich, St. Louis, MO). It should be noted that bovine pancreatic insulin shares a 100% sequence homology with mouse (*Mus musculus*) insulin. Comparative inter-species protein homology was performed using a protein basic local alignment search tool (BLAST), as originally described by Altschul *et al.* (1990). Consequently, it can be assumed that the source of insulin is irrelevant to this study and observed responses can be assumed to be physiological.

HF-fed *foz/foz* mice were found to have average serum insulin levels of 6.5 and 13.0 ng/mL at 12- and 24-weeks, respectively (Figure 4.2A). These values equate to insulin concentrations of 1.13 and 2.26 nM, respectively. Serum insulin levels in chow-fed *foz/foz* mice, however, consistently averaged 0.2 ng/mL (35 ρM) over 24 weeks (Figure

4.2A). Accordingly, 6.5 and 13 ng/mL concentrations were used to replicate hyperinsulinemic insulin levels, while 0.2 ng/mL was used as a lower range physiological concentration, in addition to un-stimulated control groups.

Bovine pancreatic insulin stock solution (1.74 µM insulin in 174 mM glacial acetic acid). Bovine pancreatic insulin (0.5 g) was added to 49.5 mL d.H_2O. Glacial acetic acid (500 µL of 1.049 $g.cm^{-3}$ stock) was added to acidify the solution and mediate insulin dissolution, after which insulin was allowed to dissolve. Solution was stored at 4°C until use. Just before use, a dilute 1:1000 intermediate working solution was created by adding 10 µL of stock solution to 9.99 mL of sterile HBSS.

30% (v/v) Sterile ethanol in d.H_2O. Ethanol (150 mL of >99.9% [v/v] stock) was added to 350 mL of d.H_2O and filter sterilised.

Rat-tail collagen coating solutions (equivalent to 5 µg/cm^2 Rat-tail collagen in sterile 30% [v/v] ethanol). Sterile rat-tail collagen was diluted in sterile 30% (v/v) ethanol and used to coat culture vessels and coverslips, as described in Table 4.1.

Table 4.1 Rat-tail collagen working concentrations and volumes used to coat coverslips and culture vessels of varying dimensions

Item	Diameter (cm)	Area (cm^2)	Coat vol (µL)	Coat vol (mL)	mg required per plate	Total µg RTC required	RTC [Working solution] (µg/mL)	RTC vol (µL of 5 mg/mL stock)	30% (v/v) Ethanol (µL)
96 well plate	0.6	0.32	100	0.1	0.0016	1.6	16.0	0.3	100
13 mmØ Coverslip	1.3	1.32	200	0.2	0.0066	6.6	33.0	1.3	199
25 mmØ Coverslip	2.5	4.90	600	0.6	0.0245	24.5	40.8	4.9	595
24 Well plate	15.6	1.90	200	0.2	0.0095	9.5	47.5	1.9	198
12 Well plate	22.1	3.80	400	0.4	0.019	19.0	47.5	3.8	396
6 Well plates	34.8	9.50	600	0.6	0.0475	47.5	79.2	9.5	591
Ti25	*N/A*	25.00	3500	3.5	0.125	125.0	35.7	25.0	3475
Ti55	10.0	55.00	5000	5	0.275	275.0	55.0	55.0	4945
Ti75	*N/A*	75.00	7500	7.5	0.375	375.0	50.0	75.0	7425

Abbreviations: Ø, diameter; RTC, rat-tail collagen; vol, volume.

4.3.2.2 Procedure

Primary hepatocytes were isolated as described in Section 2.13. Viability and quantification were assessed using 1:1 ratio of trypan blue to cell suspension. Cell viabilities of ≥95% were used for insulin stimulation experiments. Cells were seeded onto collagen-coated culture plates at ~6.5 x 10^4 viable cells/cm^2 and incubated at 37°C in 5% CO_2 and ~70% relative humidity. After 4 h, insulin was added to yield separate concentrations of 0.2, 6.5, and 13.0 ng/mL. Control plates were not supplemented with insulin. Every 8 h, cells were washed with HBSS and insulin-supplemented media changed. Prior to terminating experiments, supernatant was sampled and stored at -80°C for retrospective LDH quantification. All experiments were terminated 48 h after commencement. Experiments were conducted in triplicate or quadruplicate.

Upon termination, cells were harvested for isolation of RNA (Section 2.7.1) and total protein (Section 2.8.1). These samples were used for cDNA synthesis, real-time PCR, and western blotting, as described in Sections 2.7.2, 2.7.3, and 2.11, respectively.

Primary and secondary antibodies and primers used in this study are detailed in Tables 2.1, 2.2, and 2.3, respectively.

Culture supernatant LDH content (marker of cell injury) was quantified using a commercial kit (TOX7; Sigma-Aldrich, St. Louis, MO) as per the Manufacturer's instructions. The doses of insulin used in these experiments had no effect on cell viability.

4.3.3 Comparison of hepatic LDLR expression between *foz/foz*, MCD, and CCl_4-treated mice

To establish whether observed increases in LDLR in HF-*foz/foz* mice with NASH were due to hyperinsulinemia, and not to hepatic inflammation and fibrosis, LDLR expression was assessed, using IHC, in both MCD mice with NASH (which do not develop insulin resistance or hyperinsulinemia) and chronic CCl_4-treated mice, which develop severe liver injury, inflammation and fibrosis.

4.3.3.1 Mouse liver samples

Formalin-fixed liver samples from C57BL/6 mice fed either a MCD diet for 8 weeks, or treated with CCl_4 for 4 weeks were kindly provided by Drs Claire Larter and Nicholas Shackel, respectively. Appropriate controls were analysed for all experimental groups. Chow and HF-fed *foz/foz* mice (same mice as used in Chapter 3) were also assessed for direct comparison.

4.3.3.2 Reagents

IHC reagents were prepared as described in Section 2.6.2.

4.3.3.3 Procedure

Formalin-fixed, paraffin-embedded, liver sections (4 μm) from chow and HF-fed *foz/foz*, MCD diet-fed, and CCl_4-treated mice were mounted together on single slides; this was performed to standardise IHC staining between liver samples. IHC staining for LDLR was performed as previously described (Section 2.6.2.2, see Table 2.1 for antibody conditions).

4.3.4 Statistical analyses

Data were analysed for statistical significance using Student's *t*-test (Section 2.15), with statistical significance defined as $P<0.05$. All data are presented as mean ± standard error of the mean (SEM).

4.4 Results

4.4.1 Insulin alters increases cholesterol uptake and biosynthesis pathways in primary murine hepatocytes

Insulin concentrations simulating those observed in HF-fed *foz/foz* mice at 12 weeks (i.e. 6.5 ng/mL) and 24 weeks (13 ng/mL) (Larter *et al.* 2009), significantly elevated total cellular SREBP-2 and LDLR protein ($P<0.05$, Figure 4.3A,B) in primary murine hepatocytes. Similarly, HMGR mRNA expression was also higher following insulin exposure ($P<0.05$, Figure 4.3C) (due to the limited cellular protein available HMGR activity and protein expression were not assessed in this model system). Protein expression for the endogenous LDLR regulator protein, PCSK9, was also examined, but no immunoreactivity was observed, irrespective of insulin stimulation (results not shown). This suggests a lack of hepatocellular PCSK9 protein expression, which

corroborates the findings in Chapter 3, in which PCKS9 protein expression is only observed in non-parenchymal cells within the livers of *foz/foz* and WT mice.

Assessment of other transcriptional regulators of cholesterol metabolism, demonstrated that 6.5 and 13 ng/mL concentrations of insulin suppressed both LRH-1 and HNF-4α mRNA levels ($P<0.05$, Figure 4.4A,B). Interestingly, Shp mRNA expression was also suppressed following insulin stimulation. The suppression of HNF-4α in this model correlates with the findings of Wie *et al.* (2009), in which HNF-4α was suppressed in C57BL/6 livers and hepatocytes following insulin stimulation, in a SREBP-2-dependent manner.

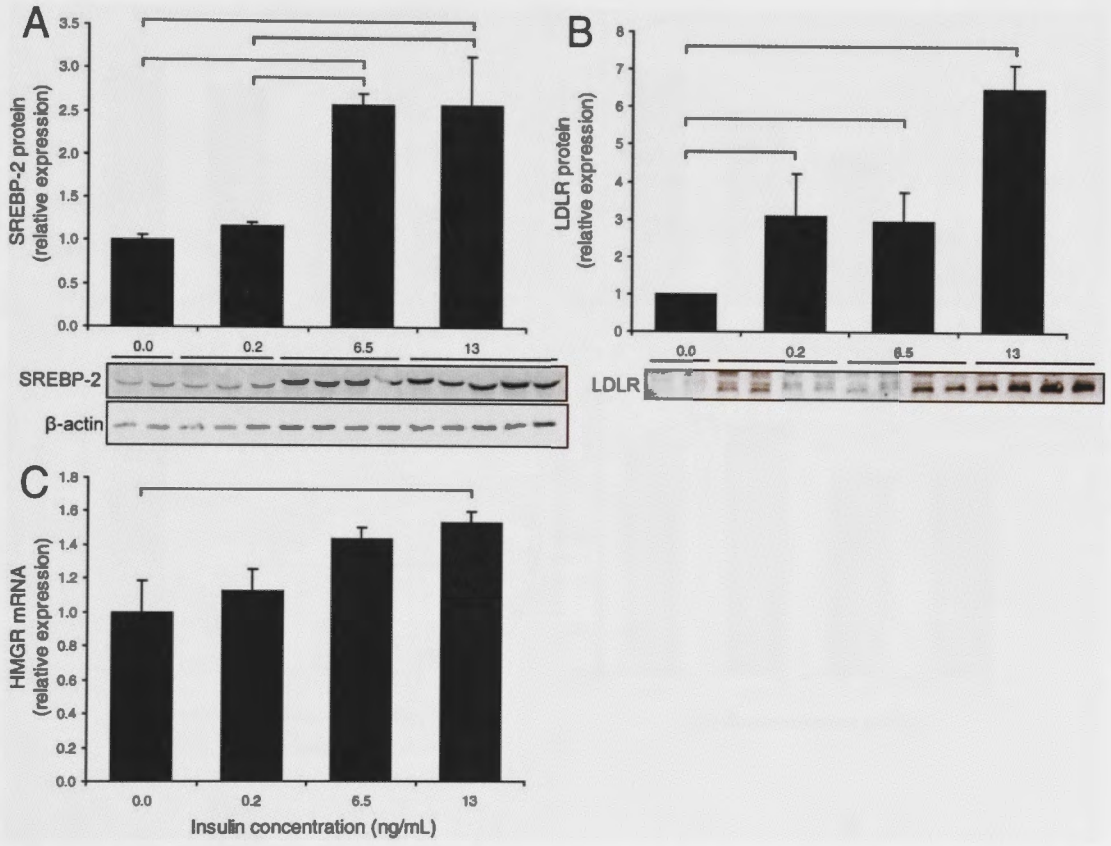

Figure 4.3 Insulin stimulation upregulates pathways of cholesterol uptake and biosynthesis in primary hepatocytes

(**A**) Total hepatocyte sterol regulatory element–binding protein (SREBP)-2, (**B**) low-density lipoprotein receptor (LDLR), and (**C**) HMG-CoA reductase (HMGR) mRNA expression in WT NOD.B10 primary hepatocytes stimulated with 0, 0.2, 6.5, and 13.0 ng/mL bovine pancreatic insulin for 48 h. Western blot quantitation was normalised to β-actin expression. Data are mean ± SEM. Bars represent $P<0.05$ between groups.

Despite suppressed LRH-1 mRNA, Cyp7a1 mRNA expression was unaltered by high concentration insulin stimulation for 48 h (Figure 4.4D). LXR-β protein levels were also unchanged, irrespective of the concentration of insulin used (data not shown). Conversely, Bsep protein expression was significantly reduced in hepatocytes stimulated by exposure to 6.5 and 13.0 ng/mL insulin ($P<0.05$, Figure 4.4E). Interestingly, at lower insulin concentrations (0.2 ng/mL), Bsep protein expression is elevated compared with untreated hepatocytes ($P<0.05$, Figure 4.4E), suggesting that lower physiological concentrations of insulin may have a differential effect on Bsep protein stabilisation, while higher insulin concentrations may augment Bsep degradation or turnover.

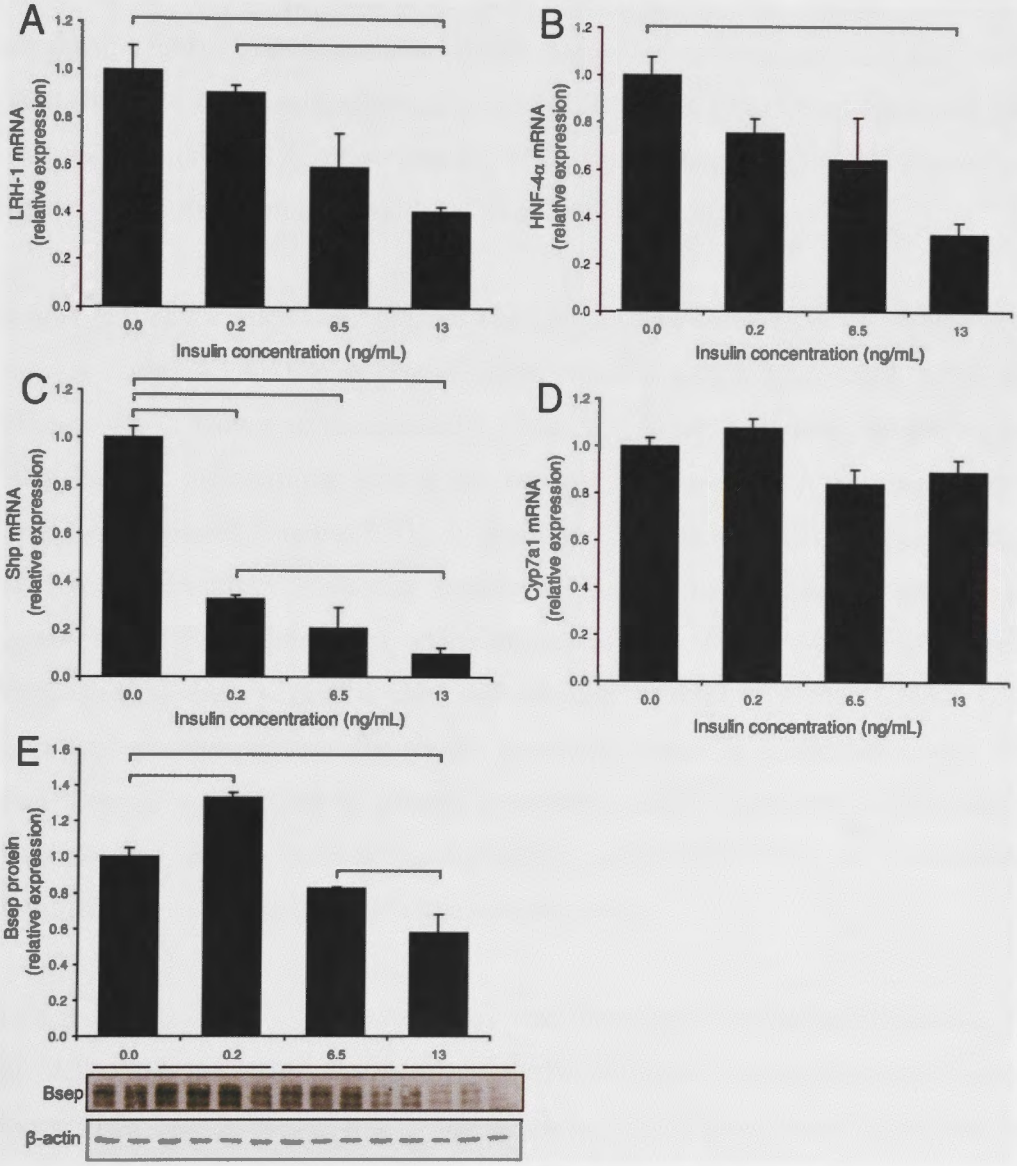

Figure 4.4 Insulin stimulation differentially alters pathways of cholesterol biotransformation and bile acid export

Legend for Figure 4.4.

(**A**) Liver receptor homolog-1 (LRH-1) mRNA, (**B**) hepatocyte nuclear factor (HNF)-4α mRNA, (**C**) short heterodimer partner (Shp) mRNA, (**D**) Cyp71 mRNA, and (**E**) bile salt exporter protein (Bsep) expression in WT NOD.B10 primary hepatocytes stimulated with 0, 0.2, 6.5, and 13.0 ng/mL bovine pancreatic insulin for 48 h. Western blot quantitation was normalised to β-actin expression. Data are mean ± SEM. Bars represent $P<0.05$, between groups.

4.4.2 LDLR over-expression in mice with NASH is unlikely due to liver injury and inflammation

Data thus far have demonstrated the ability of insulin stimulation of WT NOD.B10 primary hepatocytes to recapitulate the major changes in cholesterol homeostasis observed in HF-*foz/foz* NOD.B10 mice with diabetes and NASH (Chapter 3). To establish whether over-expression of LDLR expression observed in HF-fed *foz/foz* mice is attributable to hyperinsulinemia and not a result of liver injury-mediated SREBP-2 over-expression, LDLR expression (by IHC) was assessed in two other models of liver injury with inflammation, namely MCD-fed and CCl_4-treated mice.

Chow fed *foz/foz* mice with relatively low serum insulin levels (~0.2 ng/mL from 2-24 weeks; Figure 4.1A) display physiological vascular LDLR localisation within the liver (Figure 4.5A). However, as reported in Chapter 3, hyperinsulinemic HF-fed *foz/foz* mice with NASH over-express LDLR on hepatocyte plasma membranes in addition to vascular structures (Figure 4.5B). In contrast, livers from MCD-fed mice which show similar liver histology (steatosis, hepatocyte injury, inflammation, and fibrosis) show an apparent minor increase in *cytoplasmic* LDLR (Figure 4.5D) compared with experimental dietary (methionine and choline replete) controls (Figure 4.5C). An important distinction from the *foz/foz* model of metabolic syndrome-related NASH is that there is no increase in plasma membrane LDLR expression. It therefore seems unlikely that any effects of inflammation *per se* on SREBP-2 expression are translated to functional increases in hepatic cholesterol uptake.

LDLR expression in CCl_4-treated mice was found to be unchanged following 4 weeks of CCl_4 exposure, at which time liver inflammation and fibrosis are clearly evident. No increase in LDLR expression or alteration in LDLR localisation is evident between experimental and control groups (Figure 4.5F versus E).

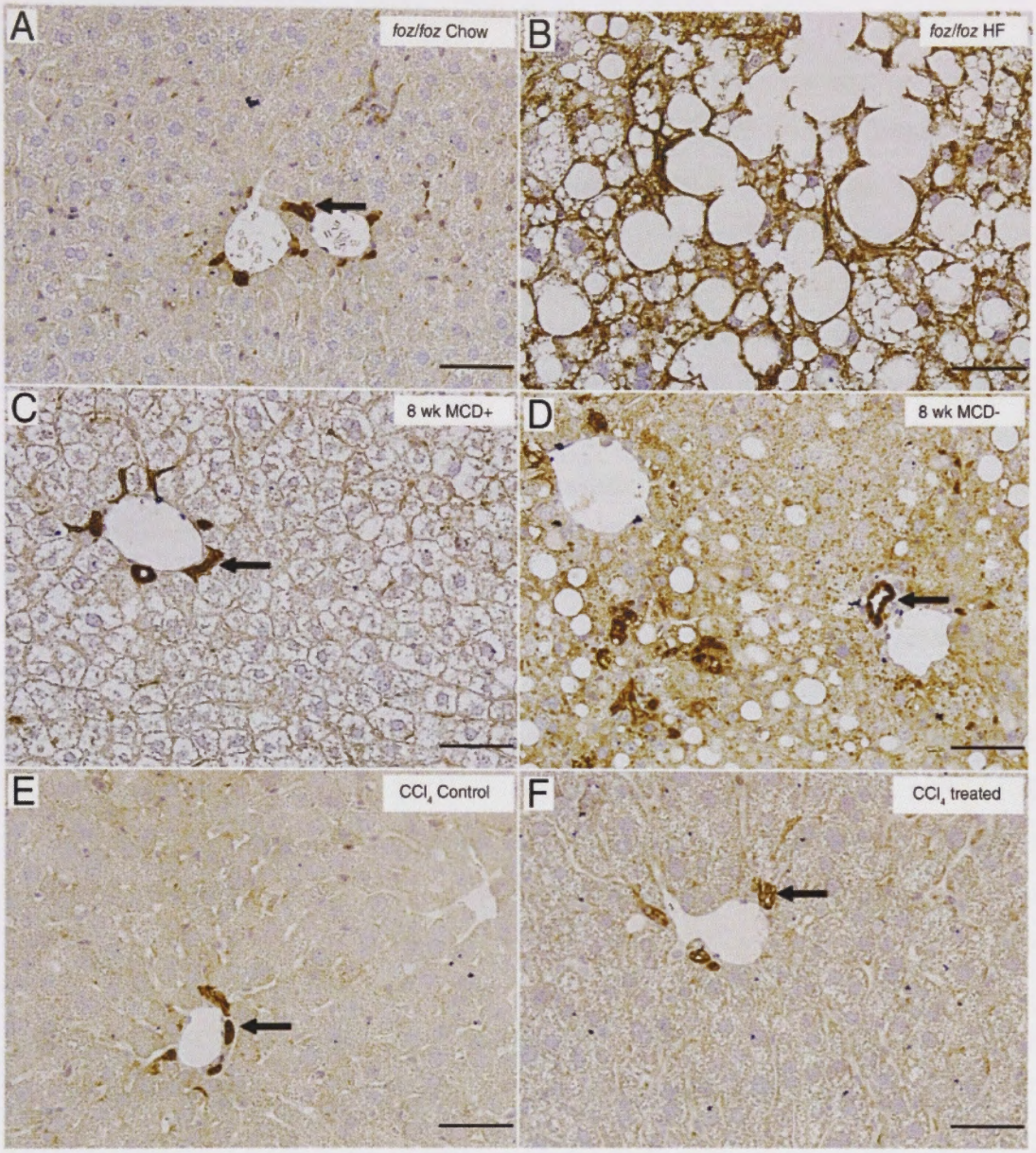

Figure 4.5 Comparison between LDLR localisation in *foz/foz*, MCD diet induced steatohepatitis and CCl_4-treated mice

LDLR localisation in (**A**) chow- and (**B**) HF-fed *foz/foz* mice at 24 weeks, (**C**) MCD control (MCD+) and (**D**) MCD-deficient (MCD-) mice at 8 weeks. (**E**) Carbon tetrachloride (CCl_4) control and (**F**) CCl_4–treated mice at 4 weeks. Arrows indicate physiological LDLR staining. Scale bars represent 20 μm.

4.5 Discussion

Metabolic syndrome (MetS) is the term used to collectively describe several "clustered" metabolic abnormalities that individually predispose to cardiovascular disease (central obesity, hypertension, glucose intolerance, dyslipidemia). According to the latest definition of MetS established by the International Diabetes Federation (Alberti *et al.* 2006), the consensual prerequisites for diagnosis are central obesity and insulin-resistance, in addition to at least two other factors: elevated serum triglycerides above 1.7 mmol/L, reduced serum HDL levels, and/or hypertension. NASH is the hepatic manifestation of MetS (Brunt 2004), with hepatic lipid accumulation one of the defining characteristics of the disease. Hepatic insulin resistance is critical to the pathophysiology and development of NAFLD (Farrell *et al.* 2008). *Foz/foz* mice, particularly when fed a HF (atherogenic) diet develop identical metabolic abnormalities, including obesity, insulin resistance and hyperinsulinemia, hyperglycemia, and decreased serum HDL (as a proportion of total serum cholesterol). Therefore the pathophysiology of the *foz/foz* model is more representative of human metabolic syndrome-related NASH than simple dietary or genetic rodent models, or the MCD dietary model in which subcutaneous fat loss, insulin sensitivity and normal or increased serum adiponectin are all opposite to the metabolic determinates of human NASH.

In the previous Chapter it was shown that livers from HF-fed *foz/foz* mice with NASH display significantly higher expression of nuclear SREBP-2 and hepatocellular LDLR protein, compared with dietary and genotype controls. Suppression of Bsep, ABCG-5 and -8, and Cyp7a/27a1 expression was also evident in these mice. In this Chapter, exposure of primary hepatocytes for 48 h to concentrations of insulin that circulate in hyperinsulinemic *foz/foz* mice induced SREBP-2, LDLR, and HMGR, as well as suppressing LRH-1, HNF-4α and Bsep gene expression. Since LRH-1 controls ABCG5/8, Bsep, Cyp7a1, Cyp8b1, MRP2, and SR-B1 expression (Freeman *et al.* 2004; Lee *et al.* 2006; Lee *et al.* 2008; Song *et al.* 2008) all of which were down-regulated in the *foz/foz* model of NASH, it seems reasonable to propose that insulin may be responsible for suppression of the pathways responsible for cholesterol biotransformation to BAs, and for cholesterol and BA export in bile.

In HF-fed *foz/foz* mice, hepatic LRH-1 protein expression failed to increase beyond baseline, whereas WT mice challenged with HF feeding display significant elevations in nuclear LRH-1 protein (Section 3.4.8). This appears to be the first evidence that an abrogated LRH-1 response (failure to increase) could be pertinent to NASH pathogenesis. While LRH-1 suppression through SREBP-2 has been previously reported by Kanayama *et al.* (2007), the present study has demonstrated that insulin concentrations which circulate in diabetic, hyperinsulinemic mice with NASH are capable of not only increasing functional LDLR expression through SREBP-2, but also suppress LRH-1 and HNF-4α, and in the process modulates genes responsible for clearance of intracellular cholesterol. One possible explanation for the abrogated LRH-1 response to HF-feeding in *foz/foz* mice may be that the down-regulatory effects of high insulin levels (via SREBP-2) counters the inductive effect of an increase in hepatic FC. Development of a "cholesterol-loaded" hepatocyte culture system would be required to test this proposal (see future directions, Chapter 8).

In vivo, nuclear LRH-1 protein levels in HF-fed *foz/foz* mice were equivalent to chow-fed controls at both 12- and 24-week time points (Figure 3.12A), while nuclear Shp protein levels were significantly increased in HF-fed *foz/foz* mice at these times (Figure 3.13C). Possible explanations for the disparity between *in vivo* and *in vitro* LRH-1 and Shp gene expression could include a differential effect of hepatocellular cholesterol loading (as observed in HF-fed *foz/foz* mice with NASH) on the regulation of LRH-1 and Shp. Alternatively, insulin stimulation may inhibit LRH-1 upregulation in diabetic *foz/foz* mice. Thus as HF-feeding induces LRH-1 expression in WT mice, high circulating insulin levels may prevent increased expression of LRH-1 in HF-fed diabetic *foz/foz* mice.

Unfortunately, due to limited protein that can be harvested from cultured hepatocytes (≤1.0 μg/μL protein), attempts to immunoblot LRH-1 and Shp proteins were unsuccessful; specifically, at least 50 μg/well of cellular protein is required for immunodetection of these peptides, and harvest protein provided less than 10 μg/well. This limitation also prevented immunoblotting for ABCG-5 and -8, LXR-α, and HMGR. Further studies using larger culture plates are needed to increase amounts of harvestable protein in order for individual protein expression to be studied. Nuclear

protein isolation would also be preferential, in order to verify increased nuclear SREBP-2 activation, and constitutes a future direction for this research.

The ability of insulin to increase SREBP-2 expression in WT NOD.B10 hepatocytes concurs with results from the Xie *et al.* study (2009), in which insulin augmented SREBP-2 expression both *in vitro* in cultured primary hepatocytes, and in *in vivo* C57BL/6 mouse livers. Insulin is a potent SREBP-1c agonist in both humans and rodents (Bobard *et al.* 2005; Dif *et al.* 2006), and is also capable of activating SREBPs through interactions with sterol response element (SRE) binding sites (Dif *et al.* 2006). Furthermore, interactions between insulin and other nuclear factors including LXR-response elements, stimulating protein-1 (Sp1), and nuclear factor-Y (NF-Y) activate SREBP-1c expression (Cagen *et al.* 2005). However, the most potent activation of SREBP-1a and -2 expression is accomplished through the activation of the mitogen activated protein (MAP) kinase pathways (Kotzka *et al.* 2000).

Insulin exerts its cellular effects predominantly through two independent pathways, namely phosphatidylinositol 3-kinase (PI3K) (Folli *et al.* 1993) and MAP kinase (Zhou *et al.* 1993a). The MAP kinase pathway is responsible for insulin-dependent activation of SREBP-2, in which insulin signalling activates downstream extracellular signal-regulated kinase (Erk)-1/-2 and results in phosphorylation of Ser^{432} and Ser^{455} of SREBP-2 (Kotzka *et al.* 2004) and Ser^{117} of SREBP-1a (Roth *et al.* 2000). Empirically phosphorylation was found to have no influence on DNA binding interactions. Instead, it augments the transcriptional efficiency of SREBP-2 (Lu *et al.* 2008). Increased transcriptional efficiency is conferred through the prevention of covalent attachment of small ubiquitin-like modifier (SUMO) at Lys^{464} sites, which lie in close proximity to Ser^{455} (Arito *et al.* 2008). SUMOylation of SREBP-2 results in constitutive attenuation of transcriptional activity through the recruitment of a co-repressor complex involving histone deacetylase 3 (HDAC3) (Arito *et al.* 2008).

In the context of the *foz/foz* mouse model of NASH, insulin stimulation of hepatocytes increases total SREBP-2 expression, as demonstrated by this study. Furthermore, insulin-dependent activation of the MAP kinase pathway involving ERK-1/-2 kinases may phosphorylate SREBP-2, preventing SUMOylation and simultaneously augmenting SREBP-2 transcriptional activity. The increased hepatic SREBP-2

activation, as described by Kanayama *et al.* (2007), is capable of inhibiting LRH-1 and HNF-4α gene expression, which negatively impacts upon ABCG-5/8, Bsep, Cyp7a1, Cyp8b1, MRP2, and SR-B1 gene expression; impaired expression of these genes was demonstrated in Chapter 3. Interestingly, reductions in hepatic LRH-1 and Shp mRNA were evident in HF-fed *foz/foz* mice at 12- and 24 weeks (Figures 3.12B and 3.13D, respectively), a finding which was corroborated in the present study. Thus, 13 ng/mL insulin suppressed HNF-4α and LRH-1 mRNA by ~2.5 fold and Shp mRNA by ~10 fold.

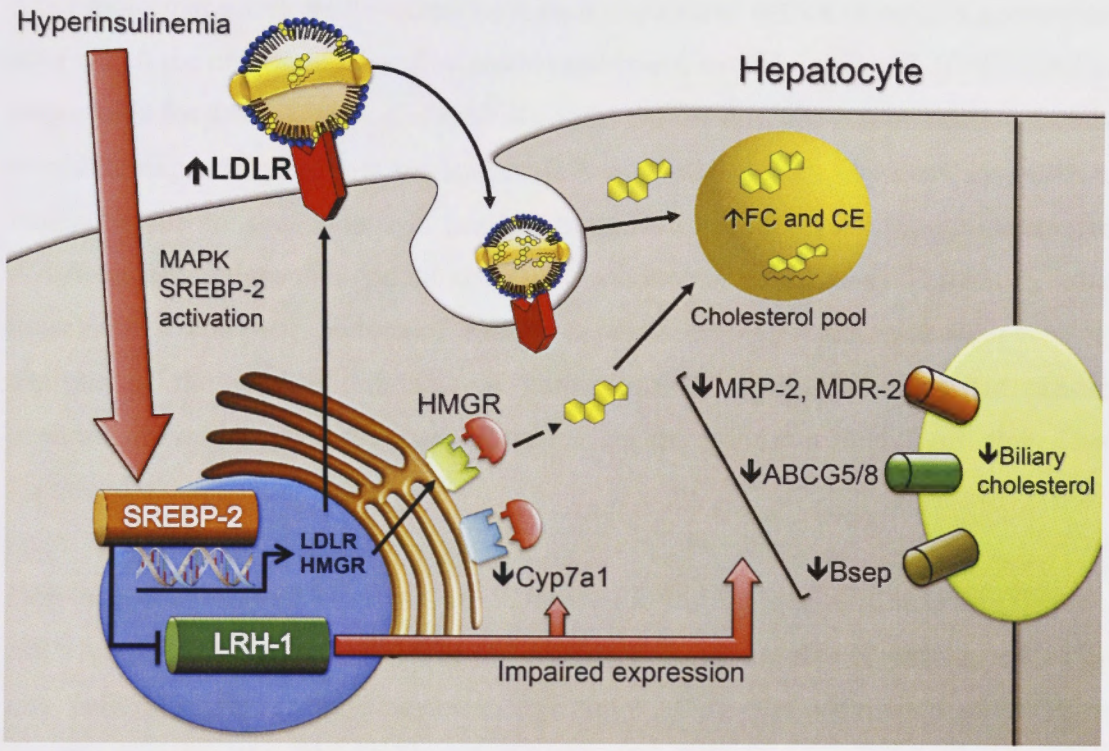

Figure 4.5 Proposed pathways of cholesterol dysregulation in *foz/foz* mice: role of hyperinsulinemia

HF-feeding induces insulin resistance, resulting in hyperinsulinemia in *foz/foz* mice, which worsens over 2-24 weeks. SREBP-2 activation is upregulated in the liver in response to increased hepatic insulin stimulation, and this results in increased hepatocellular LDLR expression, which increases LDL cholesterol uptake. Simultaneously, increased SREBP-2 expression suppresses LRH-1 transcription and effectively impairs transcription of down-stream LRH-1-responsive genes. These include Cyps involved in cholesterol to bile acid biotransformation, and canalicular protein transporters responsible for cholesterol (ABCG-5/8) and bile acid (Bsep, MRP-2) efflux from the liver. Note that, while all these changes were observed in HF-fed *foz/foz* mice with NASH, in the primary hepatocyte experiments described here, decreased Bsep was confirmed but Cyp7a1 expression was not (see text).

Abbreviations for Figure 4.5: ABCG, ATP-binding cassette protein family G; Bsep, bile salt exporter protein; CE, cholesteryl esters; Cyp, cytochrome P450; FC, free cholesterol; HMGR, HMG-CoA reductase; LDLR, low-density lipoprotein receptor; SREBP-2, sterol response element binding protein-2.

Schematic pathway constructed from data presented in Chapters 3 and 4.

Additionally, the experimental approaches undertaken in this study have not verified whether observed changes in LRH-1, Shp, and HNF-4α gene expression result from increased SREBP-2 expression or as a direct effect of insulin stimulation. In order to address this question, SREBP-2 expression could be inhibited in primary hepatocytes using molecular knock down technology, such engineered siRNA or shRNA constructs, after which the present insulin stimulation experiment could be repeated. If SREBP-2 is responsible for LRH-1, Shp, and HNF-4a gene suppression, these transcription factors would be expected to remain unchanged following stimulation. Unfortunately, siRNA manipulations are problematic in primary hepatocyte cultures due to rapid hepatocyte dedifferentiation thereafter and the short time window for experiments. Further, in order to achieve a complete picture of SREBP-2 regulation in *foz/foz* mice with NASH, analysis of the murine orthologs of human mIR-33 and -122 is needed. These experiments were beyond the scope of the current study and constitute future directions for this research.

Despite reductions in LRH-1 mRNA expression following insulin stimulation, Cyp7a1 mRNA levels did not decrease. One potential explanation for this observation could be that culturing primary hepatocytes differentially affects the expression of the Cyp enzyme superfamily, and may innately suppress Cyp7a1 gene expression. Early studies have found that composition of the hepatocyte substratum affects the expression of Cyp genes (Schuetz *et al.* 1990; Hunt *et al.* 1991). However, uniform stabilisation of Cyp gene expression is not achieved, even when more physiological substrata, such as matrigel, are used (Schuetz *et al.* 1988; Kane *et al.* 1991). Goodwin and colleagues (1996) have demonstrated that treating primary rat hepatocytes with metyrapone, a pyridol used to inhibit 11β-hydroxylase, stabilises Cyp3A2 and Cyp2C11 expression. It appears that a complex environmental system is needed to prevent rapid Cyp turnover in the *in vitro* setting. In the present study, it is plausible that Cyp7a1 mRNA is substantially lower in cultures than freshly isolated hepatocytes and, thus by 48 h, levels are unaffected by decreased LRH-1 expression in insulin-treated cells.

Given the extent of LDLR over-expression on hepatocytes in HF-fed *foz/foz* mice with NASH (Figure 3.3A,B and Figure 4.2B), LDLR expression was assessed in two other mouse model of liver injury, the MCD and CCl_4-treated mouse models. Chronic inflammation and liver injury are both features of these models. Unlike the *foz/foz* model, insulin resistance is not present in either MCD or CCl_4 treated mouse groups. There was no increase in LDLR expression and/or altered localisation in livers from MCD or CCl_4-treated mice. Thus liver injury and inflammation in MCD-fed mice and after chronic CCl_4 treatment is insufficient to upregulate LDLR expression. This finding is consistent with the proposal that hyperinsulinemia is principally responsible for augmented LDLR expression in HF-fed *foz/foz* mice with NASH. However, in order to conclusively rule out the effect of inflammation on pathways of cholesterol homeostasis, further studies are needed to compare the expression of SREBP-2, LRH-1, Shp, Bsep, and ABCG-8 between *foz/foz*, MCD-fed and chronic CCl_4-treated mice.

4.6 Summary of findings

The data presented in this study support the hypothesis that hyperinsulinemia is centrally involved in the dysregulation of cholesterol homeostasis in the HF-fed *foz/foz* mice with NASH. Persistently high levels of circulating insulin, most likely signalling through the ERK-1/-2 MAPK pathways activated by insulin receptor ligands, constitutively activates SREBP-2 leading to:

1. Increased LDLR expression, which in turn increased hepatic cholesterol uptake.
2. Decreased LRH-1 and HNF-4α expression through reciprocal inhibitory relationships, leading to suppression of Bsep.

CHAPTER 5

Hepatic cholesterol influences degree of liver injury, inflammation and fibrosis in *foz/foz* mice with non-alcoholic steatohepatitis

5.1 Introduction

In Chapter 3 it was demonstrated that feeding *foz/foz* (*Alms1* mutant) mice a HF diet containing 0.2% cholesterol induces NASH in association with the accumulation of hepatic FC and CE lipid species (Figure 3.1). Such cholesterol accumulation was attributable, at least in part, to increased LDL/VLDL cholesterol uptake via over expression of LDLR, which in turn is most likely effected by up-regulated nuclear SREBP-2. In addition to increased FC uptake, decreased biotransformation of cholesterol to form BAs and lowered expression of cholesterol and BA canalicular transporters is also evident in *foz/foz* mice; the latter appears to be a consequence of failed nuclear LRH-1 up-regulation and/or non-FXR mediated Shp upregulation. In the previous Chapter it was demonstrated that SREBP-2, LRH-1, and HNF-4α transcription factors are differentially regulated by insulin at high circulating concentrations observed in HF-fed *foz/foz* mice. We therefore hypothesise that hyperinsulinemia is a key factor mediating the dysregulated hepatic cholesterol homeostasis observed in NASH, the net effect of which culminates in cholesterol accumulation in the liver. However, whether expansion of hepatic cholesterol pools contributes to pathogenesis of liver disease in *foz/foz* mice with NASH is yet to be tested experimentally.

The lipotoxicity of excess intracellular cholesterol is well established in various cell types. Increased intracellular FC induces mitochondrial dysfunction, apoptosis and necrosis in cultured macrophages (Kellner-Weibel *et al.* 1998), while intracellular cholesterol loading of pancreatic β-cells induces apoptosis via p38 MAPK- and c-Jun *N*-terminal kinase (JNK) stress activated kinases (Lu *et al.* 2011). Similarly, apoptosis is observed in smooth muscle cells overloaded with FC (Kedi *et al.* 2009). In these cell types, apoptosis is depended on ER- and mitochondrial-stress pathway activation. In hepatocytes, Mari *et al.* (2006), similarly observed mitochondrial FC loading in obese

ob/ob and *Npc1* knockout ($Npc1^{-/-}$) transgenic mice (studies addressing activation of the ER stress pathways in *foz/foz* mice are reported in Chapter 7).

As discussed in Section 3.4.3, Npc1 is involved in intracellular trafficking of cholesterol from the late endosome/lysosome to the plasma membrane and endoplasmic reticulum (Ory 2000; Watari *et al.* 2000). Defective NPC1 protein in humans results in Niemann-Pick type C disease, a cholesterol storage disorder characterised by the early onset of jaundice and hepatosplenomegaly. Eventually, chronic liver injury and fibrosis leads to cirrhosis and liver failure (Kelly *et al.* 1993; Iturriaga *et al.* 2006; Sevin *et al.* 2007), while hepatocellular carcinoma has also been reported (Birch *et al.* 2003). In addition to the data put forward by Mari *et al.* (2006), Beltroy *et al.*(2007) demonstrated that $Npc1^{-/-}$ mice develop significant elevations in hepatic cholesterol profiles, as well as serum ALT and aspartate aminotransferase (AST) levels (which reflect liver injury). Impressively, their study identified a positive correlation between hepatic cholesterol levels and degree of liver injury (as defined by serum ALT) in $Npc1^{-/-}$ mice. In Chapter 3 we demonstrated that NPC1 mRNA expression in *foz/foz* mice is reduced by HF-feeding (Figure 3.4). However, the majority of intracellular FC in *foz/foz* mice localises to the plasma membrane and ER (Figure 3.2); the latter finding, together with NPC1 transcript data (Figure 3.4A) infers that NPC1 function is not impaired by HF-feeding and does not play an important role in NASH pathogenesis.

In addition to the $Npc1^{-/-}$ model of liver injury, several other studies employing transgenic animals have documented the effect of hepatic cholesterol loading on liver injury and inflammation. In LDLR deficient ($LDLR^{-/-}$) and ApoE knockout ($ApoE^{-/-}$) mice, severe NAFLD and NASH can be induced by cholesterol/HF-feeding (Tous *et al.* 2005; Shiri-Sverdlov *et al.* 2006; Wouters *et al.* 2008; Rull *et al.* 2009). Physiologically, ApoE lipoprotein acts in concert with ApoB (the major apolipoprotein of LDL and VLDL colloids) to facilitate chylomicron remnant uptake by the liver. Thus, $ApoE^{-/-}$ and $LDLR^{-/-}$ mice develop hyperlipidemia as a result of impaired CE-enriched VLDL and LDL uptake (Morganroth *et al.* 1975), an abnormality which leads to the development of severe atherosclerosis in these mice (Wouters *et al.* 2005). Impaired VLDL and LDL clearance from the blood may also predispose VLDL and LDL-bound FC and FFA to autooxidation, resulting in formation of oxidised LDL and VLDL, which are extremely

cytotoxic in several cell types (Reid and Mitchinson 1993; Marchant *et al.* 1996; Norata *et al.* 2003; Vaziri 2006).

More recently, Subramanian and colleagues (2011) demonstrated that C57BL/6 $LDLR^{-/-}$ mice fed HF diet containing 35.5% [w/w] carbohydrate and 36.6% [w/w] fat, and supplemented with or without 0.15% [w/w] cholesterol, develop NASH. The inclusion of dietary cholesterol exacerbates hepatic steatosis, cell death, inflammation, and fibrosis, in addition to increased hepatic triglycerides, hepatomegaly, serum insulin and serum ALT. However, unlike human NASH where SREBP-2 and CD36 expression is increased and hepatocyte ballooning is a defining characteristic (Caballero *et al.* 2009; Miquilena-Colina *et al.* 2011), SREBP-2 and CD36 gene expression are unchanged and hepatocyte ballooning is absent in cholesterol-fed $LDLR^{-/-}$ mice.

With regards to the effect of dietary cholesterol in humans, analysis of human NAFLD patients has shown that dietary lipid intake is elevated in those with NASH versus SS and lean controls (Toshimitsu *et al.* 2007). Two separate studies have found significant increases in meat consumption and dietary cholesterol levels in patients with NAFLD versus lean controls (Kim *et al.* 2010; Sathiaraj *et al.* 2011). Dietary cholesterol intake has also been found to be "superabundant" in non-obese patients with NAFLD (Yasutake *et al.* 2009). Further, a retrospective study has found that increased dietary cholesterol is associated with an elevated risk of developing liver cirrhosis (Ioannou *et al.* 2009). Together, data from animal and human studies suggest that dietary cholesterol may play an important role in the progression of NAFLD, although data provided by the non-physiological $LDLR^{-/-}$ and $ApoE^{-/-}$ mouse models restricts the direct translation of findings to the context of human NASH. However, in the *foz/foz* mouse model, which shares key pathophysiological similarities with human NASH, reported elevations in serum ALT levels (Larter *et al.* 2009) correlate strongly with the hepatic cholesterol profiles described in Chapter 3.

5.2 Purpose of study: hypotheses and aims

It is hypothesised that the accumulation of hepatic cholesterol observed in livers of HF-fed *foz/foz* mice with fatty liver (as demonstrated in Chapter 3), contributes to the initiation of NASH, and also to the progression to fibrotic liver disease. To address this hypothesis, a cholesterol-feeding experiment was devised. Specifically, the cholesterol

content of the HF diet was incrementally increased from 0% to 0.2% and 2.0% (w/w), at the expense of dietary carbohydrate. By increasing dietary cholesterol in a step-wise fashion, cholesterol-responsive pathways of liver injury could be delineated in the *foz/foz* model of NASH.

The specific aims of this part of the thesis are to:

1. Determine whether dietary cholesterol loading increases hepatic cholesterol pools in *foz/foz* and WT mice.
2. Assess whether altered hepatic cholesterol profiles affect markers of liver injury (hepatocellular injury, cell death, and inflammatory cell recruitment*) and liver fibrosis.
3. Evaluate the effects of dietary cholesterol on pathways of cholesterol homeostasis and the nuclear transcription factors involved.

***Specific molecular pathways of liver injury and inflammation will be examined in Chapter 7.**

5.3 Methods

5.3.1 Mice and diets

Female WT and *foz/foz* NOD.B10 mice (n=7-11/group) were fed HF-diet (containing either: 0, 0.2, or 2.0% [w/w] cholesterol) 24 weeks. The composition of the three diets is outline in Table 5.1. Note that all earlier experiments (Chapter 3) where "HF-diet" is mentioned used a diet containing 0.2% cholesterol (Table 5.1). Mice were maintained as described in Section 2.3. They were introduced to the HF diet at 8 weeks of age, and weighed each week thereafter. At experimental time points, mice were euthanased and tissues harvested as described in Section 2.4. Peri-ovarian white adipose tissue (WAT) from one side was also collected and weighed.

Table 5.1 Composition of diets used in this study.

Diet		23% Fat, 47% carbohydrate		
		0% cholesterol	0.2% cholesterol	2% cholesterol
Dietary component	Order code	*SF09-026*	*SF03-020*	*SF09-099*
	Ingredient	(g/100 g)		
Non-nutritive bulk	Cellulose	5.000	5.000	5.000
Vitamins and minerals	AIN trace mineral mix #93	0.140	0.140	0.140
	AIN vitamin mix #93	1.000	1.000	1.000
	Methionine	0.300	0.300	0.300
	Calcium carbonate	1.313	1.313	1.313
	Sodium chloride	0.259	0.259	0.259
	Potassium dihydrogen phosphate	0.686	0.686	0.686
	Potassium sulphate	0.163	0.163	0.163
	Potassium citrate	0.248	0.248	0.248
	Choline chloride	0.250	0.250	0.250
Protein	Casein	20.000	20.000	20.000
Carbohydrates	Sucrose	42.351	42.351	40.541
	Starch	5.190	5.000	5.000
Fats	Canola oil	5.000	5.000	5.000
	Cocoa butter	5.000	5.000	5.000
	Copha (hydrogenated vegetable oil)	13.100	13.100	13.100
Cholesterol		0.000	0.200	2.000

All diets were purchased from Specialty Feeds (Glen Forrest, WA, Australia), vacuum packed and stored at 4°C (in dark). Abbreviations: AIN, American Institute of Nutrition; SF, Specialty Feeds.

5.3.2 Procedures

Serum and hepatic lipid fractions were quantified as described in Section 2.5.

Serum insulin was quantified using a commercial kit (Millipore, Billerica, MA) as per the Manufacturer's instructions.

RnD Systems (Minneapolis, MN) ELISA kits were used to determine serum adiponectin as per the Manufacturer's instructions.

SDS-PAGE, western blotting, semi-quantitative qPCR and IHC were carried out as described in Sections 2.10, 2.11, 2.7, and 2.6.2.1, respectively. Primary and secondary antibodies and primers used for western blotting and qPCR are shown in Tables 2.1, 2.2 and 2.3, respectively.

H&E-stained sections were cut and stained by Anne Prins (John Curtin School of Medical Research, ANU, Canberra).

Liver sections were also stained for fibrosis using Sirius red, as described in Section 2.6.1.

H&E and Sirius red-stained sections were blinded and scored by an experienced liver pathologist (Associate Professor Matthew M. Yeh, Department of Pathology, University of Washington Medical Centre, Seattle, WA), using the NAFLD activity scoring (NAS) system (Mendler *et al.* 2005) and Brunt's criteria for fibrotic severity (Kleiner *et al.* 2005). In addition to histopathological assessment, Sirius red-stained liver sections were subject to quantitative image analysis using ImageJ (NIH, Bethesda, MD), as previously described (Kaemmer *et al.* 2010).

Fluorescent microscopy of frozen liver sections was conducted as previously mentioned (Section 2.14). Fluorescent images were captured using a Zeiss Axioplan2 microscope fitted with an Apotome optical sectioning module (Zeiss, GmbH, Germany). Images were analysed with AxioVision V4.8 software (Zeiss, GmbH, Germany).

All statistical analyses were carried out as described in Section 2.15.

5.4 Results

5.4.1 Effect of dietary cholesterol on anatomical parameters in *foz/foz* and WT mice

All groups of HF-fed *foz/foz* mice were significantly heavier than WT littermates from 3 weeks onwards ($P<0.05$, Figure 5.1A) but there was no effect on total body weight between genotype-matched cholesterol feeding groups (NS, Figure 5.1A). Furthermore, hepatomegaly was observed in all *foz/foz* mice irrespective of dietary cholesterol content ($P<0.05$ versus WT mice, Figure 5.1B). Relative liver weights (liver weight as percentage of body weight) increased significantly in *foz/foz* mice fed higher percentages of dietary cholesterol versus 0% cholesterol-fed mice ($P<0.05$, Figure 5.1B). Peri-ovarian white adipose tissue weights were unaffected by inclusion of cholesterol in the HF diet (Figure 5.1C), however it should be noted that the reduced adiposity in *foz/foz* mice compared to WT controls at this age has been previously

reported and is part of the phenotype of inappropriate whole-body lipid partitioning (Larter *et al.* 2009). In summary, these findings indicate that dietary cholesterol directly influences liver weight in HF-fed *foz/foz* mice, with no appreciable effect on body weight or adipose mass.

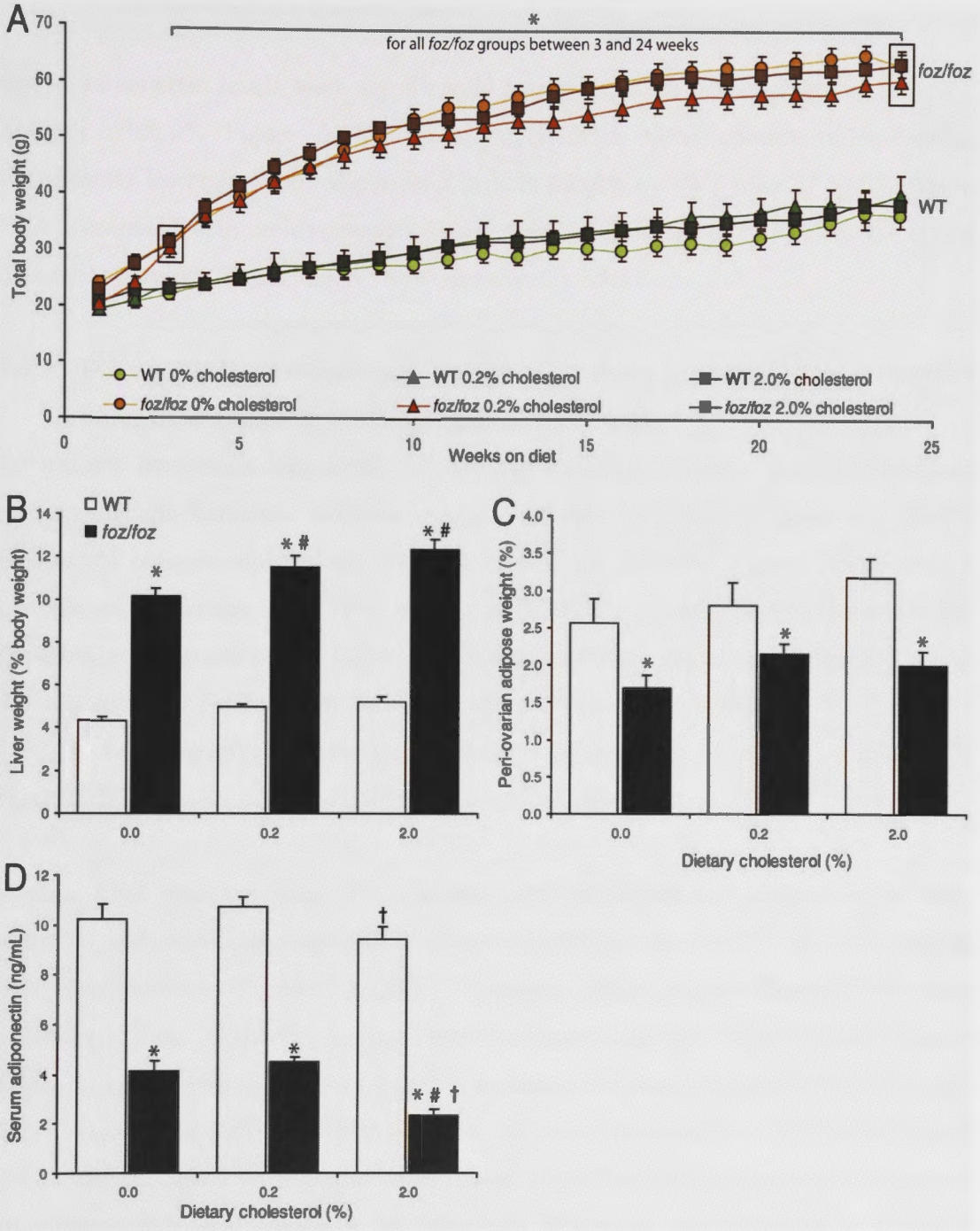

Figure 5.1 Effects of dietary cholesterol on body, liver and adipose tissue weight, and on serum adiponectin levels in *foz/foz* and WT mice.

Legend for Figure 5.1.

(**A**) Total body weight, (**B**) relative liver weight, (**C**) monolateral (RHS) peri-ovarian fat pad weight, and (**D**) serum adiponectin in *foz/foz* (■) and WT (□) mice fed HF diet, containing 0, 0.2, or 2.0% (w/w) dietary cholesterol, over 24 weeks (n=7-11/grp). Liver and adipose weights were calculated as percentages of total body weight. Data are mean ± SEM. *P<0.05, vs. diet-matched control. $^{\#}P$<0.05, vs. genotype-matched, 0.2% dietary cholesterol group. $^{\dagger}P$<0.05, vs. genotype-matched, 0% dietary cholesterol group.

Serum adiponectin levels were significantly lower in *foz/foz* mice compared with WT controls (P<0.05, Figure 5.1A). Interestingly, high (2%) cholesterol/HF-feeding significantly lowered serum adiponectin in both *foz/foz* and WT mice (P<0.05, Figure 5.1A) compared with their respective 0% cholesterol HF-controls; however, the major difference between *foz/foz* and WT mice remained evident.

5.4.2 Dietary cholesterol increases hepatic cholesterol fractions independently of other lipid species in HF-fed *foz/foz* and WT mice

To test the hypothesis that dietary cholesterol content influences hepatic cholesterol loading, hepatic lipidomic analyses were carried out. As expected, increasing dietary cholesterol content substantially elevated hepatic CE (P<0.05, Figure 5.2A), with a corresponding increase in FC (P<0.05, Figure 5.2B). Conversely, hepatic TG and DAG fractions, while significantly higher in HF-fed *foz/foz* compared to HF-fed WT mice, did not increase further with increased dietary cholesterol content (P<0.05, Figure 5.2C,D). Monoacylglyceride (MAG) fractions were found to be variably altered (NS, Figure 5.2E), but again levels failed to correlate with liver injury.

Hepatic FFA fractions were also assessed, with no significant differences in total, saturated, and mono-unsaturated FFA observed in *foz/foz* mice fed HF diet with varying cholesterol content (Figure 5.3A,B,C). Likewise, while polyunsaturated FFA were consistently less in HF-fed *foz/foz* versus corresponding WT mice (P<0.05, Figure 5.3D), there were no differences between cholesterol dietary groups of HF-fed *foz/foz* mice. Analysis of individual FFAs (Table 5.2) was also conducted. Palmitoleic acid (16:1) was the only FFA found to be increased in HF-fed *foz/foz* mice (P<0.05 between all cholesterol groups). However, no significant differences were observed in WT mice irrespective of dietary cholesterol feeding.

Since cholesterol is a precursor for oxysterol formation, hepatic oxysterols were determined using HPLC. There were no significant changes in 7-ketocholesteryl docosahexaenoate (7KD) between dietary cholesterol groups of *foz/foz* mice. 7-Hydroxycholesterol levels, however, and to a lesser extent 4-hydroxycholesterol were significantly elevated in *foz/foz* mice in association with dietary cholesterol content ($P<0.05$, Table 5.3). Other metabolites, including 25-hydroxycholesterol, 7-keto-hydroxycholesterol, and 5,6-epoxycholesterol also showed a strong trend to increase in *foz/foz* mice fed 0.2% and 2% cholesterol versus mice fed HF diet containing no cholesterol (Table 5.3), but none of these apparent changes were significant.

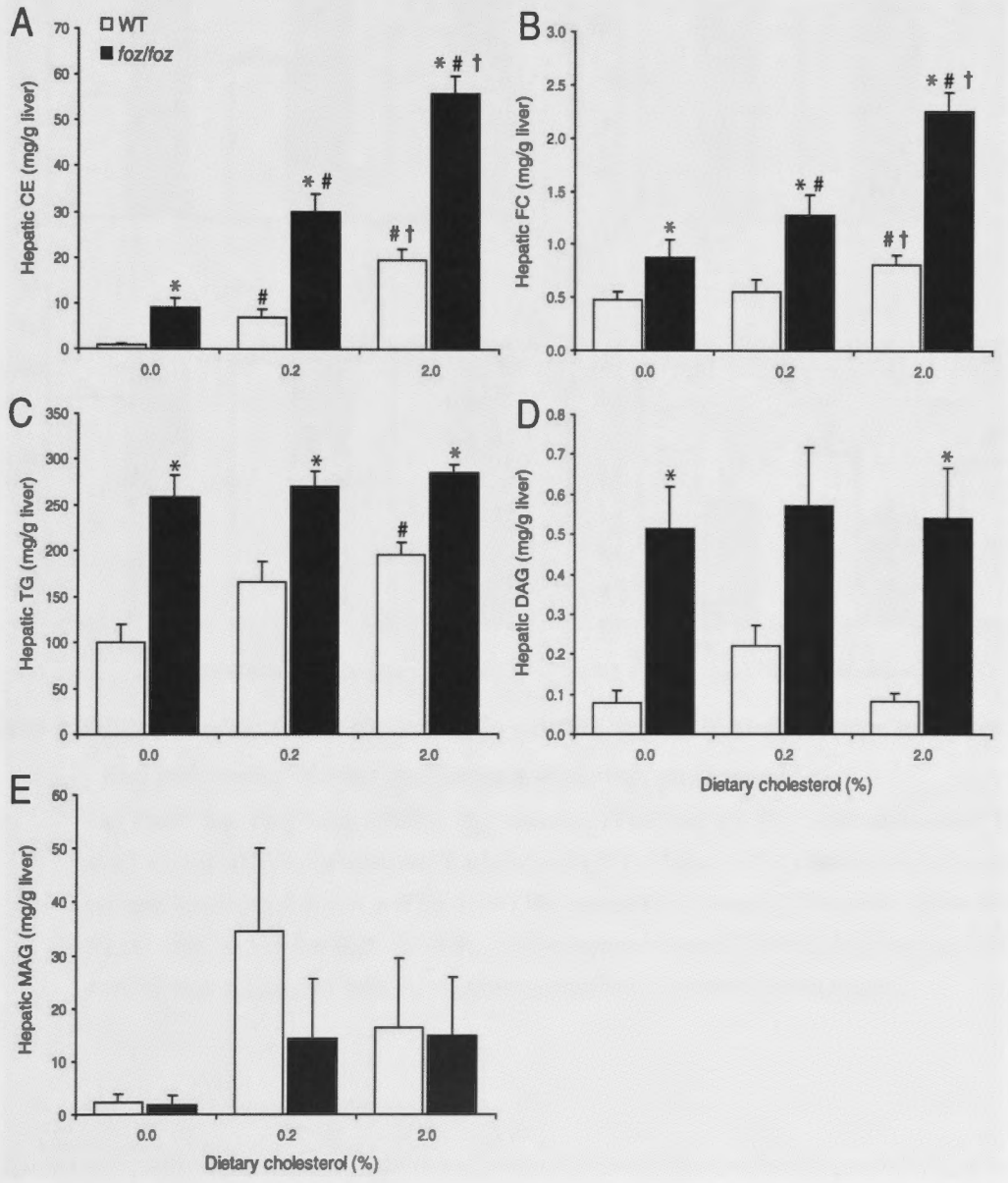

Figure 5.2 Hepatic neutral lipid profiles in *foz/foz* and wildtype mice fed HF diet containing varying percentages of dietary cholesterol

Legend for Figure 5.2.

(**A**) Hepatic cholesteryl ester (CE), (**B**) free cholesterol (FC), (**C**) triglyceride (TG), (**D**) diacylglycerides (DAG), and (**E**) monoacylglycerides (MAG) profiles in *foz/foz* (■) and WT (□) mice fed HF diet, containing 0, 0.2, or 2.0% (w/w) cholesterol, over 24 weeks (n=7-11/grp). Data are mean ± SEM. *P<0.05, vs. diet-matched control. #P<0.05, vs. genotype-matched, 0.2% dietary cholesterol group. †P<0.05, vs. genotype-matched, 0% dietary cholesterol group.

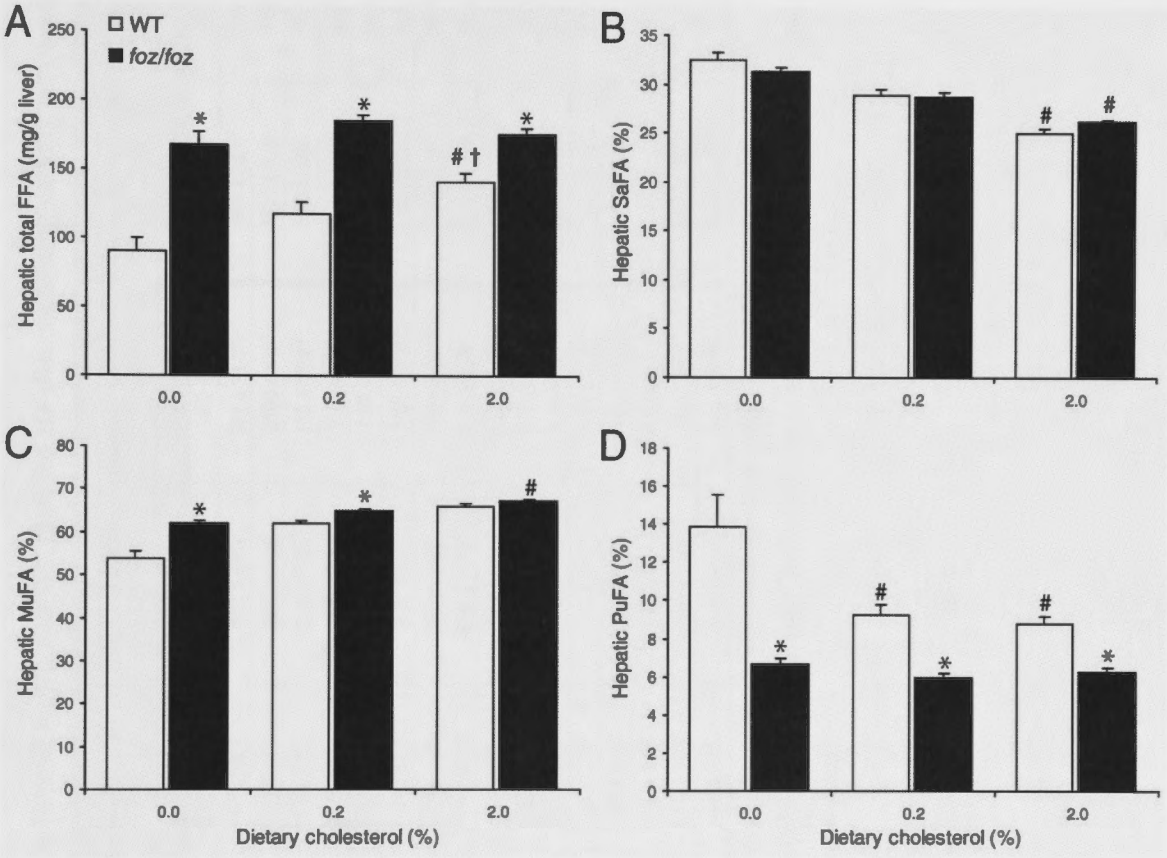

Figure 5.3 Total hepatic free fatty acid lipid profiles in *foz/foz* and wildtype mice fed HF diet containing varying percentages of dietary cholesterol

(**A**) Total free fatty acids (FFA), (**B**) saturated FFAs (SaFA), (**C**) mono-unsaturated FFAs (MuFA), and (**D**) poly-unsaturated FFAs (PuFA) in WT (□) and *foz/foz* (■) mice (n=7-11/grp) fed HF-diet containing 0.0, 0.2 or 2.0% (w/w) cholesterol for 24-weeks. FFAs were determined by HPLC. Data are mean ± SEM. *P<0.05, vs. diet-matched control. #P<0.05, vs. genotype-matched, 0.0% cholesterol groups. †P<0.05, vs. genotype-matched, 0.2% cholesterol groups.

Table 5.2 Profiles of individual free fatty acids in liver of *foz/foz* and WT mice fed HF diet containing varying percentages of dietary cholesterol

Genotype		WT			*Foz/foz*		
FFA	Unit of measurement	HF diet					
		0% Cholesterol	0.2% Cholesterol	2.0% Cholesterol	0% Cholesterol	0.2% Cholesterol	2.0% Cholesterol
Capric acid (10:0)	μg/g liver	9.77 ± 4.97	14.5 ± 2.97	19.2 ± 3.31	6.02 ± 2.99	6.57 ± 2.68	13.6 ± 0.57
Lauric acid (12:0)		402 ± 49.5	442 ± 24.5	571 ± 31.1$^{*\#\dagger}$	468 ± 33.6	443 ± 19.9	426 ± 21.6*
Myristic acid (14:0)		1340 ± 193	1860 ± 115†	2190 ± 140†	1850 ± 129	1880 ± 81.7	1740 ± 72.7
Myristoleic acid (14:1)		45.8 ± 6.57	79.6 ± 7.83†	110 ± 11.4$^{*\#\dagger}$	55.9 ± 5.06	68.11 ± 4.80	77.9 ± 6.51*
Palmitic acid (16:0)	mg/g liver	21.5 ± 3.08	26.0 ± 1.82	25.8 ± 1.35	41.3 ± 2.28*	43.0 ± 1.12*	37.5 ± 1.44*
Palmitoleic acid (16:1)		3.12 ± 0.47	5.68 ± 0.50	7.97 ± 0.54	7.18 ± 0.56*	10.8 ± 0.73*†	13.6 ± 0.95$^{*\#\dagger}$
Stearic acid (18:0)		5.31 ± 0.31	4.77 ± 0.22	5.06 ± 0.18	5.52 ± 0.24†	4.52 ± 0.09†	3.75 ± 0.10*†
Vaccenic acid (18:1)		42.0 ± 5.26	61.0 ± 5.03*†	76.9 ± 4.35$^{*\#\dagger}$	86.9 ± 5.02*	96.1 ± 2.27*	90.6 ± 1.78
Elaidic acid (18:1 trans)		3.94 ± 0.55*	6.95 ± 0.73*†	8.60 ± 0.56*†	10.3 ± 0.74*	14.2 ± 0.78*†	14.8 ± 0.55*†
Linoleic acid (18:2)		4.97 ± 0.34	5.03 ± 0.29	6.43 ± 0.37$^{\#\dagger}$	4.88 ± 0.28	5.44 ± 0.16	5.52 ± 0.18
α-Linolenic acid (18:3)		0.42 ± 0.05	0.38 ± 0.03	0.57 ± 0.05*	0.27 ± 0.02	0.29 ± 0.01	0.32 ± 0.01*
Arachidic acid (20:0)		0.80 ± 0.11*	0.88 ± 0.13*	1.46 ± 0.11*	3.25 ± 0.21*	3.63 ± 0.15*	2.85 ± 0.35*
Dihomo-γ-linolenic acid (20:3)		0.45 ± 0.02*	0.43 ± 0.02*	0.45 ± 0.02*	0.55 ± 0.04*	0.54 ± 0.01*	0.59 ± 0.02*
Arachidonic acid (20:4)		2.28 ± 0.09	1.90 ± 0.08	1.88 ± 0.09	2.33 ± 0.16	2.14 ± 0.05	1.87 ± 0.04†
Eicosapentaenoic acid (20:5)		0.35 ± 0.02	0.33 ± 0.02	0.44 ± 0.03$^{\#}$	0.27 ± 0.03	0.27 ± 0.02	0.35 ± 0.01
Docosapentaenoic acid (22:5)		0.14 ± 0.02	0.10 ± 0.01†	0.09 ± 0.01†	0.14 ± 0.01	0.12 ± 0.01	0.15 ± 0.01*
Docosahexaenoic acid (22:6)		3.02 ± 0.15	2.46 ± 0.09†	2.46 ± 0.11†	2.60 ± 0.17	2.33 ± 0.08	2.31 ± 0.07

Data (mean ± SEM) were determined using HPLC. Lipid number nomenclature is used to detail carbon chain structure (*id est* [*x*:*y*], where *x* and *y* refer to number of carbon atoms and double, unsaturated carbon bonds present in the FFA chain, respectively). $^{*}P<0.05$, vs. diet-matched control. $^{\#}P<0.05$, vs. genotype-matched, 0.2% dietary cholesterol group. $^{\dagger}P<0.05$, vs. genotype-matched, 0% dietary cholesterol group.

Table 5.3 Detectable hepatic oxysterols in *foz/foz* mice fed HF diet containing varying percentages of dietary cholesterol.

Genotype	HF-fed *foz/foz*		
Diet	0% Cholesterol	0.2% Cholesterol	2.0% Cholesterol
4-OH	23.2 ± 2.0	37.7 ± 8.19	$59.0 \pm 7.68^{\dagger}$
5,6-Epoxy	21.0 ± 6.91	22.6 ± 3.15	38.8 ± 4.03
7-KD	$5.0 \times 10^{-5} \pm 2.9 \times 10^{-5}$	0.51 ± 0.51	0.71 ± 0.71
7-Keto	12.0 ± 6.07	21.7 ± 2.51	26.8 ± 3.28
7-OH	0.77 ± 0.42	11.0 ± 5.86	$90.0 \pm 32.9^{\dagger\#}$
24-OH	1.45 ± 0.95	2.1 ± 0.58	1.84 ± 1.23
25-OH	16.3 ± 9.65	51.0 ± 17.3	60.3 ± 23.7

Oxysterol levels in HF-fed WT mice were not analysed due to insufficient tissue. All values represent μg/g wet liver. Data are mean ± SEM. $^{\#}P<0.05$, vs. 0.2% cholesterol groups. $^{\dagger}P<0.05$, vs. 0.0% cholesterol groups. Abbreviations: 4-OH, 4-hydroxy-cholesterol; 5,6-epoxy, 5,6-epoxy-cholesterol; 7-KD, 7-ketocholesteryl docosahexaenoate; 7-keto, 7-keto-cholesterol; 7-OH, 7-hydroxy-cholesterol; 24-OH, 24-hydroxy-cholesterol; 25-OH, 25-hydroxy-cholesterol.

5.4.3 Dietary cholesterol affects serum ALT levels and cholesterol fractions, but fails to alter serum TG, glucose, and insulin in HF-fed *foz/foz* mice

Restricting dietary cholesterol in HF-fed-*foz/foz* mice ameliorated liver injury, as indicated by serum ALT, while high (2%) cholesterol greatly accentuated serum ALT levels ($P<0.05$, Figure 5.4A). Interestingly, ALT levels were significantly increased in 2% cholesterol-HF-fed WT mice ($P<0.05$, Figure 5.4A) compared to their 0% cholesterol HF-fed counterparts, as reported by others (Wang *et al.* 2003). Changes in serum ALT levels in *foz/foz* and WT mice correlated with the observed patterns for serum total and HDL cholesterol, both of which were significantly elevated in *foz/foz* mice fed HF diet containing 0.2% and 2% cholesterol ($P<0.05$, Figure 5.4B,C). More impressively, the profiles of serum ALT (Figure 5.4A) showed remarkable similarities to those of hepatic FC and CE (Figure 5.2A,B). Conversely, serum TG levels were only increased in *foz/foz* mice fed 2% (w/w) cholesterol-HF ($P<0.05$, Figure 5.4D); TG levels in other groups were unchanged (Figure 5.4D).

As shown earlier, hyperglycaemia and hyperinsulinemia were both clearly evident in HF-fed *foz/foz* mice compared with genotype (WT) controls ($P<0.05$, Figure 5.4E,F), but fasting serum insulin and blood glucose levels were unchanged by modulating dietary

cholesterol content. These data suggest that loss of insulin resistance and impaired glucose tolerance are influenced by the high-sucrose/fat content of the HF diet used in this study, not its cholesterol content. Previous studies conducted in *foz/foz* mice have demonstrated that chow-fed animals show physiological serum insulin levels comparable to those of WT controls (Larter *et al.* 2009). The relevance of hyperinsulinemia to regulation of hepatic cholesterol homeostasis was discussed in the previous Chapter (4).

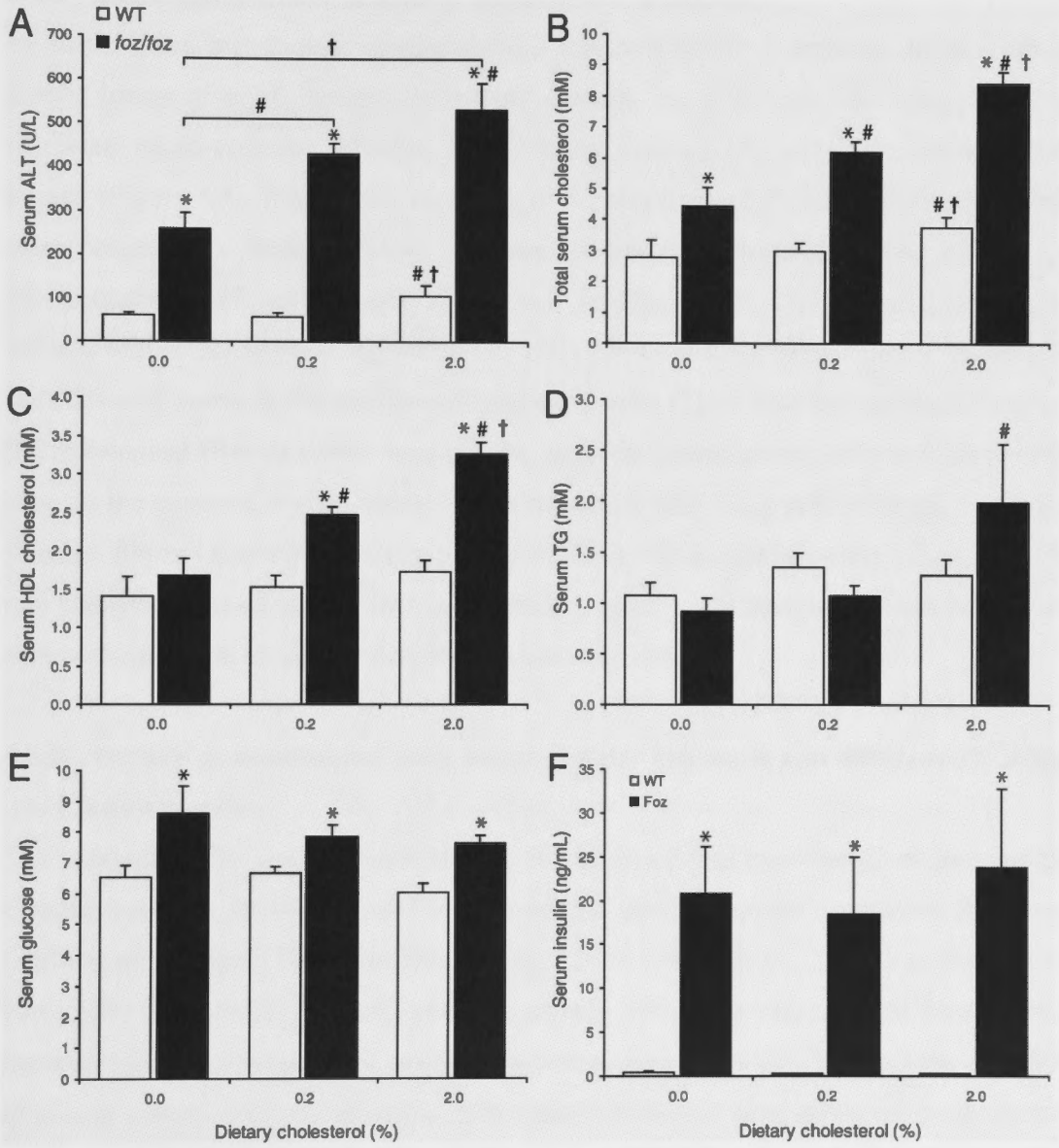

Figure 5.4 Serum ALT and metabolic indices in *foz/foz* and WT mice fed HF diet containing varying percentages of dietary cholesterol

Legend for Figure 5.4.

(**A**) Serum alanine transaminase (ALT), (**B**) total cholesterol, (**C**) HDL cholesterol, (**D**) triglyceride (TG), (**E**) fasting blood glucose, and (**F**) serum insulin in *foz/foz* (■) and WT (□) mice fed HF diet, containing varying percentages of dietary cholesterol, over 24 weeks (n=7-11/grp). Data are mean ± SEM. *P<0.05, vs. diet-matched control. $^{\#}P$<0.05, vs. genotype-matched, 0.2% dietary cholesterol group. $^{\dagger}P$<0.05, vs. genotype-matched, 0% dietary cholesterol group.

5.4.4 Histological effects of dietary cholesterol modulation

In *foz/foz* mice, histological scoring showed identical (grade 3) steatosis in each HF-fed group, irrespective of dietary cholesterol content. In WT mice, however, there was increased micro-vesicular steatosis in the 2.0% versus 0.0% and 0.2% cholesterol-HF groups (Figure 5.5). Progressive increases in hepatocellular ballooning and inflammation were observed in *foz/foz* mice in response to dietary cholesterol loading (Table 5.4); representative H&E micrographs are shown in Figure 5.5. Correspondingly, NAFLD activity scores (NAS) were highest in the 2.0% cholesterol-fed *foz/foz* group, moderate in the 0.2% and lowest in 0% cholesterol-fed *foz/foz* mice (Table 5.4). By qualitative analysis, the histological fibrosis scores were similar between dietary groups, although *foz/foz* mice showed the expected higher fibrosis score than their WT littermates (P<0.05, Table 5.4). Because fibrosis scoring is a discontinuous variable and relatively insensitive to minor but real changes in the density of matrix deposition, quantitative analysis of liver fibrosis was also performed; the results are described in Section 5.4.6.

5.4.5 Dietary cholesterol increases hepatocellular cell death and differentially affects liver inflammation

The similarity of steatosis in each HF-fed *foz/foz* group was expected given that the high carbohydrate and fat content of the diet and the insulin resistance resulting from over-nutrition are likely to be major contributing factors (Larter *et al.* 2009; Van Rooyen and Farrell 2011). However, steatosis *per se* is usually associated with minimal liver injury or hepatic inflammation and does not seem to cause hepatic fibrosis. To establish the effects of dietary cholesterol content on the pathogenesis of NASH from steatosis, we quantitated hepatocyte cell death and macrophage recruitment by IHC. Immunolabeling liver sections with M30 showed a striking increase in hepatocyte cell death in livers of *foz/foz* mice fed cholesterol-supplemented HF diets (P<0.05, Figure 5.6A,B). Thus, increasing cholesterol

content from 0.2% to 2.0% increased cell death from 12 ± 1% of counted hepatocytes to 17 ± 0.4% in HF diet-fed *foz/foz* mice, while absence of cholesterol from the high-fat diet lowered cell death to 4.5 ± 1.0% ($P<0.05$, Figure 5.6A). Interestingly, high (2%) cholesterol/HF-feeding accentuated hepatocyte cell death in WT mice from an average of 3.2 ± 0.5% cell death in 0% and 0.2% cholesterol/HF-fed WT groups to 7.7 ± 0.7% ($P<0.05$, Figure 5.6A,B).

Table 5.4 Effects of dietary cholesterol content on liver histology in *foz/foz* and WT mice.

Genotype	WT			*Foz/foz*		
Diet	HF diet					
	0% Cholesterol	0.2% Cholesterol	2.0% Cholesterol	0% Cholesterol	0.2% Cholesterol	2.0% Cholesterol
Steatosis	0.2 ± 0.1	0.1 ± 0.1	0.4 ± 0.2†	2.8 ± 0.1*	2.9 ± 0.0*	2.8 ± 0.2*
Inflammation	0.1 ± 0.1	0.6 ± 0.1†	0.3 ± 0.3	0.7 ± 0.2	0.9 ± 0.2	1.1 ± 0.3
Ballooning	0	0.3 ± 0.0	0	0.3 ± 0.2	0.5 ± 0.1	1.0 ± 0.3*†
NAS	0.3 ± 0.2	0.1 ± 0.2†	0.7 ± 0.4†	3.9 ± 0.2*	4.3 ± 0.2*†	4.8 ± 0.3$^{*\#\dagger}$
NASH	0/8	0/10	0/8, 1 borderline	0/8	1/9, 8 borderline*†	6/7 NASH, 1 borderline$^{*\#\dagger}$
Fibrosis	0:7/8; 1a:1/8	0:9/10; 2:1/10	0:8/8	1a:2/8; 2:5/8; 3:1/8*	1a:1/9; 2:8/9*	2:7/7*

Data (mean ± SEM) represent histological scores for severity steatosis, inflammation and ballooning, according to criteria of Kleiner *et al.* (2005), previously reported in this model (Larter *et al.* 2009). NAFLD activity score (NAS) and separate designation as NASH, borderline or not NASH, as well as fibrosis scoring of Sirius red-stained liver sections were determined (blinded) by an experienced liver histopathologist (MMY) according to published criteria (Kleiner *et al.* 2005). $^{*}P<0.05$, vs. diet-matched control. $^{\#}P<0.05$, vs. genotype-matched, 0.2% dietary cholesterol group. $^{\dagger}P<0.05$, vs. genotype-matched, 0% dietary cholesterol group.

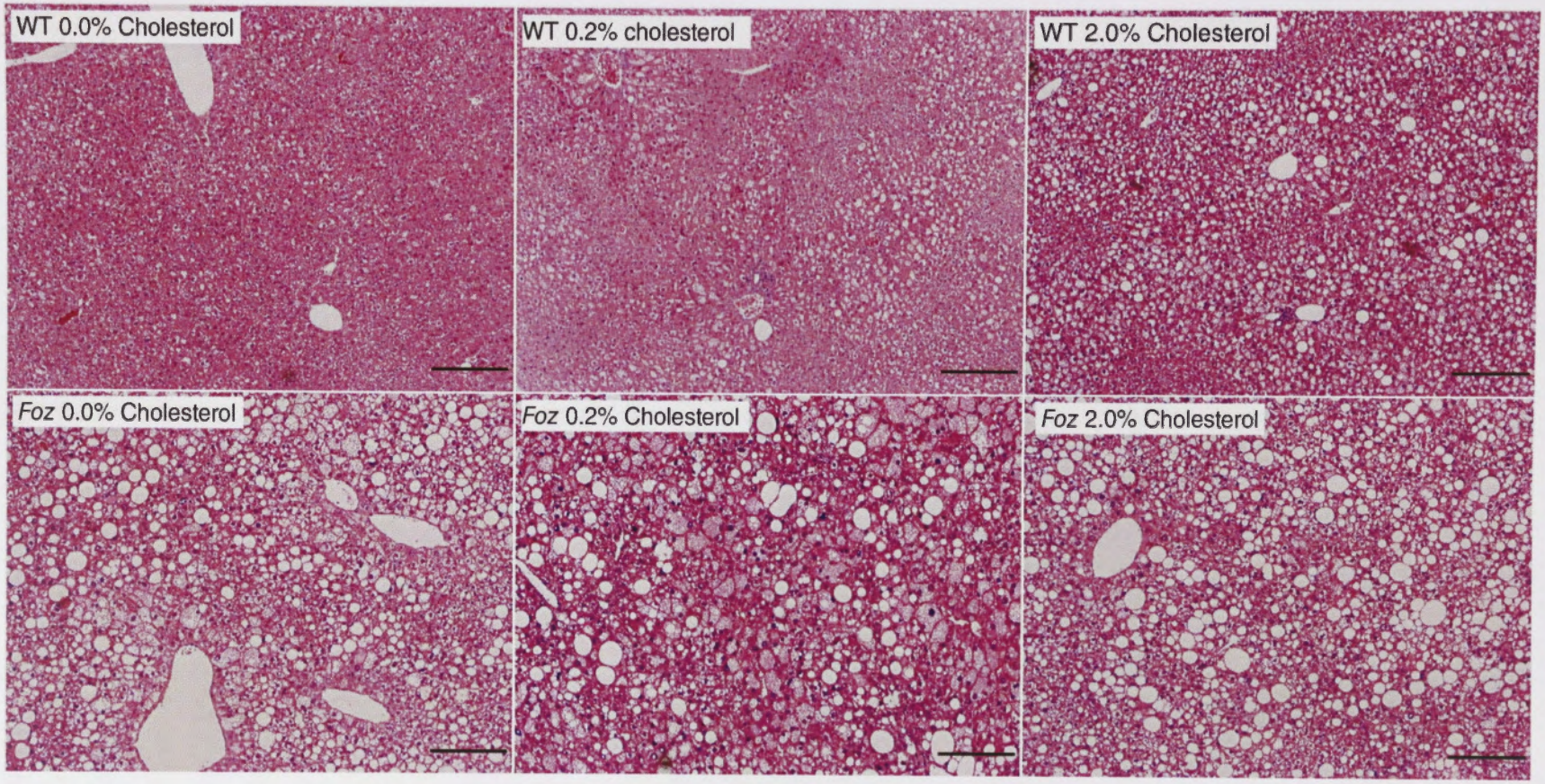

Figure 5.5 Representative H&E-stained liver sections from *foz/foz* and WT mice fed HF diet containing varying percentages of dietary cholesterol

Formalin-fixed liver sections from *foz/foz* and WT mice fed HF diet, containing varying percentages of dietary cholesterol, over 24 weeks (n=7-11/grp), were stained with haematoxylin and eosin (H&E). Histopathological scoring is represented in Table 5.4. Scale bars represent 200 μm.

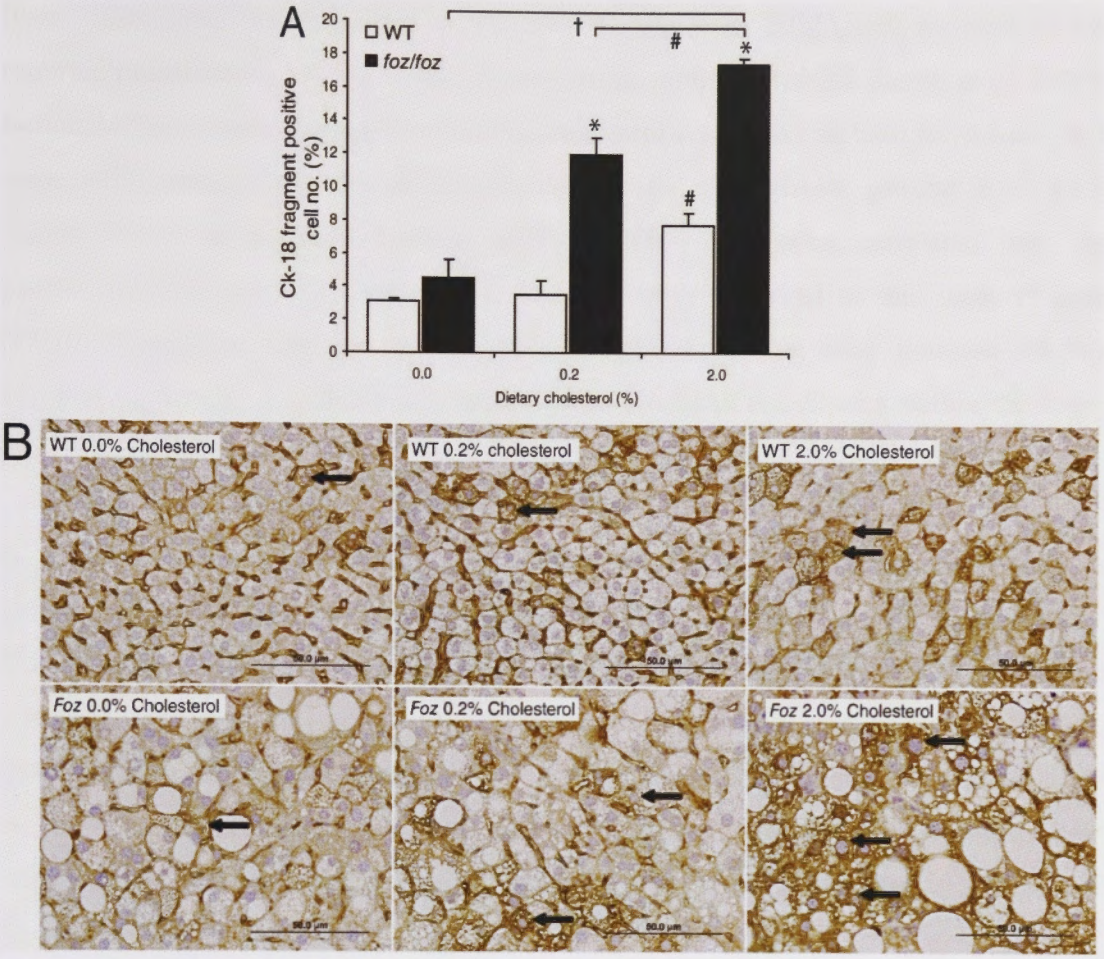

Figure 5.6 Hepatocellular cell death is increased in *foz/foz* and wildtype mice following HF-high cholesterol feeding

(**A**) Quantification of cytokeratin-18 fragmentation epitope (M30) IHC (**B**) in WT (□) and *foz/foz* (■) mice (n=7-11/grp) fed HF-diet containing 0.0, 0.2 or 2.0% (w/w) cholesterol for 24-weeks. Arrows indicate positive staining. Scale bars represent 50 μm. Data are mean ± SEM. *P<0.05, vs. diet-matched control. $^{\#}P$<0.05, vs. genotype-matched, 0.0% cholesterol groups. $^{\dagger}P$<0.05, vs. genotype-matched, 0.2% cholesterol groups.

Similarly, liver F4/80 (macrophage) immmunostaining was increasing by raising dietary cholesterol from 0% through 0.2% to 2.0% in *foz/foz* mice (P<0.05, Figure 5.7A,B). There was also an increase in hepatic macrophage infiltration for 2% cholesterol/HF-fed WT mice versus those fed 0% and 0.2% cholesterol/HF (P<0.05, Figure 5.7A). An interesting feature of livers from *foz/foz* mice is that macrophage localisation occurs predominantly around macrosteatotic (cholesterol-loaded) hepatocytes in 0.2% and 2.0% cholesterol/HF diet-fed groups (Figure 5.7B). Such localisation was not evident in 0% cholesterol/HF-fed *foz/foz* mice. Monocyte chemotactic protein-1 (MCP-1) is a

chemokine responsible for macrophage and hepatic stellate cell recruitment in the liver (Marra *et al.* 1999; Ramm *et al.* 2009; Harada *et al.* 2011), and we have earlier reported raised serum MCP-1 in the HF-fed *foz/foz* model of NASH (Larter *et al.* 2009). Serum MCP-1 levels also appeared to be cholesterol-responsive in both *foz/foz* and WT mice, with increases observed in 2.0% cholesterol-fed mice of both genotypes ($P<0.05$, Figure 5.7C). Furthermore, hepatic MCP-1 mRNA expression correlated with the profile of liver injury for both *foz/foz* and WT mice observed in this study (Figure 5.7D). These data indicate that hepatic cholesterol loading may increase MCP-1 expression, thereby contributing to increased macrophage recruitment within the livers of *foz/foz* mice with NASH.

In Chapter 3, we demonstrated that, within hepatocytes, FC accumulates on the periphery of esterified lipid droplets containing TG and CE (Figure 3.1, Section 3.4.1). To establish whether the peri-steatotic macrophage localisation observed in 0.2 and 2.0% cholesterol/HF-fed *foz/foz* mice is a result of macrophage co-localisation with FC, colocalisation studies were performed. In 0.2% cholesterol/HF-fed *foz/foz* mice, there was colocalisation of F4/80 positive cells and FC (Figure 5.8). This finding is consistent with the proposal that hepatic macrophages may participate in the phagocytosis of FC around lipid-laden hepatocytes.

Neutrophils are also evident in the hepatic inflammatory infiltrate in NASH. In these experiments, the number of neutrophils appeared to increase in *foz/foz* mice fed high (2%) dietary cholesterol, but there was not a significant difference between 0.2% and 0% cholesterol HF-fed *foz/foz* mice (Figure 5.9A,B). It is concluded that while HF feeding profoundly increases hepatic macrophage recruitment (Figure 5.7), hepatic cholesterol loading only has a minor (if any) effect on neutrophil recruitment within the liver.

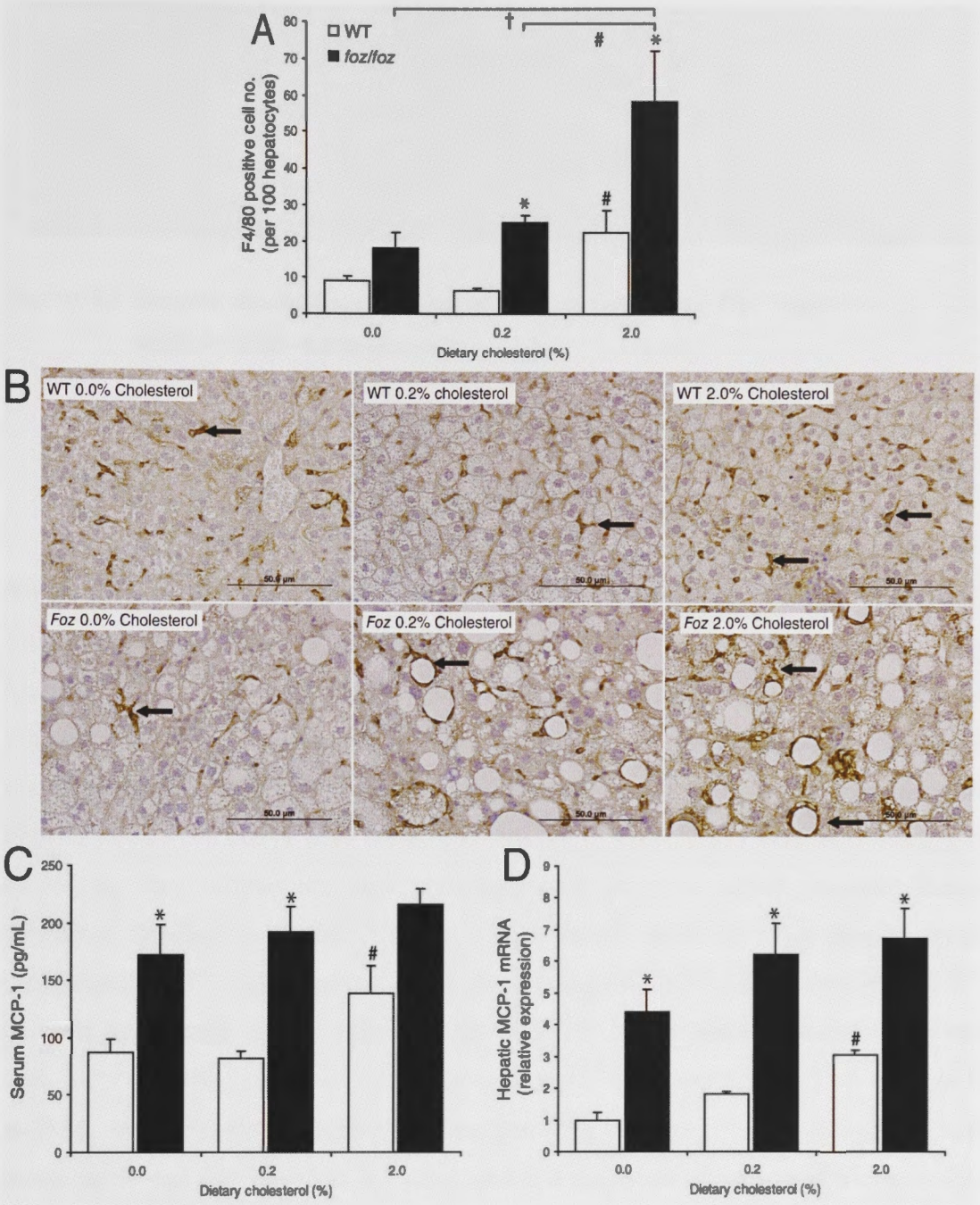

Figure 5.7 High cholesterol feeding increases hepatic macrophage recruitment and monocyte chemotactic protein-1 levels in *foz/foz* and wildtype mice

(**A**) Quantification of EGF-like module containing mucin-like hormone receptor like-1 antigen (F4/80) IHC (**B**), (**C**) serum monocyte chemotactic protein-1 (MCP-1), and (**D**) hepatic MCP-1 mRNA expression in WT (□) and *foz/foz* (■) mice (n=7-11/grp) fed HF-diet containing 0.0, 0.2 or 2.0% (w/w) cholesterol for 24-weeks. Arrows indicate positive staining. Scale bars represent 50 μm. Data are mean ± SEM. *P<0.05, vs. diet-matched control. $^{\#}P$<0.05, vs. genotype-matched, 0.0% cholesterol groups. $^{\dagger}P$<0.05, vs. genotype-matched, 0.2% cholesterol groups.

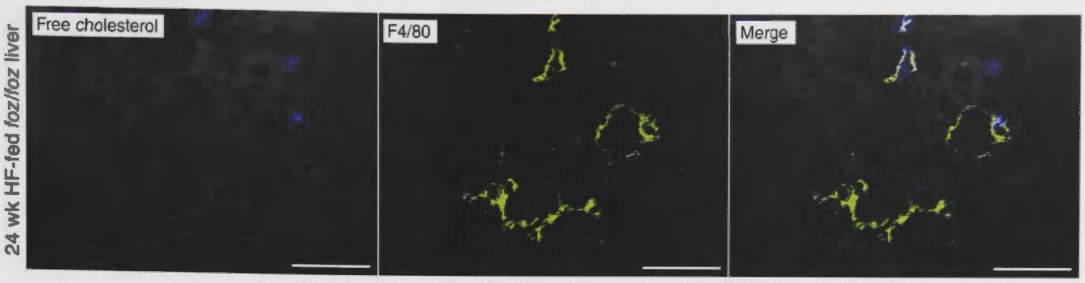

Figure 5.8 Hepatic macrophages colocalise with peri-steatotic free cholesterol in 0.2% cholesterol/HF-fed *foz/foz* mice

Frozen livers from 24 week 0.2% cholesterol/HF-fed *foz/foz* mice were sectioned (6 μm) and stained for free cholesterol (blue) using filipin and EGF-like module containing mucin-like hormone receptor like-1 antigen (F4/80) labelled using fluorescein isothiocyanate (FITC; green) as described in Section 2.14. Merged Scale bars represent 50 μm.

5.4.6 Hepatic fibrosis is altered by modulating hepatic cholesterol in *foz/foz* mice

To quantitatively evaluate liver fibrosis, whole liver protein homogenates were immunoblotted for α-smooth muscle actin (α-SMA), a marker of stellate cell activation related to hepatic fibrogenesis in NASH (Nouchi *et al.* 1991; Yamaoka *et al.* 1993; Cortez-Pinto *et al.* 2001). It has also been reported by others that MCP-1 participates in hepatic stellate cell activation following liver injury (Marra *et al.* 1999). Following their activation, they differentiate into myofibroblasts, an event which promotes matrix deposition leading to hepatic fibrosis (Olsen *et al.* 2011). α-SMA protein levels increased in all HF-fed groups of *foz/foz* mice compared to 0% cholesterol HF-fed WT controls, and values were significantly higher in 2% cholesterol-fed animals compared with 0.2% and 0% cholesterol-fed *foz/foz* mice ($P<0.05$, Figure 5.10A). This increase in α-SMA protein levels confirms that hepatic stellate cell activation occurs to a greater extent in HF-fed *foz/foz* versus WT mice, and that the extent of activation is exacerbated by increased hepatic cholesterol.

Hepatic fibrosis deposition was then measured by analysis of Sirius red-stained liver sections, using the ImageJ colourmetric deconvolution method (Kaemmer *et al.* 2010). Sirius red stains connective tissue red (Figure 5.10B). Image analysis showed progressive increases in Sirius red-positive areas in *foz/foz* mice fed HF diet containing increasing cholesterol content ($P<0.05$, Figure 5.10B; representative Sirius red-stained liver sections are shown in panel C). The area of Sirius red staining in 2% cholesterol HF-fed *foz/foz* mice was approximately double that of 0% cholesterol HF-fed *foz/foz*

mice. Collectively, these findings indicate that increased hepatic FC content modulates liver fibrosis in the *foz/foz* model of obesity and diabetes-related NASH.

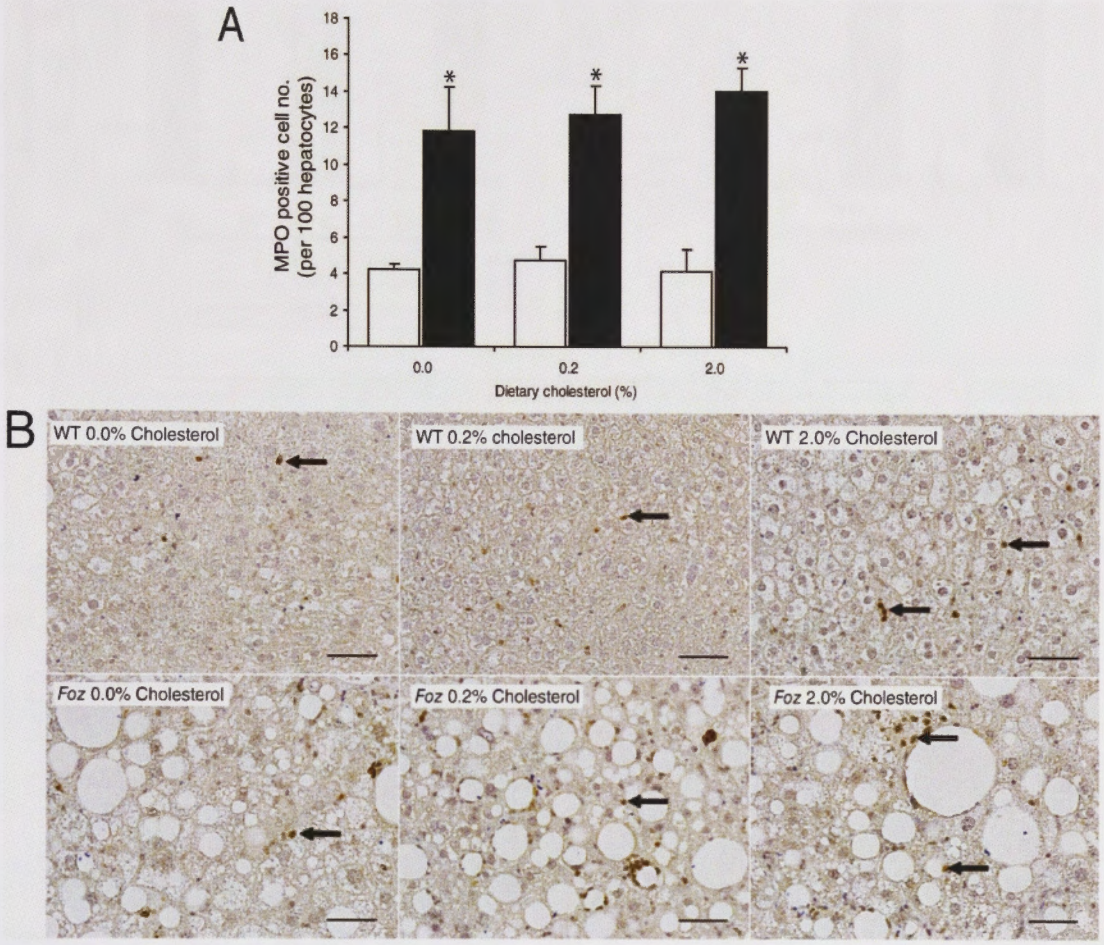

Figure 5.9 There is no change in hepatic neutrophil recruitment with high-cholesterol feeding in *foz/foz* and WT mice

(**A**) Quantification of myeloperoxidase (MPO) positive cell IHC (**B**) in WT (□) and *foz/foz* (■) mice (n=7-11/grp) fed HF-diet containing 0.0, 0.2 or 2.0% (w/w) cholesterol for 24-weeks. Arrows indicate positive staining. Scale bars represent 50 μm. Data are mean ± SEM. *P<0.05, vs. diet-matched control. $^{\#}P$<0.05, vs. genotype-matched, 0.0% cholesterol groups. $^{\dagger}P$<0.05, vs. genotype-matched, 0.2% cholesterol groups.

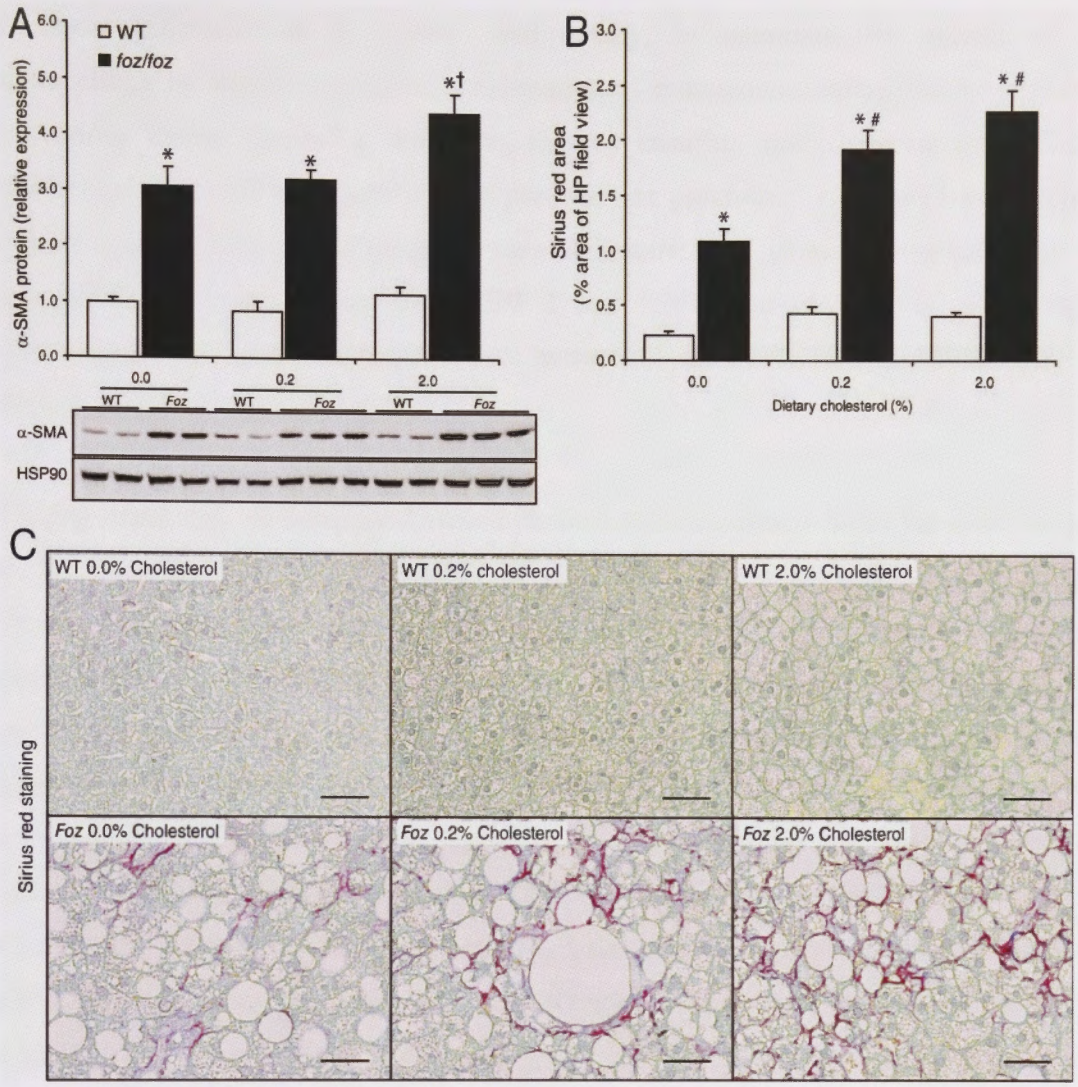

Figure 5.10 Analysis of liver fibrosis markers in *foz/foz* and wildtype mice fed HF diet containing varying percentages of dietary cholesterol

(**A**) α-Smooth muscle actin (α-SMA) protein expression and (**B**) quantitative analysis of Sirius-red stained liver sections (representative sections are shown in panel **C**) in WT (□) and *foz/foz* (■) mice (n=7-11/grp) fed HF-diet containing 0.0, 0.2 or 2.0% (w/w) cholesterol for 24-weeks. Sirius red image analysis was carried out as described in Section 2.6.1. α-SMA protein expression was normalised to heat-shock protein-90 (HSP90). Scale bars represent 50 μm. Data are mean ± SEM. *P<0.05, vs. diet-matched control. $^{\#}P$<0.05, vs. genotype-matched, 0.0% cholesterol groups. $^{\dagger}P$<0.05, vs. genotype-matched, 0.2% cholesterol groups.

5.4.7 Analysis of pathways of cholesterol homeostasis in *foz/foz* and WT mice fed varying percentages of dietary cholesterol

As previously mentioned, the liver is physiologically responsible for regulation of whole body cholesterol homeostasis in mammals. This is achieved through balanced regulation of LDL and HDL uptake, cholesterol synthesis, and forward cholesterol

transport (Dietschy *et al.* 1993). Additionally, in mammals the uptake of extracellular FC results in feedback suppression of endogenous cholesterol biosynthesis in various tissues (including the liver), thereby ensuring against excess intracellular cholesterol levels (Tabas 2002). This process, (as previously mentioned in Sections 1.4.1.1 and 1.4.1.2), is facilitated by several factors; they include the localisation of intracellular FC, the ability of SREBP-2 and HMGR to respond to intracellular cholesterol levels, and a delicate balance between nuclear SREBP-2 and LRH-1/HNF-4α transcription factor expression.

Having previously demonstrated altered cholesterol homeostasis in *foz/foz* mice fed the 0.2% cholesterol HF diet (Chapter 3), it seemed relevant to examine whether dietary cholesterol content had any separate effect on the major pathways of cholesterol homeostasis. The presence of dietary cholesterol increased hepatic expression of LDLR protein ($P<0.05$ in 0.2 and 2.0% cholesterol/HF-fed *foz/foz* mice *versus* 0% and appropriate WT controls, Figure 5.11A). Compared with WT controls, ACAT2 protein expression was also increased in all *foz/foz* mouse groups, but there was no additive effect of dietary cholesterol content ($P<0.05$ versus WT groups, Figure 5.11B). Conversely, ACAT2 mRNA gene expression was reduced in *foz/foz* and WT fed high (2%) cholesterol compared to their corresponding 0% cholesterol controls ($P<0.05$, Figure 5.11C). No significant changes in ACAT1 mRNA were observed for *foz/foz* mice, while 2% cholesterol significantly suppressed ACAT1 gene expression in WT mice compared with 0% and 0.2% cholesterol-fed controls (Figure 5.11D). Interestingly, dietary cholesterol (0.2% and 2%) significantly enhanced CEH gene expression in *foz/foz* mice ($P<0.05$), while no changes were observed in WT mice (NS, Figure 5.11E). Importantly, absence of dietary cholesterol normalised CEH mRNA in *foz/foz* mice (Figure 5.11E).

HMGR activity is inhibited post-transcriptional by phosphorylation of Ser^{872} in humans and Ser^{871} in rodents (Sato *et al.* 1993; Omkumar *et al.* 1994; Istvan *et al.* 2000). Assessment of total (pan) HMGR expression (Figure 5.12A), phosphorylated Ser^{871} of HMGR (Figure 5.12B) and the ratio between the two sub-populations (Figure 5.12C) allowed quantification of HMGR inhibition. The ratio of phosphorylated Ser^{871} HMGR:total HMGR was markedly increased in *foz/foz* mice ($P<0.05$ *versus* diet-

matched WT controls, Figure 5.12C), with no significant effect of dietary cholesterol content.

Cholesterol biotransformation pathways were differentially affected by modulating dietary cholesterol content. As shown in Chapter 3, Cyp7a1 gene expression was profoundly suppressed in *foz/foz* mice compared with diet-matched WT littermates ($P<0.05$, Figure 5.13A). In WT mice, however, Cyp7a1 mRNA levels appeared to rise in mice fed increasing amounts of dietary cholesterol, although not significantly so (Figure 5.13A). In contrast, Cyp7b1 mRNA was significantly lowered in 2% cholesterol/HF-fed WT mice versus other genotype-matched dietary groups ($P<0.05$, Figure 5.13B). In patterns similar to Cyp7a1, both Cyp7b1 and Cyp27a1 mRNA levels were markedly lower in *foz/foz* mice versus diet-matched WT controls ($P<0.05$, Figures 5.13B,C), indicating that, irrespective of hepatic cholesterol content, *foz/foz* mice exhibit impaired ability to express the enzymatic pathways responsible for biotransformation of cholesterol to bile acids.

With regards to bile acid and cholesterol export pathways, both hepatic Bsep and ABCG8 protein expression levels were suppressed in *foz/foz* mice versus WT controls ($P<0.05$, Figures 5.13D,E). Notable reductions in Bsep and ABCG8 protein were also observed in WT mice fed 2% cholesterol/HF ($P<0.05$, Figures 5.13D,E). Interestingly, reductions in Bsep and ABCG8 protein expression associated with 2% cholesterol feeding in WT mice were associated with increased liver injury (serum ALT), hepatocellular cell death, and inflammation.

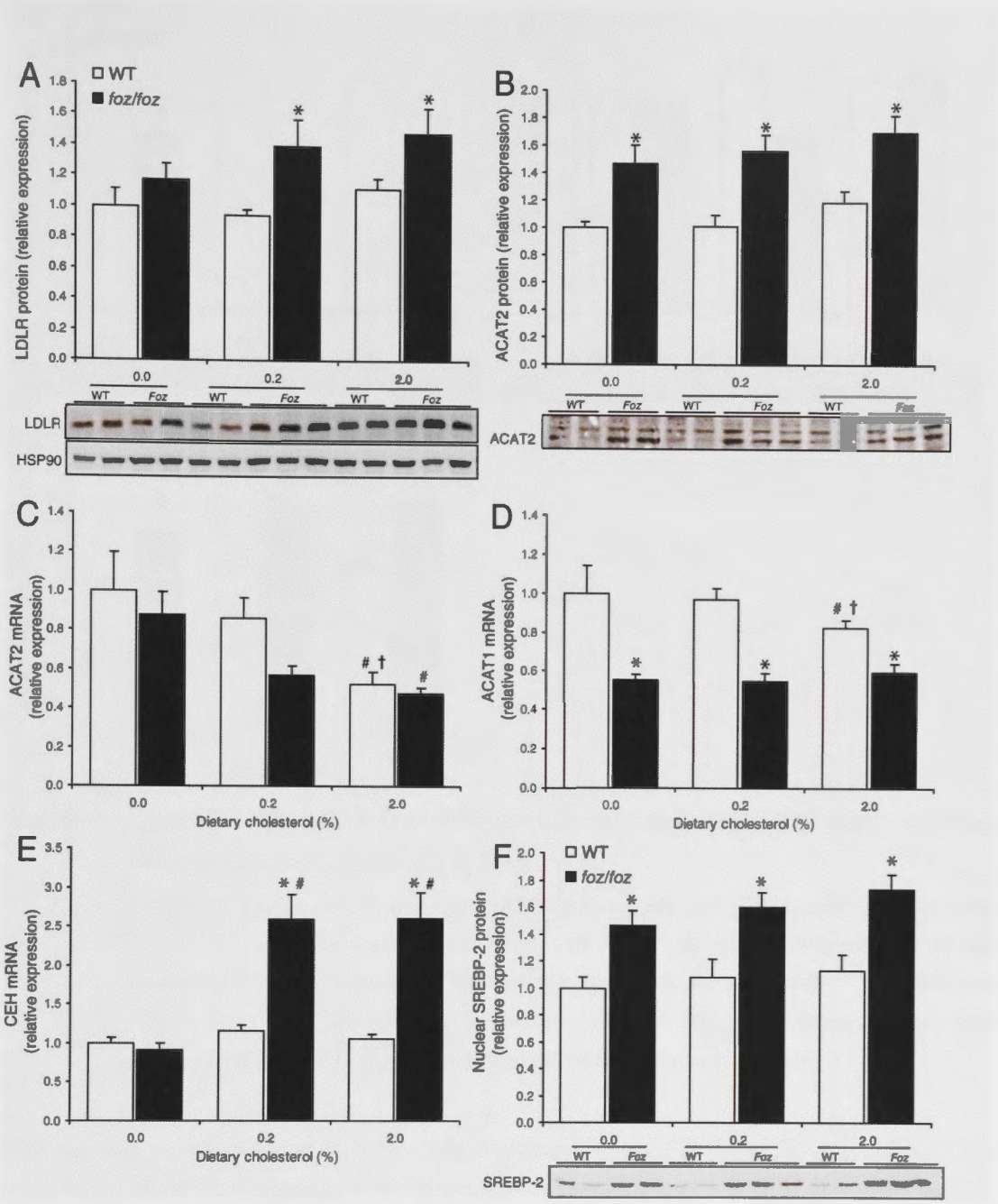

Figure 5.11 Cholesterol uptake, esterification and ester hydrolysis pathways in *foz/foz* and wildtype mice fed HF diet containing varying percentages of dietary cholesterol

(**A**) Hepatic LDLR protein, (**B**) ACAT2 protein and (**C**) mRNA, and (**D**) ACAT1 mRNA, (**E**) CEH mRNA, and (F) nuclear SREBP-2 protein in WT (□) and *foz/foz* (■) mice (n=7-11/grp) fed HF-diet containing 0.0, 0.2 or 2.0% (w/w) cholesterol for 24-weeks. Protein expression was normalised to HSP90 protein (panel A). Data are mean ± SEM. *P<0.05, vs. diet-matched control. $^{\#}P$<0.05, vs. genotype-matched, 0.0% cholesterol groups. $^{\dagger}P$<0.05, vs. genotype-matched, 0.2% cholesterol groups.

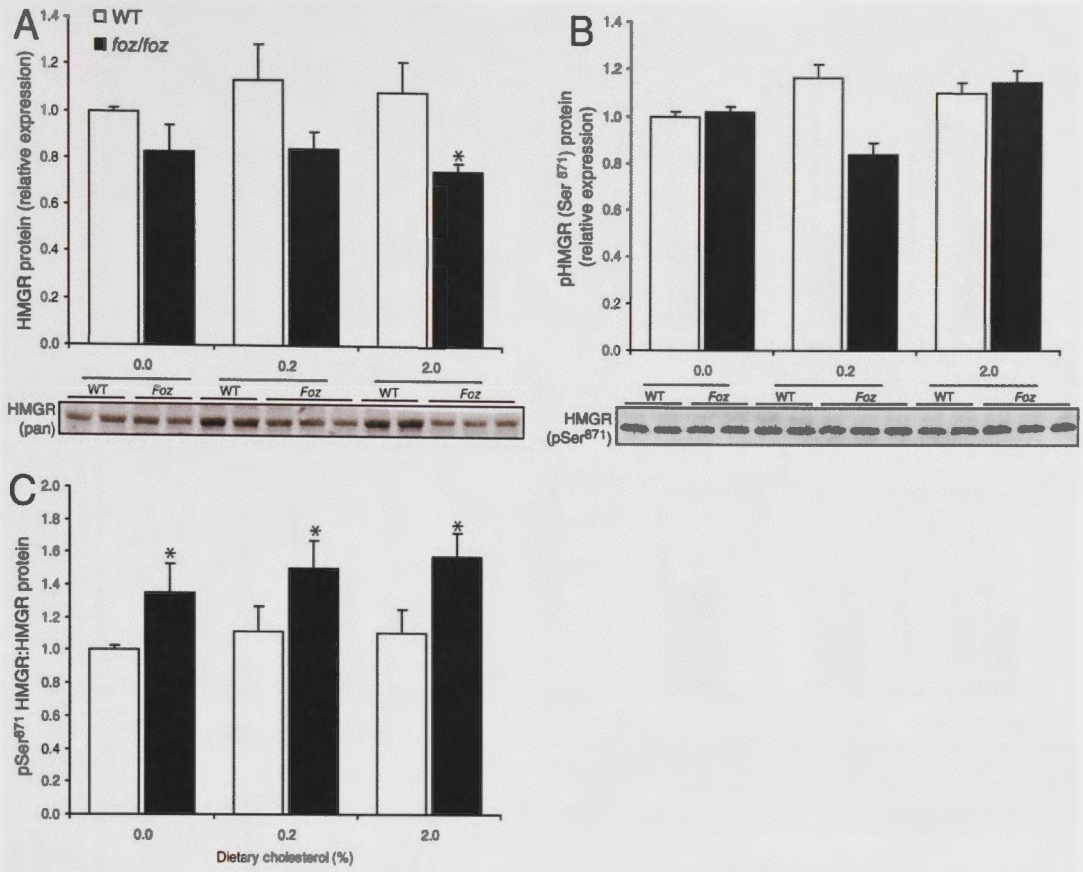

Figure 5.12 Hepatic HMG-CoA reductase protein is phosphorylated at Ser^{871} following HF, high-cholesterol feeding in *foz/foz* mice

(**A**) Hepatic expression of total (pan) HMG-CoA reductase (HMGR) and (**B**) phosphorylated Ser^{871} HMGR protein (pSer^{871}) in WT (□) and *foz/foz* (■) mice (n=7-11/grp) fed HF-diet containing 0.0, 0.2 or 2.0% (w/w) cholesterol for 24-weeks. (**C**) Ratio of Ser^{871} phosphorylated HMGR:pan HMGR protein. Data are mean ± SEM. $^{\#}P<0.05$, vs. genotype-matched, 0.0% cholesterol groups. $^{\dagger}P<0.05$, vs. genotype-matched, 0.2% cholesterol groups.

Noting that modulation of dietary cholesterol and altered hepatic FC and CE profiles were associated with differentially regulated cholesterol uptake, storage, biosynthesis, and export pathways in both *foz/foz* and WT mice (Figures 5.11, 5.12, 5.13), it was also appropriate to assay expression levels of the key nuclear transcription factors that regulate cholesterol homeostasis. Nuclear SREBP-2 protein levels were significantly higher in *foz/foz* mice versus WT controls ($P<0.05$, Figure 5.11F), and although not significant, there seemed to be an effect of hepatic cholesterol loading on nuclear SREBP-2 protein expression in *foz/foz* mice (NS, Figure 5.11F).

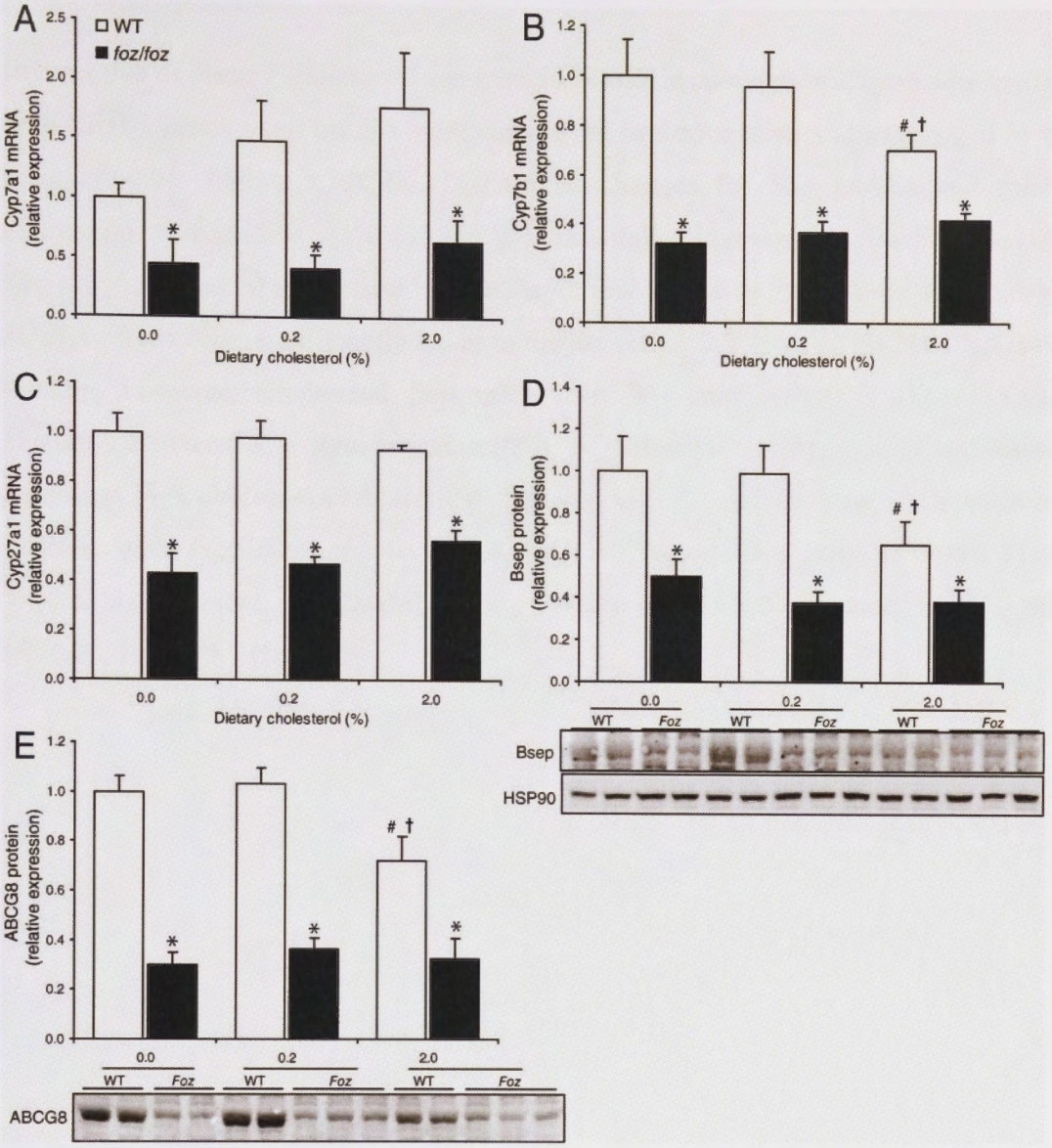

Figure 5.13 Dietary cholesterol differentially alters cholesterol biotransformation and export pathways in *foz/foz* and wildtype mice

(**A**) Hepatic Cyp7a1, (**B**) Cyp7b1, and (**C**) Cyp27a1 mRNA, (**D**) Bsep and (**E**) ABCG8 protein in WT (□) and *foz/foz* (■) mice (n=7-11/grp) fed HF-diet containing 0.0, 0.2 or 2.0% (w/w) cholesterol for 24-weeks. Protein expression was normalised to HSP90 protein (panel A). Data are mean ± SEM. *P<0.05, vs. diet-matched control. $^{\#}P$<0.05, vs. genotype-matched, 0.0% cholesterol groups. $^{\dagger}P$<0.05, vs. genotype-matched, 0.2% cholesterol groups.

In contrast, HNF-4α mRNA expression was markedly lower in *foz/foz* mice versus diet-matched WT controls, irrespective of hepatic cholesterol-loading (P<0.05, Figure 5.14B). Cholesterol-feeding, however, significantly reduced HNF-4α mRNA expression in WT mice, the extent of which was proportional to dietary cholesterol content (P<0.05, Figure 5.14B).

Irrespective of dietary cholesterol and hepatic FC/CE accumulation, expression levels of both LRH-1 protein and mRNA were suppressed in *foz/foz* mice and unchanged in WT mice ($P<0.05$, Figure 5.14C,D). Differential changes for Shp protein and mRNA expression were evident in *foz/foz* and WT mice following hepatic cholesterol loading. Shp protein appeared to increase in both *foz/foz* and WT mice (NS, Figure 5.14E), while mRNA levels, were significantly lower in *foz/foz* versus WT mice ($P<0.05$). Cholesterol feeding, however, suppressed Shp mRNA in WT mice ($P<0.05$, Figure 5.14F). Disparity between Shp protein and mRNA is indicative of Shp protein stabilisation following high cholesterol/HF feeding. Patterns of FXR mRNA were identical to Shp mRNA, with *foz/foz* expression lower than WT counterpart mice ($P<0.05$, Figure 5.14F). Furthermore, cholesterol-feeding suppressed FXR expression in WT mice ($P<0.05$, Figure 5.14F).

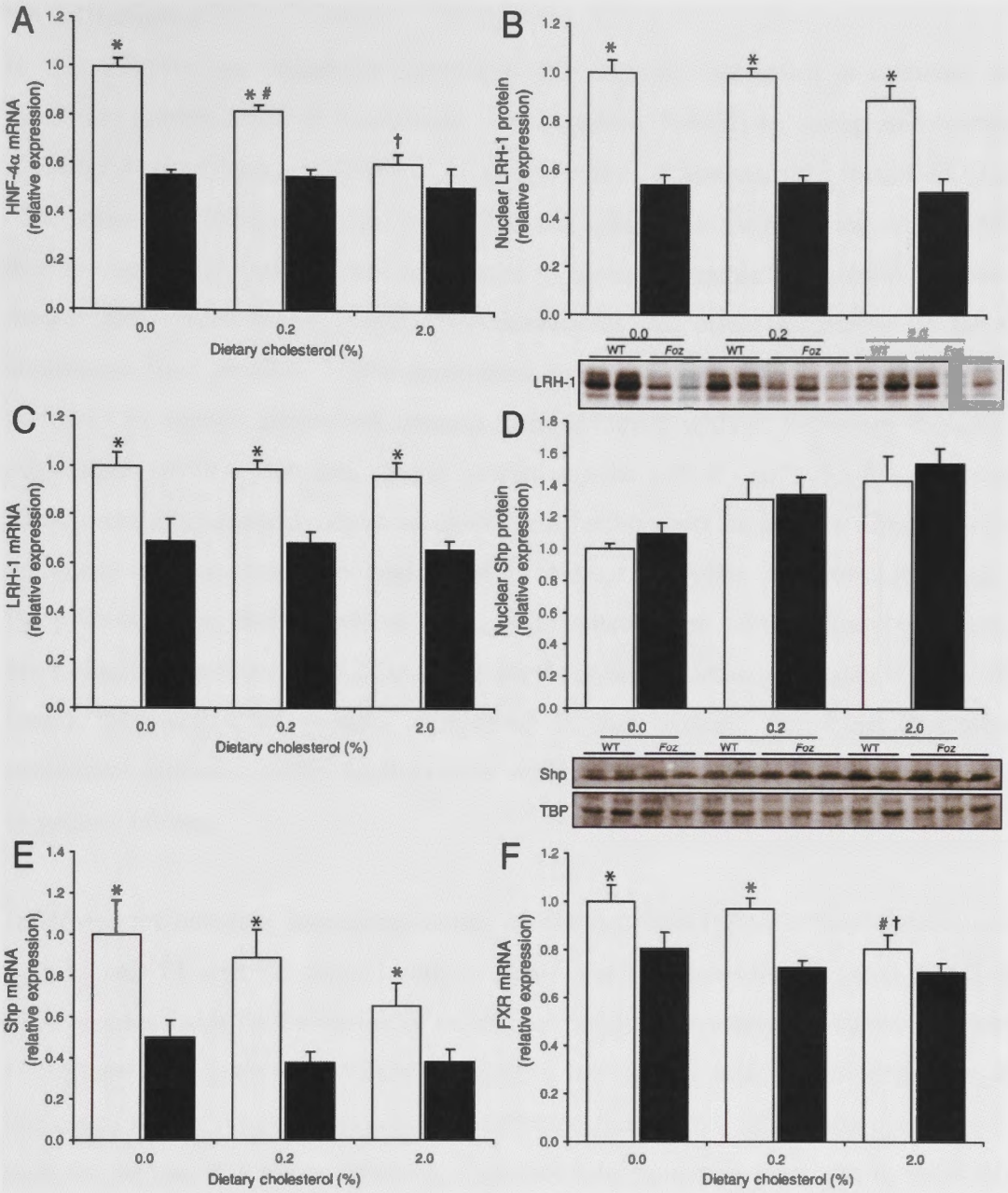

Figure 5.14 Analysis of cholesterol-regulating nuclear transcription factors in *foz/foz* and wildtype mice fed HF diet containing varying percentages of dietary cholesterol

(**A**) HNF-4α mRNA, (**B**) nuclear LRH-1 protein and (**C**) mRNA, (**D**) nuclear Shp protein and (**E**) mRNA and (**F**) FXR mRNA in WT (□) and *foz/foz* (■) mice (n=7-11/grp) fed HF-diet containing 0.0, 0.2 or 2.0% (w/w) cholesterol for 24-weeks. Protein expression was normalised to TATA box binding protein (TBP; panel E). Data are mean ± SEM. *P<0.05, vs. diet-matched control. $^{\#}P$<0.05, vs. genotype-matched, 0.0% cholesterol groups. $^{\dagger}P$<0.05, vs. genotype-matched, 0.2% cholesterol groups.

5.5 Discussion

In this Chapter, we tested the hypothesis that hepatic cholesterol is involved with mediating the transition of steatosis to steatohepatitis (NASH) by acting as a lipotoxic mediator of liver injury in NAFLD. Having previously demonstrated increased LDLR expression and reduced HMG-CoA reductase activity in *foz/foz* mice with NASH, dietary cholesterol loading was anticipated to increase hepatic cholesterol profiles in *foz/foz* mice. Such dietary cholesterol modulation did effect alterations in hepatic cholesterol lipid profiles. The experimental design of this study allowed incremental increases in hepatic cholesterol content to be achieved without important changes in other lipid species. Previous studies carried out in $LDLR^{-/-}$ and $ApoE^{-/-}$ mice have simply tested cholesterol versus no cholesterol feeding and studied the effects on liver pathology in mice genetically engineered to be inept in hepatic cholesterol handling. In the present study, three levels of dietary cholesterol were used, namely 0 (which is physiological for rodents), 0.2 (as in the previous experiments in Chapter 3) and 2.0% (w/w). Modulation of hepatic cholesterol in this manner, permitted cholesterol-responsive pathways within the liver to be studied independently of other environmental or genetic factors.

In HF-fed *foz/foz* mice, increasing dietary cholesterol from 0.2 to 2.0% (w/w) increased both hepatic FC and CE content with no significant alterations in TG, DAG, MAG and FFA profiles (with the exception of palmitoleic acid). Conversely, restriction of dietary cholesterol (0% [w/w]) significantly lowered hepatic FC and CE. Impressively, the pattern of serum ALT changes closely reflected the profiles of hepatic cholesterol in both *foz/foz* and WT mice. Moreover, hepatocellular apoptosis (assessed by M30 IHC) and hepatic macrophage infiltration all increased with cholesterol loading in the livers of *foz/foz* and WT mice, and fibrosis was elevated in *foz/foz* mice. Conversely, restricting dietary cholesterol lowered these indices. Thus, the major finding of this Chapter is the existence of a direct correlation between the extent of hepatic cholesterol accumulation and the severity of liver injury, hepatomegaly, cell death, inflammation, and fibrosis.

Removing dietary cholesterol significantly reduced liver injury in *foz/foz* mice. However, hepatic cholesterol profiles were still significantly higher in 0% cholesterol/HF-fed *foz/foz* mice versus WT littermates (Figure 5.3). Taken together,

these data support the hypothesis proposed in Chapter 3, in which hepatic cholesterol profiles, while largely reflective of dietary cholesterol, are also influenced (to a quantitatively lesser extent) by nascent cholesterol biosynthesis.

In *foz/foz* mice fed HF diet, increasing or removing dietary cholesterol failed to alter the extent of hepatic steatosis. In WT mice, high (2%) cholesterol did induce a minor, albeit significant, increase in steatosis. Cholesterol loading increased hepatocyte ballooning degeneration in *foz/foz* but not WT mice. These data suggest that, in *foz/foz* mice, dietary cholesterol has no effect on liver steatosis, which occurs in both chow and HF-feeding as the result of over-nutrition and insulin resistance, exacerbated by hypoadiponectinemia (Arsov *et al.* 2006a; Larter *et al.* 2009). Histologically, steatosis scores generally reflect hepatic TG profiles (Vuppalanchi *et al.* 2007). In this study, there was no correlation between hepatic steatosis and/or TG levels and liver injury. Our study therefore supports the non-widely held contention that hepatic TG accumulation is benign and does not contribute to NAFLD progression (Neuschwander-Tetri 2010a, 2010b). High cholesterol (2%)/HF feeding, however, significantly increased hepatomegaly (as assessed by elevations in liver weight) in *foz/foz* mice. The reasons for this increase were not studied here, but likely reflect contributions from liver CE (Figure 5.2A) and hepatic fibrosis (Figure 5.10), as well as possible expansion of hepatocyte size as part of ballooning degeneration.

NAS scores are largely reflective of the extent of steatosis because NAS is calculated from the sum of steatosis (0-3), lobular inflammation (0-3), and hepatocyte ballooning scores (0-3). Hepatocyte ballooning correlates with the degree of liver injury in steatotic *foz/foz* mouse livers. It is a key feature of NASH in humans and an independent predicator of the risk of disease progression (Matteoni *et al.* 1999; Brunt *et al.* 2004; Yeh and Brunt 2007). Others have hypothesised (without direct evidence) that steatosis contributes towards oxidative stress (Tandra *et al.* 2010) and mitochondrial dysfunction in NAFLD; the latter could exacerbate hepatic insulin resistance (Rector *et al.* 2010). If this contention is correct, hepatic steatosis may contribute to insulin resistance in the *foz/foz* model and predispose hepatocytes (and possibly adipocytes; Figure 5.15) to injury induced by hepatic cholesterol loading.

The design of the present experiments, with removal of dietary cholesterol from the HF diet, or studying dietary cholesterol in the same diet at two increasing doses, is more detailed than that of earlier studies. Use of this approach in *foz/foz* mice, in which the *Alms1* mutation perturbs appetite regulation rather than cholesterol transport function, allowed for definitive delineation of the role of cholesterol in NASH pathogenesis. Several inconsistencies exist in contemporary transgenic $LDLR^{-/-}$ and $ApoE^{-/-}$ mouse models of diet-induced NASH. $LDLR^{-/-}$ knockout mice, for example, develop hyperinsulinemia, but fail to upregulate liver SREBP-2 (Subramanian *et al.* 2011), whereas $ApoE^{-/-}$ mice develop hepatic inflammation which induces LDLR, SREBP-2, and SCAP expression (Ma *et al.* 2008), but display enhanced (not decreased) insulin-sensitivity (Hofmann *et al.* 2008). In humans, SREBP-2 is elevated in NASH versus simple steatosis and lean patients (Caballero *et al.* 2009). It is therefore plausible that hepatic LDLR may also be elevated, but to date no studies have reported on hepatic LDLR expression in human NASH. In the *foz/foz* model, the metabolic abnormalities reflect those observed in humans with metabolic syndrome, without genetic manipulation of lipid metabolism as observed in $LDLR^{-/-}$ and $ApoE^{-/-}$ mouse models. The *Alms1* mutation is unlikely to have any direct effect on hepatic lipid transport and management. As previously mentioned (Section 1.10.3), Alms1 is involved in ciliogenesis and physiological cilial functioning (Li *et al.* 2007; Jagger *et al.* 2011). Hepatocytes lack a primary cilium (De La Iglesia and Porta 1967; Seeley and Nachury 2010). Furthermore, the host laboratory has established that Alms1 localises to the centrosome basal body in neural cells cultured from the hypothalamus of WT mice and is absent in *foz/foz* mice (Heydet *et al.* 2010). The basal body is the site of attachment of primary cilia which express appetite-regulating peptides. In *foz/foz* mice, the number of neuronal cilia decreases by ~70% shortly after birth (Heydet *et al.* 2010) and it has been proposed that this loss contributes to hypothalamic leptin resistance, molecular pathways of which are clearly evident in the hypothalamus of *foz/foz* mice. Given these considerations, we believe it is unlikely that the *Alms1* mutation has any direct effect on hepatic lipid handling in *foz/foz* mice.

Cell death is a key feature of lipotoxicity (Malhi and Gores 2008), and constitutes a defining characteristic of NASH as opposed to simple steatosis (Feldstein *et al.* 2003). In this study, hepatocellular apoptosis was significantly elevated in cholesterol-laden livers, and substantially lowered in livers with suppressed cholesterol content. In

macrophages, particularly in atherosclerotic lesions, FC contributes directly to cell death by apoptosis (Guyton and Klemp 1996; Gelissen *et al.* 1998; Kellner-Weibel *et al.* 1998; Yao and Tabas 2000; Blom *et al.* 2010). However, an alternative proposal is that oxysterols may represent a lipotoxic lipid mediator in atheroma (Li *et al.* 2001; Ryan *et al.* 2005; Larsson *et al.* 2006; Lordan *et al.* 2008). It is therefore salient to note that, in addition to increased hepatic cholesterol, 7-hydroxy-cholesterol (7-OH) and 4-hydroxy-cholesterol (4-OH) were markedly increased in *foz/foz* mice in a dietary cholesterol-responsive manner ($P<0.05$, Table 5.3) with lesser increases (NS) in 7-keto and 25-hydroxycholesterol metabolites also noted. Oxysterols have been shown to be cytotoxic in several cell types (Zhou *et al.* 1993b; Lemaire-Ewing *et al.* 2005; Lee *et al.* 2007; Shibata and Glass 2010). Hepatic oxysterols are predominantly generated by autoxidation or enzymatic oxidation of cholesterol (Schroepfer 2000; Iuliano 2011). Cyp7a1 enzyme activity may explain specific elevations in hepatic 7-OH levels. Therefore, Cyp7a1 activity present in *foz/foz* mice (even if significantly lower in *foz/foz* versus WT mice), could catalyse hydroxylation of cholesterol to form 7-OH, which would subsequently accumulate due to impaired BA export (consequence of suppressed Bsep protein expression). Either intracellular FC and/or 7-OH may contribute to the increases in hepatocellular cell death observed in *foz/foz* mice. In order to correlate the pattern of liver injury with hepatic 7-OH and 4-OH oxysterol content, levels in WT mice would need to be assessed, but due to limitations on available liver tissue, oxysterol content in WT mice could not be measured in this study. Another approach to testing the individual or interactive roles of FC, 7-OH and other oxysterols in lipotoxicity would be to expose hepatocytes to them using an *in vitro* (primary hepatocyte culture) system.

While no significant changes in neutrophil recruitment were reported in this study, hepatic macrophage migration, serum MCP-1 levels and hepatic MCP-1 mRNA levels were all proportional to hepatic cholesterol levels in *foz/foz* mice. Hepatic MCP-1 expression and macrophage infiltration have been shown to increase in $LDLR^{-/-}$ mice following high (0.15%-0.25%) cholesterol/HF-feeding (Rull *et al.* 2009; Subramanian *et al.* 2011). In the present study, macrophages within the livers of 2.0% and 0.2% cholesterol/HF-fed *foz/foz* mice show increased hepatic infiltration and accumulate predominantly around macro-steatotic lesions within the liver (Figure 5.7). This phenomenon has also been reported in high cholesterol/HF-fed $LDLR^{-/-}$ mice (Wouters

et al. 2008; Subramanian *et al.* 2011). Furthermore, fluorescent colocalisation between mouse F4/80 (macrophage marker) and cholesterol (stained for using filipin) in *foz/foz* mice identified a spatial relationship between macrophages and hepatic FC deposited in the hepatocyte plasma membrane (Figure 5.8). This finding suggests that hepatic macrophages may be conscripted into the liver in response to increased deposition of FC (or oxysterols) in certain hepatocytes, or in response to hepatocytes damaged by such cholesterol accumulation (Figure 5.15). Further studies are needed to establish whether cholesterol-laden hepatocytes secrete MCP-1. If so, this would explain how peripheral macrophages are recruited to specific cholesterol-laden cells within the livers of *foz/foz* mice. The present study showed increased serum MCP-1 and total hepatic MCP-1 mRNA gene expression (Figure 5.7C,D), indicating the plausibility of this hypothesis.

Corresponding to increased hepatocellular cholesterol content, enhanced hepatic fibrosis was observed in 2.0% and 0.2% cholesterol/HF-fed *foz/foz* mice (Figure 5.10). This correlation between dietary cholesterol and liver fibrosis is consistent with data from a retrospective study in humans, where dietary cholesterol content was predictive of liver cirrhosis irrespective of etiology (Ioannou *et al.* 2009); as described in the Introduction (Section 5.1), there are similar data for NAFLD, but results are inconsistent and more studies are required. If, as demonstrated in *foz/foz* mice in this study, dietary cholesterol intake in humans predicates hepatic cholesterol loading, hepatocellular cell death and inflammation may also occur. These processes may in turn, lead to recruitment and activation of hepatic stellate cells which subsequently secrete the collagen matrix responsible for liver fibrosis, as summarised in Figure 5.15. A more detailed experimental exploration of potential pathways of cholesterol induced liver injury and inflammation is presented in Chapter 7.

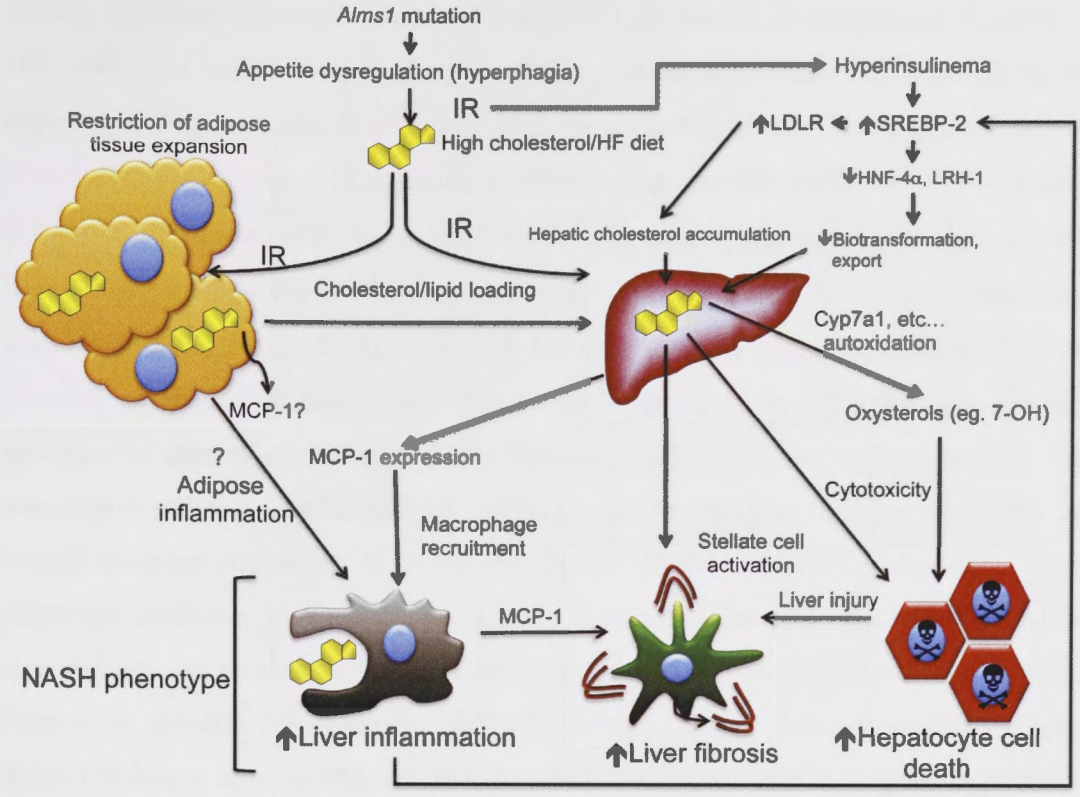

Figure 5.15 Proposed pathways of cholesterol-induced NASH in *foz/foz* mice.

The *Alms1* mutation results in hyperphagia in *foz/foz* mice. HF-feeding induces insulin resistance and steatohepatitis (NASH). Hyperinsulinemia alters cholesterol homeostasis, leading to increased cholesterol uptake and decreased biotransformation of cholesterol to BAs, as well as suppressed cholesterol and BA export. This culminates in hepatic cholesterol loading, which has pleiotropic effects, including increased cell death of hepatocytes, hepatic MCP-1 expression, macrophage recruitment, and liver fibrosis. We have not ruled out the role of cholesterol-induced adipose inflammation, which would likely increase serum MCP-1 levels and possibly contribute to hepatic cholesterol levels, as well as to insulin resistance via effects of TNFα on insulin receptor signalling. Adipose restriction as previously described in HF-fed *foz/foz* mice (Larter *et al.* 2009) limits cholesterol storage in this tissue and would likely exacerbate cholesterol loading in the liver. Note that neutrophils are not discussed in this schema, partly because they seem less responsive (or unresponsive) to hepatic cholesterol accumulation, but also for clarity. Recruitment mechanisms could include oxidative stress, chemokines (IL-6, IL-8, etc…) and high-mobility group box 1 protein (HMGB1). This is discussed in Chapter 7.

Abbreviations: 7-OH, 7-hydroxycholesterol; HF, high-fat; HNF-4α, hepatocyte nuclear factor-4α; IR, insulin resistance; LDLR, LDL receptor; LRH-1, liver receptor homolog-1; MCP-1, monocyte chemotactic protein-1; NASH, non-alcoholic steatohepatitis; SREBP-2, sterol responsive element binding protein-2.

In concert with HNF-1α and -3β, HNF-4α participates in the promotion of murine miR-122 (Xu *et al.* 2010). In the context of the present study, and unlike WT mice, *foz/foz* mice display significantly lower LRH-1 protein and mRNA expression irrespective of

dietary cholesterol content (Figure 5.14C,D). This results in suppressed Cyp7a1, 7b1, and 27a1 mRNA expression, in addition to reduced Bsep and ABCG8 protein expression (Figure 5.13). Conversely, WT mice display similar LRH-1 protein levels, although there appeared (NS) to be a reduction in the 2% cholesterol/HF-fed group (Figure 5.14). On the other hand, HNF-4α mRNA expression was significantly lower in high 2% cholesterol-fed WT mice, in a pattern which correlates with dietary cholesterol content ($P<0.05$, Figure 5.14B). As miR-122 is transcriptionally regulated by HNF-4α, lowered expression of this micro-RNA could be expected in WT mice fed increasing amounts of dietary cholesterol. More recently, miR-122a and miR-422a have been found to destabilise Cyp7a1 mRNA within human hepatocytes (Song *et al.* 2010). This would subsequently result in increased Cyp7a1 mRNA, thereby accounting for the observed increases in Cyp7a1 evident in cholesterol-fed WT mice. More detailed experiments are needed to further clarify this specific aspect of Cyp7a1 regulation in fatty liver disease. Interestingly, miR-122 is significantly down-regulated in human NASH (Cheung *et al.* 2008), which suggests that Cyp7a1 mRNA may be less stable in individuals with severe NAFLD.

5.6 Summary of findings

The key findings of this study are as follows:

1. Hepatic FC and CE lipid profiles can be modulated substantially in HF-fed *foz/foz* mice by altering dietary cholesterol content, whereas livers of WT mice are relatively refractory to dietary cholesterol loading.
2. Although there is a close correlation between FC and the pathological features of lipotoxicity, some oxysterol metabolites of cholesterol, notably 7-OH, 4-OH and 25-OH also accumulate in NASH livers. A separate, interactive or even central role for these metabolites as mediators of some features of NASH is not excluded by the present experiments.
3. Increased hepatic cholesterol is associated with increased liver injury (serum ALT), hepatocellular cell death (by apoptosis), liver macrophage infiltration, and fibrosis, the combination of which is a pathological hallmark of NASH.
4. Hepatic macrophages colocalise with FC adjacent to esterified lipid (TG and CE)-laden macro-steatotic lesions in cholesterol-fed *foz/foz* mice.
5. Neutrophils accumulate in the HF-fed *foz/foz* model of NASH, but unlike macrophages such recruitment appears unrelated to hepatic FC levels.

6. Increased inflammation may further enhance SREBP-2 and LDLR expression in *foz/foz* mice, thereby constituting an alternative pathway in addition to insulin-dependent regulation as shown in Chapter 4.

In summary, the results of this study demonstrate that hepatic FC loading, via dietary cholesterol modulation, is *ipso facto* capable of modulating hepatic injury, inflammation and fibrosis in NAFLD. These findings therefore support the overall hypothesis that hepatic cholesterol is able to mediate the pathogenesis of NASH. An alternative or additional role of oxysterol metabolites cannot be excluded and requires separate study. In the next Chapter, pharmacological interventions are used to determine whether administration of cholesterol uptake and/or biosynthesis modulating drugs can also decrease hepatic FC content and ameliorate hepatic injury. Finally, in Chapter 7, pathways of liver cholesterol-mediated injury and inflammation will be examined.

CHAPTER 6

Inhibition of cholesterol uptake and biosynthesis ameliorates liver injury in *foz/foz* mice with non-alcoholic steatohepatitis

6.1 Introduction

In Chapter 5, use of dietary cholesterol modulation to load *foz/foz* (*Alms1* mutant) hepatocytes with FC and CE resulted in significantly increased hepatocellular apoptosis, hepatic macrophage recruitment and accentuated liver fibrosis in these obese, diabetic mice with NASH. Conversely, restriction of dietary cholesterol lowered hepatic cholesterol content largely resolved liver injury (as assessed by serum ALT), hepatocellular apoptosis, inflammation, and liver fibrosis. These data support the primary hypothesis of this research, that hepatic cholesterol is involved in the pathogenesis of NASH in the *foz/foz* mouse model. To date, however, the links between hepatic cholesterol stores and liver injury, inflammation, and fibrosis in this model are largely associative, and although the dietary manipulation experiments effected changes consistent with the proposed pathogenic role of cholesterol in NASH, there are important differences between the dietary cholesterol content in rodents and humans. It has been proposed that dietary cholesterol content could be relevant to NASH pathogenesis in humans, at least in non-obese Japanese (Yasutake *et al.* 2009). Enjoji and Nakamuta (2010) have proposed that dietary cholesterol could be an effective therapeutic strategy in NASH. At the present time, there are few if any data to support this contention. A further test of the "cholesterol hypothesis" in NASH would be to use pharmacological approaches to lower hepatic cholesterol content.

In mammals, dietary sources and *de novo* biosynthesis of nascent cholesterol both contribute to bodily cholesterol pools (Vuoristo and Miettinen 1982; Luc *et al.* 1989). Further, as discussed later, cholesterol transporters regulate not only the intestinal uptake of cholesterol (discussed in Chapter 1, Sections 1.2 and 1.8), but also tissue uptake and redistribution of cholesterol. For instance, NPC1L1 which is the rate limiting transporter responsible for intestinal cholesterol uptake, is also abundantly

expressed in hepatocytes, and in livers showing NASH (Chapter 3, Section 3.4.7). Use of a cholesterol synthesis inhibitor, and/or cholesterol transport inhibitor could therefore not only lower serum cholesterol levels, but potentially remove the deposition of cholesterol that occurs in the livers of *foz/foz* mice with NASH. Further, since blocking either the cholesterol synthesis or cholesterol transport pathway could lead to reciprocal increases in the converse pathway, a combined drug strategy could be more effective than either type of agent used above.

In the present Chapter, two inhibitors were used in the *foz/foz* mouse model, namely atorvastatin and ezetimibe, to inhibit both the biosynthetic and cholesterol uptake/reclamation pathways, respectively.

6.1.1 Atorvastatin: the world's most popular hypocholesterolemic drug

Atorvastatin ([3R,5R]-7-[2-{4-fluorophenyl}-3-phenyl-4-{phenylcarbamoyl}-5-propan-2-ylpyrrol-1-yl]-3,5-dihydroxyheptanoic acid), originally termed CI-981, is a HMGR "statin" inhibitor first engineered by Bruce Roth and colleagues in 1985 (Shaw *et al.* 1990; Baumann *et al.* 1992). It is now the most popular prescribed statin worldwide (2004), and as of 2003, the largest-selling pharmaceutical drug in history (Simons 2003). Statins refer to a broad class of competitive inhibitors, which bind to the catalytic domain of HMGR, thereby preventing the conversion of HMG-CoA to mevalonic acid. In turn, this halts the biosynthesis of nascent cholesterol (Petras *et al.* 1999; Istvan and Deisenhofer 2001). There are two classes of statins, divided on the basis of inhibitor structures. Type I statins are modelled around a central decalin ring, while type II inhibitors, are characterised by the presence of fluorophenyl and methylethyl moieties (Istvan 2003).

Atorvastatin is a type II statin (see Figure 6.1Ai and Aii for spatial orientation and compound structure, respectively). The molecular backbone mimics structural aspects of HMG-CoA, while the side residues have been engineered to stabilise bonding interactions between atorvastatin and HMGR; this improves binding affinity (Clarke *et al.* 2007). The characteristic type II fluorophenyl group of atorvastatin interacts with the Arg^{590} residue of the catalytic domain of HMGR (Figure 6.2), while the hydroxyl and carboxyl moieties of the dihydroxyheptanoic acid side chain of atorvastatin interacts with Ser^{684}, Asp^{690}, Lys^{691}, and Lys^{692} residues (Figure 6.2C,D) (Istvan 2003).

Atorvastatin is further stabilised by the propan moiety attached to the central pyrrole ring; this interacts with the hydrophobic pocket created by Leu^{562}, Val^{683}, Leu^{853}, Ala^{856}, and Ala^{857} residues (Figure 6.2D) (Istvan and Deisenhofer 2001; Istvan 2002).

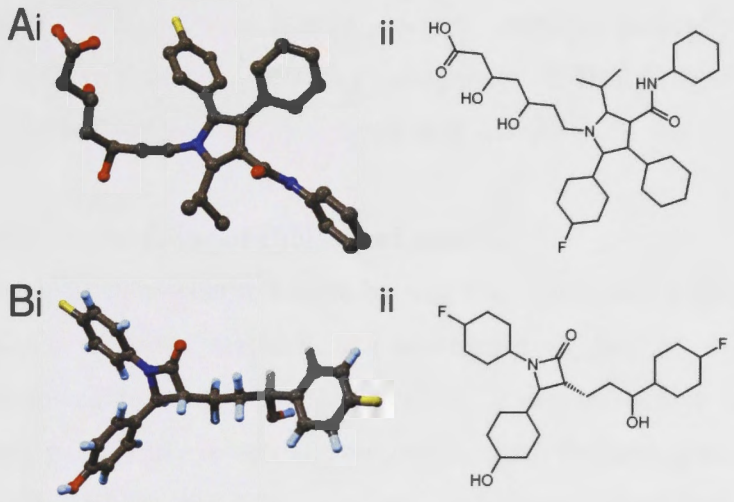

Figure 6.1 Spatial and schematic representations of atorvastatin and ezetimibe.

(**i**) Molecular ball-and-stick spatial geometry and (**ii**) schematic structure for (**A**) atorvastatin and (**B**) ezetimibe. For molecular geometry, spatial optimisation was calculated in the absence of explicit hydrogens using Chemsketch v10.02 software (ACDLabs, Toronto, ON, Canada). Images were rendered using POVray software (Cason 2004).

In humans, the efficacy of atorvastatin for lowering serum total cholesterol is between 25-45%, which is similar to Rosuvastatin, but superior to the range of 16-36% reported for simvastatin, lovastatin, fluvastatin, and pravastatin (Vaughan and Gotto 2004). With regards to murine studies, Johnston *et al.* have used atorvastatin at 20 mg/kg/day to effectively ameliorate atherosclerotic lesion development in a C57BL/6 mouse model of atherosclerosis (2000). Further, atorvastatin doses ranging from 30 mg/kg/day (Kozuki *et al.* 2011) to 60 mg/kg/day (Kanagarajan *et al.* 2008) have been published for other work.

Atorvastatin is metabolically oxidised in the gut and liver by CYP3A4 to form para- and ortho-hydroxyatorvastatin (Jacobsen *et al.* 2000; Park *et al.* 2008). In humans, this reduces the total bioavailability of atorvastatin to ~12% (Lau *et al.* 2006b). Following oxidation, para- and ortho-hydroxyatorvastatin by-products are transported across the hepatic canalicular membrane by MRP2 (See Section 1.8) and secreted in bile (Chen *et al.* 2005; Lau *et al.* 2006; Li *et al.* 2011a). Atorvastatin was selected for this study based

on its efficacy in reducing hypercholesterolemia in HF-fed *foz/foz* mice (as determined in early pilot studies; data not shown), and popularity for treating human hypercholesterolemia. The dose used (20 mg/kg/day) was identical to that used by Johnston and colleagues (2000) (see above). While 20 mg/kg/day is an order of magnitude higher than human dosage ranges, rodents generally clear drugs biotransformed by Cyp systems and biliary transporters ~5-10 fold faster than humans (Freireich *et al.* 1966; Rozman 1988; Bogaards *et al.* 2000).

6.1.2 Ezetimibe: an inhibitor of cholesterol uptake

Invented 9 years after atorvastatin, ezetimibe was discovered serendipitously as a by-product of ACAT inhibitor research. As mentioned in Section 1.2, ACAT2 is responsible for esterification of FC to form CE, a process which takes place in numerous tissues, particularly in enterocytes and the liver. Following esterification, CE containing colloids (VLDL and LDL) are subsequently trafficked into the lymphatic (for enterocytes) and the circulation (for liver-derived colloids) (Field and Mathur 1983). These circulating colloids are responsible for hypercholesterolemia (Hasler-Rapacz *et al.* 1994). Correspondingly, inhibition of ACAT activity was found to reduce hypercholesterolemia in several animal models (Bell *et al.* 1992; Matsuo *et al.* 1995), a phenomenon which sparked intensive interest in the development of ACAT inhibitors. Schering-Plough, in collaboration with Merck Sharp and Dohme, began testing novel ACAT inhibitors in the hope of developing a marketable treatment for hypercholesterolemia. Lead by Duane Burnett, this research resulted in the fortuitous discovery of a group of compounds (modelled on a 2-azetidinone backbone) which were able to lower serum cholesterol levels, ironically with no appreciable effect on ACAT activity (Burnett *et al.* 1994; Clader *et al.* 1996). Compound SCH58235 (1,1-[4-fluorophenyl]-3R)-[3-{4-fluorophenyl}-{3S}-hydroxypropyl]-[4S]-[4-hydroxyphenyl]-2-azetidinone) was subsequently developed from the basic 2-azetidinone backbone structure and found to function upstream of ACAT as a potent inhibitor of cholesterol uptake (Rosenblum *et al.* 1998). SCH58235, later termed ezetimibe (see Figure 6.1B for compound structure), binds to NPC1L1 protein present on the brush border of the intestinal mucosa and the canalicular membrane of hepatocytes (Altmann *et al.* 2004; Seedorf *et al.* 2004; Davies *et al.* 2005; Garcia-Calvo *et al.* 2005) (see Figure 3.9D for hepatic localisation).

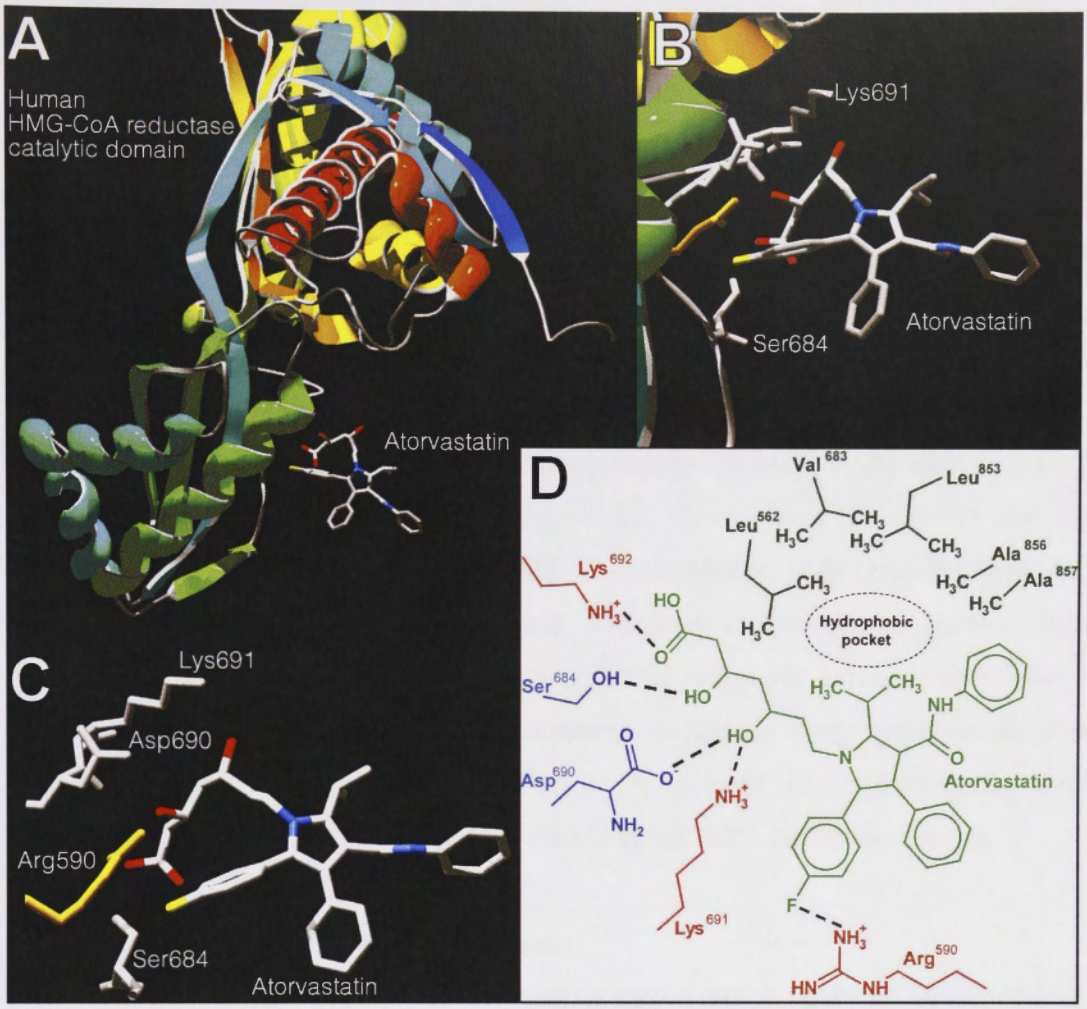

Figure 6.2 Atorvastatin binding to the catalytic domain of human HMG-CoA reductase

(**A**) X-ray crystal structure of atorvastatin bound to a single monomer of the catalytic domain of human HMG-CoA reductase (HMGR) (protein database structure 1HWK), as elucidated by Istvan and Deisenhofer (2001). Physiologically, HMGR undergoes tetramerisation, which is required for catalytic activity and in the process forms a hydrophobic pocket (Istvan 2003), which is absent in panels A-C. (**B,C**) Interaction of atorvastatin with adjacent HMGR amino acid residues (3.0 Å proximity threshold). (**D**) Schematic representation of atorvastatin (green) interacting with HMGR active-site amino acid residues. Positive and negatively charged amino acids are coloured red and blue, respectively, while hydrophobic amino acid groups are represented in black. Images were generated using DeepView Swiss-PdbViewer (Guex and Peitsch 1997), Chemsketch version 10.02 (ACDLabs, Toronto, ON, Canada), and rendered using POVray software (Cason 2004).

Ge *et al.* (2008) further described the mode of action of NPC1L1 and the role of ezetimibe in inhibiting cholesterol uptake. Under normal conditions, cholesterol binds to intestinal or canalicular NPC1L1, which contains a sterol sensing domain (SSD) similar to SREBP-2 and HMGR (Davies *et al.* 2000; Ioannou 2000; Yu 2008). NPC1L1 is subsequently internalised by receptor-mediated endocytosis, a process which involves

microfilaments and the clathrin/AD-2 complex. Endocytosis of the cholesterol/NPC1L1 complex culminates in intracellular cholesterol absorption and NPC1L1 receptor recycling back to the plasma membrane (specifically the canalicular surface, or apical pole, in the case of hepatocytes) (Ge *et al.* 2008). Ezetimibe competitively binds to NPC1L1, thereby preventing endocytosis and inhibiting intracellular cholesterol absorption (Ge *et al.* 2008).

6.2 Purpose of study: hypotheses and aims

In the previous Chapter, it was shown that hepatic cholesterol loading increases serum ALT levels, liver cell death by apoptosis, hepatic macrophage recruitment and liver fibrosis in HF-fed *foz/foz* mice with NASH. This allowed us to develop the hypothesis underlying the present experiments, that inhibition of cholesterol uptake and/or biosynthesis, using ezetimibe and atorvastatin should reduce the extent of liver injury in these mice. To test this hypothesis, cholesterol-modulating drugs were administered orally for 8 weeks following onset of NASH at 16 weeks in HF-fed *foz/foz* mice. As in Chapter 3 experiments, this particular HF diet contains 0.2% (w/w) cholesterol.

The specific aims of this part of the thesis are:

1. Assess whether cholesterol-modulating agents are capable of altering hepatic cholesterol profiles.
2. Determine whether such changes are accompanied by improved liver pathology, as assessed for injury by serum ALT values and hepatocellular apoptosis, inflammation by macrophage infiltration, and liver fibrosis.

6.3 Methods

6.3.1 Mice

From 8 weeks of age, female WT and *foz/foz* NOD.B10 mice (n=8-11/group) were fed either chow or HF diet (containing 0.2% [w/w] cholesterol) for 16 weeks. After this time, atorvastatin, ezetimibe, or a combination of the two were added to diets and mice were fed for a further 8 weeks. As positive controls mice were fed the HF diet (inhibitor vehicle only) for a total of 24 weeks. In a small pilot study (see results shown in Table 6.1) drug doses used in this study where shown to lower serum cholesterol and ALT values. Details regarding addition of drug to the diet are discussed below.

Table 6.1 Atorvastatin and ezetimibe pilot study serum data

Female *foz/foz* mice (n=3/grp) were fed high fat (HF) diet for 16 weeks, after which atorvastatin (20 mg/kg/day) and/or ezetimibe (5 mg/kg/day) was introduced into diet and administered for an additional 8 weeks. Positive control mice (vehicle) only received HF diet. Mice were tail-bled prior to drug administration (0 weeks) and again at 4 weeks and 8 weeks during drug treatment. Serum alanine transaminase (ALT), total cholesterol (TC), HDL cholesterol (HDL-C), and triglyceride (TG) levels were assessed as described in Section 2.5.

Treatment	Week	ALT (U/L)	TC (mmol/L)	HDL-C (mmol/L)	TG (mmol/L)
Vehicle	0	705 ± 71.1	8.11 ± 0.66	2.96 ± 0.28	2.30 ± 0.41
	4	588 ± 168	7.9 ± 0.87	2.98 ± 0.38	1.84 ± 0.09
	8	590 ± 15.0	7.8 ± 0.06	2.08 ± 0.04	1.81 ± 0.07
Atorvastatin (20 mg/kg/day)	0	750 ± 275	7.22 ± 0.13	2.48 ± 0.17	1.94 ± 0.62
	4	520 ± 154	6.99 ± 0.40	2.90 ± 0.13	1.62 ± 0.29
	8	317 ± 89.4*	4.79 ± 0.23*	2.08 ± 0.04*	0.86 ± 0.16*
Ezetimibe (5 mg/kg/day)	0	879 ± 233	9.42 ± 0.45	3.54 ± 0.14	1.90 ± 0.06
	4	368 ± 64.2*	6.89 ± 0.17*	3.01 ± 0.08*	1.30 ± 0.12*
	8	300 ± 37.2*	4.09 ± 0.10*,#	1.76 ± 0.05*,#	0.89 ± 0.07*,#

Data are mean ± SEM. *P<0.05, vs. treatment-matched, 0 week group. #P<0.05, vs. treatment-matched, 4 week group.

6.3.2 Addition of drugs to diet

6.3.2.1 Reagents

Chow and HF diet were purchased from Specialty Feeds (Glen Forrest, WA, Australia) (Section 2.3). The HF diet used in this study contained 0.2% (w/w) cholesterol (as used in Chapters 3, 4, and 5; for composition see Table 5.1).

Atorvastatin working solution (10 mg/mL atorvastatin in 30% [v/v] ethanol). Commercially available atorvastatin tablets prepared for human use (Lipitor®, Pfizer, West Ryde, NSW, Australia) (2 x 80 mg) were ground up, with coating and excipient allowed to dissolve in d.H_2O (11.2 mL). Ethanol (4.8 mL of >99% [v/v] stock) was subsequently added to assist statin dissolution. Solution was mixed thoroughly using a magnetic stirrer bar and prepared just before use.

Ezetimibe working solution (2 mg/mL ezetimibe in 30% [v/v] ethanol). Commercially available ezetimibe tablets prepared for human use (Ezeterol®, Schering-Plough, Whitehouse Station, NJ) (2 x 10 mg) were ground up, with coating and excipient allowed to dissolve in d.H_2O (6.0 mL). Ethanol (3.0 mL of >99% [v/v] stock) was

added and the solution was mixed thoroughly using a magnetic stirrer bar. Working solution was prepared just before use.

HF diet was supplemented with atorvastatin and/or ezetimibe working solution, at dosages calculated (from known levels of daily food consumption) to result in each mouse receiving:

i. Atorvastatin 20 mg/kg/day, or
ii. Ezetimibe 5 mg/kg/day, or
iii. Combined atorvastatin 20 mg/kg/day and ezetimibe 5 mg/kg/day

The exact amount of atorvastatin and/or ezetimibe working solution added to diet was calculated weekly and was based on the average *foz/foz* and WT body weights observed for the preceding week. An example of the methodology used to calculate the exact volume of atorvastatin drug used to supplement HF diet for a cage of 16 week *foz/foz* mice is included below:

- Assuming *foz/foz* mouse body weight is ~55 g at 16 weeks post HF-feeding (see Figure 6.3A,B) and the average diet consumption for female *foz/foz* mice is ~4.5 g/day (Arsov 2006), then the volume of atorvastatin working solution needed to supplement 100 g of HF diet was calculated as follows:

$$\text{Atorvastatin required} = 20 \text{ mg/kg/day}$$

$$= 1.1 \frac{\text{mg}}{\frac{55 \text{ g mouse}}{\text{day}}}$$

$$\therefore \text{if 4.5 g of diet consumed each day, then: } 0.244 \text{ mg/g diet}$$

$$= 24.4 \frac{\text{mg}}{100 g \text{ of HF diet}}$$

$$= 2.44 \text{ mL of 10 mg/mL atorvastatin solution}$$

Ezetimibe and combination delivery doses were calculated weekly in identical manner. To ensure equivalent daily dosages, based on the different rates of dietary consumption between genotypes, separate calculations were carried out for *foz/foz* and WT cages.

Once calculated, working solution volumes were carefully spray-applied to pre-weighed 100 g portions of diet using a small air pump and 1 mL pipette tip. Diet pellets were

rotated mid-way though the procedure to ensure homogenous drug coverage. Following application, treated diets were air-dried over night in a fume hood to assist ethanol evaporation. All diets were prepared under clean conditions and stored at 4°C until use (atorvastatin and ezetimibe are stable at room temperature). The prepared 100 g portions of drug-supplemented diets were typically consumed within 7 days of preparation. Note that the host laboratory has extensive experience in the use of this approach to oral drug administration, as published repeatedly (Ip *et al.* 2003; Ip *et al.* 2004; Teoh *et al.* 2010).

6.3.3 Harvesting

Mice were maintained as described in Section 2.3 and weighed weekly from the introduction of HF diets at 8 weeks of age. At experimental time points (24 weeks on drug or control diet), mice were harvested as described in Section 2.4. In addition to the standard harvesting methodology, peri-ovarian white adipose tissue (WAT) from one side, and interscapular dorsal adipose tissue were also collected. Following isolation, dorsal adipose tissue was dissected to separate brown adipose tissue (BAT) from adjacent WAT. BAT was weighed separately.

6.3.4 Procedures

Serum and hepatic lipid fractions were quantified as described in Section 2.5.

Serum insulin was quantified using a commercial ELISA kit (Millipore, Billerica, MA), as per Manufacturer's instructions.

RnD Systems (Minneapolis, MN) ELISA kits were used to determine serum adiponectin as per Manufacturer's instructions.

SDS-PAGE, western blotting, semi-quantitative qPCR and IHC were carried out as described in Sections 2.10, 2.11, 2.7, and 2.6.2.1, respectively. The primary antibodies and primers used for western blotting and qPCR are shown in Tables 2.1 and 2.3, respectively.

H&E sections were cut and stained by Anne Prins (John Curtin School of Medical Research, ANU, Canberra).

Liver sections were also stained for fibrosis using Sirius red, as described in Section 2.6.1.

H&E and Sirius red-stained sections were blinded and scored by an experienced liver pathologist (Associate-Professor Matthew M. Yeh, Department of Pathology, University of Washington Medical Centre, Seattle, WA), using the NAS scoring system (Mendler *et al.* 2005) and Brunt's criteria for fibrotic severity (Kleiner *et al.* 2005).

In addition to histopathological assessment, Sirius red-stained liver sections were subjected to quantitative image analysis using ImageJ (NIH, Bethesda, MD), as previously described (Kaemmer *et al.* 2010).

All statistical analyses were carried out as described in Section 2.15.

6.4 Results

6.4.1 Effect of cholesterol modulation on body and tissue weights and serum adiponectin in chow and HF-fed *foz/foz* and WT mice

In this study, and as previously reported in Chapter 5, *foz/foz* mice fed chow or HF diet were significantly heavier than their WT controls ($P<0.05$, Figure 6.3). The introduction of atorvastatin and/or ezetimibe (at 16 weeks of feeding) into the chow or HF diet had no appreciable effect on total body weight over the 8 week treatment period in either chow or HF-fed mice (Figure 6.3A,B). By 24 weeks, *foz/foz* mice body weight averaged 51 ± 2.0 g *versus* 27 ± 1.4 g for WT counterparts. It should be noted that total body weights for *foz/foz* mice described in this study were ~18% lower than those described in Chapter 5 (Figure 5.1A), which averaged 62 ± 2.0 g by 24 weeks of HF (0.2% cholesterol) feeding. Possible reasons for this disparity in body weights between studies are considered in the discussion. Chow-fed mice were included in this study to act as dietary controls; however, there were no significant effects of atorvastatin and/or ezetimibe treatment in chow-fed *foz/foz* and WT mice for any of the measurements in this study, and, for clarity, readouts from these groups are not shown. Thus, all subsequent reference to WT and *foz/foz* mice refers to HF-fed animals.

Atorvastatin and ezetimibe treatment reduced liver weight in *foz/foz* mice ($P<0.05$, Figure 6.4A), with additional additive effects of combined atorvastatin and ezetimibe ($P<0.05$, Figure 6.4A). Conversely, peri-ovarian adipose tissue weights were elevated in HF-fed *foz/foz* mice treated with atorvastatin and ezetimibe *versus* vehicle and genotype controls ($P<0.05$, Figure 6.4B), while subcutaneous WAT tissue weights, although greater in *foz/foz* mice compared to WT controls ($P<0.05$), were relatively unchanged following drug treatment (NS, Figure 6.4C). Ezetimibe and combination treatment also increased brown adipose tissue (BAT) weights for HF-fed *foz/foz* mice ($P<0.05$, Figure 6.4E). Atorvastatin increased total dorsal adipose pad (BAT and adjacent WAT) weights in HF-fed *foz/foz* mice ($P<0.05$, Figure 6.4D), total dorsal adipose weights were comparable to vehicle controls in ezetimibe and combination-treated *foz/foz* mice ($P<0.05$, Figure 6.4D). In summation, these findings are interpreted as indicating that the ratio of dorsal BAT:WAT may be differentially altered following statin and ezetimibe treatment. This aspect will be considered further in the Discussion (Section 6.5).

As demonstrated in Chapter 5 and previously reported for the mice used in Chapter 3 (Larter *et al.* 2009), HF-fed *foz/foz* mice develop profound hypoadiponectinemia compared with WT counterparts ($P<0.05$, Figure 6.4F). However, 8 week atorvastatin and ezetimibe treatment significantly increased serum adiponectin levels, by ~2-fold. A minor, albeit non-significant, additional increase in serum adiponectin was also observed for combination drug-treated mice, suggesting that there may be an additive effect of atorvastatin and ezetimibe on adiponectin expression (Figure 6.4F). Importantly, these increases in circulating adiponectin may partially explain (or be explained by – see Discussion, Section 6.5) the increased peri-ovarian adipose weights in drug-treated *foz/foz* mice (Figure 6.4B). However, further analysis of adiponectin gene expression and adipose tissue metabolism is needed to clarify this hypothesis.

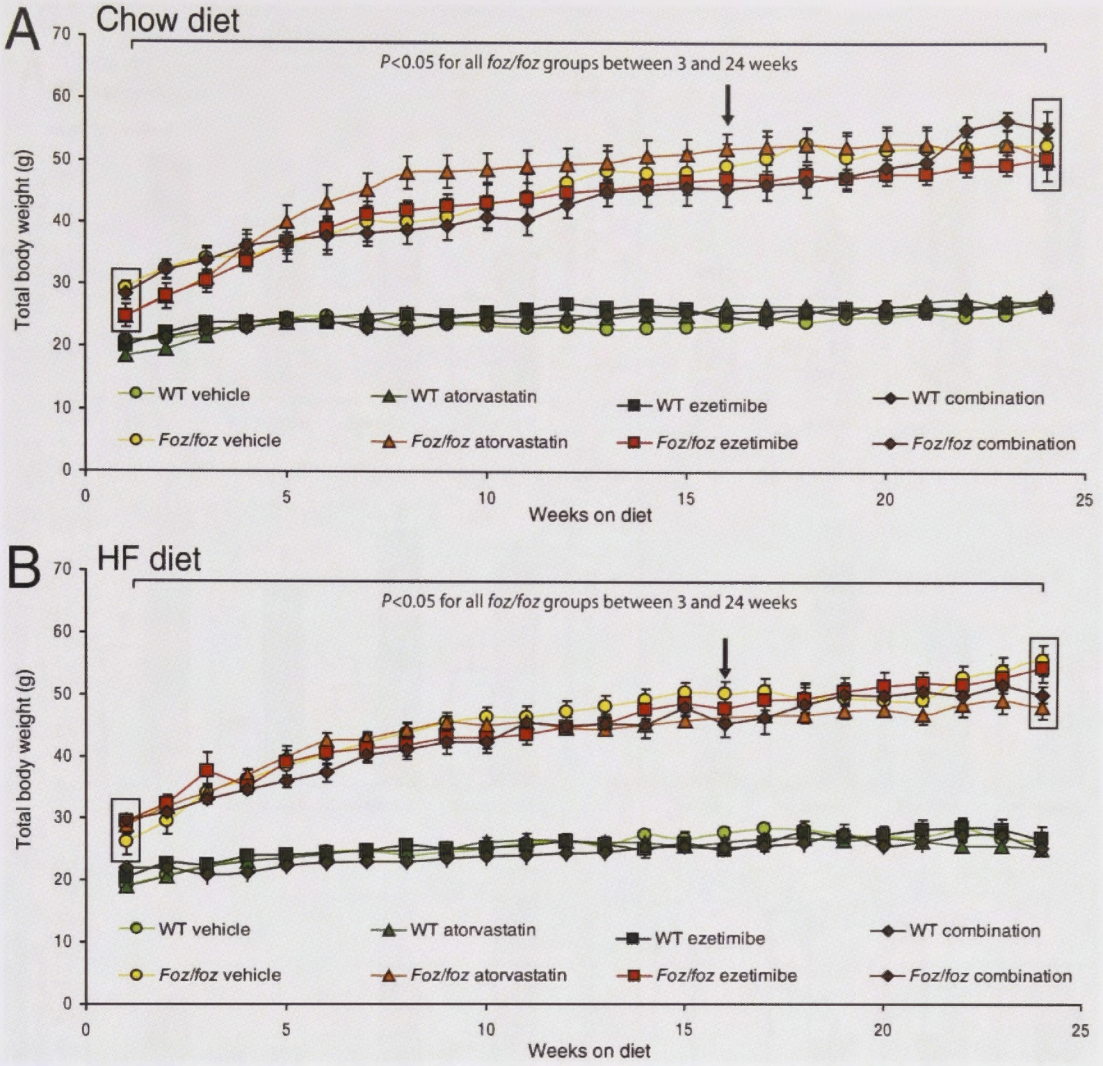

Figure 6.3 Growth curves for chow and high fat-fed *foz/foz* and WT mice treated with or without atorvastatin and/or ezetimibe.

Foz/foz and WT mice (n=8-11/grp) were fed either (**A**) chow or (**B**) HF diet (containing 0.2% [w/w] cholesterol) for 16 weeks, after which atorvastatin (20 mg/kg/day) and/or ezetimibe (5 mg/kg/day) were introduced to the chow and HF diets, and mice fed for an additional 8 weeks (see Section 6.3.2 dosage and methods). Control (vehicle) mice were fed un-supplemented chow or HF diet. Arrows indicate the introduction of drug-treated diets in experimental groups. All *foz/foz* mouse groups were significantly heavier than WT controls (P<0.05). Data are mean ± SEM.

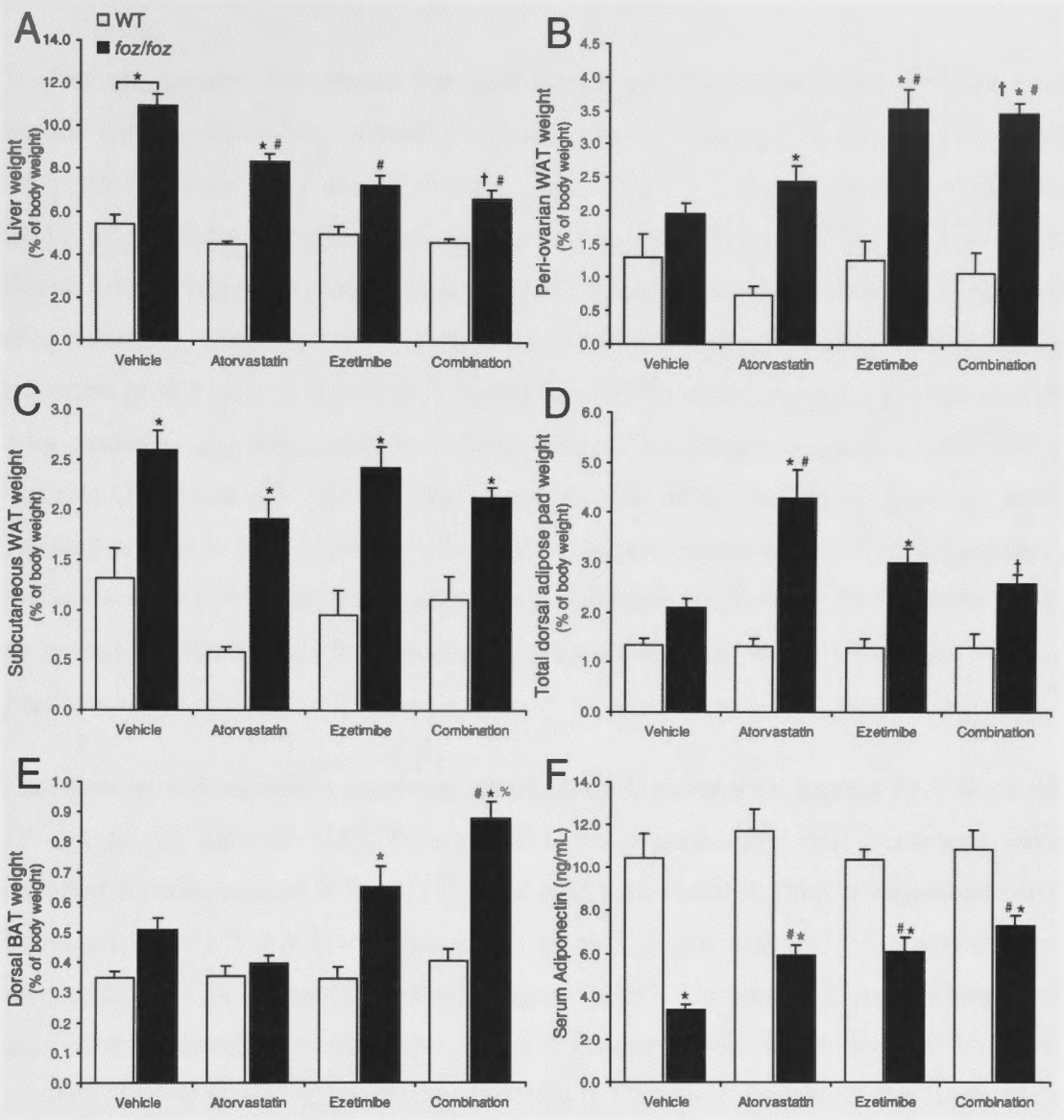

Figure 6.4 Tissue weights and serum adiponectin levels in HF-fed *foz/foz* and wildtype mice treated with or without atorvastatin and/or ezetimibe

(**A**) Liver, (**B**) peri-ovarian white adipose (WAT) and (**C**) subcutaneous WAT weights from one side, (**D**) total dorsal adipose tissue and (**E**) brown adipose tissue (BAT) weights (as percentage of body weight) for *foz/foz* (■) and WT (□) mice fed high fat (HF) diet for 16 weeks, after which atorvastatin (20 mg/kg/day) and/or ezetimibe (5 mg/kg/day) was introduced into diet and administered for an additional 8 weeks (see Section 6.3.2). (**F**) Serum adiponectin levels in HF-fed *foz/foz* and WT mice treated with atorvastatin and/or ezetimibe. Data are mean ± SEM. $^{*}P<0.05$, vs. treatment-matched, genotype control. $^{\#}P<0.05$, vs. genotype-matched, vehicle group. $^{\dagger}P<0.05$, vs. genotype-matched, atorvastatin treatment group. $^{\%}P<0.05$, vs. genotype-matched, ezetimibe treatment group.

6.4.2 Atorvastatin and ezetimibe alter hepatic lipid profiles in HF-fed *foz/foz* mice

To test the primary hypothesis that atorvastatin and ezetimibe treatment influences hepatic cholesterol loading, hepatic lipidomic analyses were conducted. As anticipated from pilot studies of serum cholesterol (see Table 6.1), atorvastatin and ezetimibe treatment markedly reduced hepatic CE content in both *foz/foz* and WT mice ($P<0.05$, Figure 6.5A). Hepatic FC levels were also reduced in *foz/foz* mice following 8 weeks of drug treatment ($P<0.05$, Figure 6.5B), but there was no appreciable effect of drug treatment in WT mice (Figure 6.5B). While hepatic TG levels also tended to decrease in drug-treated *foz/foz* mice, such reductions were not significant compared with vehicle controls (Figure 6.5C). On the other hand, hepatic DAG and MAG fractions were variably altered in HF-fed *foz/foz* mice following atorvastatin and ezetimibe treatment. Increases were only observed in atorvastatin and ezetimibe-treated *foz/foz* mice, while no changes were observed for combination drug-treated mice and WT controls ($P<0.05$, Figure 6.5D,E).

Atorvastatin and ezetimibe treatment significantly lowered total hepatic FFA levels in HF-fed *foz/foz* mice ($P<0.05$, Figure 6.6A), while lesser (and NS) reductions were apparent in drug-treated WT mice (Figure 6.6A). In contrast, drug treatment actually increased hepatic SaFA levels marginally in both *foz/foz* and WT mice *versus* their respective vehicle controls ($P<0.05$, Figure 6.6B). Combination atorvastatin and ezetimibe treatment decreased hepatic MuFA content in HF-fed *foz/foz* and WT mice ($P<0.05$, Figure 6.6C). As previously reported in Chapter 5, hepatic PuFA levels were significantly lower in *foz/foz* mice versus WT controls ($P<0.05$, Figure 6.6D), and drug treatment had no effect on hepatic PuFA profiles in *foz/foz* mice (Figure 6.6D).

Individual FFAs were also quantified in this study (Table 6.2). Drug treatment had no overall effect on FFA levels in WT mice (Table 6.2). Conversely, atorvastatin and ezetimibe treatment generally lowered levels of hepatic saturated and *trans* long chain unsaturated FFAs (stearic acid [18:0] was an exception) in *foz/foz* animals. Specifically, palmitic (16:0), palmitoleic (16:1), oleic (18:1), elaidic (18:1 *trans*), and arachidic acid (20:0) were all decreased in drug-treatment groups ($P<0.05$ for all combination-treated *foz/foz* mice, Table 6.2). The most profound changes in these FFA were observed for combination drug-treated *foz/foz* mice, with palmitoleic levels lowered ~2-fold, while palmitoleic, elaidic, and arachidic acid decreased ~3-4 fold compared with genotype-

matched vehicle controls ($P<0.05$ for all combination-treated *foz/foz* mice, Table 6.2). Quantification of hepatic oxysterols is underway.

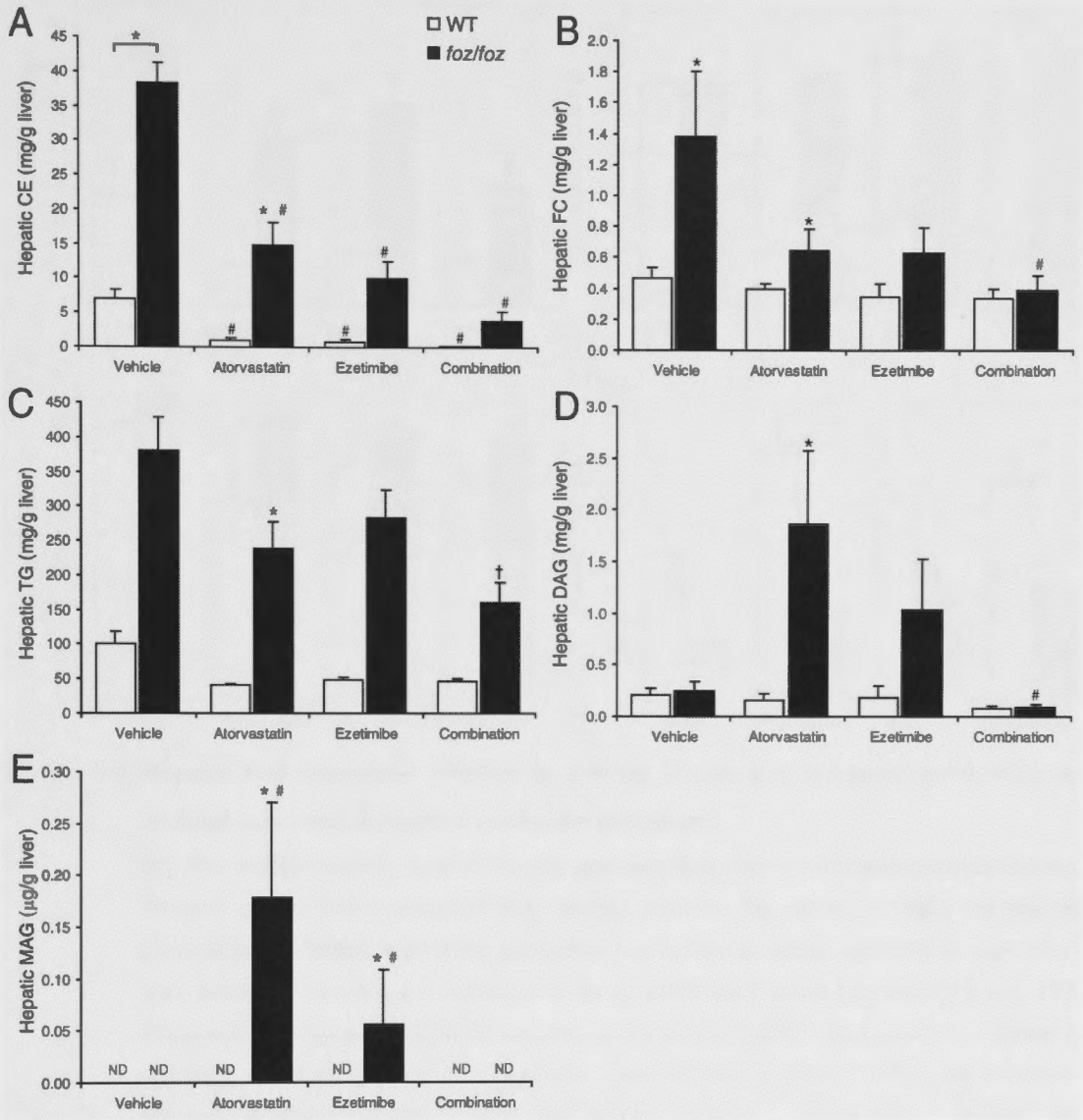

Figure 6.5 Hepatic neutral lipids in *foz/foz* and wildtype mice, with or without atorvastatin and/or ezetimibe treatment

(**A**) Hepatic cholesteryl ester (CE), (**B**) free cholesterol (FC), (**C**) triglyceride (TG), (**D**) diacylglycerides (DAG), and (**E**) monoacylglycerides (MAG) lipid profiles in *foz/foz* (■) and WT (□) mice fed high fat (HF) diet for 16 weeks, after which atorvastatin (20 mg/kg/day) and/or ezetimibe (5 mg/kg/day) were introduced into diet and administered for an additional 8 weeks (see Section 6.3.2). Lipid fractions were detected using HPLC (see Section 2.5). MAGs were not detected (ND) in most samples. Data are mean ± SEM. $^{*}P<0.05$, vs. treatment-matched, genotype control. $^{\#}P<0.05$, vs. genotype-matched, vehicle group. $^{\dagger}P<0.05$, vs. genotype-matched, atorvastatin treatment group.

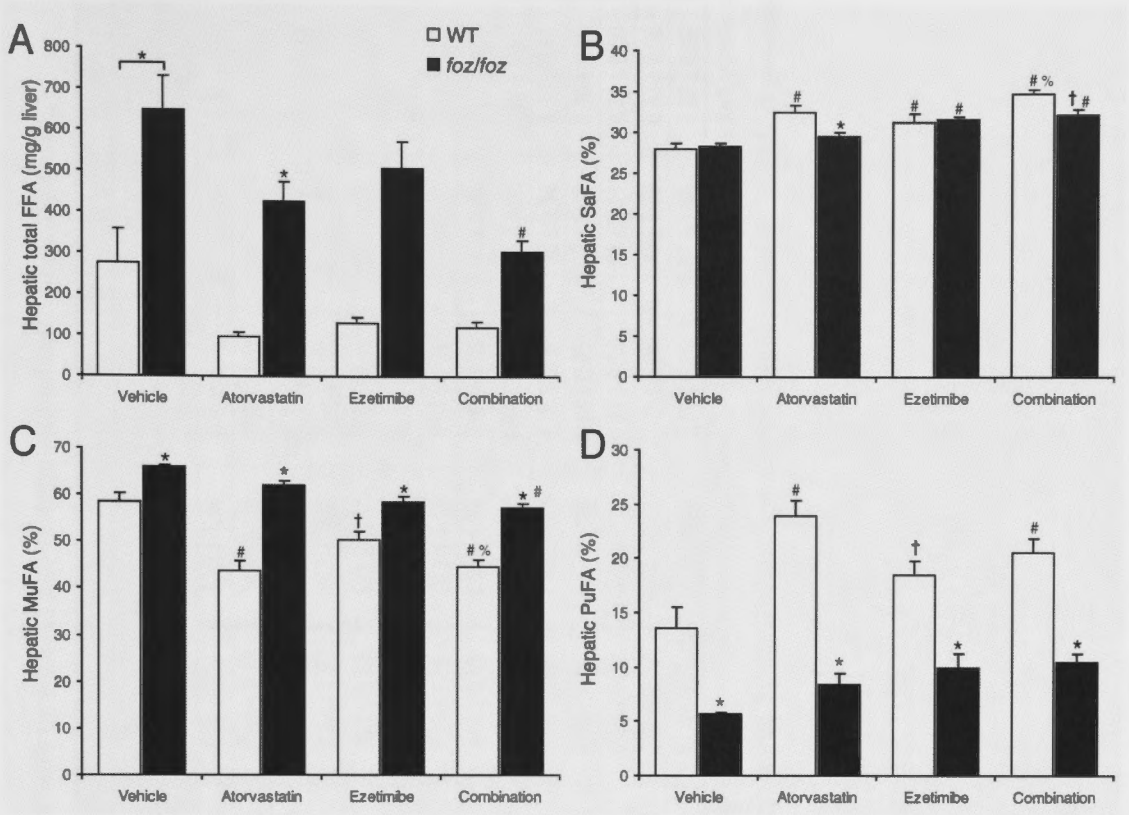

Figure 6.6 Hepatic free fatty acid profiles in HF-fed *foz/foz* and wildtype mice, with or without atorvastatin and/or ezetimibe treatment

(**A**) Total hepatic free fatty acids (FFA), (**B**) saturated FFAs (SaFA), (**C**) mono-unsaturated FFAs (MuFA), and (**D**) poly-unsaturated FFAs (PuFA) in *foz/foz* (■) and WT (□) mice fed high fat (HF) diet for 16 weeks, after which atorvastatin (20 mg/kg/day) and/or ezetimibe (5 mg/kg/day) were introduced into diet and administered for an additional 8 weeks (see Section 6.3.2). FFA levels were assessed using HPLC as described in Section 2.5. SaFA, MuFA, and PuFA content is expressed as percentage of total FFA content. Data are mean ± SEM. $^{*}P<0.05$, vs. treatment-matched, genotype control. $^{\#}P<0.05$, vs. genotype-matched, vehicle group. $^{\dagger}P<0.05$, vs. genotype-matched, atorvastatin treatment group. $^{\%}P<0.05$, vs. genotype-matched, ezetimibe treatment group.

Table 6.2 Individual free fatty acids in livers of HF-fed *foz/foz* and WT mice with or without atorvastatin and/or ezetimibe treatment

Genotype		WT				*Foz/foz*			
FFA	Unit of measurement	HF diet							
		Vehicle	Atorvastatin	Ezetimibe	Combination	Vehicle	Atorvastatin	Ezetimibe	Combination
Myristic acid (14:0)	mg/g liver	4.79 ± 0.79	1.59 ± 0.29	2.41 ± 0.43	2.50 ± 0.37	7.48 ± 1.14	5.86 ± 0.70*	9.34 ± 1.06*	4.87 ± 0.63
Palmitic acid (16:0)		56.7 ± 12.9	19.2 ± 8.88	29.9 ± 2.96	25.48 ± 3.53	149 ± 22.0*	100 ±12.5*	124 ±17.2	75.4 ± 7.45#
Palmitoleic acid (16:1)		11.3 ± 2.77	2.28 ± 1.14	3.33 ± 0.40	3.11 ± 0.49	43.8 ± 6.68*	18.8 ± 2.61*,#	20.8 ± 3.52#	11.8 ± 1.49#
Stearic acid (18:0)		13.2 ± 1.79	8.51 ± 1.60	10.4 ± 1.08	12.44 ± 1.57	15.7 ± 3.02	13.2 ± 0.81	19.0 ± 2.14	14.6 ± 1.33
Oleic acid (18:1)		139 ± 28.5	36.7 ± 17.9	58.5 ± 7.67	46.3 ± 6.60	330 ± 47.9*	217 ± 24.8*	252 ± 34.7	148 ± 15.0#
Elaidic acid (18:1 trans)		14.1 ± 3.27	3.96 ± 1.61	5.20 ± 0.57	4.96 ± 0.76	52.6 ± 8.18*	31.1 ± 4.40*	30.2 ± 5.46#	16.5 ± 1.88#
Linoleic acid (18:2)		15.3 ± 1.54	7.48 ± 3.72	9.08 ± 0.91	7.75 ± 1.18	20.1 ± 3.19	16.3 ± 1.34	23.4 ± 2.30	14.3 ± 1.38
α-Linolenic acid (18:3)		1.19 ± 0.14	0.42 ± 0.24	0.54 ± 0.09	0.43 ± 0.11	0.95 ± 0.15	0.96 ± 0.08	2.01 ± 0.32	1.02 ± 0.17
Arachidic acid (20:0)		2.88 ± 0.51	0.97 ± 0.39	1.14 ± 0.15	1.16 ± 0.16	11.3 ± 1.92*	8.37 ± 1.22*	7.51 ± 1.95	3.26 ± 0.31#
Dihomo-γ-linolenic acid (20:3)		1.24 ± 0.19	0.86 ± 0.20	0.74 ± 0.05	0.82 ± 0.09	1.42 ± 0.21	1.28 ± 0.08	1.36 ± 0.14	1.10 ± 0.11
Arachidonic acid (20:4)		4.89 ± 0.44	5.16 ± 1.17	5.48 ± 0.35	6.63 ± 0.84	5.97 ± 0.92	5.88 ± 0.25	5.97 ± 0.49	6.30 ± 0.76
Eicosapentaenoic acid (20:5)		0.92 ± 0.10	0.57 ± 0.15	0.73 ± 0.07	0.59 ± 0.08	0.80 ± 0.15	0.57 ± 0.04	1.27 ± 0.21	0.74 ± 0.09
Docosapentaenoic acid (22:5)		0.67 ± 0.22	0.34 ± 0.17	0.26 ± 0.03	0.36 ± 0.04	0.41 ± 0.08	0.35 ± 0.04	1.19 ± 0.35	0.42 ± 0.06
Docosahexaenoic acid (22:6)		8.00 ± 1.06	6.77 ± 1.80	6.69 ± 0.54	7.34 ± 0.79	6.59 ± 0.95	6.99 ± 0.38	9.67 ± 1.43	6.99 ± 0.82

Data (mean ± SEM) were determined using HPLC (see Section 2.5). Lipid number nomenclature is used to detail carbon chain structure (*id est* [*x*:*y*], where *x* and *y* refer to number of carbon atoms and double, unsaturated carbon bonds present in the FFA chain, respectively). **P*<0.05, vs. treatment-matched, genotype control. #*P*<0.05, vs. genotype-matched, vehicle group.

6.4.3 Atorvastatin and ezetimibe treatment lowers serum ALT, cholesterol, and insulin, but fails to alter serum TG and glucose in HF-fed *foz/foz* mice

In Chapter 5, we demonstrated a direct correlation between hepatic cholesterol profiles and the pattern of liver injury. In the present experiments, atorvastatin and/or ezetimibe treatment markedly reduced serum ALT in HF-fed *foz/foz* mice. Furthermore, an additive effect of the two drugs was observed; mice treated with combination atorvastatin and ezetimibe showed ALT levels reduced ~3.5-fold *versus* vehicle control ($P<0.05$, Figure 6.7). This pattern of serum ALT change, which is very similar to that demonstrated in dietary cholesterol experiments from Chapter 5, was again remarkably similar to the corresponding profiles of hepatic FC and CE (Figure 6.5 A,B) in drug-treated mice. Additionally, atorvastatin and ezetimibe treatment significantly lowered serum total and HDL cholesterol levels in *foz/foz* mice, although no significant changes were seen in WT mice for any of the drug treatment groups ($P<0.05$, Figure 6.7B,C). Serum TG levels appeared to decrease in atorvastatin-treated *foz/foz* and WT mice (NS), but levels were unchanged in other treatment groups (Figure 6.7D).

In HF-fed *foz/foz* mice, blood glucose tended to be higher than in WT controls (Figure 6.7E), but despite earlier findings in similar experiments (Larter *et al.* 2009) this change was not significant (possible explanations for this difference between experiments will be proposed in the Discussion [Section 6.5]). Atorvastatin and ezetimibe treatment had no effect on serum glucose levels for either *foz/foz* or WT mice (Figure 6.7E). Serum insulin levels, however, declined in *foz/foz* mice treated with atorvastatin and ezetimibe; no additive effect was observed ($P<0.05$, Figure 6.7F). We interpret this change as indicating that drug treatment could improve insulin-sensitivity in *foz/foz* mice, either directly through pharmacological action, as demonstrated in other studies (Deushi *et al.* 2007; Nomura *et al.* 2009; Calisto *et al.* 2010; Zhang *et al.* 2010), or indirectly as a result of decreased hepatic lipid loading (as demonstrated in Figure 6.5A,B,C).

6.4.4 Histological effects of pharmacological cholesterol modulation of liver cholesterol stores

Blinded histological scoring of H&E stained liver sections was carried out by an experienced liver histopathologist, as previously described (Section 2.6). Atorvastatin and

ezetimibe treatment for 8 weeks improved NAFLD pathology in *foz/foz* mice. Hepatic steatosis and ballooning scores appeared to be lower in drug-treated groups, albeit not significantly (Table 6.3); representative H&E micrographs are shown in Figure 6.8. Inflammatory scores, however, were significantly reduced in drug-treated *foz/foz* mice. In particular, combination treatment almost normalised inflammatory scores compared with WT controls ($P<0.05$, Table 6.3). The minor improvements in steatosis and ballooning, factored together with inflammatory scores, resulted in significant reductions in NAS score for drug-treated *foz/foz* mice *versus* vehicle controls ($P<0.05$, Table 6.3). More impressively, improvements in liver pathology conferred by combination drug treatment changed the designation as definite NASH from 100% for vehicle-treated *foz/foz* mice to 22% for combination treated mice ($P<0.05$, Table 6.3); 67% of combination-treated *foz/foz* mice were classified as having simple steatosis.

Significant reductions in histological fibrosis scoring were also observed for ezetimibe and combination drug treated *foz/foz* mice *versus* vehicle controls ($P<0.05$, Table 6.3). Meanwhile, morphometric analysis of liver fibrosis (using sirius red staining) has been completed, and results are described later (Section 6.4.6, Figure 6.11). In summation, these data indicate that 8 week treatment with atorvastatin and ezetimibe improves histological severity of liver injury in *foz/foz* mice, including both inflammation and fibrosis. Furthermore, an additive effect of these cholesterol-lowering agents is evident.

6.4.5 Pharmacological modulation of cholesterol stores decreases hepatocyte cell death and the phenotype of liver inflammation

As mentioned in Section 6.4.4, qualitative histological scoring showed an overall improvement in liver pathology (NASH to "non-NASH") in atorvastatin and ezetimibe treated *foz/foz* mice fed HF diet. Given the strong correlation between hepatic cholesterol profiles and hepatocellular apoptosis and macrophage infiltration demonstrated in Chapter 5, we sought to determine whether atorvastatin and/or ezetimibe treatment affected hepatocyte cell death and macrophage recruitment in livers of HF-fed *foz/foz* and WT mice, using IHC. Ezetimibe and combination treatment significantly lowered M30 positive staining in *foz/foz* mice *versus* genotype-matched vehicle controls ($P<0.05$, Figure 6.9A,B); the effect of atorvastatin monotherapy treatment appeared qualitatively similar but was not

significant (Figure 6.9A,B). By analysis of variance, there was no significant difference in hepatocellular apoptosis between ezetimibe and combination treated *foz/foz* mice.

Drug treatment also lowered serum MCP-1 levels from 193 ± 23.1 pg/mL in HF-fed *foz/foz* vehicle controls, to a mean 113 ± 12.0 pg/mL for drug treatment groups ($P<0.05$, Figure 6.10A). Hepatic macrophage recruitment was assessed using two techniques, namely semi-quantitative qPCR of cluster of differentiation 68 (CD68) gene expression and F4/80 IHC, as previously described in Chapter 5 (Section 5.4.5). CD68, also known as macrosialin, is a ~115 kDa glycoprotein expressed by macrophages (Holness *et al.* 1993; Ramprasad *et al.* 1995). Furthermore, CD68 is significantly upregulated during macrophage activation and has been used as a marker of such activation (Rabinowitz and Gordon 1991; Ramprasad *et al.* 1996; Gordon 1999).

In the present experiments, hepatic CD68 mRNA expression levels were increased in *foz/foz* mice compared with WT controls, but atorvastatin and ezetimibe treatment failed to lower such expression (NS, Figure 6.10B). On the other hand, combined drug treatment significantly lowered CD68 mRNA expression in *foz/foz* mice compared with vehicle controls ($P<0.05$, Figure 6.10C). Notwithstanding this effect on CD68 expression, a differential effect on liver macrophage recruitment was observed. Atorvastatin and combination drug treatment appeared to variably increase F4/80 positive hepatic macrophage recruitment (NS, Figure 6.10B,C). Predominant localisation of macrophages around macrosteatotic (cholesterol-loaded) hepatocytes was observed only in HF-fed *foz/foz* vehicle and atorvastatin monotherapy groups. In livers of ezetimibe and combination-treated *foz/foz* mice, macrophage localisation appeared more random with little to no focus on lipid-laden hepatocytes (Figure 6.10C). We interpret these results as indicating that, in addition to histological improvement in liver injury, combination atorvastatin and ezetimibe therapy reduces macrophage activation in *foz/foz* mice.

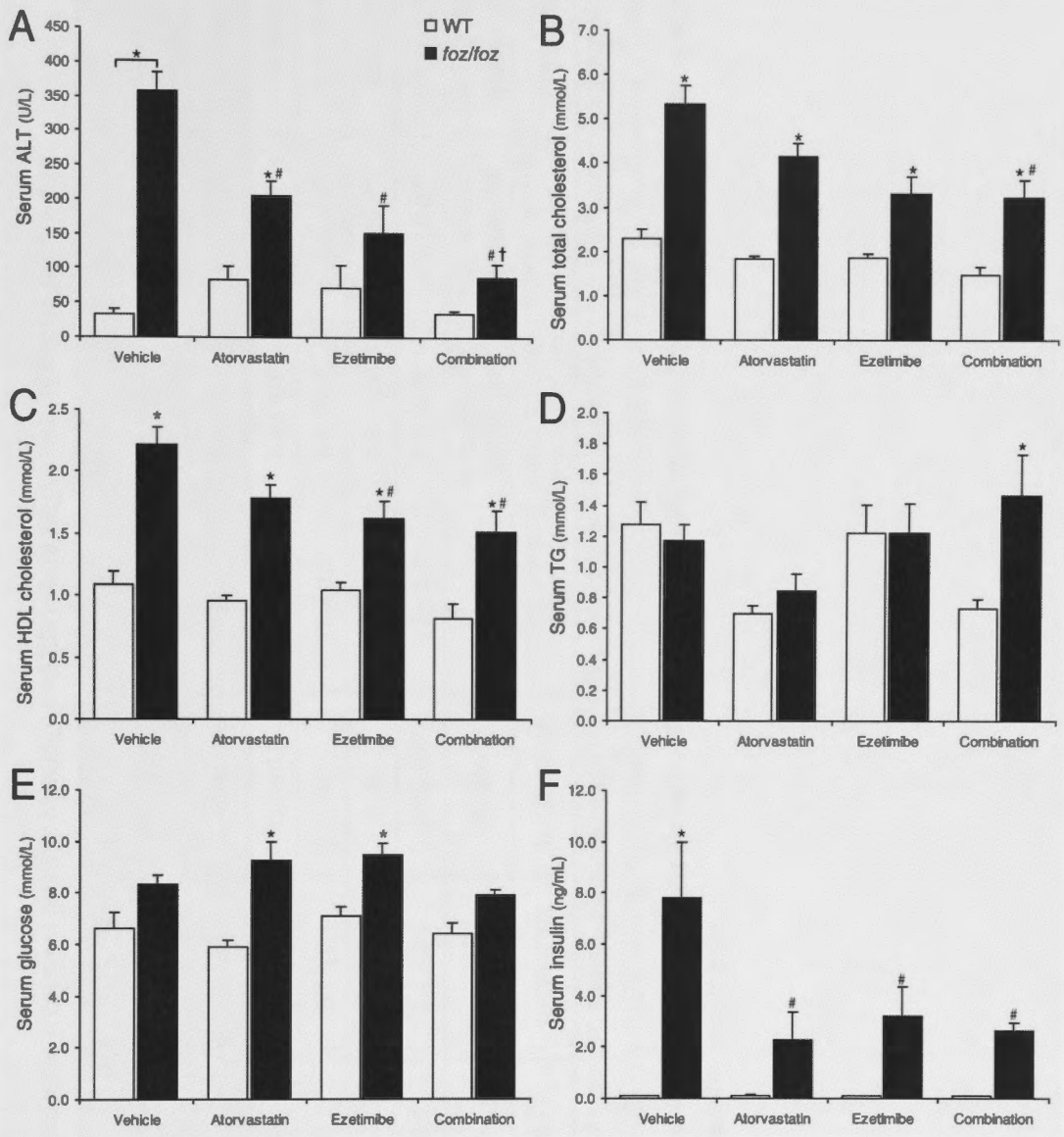

Figure 6.7 Serum ALT, total and HDL cholesterol, glucose and insulin in HF-fed *foz/foz* and wildtype mice with or without atorvastatin and/or ezetimibe treatment

Serum (**A**) alanine transaminase (ALT), (**B**) total cholesterol, (**C**) HDL cholesterol, (**D**) triglycerides (TG), (**E**) fasting blood glucose, and (**F**) serum insulin levels in *foz/foz* and WT mice fed high fat (HF) diet for 16 weeks, after which atorvastatin (20 mg/kg/day) and/or ezetimibe (5 mg/kg/day) were introduced into diet and administered for an additional 8 weeks (see Section 6.3.2). (**F**) Serum insulin levels in atorvastatin and/or ezetimibe-treated *foz/foz* (■) and WT (□) mice. Data are mean ± SEM. $^{*}P<0.05$, vs. treatment-matched, genotype control. $^{\#}P<0.05$, vs. genotype-matched, vehicle group. $^{\dagger}P<0.05$, vs. genotype-matched, atorvastatin treatment group. $^{\%}P<0.05$, vs. genotype-matched, ezetimibe treatment group.

Table 6.3 Effects of atorvastatin and/or ezetimibe treatment on liver histology and fibrosis in *foz/foz* and WT mice fed HF diet

Genotype	WT				*Foz/foz*			
Diet	HF diet							
	Vehicle	Atorvastatin	Ezetimibe	Combination	Vehicle	Atorvastatin	Ezetimibe	Combination
Steatosis	0.2 ± 0.1	0.2 ± 0.1	0.3 ± 0.1	0.6 ± 0.3	2.6 ± 0.2*	2.2 ± 0.3*	2.2 ± 0.2*	1.8 ± 0.3*
Inflammation	0.1 ± 0.1	0.1 ± 0.1	0.1 ± 0.1	0	1.6 ± 0.2*	1.3 ± 0.3*	0.9 ± 0.2#	0.3 ± 0.2#
Ballooning	0	0	0	0	2.0 ± 0.0*	1.6 ± 0.3*	1.8 ± 0.1*	1.8 ± 0.2*
NAS	0.3 ± 0.2	0.3 ± 0.2	0.4 ± 0.6	0.6 ± 0.4	6.3 ± 0.2*	5.1 ± 0.6*	4.9 ± 0.3*,#	4.0 ± 0.3*,#,†
NASH	0/8; SS:1/8	0/8	0/8; SS:2/8	0/8; SS:3/8	8/8*	8/10; SS:1/10; Neither:1/10*	7/10; SS:1/10; Neither:2/10	2/9; SS:6/9; Neither:1/9#
Fibrosis	0:7/8; 1a:1/8	0:8/8	1b:1/8; 2:1/8	1a:1/8; 1b:2/8	1b:1/8; 2:6/8; 3:1/8*	0:1/10; 1a:3/10; 1b:1/10; 2:5/10*	0:5/10; 1a:4/10; 2:1/10#	0:6/9; 2:3/9#

Data (mean ± SEM) represent histological scores for severity steatosis, inflammation and ballooning, according to criteria of Kleiner *et al.* (2005), previously reported in this model (Larter *et al.* 2009). NAFLD activity score (NAS) and designation as NASH, borderline or not NASH (simple steatosis [SS]), as well as fibrosis scoring of Sirius red-stained liver sections were determined (blinded) by an experienced liver histopathologist (MMY) according to published criteria (Kleiner *et al.* 2005). *$P<0.05$, vs. treatment-matched, genotype control. #$P<0.05$, vs. genotype-matched, vehicle group.

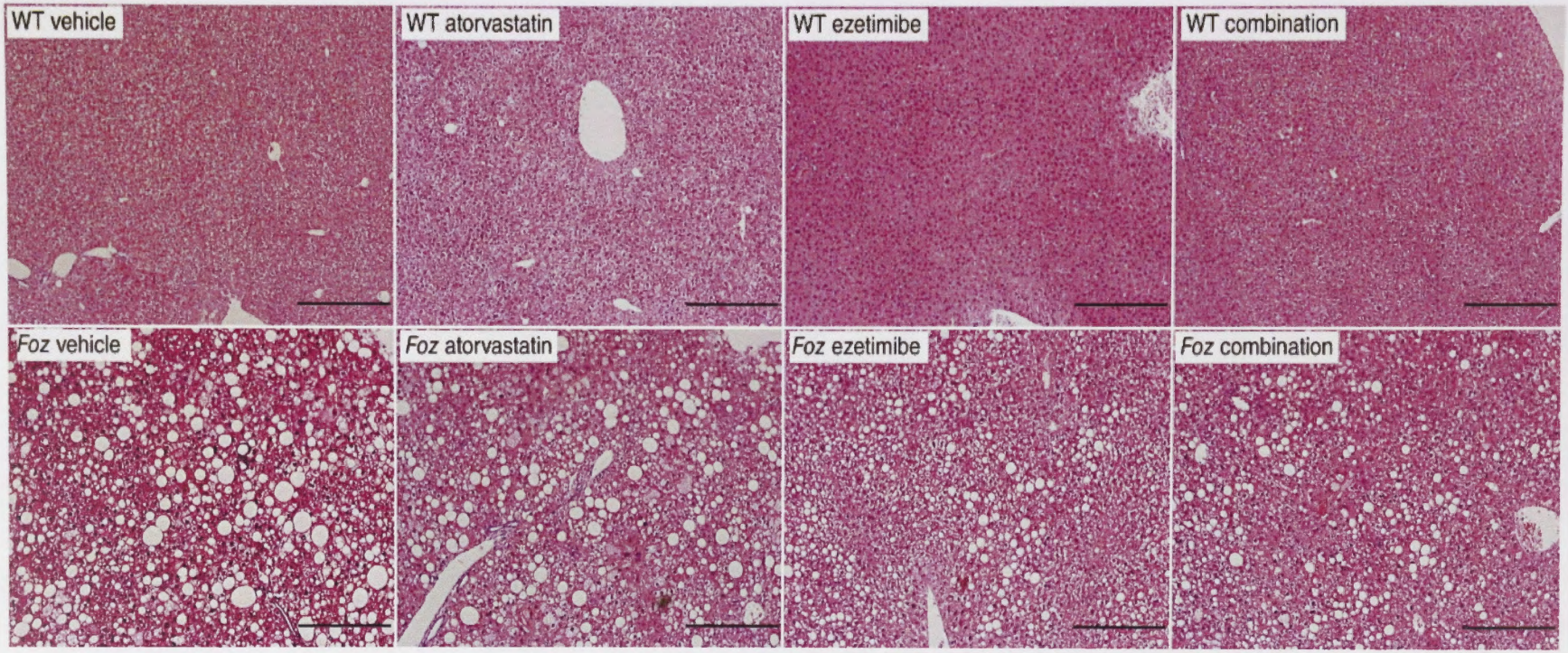

Figure 6.8 Representative H&E sections obtained from HF-fed *foz/foz* and wildtype mice, with or without atorvastatin and/or ezetimibe treatment

Formalin-fixed liver sections from *foz/foz* and WT mice were stained with haematoxylin and eosin. Mice were fed high fat (HF) diet for 16 weeks, after which 20 mg/kg/day atorvastatin and/or 5 mg/kg/day ezetimibe was introduced into diet and administered for an additional 8 weeks (see Section 6.3.2) (n=8-11/grp). Histological scoring is presented in Table 6.3. Scale bars represent 500 μm. No histological differences in haematoxylin and eosin staining were evident in chow-fed *foz/foz* and WT (data not shown).

6.4.6 Hepatic fibrosis is altered by pharmacological modulation of hepatic cholesterol biosynthesis and redistribution in *foz/foz* mice

α-SMA protein levels were variably altered by atorvastatin and ezetimibe treatment in *foz/foz* mice. Although dug treatment appeared to reduce α-SMA expression, changes were not significant (Figure 6.11A). Hepatic collagen-α1 mRNA expression, however, was significantly lower in atorvastatin and ezetimibe-treated *foz/foz* mice compared with vehicle controls, while the most impressive reduction was observed for combination treated *foz/foz* mice ($P<0.05$, Figure 6.11B). Hepatic fibrosis deposition was then measured by analysis of Sirius red-stained liver sections, using the ImageJ colourmetric deconvolution method (Kaemmer *et al.* 2010). *Foz/foz* vehicle controls averaged 1.0 ± 0.1% fibrosis per liver. This value was significantly lowered (~2.5-fold) following atorvastatin and ezetimibe drug treatment ($P<0.05$, Figure 6.11C,D). These findings indicate that pharmacological modulation of *de novo* cholesterol biosynthesis and cholesterol redistribution following NASH onset is capable of reducing hepatic fibrosis, and possibly attenuates hepatic stellate cell activation. It is noted here that the fibrosis observed in HF-fed *foz/foz* controls was significantly lower than that described in Chapter 5 ($P<0.05$, 1.9 ± 0.2%), and possible reasons for this modulation of disease phenotype will be discussed later (Section 6.5).

6.4.7 Analysis of pathways of cholesterol homeostasis in *foz/foz* and WT mice fed treated with atorvastatin and ezetimibe

Given the extent of hepatic cholesterol reduction in drug-treated *foz/foz* mice, pathways of cholesterol homeostasis were investigated to establish whether atorvastatin and/or ezetimibe affect such pathways. As previously described in the *foz/foz* model (Chapter 3 and 5), LDLR expression was significantly upregulated in all *foz/foz* mice compared with treatment-matched controls ($P<0.05$, Figure 6.12A), and (as expected) drug treatment had no significant effect on LDLR expression (Figure 6.12A). On the other hand, gene expression pathways of cholesterol esterification and cholesteryl ester hydrolysis were differentially regulated. ACAT2 protein levels were markedly lower in drug treatment groups and WT controls *versus* vehicle *foz/foz* mice ($P<0.05$; Figure 6.12B), but atorvastatin and ezetimibe treatment progressively lowered ACAT2 expression, which was completely normalised by combination treatment ($P<0.05$, Figure 6.12B). Interestingly,

ACAT2 mRNA levels were relatively unchanged for atorvastatin and ezetimibe monotherapy compared with vehicle controls, but combination treatment did result in a significant increase in ACAT2 mRNA expression for both WT and *foz/foz* mice ($P<0.05$, Figure 6.12C). Conversely, no remarkable differences were observed for ACAT1 and CEH mRNA expression, irrespective of drug-treatment (NS, Figure 6.12D).

Microsomal triglyceride transfer protein (MTTP), a marker of hepatic VLDL assembly, is required for apoB-100 secretion in hepatocytes (Raabe *et al.* 1999; Hussain 2000; Chen *et al.* 2008). Hepatic MTTP mRNA levels appeared to be increased in both *foz/foz* and WT mice treated with atorvastatin and ezetimibe (Figure 6.13D), which we interpret as possibly indicating drug treatment increases hepatic forward cholesterol transport in both *foz/foz* and WT. The fall in serum insulin levels, indicating increased insulin sensitivity, would be consistent with this effect since VLDL formation and secretion decreases with insulin resistance.

Total HMGR protein expression was increased in *foz/foz* mice following atorvastatin, ezetimibe, and combination drug treatment ($P<0.05$, Figure 6.13A). Phosphorylated Ser^{871} HMGR protein levels also increased proportionally in atorvastatin and ezetimibe groups, however, values dropped significantly in combination treated *foz/foz* and WT mice ($P<0.05$, Figure 6.13B). Assuming the expressed ratio of total:phosphorylated Ser^{871} HMGR reflects the proportion of active HMGR protein, levels of active HMGR protein appear to increase significantly in combination drug-treated *foz/foz* mice ($P<0.05$, Figure 6.13C). These data correspond to the normalisation of hepatic FC levels observed in combination atorvastatin and ezetimibe treated *foz/foz* mice (Figure 6.5B). It is plausible that such drug treatment is capable of restoring HMGR activity, however, the activity of HMGR was not assessed in this study and needs to be quantified to verify this hypothesis.

With regards to pathways of cholesterol biotransformation to bile acids, expression levels of Cyp7a1, Cyp7b1 and Cyp27a1 were relatively unchanged compared with vehicle controls in both *foz/foz* and WT mice following separate atorvastatin and ezetimibe treatment (NS, Figure 6.14). However, increases in Cyp7a1 and Cyp27a1 mRNA were observed in combination drug-treated *foz/foz* and WT mice ($P<0.05$, Figure 6.14A,C). As

previously described in Chapters 3 and 5, levels of Cyp7a1, Cyp7b1 and Cyp27a1 appeared lower in HF-fed *foz/foz* versus WT mice, although levels were not significantly different between groups (Figure 6.14A,B,C). Taken together, these finding suggest that combined atorvastatin and ezetimibe treatment may augment pathways responsible for the biotransformation of cholesterol to BAs, and in particular may reinstate the classical bile acid biosynthetic pathway in HF-fed *foz/foz* mice. This change could be in response to the fall in serum insulin, and could contribute to the normalisation of hepatic FC observed in combination drug-treated mice (Figure 6.5B).

While pathways responsible for the classical biotransformation of cholesterol to BA increased in combination drug-treated *foz/foz* and WT mice, Bsep expression was similar for all treatment groups, irrespective of drug treatment or genotype (Figure 6.14D). ABCG8 expression was also examined; although levels trended to be lower in vehicle and atorvastatin-treated *foz/foz* mice compared to WT controls (Figure 6.14E), these apparent changes were not significant; ezetimibe and combined drug treatment resulted in minor, non-significant increases in ABCG8 expression in *foz/foz* mice (Figure 6.14E). These data further support the proposal that combined atorvastatin and ezetimibe treatment is capable of partially restoring physiological cholesterol homeostasis in HF-fed *foz/foz* mice, but a further investigation of the transcriptional and/or post-translational mechanisms involved is beyond the scope of the present work.

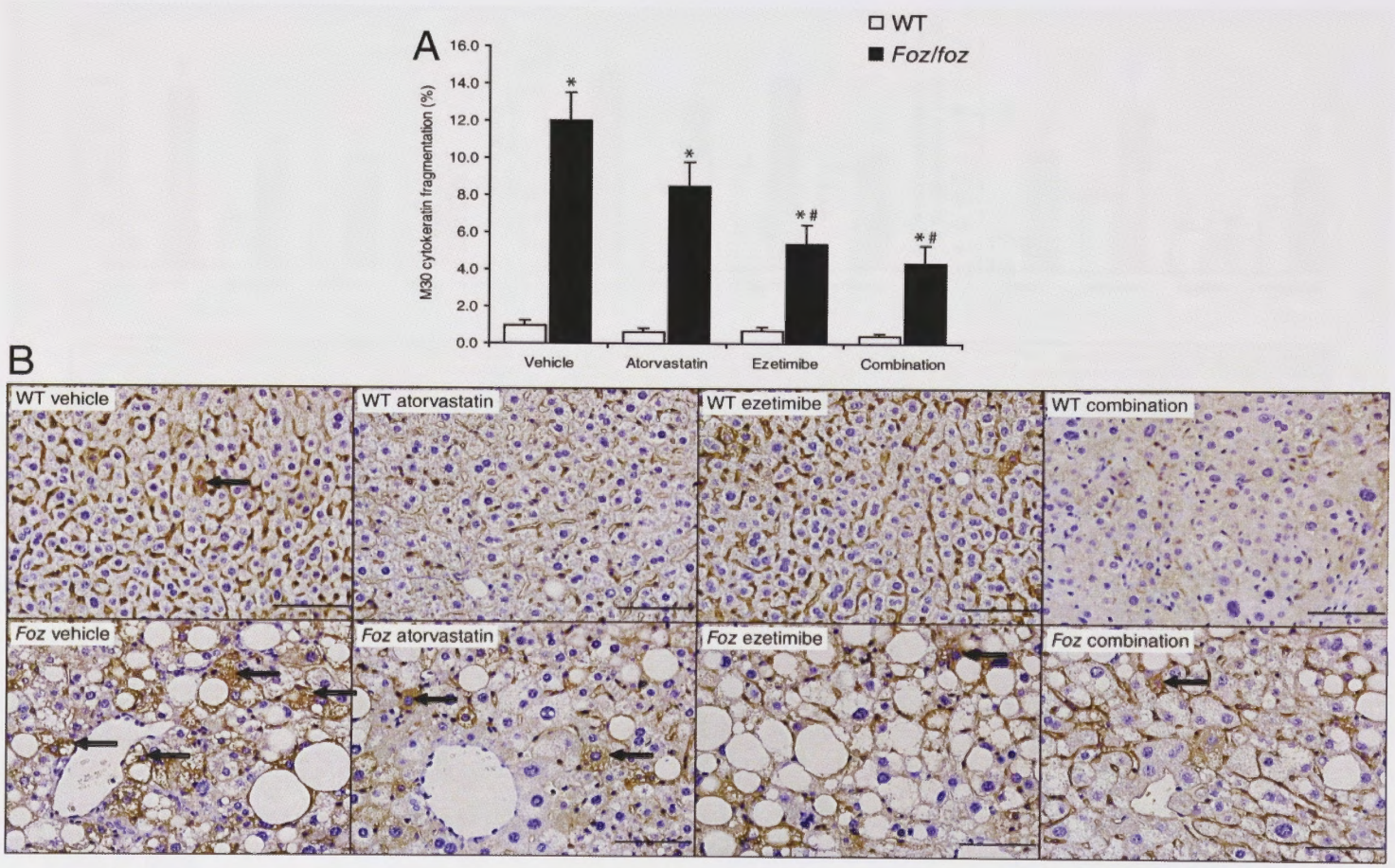

Figure 6.9 Inhibition of cholesterol uptake and/or biotransformation decreases hepatocellular cell death in HF-fed *foz/foz* mice

(**A**) Quantification of cytokeratin-18 fragment (M30)-positive cells for HF-fed *foz/foz* and WT mice. (**B**) Representative immunohistochemistry. Drug treatment and experimental design are described in Section 5.3.1. Scale bars represent 50 μm. Arrows indicate positive staining. Data are mean ± SEM. *$P<0.05$, vs. treatment-matched, genotype control. $^{\#}P<0.05$, vs. genotype-matched, vehicle control.

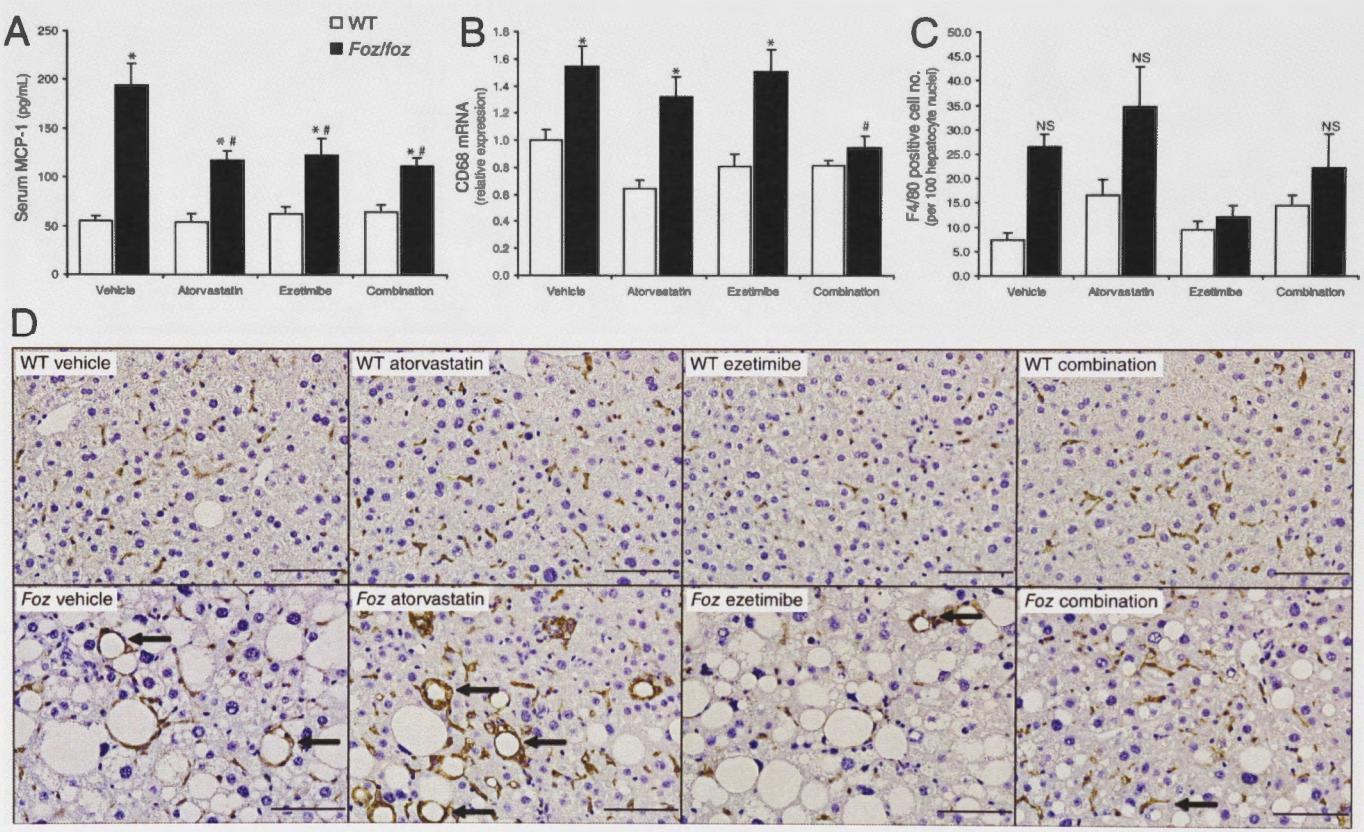

Figure 6.10 Atorvastatin and ezetimibe treatment differentially alter serum MCP-1 levels and hepatic macrophage recruitment in *foz/foz* and wildtype mice

(**A**) Serum MCP-1, (**B**) cluster of differentiation 68 (CD68) mRNA expression, and (**C**) quantification of F4/80-positive cell immunohistochemistry (representative panels shown in **D**) for HF-fed *foz/foz* and WT mice treated with atorvastatin and/or ezetimibe. Drug treatment and experimental design are described in Section 6.3.2. Scale bars represent 50 μm. Arrows indicate positive staining. Data are mean ± SEM. **P*<0.05, vs. treatment-matched, genotype control. #*P*<0.05, vs. genotype-matched, vehicle control. NS, non-significant.

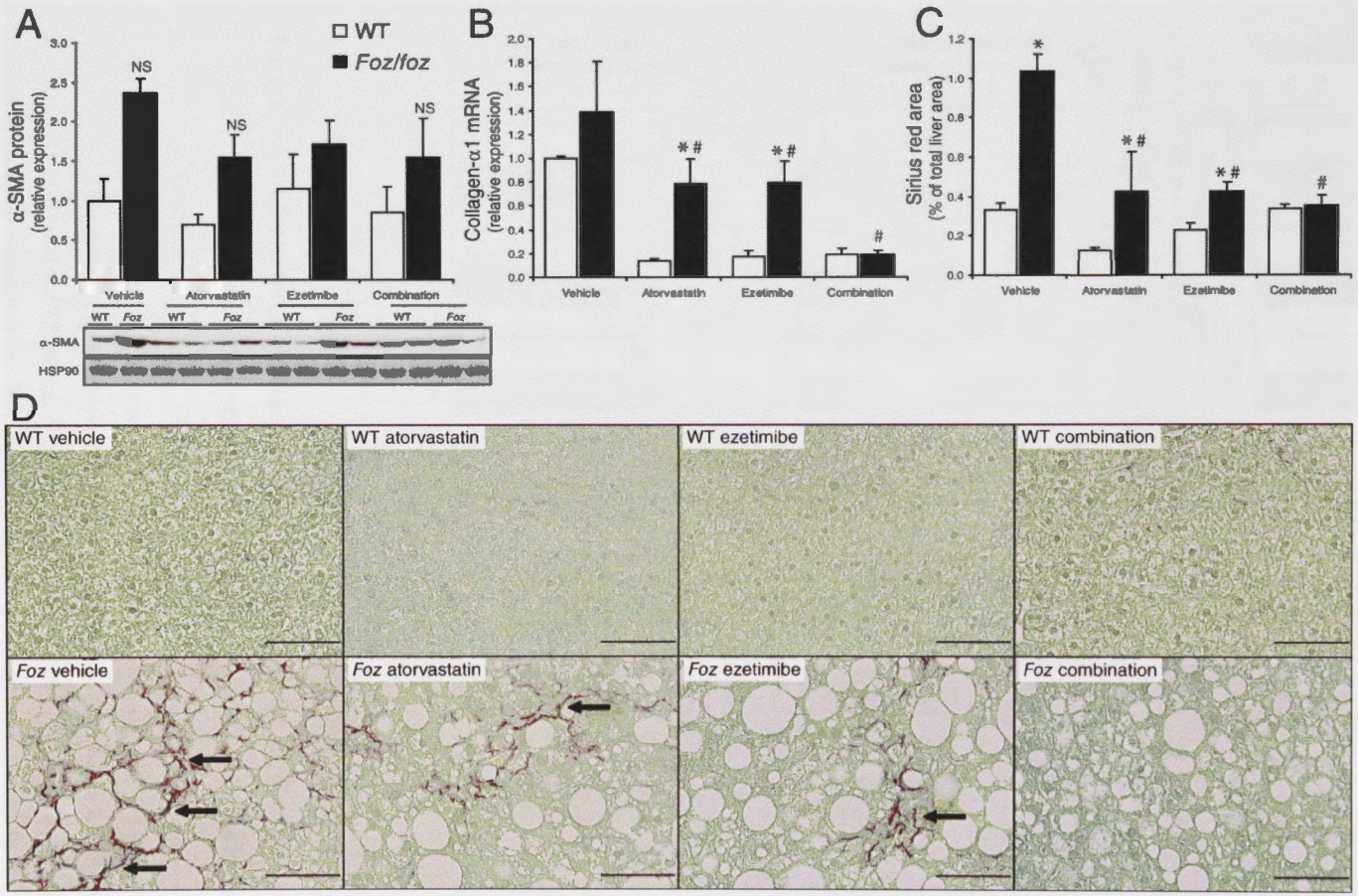

Figure 6.11 Analysis of liver fibrosis markers in HF-fed *foz/foz* and wildtype mice treated with or without atorvastatin and/or ezetimibe

(**A**) α-Smooth muscle actin (α-SMA) protein expression, (**B**) collagen-a1 mRNA expression, and (**C**) quantitative analysis of Sirius-red stained liver sections (representative sections are shown in panel **D**) in HF-fed *foz/foz* (■) and WT (□) mice (n=8-11/grp) treated with or without atorvastatin and/or ezetimibe. Sirius red image analysis was carried out as described in Section 2.6.1. α-SMA protein expression was normalised to heat-shock protein-90 (HSP90). Data in panels A-C are mean ± SEM. Scale bars represent 50 μm. *P<0.05, vs. treatment-matched, genotype control. $^{\#}P$<0.05, vs. genotype-matched, vehicle control.

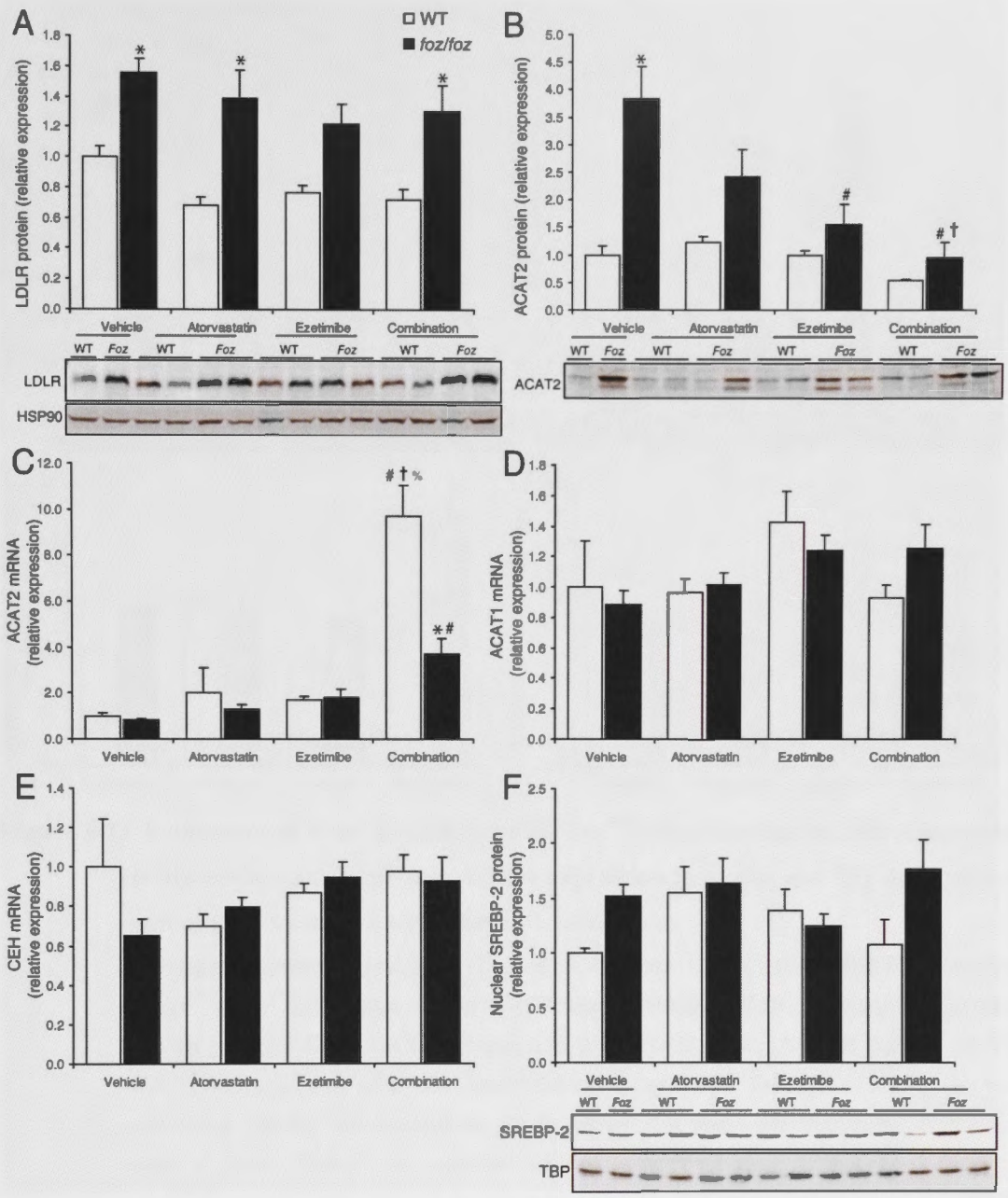

Figure 6.12 Cholesterol uptake, esterification and ester hydrolysis pathways in HF-fed *foz/foz* and wildtype mice, with or without atorvastatin and/or ezetimibe treatment

(**A**) Hepatic LDLR protein, (**B**) ACAT2 protein and (**C**) mRNA, and (**D**) ACAT1 mRNA, (**E**) CEH mRNA, and (**F**) nuclear SREBP-2 protein in WT (□) and *foz/foz* (■) mice fed high fat (HF) diet for 16 weeks, after which atorvastatin (20 mg/kg/day) and/or ezetimibe (5 mg/kg/day) were introduced into diet and administered for an additional 8 weeks (see Section 6.3.2). Nuclear SREBP-2 protein levels were normalised to TATA box-binding protein (TBP) expression. Data are mean ± SEM. $^{*}P<0.05$, vs. treatment-matched, genotype control. $^{\#}P<0.05$, vs. genotype-matched, vehicle group. $^{\dagger}P<0.05$, vs. genotype-matched, atorvastatin treatment group. $^{\%}P<0.05$, vs. genotype-matched, ezetimibe treatment group.

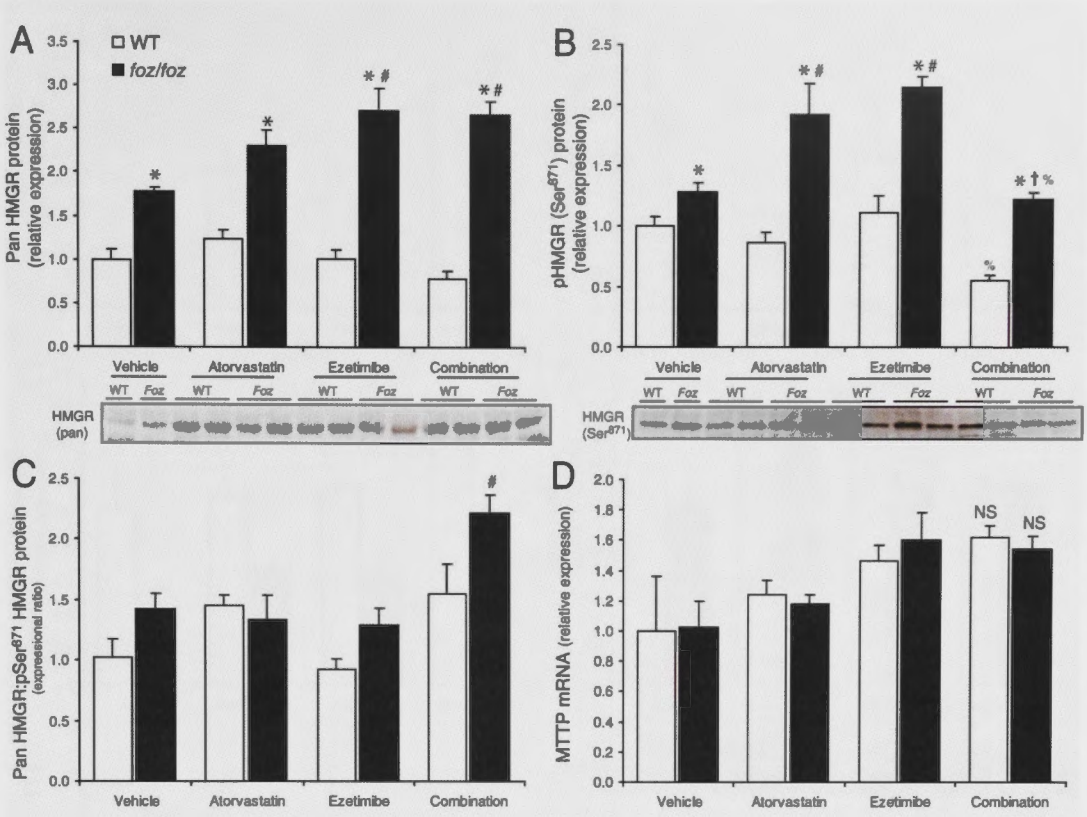

Figure 6.13 Expression of total HMGR protein, Ser^{871} phosphorylation, and microsomal triglyceride transfer protein mRNA expression in *foz/foz* and WT mice with or without atorvastatin and/or ezetimibe treatment

(**A**) Hepatic expression of total (pan) HMG-CoA reductase (HMGR), (**B**) HMGR phosphorylated at Ser^{871} (pSer^{871}), (**C**) ratio of total HMGR:pSer^{871} HMGR, and (D) microsomal triglyceride transfer protein (MTTP) mRNA expression in WT (□) and *foz/foz* (■) mice fed high fat (HF) diet for 16 weeks, after which atorvastatin (20 mg/kg/day) and/or ezetimibe (5 mg/kg/day) were introduced into diet and administered for an additional 8 weeks (see Section 6.3.2). Data are mean ± SEM. *P<0.05, vs. treatment-matched, genotype control. $^{\#}P$<0.05, vs. genotype-matched, vehicle group. $^{\dagger}P$<0.05, vs. genotype-matched, atorvastatin treatment group. $^{\%}P$<0.05, vs. genotype-matched, ezetimibe treatment group. NS, non-significant.

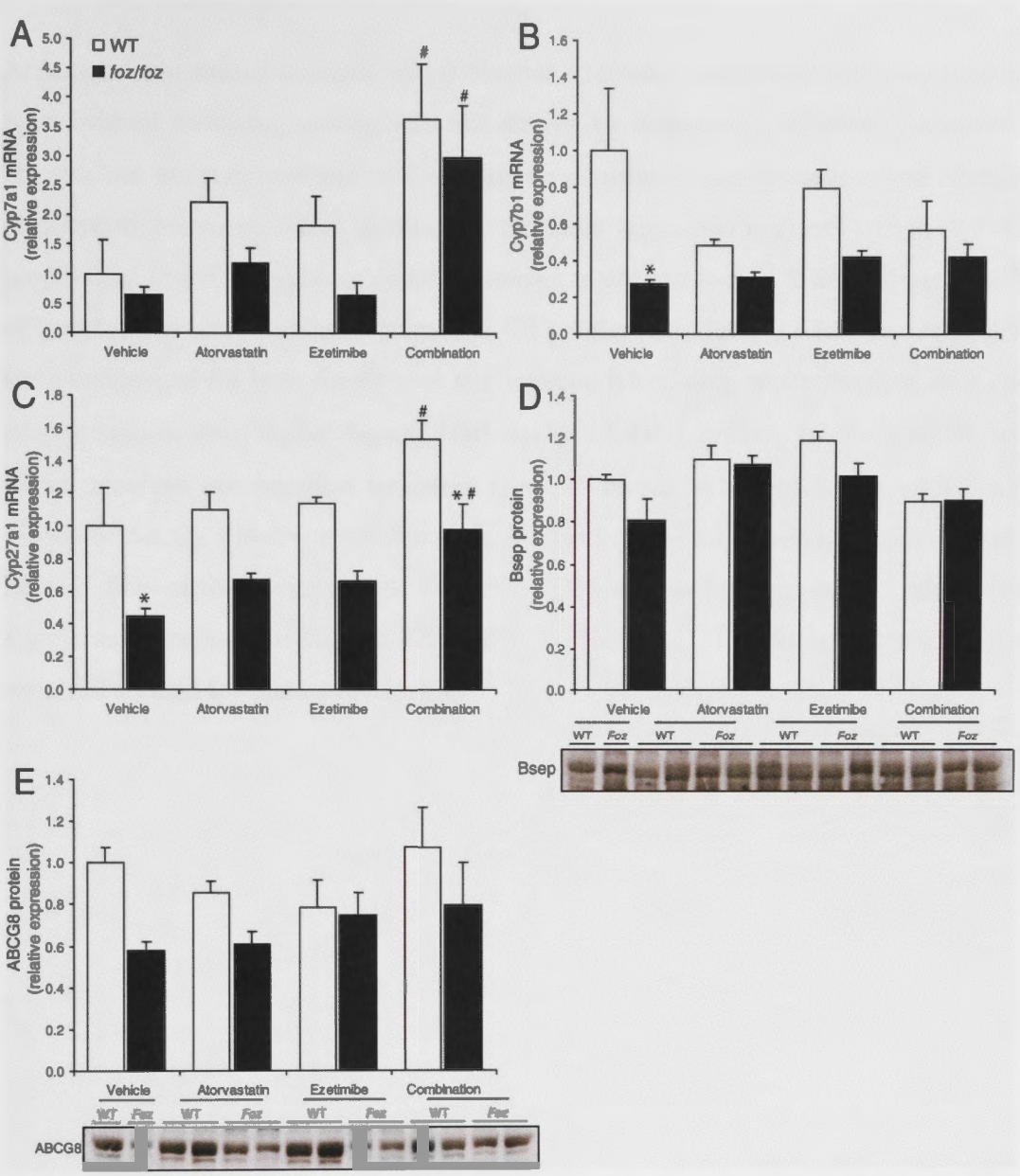

Figure 6.14 Atorvastatin and ezetimibe treatment minimally alter cholesterol biotransformation and export pathways in *foz/foz* and wildtype mice

(**A**) Hepatic Cyp7a1, (**B**) Cyp7b1, and (**C**) Cyp27a1 mRNA, (**D**) Bsep, and (**E**) ABCG8 protein in WT (□) and *foz/foz* (■) mice fed high fat (HF) diet for 16 weeks, after which atorvastatin (20 mg/kg/day) and/or ezetimibe (5 mg/kg/day) were introduced into diet and administered for an additional 8 weeks (see Section 6.3.2). Data are mean ± SEM. **P*<0.05, vs. treatment-matched, genotype control. $^{\#}P$<0.05, vs. genotype-matched, vehicle group. $^{\dagger}P$<0.05, vs. genotype-matched, atorvastatin treatment group. $^{\%}P$<0.05, vs. genotype-matched, ezetimibe treatment group.

Although only minor changes in cholesterol biotransformation and export pathways were evident following atorvastatin and ezetimibe treatment, expression levels of the key nuclear transcription factors that regulate cholesterol homeostasis could change in response to decreased serum insulin. We therefore quantified nuclear (active) SREBP-2 protein and found variable expression between treatment groups, but no apparent effect of genotype or drug treatment (Figure 6.12F). Likewise, nuclear LRH-1 protein levels were unchanged for both *foz/foz* and WT irrespective of drug treatment (Figure 6.15B), despite significantly higher hepatic HNF-4α and LRH-1 mRNA levels in *foz/foz* mice which received combination treatment ($P<0.05$ *versus* vehicle controls with NASH, Figure 6.15A,C). Finally, administration of atorvastatin and ezetimibe had no effect on hepatic Shp mRNA levels (NS, Figure 6.15D), and only an apparent minor (non-significant), increase in hepatic FXR mRNA (Figure 6.15F). Nuclear protein extracts were not studied for these experiments.

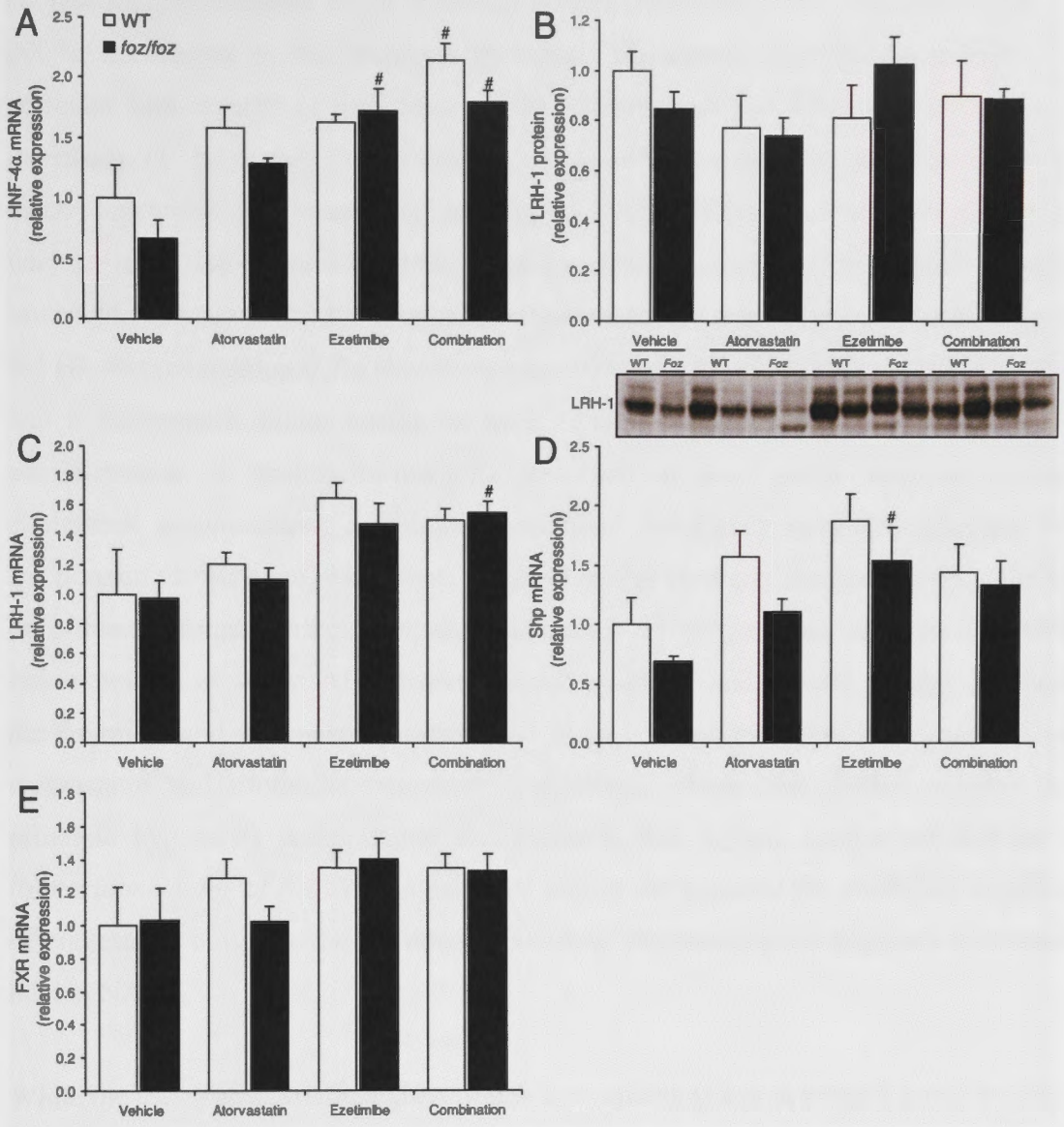

Figure 6.15 Analysis of cholesterol-regulating nuclear transcription factors in *foz/foz* and wildtype mice with or without atorvastatin and/or ezetimibe treatment

(**A**) HNF-4α mRNA, (**B**) nuclear LRH-1 protein and (**C**) mRNA, (**D**) Shp mRNA and (**E**) mRNA and (**F**) FXR mRNA protein in WT (□) and *foz/foz* (■) mice fed high fat (HF) diet for 16 weeks, after which atorvastatin (20 mg/kg/day) and/or ezetimibe (5 mg/kg/day) were introduced into diet and administered for an additional 8 weeks (see Section 6.3.2). Data are mean ± SEM. **P*<0.05, vs. treatment-matched, genotype control. $^{\#}P$<0.05, vs. genotype-matched, vehicle group. $^{\dagger}P$<0.05, vs. genotype-matched, atorvastatin treatment group. $^{\%}P$<0.05, vs. genotype-matched, ezetimibe treatment group.

6.5 Discussion

In earlier Chapters, we demonstrated that dysregulated cholesterol homeostasis is a dominant feature in the *foz/foz* mouse model of NASH, recapitulating hepatic

cholesterol accumulation found in human NASH (Puri *et al.* 2007; Caballero *et al.* 2009). In Chapter 5, the increases in hepatic cholesterol fractions were shown to correlate with severity of liver injury, liver inflammation and fibrosis in *foz/foz* mice; increasing FC by dietary means exacerbated liver injury, whereas normalising FC by dietary exclusion ameliorated the severity of NAFLD/NASH. In order to determine whether inhibition of cholesterol biosynthesis and/or cholesterol redistribution likewise lowered hepatic cholesterol stores to likewise ameliorate liver injury, *foz/foz* mice were fed HF diet (containing 0.2% cholesterol) for 16 weeks (to allow onset of NASH), after which atorvastatin and/or ezetimibe were administered for 8 weeks. Such 8 week administration of cholesterol-lowering treatment at least partly resolved hepatic cholesterol accumulation; combination treatment completely normalised hepatic FC fractions in *foz/foz* mice, while liver CE content was similarly markedly reduced in all drug-treated groups. Furthermore, each cholesterol-lowering regime was associated with improvements in serum ALT, hepatocellular apoptosis and hepatic fibrosis in obese *foz/foz* mice, and the most consistent and impressive effects were with combination atorvastatin and ezetimibe treatment. Collectively, these data further support the principle hypothesis underpinning this research, that *hepatic cholesterol acts as a lipotoxic mediator of NASH.* The data also inform the potential for combined targeting of cholesterol biosynthesis and uptake as a new pharmacological approach to reverse human NASH.

While the use of atorvastatin and ezetimibe individually is not an entirely novel NAFLD therapy, the successful combined use of these agents in reducing hepatic cholesterol fractions and improving NAFLD severity in the *foz/foz* model provides evidence to project their further study in clinical trials of NASH. Atorvastatin and ezetimibe each effectively lower serum total cholesterol levels in humans and rodents (Marais *et al.* 1997; Mathur *et al.* 2007; Enjoji *et al.* 2010; Zhang *et al.* 2010; Muraoka *et al.* 2011), and atorvastatin has become the most prescribed (and profitable) drug in history because of its protection against cardiovascular events (Simons 2003). Use of statins in patients with NAFLD is primarily targeted at preventing cardiovascular events, and their use has been found to be safe in this context (Chitturi and Farrell 2007; Bader 2010; Rzouq *et al.* 2010). Use of statins to combat NASH has been confined to a few, very small open studies, with no consistent evidence of efficacy. It is also important to note that statin treatment has also been shown to have additional beneficial effects including anti-

inflammatory action (Cowled *et al.* 2007) and endothelial protection, effects which contribute to hepato-protection against ischemia reperfusion injury (IRI) (Ajamieh and Teoh, unpublished data, 2011)(Yokota *et al.* 2003).

In 2006, Yamagishi and colleagues put forward a hypothesis proposing ezetimibe as a potential therapy for human NAFLD. The rationale for this was based on two factors. Firstly, empirical findings demonstrated that loss of NPC1L1 function protected against NAFLD in mice (Jia *et al.* 2010); hepatic NPC1L1 expression in HF-fed *foz/foz* mice with NASH was demonstrated in Section 3.4.7 (see Figure 3.9). Secondly, in humans NPC1L1 protein is predominantly (96-99%) expressed in liver *versus* intestine (1-4%); the inverse relationship is true for mice (Davies *et al.* 2005; Jia *et al.* 2010). Hughes *et al.* (2006), then published a letter detailing the fact that ezetimibe therapy (administered as treatment for cardiovascular risk disease, a common co-morbidity in patients with NAFLD), over an 8 month period, decreased both serum total cholesterol and serum transaminase levels in NAFLD, thereby demonstrating an improvement in liver injury. However, such improvement was attributed to potential anti-inflammatory effect of the antioxidant metabolic phenol by-products of ezetimibe (Hughes *et al.* 2006). More recently, Yoneda *et al.* (2010) conducted a pilot study, in which ten NASH patients were treated with 10 mg/day ezetimibe over a 6 month period. Ezetimibe treatment reduced transaminases and NAS score, while 60% of individuals treated showed an improvement in fibrosis score (Yoneda *et al.* 2010).

In regards to animal studies, Zheng *et al.* (2008) reported significant improvements in liver size, steatosis, steatohepatitis, and serum ALT in a HF (0.12% cholesterol)-fed C57Bl/6J mouse model of NAFLD, following 4 weeks of ezetimibe (5.3 mg/kg/day) monotherapy. In the present study, the doses of atorvastatin and ezetimibe used were based on previously documented atorvastatin and ezetimibe doses in mice, reinforced by the results of a pilot study examining serum ALT and total cholesterol levels at 4- and 8-week time points (Table 6.1). The pilot study (n=3/grp) consisted of female *foz/foz* mice fed HF diet for 16 weeks, after which atorvastatin (20 mg/kg/day) and ezetimibe (5 mg/kg/day) were added to HF diet as previously described (Section 6.3.2). These dosages were found to decrease serum cholesterol and ALT after 8 weeks of treatment (P<0.05 *versus* levels before drug administration, Table 6.1). Among many previous studies, the following doses of atorvastatin have been used: 8 mg/kg/day (Holub *et al.*

2004), 20 mg/kg/day (Wang *et al.* 2011), 30 mg/kg/day (Kozuki *et al.* 2011), and 60 mg/kg/day (Kanagarajan *et al.* 2008). Ezetimibe has been previously dosed in mice at 5 mg/kg/day (Nozaki *et al.* 2009) and 8-20 mg/kg/day (Wang *et al.* 2008). Given the ranges used in these experiments, the doses used in this study can be regarded as "mid-range" or "moderate" in comparison. Additionally, the actual doses of atorvastatin and ezetimibe delivered to each mouse in this study could vary from the calculated amount; in most cases they were probably less than 20 mg/kg/day for atorvastatin, and 5 mg/kg/day for ezetimibe. This assumption is based on the fact that these drugs only coated the food pellets of supplemented diets and were not incorporated homogeneously. The calculations used to work out drug doses assume that drug content is consistent throughout the diet consumed within one day. With this design, once the outer layers of food pellets are consumed, drug delivery is halted. While this limitation could have been overcome by intraperitoneal (IP) injection, this method of drug administration requires daily mouse handling, imparting unnecessary stress (Ryabinin *et al.* 1999; Advani *et al.* 2009), which may also alter feeding habits. Irrespective of the limitations of the methodology used in this study, significant reductions in serum total cholesterol, as well as hepatic FC and CE were observed for drug-treated mice, indicating expected pharmacological effects of the drugs. Further, body weights were consistently heavier in drug-treated *foz/foz* mice than in WT controls, indicating little if any impact on obesity.

The combination of ezetimibe and atorvastatin was more efficacious than ezetimibe or atorvastatin monotherapy in attenuating liver injury and improving liver pathology of obese *foz/foz* mice. This could indicate that cholesterol biosynthesis, as well as, cholesterol uptake each contribute importantly to hepatic cholesterol fractions involved in the pathogenesis of NASH in *foz/foz* mice. Alternatively, each "blocker" is known to promote feedback upregulation of the alternate pathway, that is, statins increase NPC1L1, while ezetimibe increases HMGR activity (Sudhop *et al.* 2002; Tremblay *et al.* 2011). Interestingly, blocking cholesterol uptake and biosynthesis using combined atorvastatin and ezetimibe treatment, resulted in significant elevations in active HMGR (Figure 6.13C). This may constitute an adaptive response to restricted intercellular cholesterol pools in combination drug treated *foz/foz* mice. However, the role of cholesterol uptake and biosynthetic pathways in contributing to hepatocellular cholesterol accumulation and mediating NASH pathogenesis may differ in humans. In a

small Budapest study (Abel *et al.* 2009), 26 patients were assigned 20 mg/day simvastatin monotherapy, while 19 received a combination of ezetimibe and simvastatin (each at 10 mg/day). The primary objective of that study was to determine the safety and efficacy of combined ezetimibe and statin treatment in individuals with NAFLD and increased cardiovascular risk disease. While the combination treated groups showed significant improvements in serum ALT and AST levels, simvastatin monotherapy was more efficacious in reducing transaminases than drug combination (Abel *et al.* 2009). It is also possible that the ratio of statin:ezetimibe used in combination therapy may be important. In the Abel study (2009), the dose of simvastatin used in combination treatment was only 50% that used in monotherapy treatment groups.

In HF-fed obese *foz/foz* mice, atorvastatin treatment resulted in a marginal increase in hepatic macrophage infiltration. It is plausible that during the 8 week period of cholesterol biosynthesis and uptake inhibition, macrophages were recruited into the liver to assist in apoptotic cell clearance by phagocytosis. This would explain the morphology of macrophages noted in vehicle and atorvastatin-treated *foz/foz* mice. In ezetimibe and combination-treated mice, however, macrophages did not show predominant localisation around macrosteatotic hepatocytes (Figure 6.10). Given that livers from these mice contained significantly lower amounts of FC (Figure 6.5B), it may be assumed that ezetimibe treatment allows faster resolution of the hepatic cholesterol burden, thereby allowing more rapid macrophage-dependent clearance of dead or dying hepatocytes. The randomly distributed F4/80 positive cells present in ezetimibe and combination-treated *foz/foz* mice may constitute remnants of the original recruited population. It is important to note that the morphology of most F4/80 positive cells in combination-treated *foz/foz* livers does not resemble that of macrophages in the process of phagocytosis, as is clearly evident in livers of vehicle and atorvastatin-treated *foz/foz* mice (Figure 6.10). However, further studies to phenotype the macrophages present in this NASH model and after different treatments is required to establish the functional implications of these morphological observations.

Among possible explanations for the changes in non-cholesterol lipids, we studied adipose sites, adiponectin and insulin sensitivity. The first interesting finding was that atorvastatin and ezetimibe treatment of HF-fed *foz/foz* mice increased serum adiponectin levels ($P<0.05$, Figure 6.4F), along with corresponding changes in peri-ovarian adipose

weight ($P<0.05$, Figure 6.4B). Given that one of the primary functions of adipose tissue is to store FC (Angel 1970; Farkas *et al.* 1973), the cholesterol storage capacity of adipose tissue may also play a role in cholesterol-mediated liver injury. It is possible that statin and ezetimibe treatment improves either overall adipose tissue function, and in turn promotes adiponectin expression, or statin/ezetimibe treatment is directly involved in the regulation of bodily lipid partitioning. The latter is unlikely since subcutaneous WAT weights were unchanged in the present experiments, irrespective of drug treatment (Figure 6.4C). Alternatively, inhibition of cholesterol biosynthesis and uptake over the 8 week treatment period may specifically improve visceral adipose function. Increased visceral fat pad storage is a potential explanation for the reductions in liver weight observed in drug-treated *foz/foz* mice (Figure 6.4A), since hepatic lipid stores (including cholesterol and TG) may be redistributed to visceral WAT. The reduction in liver mass may also be assisted by the direct inhibition of cholesterol biosynthesis and uptake by atorvastatin and ezetimibe, respectively. Interestingly, BAT tissue weights also increased following atorvastatin and/or ezetimibe treatment in HF-fed *foz/foz* mice. Furthermore, whereas the modest expansion of BAT in untreated *foz/foz* mice likely reflects increased lipid storage, the appearance of BAT in drug treated mice (dark brown) is consistent with increased thermogenic function. However, no apparent changes were observed for WT mice, irrespective of drug treatment. Physiologically, BAT serves as the primary energy source for bodily thermoregulation in mammals, especially in those like rodents which lack the capacity to shiver. In BAT tissue, cellular respiration is highly exothermic and increases body temperature. Located interscapularly, murine BAT weights indicate thermogenic function in mice (Bazin *et al.* 1985; Mercer and Trayhurn 1987; Trayhurn and Jennings 1988). Therefore, from the results of this study, it could be inferred that atorvastatin and/or ezetimibe treatment increases the thermogenic capacity and basal metabolic rate in HF-fed *foz/foz* mice. However this study would need to be repeated using metabolic cages to establish whether changes in metabolic rate can be produced by atorvastatin and ezetimibe treatment.

In addition to the above changes in adipose storage and function, the cholesterol-lowering agents used here could have improved insulin sensitivity. Inhibition of hepatic NPC1L1 (using ezetimibe, and a "knockdown" strategy with shRNA) has been shown to improve insulin sensitivity in Zucker obese fatty rats as assessed by increased

serine/threonine protein kinase phosphorylation, decreased JNK activation and reduced in ER stress (Nomura *et al.* 2009). In the following Chapter, we demonstrate that JNK activation is increased in *foz/foz* mice with NASH, and attenuated following atorvastatin and ezetimibe treatment. It is plausible that ezetimibe, by inhibition of NPC1L1, may likewise contribute to improved insulin sensitivity both in liver and adipose tissues of HF-fed *foz/foz* mice. This would account for the observed reduction in serum insulin, and may further explain decreased hepatic TG levels via lowered adipose lipolysis and hepatic lipogenesis. However, these specific aspects were beyond the scope of the present study and require further investigation. Furthermore, the contribution of decreased steatosis would also need to be explored. In particular, Akt phosphorylation, an intermediate of insulin signalling pathway, as well as SREBP-1c and carbohydrate response element binding protein (ChREBP) should be determined in atorvastatin and ezetimibe-treated *foz/foz* mice to establish whether this is the case.

Atorvastatin and ezetimibe monotherapy decreased hepatic CE fractions 2.5- and 4.0-fold, respectively, in HF-fed *foz/foz* mice compared with vehicle controls. An even more impressive ~10-fold reduction in hepatic CE was observed in combination drug-treated *foz/foz* mice ($P<0.05$, Figure 6.5A). In contrast, the effect of atorvastatin and ezetimibe monotherapy on hepatic FC was comparable; atorvastatin and ezetimibe monotherapy and combination treatment resulted in ~2-4-fold reductions in FC in HF-fed *foz/foz* mice *versus* genotype-matched vehicle controls (Figure 6.5B). In the previous Chapter, oxysterols were also found to correlate with patterns of liver injury in *foz/foz* mice. Unfortunately, in this study oxysterol analyses are not yet completed. The results may provide evidence to implicate or refute oxysterol involvement in NASH pathogenesis.

Atorvastatin and ezetimibe treatment had differential effects on pathways of cholesterol homeostasis in *foz/foz* mice. The cholesterol uptake pathway, namely LDLR, was unchanged, while cholesterol storage and CE hydrolysis pathways were variably altered. Hepatic ACAT2 protein levels were significantly decreased, most likely in response to lowered hepatic accumulation of CE and FC in drug-treated *foz/foz* mice. Despite this, ACAT2 mRNA was actually increased in combination-treated *foz/foz* and WT mice. A plausible explanation is that combination drug treatment induces VLDL export from the livers and in favour of this, MTTP mRNA levels were increased (Figure 6.13D). Also likely in response to falls in cholesterol pool size, Cyp7a1 and Cyp27a1 mRNA levels

were elevated in combination-treated *foz/foz* mice compared to genotype-matched controls, suggesting that pathways of cholesterol to bile acid biotransformation can be augmented in these mice by drug treatment, thereby assisting in hepatic clearance of FC. The resultant BA formation would account for the observed increase in FXR mRNA (Figure 6.14E).

In contrast to esterification and biotransformation, there were no remarkable changes in pathways of cholesterol/BA export for atorvastatin and ezetimibe-treated mice. Despite unchanged nuclear LRH-1 protein levels (Figure 6.14B), drug treatment restored HNF-4α and LRH-1 mRNA levels in both *foz/foz* and WT mice. It is possible that longer term therapy would raise/restore nuclear LRH-1 protein levels in obsess *foz/foz* mice. Nevertheless, this study demonstrates that, with atorvastatin and ezetimibe treatment, HNF-4α and LRH-1 mRNA levels increase as NASH severity decreases; reciprocal changes that mirror the decrease in hepatic cholesterol stores. Although atorvastatin and ezetimibe each produced the anticipated reductions in hepatic cholesterol levels, an unexpected observation was that their effects also extended to hepatic TG and total FFA lipids, albeit these decreased to a lesser extent than CE. As previously reported, hepatic TG fractions are not thought to play a direct role in NASH pathogenesis (Neuschwander-Tetri 2010a, 2010b).

Despite the exciting new data brought forward by this section of research, this study was subject to several logistical difficulties. Most notably, *foz/foz* mice used in these experiments weighed ~18% less than those described in Chapter 5 ($P<0.05$, Figure 6.3A,B *versus* Figure 5.1A). There is an unfortunate logistical explanation for this (other than phenotypic drift in obesity severity in our *foz/foz* colony). Firstly, this study coincided with upgrades to The Canberra Hospital (TCH) Animal House and construction of the neighbouring Canberra Women's and Children's Hospital. In addition to the considerable ambient noise, it was necessary to move our TCH mouse colony to a temporary (suboptimal) animal facility located 15 km away on the Australian National University campus. Mice were subsequently returned to TCH for harvests at experimental endpoints (the upgrade to the TCH animal facility was delayed, and not completed until the conclusion of this study). Secondly, during the initial move, mice in several cages assigned to this study, notably both *foz/foz* and WT, began grinding down food pellets, apparently using it as nesting material. Additional sterile

aspen shavings and Enviro-dri® nesting material was subsequently introduced into the cages to assist acclimation and remediate the situation. In a few cages, grinding of the diet did continue until the time of termination. Such grinding (powdering) of food pellets posed a problem since drug delivery was largely dependent on mice eating the outer layer of these food pellets, containing the applied drug (see earlier in Section 6.3.2). In effect, this meant the security (reproducibility) of drug delivery was no longer guaranteed. However, as speculated earlier this is more likely to have resulted in under-delivery of drug than intake in excess of that calculated.

It is conceivable that ambient noise (building construction, vibration) and moving the mice altered feeding patterns and induced behavioural stress, either or both of which resulted in lower total body weight and a less severe NASH phenotype; this is evident in the trend for lower serum ALT (357 ± 57 U/L for HF-fed *foz/foz* vehicle this study *versus* 430 ± 26 U/L for HF [0.2% cholesterol]-fed *foz/foz* mice in Chapter 5), macrophage infiltration, and liver fibrosis. However, from the point of view of the controlled nature of this study, all mice, both positive genotype controls and experimental groups were subject to the same conditions (housing, transport, mode of food delivery, caging, temperature, humidity, handling). We are therefore confident that the effects of atorvastatin and ezetimibe treatment occurred independently of external factors.

Another logistic challenge of this study was the large number of animal groups. This posed a problem for quantifying protein expression by western blotting. As each SDS-PAGE gel can only be loaded with 14 samples, the overall number of samples that can be analysed (by direct comparison on the same gel) for each of the 8 groups used in this study was restricted. Furthermore, comparison western blots needed for inter-group comparisons were confined to a maximum of 1-2 samples on combination gels. This explains the apparent extent of sample variation observed for the various samples quantified using western blotting (see Figures 6.11A, 6.12F, 6.14D,E, 6.15B). Nevertheless, multiple gels were run simultaneously, with *foz/foz* and WT mice assessed separately and then together to ensure that at least 6-8 samples/group were analysed (all westerns were repeated at least twice).

In conclusion, drug treatment designed to lower hepatic cholesterol stores, achieved that objective, and in doing so decreased liver injury, inflammation and fibrosis in NASH. These results provide further support to implicate cholesterol as a lipotoxic mediator of NASH in obese, diabetic *foz/foz* mice. While we have not excluded additional roles for FFA (particularly long chain saturated FA; and decreased PuFAs) and oxysterol species, these data may provide insight into human NAFLD. Noting that the liver improvement included both hepatocellular injury and apoptosis, and also liver inflammation and fibrosis, further attention should be given to how cholesterol could engage a pro-inflammatory and pro-fibrotic stimulus. This will be addressed in the next Chapter (7).

6.6 Summary of findings

The primary findings of this study are outlined below:

1. Atorvastatin and/or ezetimibe significantly lower hepatic FC and CE lipid profiles in HF-fed *foz/foz* mice, with most impressive effects for combined therapy.
2. Reductions in hepatic FC and CE levels are associated with decreased liver injury (serum ALT), hepatocellular cell death, liver macrophage infiltration, and fibrosis.
3. Atorvastatin and/or ezetimibe treatment increases serum adiponectin levels, with concomitant reductions in serum insulin levels, suggesting that drug treatment may improve adipose function and increase insulin-sensitivity.
4. There were also changes in hepatic TG and some saturated FFA species after atorvastatin and/or ezetimibe treatments, which were tentatively attributed to improved adipose function (raised serum adiponectin) and insulin sensitivity, but this aspect and the significance of the FFA changes requires further study.

CHAPTER 7

Pathways of cholesterol-mediated liver injury in *foz/foz* mice with non-alcoholic steatohepatitis

7.1 Introduction

Despite uncertainty regarding the exact molecular pathways involved in liver injury during NASH pathogenesis, most patients with this disorder exhibit evidence of caspase 3-mediated hepatocellular apoptosis, histological and cytokine evidence of liver inflammation, and (in those with more severe forms of the disease) liver fibrosis, whereas those with simple steatosis do not (Haukeland *et al.* 2001; Perez-Aguilar 2005; Ramalho *et al.* 2006; Wieckowska *et al.* 2006; Ferreira *et al.* 2011; Singh *et al.* 2011). *c*-Jun *N*-terminal kinase (JNK) activation is well documented in human NASH and rodent steatohepatitis models (MCD and CDAA diet-induced)*; it is a potent activator of caspase 3-mediated (apoptosis) cell death (Yang *et al.* 2001; Malhi *et al.* 2006; Schattenberg *et al.* 2006; Ferreira *et al.* 2011; Sharma *et al.* 2011; Wree *et al.* 2011). Liver inflammation and fibrotic severity in NASH have also been correlated with activation of nuclear factor-κB (NF-κB) in both humans (Ribeiro *et al.* 2004) and animal models (Nanji *et al.* 1999; Dela Pena *et al.* 2005; Wouters *et al.* 2008). In the MCD model, NF-κB activation was necessary for inflammatory recruitment and occurred independently of TNF-α or TNF receptor-1 (TNFR1) (Dela Pena *et al.* 2005).

***Footnote**: We would argue that the MCD and choline deficient amino acid defined (CDAA) models are caused by nutritional depletion and do not fall logically into obesity/insulin-resistance-related NASH.

Given the substantially increased hepatocellular apoptosis and inflammation observed in cholesterol-loaded *foz/foz* mouse livers with NASH, we hypothesised that JNK and NF-κB are pathways involved in cholesterol-mediated liver injury and inflammatory cell recruitment. Details pertaining to the major pathways of cell death and inflammation and their signalling are described next, acknowledging that pathway reviews are not exhaustive. Instead, the aim is to provide a mechanistic overview of the potential pro-inflammatory/apoptotic pathways studied in this Chapter.

7.1.1 The JNK proapoptotic pathway

JNK activation can be initiated by cellular stress and injury, inducing an apoptotic response (Liu *et al.* 2002a). Kluwe *et al.* (2010) have identified JNK activation in fibrotic liver samples from patients with chronic hepatitis C and NASH, as well as in mice administered CCl_4 or subject to bile duct ligation. Other recent investigations have identified JNK activation specifically in NASH patients *versus* those with SS (Puri *et al.* 2008; Ferreira *et al.* 2011).

JNK proteins are members of the mitogen activate protein kinase (MAPK) superfamily, which respond to cytokine death receptor activation and directly to cellular stress signals. In the latter context, they are also referred to as stress-activated protein kinases (SAPK). Potential JNK-activating stressors include oxidant stress, shearing (physical) stress, heat stress, ultra-violet radiation, and ER (metabolic) stress. Signalling via growth factors, some other cytokines and toll-like receptors (TLR) may also involve activation of the JNK cascade. Three JNK genes (JNK-1, -2, and -3) each produce 46- and 54 kDa isoforms, and these appear to function identically. JNK-1 and -2 are ubiquitously expressed in mammals and have subsequently been assessed in this study.

JNK activation is either initiated by upstream death receptor signalling (extrinsic pathways, see Figures 7.1A and 7.2) or via intrinsic (stress) pathways; the latter particularly involve mitochondrial events. Signalling via the extrinsic pathways results in activation of TNF receptor-associated factor-2 (TRAF2) and/or generation of reactive oxygen species (ROS) (Natoli *et al.* 1997; Reinhard *et al.* 1997). In turn, these factors induce apoptosis signal-regulating kinase 1 (ASK1), which subsequently, in a scaffold protein-dependent fashion, activates mitogen-activated protein kinase kinase-4/-7 (MKK4/7) (Ichijo *et al.* 1997). MKK4/7 activates JNK by phosphorylation (Deacon and Blank 1997; Cuenda and Dorow 1998). Once activated, JNK can either undergo nuclear translocation to promote transcription of pro-apoptotic factors, or alternatively to target mitochondrial apoptotic events (Lei *et al.* 2002). The latter is triggered by active JNK activation of Bim, a pro-apoptotic protein, which along with JNK, phosphorylates Bcl2 and/or Bcl-X_L, thereby inhibiting the anti-apoptotic functioning of these proteins (Deng *et al.* 2001; Lei and Davis 2003; Putcha *et al.* 2003). Separately, JNK cleaves Bid into a smaller protein known as jBid, which enters the mitochondria and results in the release of mitochondrial Smac/DIABLO (Deng *et al.* 2003). Cytosolic Smac/DIABLO

interferes with the interaction of TRAF2 and *c*-IAP1 present in the TNF receptor-1 (TNFR1) complex (see Figure 7.2F), thereby initiating caspase 8 activity. This triggers activation of the caspase cascade to culminate in cellular apoptosis (Deng *et al.* 2003) (Figure 7.1A). Activated JNK also phosphorylates *c*-Jun, thereby forming *c*-Jun:*c*-fos heterodimers that serve as the activating protein-1 (AP-1) early response transcription factor (Botteron and Dobbelaere 1998; Humar *et al.* 2007). Many NF-κB p65 regulated genes also have an AP-1 recognition site in their promoter regions. In this way, JNK signalling via AP-1 may augment the proinflammatory effects of NF-κB p65 (discussed next).

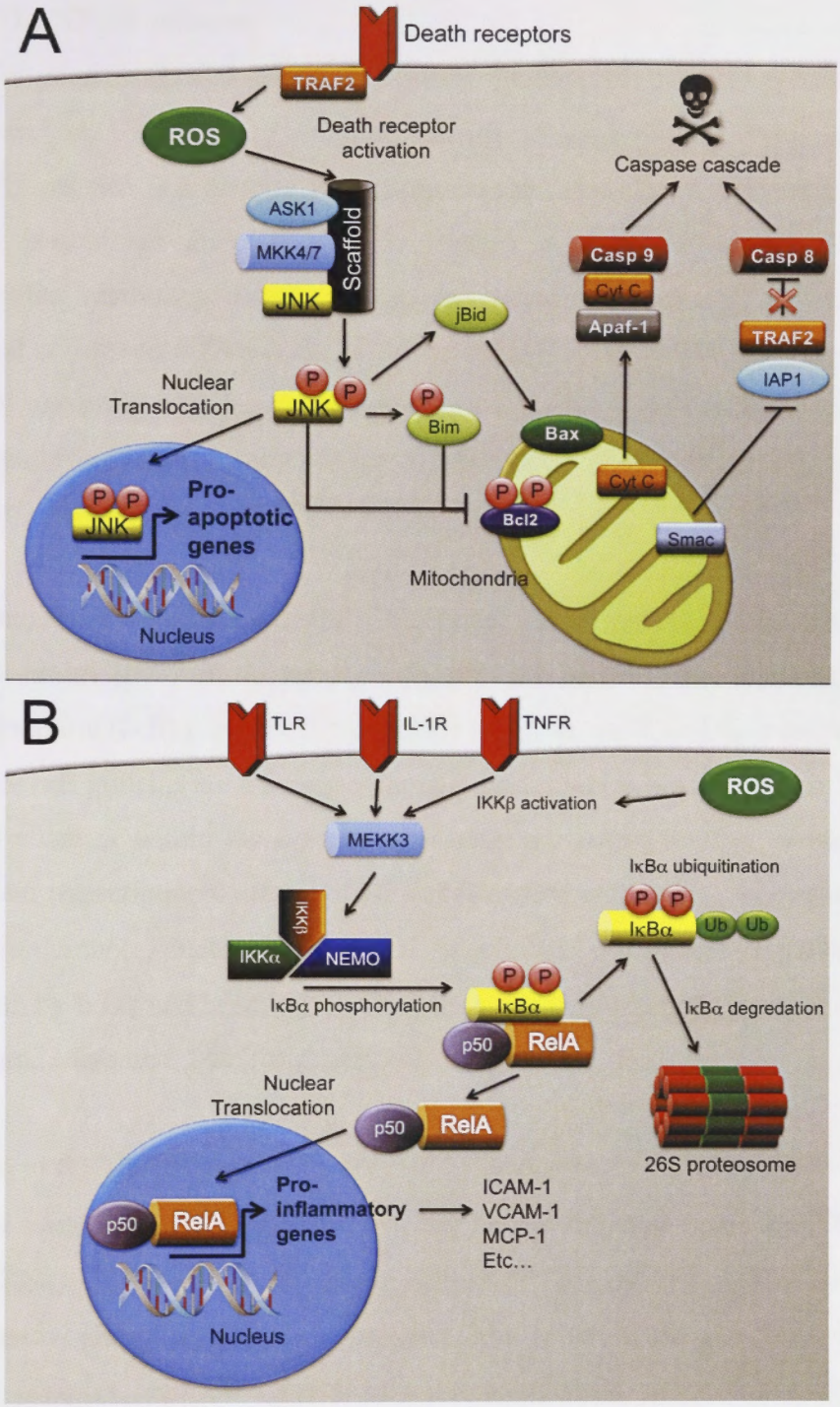

Figure 7.1 JNK and NF-κB p65 (RelA) activation pathways

Schematic representation of (**A**) JNK and (**B**) NF-κB activation pathways. Molecular details of the activation steps in these signaling pathways are detailed in Sections 7.1.1 and 7.1.2.

Abbreviations: Apaf1, apoptotic peptidase activating factor 1; ASK1, apoptosis signal-regulating kinase; Casp, caspase ; Cyt C, cytochrome C; IκBα; NF-κB inhibitor-α; IKK; IκB kinase; IL-1R, interleukin-1 receptor; JNK, *c*-Jun *N*-terminal kinase; MEKK, mitogen activated protein kinase kinase; NEMO, NF-κB essential modulator; ROS, reactive oxygen species; TLR, toll-like receptor; TRAF2, TNF receptor-associated factor 2; Ub, ubiquitin.

7.1.2 The NF-κB pathway

NF-κB is composed of 5 peptides (NFKB1 [p50/p105], NFKB2 [p52/p100], RelA [p65], c-Rel and RelB). These form homodimeric or heterodimeric complexes (Gilmore 2006). NF-κB p65 is a 65 kDa transcriptional regulator highly expressed in the liver; p65:p65 homodimer and p65:p50 heterodimer tend to be proinflammatory and proapoptotic, whereas p50:p50 tends to upregulate anti-apoptotic, anti-inflammatory genes and cell survival (Ivanov *et al.* 1995; Aoudjit *et al.* 1997). Accordingly, NF-κB p65 is of particular relevance in NASH, since it is able to modulate the expression of pro-inflammatory and pro-apoptotic genes associated with liver injury and inflammation (Ban *et al.* 2007; Videla *et al.* 2009).

NF-κB members are expressed within the cytoplasm of most cells (Hayden and Ghosh 2004; Nishikori 2005). In the resting state, they are bound to and regulated by several NF-κB inhibitor (IκB) proteins; these include IkBα, -β and ε, and their precursors, p100 and p105. IκB proteins are a family of small peptides which bind and detain the NF-κB-p65/p50 complex within the cytoplasm, thereby preventing nuclear translocation and subsequent transcriptional effects of NF-κB (Huxford *et al.* 1998; Jacobs and Harrison 1998). Furthermore, nuclear DNA-bound NF-κB can be displaced and returned to the cytoplasm by IκBα and IκBε, which are able shuttle between the nucleus and cytoplasm (Huang and Miyamoto 2001; Birbach *et al.* 2002).

Initiation of the NF-κB pathway is effected by activation of IκB kinase (IKK) complex, which is comprised of IKKα and IKKβ and NF-κB essential modifier (NEMO) (also called IKKγ) (Yamaoka *et al.* 1998; Karin and Ben-Neriah 2000). This complex subsequently phosphorylates IκB proteins. The latter dissociate from the NF-κB-p65/p50 complex, and are subsequently polyubiquinated which targets them to 26S proteosome for proteolysis (Hayden and Ghosh 2004; Scheidereit 2006). The dissociated NF-κB heterodimer subsequently enters the nucleus (by an active transporter) where it binds to DNA recognition sites to promote the transcription of NF-κB responsive genes.

Nuclear p65 promotes the transcription of several hundred proinflammatory genes, including COX-2, ICAM-1, iNOS, MCP-1, proIL-1β, proIL-18, TNF-α, and VCAM-1

(Shu *et al.* 1993; Aoudjit *et al.* 1997; Martin *et al.* 1997; Goto *et al.* 1999; Ping *et al.* 1999). ProIL-1β and proIL-18 are involved in the inflammasome pathway (Figure 7.4), which is described later in Section 7.1.4.

7.1.3 TNF and TNF-related pathways of NF-κB and JNK activation

Like JNK, and often in parallel with JNK activation, NF-κB is initiated by several stress-related stimuli, including ROS, oxidised LDL, and signalling via TNF-α receptor 1 (TNFR1), and related members of the TNF superfamily of "death-activated" receptors (DR). There are ~40 ligand-receptor molecules related to the TNF superfamily of genes (Aggarwal 2003), including FasL/Fas, and TNF-related apoptosis inducing ligand (TRAIL) and its cognate receptors (Brand *et al.* 1997; Muroya *et al.* 2003; Clark and Valente 2004). As of 2003,

TNF-α is responsible for mediating an array of gene responses, and these are induced through TNFR1 and TNFR2 receptor signalling. Signalling through TNFR1 (as well as DR3 and -6) activates TNFR1-associated DEATH domain protein (TRADD), which in turn signals TNF receptor-associated factor 2 (TRAF2) to activate NF-κB p65 via replication protein A interacting protein (RIP), or JNK through the glucokinase (GCK)-MEKK1/4-MKK4/7 axis (Hsu *et al.* 1995; Baker and Reddy 1998; Kieser *et al.* 1999; Park *et al.* 2001) (Figure 7.2). Alternatively, TRADD is capable of activating FAS-associated death domain (FADD) to subsequently induce the caspase-8 cascade, culminating in caspase-3 activation and apoptosis (Srinivasula *et al.* 1997) (Figure 7.2). TNFR2 also signals through TRAF2, but this not dependent on the TRADD intermediate; as a result, it is not capable of triggering the FADD cascade (Shu *et al.* 1996; Depuydt *et al.* 2005). In contrast, FasL and TRAIL signalling through CD95 (Fas), DR4 and –5 receptors (or TRAIL murine Killer in mouse [Killer]) only proceeds through the FADD cascade, thereby terminating in the induction of apoptosis (Rytomaa *et al.* 1999; Kischkel *et al.* 2000; Roth and Reed 2004; Thomas *et al.* 2004) (Figure 7.2). However, these receptors do have JNK and NF-κB p65 activation potentials, which proceed through RIP signalling (Lin *et al.* 2000).

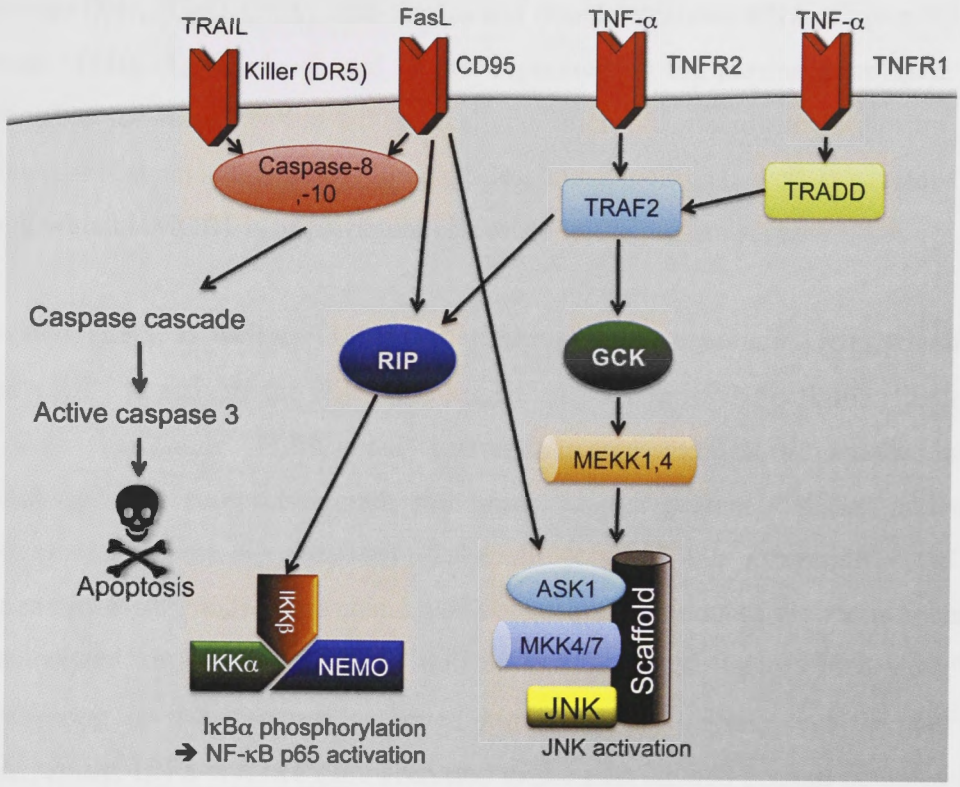

Figure 7.2 Tumour necrosis factor-related signaling pathways involved in JNK and NF-κB p65 (RelA) activation

Molecular details of the activation steps in these signaling pathways are detailed in Section 7.1.3. Abbreviations: ASK1, apoptosis signal-regulating kinase; CD95, TNF receptor superfamily member 6; DR, death receptor; FasL; Fas ligand; GCK, glucokinase; IκBα; NF-κB inhibitor-α; IKK; IκB kinase; IL-1R, interleukin-1 receptor; JNK, *c*-Jun *N*-terminal kinase; MEKK, mitogen activated protein kinase kinase; NEMO, NF-κB essential modulator; RIP, replication protein A interacting protein; TNF, tumour necrosis factor; TNFR, TNF receptor; TRADD, TNF receptor type 1-associated DEATH domain protein; TRAF2, TNF receptor-associated factor 2; TRAIL, TNF-related apoptosis-inducing ligand.

7.1.3.1 TLR pathways of NF-κB and JNK activation

Toll-like receptors (TLR) constitute a family of receptors involved in pro-inflammatory signalling in the innate immune system. They are responsible for the recognition of pathogen-associated molecular patterns (PAMPs) (Akira *et al.* 2006; Kaisho and Akira 2006). TLRs may be triggered by exogenous stimuli, such as pathogens, or endogenous agonists, such as sterile tissue damage (Jiang *et al.* 2005); in the later case, the molecules that can serve as TLR ligands are termed danger-associated molecular patterns (DAMPs). There are 9 known TLR receptors (1-9), four of which (TLRs 3, 7, 8, and 9) are present on the endosomal membrane and are responsible for viral particle surveillance, which includes the detection of deoxy-cytidylate-phosphate-deoxy-

guanylate DNA (CpG-DNA), and single- and double-stranded RNA (Figure 7.3). In contrast, TLRs -1, -2, -4, -5, and -6 are expressed on the plasma membrane and are responsible for the detection of extracellular microbial pathogens. Relevant PAMPs include: LPS, diacyl- and triacyl lipopeptides, and flagellin, as well as several DAMPs, among which HMGB1 is of particular relevance to the present review.

Activated TLR3, as well as TLR4, signal through adaptor protein TRIF, which in turn recruits RIP1 to activate the IKK complex, thereby activating NF-κB p65 (Figures 7.1B and 7.3). The other TLRs, once activated signal through a cascade involving Toll/interleukin-1 receptor domain containing adaptor protein (TIRAP) and myeloid differentiation factor 88 (Myd88) (Takeuchi *et al.* 2000; Fitzgerald *et al.* 2001; Bannerman *et al.* 2002). Activated Myd88 subsequently induces the recruitment of IL-1R-associated kinase (IRAK) 4, as well as IRAK1. These factors bind TRAF-6 and transforming growth factor-β activated kinase (TAK)-1 (Seki and Brenner 2008). Subsequently, IRF5 and IRF7 are recruited to the post-Myd88 protein complex (Figure 7.3). IRF7 recruitment is dependent upon on TLR7 and TLR9 signalling (Dai *et al.* 2004; Uematsu *et al.* 2005; Seki and Brenner 2008) (Figure 7.3). The IRAK1/4/TRAF6/TAK1/IRF5/7 complex is responsible for downstream Myd88-dependent activation of JNK and NF-κB p65 pathways (Barton and Medzhitov 2003; Wietek *et al.* 2003; Greene *et al.* 2005; Sabroe *et al.* 2005; Kawai and Akira 2007; Guleng *et al.* 2010) (Figure 7.3).

Studies in human with NASH and animal models of nutritional-depletion fatty liver disease have demonstrated that TLR signalling is important for steatohepatitis pathogenesis (Szabo *et al.* 2005; Miura *et al.* 2010; Shanab *et al.* 2011).

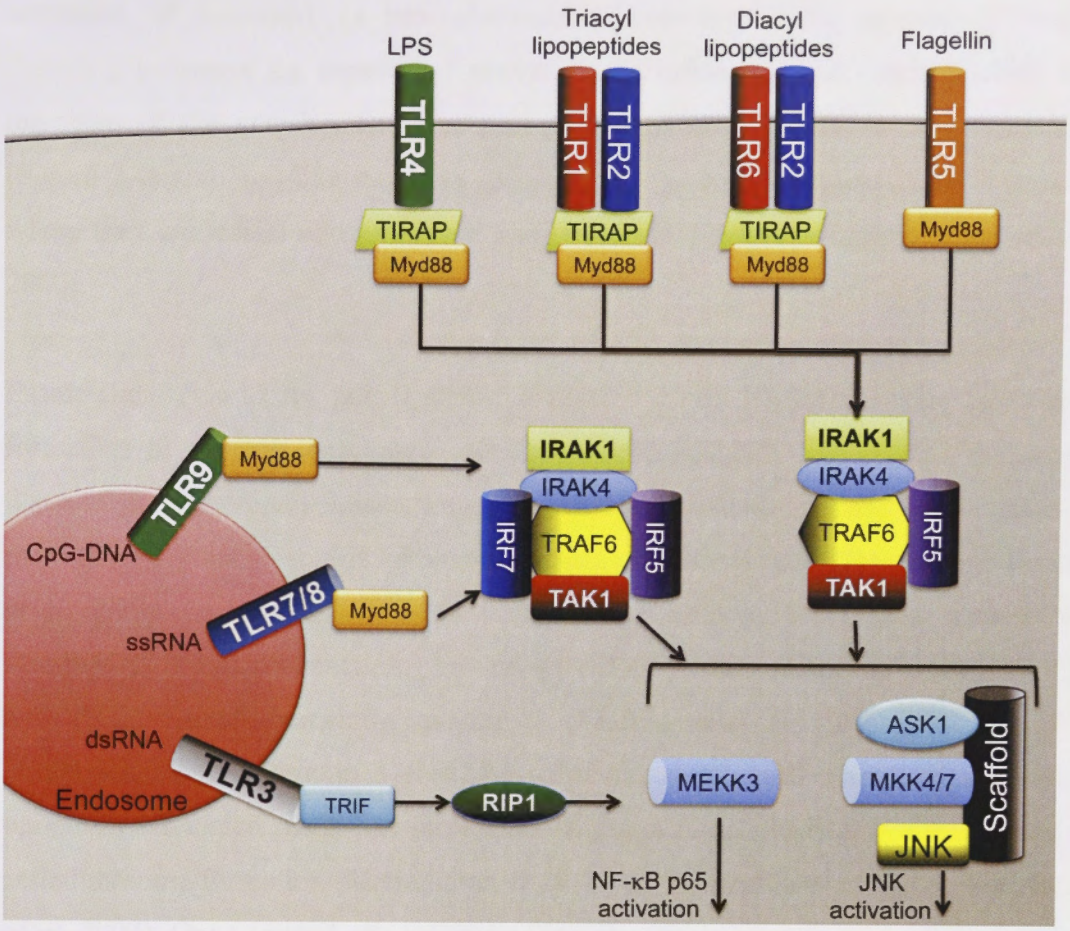

Figure 7.3 Toll-like receptor (TLR) signaling pathways involved in JNK and NF-κB p65 activation

Molecular details of the activation steps in these signaling pathways are detailed in Section 7.1.4. Abbreviations: ASK1, apoptosis signal-regulating kinase; CpG-DNA, deoxy-cytidylate-phosphate-deoxy-guanylate deoxyribonucleic acid; dsRNA, double stranded ribonucleic acid; IRAK, interleukin-1 receptor-associated kinase; IRF, interferon regulatory factor; JNK, *c*-Jun *N*-terminal kinase; LPS, lipopolysaccharide; MEKK, mitogen activated protein kinase kinase; Myd88, myeloid differentiation primary response gene-88; RIP, replication protein A interacting protein; ssRNA, single stranded ribonucleic acid; TAK1, TGF beta activated kinase-1; TIRAP; toll-interleukin 1 receptor domain-containing adapter protein; TLR, toll-like receptor; TRAF, TNF receptor-associated factor; TRIF, toll-interleukin-1 receptor-domain adaptor protein.

7.1.4 The inflammasome

The inflammasome is a pro-inflammatory element of the innate immune system responsible for the caspase-1-dependent activation of IL-1β and IL-18, as well as the induction of cellular pyroptosis, a form of cell death involved in antimicrobial immune responses (Mariathasan and Monack 2007). The inflammasome consists of several protein components forming a scaffold, and these interact and are responsible for the

activation of caspase-1 (a pro-inflammatory caspase) in the cytosol. Several signaling pathways are capable of activating the inflammasome. These include most members of the germline-encoded pattern-recognition receptors, notably, the TLRs (Figure 7.4) and Nod-like receptors (NLRs). The NLRs are present in the cytoplasm, where they are tasked with microbial and/or foreign particle surveillance (Sirard *et al.* 2007).

Extracellular (via TLRs, etc…) and/or intracellular (via NLRs) signaling initiates the formation of caspase-recruitment domain (CARD)-CARD domain and pyrin–pyrin domain protein-protein interactions that involve various proteins responsible for procaspase-1 activation; this complex is what is known as the inflammasome (Franchi *et al.* 2009). Various NLRs may be involved in CARD signaling. They include NLR family CARD domain-containing protein 4 (NLRC4) (also called IPAF), NACHT, LRR and PYD domains-containing protein 1 (NLRP1) and NACHT, LRR and PYD domains-containing protein 3 (NALP3) (Franchi *et al.* 2009). The adaptor protein, apoptosis-associated speck-like protein containing a CARD (ASC), is also required for inflammasome formation (Mariathasan *et al.* 2006; Sutterwala *et al.* 2006; Willingham *et al.* 2007). Once formed, the inflammasome is capable of activating procaspase-1. In turn, caspase-1 is responsible for the activation of pro-IL-1β and pro-IL-18, forming IL-1β and IL-18 respectively, which are subsequently secreted from the cell (Pirhonen *et al.* 1999; Sansonetti *et al.* 2000) (Figure 7.4). Co-expression of IL-1β and IL-18 or their detection in the circulation is often taken as a molecular finger print of inflammasome activation.

Three types of inflammasome have been described. Their characterisation is based on the NLR protein involved in the CARD/pyrin domain complex formation, namely the NLRC4, NLRP1, and NALP3 inflammasomes. The NLRC4 inflammasome is largely responsible for bacterial/TLR5-dependent (flagellin signaling) activation of the pyroptotic pathways (McCoy *et al.* 2010; Miao *et al.* 2010), whereas the NLRP1 inflammasome is responsive to muramyl dipeptide (MDP) bacterial cell wall components (Chamaillard *et al.* 2003; Franchi *et al.* 2009). The NALP3 inflammasome, however, is more complex. Since this has recently been found to be up-regulated in an MCD mouse model of steatohepatitis, it will be described in more detail here (Csak *et al.* 2011a).

The NALP3 inflammasome can be activated by extracellular ATP, which acts upon purinergic ATP-gated P2X7 receptor (P2X7R). This results in formation of a cation channel, which alters physiological ionic gradients and releases intracellular potassium ions (Figure 7.4) (Verhoef *et al.* 2004; Petrilli *et al.* 2007; Qu *et al.* 2007; Qu *et al.* 2009). Once activated by extracellular ATP, P2X7R may also co-activate pannexin-1, which in turn is responsible for the uptake of extracellular microbial matter (Franchi *et al.* 2009). The latter may lead to the activation of the NALP3 inflammasome. Additionally, endocytosed crystalline and particulate matter may damage the endosome/lysosomal pathway and activate the NALP3 inflammasome. Cholesterol crystals are included in this category and have been documented to activate the NALP3 inflammasome (Duewell *et al.* 2010; Rajamaki *et al.* 2010; Adamson and Leitinger 2011; Masters *et al.* 2011)(Figure 7.4).

Activated IL-1β and IL-18 are responsible for numerous proinflammatory responses, including: activation of Th1 and Th2 cellular responses, induction of interferon (IFN)-γ and IL-11, endothelial cell activation, and amplification of the inflammasome by induction of IL-8, IL-1β and TNF (Jander and Stoll 1998; Mencacci *et al.* 2000; Netea *et al.* 2000; Chen *et al.* 2011).

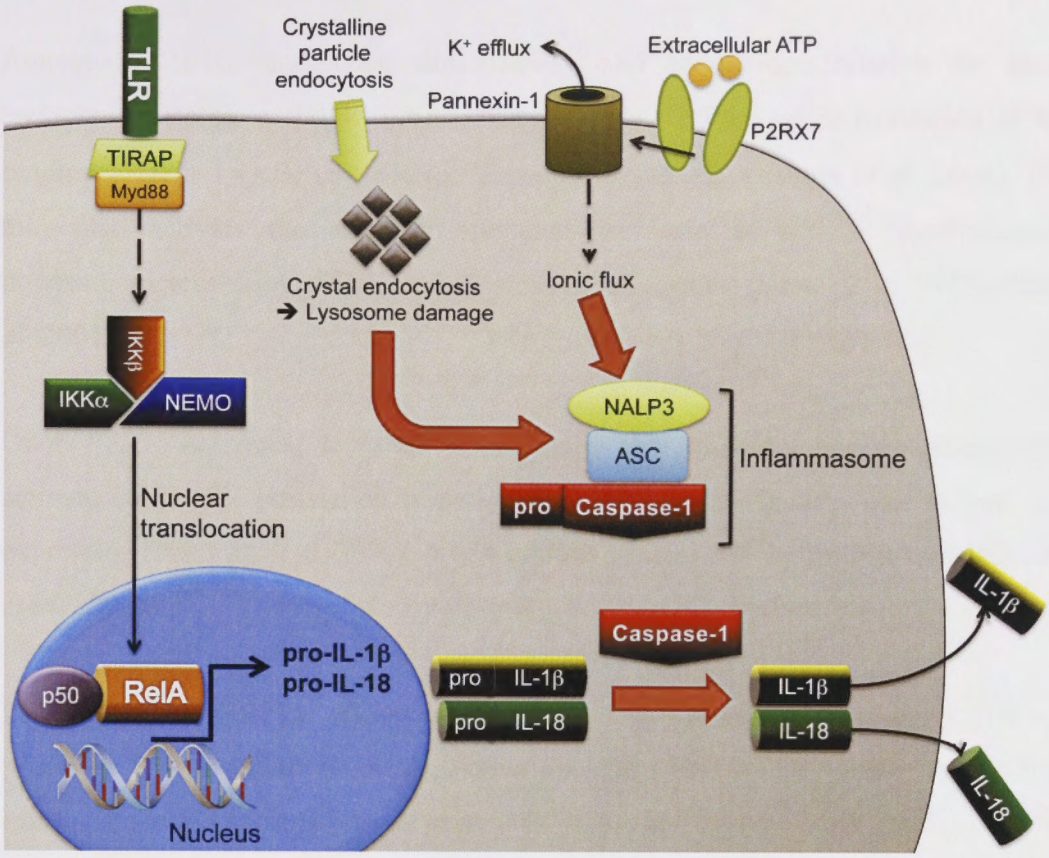

Figure 7.4 The inflammasome pathway responsible for IL-1β and IL-18 activation

Molecular details of the activation steps in these signaling pathways are detailed in Section 7.1.5. Abbreviations: ASC, apoptosis-associated speck-like protein containing a CARD; ATP, Adenosine-5'-triphosphate; IκBα; NF-κB inhibitor-α; IKK; IκB kinase; IL-1R, interleukin-1 receptor; IL, interleukin; Myd88, myeloid differentiation primary response gene-88; NALP3, NACHT, LRR and PYD domains-containing protein 3; NEMO, NF-κB essential modulator; P2RX7, purinergic receptor P2X, ligand-gated ion channel, 7; TIRAP; toll-interleukin 1 receptor domain-containing adapter protein; TLR, toll-like receptor.

7.1.5 The unfolded protein response (UPR)

The unfolded protein response (UPR) is a cellular stress response triggered by several events, including protein unfolding/misfolding, hypoxia, low ATP levels, ER calcium depletion, and protein/sterol over-expression (Mori *et al.* 1996; Welihinda *et al.* 1999; Caspersen *et al.* 2000; Bonilla *et al.* 2002; Koumenis *et al.* 2002; Li and Holbrook 2004). These events cause dissociation of GRP78 from the three UPR sensors, inositol-requiring enzyme 1α (IRE1α) (Figure 7.5A), protein kinase RNA-like endoplasmic reticulum kinase (PERK) (Figure 7.5B), and activating transcription factor-6 (ATF6) (Figure 7.5C) (Schroder and Kaufman 2005). Dissociation of GRP78 activates these sensors, which are responsible for the three arms of the UPR response (Figure 7.5).

Activated IRE1α undergoes dimerisation and autophosphorylation to generate endogenous RNase activity; in turn, this is responsible for splice truncation of X-box binding protein 1 (XBP1S) mRNA (Zhang *et al.* 2005; Yoshida *et al.* 2006). IRE1α may also activate the extrinsic apoptosis pathway, in which TRAF2-dependent downstream activation of JNK and caspase-12 takes place (Urano *et al.* 2000; Zhang *et al.* 2001a).

Once PERK activates, it forms homodimers that undergo autophosphorylation to activate eukaryotic translation initiation factor 2 (eIF2α). In turn, this induces ATF4 expression (Harding *et al.* 2000). ATF4 inhibits general cellular mRNA translation (Lim *et al.* 2000).

Dissociation of GRP78, allows ATF6 processing by the Golgi complex. Here, the proteases S1P and S2P cleave an active 50 kDa (p50) ATF6 domain that is free to translocate to the nucleus (Okada *et al.* 2003; Shen and Prywes 2004, 2005).

Xbp1s, ATF4 and ATF6, as well as other unlisted factors, are responsible for three dominant cell responses to UPR. The *folding pathway* induces increased expression of molecular chaperones, including GRP78, which assist in ER protein folding. Alternatively, the cell may respond by increasing ER-associated protein degradation (*ERAD*), whereby gene products target and degrade unfolded proteins in the ER (Schroder and Kaufman 2005). These pathways are predominantly regulated by nuclear ATF6 and Xbp1s. Prolonged UPR results in the activation of the intrinsic apoptosis pathway; this ATF6 and ATF4-dependent process induces C/EBP-homologous protein (Chop) expression. In turn, Chop inhibits B-cell lymphoma 2 (Bcl-2) and induces apoptosis (Schroder and Kaufman 2005).

Puri and colleagues (2008) have shown that some UPR components are upregulated in NAFLD patients, particularly sXBP-1 and GRP78 mRNA, although sXBP-1 protein was decreased in NASH subjects compared to those with lean or SS livers. Interestingly, in *db/db* mice fed a MCD diet for 4 weeks to cause steatohepatitis, an overall upregulation of the UPR pathways was evident (Rinella *et al.* 2011). In the host laboratory, MCD-feeding of C57BL/6 WT mice had no effect on GRP96 or

selenoprotein S (SEPS-1) (alternative ER chaperones to GRP78), but was associated with increased Chop protein expression. *In vitro* studies showed that, as known from other studies, methionine deficiency causes upregulation of Chop directly rather than via operation of ER stress (Larter et al., unpublished data, 2008). In summary, studies of the effects of MCD on ER stress responses have produced conflicting data. Further, with the exception of one study (Pfaffenbach *et al.* 2010), there is little information on whether administration of pharmacological chaperones, such as 4-phenylbutyrate or tauroursodeoxycholic acid (TUDCA), protect mice in this model from hepatocellular apoptosis.

In regards to the effect of hepatic cholesterol-loading on UPR activation, loading human hepatic L02 cells with cholesterol, using LDL and an ACAT inhibitor, significantly increased the gene expression of GRP78, Chop, ATF4 and ATF6, and XBP1S mRNA (Li *et al.* 2009).

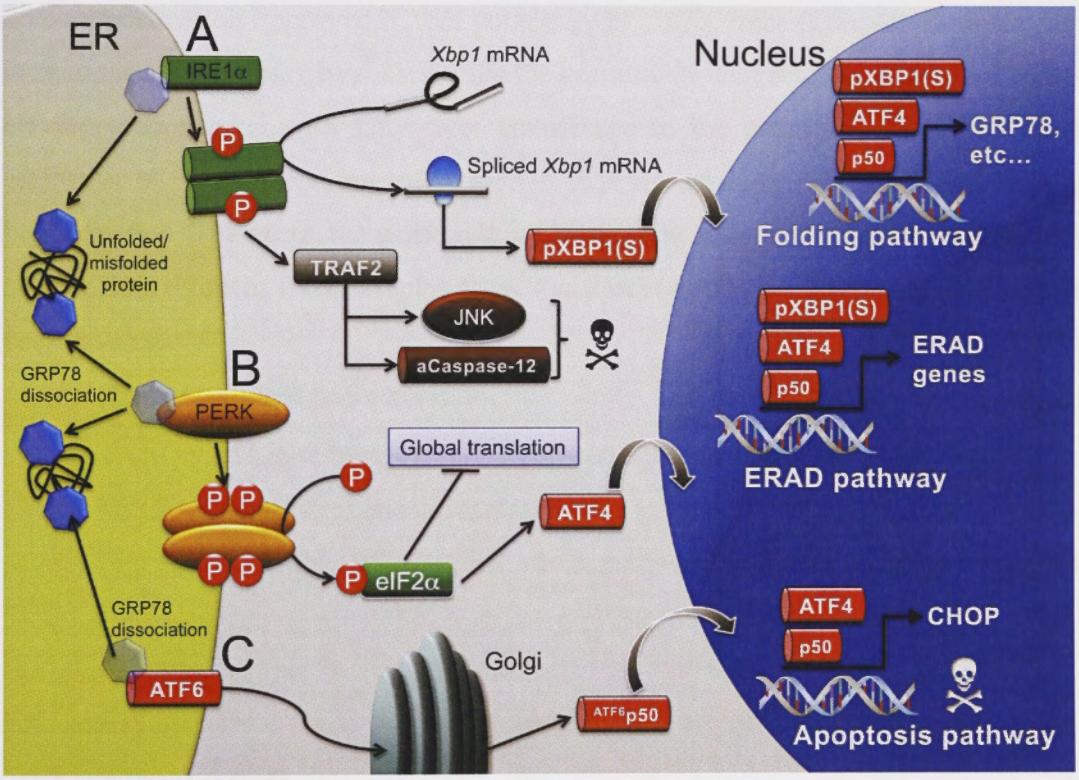

Figure 7.5 Mammalian unfolded protein response (UPR) pathways

Molecular details of the activation steps in these signaling pathways are detailed in Section 7.1.5.

Abbreviation list for Figure 7.5: aCaspase-12, active caspase-12; ATF, activating transcription factor; Chop, C/EBP-homologous protein; eIF2α, eukaryotic translation initiation factor 2α; ERAD, endoplasmic reticulum associated protein degradation; GRP78, glucose-regulated protein-78 (also known as binding immunoglobulin protein [Bip]); IRE1α, inositol-requiring enzyme 1α; JNK, *c*-Jun *N*-terminal kinase; PERK, protein kinase RNA-like endoplasmic reticulum kinase; pXBP1(S), splice truncation of X-box binding protein 1; TRAF2, necrosis factor receptor-associated factor 2.

7.2 Purpose of study: hypotheses and aims

In Chapters 3, 5 and 6, we reported that hepatic cholesterol accumulates in *foz/foz* mice. Two approaches were used to confirm a direct relationship between hepatic cholesterol content and severity of liver injury in this model. Firstly, dietary cholesterol modulation experiments verified that NASH severity can be exacerbated or ameliorated depending on whether hepatic cholesterol loading is increased or decreased, respectively (Chapter 5). Secondly, pharmacological modulation of cholesterol biosynthesis and/or uptake/reclamation improved NASH pathology in *foz/foz* mice (Chapter 6). While these data support the primary hypothesis that the accumulation of free cholesterol in livers of HF-fed *foz/foz* mice with fatty liver contributes to the pathogenesis of NASH, the pathways of liver injury and inflammation that are activated by cholesterol have yet been clarified. Therefore, the work in this Chapter was to analyse pathways of cell death and inflammation in liver samples from the previous studies. Particular attention has been given to:

1. JNK and NF-κB p65 activation.
2. TNF- and TLR-related signalling pathways that activate JNK and NF-κB p65
3. Inflammasome component expression.
4. Expression of the UPR and ER stress pathways in livers of *foz/foz* mice with NASH.

7.3 Methods

7.3.1 Mice and diets

Study 1: From 8 weeks of age, female WT and *foz/foz* NOD.B10 mice were fed either chow or HF-diet (containing 0.2% cholesterol) for 12 wks (n=7-10/group) or 24 wks (n=5/group), as described in Section 3.3.1. Note that these are the same mice as described in Chapter 3, for which metabolic data have been published (Larter *et al.* 2009).

Study 2: Female WT and *foz/foz* NOD.B10 mice (n=7-11/group) were fed HF-diet (containing either: 0, 0.2, or 2.0% [w/w] cholesterol) 24 weeks. The composition of the three diets is outlined in Table 4.1. They were introduced to the HF diet at 8 weeks of age, and weighed each week thereafter. Peri-ovarian white adipose tissue (WAT) from one side was also collected and weighed. These are the same mice as described in Chapter 5.

Study 3: From 8 weeks of age, female WT and *foz/foz* NOD.B10 mice (n=8-11/group) were fed HF diet (containing either: 0.2% [w/w] cholesterol) for 16 weeks, after which atorvastatin (20 mg/kg/day), ezetimibe (5 mg/kg/day) ezetimibe, or a combination of the two (in the same dose regime) were added to diets. Mice were then fed for a further 8 weeks. Control (vehicle) mice were fed the same HF diet for a total of 24 weeks. Details relating to drug/diet preparation are described in Section 6.3.2. These are the same mice as described in Chapter 6.

All mice were maintained as described in Section 2.3, and at experimental time points mice were harvested as described in Section 2.4.

7.3.2 Procedures

RnD Systems (Minneapolis, MN) ELISA kits were used to determine serum IL-1β and TNF-α levels, while serum IL-18 levels were quantified using assay kits purchased from Medical & Biological Laboratories Co., Ltd. (Nagoya, Japan). Assays were carried out in accordance with the respective Manufacturer's instructions.

SDS-PAGE, western blotting, semi-quantitative qPCR and IHC were carried out as described in Sections 2.10, 2.11, 2.7, and 2.6.2.1, respectively. Primary and secondary antibodies and primers used for western blotting and qPCR are shown in Tables 2.1, 2.2 and 2.3, respectively.

All statistical analyses were carried out as described in Section 2.15.

7.4 Results

7.4.1 JNK activation is responsive to hepatic cholesterol levels in HF-fed *foz/foz* and WT mice

The host laboratory, as well as others, have demonstrated JNK activation in MCD diet-fed mice with steatohepatitis (Schattenberg *et al.* 2006; Larter *et al.* 2008a; Aghazadeh and Yazdanparast 2010; Soon *et al.* 2010). In Chapters 5 and 6, we demonstrated that cholesterol loading increased liver injury and hepatocyte cell death in the *foz/foz* model. Conversely, dietary and pharmacological lowering of hepatic cholesterol fractions improved liver pathology and decreased hepatocellular apoptosis. Since JNK activation can descend on caspase-3-dependent apoptosis (Roulston *et al.* 1998), it seemed particularly important to establish whether any relationship exists between hepatic FC levels and JNK activation. In both dietary cholesterol and atorvastatin/ezetimibe pharmacological experiments, pan JNK-1/2 46- and 54 kDa isoform expression was very similar between groups, as expected for these constitutive proteins (Figure 7.6A,B and 7.7A,B). Conversely, JNK-1/2 activation (as assessed by phospho-JNK-1/2 [pJNK] immunoblotting) correlated closely with hepatic FC levels. In the dietary cholesterol experiment, both 46 kDa and 54 kDa pJNK-1/2 levels were significant increased in *foz/foz* mice ($P<0.05$, Figure 7.6C,D). Further, when expressed as a ratio of pan JNK expression, which is a more accurate way to express JNK activation levels, pJNK:pan JNK was also significantly elevated in the 2% cholesterol-fed WT group, for both 46- and 54 kDa isoforms ($P<0.05$, Figure 7.6E,F). In addition to the patterns of JNK activation for *foz/foz* and WT mice correlating with profiles of liver cholesterol (Figure 5.2A,B), similar correlations are also evident with serum ALT (Figure 5.4) and hepatocyte apoptosis (Figure 5.6).

In contrast to the effects of dietary cholesterol loading, atorvastatin and/or ezetimibe treatment significantly reduced 46 kDa and 54 kDa pJNK-1/2 expression in drug-treated HF-fed *foz/foz* mice *versus* genotype-matched vehicle controls ($P<0.05$, Figure 7.7C,D). Expressing pJNK as a ratio of total JNK expression mirrored this result, with 2-, 3-, and 4.5-fold reductions in JNK activation observed for atorvastatin and ezetimibe monotherapy and combined drug-treated *foz/foz* mice, respectively, compared with genotype-matched vehicle controls ($P<0.05$, Figure 7.7E,F). As observed for the dietary cholesterol feeding experiments, profiles of JNK activation in atorvastatin- and ezetimibe-treated *foz/foz* mice bear striking similarity to patterns of hepatic cholesterol

content (Figure 6.5A,B). Collectively, these data are consistent with the proposal that JNK activation may constitute the primary pathway responsible for cholesterol-induced cell death in this metabolic syndrome model of NASH.

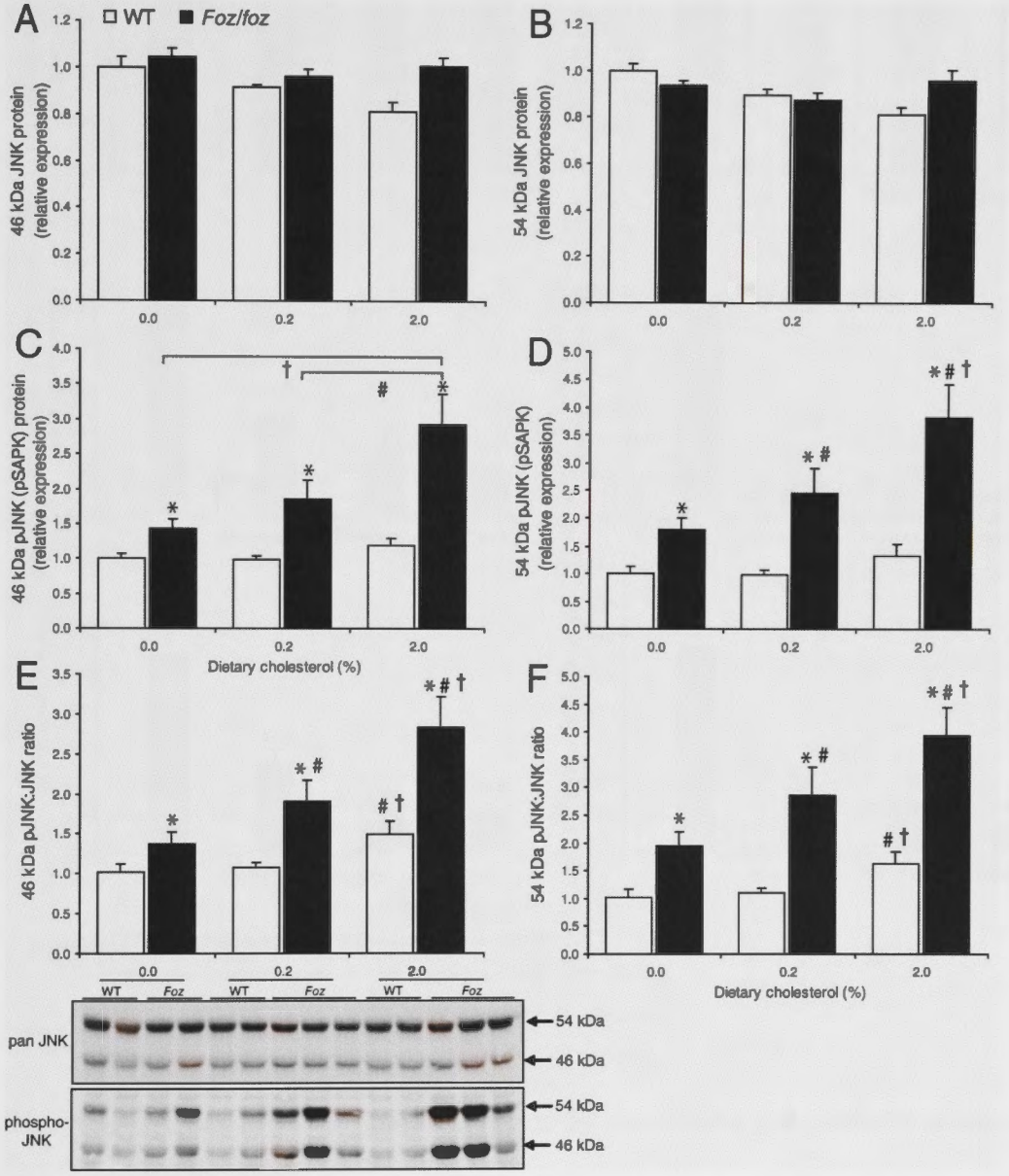

Figure 7.6 Hepatic cholesterol loading activates cell stress activated JNK in *foz/foz* and WT mice

(**A**) Total (pan) 46 kDa and (**B**) 54 kDa *c*-Jun *N*-terminal kinase-1 (JNK) protein, as well as phosphorylated (**C**) 46 kDa and (**D**) 54 kDa JNK protein expression in WT (□) and *foz/foz* (■) mice (n=7-11/grp) fed HF-diet containing 0.0, 0.2 or 2.0% (w/w) cholesterol for 24-weeks. (**E**) Ratio of 46 kDa and (**F**) 54 kDa phosphorylated JNK protein: total (pan) JNK protein. Representative western blots are shown in panel E. Data are mean ± SEM. *P<0.05, vs. diet-matched control. $^{\#}P$<0.05, vs. genotype-matched, 0.2% dietary cholesterol group. $^{\dagger}P$<0.05, vs. genotype-matched, 0% dietary cholesterol group.

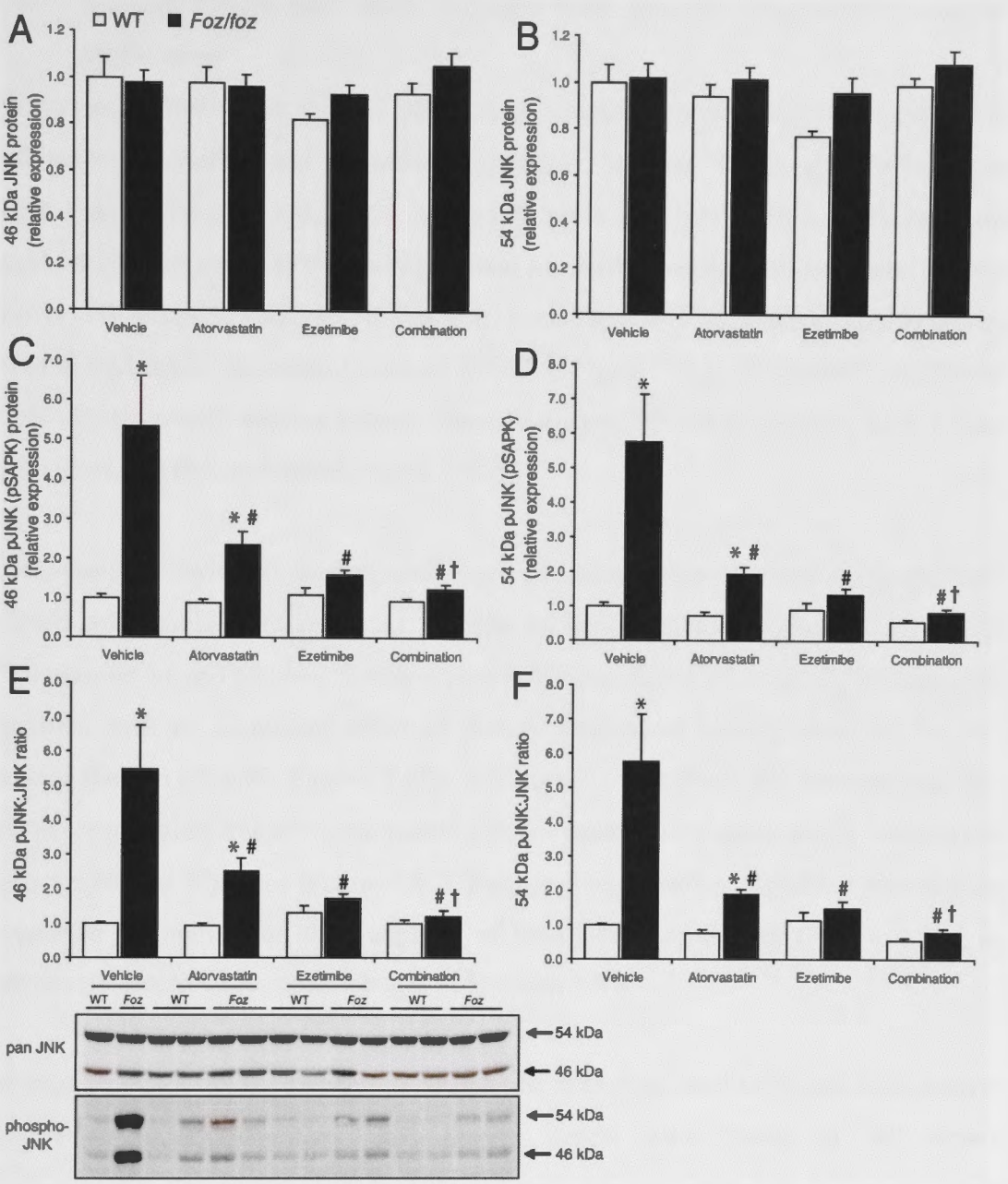

Figure 7.7 Hepatic JNK activation is reduced by atorvastatin and ezetimibe treatment of *foz/foz* mice

(**A**) Total (pan) 46 kDa and (**B**) 54 kDa *c*-Jun *N*-terminal kinase-1 (JNK) protein, as well as phosphorylated (**C**) 46 kDa and (**D**) 54 kDa JNK protein expression in *foz/foz* (■) and WT (□) mice fed high fat (HF) diet for 16 weeks, after which atorvastatin (20 mg/kg/day) and/or ezetimibe (5 mg/kg/day) were introduced into diet and administered for an additional 8 weeks (see Section 6.3.2). (**E**) Ratio of 46 kDa and (**F**) 54 kDa phosphorylated JNK protein: total (pan) JNK protein. Representative western blots are shown in panel E. Data are mean ± SEM. $^{*}P<0.05$, vs. treatment-matched, genotype control. $^{\#}P<0.05$, vs. genotype-matched, vehicle group. $^{\dagger}P<0.05$, vs. genotype-matched, atorvastatin treatment group.

7.4.2 Nuclear NF-κB p65 levels increase with hepatic cholesterol loading in *foz/foz* mice

As previously mentioned, NF-κB p65 acts as a nuclear transcription factor promoting inflammatory cytokine and chemokine expression. Nuclear NF-κB p65 is responsible for the activation of IL-1β, IL-18, MCP-1 (Ping *et al.* 1999), TNF-α, VCAM-1 and ICAM-1 (Zhang *et al.* 2002), among several hundred proinflammatory genes. Nuclear (active) NF-κB p65 protein in HF-fed *foz/foz* mice appeared to be responsive to dietary loading of hepatic cholesterol content ($P<0.05$, Figure 7.8A). Conversely, 0.2% and 2.0% cholesterol/HF-feeding actually lowered nuclear NF-κB p65 protein in WT mice ($P<0.05$ *versus* 0% cholesterol, Figure 7.8A).

Cytoplasmic NF-κB p65 protein levels were also quantified to determine whether total NF-κB p65 levels were raised in addition to increased nuclear (activation) levels. Cytoplasmic NF-κB p65 levels were higher in HF-fed *foz/foz* mice *versus* WT genotype controls, with no additional effect of dietary cholesterol loading observed for this protein fraction ($P<0.05$, Figures 7.8B). IHC staining for NF-κB p65 revealed that NF-κB p65 expression was restricted to non-parenchymal cell fractions within the livers of both *foz/foz* and WT mice (Figure 7.8C). Furthermore, NF-κB p65-positive stained cells appear to accumulate on the periphery of lipid-laden hepatocytes (Figure 7.8C), as previously described for macrophages in Sections 5.4.5.

In order to establish the pathways to NF-κB p65 activation, total IκBα and IκBβ protein expression were quantified. IκBα protein levels were lower in all dietary cholesterol/HF-fed *foz/foz* groups compared with treatment-matched WT counterparts ($P<0.05$, Figure 7.8D). Conversely, IκBβ protein levels were unchanged regardless of genotype or dietary cholesterol content (Figure 7.8E). These findings indicate that IκBα expression is destabilised in *foz/foz* mice, and in 2.0% cholesterol/HF-fed WT mice (Figure 7.8D). This fall represents the likely effector route to nuclear NF-κB p65 activation in *foz/foz* mice with NASH.

The effects of NF-κB p65 activation in NASH were then assessed through VCAM-1 and ICAM-1 protein expression. In concert with activation of NF-κB p65, total hepatic

VCAM-1 protein expression appeared responsive to dietary cholesterol content in *foz/foz* mice, and 2% cholesterol HF-feeding also significantly increased ICAM-1 expression in *foz/foz* mice with NASH ($P<0.05$ *versus* genotype and dietary controls, Figures 7.8F,G).

NF-κB p65 pathways were also assessed in atorvastatin and/or ezetimibe-treated mice described in Chapter 6. Atorvastatin or ezetimibe monotherapy lowered nuclear NF-κB p65 protein levels in obese HF-fed *foz/foz* mice. However, even more profound reduction was observed with combination atorvastatin and ezetimibe treatment ($P<0.05$, Figure 7.9A). There was an impressive inverse relationship between total IκBα protein and nuclear NF-κB p65 in this set of experiments; thus, IκBα levels were significantly raised in ezetimibe and combination atorvastatin and ezetimibe treated *foz/foz* mice ($P<0.05$, Figure 7.9B). It is plausible that combined atorvastatin and ezetimibe treatment stabilises IκBα protein, but the alternative explanation is that the lowering of hepatic FC or other cholesterol pools removes the incitement to NF-κB activation via one or more of the pathways outlined in the introduction to this Chapter.

As expected from the suppression of NF-κB activation, hepatic VCAM-1 and ICAM-1 protein levels were also reduced in atorvastatin and ezetimibe-treated HF-fed *foz/foz* mice. As for the reduction in hepatic FC, the largest reduction for these two adhesion molecules was observed in combination drug-treated *foz/foz* mice ($P<0.05$ *versus* genotype-matched vehicle controls, Figure 7.9C,D).

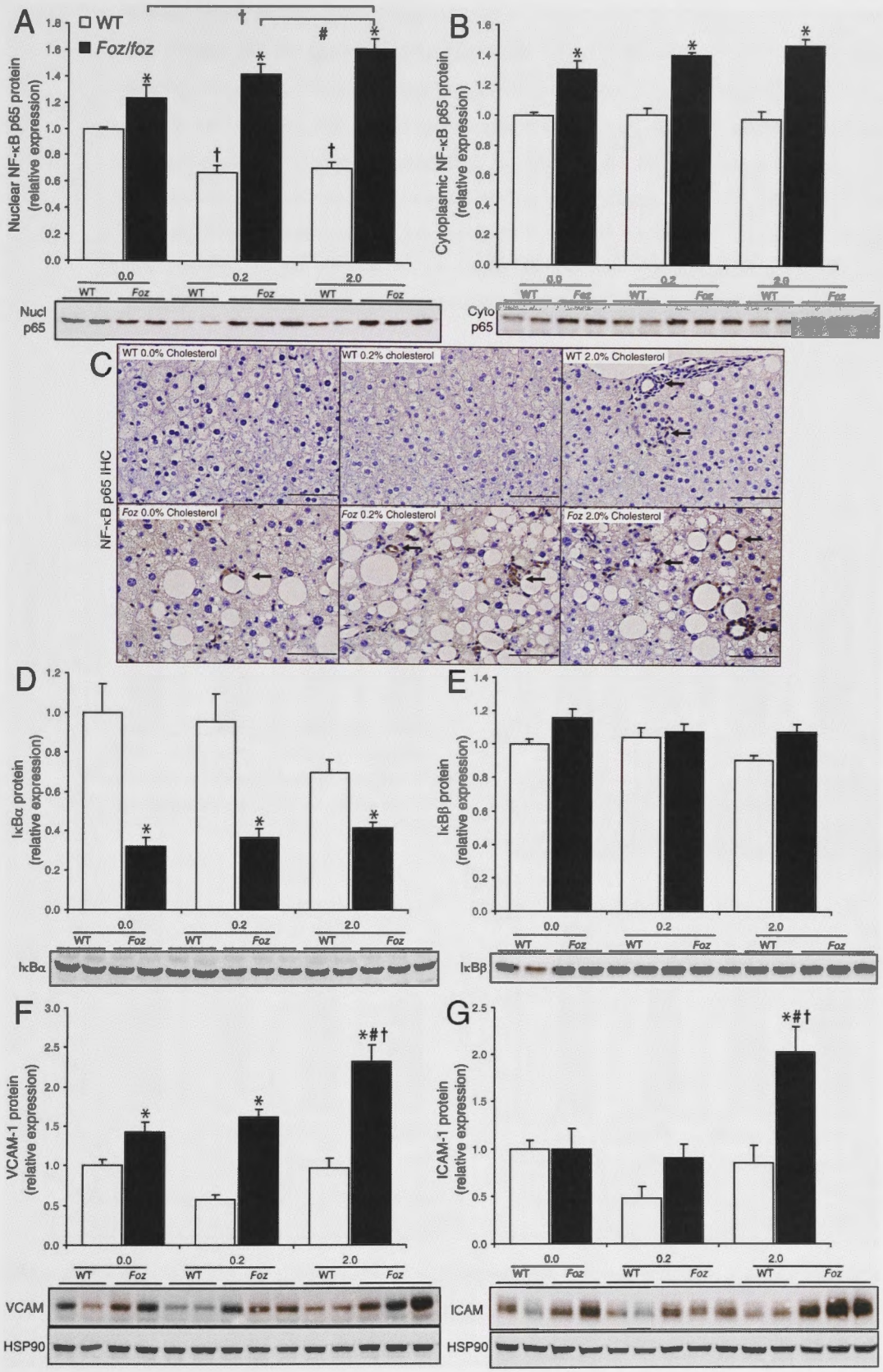

Figure 7.8 Hepatic cholesterol loading increases nuclear factor κ-B p65 activation and downstream inflammatory pathways in *foz/foz* and wildtype mice

Legend for Figure 7.8.

(**A**) Nuclear and (**B**) cytoplasmic nuclear factor κ-B p65 (NF-κB p65), (**C**) NF-κB p65 IHC staining, (**D**) nuclear factor of κ light polypeptide gene enhancer in B-cells inhibitor (IκB)-α and (**E**) -β, (**F**) vascular cell adhesion molecule 1 (VCAM-1), and (**G**) inter-cellular adhesion molecule-1 (ICAM-1) protein expression in WT (□) and *foz/foz* (■) mice (n=7-11/grp) fed HF-diet containing 0.0, 0.2 or 2.0% (w/w) cholesterol for 24-weeks. House keeping gene (HSP90) western blots are shown in panels F and G for clarity, but were similar for all westerns. Scale bars represent 50 μm. Data are mean ± SEM. *P<0.05, vs. diet-matched control. $^{\#}P$<0.05, vs. genotype-matched, 0.2% dietary cholesterol group. $^{\dagger}P$<0.05, vs. genotype-matched, 0% dietary cholesterol group.

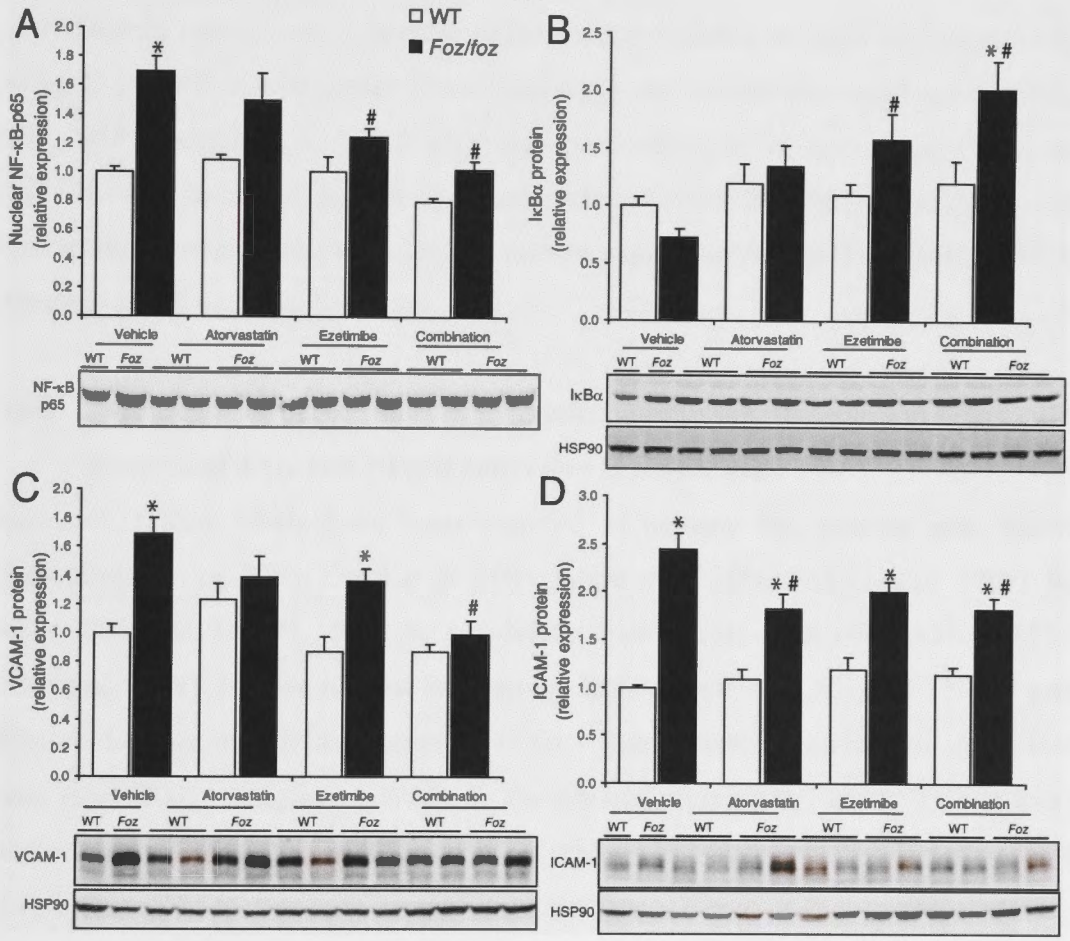

Figure 7.9 Modulation of cholesterol biosynthesis and uptake reduces nuclear factor κ-B p65 activation and associated inflammatory pathways in HF-fed *foz/foz* mice

Legend for Figure 7.9.

(**A**) Nuclear and (**B**) nuclear factor of κ light polypeptide gene enhancer in B-cells inhibitor (IκB)-α, (**C**) vascular cell adhesion molecule 1 (VCAM-1), and (**D**) inter-cellular adhesion molecule-1 (ICAM-1) protein expression in *foz/foz* (■) and WT (□) mice fed high fat (HF) diet for 16 weeks, after which atorvastatin (20 mg/kg/day) and/or ezetimibe (5 mg/kg/day) were introduced into diet and administered for an additional 8 weeks (see Section 6.3.2). House keeping gene (HSP90) western blots are shown in panels C and D for clarity, but were similar for all westerns. Data are mean ± SEM. $^{*}P<0.05$, vs. treatment-matched, genotype control. $^{\#}P<0.05$, vs. genotype-matched, vehicle group. $^{\dagger}P<0.05$, vs. genotype-matched, atorvastatin treatment group.

Taken together, these data indicate that the extent of NF-κB p65 activation is proportional to hepatic total and FC levels. Such activation may, therefore, at least partly explain recruitment of hepatic inflammation observed in these cholesterol-laden *foz/foz* livers with NASH. Since several pathways are capable of activating NF-κB and JNK, TNF superfamily and TLR pathways were subsequently assessed in *foz/foz* and WT livers from both the dietary cholesterol feeding experiment and atorvastatin/ezetimibe pharmacological intervention experiments. The results will be described in the next two Sections.

7.4.3 Activation of TNF and TNF-related pathways do not correlate with patterns of JNK and NF-κB activation in *foz/foz* mice

Increased TNF-α levels have been reported in humans and rodents with NASH (Bahcecioglu *et al.* 2005; Diehl *et al.* 2005; Abiru *et al.* 2006; Farrell *et al.* 2009), but serum TNF and TNFR1 levels do not discriminate NASH from not NASH NAFLD (Hui *et al.* 2004). Further, at least three groups have shown that TNF-α or TNFR1 gene deletion does not modify the phenotype of fatty liver disease (Memon *et al.* 2001; Dela Pena *et al.* 2005; Deng *et al.* 2005). In the present experiments, serum TNF-α levels were variably detected in *foz/foz* mice in both the dietary cholesterol feeding experiment and pharmacological study; this large variability was attributable to the borderline range of detection, such that TNF-α was undetectable in several *foz/foz* and WT mice in both studies. More importantly, serum TNF-α profiles for various groups of *foz/foz* mice were similar and failed to correlate with the pattern of liver injury (Figures 7.10A, 7.11A). Hepatic TNF-α mRNA levels likewise showed no remarkable changes between genotype, dietary or pharmacological treatment groups (Figures 7.10B and 7.11B).

Similar unchanged expression was observed for the hepatic gene expression of TNF receptors, TNFR1 and TNFR2 (Figures 7.10C,D).

In the atorvastatin and ezetimibe study, there was a trend for TNFR1 expression to appear higher in *foz/foz* vehicle controls *versus* WT genotype controls, and in genotype-matched *foz/foz* treatment groups, but none of these apparent changes were significant compared with the appropriate drug-treatment or genotype controls (Figure 7.11C). TNFR2 gene expression was significantly elevated in ezetimibe monotherapy treated HF-fed *foz/foz* mice compared to genotype-matched vehicle controls, but whether this outlying finding (among many comparisons) has biological significance is unclear ($P<0.05$, Figure 7.11D).

While there was also a trend for hepatic TRAIL mRNA expression to rise in *foz/foz* and WT mice fed increasing amounts of dietary cholesterol, these increases were not significant (Figure 7.10E). On the other hand, gene expression for Killer, the only TRAIL DR in mice (there are two in humans), did seem to increase (but again not significantly) in 0% and 0.2% cholesterol/HF-fed *foz/foz* mice compared with diet-matched genotype controls. In mice fed 2% cholesterol/HF diet, the increase in Killer mRNA expression in *foz/foz* mice was significant compared to WT controls ($P<0.05$, Figure 7.10F). Conversely, atorvastatin and/or ezetimibe treatment clearly had no significant effect on hepatic TRAIL or Killer mRNA expression in HF-fed *foz/foz* mice (Figure 7.11E,F).

Collectively, these data provide no good evidence that TNF-α and TRAIL signalling through the TNF superfamily death receptors could account for increased activation of JNK and NF-κB in HF-fed *foz/foz* mice with NASH. Gene expression for the TLR superfamily was subsequently assessed to determine whether these genes are involved in JNK and NF-κB signalling.

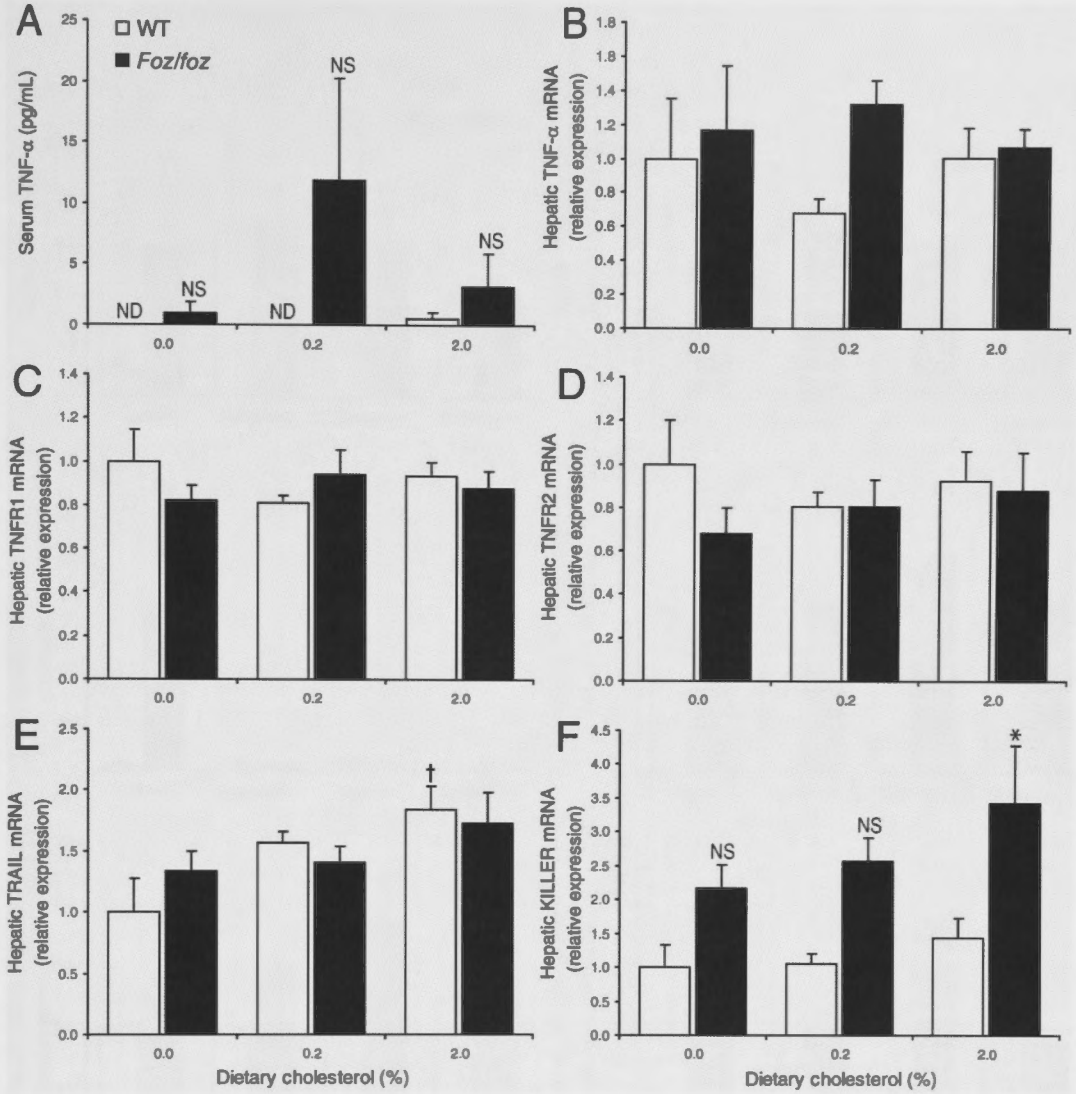

Figure 7.10 Dietary cholesterol feeding differentially alters TNF- and TNF-related pathways in HF-fed *foz/foz* mice

(**A**) Serum TNF-α levels, (**B**) hepatic TNF-α, (**C**) TNF receptor-1 (TNFR1), (**D**) TNF receptor-2 (TNFR2), (**E**) TNF-related apoptosis inducing ligand (TRAIL), and (**F**) Killer mRNA in WT (□) and *foz/foz* (■) mice (n=7-11/grp) fed HF-diet containing 0.0, 0.2 or 2.0% (w/w) cholesterol for 24-weeks. Data are mean ± SEM. $^{*}P<0.05$, vs. diet-matched control. $^{\#}P<0.05$, vs. genotype-matched, 0.2% dietary cholesterol group. $^{\dagger}P<0.05$, vs. genotype-matched, 0% dietary cholesterol group. NS, not significant. ND, not detected.

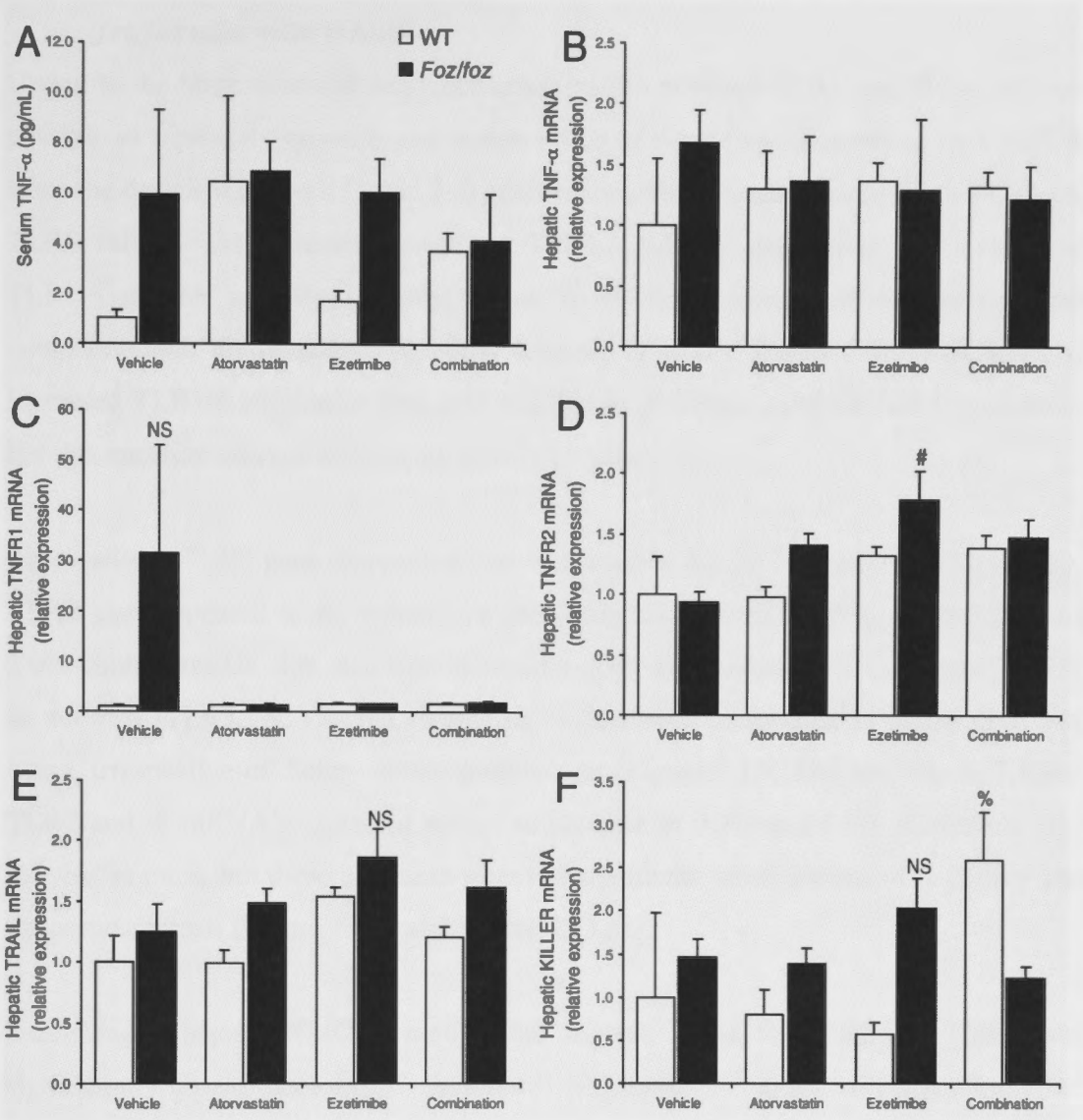

Figure 7.11 Atorvastatin and/or ezetimibe treatment differentially alters TNF- and TNF-related pathways in HF-fed *foz/foz* mice

(**A**) Serum TNF-α levels, (**B**) hepatic TNF-α, (**C**) TNF receptor-1 (TNFR1), (**D**) TNF receptor-2 (TNFR2), (**E**) TNF-related apoptosis inducing ligand (TRAIL), and (**F**) Killer mRNA in *foz/foz* (■) and WT (□) mice fed high fat (HF) diet for 16 weeks, after which atorvastatin (20 mg/kg/day) and/or ezetimibe (5 mg/kg/day) were introduced into diet and administered for an additional 8 weeks (see Section 6.3.2). Data are mean ± SEM. $^{*}P<0.05$, vs. treatment-matched, genotype control. $^{\#}P<0.05$, vs. genotype-matched, vehicle group. $^{\dagger}P<0.05$, vs. genotype-matched, atorvastatin treatment group.

7.4.4 Dietary cholesterol feeding differentially alters TLR gene expression in *foz/foz* mice with NASH

Owing to the large extent of sequence conservation between TLR1 and TLR6, it is not possible to separately quantify expression levels of these two receptors using RT-PCR, since the designed primers (Table 2.3) crossed the exonic boundaries for both TLR1 and TLR6 mRNA. As a result, combined TLR1/6 mRNA expression was quantified. TLR1/6 mRNA was significantly higher in 0.2% cholesterol/HF-fed *foz/foz* mice compared with diet-matched genotype controls ($P<0.05$, Figure 7.12A). A trend to increased TLR1/6 expression was also evident in 2% cholesterol/HF-fed *foz/foz* mice, but this apparent change was not significant (Figure 7.12A).

Impressively, TLR2 gene expression was increased in *foz/foz* mice *versus* WT controls. TLR2 also appeared to be responsive to dietary cholesterol feeding, with 0.2% and 2.0% cholesterol/HF diet stepwise increasing gene expression ($P<0.05$, Figure 7.12B). In contrast, TLR3, -4, -5, and -9 mRNA levels were unchanged in *foz/foz* and WT livers, irrespective of dietary cholesterol content (Figure 7.12C,D,E and Figure 7.13B). TLR7 and -8 mRNA expression tended to increase in 0.2% and 2.0% cholesterol/HF-fed *foz/foz* mice, but these increases were not significant when compared to dietary and genotype controls (Figure 7.12F and Figure 7.13A).

Interestingly, hepatic HMGB1 protein, the cognate ligand for TLR2 and TLR4, was significantly up-regulated in 0% cholesterol HF-fed *foz/foz versus* correspondingly fed WT mice. Further, increasing dietary cholesterol to 0.2 and 2.0%, stepwise elevated hepatic HMGB1 protein expression, with changes between *foz/foz* and WT mice being significant for 0.2% cholesterol but not 2% cholesterol.

Once activated, all TLR receptors, except TLR3, share the common Toll/IL-1 receptor domain-containing adaptor, Myd88. Myd88 mRNA levels were assessed and no significant differences were observed in livers of *foz/foz* and WT, irrespective of dietary cholesterol feeding (Figure 7.13D).

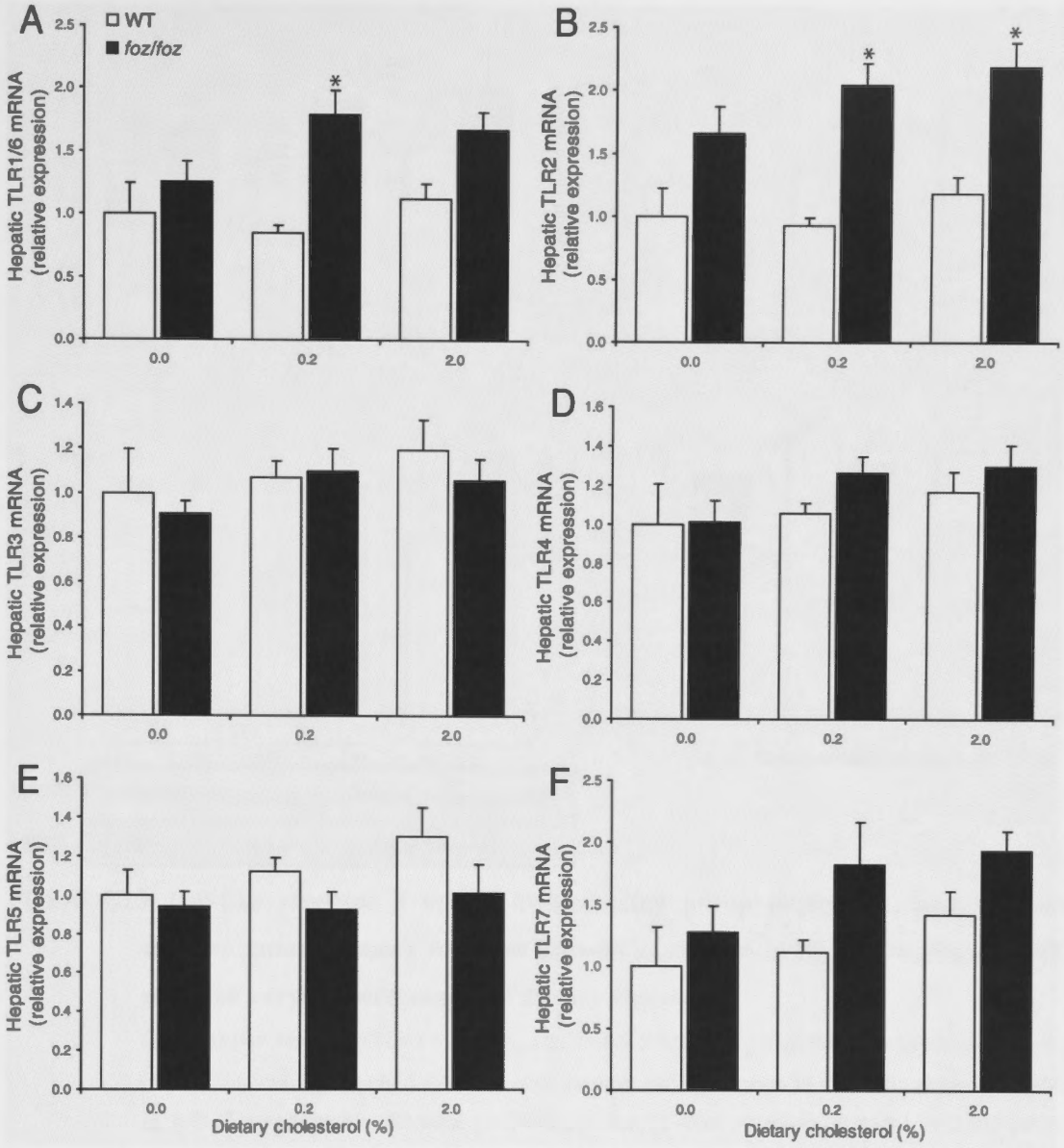

Figure 7.12 Toll-like receptor 1-7 gene expression in HF-fed *foz/foz* and WT mice fed varying percentages of dietary cholesterol

(**A**) Toll-like receptor (TLR)-1/6 mRNA (see text), (**B**) TLR2, (**C**) TLR3, (**D**) TLR4, (**E**) TLR5, and (**F**) TLR7 mRNA in WT (□) and *foz/foz* (■) mice (n=7-11/grp) fed HF-diet containing 0.0, 0.2 or 2.0% (w/w) cholesterol for 24-weeks. TLR1 and -6 were not assessed separately due to high degree of sequence conservation. Data are mean ± SEM. *P<0.05, vs. diet-matched control. $^{\#}P$<0.05, vs. genotype-matched, 0.2% dietary cholesterol group. $^{\dagger}P$<0.05, vs. genotype-matched, 0% dietary cholesterol group.

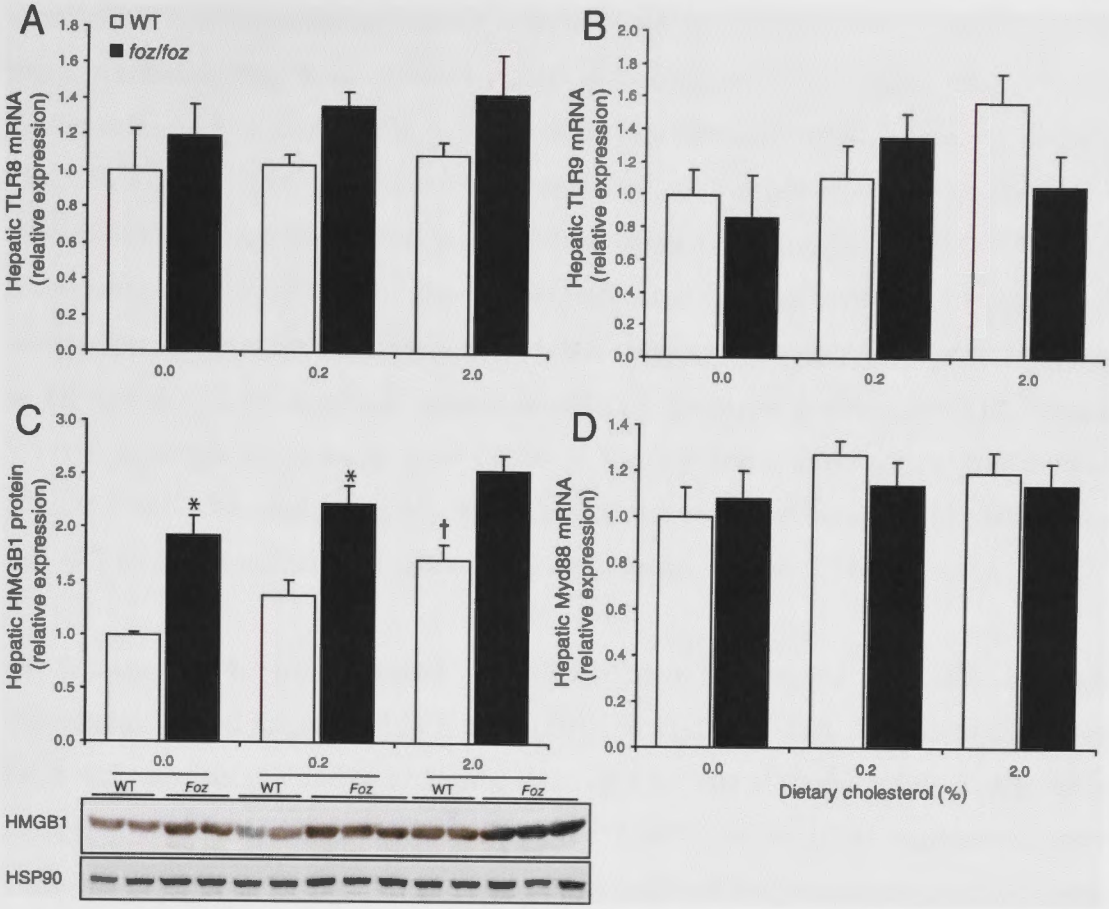

Figure 7.13 Toll-like receptor 8 and-9, high-mobility group protein-B1, and myeloid differentiation primary response gene-88 expression in HF-fed *foz/foz* and WT mice fed varying percentages of dietary cholesterol

(**A**) Toll-like receptor (TLR)-8 mRNA, (**B**) TLR9 mRNA, (**C**) high-mobility group protein-B1 (HMGB1), and (**D**) myeloid differentiation primary response gene-88 (Myd88) gene expression in WT (□) and *foz/foz* (■) mice (n=7-11/grp) fed HF-diet containing 0.0, 0.2 or 2.0% (w/w) cholesterol for 24-weeks. Data are mean ± SEM. *P<0.05, vs. diet-matched control. $^{\#}P$<0.05, vs. genotype-matched, 0.2% dietary cholesterol group. $^{\dagger}P$<0.05, vs. genotype-matched, 0% dietary cholesterol group.

7.4.5 Atorvastatin and/or ezetimibe treatment reduces TLR2 and HMGB1 gene expression, but does not alter TLR4, -9 and Myd88 mRNA levels

Since upregulated TLR2 and HMGB1 gene expression were observed in *foz/foz* and WT fed HF/high cholesterol diets, these genes were assessed in atorvastatin and/or ezetimibe-treated animals. Although no changes had previously been observed in *foz/foz* mice with NASH (Figures 7.12D and 7.13B,D), TLR4, -9 and Myd88 gene expression were also examined in atorvastatin and/or ezetimibe-treated mice, since these pathways have been previously shown to be involved in steatohepatitis pathogenesis in other models (Miura *et al.* 2010; Rivera *et al.* 2010; Csak *et al.* 2011b). Treatment with

atorvastatin and/or ezetimibe lowered hepatic TLR2 mRNA levels in HF-fed *foz/foz* mice; combined drug treatment also significantly reduced TLR2 mRNA expression in *foz/foz* mice, in fact normalising levels to those of treatment-matched genotype controls ($P<0.05$, Figure 7.14A). TLR4 mRNA levels were unchanged in *foz/foz* and WT mice irrespective of atorvastatin and/or ezetimibe treatment (Figure 7.14B). TLR9 mRNA levels were variably altered by pharmacological modulation of cholesterol biosynthesis and/or uptake. Atorvastatin and ezetimibe monotherapy *increased* TLR9 mRNA levels in HF-fed *foz/foz* mice *versus* treatment-matched genotype controls ($P<0.05$, Figure 7.14C), although no changes were observed for combined drug-treated *foz/foz* mice (Figure 7.14C). No changes in Myd88 gene expression were observed in HF-fed *foz/foz* and WT mice, regardless of drug treatment or genotype (Figure 7.14E).

In Section 7.4.4, we observed an upregulation in hepatic HMGB1 in high cholesterol/HF-fed *foz/foz* and WT mice ($P<0.05$, Figure 7.13C). Treatment of *foz/foz* mice with atorvastatin and/or ezetimibe decreased hepatic HMGB1 levels significantly compared to vehicle controls ($P<0.05$, Figure 7.14D); for HMGB1 expression, there were no differences between monotherapy and combined drug treatment groups (Figure 7.14D).

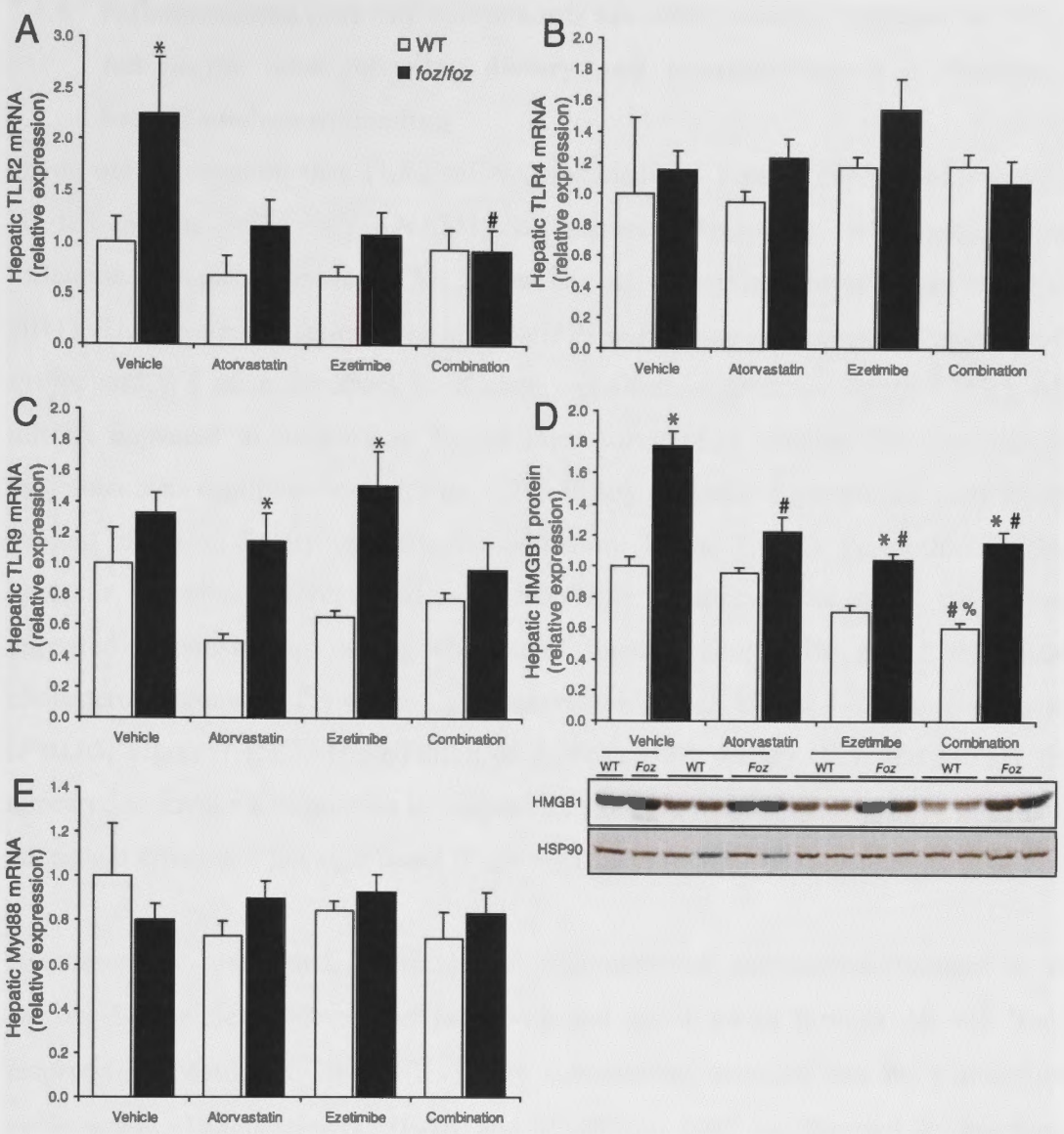

Figure 7.14 TLR2, -4, -9, HMGB1, and Myd88 gene expression in HF-fed *foz/foz* and WT mice with or without atorvastatin and/or ezetimibe treatment

(**A**) Toll-like receptor (TLR)-2 mRNA, (**B**) TLR4 mRNA, (**C**) TLR9 mRNA, (**D**) high-mobility group protein-B1 (HMGB1) protein, and (**E**) myeloid differentiation primary response gene-88 (Myd88) mRNA expression in *foz/foz* (■) and WT (□) mice fed high fat (HF) diet for 16 weeks, after which atorvastatin (20 mg/kg/day) and/or ezetimibe (5 mg/kg/day) were introduced into diet and administered for an additional 8 weeks (see Section 6.3.2). Data are mean ± SEM. *P<0.05, vs. treatment-matched, genotype control. $^{\#}P$<0.05, vs. genotype-matched, vehicle group. $^{\dagger}P$<0.05, vs. genotype-matched, atorvastatin treatment group.

7.4.6 Inflammasome pathway components are differentially regulated in HF-fed *foz/foz* mice following dietary and pharmacological modulation of hepatic cholesterol loading

Given our observation that TLR2 mRNA and HMGB1 protein expression increase in HF-fed *foz/foz* mice with NASH, it seemed relevant to investigate hepatic inflammasome pathways since TLR2 signalling activates this pathway (Jones and Weiss 2011). There were no differences in hepatic NALP3 gene expression between HF-fed *foz/foz* and WT mice, irrespective of dietary cholesterol feeding (Figure 7.15A). ASC mRNA appeared to increase in *foz/foz* mice *versus* diet-matched WT controls (the difference was significant only for the 0.2% dietary cholesterol group), but there was no evident effect of dietary cholesterol modulation (Figure 7.15B). Pannexin-1 mRNA, however, was clearly upregulated in HF-fed *foz/foz* mice compared to WT controls and appeared responsive to dietary cholesterol loading; thus 0.2% and 2.0% dietary cholesterol augmented Pannexin-1 gene expression, albeit effects were relatively small ($P<0.05$, Figure 7.15C). The addition of 0.2% and 2% dietary cholesterol in HF diet appeared to invoke a minor rise in caspase-1 mRNA in *foz/foz* mice, but this apparently consistent effect was not significant (Figure 7.15D).

As previously mentioned, activation of inflammasome pathways culminates in the caspase-1-dependent cleavage of pro-IL-1β and pro-IL-18 to form IL-1β and IL-18, respectively. Mature IL-1β and IL-18 are subsequently secreted into the extracellular environment. Diagnostically, IL-1β and IL-18 can both be detected in the blood following inflammasome activation (Imamura *et al.* 2009). In the dietary cholesterol feeding experiment, hepatic IL-1β mRNA expression tended to be higher in HF-fed *foz/foz* mice *versus* WT control, while 2% cholesterol feeding appeared to augment IL-1β mRNA expression in *foz/foz* mice, albeit increases were not statistically significant (Figure 7.15E). Similarly, serum IL-18 levels were heightened in 0.2% and 2.0% cholesterol/HF-fed *foz/foz* mice compared to diet-matched WT controls, but increases were not significant, as assessed by ANOVA (the difference between serum IL-18 levels in 2% cholesterol/HF-fed *foz/foz* mice *versus* corresponding WT dietary controls may be an artefact of the unexplained very low levels of serum IL-18 for the controls in this dietary group) (Figure 7.15F).

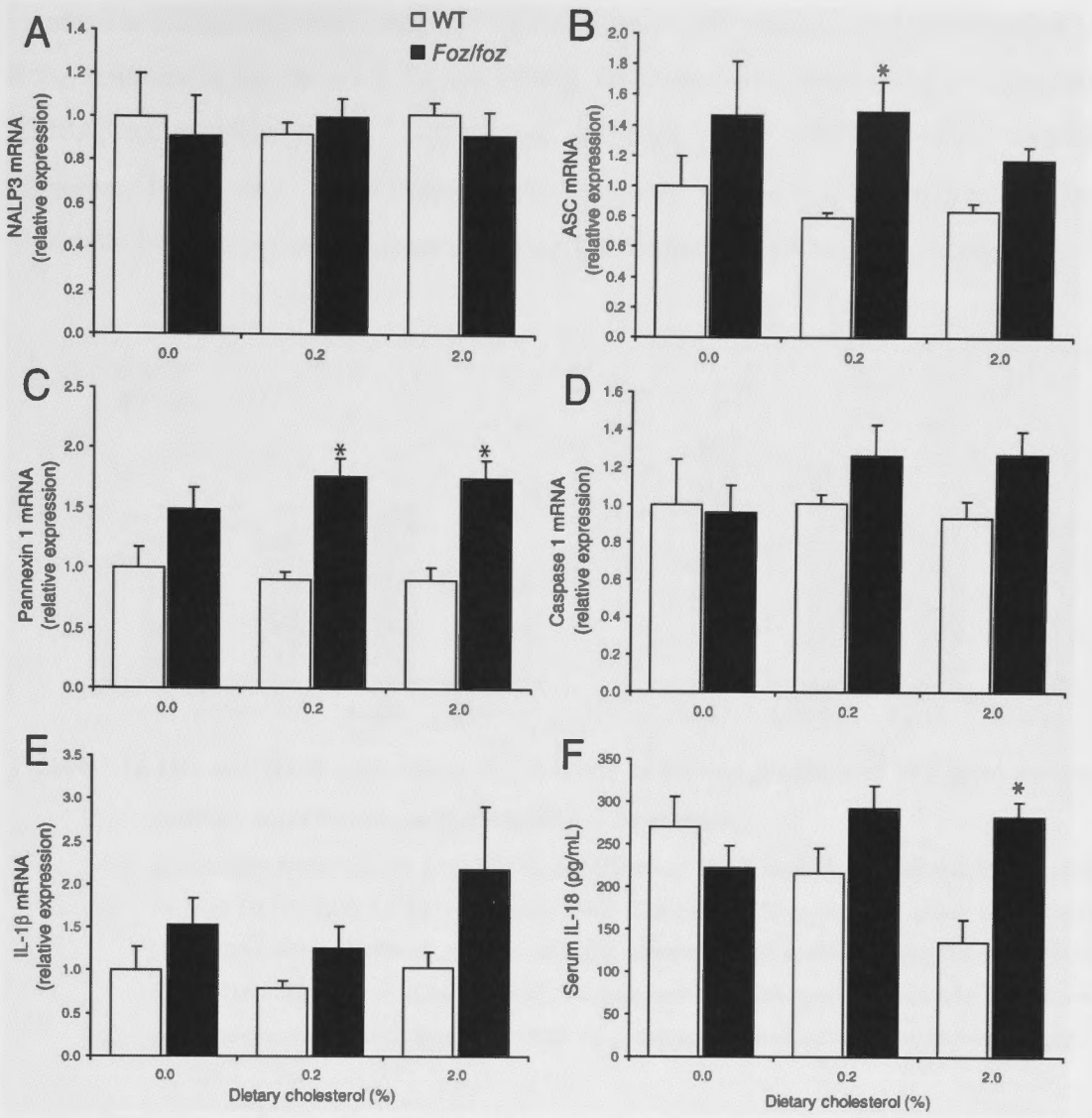

Figure 7.15 Inflammasome-associated gene expression, and serum IL-18 levels in HF-fed *foz/foz* and WT mice fed varying percentages of dietary cholesterol

(**A**) NACHT, LRR and PYD domains-containing protein 3 (NALP3) mRNA, (**B**) apoptosis-associated speck-like protein containing a CARD (ASC) mRNA, (**C**) Pannexin-1 mRNA, (**D**) caspase-1 mRNA, (**E**) interleukin (IL)-1β mRNA, and (**F**) serum IL-18 levels in WT (□) and *foz/foz* (■) mice (n=7-11/grp) fed HF-diet containing 0.0, 0.2 or 2.0% (w/w) cholesterol for 24-weeks. Data are mean ± SEM. *P<0.05, vs. diet-matched control. $^{\#}P$<0.05, vs. genotype-matched, 0.2% dietary cholesterol group. $^{\dagger}P$<0.05, vs. genotype-matched, 0% dietary cholesterol group.

In regards to atorvastatin and/or ezetimibe-treated animals, cholesterol-lowering therapy was not associated with any significant increases in hepatic IL-1β mRNA expression in either *foz/foz* or WT mice (Figure 7.16A). Serum IL-18 levels, however, tended to decrease after atorvastatin administration in HF-fed *foz/foz* mice, while the more

impressive reductions were observed with ezetimibe monotherapy and combination drug-treatment in *foz/foz* mice (Figure 7.16B). Attempts were made, using a commercial ELISA, to quantify serum IL-1β levels in dietary and pharmacological studies. However, IL-1β was not detected in any samples, regardless of genotype, dietary cholesterol content, or atorvastatin and/or ezetimibe treatment (data not shown).

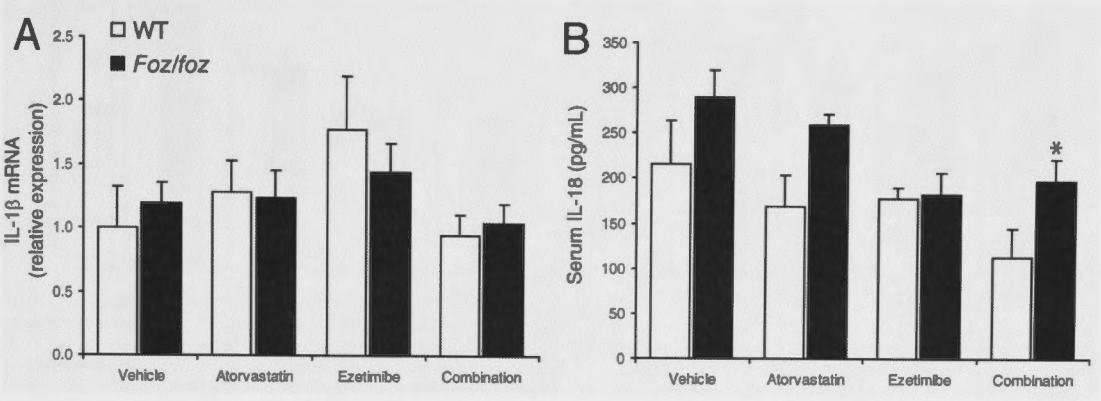

Figure 7.16 Hepatic IL-1β and serum IL-18 levels in HF-fed *foz/foz* and WT mice with or without atorvastatin and/or ezetimibe treatment

(**A**) Hepatic interleukin (IL)-1β mRNA, and (**B**) serum IL-18 levels *foz/foz* (■) and WT (□) mice fed high fat (HF) diet for 16 weeks, after which atorvastatin (20 mg/kg/day) and/or ezetimibe (5 mg/kg/day) were introduced into diet and administered for an additional 8 weeks (see Section 6.3.2). Data are mean ± SEM. *$P<0.05$, vs. treatment-matched, genotype control. $^{\#}P<0.05$, vs. genotype-matched, vehicle group. $^{\dagger}P<0.05$, vs. genotype-matched, atorvastatin treatment group.

7.4.7 Pathways of ER stress are differentially altered during NASH progression in HF-fed *foz/foz* mice

Pathways of ER stress were studies in 12- and 24-week HF and chow-fed *foz/foz* mice, as described in Chapter 3. As previously mentioned Section 7.1.5, GRP78 is the major ER chaperone involved in the initiation of the three UPR pathway arms (see Figure 7.5). GRP78 protein levels appeared to decrease, although not significantly, in both HF-fed *foz/foz* and WT mice at 12- and 24 week time points (Figure 7.17A). In contrast, differential responses were observed for the gene expression of the 3 UPR arm activators. IRE1α mRNA was unchanged in *foz/foz* and WT mice, irrespective of diet or time (Figure 7.17B). Conversely, PERK and ATF6 mRNA levels were significantly higher in HF-fed *foz/foz* mice at both 12- and 24 weeks ($P<0.05$, Figure 7.17C,D), times at which NASH and fibrotic NASH are observed in these animals. Importantly, however, the opposite was observed for the biologically more relevant Chop protein,

nuclear expression of which was significantly lower in the mice with NASH compared with dietary controls ($P<0.05$, Figure 7.17E). On the other hand, Chop mRNA increased significantly in HF-fed *foz/foz* mice with NASH ($P<0.05$, Figure 7.17F).

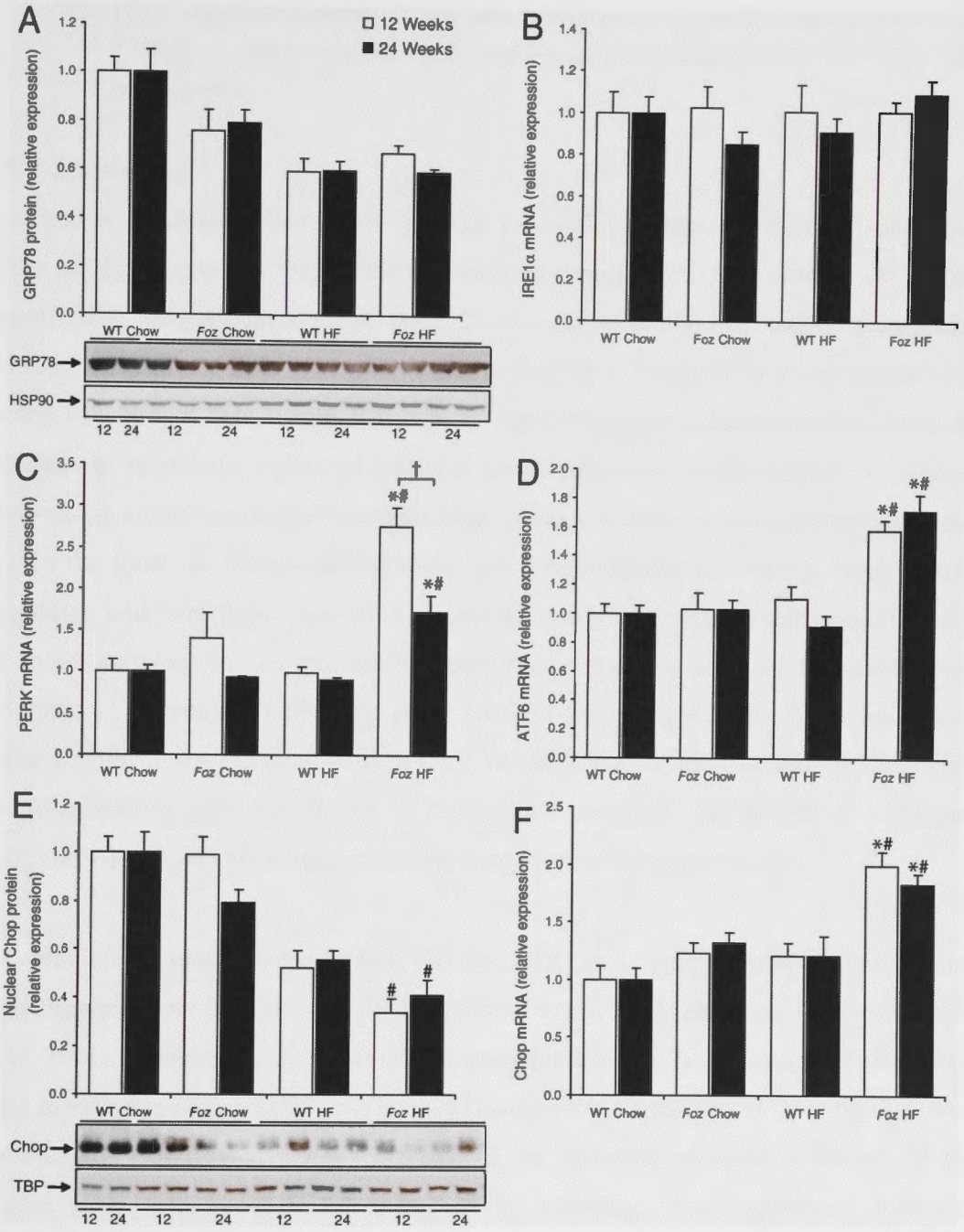

Figure 7.17 ER stress pathways are differentially regulated in HF-fed *foz/foz* with NASH versus wildtype mice.

Legend for Figure 7.17.

(**A**) 78 kDa glucose-regulated protein (GRP78), (**B**) inositol-requiring enzyme 1α (IRE1α) mRNA, (**C**) PKR-like ER kinase (PERK) mRNA, (**D**) eukaryotic translation initiation factor 2 (eIF2α) mRNA, (**E**) nuclear C/EBP- homologous (Chop) protein and (**F**) Chop mRNA expression at 12- (□) and 24-weeks (■) in WT and *foz/foz* mice fed chow or HF (0.2% cholesterol) diet. Western blot quantitation was normalised to house keeping gene expression (TATA box binding protein [TBP] or heat-shock protein-90 [HSP90]). Data are mean ± SEM. $^{*}P<0.05$, vs. diet-matched control. $^{\#}P<0.05$, vs. genotype-matched control. $^{\dagger}P<0.05$, vs. time-matched control.

7.5 Discussion

In Chapter 5, dietary cholesterol loading experiments demonstrated an association between the degree of hepatic cholesterol accumulation and severity of NASH. Specifically, the patterns of serum ALT, hepatocyte apoptosis and hepatic macrophage infiltration faithfully paralleled the profiles of hepatic CE and FC in obese *foz/foz* mice. In the following Chapter, pharmacological approaches were undertaken in successful attempts to remediate hepatic cholesterol accumulation in HF-fed *foz/foz* mice. Such atorvastatin and/or ezetimibe treatment for 8 weeks not only reduced cholesterol content within the livers of HF-fed *foz/foz* mice, but concomitantly suppressed hepatocellular apoptosis, and liver injury (serum ALT levels), and modulated macrophage infiltration in these animals. In the present Chapter, we sought to identify the cholesterol-responsive molecular pathways that mediate hepatocyte cell death and liver inflammation in *foz/foz* mice with NASH. We first studied the cardinal cell death and proinflammatory pathways linked to lipotoxicity generally and NASH in particular, JNK and NF-κB p65 activation, using the livers for earlier experiments.

As previously mentioned (Section 7.1.1), JNK is a proapoptotic protein kinase signalling pathway (Zanke *et al.* 1998; Tournier *et al.* 2000; Liu *et al.* 2002b; Schwabe *et al.* 2004). In this study, the ratio of phosphorylated:pan JNK protein (pJNK:JNK) was used to estimate JNK activation. The 46 kDa and 54 kDa isoforms of hepatic JNK were both strongly activated (phosphorylated) in the livers of cholesterol-loaded HF-fed *foz/foz* mice with NASH. Moreover, JNK activation was suppressed following atorvastatin and/or ezetimibe treatment for 8 weeks in these animals (Figure 7.7). The consistency of changes in FC, JNK activation and M30 IHC staining for cytokeratin-18 fragmentation (see Figures 5.6 and 6.9), as well as profiles of serum ALT (Figures 5.4A and 6.7A) and hepatic macrophage infiltration emphasise the likely causative role for

FC in activating JNK as a cell death pathway in this model. On the other hand, JNK activation failed to correlate with profiles of hepatic FFA, DAG, MAG, and TG lipid fractions (Figures 5.2, 5.3, 6.5, and 6.6). Taken together these data suggest that JNK activation appears to be responsive to hepatic cholesterol content, not to FFA, which in isolated cell systems can activate JNK and apoptosis (Malhi *et al.* 2006).

Cholesterol-dependent JNK activation has been previously documented in pancreatic β-cells and macrophages (Devries-Seimon *et al.* 2005; Bao *et al.* 2006; Li *et al.* 2008; Lu *et al.* 2011). Additionally, increased JNK and caspase-3 pathway activation have been reported in $ApoE^{-/-}$ mice fed 0.21% dietary cholesterol (Sinha-Hikim *et al.* 2011). Further, recent studies by Henkel and colleagues (2011) from Richard Green's laboratory have demonstrated JNK activation in FVB/NJ mice fed 1.2% cholesterol for 12 weeks. More impressively, these results were also accompanied by a reduction in hepatic Cyp7a1 expression and accumulation of hepatic cholesterol (Henkel *et al.* 2011), which corroborate the observations of hepatic cholesterol accumulation, suppressed Cyp7a1 mRNA and increased JNK activation in HF-fed *foz/foz* mice, presented here and in Chapters 3, 5, and 6. Taken together, these data suggest that JNK activation may be responsive to intracellular cholesterol accumulation within the livers of both *foz/foz* (the present work) and WT mice (work of Henkel *et at.* 2011); it therefore could constitute the major pathway responsible for increased hepatocellular cell death observed in NASH (Figures 5.6 and 6.9). This proposal is strongly supported by the direct correlation between JNK activation and profiles of liver injury in *foz/foz* and WT mice.

There were some similarities and some differences between the patterns of JNK and NF-κB activation in these analyses. Nuclear (active) NF-κB p65 protein levels fell in WT mice fed 0.2% and 2% dietary cholesterol (Figure 7.8A) compared with 0% cholesterol/HF-fed WT mice, whereas liver injury was significantly elevated in 2% cholesterol-fed WT mice (Figures 5.4A, 5.6, and 5.7). Overall, however, hepatic cholesterol loading appeared to activate NF-κB p65 activity in HF-fed *foz/foz* mice, as assessed by quantification of nuclear p65 protein levels ($P<0.05$, Figure 7.8A) and raised cytoplasmic NF-κB p65 protein (Figure 7.8B). The fall in IκBα (not IκBβ) levels (Figure 7.8D) in *foz/foz* mice *versus* WT controls, again proportional to hepatic cholesterol levels, is also consistent with the assertion that there is a direct relationship

between hepatic FC levels and NF-κB activation, albeit the pathway(s) activated require further consideration.

The cholesterol-responsiveness of NF-κB p65 activation in this NASH model, as determined through quantification of nuclear p65 protein levels, was further demonstrated in drug-treated HF-fed *foz/foz* mice. Thus, nuclear p65 levels were significantly lowered by ezetimibe monotherapy and by combined ezetimibe and atorvastatin treatment (Figure 7.9A), both treatments which substantially lowered hepatic cholesterol content. Impressively, these treatments also stabilised IκBα protein in HF-fed *foz/foz* mice (Figure 7.9B), tightening the nexus between cholesterol and NF-κB activation. In a separate study, combined ezetimibe and simvastatin treatment has been shown to reduce atherosclerotic plaque density in rabbits fed atherogenic HF diet (Gomez-Garre *et al.* 2009). Importantly, amelioration of arterial atherosclerosis was accompanied by reductions of NF-κB p65 activation in peripheral blood leukocytes, as determined by electrophoretic mobility shift assay, and arterial MCP-1 gene expression (Gomez-Garre *et al.* 2009).

The study of NF-κB p65 localisation in the present experiments showed that this proinflammatory mediator is expressed predominantly by hepatic NPC cell fractions. Wang *et al.* (2011b) have demonstrated that treating human U937 promonocytic cells with oxidised LDL increased intracellular cholesterol content, and destabilised and degraded total IκBα protein so as to increase nuclear NF-κB p65. Similarly, Zhu and colleagues (2008) reported increased NF-κB p65 activation in cholesterol-laden Abca1 knock-out ($Abca1^{-/-}$) macrophages. Furthermore, NF-κB activation in cholesterol-laden $Abca1^{-/-}$ macrophages appeared to be hypersensitive to LPS stimulation in a Myd88-dependent fashion (Zhu *et al.* 2008). These data clearly indicate a role of TLR signalling in cholesterol-mediated NF-κB p65 activation, as discussed later in this Section.

Subsequent assessment of NF-κB p65-responsive proinflammatory genes, including VCAM-1, ICAM-1 and MCP-1 revealed significantly elevated gene expression in obese, diabetic *foz/foz* mice with NASH (Figures 7.8E,F; 7.9C,D; 5.7C,D; 6.10A). Activation of these genes correlated with increased nuclear NF-κB p65 levels, which as previously mentioned are thought to be responsive to hepatic cholesterol deposition.

Rull *et al.* (2009) have also reported increased hepatic MCP-1 expression in $LDLR^{-/-}$ C57BL/6J mice, following 0.25% cholesterol/HF feeding; this was accompanied by liver inflammation as well as steatosis. Dual $LDLR^{-/-}$ and MCP-1 knockout ($MCP\text{-}1^{-/-}$) mice fed the same diet were refractory to hepatic inflammation and steatosis. Furthermore, MCP-1 protein was localised around lipid-laden hepatocytes in $LDLR^{-/-}$ mice (Rull *et al.* 2009), a finding which is similar to our observation of increased NF-κB p65 expression in NPC cells adjacent to lipid-laden hepatocytes (Figure 7.8C). Collectively, we interpret these data as indicating that NF-κB p65 is activated in NPCs (most likely macrophages) in response to hepatic cholesterol-loading. In turn, this change most likely results in increased proinflammatory responses and heightened macrophage recruitment in HF-fed *foz/foz* mice with NASH.

JNK and NF-κB p65 are the "messengers" in all signalling pathways that arise from cell stressors, such as lipotoxic molecules, and/or by activation of cell surface receptors; the latter include the TNF receptor superfamily and TLRs (see Sections 7.1.1 to 7.1.5). We, therefore sought to determine which signalling pathway(s) were responsible for the activation of JNK and NF-κB p65 within the livers of *foz/foz* mice. We canvassed several molecular processes of contemporary interest. Firstly, we sought to assess the role of the TNF- and TNF-related signalling pathways. Previous studies have demonstrated increased serum TNF-α levels in human and animals with NASH (Fan *et al.* 2003; Hui *et al.* 2004; Bahcecioglu *et al.* 2005; Abiru *et al.* 2006; Zou *et al.* 2006), albeit most of these human studies found no difference between levels in NAFLD cases with and without NASH.

In our studies, serum and hepatic TNF-α levels likewise failed to correlate (increase) with the degree of liver injury, apoptosis, inflammation or fibrosis observed in HF-fed *foz/foz* mice with NASH (Figures 7.10A,B and 7.11A,B). Likewise, hepatic TNF receptor expression was unchanged in these animals, regardless of liver injury. In regards to other TNF-related signalling pathways, the only interesting change was observed for hepatic Killer (orthologous to human DR5) expression, which was increased in HF-fed *foz/foz* mice fed 2% cholesterol (Figure 7.10F). However, in the atorvastatin and ezetimibe study, Killer expression was variably altered (Figure 7.11F). It is plausible that TRAIL is secreted by liver lymphocytes (particularly natural killer cells) and Kupffer cells or circulating mononuclear cells and could activate hepatocyte

Killer, in turn triggering the caspase cascade (Figure 7.2). On the other hand, Killer signalling does not inevitably lead to cell death in the liver. In fact, Killer$^{-/-}$ mice are refractory to liver injury and apoptosis in hepatic ischaemia-reperfusion injury (Teoh *et al.* unpublished data, 2009).

To assess the role of TRAIL/Killer in metabolic syndrome-related NASH, further experiments will be performed in our C57BL/6 Killer$^{-/-}$ and TRAIL$^{-/-}$ mice, using bone marrow chimeras (with WT C57BL/6 mice) recently created in the host laboratory (Ajamieh, Teoh, and Farrell, unpublished data, 2011). Nonetheless, the global findings from the dietary and pharmacological modulation experiments suggest that the TNF- and TNF-related pathways do not play a significant role in mediating liver injury in the HF-fed *foz/foz* model of NASH.

In the absence of a satisfactory explanation from TNF signalling, TLR activation seemed the most plausible origin of JNK and NF-κB p65 activation. We therefore examined the TLR and Myd88 gene expression. TLR receptor and down-stream Myd88 gene expression was unchanged in *foz/foz* mice with NASH. The important positive finding was that the TLR2/4 ligand, HMGB1, was upregulated in both *foz/foz* and WT mice, in a cholesterol-responsive manner ($P<0.05$, Figures 7.13C and 7.14D). Furthermore, TLR2 expression itself tended to increase in *foz/foz* mice according to hepatic cholesterol content. These findings are consistent with the idea that the HMGB1/TLR2 pathway is important in the cholesterol-dependent activation of JNK and NF-κB p65 in NASH. In atherosclerosis, HMGB1 involvement has been previously documented. Thus, in endothelial cells derived from Sprague-Dawley rats, Yang *et al.* (2010) reported that atorvastatin inhibited HMGB1-dependent activation of TLR4, with its downstream upregulation of NF-κB p65-dependent ICAM-1 and E-selectin expression. Our findings support our suggestion that atorvastatin may partially contribute to decreased hepatic HMGB1 expression in drug-treated *foz/foz* mice (Figure 7.14D). Ezetimibe, which has no known (documented) effect on HMGB1, also decreased total HMGB1 expression in HF-fed *foz/foz* mice. It therefore seems more likely that the treatment-induced reduction in hepatic cholesterol content, achieved by administration of atorvastatin and/or ezetimibe, abrogated hepatic HMGB1 expression either as a direct result of reduced hepatic cholesterol loading or by virtue of lowered hepatic inflammation and cell death.

Our favoured interpretation of these data is that HMGB1 is directly responsive to increases in hepatic cholesterol loading. Li and colleagues (2011b) recently demonstrated that hepatocytes secrete HMGB1 in response to FFA stimulation, with the most impressive results observed for palmitic acid (saturated FFA) stimulation. The same workers subsequently demonstrated that TLR4 and Myd88 function is essential for NAFLD onset in HF-fed C57BL/10SNJ mice, with TLR4 ($TLR4^{-/-}$) and Myd88 ($Myd88^{-/-}$) knockout mice found to be refractory to NAFLD onset. Thus, during HF feeding for 12 weeks, hepatic macrophage infiltration, myeloperoxidase activity and serum ALT levels remained unchanged in $TLR4^{-/-}$ and $Myd88^{-/-}$ mice, whereas all of these indices increased significantly in control mice. Importantly, $TLR4^{-/-}$ mice are also resistant to MCD diet-induced steatohepatitis (Szabo *et al.* 2005). On the other hand, the role of TLR2 in NAFLD progression is less clear, and this is an important point because TLR2, and not TLR4 was induced in our model. In two separate studies, TLR2 knockout ($TLR2^{-/-}$) mice fed MCD diet display elevated hepatic steatosis, accompanied by increased serum ALT, TNF-α, and hepatic collagen-α1 mRNA levels compared to $TLR2^{+/+}$ controls (Szabo *et al.* 2005; Rivera *et al.* 2010). In contrast, TLR2 signalling has been shown to be important in the progression of atherosclerosis (Mullick *et al.* 2005). The obvious explanation for these discrepancies is that TLR4 activation is model-specific and unrelated to cholesterol-induced lipotoxicity, which we and other propose is an important mechanism of metabolic syndrome-related NASH and atherosclerosis.

In regards to the role of TLR9 in NASH pathogenesis, studies by Miura *et al.* (2010), using C57BL/6 $TLR9^{-/-}$ mice fed choline-deficient *L*-amino acid defined diet demonstrated that TLR9 signalling is involved in the development of steatohepatitis and hepatic fibrosis. Their further findings identified that Kupffer cell TLR-dependent IL-1β expression results in HSC activation, as well as induction of both hepatocellular steatosis and apoptosis. In our obese insulin-resistant, diabetic and hypoadiponectinemic mice with NASH, however, we found no significant increases in TLR9 gene expression (Figure 7.13B and 7.14C). It remains plausible that circulating unmethylated CpG oligonucleotides as TLR9 ligands may contribute TLR9 signalling in the HF-fed *foz/foz* model, since increased expression is not essential for this pathway, or a selective increase in TLR protein on Kupffer cells may not have been detected by the methods used here. On the other hand, it is possibly more likely that TLR9 upregulation and

participation in steatohepatitis pathogenesis is also model specific, and not relevant to NASH with metabolic syndrome.

Some studies have demonstrated that high-cholesterol feeding can increase intestinal permeability (Thomson *et al.* 1987; Thomson and Keelan 1989). This could increase exposure to gut-derived endotoxin (LPS) and subsequently increase hepatic TLR signalling, thereby driving JNK and NF-κB signalling in the liver. One of the limitations of the present study is the limited quantification of TLR ligands. While HMGB1 protein expression was quantifiable, the exogenous TLR ligands (LPS, CpG DNA, etc…) could not be assessed by the methods at our disposal, and these may play an important role in TLR signalling in *foz/foz* mice. Despite this limitation, our collective findings indicate that HMGB1 is a likely candidate for involvement in NASH pathogenesis in *foz/foz* mice. Although we failed to observe any changes in TLR4 expression, it is highly plausible that HMGB1/TLR2/4 signalling could be an important mediator of necroinflammation in the *foz/foz* mouse model. On the other hand, upregulation of TLR2 may constitute an adaptive response to liver injury and inflammation induced by hepatic cholesterol loading, if, as in the MCD model, TLR2 plays a protective role in steatohepatitis development in metabolic forms of NAFLD. Further studies are needed to elucidate the exact roles of TLR2 and TLR4 in NASH pathogenesis in the *foz/foz* model of NASH (see Section 8.1.4 for future directions).

The observed increased HMGB1 expression and NF-κB p65 activation (nuclear protein), led us to analyse the inflammasome pathway. This was pursued by semi-quantification of gene expression of the various inflammasome components, in addition to serum IL-1β and IL-18. NALP3 inflammasome components were differentially altered in HF-fed *foz/foz* mice. Pannexin-1 gene expression increased in *foz/foz* mice fed 0.2 and 2% cholesterol/HF diets, while the gene expression data for NALP3, ASC, caspase-1 and IL-1β were variable and failed to correlate with or reflect the clear profiles of liver injury and liver inflammation in *foz/foz* mice. Recent studies have identified NALP3 inflammasome activation in both MCD-fed C57BL/6 and humans with NASH (Csak *et al.* 2011a). Csak *et al.* (2011a) also reported increased IL-1β expression in MCD-fed C57BL/6 mice with steatohepatitis. In our studies, serum IL-1β levels were not detected despite using undiluted samples for its assay. Serum IL-18, the other major cytokine product produced by inflammasome activation (Figure 7.4),

appeared to increase in cholesterol-loaded *foz/foz* mice (Figure 7.15F), and declined in atorvastatin and/or ezetimibe-treated HF-fed *foz/foz* mice (Figure 7.16B). These preliminary findings indicate that the inflammasome pathway seems less important than HMGB1/TLR2/4 signalling via JNK and NF-κB p65 during NASH pathogenesis. However, further investigations, specifically examining protein levels and caspase-1 activity, are needed to conclusively rule out inflammasome recruitment and functioning during the pathogenesis of steatohepatitis related to insulin resistance and metabolic syndrome.

Lastly, we examined the UPR response in the obese *foz/foz* model of NASH. Loading macrophages with FC activates JNK, in a UPR-dependent fashion (Devries-Seimon *et al.* 2005; Li *et al.* 2008). Our studies, however, have found that pathways of ER stress appear to be differentially and inconsistently altered in *foz/foz* mice with NASH. While PERK and ATF6 mRNA levels were significantly higher in HF-fed *foz/foz* mice than WT controls, total GRP78 and nuclear Chop protein levels decreased significantly compared with WT mice (Figure 7.15). Further, preliminary studies carried out by an international collaborator (Professor Isabelle Leclercq, Gastroenterology Laboratory, Université catholique de Louvain, Brussels, Belgium) have failed to identify increased TRAF2 expression, pXBP1 mRNA splicing, or eIF-2α phosphorylation in HF-fed *foz/foz* mice with NASH (Isabelle Leclercq, unpublished data, 2010). While further studies are needed to determine the role of UPR responses in non-parenchymal cells *versus* hepatocytes in HF-fed *foz/foz* mice with NASH, the current data find no support for the speculation that the UPR response is critical for JNK activation in NAFLD (Dara *et al.* 2011; Ji *et al.* 2011).

The primary aim of this Chapter was to identify the pathways involved in cholesterol-dependent liver injury and inflammation. Assessment of several pathways known to mediate cell death and pro-inflammatory gene expression identified hepatic cholesterol-responsive increases for both JNK and NF-κB p65. In trying to understand the origins of such activation, the further analysis of the various signalling cascades identified increased hepatic HMGB1 and TLR2 expression as the only molecules whose expression consistently followed hepatic FC levels, JNK and NF-κB p65 activation, as well as the disease phenotype of liver injury, cell death, inflammation, and fibrosis. Accordingly, we propose the following hypotheses for further study, that hepatic

cholesterol loading induces HMGB1 expression, which subsequently signals through TLR2 and/or TLR4, thereby activating JNK in hepatocytes and NF-κB p65 in Kupffer cells and recruited macrophages. Another possibility is that FC-mediated Kupffer cell activation releases DR-signalling cytokines (including FasL/Fas, which has not yet been pursued in this study) in proximity to hepatocytes, thereby activating JNK and NF-κB p65 in the cholesterol-loaded hepatocytes.

7.6 Summary of findings

The key findings of this study are outlined below:

1. Both NF-κB p65 and JNK-1/2 activation are reproducibly modulated by hepatic cholesterol levels in *foz/foz* mice, and their activation correspondingly is tightly linked to liver injury, hepatic apoptosis, liver inflammation, and fibrosis in NASH.
2. TNF and TNF-related pathways are unaffected by hepatic cholesterol-loading, but dietary cholesterol increases mouse Killer (ortholog to human TRAIL DR5) mRNA.
3. Hepatic TLR2 mRNA and HMGB1 protein levels increase within the livers of cholesterol-laden *foz/foz* mice with NASH, consistent with a proposed role for HMGB1 in signalling TLR2/4 during cholesterol-induce liver injury/inflammation in NASH.
4. Hepatic inflammasome components are differentially altered in *foz/foz* mice with NASH and may play an augmentary or supportive (as opposed to primary) role in cholesterol-induced liver inflammation.
5. PERK and AFT6 sensors are upregulated in *foz/foz* mice with NASH, but subsequent UPR response genes are unchanged or down-regulated in *foz/foz* mice with NASH. Thus, evidence for UPR/ER stress-related cell death and inflammation signalling in *foz/foz* mice with NASH is unconvincing.

CHAPTER 8

General discussion

8.1 Key findings of this research for perspectives on metabolic syndrome and NASH

The broad aim of the research presented in this thesis was to identify whether hepatic cholesterol acts as a lipotoxic mediator of NASH pathogenesis. Unlike many other animal models of fatty liver, *foz/foz* mice develop NASH in the context of metabolic syndrome (hyperphagic obesity, insulin-resistant diabetes, hypoadiponectinemia, dyslipidemia). Lipidomic characterisation of the model revealed significantly increased hepatic CE and FC lipid fractions in *foz/foz* mice with NASH compared to both dietary and genetic controls. Accordingly, the principle experimental aims of this research were: i) to elucidate the mechanisms responsible for this increase in hepatic cholesterol in *foz/foz* mice with NASH, and ii) to determine the effect of hepatic cholesterol accumulation on key aspects of NASH pathology (liver cell injury, inflammatory cell recruitment, fibrosis), and iii) to establish whether reversal of hepatic cholesterol stores could improve liver injury in NASH.

The first experimental aim was addressed through detailed characterisation of the various pathways involved in hepatic cholesterol homeostasis (described in Chapter 3). These studies identified several pathways that were altered inappropriately for the state of cholesterol accumulation in the livers of *foz/foz* mice with NASH. Specifically, operation of these dysregulated pathways would account for increased uptake of cholesterol into the liver and the failure of its biotransformation to bile acids, followed by impaired canalicular excretion of both cholesterol itself, and of bile acids into bile.

In Chapter 4, we were able to replicate several of these key changes *in vitro,* with experiments that used primary hepatocytes challenged with insulin at concentrations observed in hyperinsulinemic HF-fed *foz/foz* mice. An important implication of hyperinsulinemia-dependent cholesterol dysregulation is for the critical mechanistic link between insulin resistance (and associated hyperinsulinemia) and type 2 diabetes, and resultant cardiovascular risk in patients with NAFLD (Figure 8.1A,B). A literature

review failed to find earlier appreciations that the central role of the liver in metabolic syndrome may embrace disordered hepatic cholesterol metabolism resulting from insulin resistance, rather than (just) circulating dyslipidemia with steatosis (TG accumulation). The present findings therefore represent a conceptual advance in understanding why NASH and metabolic syndrome/type 2 diabetes are so closely related.

Chapters 5 and 6 addressed the second experimental aim, using two different experimental approaches to determine the effect of hepatic cholesterol loading on NASH pathology in *foz/foz* mice. In the first approach, manipulation of dietary cholesterol content (Chapter 5) was used to exacerbate or mitigate hepatic cholesterol loading, while the second intervention (Chapter 6) examined the effect of pharmacological inhibition of cholesterol biosynthesis and/or uptake/reclamation pathways. The combined results from these studies revealed that the profiles of hepatic cholesterol content strongly correlate with and seem likely to largely determine the patterns of liver injury (serum ALT), hepatocellular apoptosis, inflammation, as well as fibrosis in NASH. By use of the dual intervention approach (dietary and pharmacological), these results strongly support the underlying primary hypothesis of this research that *hepatic cholesterol does contribute to increased liver injury during NASH progression*. Subsequently, the mechanisms of inflammation and cell death that could be provoked by FC (or oxysterols) were explored in Chapter 7. We found that JNK and NF-κB p65 activation pathways are largely responsive to hepatic cholesterol content in HF-fed *foz/foz* mice with NASH. Preliminary data presented in Chapter 7 also suggests that hepatic FC loading may induce HMBG1 and TLR2 expression to initiate the observed JNK and NF-κB p65 activation (Figure 8.1C). HMGB1 is a cognate ligand of TLR4 and TLR2. In this work, any role for ER stress and the inflammasome was largely discounted by the comprehensive measurements of molecules involved in these two processes, expression levels of which were monotonously unchanged during manipulated changes in expression of the NASH phenotype. In the current Chapter, the potential clinical and mechanistic relevance of these results for NAFLD will be discussed, as well as important future directions.

One of the most interesting findings to emerge from this study is that hyperinsulinemia alters hepatic cholesterol homeostasis. While insulin-dependent regulation of

hepatocellular SREBP-2 was first demonstrated by Xie *et al.* (2009), the present study appears to be the first research to link hyperinsulinemic-dependent SREBP-2 augmentation to perturbed pathways of hepatic cholesterol homeostasis relevant to metabolic syndrome and NASH. In our studies, hyperinsulinemia-dependent alteration of pathways of hepatic cholesterol uptake, biotransformation to bile acids, and bile acid and cholesterol export explains why hepatic cholesterol accumulation and hypercholesterolemia occur in *foz/foz* mice with NASH (Figure 3.1A). In the earliest stags of hepatic cholesterol accumulation, increased HMGR activity and substrate loading may also play a role. More importantly, these data provide mechanistic insights into the inexorable link between type 2 diabetes and increased cardiovascular risk disease in NASH patients, among whom myocardial infarction constitutes one of the leading causes of death (Argo and Caldwell 2009; Wong *et al.* 2011), while incident cases of type 2 diabetes increase 2-3 fold in the 3 years after diagnosis of NASH. Small but seminal studies by Puri *et al.* (2007) and Caballero *et al.* (2009) were the first to demonstrate increased hepatic cholesterol accumulation in NASH patients. Caballero and colleagues (2009) also identified increased SREBP-2 expression in these individuals, a change which is corroborated by our studies in HF-fed *foz/foz* mice with NASH. Unfortunately, there do not yet appear to be other studies which have further characterised pathways of cholesterol homeostasis in patients with NASH. We propose that, in addition to increased hepatic FC accumulation and SREBP-2 expression, pathways of cholesterol uptake, biotransformation and export are likely suppressed in these individuals, thereby explaining the increases in hepatic cholesterol accumulation. This requires careful approaches to both lipidomic and pathway analyses in human liver, and/or in animal models where NASH results from metabolic syndrome.

Our proposal that, in patients with metabolic syndrome and type 2 diabetes, hyperinsulinemia perturbs bodily cholesterol homeostasis has conceptual implications for the function of the liver as a lipid storage organ. If because of insulin resistance, physiological regulation of hepatic cholesterol turnover is lost in ways that are proposed to occur in the *foz/foz* model of NASH, the normal hepatic phenotype related to cholesterol regulation must be replaced by a more "adipocytic" phenotype. In this way the liver becomes a cholesterol storage tissue, with little to no catabolic/export functioning, and the corresponding suppression of BA synthesis has other implications, for example for gallstone formation. This theory is supported by our observations of

reduced expression of key nuclear receptors in *foz/foz* mice; HNF-4α, LXR and LRH-1 are all markedly decreased in *foz/foz* mice with NASH (see Chapter 3). Such dysregulation of specialised hepatic function would effectively result in cholesterol accumulation elsewhere, such as the vascular endothelium, thereby accelerating atherosclerosis. As well, hepatic FC accumulation exacerbates liver injury, inflammation, and fibrosis (as demonstrated in our *foz/foz* mouse model [Chapters 5 and 6]). This concept would explain why insulin resistance, diabetes and metabolic syndrome are so strongly associated with NASH (Scheen and Luyckx 2003; Friis-Liby *et al.* 2004).

The only generally accepted management for patients with NASH is lifestyle intervention, in which physical activity is increased, energy intake reduced, and high sugar and fat diets are replaced by those containing minimal saturated fats and simple sugars, more complex (low glycaemic index) carbohydrates, unsaturated fats and higher fibre content. These changes improve liver function tests, reduce steatosis and increase insulin sensitivity, which also reduce cardiovascular risk factors. Among, pharmacological approaches, insulin-sensitising agents, such as pioglitazone and dipeptidyl peptidase IV inhibitors have demonstrated modest efficacy in ameliorating NASH in humans and in some animal studies, in association with improved insulin-sensitivity. Insulin resistance is not only a hallmark of NASH, but may also constitute a critical factor in progression of liver pathology to NASH. Unfortunately, most insulin-sensitising agents are associated with adverse effects and, as a result of their modest or transient efficacy (e.g. metformin and pioglitazone) none have been approved for NASH treatment. To further examine the proposed link between hyperinsulinemia and cholesterol-dependent NASH pathogenesis, HF-fed *foz/foz* mice could be treated with insulin-sensitising agents, and the effects of insulin sensitisation on intrahepatic cholesterol stores examined. Studies conducted by Dr Claire Larter (several readouts were carried out by the candidate) in the host laboratory, have demonstrated that dietary intervention (switching HF to chow) after NASH onset is capable of reversing NASH pathology, in association with decreased insulin-resistance and hepatic cholesterol content (paper submitted, see publication list, pg XIV). Likewise, use of a PPARα agonist (Wy-14,643) appeared to improve insulin sensitivity in the HF-fed *foz/foz* model with corresponding reductions of steatosis and fibrosis, but with no changes in liver

inflammation (Larter *et al.* 2011). Additional experiments examining the effect of exercise on *foz/foz* mouse NASH pathology have been planned.

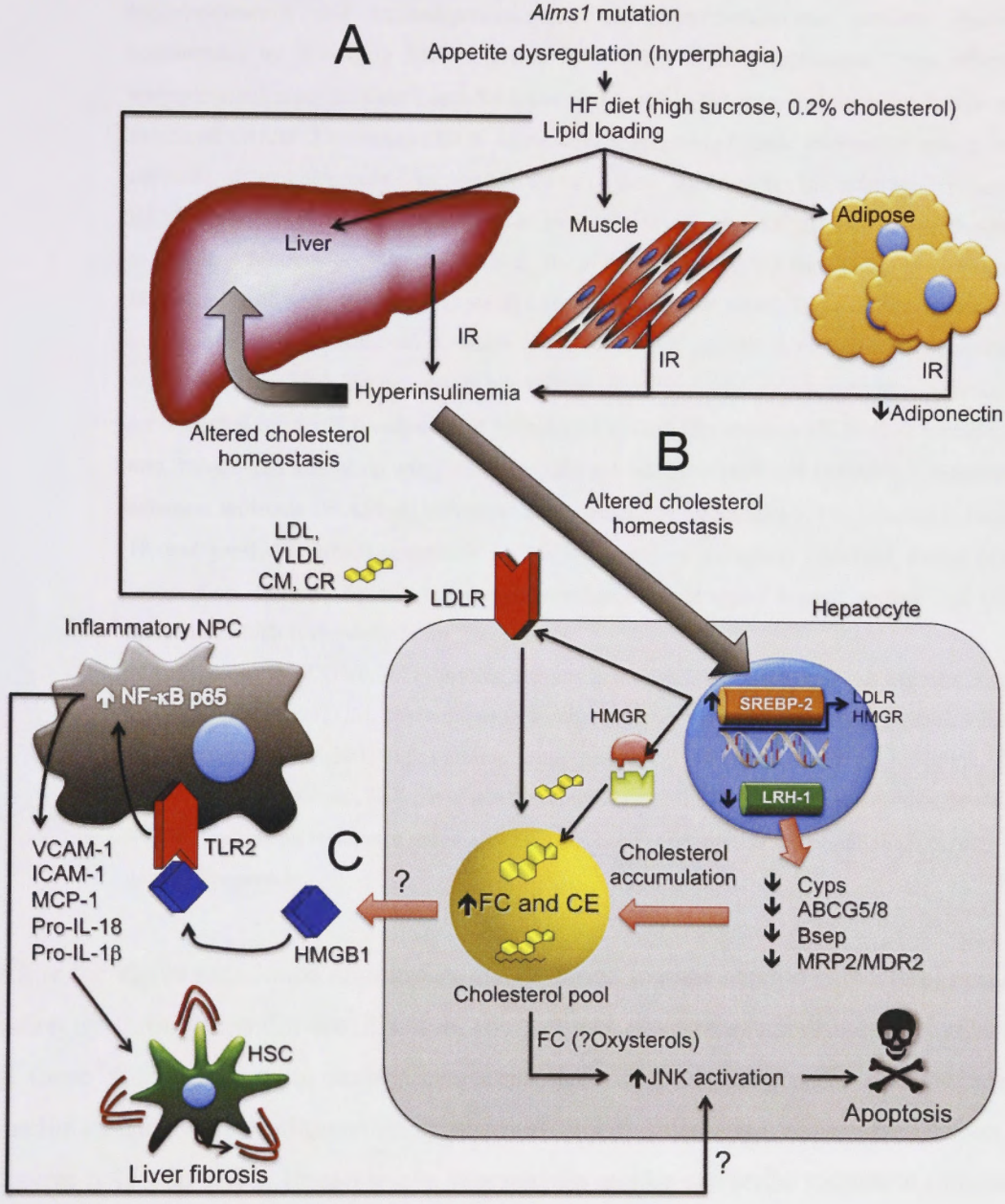

Figure 8.1 Proposed pathways of cholesterol-mediated liver injury in HF-fed *foz/foz* mice with NASH

Figure legend on next page.

Legend for Figure 8.1.

(**A**) High fat (HF)-feeding (containing high simple sugar content and 0.2% cholesterol) and lack of exercise cause over-nutrition which results in excessive lipid-loading of adipose, muscle and hepatic tissue. In turn, this induces insulin resistance (IR) in *foz/foz* mice, leading to hyperinsulinemia and hypoadiponectinemia. (**B**) Hyperinsulinemia perturbs cholesterol homeostasis by increasing SREBP-2 and suppressing LRH-1 expression. Other effects on transcriptional regulators such as LXRβ are also possible but were not clear cut in this study. Increased SREBP-2 increases LDLR expression, augmenting hepatic cholesterol uptake. In the absence of compensatory (increased) LRH-1 gene expression, no adaptive changes to HF/cholesterol-feeding take place, such as increased expression of Cyps involved in cholesterol to bile acid biotransformation, ABCG5/8, Bsep, MRP2 and MDR2 canalicular transporters. In fact, these pathways are under-expressed in HF-fed *foz/foz* mice. These events culminate in hepatic cholesterol accumulation, which (**C**) induces JNK activation, resulting in hepatocellular cell death, while HMGB1 expression and release (possibly for necrotic hepatocytes) signals non-parenchymal cell (NPC) activation of NF-κB p65 via toll-like receptor (TLR)-2/-4 signalling. In turn, NF-κB p65 activation upregulates vascular cell adhesion molecule (VCAM)-1, intercellular adhesion molecule (ICAM)-1, monocyte chemotactic protein (MCP)-1, pro-interleukin (proIL)-1β and proIL-18, which contribute to the inflammatory pathology observed during NASH progression. Chronic hepatic inflammation subsequently triggers hepatic stellate cell (HSC) activation which is responsible for fibrogenesis.

Abbreviations: ABCG5/8, ATP-binding cassette protein-G5/G8; Bsep, bile salt exporter protein; CE, cholesteryl ester; CM, chylomicron; CR, chylomicron remnants; Cyp, cytochrome p450; FC, free cholesterol; HMGB1, high-mobility group protein B1; HMGR, HMG-CoA reductase; JNK, c-Jun *N*-terminal kinase; LDL, low density lipoprotein; MDR2, multi-drug resistance protein 2; MRP2, multi-drug resistance associated protein 2; NF-κB, nuclear factor-κB; VLDL, very low density lipoprotein.

While the above mentioned approaches are designed to alter hepatic cholesterol content indirectly through insulin-sensitisation, more direct pharmacological approaches, such as those with atorvastatin and/or ezetimibe described in Chapter 6, also improved insulin resistance and adiponectin expression in HF-fed *foz/foz* mice (see Chapter 6, Figures 6.4F and 6.7F). Impressively, atorvastatin and/or ezetimibe treatment mitigated NASH severity in HF-fed *foz/foz* mice by reducing liver injury, apoptosis, inflammation and fibrosis; these changes were closely associated with and likely attributable to decreased activation of JNK and NF-κB p65. Preliminary data are consistent with the proposal that this process is TLR2/4 and HMGB1-dependent. Interestingly, atorvastatin and/or ezetimibe also appeared to improve adipose tissue functioning, as determined by increases in serum adiponectin (Figure 6.4F). It is plausible that the increase in serum adiponectin is an important factor contributing to improved insulin sensitivity. In

addition to the expected reductions in hepatic cholesterol stores (Figure 6.), visceral adipose weights were altered by atorvastatin and/or ezetimibe treatment (Figure 6.4B). It is possible that atorvastatin and/or ezetimibe treatment improves adipose inflammation in *foz/foz* mice and further increases insulin sensitivity and adiponectin secretion, thereby improving the overall NASH phenotype. In addition, a role of altered FFA composition secondary to improved insulin sensitivity is not excluded by the present studies, as discussed in Chapter 6. Specifically, the role of accumulated saturated long chain FFA and depletion of very long chain polyunsaturates merits further separate study.

Another important consideration for the lipotoxic pathogenesis of NASH is that preliminary oxysterol data presented in Chapter 5, suggests that the patterns of certain hepatic oxysterol compounds show positive correlation with profiles of hepatic CE and FC, as well as liver injury and NASH pathology. A key piece of missing data is analysis of oxysterols from the drug intervention experiment (Chapter 6). Most likely this will show global reduction in oxysterols in parallel with the changes in FC and CE, but selective change that paralleled that NASH phenotype would be informative as to one or more lipotoxic oxysterol species. Whatever the results, future studies are planned to examine the role of oxysterols as lipotoxic species in the HF-fed *foz/foz* model of NASH. Finally, it may be useful to stress that while the global results of the present thesis provide strong support for a role of FC in NASH pathogenesis, they by no means exclude roles for other lipotoxic molecules, acting in some cases where FC does not accumulate, or acting synergistically with FC to sensitise hepatocytes to cytokine or lipid-mediated cell death.

8.2 Future directions

Although the results presented in this thesis have addressed several aspects pertinent to the role of cholesterol in NASH pathogenesis, several questions have arisen from these studies. The major future directions are described below.

8.2.1 Assessment of oxysterols and bile acids for HF-fed *foz/foz* mice with NASH

Analysis of the pathways of hepatic cholesterol homeostasis in this work revealed compelling evidence for perturbed nuclear receptor expression in *foz/foz* mice with NASH (see Chapter 3). While some of these changes were explained by

hyperinsulinemia, further research is needed to determine the specific roles of hepatic cholesterol, oxysterols, and BAs in regulating nuclear receptor expression and activity in metabolic syndrome, and to assess whether pathways of feedback/feedforward regulation are altered. Furthermore, compositional analysis of hepatic oxysterol and BA are needed to obtain a more comprehensive picture of cholesterol homeostasis in animals with NASH. For example, while Cyps 7a1, 7b1, 27a1 mRNA expression in *foz/foz* and WT mice was described in Chapters 4, 5, and 6, these analyses only provide a superficial assessment of the pathways of hepatic biotransformation of cholesterol to bile acids, all of which appear to be down-regulated during NASH pathogenesis. HPLC and mass spectroscopic analysis of hepatic and serum BAs, composition of bile and faecal cholesterol and bile acid content is needed to verify the assumptions made from pathway (gene expression) analysis. The results could provide additional mechanistic data, explaining the regulation of expression and activation of the nuclear receptors involved in cholesterol homeostasis. Ideally we need to study the interactions between nuclear receptors in the presence of varying levels of FC, but this is difficult to model *in vitro* where differentiated functions of hepatocytes are lost rapidly in culture.

8.2.2 What role does LRH-1 play in NASH pathogenesis?

While we demonstrated that LRH-1 mRNA levels are suppressed by insulin stimulation, we were not been able to resolve whether this occurs as a direct result of insulin stimulation or as a down-stream effect of SREBP-2-dependent inhibition; the latter indirect effect has been described by Kanayama *et al.* (2007). To the best of the candidate's knowledge, no studies have examined LRH-1 in human or other rodent models of NAFLD. However, the findings presented in Chapter 4 indicate that there may be a direct link between hyperinsulinemia related to insulin resistance and LRH-1 suppression in metabolic syndrome. Accordingly, it would be interesting to determine the role of LRH-1 in human NAFLD, with careful correlation to disease phenotype (severity).

In preliminary studies, we attempted to reinstate LRH-1 function in HF-fed *foz/foz* mice using two novel LRH-1 agonists JS/5197/16C and JS/5197/74A (kindly supplied by Professor Richard Whitby, University of Southampton, Southampton, UK). Unfortunately, the LRH-1 agonist compounds designed in Professor Whitby's

laboratory, as previously described (Whitby *et al.* 2011), specificially target human LRH-1 expression. Attempts to promote murine hepatocellular LRH-1 expression in primary cultures have proven unsuccessful, using the agonists at both the recommended concentrations or 10-fold higher. Alternatively, we plan to using knock-in strategies (adenovirus or retrovirus) to over-express LRH-1 protein in *foz/foz* hepatocytes, and determine whether cholesterol biotransformation and export pathways are reinstated as a result of increased LRH-1 expression.

8.2.3 Ultra-structural studies of hepatic cholesterol localisation and its effect on cellular functioning

In Chapter 3 we outlined preliminary cholesterol localisation studies. The majority of hepatic FC appeared to localise to the hepatocellular plasma membrane, with some partial localisation to ER and mitochondria. However, we have not ruled out the presence of crystallised cholesterol within the livers of *foz/foz* mice with NASH. Studies have found that at heightened concentrations, membrane-bound cholesterol is susceptible to crystallisation, yielding cholesterol monohydrate crystals (Phillips 1990; Huang *et al.* 1999). It is noted that mitochondrial crystals, first reported by Sanyal and colleagues (2001) have been observed repeatedly in human NASH (Caldwell *et al.* 2009), although their chemical nature and pathogenic significance remains unclear. Since cholesterol crystals are capable of activating inflammasome responses (Duewell *et al.* 2010; Rajamaki *et al.* 2010; Dunne 2011) (see Section 7.1.4) and cell death (Kockx *et al.* 1996; Kiyak 1997; Kellner-Weibel *et al.* 1998), this aspect warrants further study. Accordingly, we plan to use electron microscopy (EM) to examine fixed liver sections for the presence of cholesterol crystals in the mitochondria and other sites. Digitonin, a naturally occurring detergent, has proven to be useful in staining FC in EM studies (Okros 1968; Napolitano *et al.* 1972; Bonvicini *et al.* 1978; Sharawy *et al.* 1979). Additionally, the inherent resolution of EM will be particularly useful in further resolving the subcellular localisation of FC lipid fractions in animals with NASH.

Further, we have not determined the extent of cholesterol colocalisation within the endosome/lysosomal pathway. Studies by Beltroy *et al.* (2007) have identified that excess lysosomal FC may contribute to cell death within hepatocytes. Since we have proposed that the major source of hepatic cholesterol in *foz/foz* mice originates from LDL-bound cholesterol, the LDLR-mediated endosomal/lysosomal uptake pathway

may be of significant importance in mediating cholesterol-dependent hepatocellular cell death. Additionally, since cholesterol is an important determinant of membrane fluidity (Lande *et al.* 1995), we propose that plasma membrane-bound cholesterol may interfere with physiological membrane functioning, intercellular communication and signalling in *foz/foz* mice with NASH. Through the use of multi-photon scanning fluorescence microscopy and diphenylhexatriene staining (Ludi and Hasselbach 1982; Chazotte 1994), the fluid dynamics of membranes from HF-fed *foz/foz* mice could be compared with chow-fed and WT counterparts to determine whether membrane dysfunction is occurring. Alternatively, electron-spin and freeze-fracture studies could be implemented to determine the effects of excess plasma membrane cholesterol on membrane fluidity and functioning, as previously described by Martin *et al.* (1978). At a functional level, the mitochondrial/liposomal compartments are integrally involved with autophagy, a process which partially protects energy-depleted hepatocytes from necrotic (pro-inflammatory) cell death by coating apoptotic bodies suitable for macrophage ingestion (see review of hepatic autophagy by Mark Czaja (2011)]). Thus, studies of autophagy-related gene expression (e.g. lysosome-associated membrane proteins, beclin-1, autophagy-related genes, etc…) and ultrastructural morphology would be of interest in the *foz/foz* model of NASH.

Trafficking of CE-derived FC to the plasma membrane initiates apoptosis in cholesterol-loaded macrophages (Kellner-Weibel *et al.* 1999). From our preliminary studies we have identified that the majority of hepatocellular cholesterol resides in plasma membrane. To establish whether cholesterol accumulation within this compartment is important in hepatocellular apoptosis, future experiments could include interventions designed to restrict intracellular FC trafficking and/or CE hydrolysis to FC, using Niemann Pick C1/2 and ACAT small molecule inhibitors or siRNA knockdown strategies. These experiments would be initially trialled in *in vitro* model systems, using cholesterol-laden hepatocytes. Depending on the outcome, *in vivo* approaches could then be employed with relevant vehicles for molecular manipulations.

8.2.4 Further characterisation of cholesterol-induced pathways of liver injury

The findings presented in Chapter 7 suggest that TLR2 activation may be involved in cholesterol-dependent JNK and NF-κB p65 activation in *foz/foz* mice. However, in their current form these results are only correlative; they require additional (interventional)

experiments to validate and delineate the extent of pathway involvement. Furthermore, TLR2 deficiency has been shown to augment liver injury in MCD diet fed mice with NASH. Other studies involving nutritional depletion models (MCD, choline defined amino acid diet) models have implicated TLR4 and TLR9 in steatohepatitis pathogenesis (Gabele *et al.* 2011). Li *et al.* (2011b) have demonstrated that hepatocellular HMGB1 and TLR4 interactions are important in the activation of hepatic NF-κB p65. In this thesis, we have demonstrated that HMGB1 appears to be responsive to hepatic cholesterol content. Current experiments underway in the host laboratory are directed at determining whether TLR9, TLR4, and Myd88 knockout *foz/foz* mice develop NASH. Furthermore, bone marrow chimeras will be established to determine the extent of Kupffer cell *versus* hepatocyte involvement in NASH pathogenesis. It is anticipated that the results of these studies could delineate the pathogenic pathways of cholesterol-dependent necroinflammation in NASH. It is also worth emphasising again that while some pathways to liver injury in steatohepatitis are likely to be held in common by numerous aetiologies (alcohol, nutritional depletion, drug toxicity, metabolic syndrome) other may be specific or at least nuanced to specific causes. In this respect, JNK and NF-κB p65 activation appears essential in all types of steatohepatitis; and has been shown to be essential in MCD steatohepatitis (Dela Pena *et al.* 2005; Schattenberg *et al.* 2006) and occur in both human NASH and the *foz/foz* model. Others like the inflammasome (Csak *et al.* 2011a), oxidative stress (Leclercq *et al.* 2000; Robertson *et al.* 2001), and ER stress may be model-specific as they have not yet been faithfully recapitulated (to a convincing extent) in human NASH *versus* not NASH, and they do not appear to operate in obese diabetic *foz/foz* mice with NASH.

8.2.5 Alternative interventions to restitute cholesterol homeostasis in *foz/foz* mice with NASH

A major factor contributing to hepatic cholesterol accumulation in *foz/foz* mice with NASH appears to be suppression of cholesterol biotransformation and export pathways (see Chapter 3). Guggulsterone, a natural plant sterol derived from *Commiphora mukul* (colloquially known as Guggul tree), functions as an FXR agonist (Urizar *et al.* 2002). Guggul tree resin has been used as a traditional Indian medicine for the treatment of obesity and related hyperlipidemia (Dev 1997). In preliminary *in vitro* studies conducted by the candidate, primary murine hepatocytes were treated with either guggulsterone (4,17[20]-pregnadiene-3,16-dione) or the experimental FXR agonist,

GW4064 (3-[2,6-Dichlorophenyl]-4-[3-carboxy-2-chlorostilben-4-yl] oxymethyl-5-isopropylisoxazole) (Figure 8.2A). Guggulsterone significantly suppressed FXR protein expression, and correspondingly increased expression of Cyp7a1 mRNA and Bsep protein ($P<0.05$, Figure 8.2B,C). We are currently planning experiments involving guggulsterone administration in *foz/foz* mice following onset of NASH, using a similar treatment protocol to that described for atorvastatin and ezetimibe administration (detailed in Chapter 6). Further studies involving a combination of guggulsterone and ezetimibe treatment *in vivo* may also be useful. This combined treatment regime would be expected to decreased cholesterol uptake/reclamation (ezetimibe functioning) while promoting biotransformation and export of hepatic cholesterol fractions (guggulsterone functioning), thereby directed at the two major sites of disordered hepatic cholesterol homeostasis that were identified in the present work. Additional approaches that attempt to resolve insulin resistance while pharmacologically reversing disordered hepatic cholesterol accumulation might include a restrictive or nutritionally more optimal diet (no cholesterol, low saturated FA and simple sugar) as well as exercise.

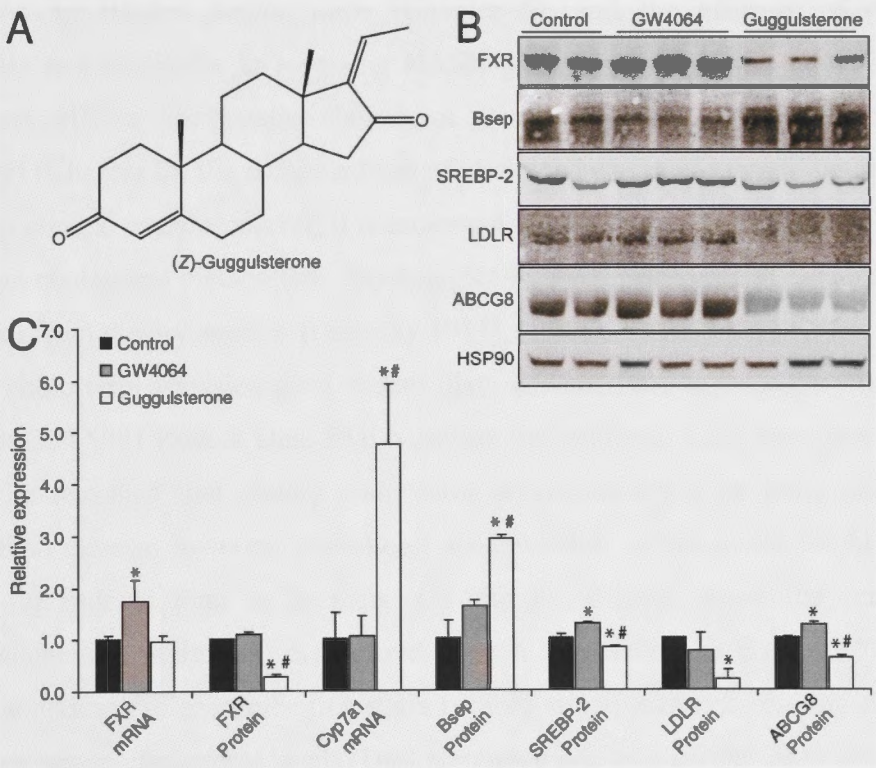

Figure 8.2 Guggulsterone differentially regulates pathways of cholesterol homeostasis in WT hepatocytes

Legend for Figure 8.2.

(**A**) Structure of guggulsterone (*Z*-geometric isomer shown). WT NOD.B10 hepatocytes were isolated and cultured from 8 week old female NOD.B10 mice (Section 2.13). Cells were exposed to GW4064, a FXR agonist (2 μM) and FXR antagonist guggulsterone (10 μM) for 30 h, and harvested for qPCR (Sections 2.7.5) and western blotting (Section 2.11). (**B**) Representative western blotting for bile salt exporter protein (Bsep), farnesoid X receptor (FXR), sterol responsive element binding protein (SREBP)-2, low density lipoprotein receptor (LDLR), ATP-binding cassette protein (ABC)-G8, and heat-shock protein (HSP)-90. (**C**) Quantified gene expression (relative) for FXR, Cyp7a1, Bsep, SREBP-2, LDLR, and ABCG8. Experiment was conducted in triplicate (n=3/treatment). Data are mean ± SEM. $^{*}P<0.05$, vs. control cells. $^{\#}P<0.05$, vs. GW4064-treated cells.

8.2.6 Combined statin and ezetimibe therapy: potential treatment for human NASH

As previously described (see Section 6.5), recent open studies have demonstrated the efficacy of ezetimibe treatment in improving NAFLD severity in humans, including lowered inflammation (Park *et al.* 2011) and (in one very small study) fibrosis (Yoneda *et al.* 2010). Given the extent to which cholesterol appears to mediate NASH progression in HF-fed *foz/foz* mice (Chapter 5), and the efficacy of combined atorvastatin and ezetimibe in reversing NASH pathogenesis in these mice (including both direct effects on hepatic cholesterol stores and indirect effects on insulin sensitivity) (Chapter 6), the combined use of statin and ezetimibe should be considered for human clinical trials. However, it is important to note the differences between rodent and human cholesterol metabolism. Physiologically, humans acquire greater amounts of cholesterol from dietary sources (Dietschy 1984), whereas rodents tend to biosynthesise required cholesterol (physiological rodent diets contain little to no cholesterol [~200 PPM, Lab Diet 5001 Rodent Diet, PMI Nutrition International, LLC, Brentwood, MO]). It could be reasoned that dietary cholesterol restriction might be more effective in humans than mice in lowering cholesterol accumulation, while statins might be more effective in rodents than in humans. On the other hand, ezetimibe (cholesterol uptake/reclamation inhibition) may prove to be more relevant in humans. It is worth noting that addition of ezetimibe to a statin is more effective than increasing statin dose at lowering serum cholesterol levels (Daskalopoulou and Mikhailidis 2006; Friedman *et al.* 2011). Further, combination statin and ezetimibe treatment was more effective at decreasing MCP-1 and TNF-α secretion from peripheral blood mononuclear cells of patients with insulin resistance (Krysiak and Okopien 2011). It is also important to note

that genetic causes of hypercholesterolemia are common and may contribute to NAFLD progression in humans (Arnett *et al.* 2005; Moutzouri *et al.* 2011). These factors further support investigation of the use of combined atorvastatin and ezetimibe treatment for NAFLD (Lioudaki *et al.* 2011).

8.3 Concluding remarks

There is increasing evidence to suggest that the progression of NAFLD to NASH occurs as a result of lipotoxic lipid accumulation in a steatotic liver, as opposed to two separate "hits" (Larter *et al.* 2010; Neuschwander-Tetri 2010a, 2010b; Fuchs and Sanyal 2011). Unfortunately, the complex interaction between metabolic syndrome and NAFLD progression, and lack of animal models that faithfully reflect both the pathophysiological determinants of human NASH (obesity, insulin resistance, metabolic syndrome, hypoadiponectinemia) and the appropriate pathology, has impeded the identification of the lipid species involved. These limitations may be partially overcome by use of the hyperphagic *foz/foz* mouse model of NASH (Larter and Yeh 2008), but HF-fed C57BL/6 also develop NASH without having an appetite regulation defect ((Ito *et al.* 2007); Larter *et al.*, unpublished data, 2009). In this thesis, we determined that insulin resistance which is a hallmark of NASH (Sanyal *et al.* 2001; Chitturi *et al.* 2002), is an important determinant of altered cholesterol metabolism in *foz/foz* with NASH. The mechanism involves high serum insulin concentrations that alter nuclear receptor expression to promote hepatic cholesterol accumulation. The effects of hepatic cholesterol accumulation were determined by loading *foz/foz* mouse livers with cholesterol, through dietary cholesterol manipulation. The severity of liver injury, cell death, inflammation, and fibrosis were largely reflective of hepatic cholesterol content and failed to correlate with other lipid species (TG, DAG, MAG, FFAs); these findings indicate that hepatic cholesterol does contribute to progression of NASH. Pharmacological inihibition of cholesterol biosynthesis and/or uptake/reclamation pathways lowered hepatic cholesterol content and improved overall liver pathology. Finally, analysis of mechanistic pathways for liver inflammation and cell death indicated that hepatic cholesterol activates JNK and NF-κB p65, most likely through pathways involving induction of HMGB1 which signals through TLR2/4. While not all of the pathways identified in this study are novel, our findings have reinforced previous observations of cholesterol lipotoxicity in animal models of NAFLD, and FC accumulation in human NASH livers. Further, they provide additional mechanistic data

to support the hypothesis that cholesterol acts as a "death-sterol" responsible for augmenting hepatic necroinflammation during NASH pathogenesis. Importantly, these pathways may constitute potential therapeutic targets for the treatment of human NASH.

In summary, lipotoxicity has long been suspected in NASH (Bass and Merriman 2007). The studies in this thesis have demonstrated that cholesterol is a key lipotoxic mediator in NASH pathogenesis, and have given insight into critical disease pathways and ways to interrupt them therapeutically.

References

Abel, T., Feher, J., Dinya, E., Eldin, M. G. and Kovacs, A. (2009). "Safety and efficacy of combined ezetimibe/simvastatin treatment and simvastatin monotherapy in patients with non-alcoholic fatty liver disease." *Med Sci Monit* **15**(12): MS6-11.

Abifadel, M., Varret, M., Rabes, J. P., Allard, D., Ouguerram, K., Devillers, M., Cruaud, C., Benjannet, S., Wickham, L., Erlich, D., Derre, A., Villeger, L., Farnier, M., Beucler, I., Bruckert, E., Chambaz, J., Chanu, B., Lecerf, J. M., Luc, G., Moulin, P., Weissenbach, J., Prat, A., Krempf, M., Junien, C., Seidah, N. G. and Boileau, C. (2003). "Mutations in PCSK9 cause autosomal dominant hypercholesterolemia." *Nat. Genet.* **34**(2): 154-156.

Abiru, S., Migita, K., Maeda, Y., Daikoku, M., Ito, M., Ohata, K., Nagaoka, S., Matsumoto, T., Takii, Y., Kusumoto, K., Nakamura, M., Komori, A., Yano, K., Yatsuhashi, H., Eguchi, K. and Ishibashi, H. (2006). "Serum cytokine and soluble cytokine receptor levels in patients with non-alcoholic steatohepatitis." *Liver Int.* **26**(1): 39-45.

Abrahamsson, A., Gustafsson, U., Ellis, E., Nilsson, L. M., Sahlin, S., Bjorkhem, I. and Einarsson, C. (2005). "Feedback regulation of bile acid synthesis in human liver: importance of HNF-4alpha for regulation of CYP7A1." *Biochem. Biophys. Res. Commun.* **330**(2): 395-399.

Adamson, S. and Leitinger, N. (2011). "Phenotypic modulation of macrophages in response to plaque lipids." *Curr. Opin. Lipidol.* **22**(5): 335-342.

Advani, T., Koek, W. and Hensler, J. G. (2009). "Gender differences in the enhanced vulnerability of BDNF+/- mice to mild stress." *Int. J. Neuropsychopharmacol.* **12**(5): 583-588.

Aggarwal, B. B. (2003). "Signalling pathways of the TNF superfamily: a double-edged sword." *Nat. Rev. Immunol.* **3**(9): 745-756.

Aghazadeh, S. and Yazdanparast, R. (2010). "Inhibition of JNK along with activation of ERK1/2 MAPK pathways improve steatohepatitis among the rats." *Clin. Nutr.* **29**(3): 381-385.

Ahlberg, J., Angelin, B., Bjorkhem, I., Einarsson, K. and Leijd, B. (1979). "Hepatic cholesterol metabolism in normo- and hyperlipidemic patients with cholesterol gallstones." *J. Lipid Res.* **20**(1): 107-115.

Akira, S., Uematsu, S. and Takeuchi, O. (2006). "Pathogen recognition and innate immunity." *Cell* **124**(4): 783-801.

Alberti, G., Zimmet, P., Shaw, J. and Grundy, S. M. (2006). The IDF consensus worldwide definition of metabolic syndrome. Brussels, IDF Communications.

Alberti, S., Schuster, G., Parini, P., Feltkamp, D., Diczfalusy, U., Rudling, M., Angelin, B., Bjorkhem, I., Pettersson, S. and Gustafsson, J. A. (2001). "Hepatic cholesterol metabolism and resistance to dietary cholesterol in LXRbeta-deficient mice." *J. Clin. Invest.* **107**(5): 565-573.

Alger, H. M., Brown, J. M., Sawyer, J. K., Kelley, K. L., Shah, R., Wilson, M. D., Willingham, M. C. and Rudel, L. L. (2010). "Inhibition of acyl-coenzyme A:cholesterol acyltransferase 2 (ACAT2) prevents dietary cholesterol-associated steatosis by enhancing hepatic triglyceride mobilization." *J. Biol. Chem.* **285**(19): 14267-14274.

Altmann, S. W., Davis Jr, H. R., Zhu, L., Yao, X., Hoos, L. M., Tetzloff, G., Iyer, S. P. N., Maguire, M., Golovko, A., Zheng, M., Wang, L., Murgolo, N. and Graziano, M. P. (2004). "Niemann-Pick C1 like 1 protein is critical for intestinal cholesterol absorption." *Science* **46**: 1034-1039.

Altschul, S. F., Gish, W., Miller, W., Myers, E. W. and Lipman, D. J. (1990). "Basic local alignment search tool." *J. Mol. Biol.* **215**(3): 403-410.

Anonymous (2004). "Clash of the statins? A trial pitting two popular statins against each other helps answer a far more important question: how low should cholesterol go?" *Harv. Heart Lett.* **14**(6): 5.

Aoudjit, F., Brochu, N., Belanger, B., Stratowa, C., Hiscott, J. and Audette, M. (1997). "Regulation of intercellular adhesion molecule-1 gene by tumor necrosis factor-alpha is mediated by the nuclear factor-kappaB heterodimers p65/p65 and p65/c-Rel in the absence of p50." *Cell Growth Differ.* **8**(3): 335-342.

Arito, M., Horiba, T., Hachimura, S., Inoue, J. and Sato, R. (2008). "Growth factor-induced phosphorylation of sterol regulatory element-binding proteins inhibits sumoylation, thereby stimulating the expression of their target genes, low density lipoprotein uptake, and lipid synthesis." *J. Biol. Chem.* **283**(22): 15224-15231.

Arsov, T. (2006). Genetic and phenotype analysis of Fat Aussie: a mouse model of Alström syndrome. *John Curtin School of Medical Research.* Canberra, Australian National University. **PhD:** 320.

Arsov, T., Larter, C. Z., Nolan, C. J., Petrovsky, N., Goodnow, C. C., Teoh, N. C., Yeh, M. M. and Farrell, G. C. (2006a). "Adaptive failure to high-fat diet characterizes steatohepatitis in Alms1 mutant mice." *Biochem. Biophys. Res. Commun.* **342**(4): 1152-1159.

Arsov, T., Silva, D. G., O'Bryan, M. K., Sainsbury, A., Lee, N. J., Kennedy, C., Manji, S. S., Nelms, K., Liu, C., Vinuesa, C. G., de Kretser, D. M., Goodnow, C. C. and Petrovsky, N. (2006b). "Fat aussie--a new Alstrom syndrome mouse showing a critical role for ALMS1 in obesity, diabetes, and spermatogenesis." *Mol. Endocrinol.* **20**(7): 1610-1622.

Avramoglu, R. K., Basciano, H. and Adeli, K. (2006). "Lipid and lipoprotein dysregulation in insulin resistant states." *Clin. Chim. Acta* **368**(1-2): 1-19.

Bader, T. (2010). "The myth of statin-induced hepatotoxicity." *Am. J. Gastroenterol.* **105**(5): 978-980.

Bahcecioglu, I. H., Yalniz, M., Ataseven, H., Ilhan, N., Ozercan, I. H., Seckin, D. and Sahin, K. (2005). "Levels of serum hyaluronic acid, TNF-alpha and IL-8 in patients with nonalcoholic steatohepatitis." *Hepatogastroenterology.* **52**(65): 1549-1553.

Baker, S. J. and Reddy, E. P. (1998). "Modulation of life and death by the TNF receptor superfamily." *Oncogene* **17**(25): 3261-3270.

Balasubramaniam, S., Goldstein, J. L. and Brown, M. S. (1977a). "Regulation of cholesterol synthesis in rat adrenal gland through coordinate control of 3-hydroxy-3-methylglutaryl coenzyme A synthase and reductase activities." *Proc. Natl. Acad. Sci. U. S. A.* **74**(4): 1421-1425.

Balasubramaniam, S., Goldstein, J. L., Faust, J. R., Brunschede, G. Y. and Brown, M. S. (1977b). "Lipoprotein-mediated regulation of 3-hydroxy-3-methylglutaryl coenzyme A reductase activity and cholesteryl ester metabolism in the adrenal gland of the rat." *J. Biol. Chem.* **252**(5): 1771-1779.

Ballantyne, C. M. (2008). *Clinical lipidology: a companion to Braunwald's heart disease*, Elsvier Health Sciences.

Bamberger, M. J. and Lane, M. D. (1988). "Assembly of very low density lipoprotein in the hepatocyte." *J. Biol. Chem.* **263**(24): 11868-11878.

Ban, J. O., Hwang, I. G., Kim, T. M., Hwang, B. Y., Lee, U. S., Jeong, H. S., Yoon, Y. W., Kimz, D. J. and Hong, J. T. (2007). "Anti-proliferate and pro-apoptotic effects of 2,3-dihydro-3,5-dihydroxy-6-methyl-4H-pyranone through inactivation of NF-kappaB in human colon cancer cells." *Arch. Pharmacal Res.* **30**(11): 1455-1463.

Bannerman, D. D., Erwert, R. D., Winn, R. K. and Harlan, J. M. (2002). "TIRAP mediates endotoxin-induced NF-kappaB activation and apoptosis in endothelial cells." *Biochem. Biophys. Res. Commun.* **295**(1): 157-162.

Bao, L., Li, Y., Deng, S. X., Landry, D. and Tabas, I. (2006). "Sitosterol-containing lipoproteins trigger free sterol-induced caspase-independent death in ACAT-competent macrophages." *J. Biol. Chem.* **281**(44): 33635-33649.

Barrasa, J. I., Olmo, N., Perez-Ramos, P., Santiago-Gomez, A., Lecona, E., Turnay, J. and Antonia Lizarbe, M. (2011). "Deoxycholic and chenodeoxycholic bile acids induce apoptosis via oxidative stress in human colon adenocarcinoma cells." *Apoptosis* **16**(10): 1054-1067.

Barton, G. M. and Medzhitov, R. (2003). "Toll-like receptor signaling pathways." *Science* **300**(5625): 1524-1525.

Bass, N. M. and Merriman, R. B. (2007). Fatty Acid Metabolism and Lipotoxicity in the Pathogenesis of NAFLD/NASH. *Fatty Liver Disease*, Blackwell Publishing Ltd: 109-122.

Bazin, R., Ricquier, D., Dupuy, F., Hoover-Plow, J. and Lavau, M. (1985). "Thermogenic and lipogenic activities in brown adipose tissue of I-strain mice." *Biochem. J.* **231**(3): 761-764.

Becker-Andre, M., Andre, E. and DeLamarter, J. F. (1993). "Identification of nuclear receptor mRNAs by RT-PCR amplification of conserved zinc-finger motif sequences." *Biochem. Biophys. Res. Commun.* **194**(3): 1371-1379.

Bellentani, S., Dalle Grave, R., Suppini, A. and Marchesini, G. (2008). "Behavior therapy for nonalcoholic fatty liver disease: The need for a multidisciplinary approach." *Hepatology* **47**(2): 746-754.

Bellentani, S. and Marino, M. (2009). "Epidemiology and natural history of non-alcoholic fatty liver disease (NAFLD)." *Ann. Hepatol.* **8 Suppl 1**: S4-8.

Bellentani, S., Scaglioni, F., Marino, M. and Bedogni, G. (2010). "Epidemiology of non-alcoholic fatty liver disease." *Dig. Dis.* **28**(1): 155-161.

Beltroy, E. P., Liu, B., Dietschy, J. M. and Turley, S. D. (2007). "Lysosomal unesterified cholesterol content correlates with liver cell death in murine Niemann-Pick type C disease." *J. Lipid Res.* **48**(4): 869-881.

Benedetti, A., Alvaro, D., Bassotti, C., Gigliozzi, A., Ferretti, G., La Rosa, T., Di Sario, A., Baiocchi, L. and Jezequel, A. M. (1997). "Cytotoxicity of bile salts against biliary epithelium: a study in isolated bile ductule fragments and isolated perfused rat liver." *Hepatology* **26**(1): 9-21.

Berge, K. E., Tian, H., Graf, G. A., Yu, L., Grishin, N. V., Schultz, J., Kwiterovich, P., Shan, B., Barnes, R. and Hobbs, H. H. (2000). "Accumulation of dietary cholesterol in sitosterolemia caused by mutations in adjacent ABC transporters." *Science* **290**: 1771-1777.

Berry, M. N., Grivell, A. R., Grivell, M. B. and Phillips, J. W. (1997). "Isolated hepatocytes--past, present and future." *Cell Biol. Toxicol.* **13**(4-5): 223-233.

Bieghs, V., Wouters, K., van Gorp, P. J., Gijbels, M. J., de Winther, M. P., Binder, C. J., Lutjohann, D., Febbraio, M., Moore, K. J., van Bilsen, M., Hofker, M. H. and Shiri-Sverdlov, R. (2010). "Role of scavenger receptor A and CD36 in

diet-induced nonalcoholic steatohepatitis in hyperlipidemic mice." *Gastroenterology* **138**(7): 2477-2486, 2486 e2471-2473.

Birbach, A., Gold, P., Binder, B. R., Hofer, E., de Martin, R. and Schmid, J. A. (2002). "Signaling molecules of the NF-kappa B pathway shuttle constitutively between cytoplasm and nucleus." *J. Biol. Chem.* **277**(13): 10842-10851.

Birch, N. C., Radio, S. and Horslen, S. (2003). "Metastatic hepatocellular carcinoma in a patient with niemann-pick disease, type C." *J. Pediatr. Gastroenterol. Nutr.* **37**(5): 624-626.

Bischoff, E. D., Daige, C. L., Petrowski, M., Dedman, H., Pattison, J., Juliano, J., Li, A. C. and Schulman, I. G. (2010). "Non-redundant roles for LXRalpha and LXRbeta in atherosclerosis susceptibility in low density lipoprotein receptor knockout mice." *J. Lipid Res.* **51**(5): 900-906.

Blann, A. D., Faragher, E. B. and McCollum, C. N. (1997). "Increased soluble P-selectin following myocardial infarction: a new marker for the progression of atherosclerosis." *Blood Coagul. Fibrinolysis* **8**(7): 383-390.

Bloch, K. (1965). "The biological synthesis of cholesterol." *Science* **150**: 19-28.

Blom, T., Back, N., Mutka, A. L., Bittman, R., Li, Z., de Lera, A., Kovanen, P. T., Diczfalusy, U. and Ikonen, E. (2010). "FTY720 stimulates 27-hydroxycholesterol production and confers atheroprotective effects in human primary macrophages." *Circ. Res.* **106**(4): 720-729.

Bobard, A., Hainault, I., Ferre, P., Foufelle, F. and Bossard, P. (2005). "Differential regulation of sterol regulatory element-binding protein 1c transcriptional activity by insulin and liver X receptor during liver development." *J. Biol. Chem.* **280**(1): 199-206.

Bohan, A., Chen, W. S., Denson, L. A., Held, M. A. and Boyer, J. L. (2003). "Tumor necrosis factor alpha-dependent up-regulation of Lrh-1 and Mrp3(Abcc3) reduces liver injury in obstructive cholestasis." *J. Biol. Chem.* **278**(38): 36688-36698.

Bonilla, M., Nastase, K. K. and Cunningham, K. W. (2002). "Essential role of calcineurin in response to endoplasmic reticulum stress." *EMBO J.* **21**(10): 2343-2353.

Bonvicini, F., Gautier, A., Gardiol, D. and Borel, G. A. (1978). "Cholesterol in acute cholestasis induced by taurolithocholic acid. A cytochemical study in transmission and scanning electron microscopy." *Lab. Invest.* **38**(4): 487-495.

Botteron, C. and Dobbelaere, D. (1998). "AP-1 and ATF-2 are constitutively activated via the JNK pathway in Theileria parva-transformed T-cells." *Biochem. Biophys. Res. Commun.* **246**(2): 418-421.

Bowden, K. and Ridgway, N. D. (2008). "OSBP negatively regulates ABCA1 protein stability." *J. Biol. Chem.* **283**(26): 18210-18217.

Bramlett, K. S., Yao, S. and Burris, T. P. (2000). "Correlation of farnesoid X receptor coactivator recruitment and cholesterol 7alpha-hydroxylase gene repression by bile acids." *Mol. Genet. Metab.* **71**(4): 609-615.

Brand, K., Eisele, T., Kreusel, U., Page, M., Page, S., Haas, M., Gerling, A., Kaltschmidt, C., Neumann, F. J., Mackman, N., Baeurele, P. A., Walli, A. K. and Neumeier, D. (1997). "Dysregulation of monocytic nuclear factor-kappa B by oxidized low-density lipoprotein." *Arterioscler. Thromb. Vasc. Biol.* **17**(10): 1901-1909.

Brown, A., Wiggins, D. and Gibbons, G. F. (1999). "Manipulation of cholesterol and cholesteryl ester synthesis has multiple effects on the metabolism of apolipoprotein B and the secretion of very-low-density lipoprotein by primary hepatocyte cultures." *Biochim. Biophys. Acta* **1440**(2-3): 253-265.

Brown, A. M. and Gibbons, G. F. (1997). "The effect of ACAT inhibition on VLDL secretion in rats fed a diet rich in fish-oil." *Biochem. Soc. Trans.* **25**(4): S688.

Brown, M. S., Anderson, R. G. W. and Goldstein, J. L. (1983). "Recycling receptors: the round-trip itinerary of migrant membrane proteins." *Cell* **32**: 663-667.

Brown, M. S. and Goldstein, J. L. (1997). "The SREBP pathway: regulation of cholesterol metabolism by proteolysis of a membrane-bound transcription factor." *Cell* **89**: 331-340.

Brown, M. S., Goldstein, J. L. and Siperstein, M. D. (1973). "Regulation of cholesterol synthesis in normal and malignant tissue." *Fed. Proc.* **32**(12): 2168-2173.

Browning, J. D. and Horton, J. D. (2004). "Molecular mediators of hepatic steatosis and liver injury." *J. Clin. Invest.* **114**(2): 147-152.

Browning, J. D., Szczepaniak, L. S., Dobbins, R., Nuremberg, P., Horton, J. D., Cohen, J. C., Grundy, S. M. and Hobbs, H. H. (2004). "Prevalence of hepatic steatosis in an urban population in the United States: impact of ethnicity." *Hepatology* **40**(6): 1387-1395.

Brunt, E. M. (2004). "Nonalcoholic steatohepatitis." *Semin. Liver Dis.* **24**(1): 3-20.

Brunt, E. M., Neuschwander-Tetri, B. A., Oliver, D., Wehmeier, K. R. and Bacon, B. R. (2004). "Nonalcoholic steatohepatitis: histologic features and clinical correlations with 30 blinded biopsy specimens." *Hum. Pathol.* **35**(9): 1070-1082.

Burnett, J. R. and Hooper, A. J. (2008). "Common and rare gene variants affecting plasma LDL cholesterol." *Clin Biochem Rev* **29**(1): 11-26.

Burnett, J. R., Wilcox, L. J., Telford, D. E., Kleinstiver, S. J., Barrett, P. H., Newton, R. S. and Huff, M. W. (1999). "Inhibition of ACAT by avasimibe decreases both VLDL and LDL apolipoprotein B production in miniature pigs." *J. Lipid Res.* **40**(7): 1317-1327.

Caballero, F., Bataller, R., Lacy, A., Fernandez-Checa, J. C., Caballeria, J. and Garcia-Ruiz, C. (2009). "Enhanced free cholesterol, SREBP-2 and StAR expression in human NASH." *J. Hepatol.* **50**: 789-796.

Caccamo, G., Bonura, F., Vitale, G., Novo, G., Evola, S., Evola, G., Grisanti, M. R. and Novo, S. (2010). "Insulin resistance and acute coronary syndrome." *Atherosclerosis* **211**(2): 672-675.

Cagen, L. M., Deng, X., Wilcox, H. G., Park, E. A., Raghow, R. and Elam, M. B. (2005). "Insulin activates the rat sterol-regulatory-element-binding protein 1c (SREBP-1c) promoter through the combinatorial actions of SREBP, LXR, Sp-1 and NF-Y cis-acting elements." *Biochem. J.* **385**(Pt 1): 207-216.

Caldwell, S. H., de Freitas, L. A., Park, S. H., Moreno, M. L., Redick, J. A., Davis, C. A., Sisson, B. J., Patrie, J. T., Cotrim, H., Argo, C. K. and Al-Osaimi, A. (2009). "Intramitochondrial crystalline inclusions in nonalcoholic steatohepatitis." *Hepatology* **49**(6): 1888-1895.

Calisto, K. L., Carvalho Bde, M., Ropelle, E. R., Mittestainer, F. C., Camacho, A. C., Guadagnini, D., Carvalheira, J. B. and Saad, M. J. (2010). "Atorvastatin improves survival in septic rats: effect on tissue inflammatory pathway and on insulin signaling." *PLoS ONE* **5**(12): e14232.

Cason, C. (2004). Persistence of Vision Raytracer. Williamstown, Victoria, Australia.

Caspersen, C., Pedersen, P. S. and Treiman, M. (2000). "The sarco/endoplasmic reticulum calcium-ATPase 2b is an endoplasmic reticulum stress-inducible protein." *J. Biol. Chem.* **275**(29): 22363-22372.

Celis, J. E., Lauridsen, J. B. and Basse, B. (1994). Determination of antibody specificity by Western blotting and immunoprecipitation. *Cell Biology: A laboratory handbook*. Celis, J. E. New York, Academic Press. **2:** 305-313.

Chamaillard, M., Girardin, S. E., Viala, J. and Philpott, D. J. (2003). "Nods, Nalps and Naip: intracellular regulators of bacterial-induced inflammation." *Cell. Microbiol.* **5**(9): 581-592.

Chang, C. C. Y., Sakashita, N., Ornvold, K., Lee, O., Chang, E. T., Dong, R., Lin, S., Lee, C. Y. G., Strom, S., Kashyap, R., Fung, J., Farese Jr., R. V., Patoiseau, J. F., Delhon, A. and Chang, T. Y. (2000). "Immunological quantitation and localization of ACAT-1 and ACAT-2 in human liver and small intestine." *J. Biol. Chem.* **275**: 28083-28092.

Charman, M., Kennedy, B. E., Osborne, N. and Karten, B. (2010). "MLN64 mediates egress of cholesterol from endosomes to mitochondria in the absence of functional Niemann-Pick Type C1 protein." *J. Lipid Res.* **51**(5): 1023-1034.

Chaya, D., Fougere-Deschatrette, C. and Weiss, M. C. (1997). "Liver-enriched transcription factors uncoupled from expression of hepatic functions in hepatoma cell lines." *Mol. Cell. Biol.* **17**(11): 6311-6320.

Chazotte, B. (1994). "Comparisons of the relative effects of polyhydroxyl compounds on local versus long-range motions in the mitochondrial inner membrane. Fluorescence recovery after photobleaching, fluorescence lifetime, and fluorescence anisotropy studies." *Biochim. Biophys. Acta* **1194**(2): 315-328.

Chen, C., Mireles, R. J., Campbell, S. D., Lin, J., Mills, J. B., Xu, J. J. and Smolarek, T. A. (2005). "Differential interaction of 3-hydroxy-3-methylglutaryl-coa reductase inhibitors with ABCB1, ABCC2, and OATP1B1." *Drug Metab. Dispos.* **33**(4): 537-546.

Chen, G., Izzo, J., Demizu, Y., Wang, F., Guha, S., Wu, X., Hung, M. C., Ajani, J. A. and Huang, P. (2009). "Different redox states in malignant and nonmalignant esophageal epithelial cells and differential cytotoxic responses to bile acid and honokiol." *Antioxid. Redox Signaling* **11**(5): 1083-1095.

Chen, M., Wang, H., Chen, W. and Meng, G. (2011). "Regulation of adaptive immunity by the NLRP3 inflammasome." *Int. Immunopharmacol.* **11**(5): 549-554.

Chen, W. and Chiang, J. Y. (2003). "Regulation of human sterol 27-hydroxylase gene (CYP27A1) by bile acids and hepatocyte nuclear factor 4alpha (HNF4alpha)." *Gene* **313**: 71-82.

Cheung, O., Puri, P., Eicken, C., Contos, M. J., Mirshahi, F., Maher, J. W., Kellum, J. M., Min, H., Luketic, V. A. and Sanyal, A. J. (2008). "Nonalcoholic steatohepatitis is associated with altered hepatic MicroRNA expression." *Hepatology* **48**(6): 1810-1820.

Chiang, J. Y., Kimmel, R. and Stroup, D. (2001). "Regulation of cholesterol 7alpha-hydroxylase gene (CYP7A1) transcription by the liver orphan receptor (LXRalpha)." *Gene* **262**(1-2): 257-265.

Chien, K. L., Liau, C. S., Chen, M. F., Lee, Y. T., Jeng, J. S., Hwang, B. S. and Su, T. C. (2008). "Primary hypercholesterolemia, carotid atherosclerosis and insulin resistance among Chinese." *Lipids* **43**(2): 117-124.

Childs, S., Yeh, R. L., Georges, E. and Ling, V. (1995). "Identification of a sister gene to P-glycoprotein." *Cancer Res.* **55**: 2029-2034.

Chitturi, S., Abeygunasekera, S., Farrell, G. C., Holmes-Walker, J., Hui, J. M., Fung, C., Karim, R., Lin, R., Samarasinghe, D., Liddle, C., Weltman, M. and George, J. (2002). "NASH and insulin resistance: Insulin hypersecretion

and specific association with the insulin resistance syndrome." *Hepatology* **35**(2): 373-379.

Chitturi, S. and Farrell, G. C. (2007). Drug induced liver disease. *Schiff's diseases of the liver*. Schiff, E. R., Sorrell, M. F. and Maddrey, W. C. New York, Lippincott Williams and Wilkins. **10th edn.:** 923-1004.

Chitturi, S., Farrell, G. C., Hashimoto, E., Saibara, T., Lau, G. K. and Sollano, J. D. (2007). "Non-alcoholic fatty liver disease in the Asia-Pacific region: definitions and overview of proposed guidelines." *J. Gastroenterol. Hepatol.* **22**(6): 778-787.

Chitturi, S., Wong, V. W. and Farrell, G. (2011). "Nonalcoholic fatty liver in Asia: Firmly entrenched and rapidly gaining ground." *J. Gastroenterol. Hepatol.* **26 Suppl 1**: 163-172.

Chomczynski, P. and Sacchi, N. (2006). "The single-step method of RNA isolation by acid guanidinium thiocyanate-phenol-chloroform extraction: twenty-something years on." *Nat. Protoc.* **1**(2): 581-585.

Clark, R. A. and Valente, A. J. (2004). "Nuclear factor kappa B activation by NADPH oxidases." *Mech. Ageing Dev.* **125**(10-11): 799-810.

Clarke, R. M., O'Connell, F., Lyons, A. and Lynch, M. A. (2007). "The HMG-CoA reductase inhibitor, atorvastatin, attenuates the effects of acute administration of amyloid-beta1-42 in the rat hippocampus in vivo." *Neuropharmacology* **52**(1): 136-145.

Clayton, D. F. and Darnell, J. E., Jr. (1983). "Changes in liver-specific compared to common gene transcription during primary culture of mouse hepatocytes." *Mol. Cell. Biol.* **3**(9): 1552-1561.

Clement, J. (1976). "[Digestion and absorption of dietary triglycerides]." *J. Physiol. (Paris)* **72**(2): 137-170.

Coenen, K. R. and Hasty, A. H. (2007). "Obesity potentiates development of fatty liver and insulin resistance, but not atherosclerosis, in high-fat diet-fed agouti LDLR-deficient mice." *Am. J. Physiol. Endocrinol. Metab.* **293**(2): E492-499.

Cohen, D. E. (1999). "Hepatocellular transport and secretion of biliary lipids." *Curr. Opin. Lipidol.* **10**(4): 295-302.

Cohen, J., Pertsemlidis, A., Kotowski, I. K., Graham, R., Garcia, C. K. and Hobbs, H. H. (2005). "Low LDL cholesterol in individuals of African descent resulting from frequent nonsense mutations in PCSK9." *Nat. Genet.* **37**(2): 161-165.

Collin, G. B., Cyr, E., Bronson, R., Marshall, J. D., Gifford, E. J., Hicks, W., Murray, S. A., Zheng, Q. Y., Smith, R. S., Nishina, P. M. and Naggert, J. K. (2005). "Alms1-disrupted mice recapitulate human Alstrom syndrome." *Hum. Mol. Genet.* **14**(16): 2323-2333.

Collin, G. B., Marshall, J. D., Ikeda, A., So, W. V., Russell-Eggitt, I., Maffei, P., Beck, S., Boerkoel, C. F., Sicolo, N., Martin, M., Nishina, P. M. and Naggert, J. K. (2002). "Mutations in ALMS1 cause obesity, type 2 diabetes and neurosensory degeneration in Alstrom syndrome." *Nat. Genet.* **31**(1): 74-78.

Cooper, A. D. and Yu, P. Y. (1978). "Rates of removal and degradation of chylomicron remnants by isolated perfused rat liver." *J. Lipid Res.* **19**(5): 635-643.

Cortez-Pinto, H., Baptista, A., Camilo, M. E. and de Moura, M. C. (2001). "Hepatic stellate cell activation occurs in nonalcoholic steatohepatitis." *Hepatogastroenterology.* **48**(37): 87-90.

Corton, J. M., Gillespie, J. G. and Hardie, D. G. (1994). "Role of the AMP-activated protein kinase in the cellular stress response." *Curr. Biol.* **4**: 315-324.

Costet, P., Cariou, B., Lambert, G., Lalanne, F., Lardeux, B., Jarnoux, A. L., Grefhorst, A., Staels, B. and Krempf, M. (2006). "Hepatic PCSK9 expression is regulated by nutritional status via insulin and sterol regulatory element-binding protein 1c." *J. Biol. Chem.* **281**(10): 6211-6218.

Cowled, P. A., Khanna, A., Laws, P. E., Field, J. B., Varelias, A. and Fitridge, R. A. (2007). "Statins inhibit neutrophil infiltration in skeletal muscle reperfusion injury." *J. Surg. Res.* **141**(2): 267-276.

Cryer, A. (1981). "Tissue lipoprotein lipase activity and its action in lipoprotein metabolism." *Int. J. Biochem.* **13**: 525-541.

Csak, T., Ganz, M., Pespisa, J., Kodys, K., Dolganiuc, A. and Szabo, G. (2011a). "Fatty acids and endotoxin activate inflammasome in hepatocytes which release danger signals to activate immune cells in steatohepatitis." *Hepatology.*

Csak, T., Velayudham, A., Hritz, I., Petrasek, J., Levin, I., Lippai, D., Catalano, D., Mandrekar, P., Dolganiuc, A., Kurt-Jones, E. and Szabo, G. (2011b). "Deficiency in myeloid differentiation factor-2 and Toll-like receptor 4 expression attenuates non-alcoholic steatohepatitis and fibrosis in mice." *Am. J. Physiol. Gastrointest. Liver Physiol.*

Cuenda, A. and Dorow, D. S. (1998). "Differential activation of stress-activated protein kinase kinases SKK4/MKK7 and SKK1/MKK4 by the mixed-lineage kinase-2 and mitogen-activated protein kinase kinase (MKK) kinase-1." *Biochem. J.* **333 (Pt 1)**: 11-15.

Czaja, M. J. (2011). "Functions of autophagy in hepatic and pancreatic physiology and disease." *Gastroenterology* **140**(7): 1895-1908.

Dai, J., Megjugorac, N. J., Amrute, S. B. and Fitzgerald-Bocarsly, P. (2004). "Regulation of IFN regulatory factor-7 and IFN-alpha production by enveloped virus and lipopolysaccharide in human plasmacytoid dendritic cells." *J. Immunol.* **173**(3): 1535-1548.

Dara, L., Ji, C. and Kaplowitz, N. (2011). "The contribution of endoplasmic reticulum stress to liver diseases." *Hepatology* **53**(5): 1752-1763.

Daskalopoulou, S. S. and Mikhailidis, D. P. (2006). "Reaching goal in hypercholesterolaemia: dual inhibition of cholesterol synthesis and absorption with simvastatin plus ezetimibe." *Curr. Med. Res. Opin.* **22**(3): 511-528.

Davies, J. P., Levy, B. and Ioannou, Y. A. (2000). "Evidence for a Niemann-pick C (NPC) gene family: identification and characterization of NPC1L1." *Genomics* **65**(2): 137-145.

Davies, J. P., Scott, C., Oishi, K., Liapis, A. and Ioannou, Y. A. (2005). "Inactivation of NPC1L1 causes multiple lipid transport defects and protects against diet-induced hypercholesterolemia." *J. Biol. Chem.* **280**(13): 12710-12720.

Davis, G. C., Elhammer, A., Russell, D. W., Schneider, W. J., Kornfeld, S., Brown, M. S. and Goldstein, J. L. (1986). "Deletion of clustered *O*-linked carbohydrates does not impair function of low density lipoprotein receptor in transfected fibroblasts." *J. Biol. Chem.* **261**(6): 2828-2838.

Day, C. P. (2002). "NASH-related liver failure: one hit too many?" *Am. J. Gastroenterol.* **97**(8): 1872-1874.

Day, C. P. and James, O. F. (1998). "Steatohepatitis: a tale of two "hits"?" *Gastroenterology* **114**(4): 842-845.

De La Iglesia, F. A. and Porta, E. A. (1967). "Ciliated biliary epithelial cells in the livers of non-human primates." *Experientia* **23**(1): 49-51.

Deacon, K. and Blank, J. L. (1997). "Characterization of the mitogen-activated protein kinase kinase 4 (MKK4)/c-Jun NH2-terminal kinase 1 and MKK3/p38 pathways

regulated by MEK kinases 2 and 3. MEK kinase 3 activates MKK3 but does not cause activation of p38 kinase in vivo." *J. Biol. Chem.* **272**(22): 14489-14496.

DeFronzo, R. A. (2010). "Insulin resistance, lipotoxicity, type 2 diabetes and atherosclerosis: the missing links. The Claude Bernard Lecture 2009." *Diabetologia* **53**(7): 1270-1287.

del Castillo-Olivares, A. and Gil, G. (2000a). "Alpha 1-fetoprotein transcription factor is required for the expression of sterol 12alpha -hydroxylase, the specific enzyme for cholic acid synthesis. Potential role in the bile acid-mediated regulation of gene transcription." *J. Biol. Chem.* **275**(23): 17793-17799.

del Castillo-Olivares, A. and Gil, G. (2000b). "Role of FXR and FTF in bile acid-mediated suppression of cholesterol 7alpha-hydroxylase transcription." *Nucleic Acids Res.* **28**(18): 3587-3593.

Dela Pena, A., Leclercq, I., Field, J., George, J., Jones, B. and Farrell, G. (2005). "NF-kappaB activation, rather than TNF, mediates hepatic inflammation in a murine dietary model of steatohepatitis." *Gastroenterology* **129**(5): 1663-1674.

Deng, Q. G., She, H., Cheng, J. H., French, S. W., Koop, D. R., Xiong, S. and Tsukamoto, H. (2005). "Steatohepatitis induced by intragastric overfeeding in mice." *Hepatology* **42**(4): 905-914.

Deng, R., Yang, D., Yang, J. and Yan, B. (2006). "Oxysterol 22(R)-hydroxycholesterol induces the expression of the bile salt export pump through nuclear receptor farsenoid X receptor but not liver X receptor." *J. Pharmacol. Exp. Ther.* **317**(1): 317-325.

Deng, X., Xiao, L., Lang, W., Gao, F., Ruvolo, P. and May, W. S., Jr. (2001). "Novel role for JNK as a stress-activated Bcl2 kinase." *J. Biol. Chem.* **276**(26): 23681-23688.

Deng, Y., Ren, X., Yang, L., Lin, Y. and Wu, X. (2003). "A JNK-dependent pathway is required for TNFalpha-induced apoptosis." *Cell* **115**(1): 61-70.

Denis, M., Haidar, B., Marcil, M., Bouvier, M., Krimbou, L. and Genest, J. (2004a). "Characterization of oligomeric human ATP binding cassette transporter A1." *J. Biol. Chem.* **279**(40): 41529-41536.

Denis, M., Haidar, B., Marcil, M., Bouvier, M., Krimbou, L. and Genest, J., Jr. (2004b). "Molecular and cellular physiology of apolipoprotein A-I lipidation by the ATP-binding cassette transporter A1 (ABCA1)." *J. Biol. Chem.* **279**(9): 7384-7394.

Depuydt, B., van Loo, G., Vandenabeele, P. and Declercq, W. (2005). "Induction of apoptosis by TNF receptor 2 in a T-cell hybridoma is FADD dependent and blocked by caspase-8 inhibitors." *J. Cell Sci.* **118**(Pt 3): 497-504.

Deushi, M., Nomura, M., Kawakami, A., Haraguchi, M., Ito, M., Okazaki, M., Ishii, H. and Yoshida, M. (2007). "Ezetimibe improves liver steatosis and insulin resistance in obese rat model of metabolic syndrome." *FEBS Lett.* **581**(29): 5664-5670.

Dev, S. (1997). "Ethnotherapeutics and modern drug development: the potential of ayurveda." *Curr. Sci.* **73**(11): 909-928.

Devries-Seimon, T., Li, Y., Yao, P. M., Stone, E., Wang, Y., Davis, R. J., Flavell, R. and Tabas, I. (2005). "Cholesterol-induced macrophage apoptosis requires ER stress pathways and engagement of the type A scavenger receptor." *J. Cell Biol.* **171**(1): 61-73.

Diehl, A. M., Li, Z. P., Lin, H. Z. and Yang, S. Q. (2005). "Cytokines and the pathogenesis of non-alcoholic steatohepatitis." *Gut* **54**(2): 303-306.

Dietschy, J. M. (1984). "Regulation of cholesterol metabolism in man and in other species." *Klin. Wochenschr.* **62**(8): 338-345.

Dietschy, J. M., Turley, S. D. and Spady, D. K. (1993). "Role of liver in the maintenance of cholesterol and low density lipoprotein homeostasis in different animal species, including humans." *J. Lipid Res.* **34**(10): 1637-1659.

Dif, N., Euthine, V., Gonnet, E., Laville, M., Vidal, H. and Lefai, E. (2006). "Insulin activates human sterol-regulatory-element-binding protein-1c (SREBP-1c) promoter through SRE motifs." *Biochem. J.* **400**(1): 179-188.

Duewell, P., Kono, H., Rayner, K. J., Sirois, C. M., Vladimer, G., Bauernfeind, F. G., Abela, G. S., Franchi, L., Nunez, G., Schnurr, M., Espevik, T., Lien, E., Fitzgerald, K. A., Rock, K. L., Moore, K. J., Wright, S. D., Hornung, V. and Latz, E. (2010). "NLRP3 inflammasomes are required for atherogenesis and activated by cholesterol crystals." *Nature* **464**(7293): 1357-1361.

Dunne, A. (2011). "Inflammasome activation: from inflammatory disease to infection." *Biochem. Soc. Trans.* **39**(2): 669-673.

Duran-Sandoval, D., Mautino, G., Martin, G., Percevault, F., Barbier, O., Fruchart, J. C., Kuipers, F. and Staels, B. (2004). "Glucose regulates the expression of the farnesoid X receptor in liver." *Diabetes* **53**(4): 890-898.

Eberle, D., Hegarty, B., Bossard, P., Ferre, P. and Foufelle, F. (2004). "SREBP transcription factors: master regulators of lipid homeostasis." *Biochimie* **86**(11): 839-848.

Edwards, P. A., Tabor, D., Kast, H. R. and Venkateswaran, A. (2000). "Regulation of gene expression by SREBP and SCAP." *Biochim. Biophys. Acta* **1529**(1-3): 103-113.

Ehehalt, R., Jochims, C., Lehmann, W. D., Erben, G., Staffer, S., Reininger, C. and Stremmel, W. (2004). "Evidence of luminal phosphatidylcholine secretion in rat ileum." *Biochim. Biophys. Acta* **1682**(1-3): 63-71.

Endemann, G., Stanton, L. W., Madden, K. S., Bryant, C. M., White, R. T. and Protter, A. A. (1993). "CD36 is a receptor for oxidized low density lipoprotein." *J. Biol. Chem.* **268**(16): 11811-11816.

Enjoji, M., Machida, K., Kohjima, M., Kato, M., Kotoh, K., Matsunaga, K., Nakashima, M. and Nakamuta, M. (2010). "NPC1L1 inhibitor ezetimibe is a reliable therapeutic agent for non-obese patients with nonalcoholic fatty liver disease." *Lipids Health Dis.* **9**: 29.

Enjoji, M. and Nakamuta, M. (2010). "Is the control of dietary cholesterol intake sufficiently effective to ameliorate nonalcoholic fatty liver disease?" *World J. Gastroenterol.* **16**(7): 800-803.

Ericsson, J., Jackson, S. M., Lee, B. C. and Edwards, P. A. (1996). "Sterol regulatory element binding protein binds to a cis element in the promoter of the farnesyl diphosphate synthase gene." *Proc. Natl. Acad. Sci. U. S. A.* **93**(2): 945-950.

Fan, J. G., Xu, Z. J., Wang, G. L., Ding, X. D., Tian, L. Y. and Zheng, X. Y. (2003). "[Change of serum endotoxin level in the progress of nonalcoholic steatohepatitis in rats]." *Zhonghua Gan Zang Bing Za Zhi* **11**(2): 73-76.

Farrell, G. C. and Larter, C. Z. (2006). "Nonalcoholic fatty liver disease: from steatosis to cirrhosis." *Hepatology* **43**(2 Suppl 1): S99-S112.

Farrell, G. C., Larter, C. Z., Hou, J. Y., Zhang, R. H., Yeh, M. M., Williams, J., dela Pena, A., Francisco, R., Osvath, S. R., Brooling, J., Teoh, N. and Sedger, L. M. (2009). "Apoptosis in experimental NASH is associated with p53 activation and TRAIL receptor expression." *J. Gastroenterol. Hepatol.* **24**(3): 443-452.

Farrell, G. C., Teoh, N. C. and McCuskey, R. S. (2008). "Hepatic microcirculation in fatty liver disease." *Anat Rec (Hoboken)* **291**(6): 684-692.

Fayard, E., Auwerx, J. and Schoonjans, K. (2004). "LRH-1: an orphan nuclear receptor involved in development, metabolism and steroidogenesis." *Trends Cell Biol.* **14**(5): 250-260.

Feldstein, A. E., Canbay, A., Angulo, P., Taniai, M., Burgart, L. J., Lindor, K. D. and Gores, G. J. (2003). "Hepatocyte apoptosis and fas expression are prominent features of human nonalcoholic steatohepatitis." *Gastroenterology* **125**(2): 437-443.

Ferdinandusse, S. and Houten, S. M. (2006). "Peroxisomes and bile acid biosynthesis." *Biochim. Biophys. Acta* **1763**: 1427-1440.

Fernandez, A., Llacuna, L., Fernandez-Checa, J. C. and Colell, A. (2009). "Mitochondrial cholesterol loading exacerbates amyloid beta peptide-induced inflammation and neurotoxicity." *J. Neurosci.* **29**(20): 6394-6405.

Ferreira, D. M., Castro, R. E., Machado, M. V., Evangelista, T., Silvestre, A., Costa, A., Coutinho, J., Carepa, F., Cortez-Pinto, H. and Rodrigues, C. M. (2011). "Apoptosis and insulin resistance in liver and peripheral tissues of morbidly obese patients is associated with different stages of non-alcoholic fatty liver disease." *Diabetologia* **54**(7): 1788-1798.

Field, F. J., Born, E., Murthy, S. and Mathur, S. N. (2001a). "Gene expression of sterol regulatory element-binding proteins in hamster small intestine." *J. Lipid Res.* **42**(1): 1-8.

Field, F. J., Born, E., Murthy, S. and Mathur, S. N. (2001b). "Regulation of sterol regulatory element-binding proteins in hamster intestine by changes in cholesterol flux." *J. Biol. Chem.* **276**(20): 17576-17583.

Field, F. J. and Mathur, S. N. (1983). "Regulation of acyl CoA:cholesterol acyltransferase by 25-hydroxycholesterol in rabbit intestinal microsomes and absorptive cells." *J. Lipid Res.* **24**(8): 1049-1059.

Fielding, C. J. and Fielding, P. E. (1995). "Molecular physiology of reverse cholesterol transport." *J. Lipid Res.* **36**: 211-228.

Fisher, E. A. and Ginsberg, H. N. (2002). "Complexity in the secretory pathway: the assembly and secretion of apolipoprotein B-containing lipoproteins." *J. Biol. Chem.* **277**: 17377-17380.

Fitzgerald, K. A., Palsson-McDermott, E. M., Bowie, A. G., Jefferies, C. A., Mansell, A. S., Brady, G., Brint, E., Dunne, A., Gray, P., Harte, M. T., McMurray, D., Smith, D. E., Sims, J. E., Bird, T. A. and O'Neill, L. A. (2001). "Mal (MyD88-adapter-like) is required for Toll-like receptor-4 signal transduction." *Nature* **413**(6851): 78-83.

Folli, F., Saad, M. J., Backer, J. M. and Kahn, C. R. (1993). "Regulation of phosphatidylinositol 3-kinase activity in liver and muscle of animal models of insulin-resistant and insulin-deficient diabetes mellitus." *J. Clin. Invest.* **92**(4): 1787-1794.

Franchi, L., Eigenbrod, T., Munoz-Planillo, R. and Nunez, G. (2009). "The inflammasome: a caspase-1-activation platform that regulates immune responses and disease pathogenesis." *Nat. Immunol.* **10**(3): 241-247.

Fredrickson, D. S., Levy, R. I. and Lees, R. S. (1967). "Fat transport in lipoproteins - An integrated approach to mechanisms and disorders." *N. Engl. J. Med.* **276**(34-44).

Freeman, L. A., Kennedy, A., Wu, J., Bark, S., Remaley, A. T., Santamarina-Fojo, S. and Brewer Jr., H. B. (2004). "The orphan nuclear receptor LRH-1 activates the ABCG5/ABCG8 intergenic promoter." *J. Lipid Res.* **45**: 1197-1206.

Friedman, H. S., Rajagopalan, S., Barnes, J. P. and Roseman, H. (2011). "Combination therapy with ezetimibe/simvastatin versus statin monotherapy for low-density lipoprotein cholesterol reduction and goal attainment in a real-world clinical setting." *Clin. Ther.* **33**(2): 212-224.

Friis-Liby, I., Aldenborg, F., Jerlstad, P., Rundstrom, K. and Bjornsson, E. (2004). "High prevalence of metabolic complications in patients with non-alcoholic fatty liver disease." *Scand. J. Gastroenterol.* **39**(9): 864-869.

Furuyama, N. and Fujisawa, Y. (2000). "Regulation of collagenolytic cysteine protease synthesis by estrogen in osteoclasts." *Steroids* **65**(7): 371-378.

Gabele, E., Dostert, K., Dorn, C., Patsenker, E., Stickel, F. and Hellerbrand, C. (2011). "A new model of interactive effects of alcohol and high-fat diet on hepatic fibrosis." *Alcohol. Clin. Exp. Res.* **35**(7): 1361-1367.

Galatola, G., Jazrawi, R. P., Bridges, C., Joseph, A. E. and Northfield, T. C. (1991). "Direct measurement of first-pass ileal clearance of a bile acid in humans." *Gastroenterology* **100**(4): 1100-1105.

Garcia-Calvo, M., Lisnock, J., Bull, H. G., Hawes, B. E., Burnett, D. A., Braun, M. P., Crona, J. H., Davis, H. R., Jr., Dean, D. C., Detmers, P. A., Graziano, M. P., Hughes, M., Macintyre, D. E., Ogawa, A., O'Neill K, A., Iyer, S. P., Shevell, D. E., Smith, M. M., Tang, Y. S., Makarewicz, A. M., Ujjainwalla, F., Altmann, S. W., Chapman, K. T. and Thornberry, N. A. (2005). "The target of ezetimibe is Niemann-Pick C1-Like 1 (NPC1L1)." *Proc. Natl. Acad. Sci. U. S. A.* **102**(23): 8132-8137.

Gauthier, M. A., Simard, P., Zhang, Z. and Zhu, X. X. (2007). "Bile acids as constituents for dental composites: in vitro cytotoxicity of (meth)acrylate and other ester derivatives of bile acids." *J. Royal Soc. Interface* **4**(1145-1150).

Gavey, K. L., Noland, B. J. and Scallen, T. J. (1981). "The participation of sterol carrier protein-2 in the conversion of cholesterol to cholesterol ester by rat liver microsomes." *J. Biol. Chem.* **256**(2).

Gaynes, B. I. and Watkins, J. B., 3rd (1989). "Carbon tetrachloride and the sorbitol pathway in the diabetic mouse." *Comp. Biochem. Physiol. B* **94**(1): 213-217.

Ge, L., Wang, J., Qi, W., Miao, H. H., Cao, J., Qu, Y. X., Li, B. L. and Song, B. L. (2008). "The cholesterol absorption inhibitor ezetimibe acts by blocking the sterol-induced internalization of NPC1L1." *Cell Metab.* **7**(6): 508-519.

Gelissen, I. C., Hochgrebe, T., Wilson, M. R., Easterbrook-Smith, S. B., Jessup, W., Dean, R. T. and Brown, A. J. (1998). "Apolipoprotein J (clusterin) induces cholesterol export from macrophage-foam cells: a potential anti-atherogenic function?" *Biochem. J.* **331 (Pt 1)**: 231-237.

Gentile, C. L. and Pagliassotti, M. J. (2008). "The role of fatty acids in the development and progression of nonalcoholic fatty liver disease." *J. Nutr. Biochem.* **19**(9): 567-576.

Gerin, I., Clerbaux, L. A., Haumont, O., Lanthier, N., Das, A. K., Burant, C. F., Leclercq, I. A., MacDougald, O. A. and Bommer, G. T. (2010). "Expression of miR-33 from an SREBP2 intron inhibits cholesterol export and fatty acid oxidation." *J. Biol. Chem.* **285**(44): 33652-33661.

Gerloff, T., Stieger, B., Hagenbuch, B., Madon, J., Landmann, L., Roth, J., Hofmann, A. F. and Meier, P. J. (1998). "The sister of P-glycoprotein represents the canalicular bile salt export pump of mammalian liver." *J. Biol. Chem.* **273**(16): 10046-10050.

German, J. B., Smilowitz, J. T. and Zivkovic, A. M. (2006). "Lipoproteins: when size really matters." *Curr. Opin. Colloid Interface Sci.* **11**: 171-183.

Gil, G., Faust, J. R., Chin, D. J., Goldstein, J. L. and Brown, M. S. (1985). "Membrane-bound domain of HMG-CoA reductase is required for sterol-enhanced degradation of the enzyme." *Cell* **41**: 249-258.

Gill, S., Chow, R. and Brown, A. J. (2008). "Sterol regulators of cholesterol homeostasis and beyond: the oxysterol hypothesis revisited and revised." *Prog. Lipid Res.* **47**: 391-404.

Gillespie, J. G. and Hardie, D. G. (1992). "Phosphorylation and inactivation of HMG-CoA reductase at the AMP-activated protein kinase site in response to fructose treatment of isolated rat hepatocytes." *FEBS J.* **306**(1): 59-62.

Gilmore, T. D. (2006). "Introduction to NF-kappaB: players, pathways, perspectives." *Oncogene* **25**(51): 6680-6684.

Goldstein, J. L. and Brown, M. S. (1990). "Regulation of the mevalonate pathway." *Nature (Lond.)* **343**: 425-430.

Goldstein, J. L., DeBose-Boyd, R. A. and Brown, M. S. (2008). "Protein sensors for membrane sterols." *Cell* **124**: 35-47.

Gomez-Garre, D., Munoz-Pacheco, P., Gonzalez-Rubio, M. L., Aragoncillo, P., Granados, R. and Fernandez-Cruz, A. (2009). "Ezetimibe reduces plaque inflammation in a rabbit model of atherosclerosis and inhibits monocyte migration in addition to its lipid-lowering effect." *Br. J. Pharmacol.* **156**(8): 1218-1227.

Goodwin, B., Jones, S. A., Price, R. R., Watson, M. A., McKee, D. D., Moore, L. B., Galardi, C., Wilson, J. G., Lewis, M. C., Roth, M. E., Maloney, P. R., Willson, T. M. and Kliewer, S. A. (2000). "A regulatory cascade of the nuclear receptors FXR, SHP-1, and LRH-1 represses bile acid biosynthesis." *Mol. Cell* **6**(3): 517-526.

Goodwin, B., Liddle, C., Murray, M., Tapner, M., Rooney, T. and Farrell, G. C. (1996). "Effects of metyrapone on expression of CYPs 2C11, 3A2, and other 3A genes in rat hepatocytes cultured on matrigel." *Biochem. Pharmacol.* **52**(2): 219-227.

Goodwin, B., Watson, M. A., Kim, H., Miao, J., Kemper, J. K. and Kliewer, S. A. (2003). "Differential regulation of rat and human CYP7A1 by the nuclear oxysterol receptor liver X receptor-alpha." *Mol. Endocrinol.* **17**(3): 386-394.

Gordon, D. A., Jamil, H., Sharp, D., Mullaney, D., Yao, Z., Gregg, R. E. and Wetterau, J. (1994). "Secretion of apolipoprotein B-containing lipoproteins from HeLa cells is dependent on expression of the microsomal triglyceride transfer protein and is regulated by lipid availability." *Proc. Natl. Acad. Sci. U. S. A.* **91**(16): 7628-7632.

Gordon, S. (1999). "Macrophage-restricted molecules: role in differentiation and activation." *Immunol. Lett.* **65**(1-2): 5-8.

Goto, M., Katayama, K. I., Shirakawa, F. and Tanaka, I. (1999). "Involvement of NF-kappaB p50/p65 heterodimer in activation of the human pro-interleukin-1beta gene at two subregions of the upstream enhancer element." *Cytokine* **11**(1): 16-28.

Gould, E. A., Buckley, A. and Cammack, N. (1985). "Use of the biotin-streptavidin interaction to improve flavivirus detection by immunofluorescence and ELISA tests." *J. Virol. Methods* **11**(1): 41-48.

Greene, C. M., Carroll, T. P., Smith, S. G., Taggart, C. C., Devaney, J., Griffin, S., O'Neill S, J. and McElvaney, N. G. (2005). "TLR-induced inflammation in cystic fibrosis and non-cystic fibrosis airway epithelial cells." *J. Immunol.* **174**(3): 1638-1646.

Guan, G., Dai, P. H., Osborne, T. F., Kim, J. B. and Shechter, I. (1997). "Multiple sequence elements are involved in the transcriptional regulation of the human squalene synthase gene." *J. Biol. Chem.* **272**(15): 10295-10302.

Guex, N. and Peitsch, M. C. (1997). "SWISS-MODEL and the Swiss-PdbViewer: an environment for comparative protein modeling." *Electrophoresis* **18**(15): 2714-2723.

Guleng, B., Lian, Y. M. and Ren, J. L. (2010). "Mindin is upregulated during colitis and may activate NF-kappaB in a TLR-9 mediated manner." *World J. Gastroenterol.* **16**(9): 1070-1075.

Guyton, J. R. and Klemp, K. F. (1996). "Development of the lipid-rich core in human atherosclerosis." *Arterioscler. Thromb. Vasc. Biol.* **16**(1): 4-11.

Harada, K., Chiba, M., Okamura, A., Hsu, M., Sato, Y., Igarashi, S., Ren, X. S., Ikeda, H., Ohta, H., Kasashima, S., Kawashima, A. and Nakanuma, Y. (2011). "Monocyte chemoattractant protein-1 derived from biliary innate immunity contributes to hepatic fibrogenesis." *J. Clin. Pathol.* **64**(8): 660-665.

Harding, H. P., Novoa, I., Zhang, Y., Zeng, H., Wek, R., Schapira, M. and Ron, D. (2000). "Regulated translation initiation controls stress-induced gene expression in mammalian cells." *Mol. Cell* **6**(5): 1099-1108.

Hardwick, D. C. (1966). "The fate of acetyl groups derived from glucose in the isolated perfused goat udder." *Biochem. J.* **99**(1): 228-231.

Hashimoto, E., Yatsuji, S., Tobari, M., Taniai, M., Torii, N., Tokushige, K. and Shiratori, K. (2009). "Hepatocellular carcinoma in patients with nonalcoholic steatohepatitis." *J. Gastroenterol.* **44 Suppl 19**: 89-95.

Hashizume, H., Sato, K., Takagi, H., Hirokawa, T., Kojima, A., Sohara, N., Kakizaki, S., Mochida, Y., Shimura, T., Sunose, Y., Ohwada, S. and Mori, M. (2007). "Primary liver cancers with nonalcoholic steatohepatitis." *Eur. J. Gastroenterol. Hepatol.* **19**(10): 827-834.

Haukeland, J. W., Konopski, Z., Bell, H. and Raknerud, N. (2001). "[Non-alcoholic steatohepatitis]." *Tidsskr. Nor. Laegeforen.* **121**(20): 2377-2380.

Havel, R. J. (1998). "Receptor and non-receptor mediated uptake of chylomicron remnants by the liver." *Atheroscler. Suppl.* **141**(1): S1-S7.

Havel, R. J. and Hamilton, R. L. (2004). "Hepatic catabolism of remnant lipoproteins: where the action is." *Arterioscler. Thromb. Vasc. Biol.* **24**: 213-215.

Hayden, M. S. and Ghosh, S. (2004). "Signaling to NF-kappaB." *Genes Dev.* **18**(18): 2195-2224.

Hayhurst, G. P., Lee, Y. H., Lambert, G., Ward, J. M. and Gonzalez, F. J. (2001). "Hepatocyte nuclear factor 4alpha (nuclear receptor 2A1) is essential for maintenance of hepatic gene expression and lipid homeostasis." *Mol. Cell. Biol.* **21**(4): 1393-1403.

Hedley, A. A., Ogden, C. L., Johnson, C. L., Carroll, M. D., Curtin, L. R. and Flegal, K. M. (2004). Prevalence of Overweight and Obesity Among US Children, Adolescents, and Adults, 1999-2002. **291:** 2847-2850.

Henkel, A. S., Anderson, K. A., Dewey, A. M., Kavesh, M. H. and Green, R. M. (2011). "A chronic high-cholesterol diet paradoxically suppresses hepatic CYP7A1 expression in FVB/NJ mice." *J. Lipid Res.* **52**(2): 289-298.

Heydet, D., Larter, C. Z. and Farrell, G. C. (2010). "Roles of neuronal primary cilium and leptin receptor in leptin resistance in obese mice with NAFLD." *J. Gastroenterol. Hepatol.* **25**(Suppl. 3): A7.

Hilser, V. J. and Thompson, E. B. (2011). "Structural dynamics, intrinsic disorder and allostery in nuclear receptors as transcription factors." *J. Biol. Chem.*

Hino, A., Morita, M., Une, M., Fujimura, K. and Kuramoto, T. (2001). "Effects of deoxycholic acid and its epimers on lipid peroxidation in isolated rat hepatocytes." *J Biochem* **129**(5): 683-689.

Hoff, J. (2000). "Methods of blood collection in the mouse." *Lab. Anim.* **29**(10): 47-53.

Hofmann, A. F. (2001). The limited utility of conjugated bile acid replacement therapy in short bowel syndrome. *Biology of Bile Acids in Health and Disease - XVI International Bile Acid Meeting (Falk Symposium, Volume 120)*. van Berge Henegouwen, G. P., Keppler, D., Leuschner, U., Paumgartner, G. and Stiehl, A. Dordrecht, The Netherlands, Kluwer Academic Publishers.

Hofmann, S. M., Perez-Tilve, D., Greer, T. M., Coburn, B. A., Grant, E., Basford, J. E., Tschop, M. H. and Hui, D. Y. (2008). "Defective lipid delivery modulates glucose tolerance and metabolic response to diet in apolipoprotein E-deficient mice." *Diabetes* **57**(1): 5-12.

Holub, J. M., O'Toole-Colin, K., Getzel, A., Argenti, A., Evans, M. A., Smith, D. C., Dalglish, G. A., Rifat, S., Wilson, D. L., Taylor, B. M., Miott, U., Glersaye, J., Lam, K. S., McCranor, B. J., Berkowitz, J. D., Miller, R. B., Lukens, J. R., Krumpe, K., Gupton, J. T. and Burnham, B. S. (2004). "Lipid-lowering effects of ethyl 2-phenacyl-3-aryl-1H-pyrrole- 4-carboxylates in rodents." *Molecules* **9**(3): 134-157.

Horie, T., Ono, K., Horiguchi, M., Nishi, H., Nakamura, T., Nagao, K., Kinoshita, M., Kuwabara, Y., Marusawa, H., Iwanaga, Y., Hasegawa, K., Yokode, M., Kimura, T. and Kita, T. (2010). "MicroRNA-33 encoded by an intron of sterol regulatory element-binding protein 2 (Srebp2) regulates HDL in vivo." *Proc. Natl. Acad. Sci. U. S. A.* **107**(40): 17321-17326.

Hornick, C. A. (2002). Lipids II: Phospholipids, glycosphingolipids, and cholesterol. *Medical biochemistry*. Hayhurst, J. San Diego, California, USA, Harcourt/Academic Press: 401-427.

Horton, J. D., Goldstein, J. L. and Brown, M. S. (2002). "SREBPs: activators of the complete program of cholesterol and fatty acid synthesis in the liver." *J. Clin. Invest.* **109**(9): 1125-1131.

Hozoji-Inada, M., Munehira, Y., Nagao, K., Kioka, N. and Ueda, K. (2011). "Liver X receptor beta (LXRbeta) interacts directly with ATP-binding cassette A1 (ABCA1) to promote high density lipoprotein formation during acute cholesterol accumulation." *J. Biol. Chem.* **286**(22): 20117-20124.

Hsu, H., Xiong, J. and Goeddel, D. V. (1995). "The TNF receptor 1-associated protein TRADD signals cell death and NF-kappa B activation." *Cell* **81**(4): 495-504.

Hua, X., Yokoyama, C., Wu, J., Briggs, M. R., Brown, M. S., Goldstein, J. L. and Wang, X. (1993). "SREBP-2, a second basic-helix-loop-helix-leucine zipper protein that stimulates transcription by binding to a sterol regulatory element." *Proc. Natl. Acad. Sci. U. S. A.* **90**(24): 11603-11607.

Huang, J., Buboltz, J. T. and Feigenson, G. W. (1999). "Maximum solubility of cholesterol in phosphatidylcholine and phosphatidylethanolamine bilayers." *Biochim. Biophys. Acta* **1417**(1): 89-100.

Huang, T. T. and Miyamoto, S. (2001). "Postrepression activation of NF-kappaB requires the amino-terminal nuclear export signal specific to IkappaBalpha." *Mol. Cell. Biol.* **21**(14): 4737-4747.

Hughes, E. A., Tracey, I., Singhal, S. and Patel, J. (2006). "Unexpected beneficial effect in the use of ezetimibe in non-alcoholic fatty liver disease." *Med. Hypotheses* **67**(6): 1463-1464.

Hui, D. Y. (1996). "Molecular biology of enzymes involved with cholesterol ester hydrolysis in mammalian tissues." *Biochim. Biophys. Acta* **1303**: 1-14.

Hui, J. M., Hodge, A., Farrell, G. C., Kench, J. G., Kriketos, A. and George, J. (2004). "Beyond insulin resistance in NASH: TNF-alpha or adiponectin?" *Hepatology* **40**(1): 46-54.

Humar, M., Loop, T., Schmidt, R., Hoetzel, A., Roesslein, M., Andriopoulos, N., Pahl, H. L., Geiger, K. K. and Pannen, B. H. (2007). "The mitogen-activated protein kinase p38 regulates activator protein 1 by direct phosphorylation of c-Jun." *Int. J. Biochem. Cell Biol.* **39**(12): 2278-2288.

Hunt, C. M., Guzelian, P. S., Molowa, D. T. and Wright, S. A. (1991). "Regulation of rat hepatic cytochrome P450IIE1 in primary monolayer hepatocyte culture." *Xenobiotica* **21**(12): 1621-1631.

Huxford, T., Huang, D. B., Malek, S. and Ghosh, G. (1998). "The crystal structure of the IkappaBalpha/NF-kappaB complex reveals mechanisms of NF-kappaB inactivation." *Cell* **95**(6): 759-770.

Hylemon, P. B., Pandak, W. M. and Vlahcevic, Z. R. (2001). Regulation of hepatic cholesterol homeostasis. *The liver: biology and pathobiology*. Arias, I. M., Boyer, J. L., Fausto, N.*et al.* Philadelphia, Pa., Lippincott Williams & Wilkins: 231-247.

Ichijo, H., Nishida, E., Irie, K., ten Dijke, P., Saitoh, M., Moriguchi, T., Takagi, M., Matsumoto, K., Miyazono, K. and Gotoh, Y. (1997). "Induction of apoptosis by ASK1, a mammalian MAPKKK that activates SAPK/JNK and p38 signaling pathways." *Science* **275**(5296): 90-94.

Imamura, M., Tsutsui, H., Yasuda, K., Uchiyama, R., Yumikura-Futatsugi, S., Mitani, K., Hayashi, S., Akira, S., Taniguchi, S., Van Rooijen, N., Tschopp, J., Yamamoto, T., Fujimoto, J. and Nakanishi, K. (2009). "Contribution of TIR domain-containing adapter inducing IFN-beta-mediated IL-18 release to LPS-induced liver injury in mice." *J. Hepatol.* **51**(2): 333-341.

Ioannou, G. N., Morrow, O. B., Connole, M. L. and Lee, S. P. (2009). "Association between dietary nutrient composition and the incidence of cirrhosis or liver cancer in the United States population." *Hepatology* **50**(1): 175-184.

Ip, E., Farrell, G., Hall, P., Robertson, G. and Leclercq, I. (2004). "Administration of the potent PPARalpha agonist, Wy-14,643, reverses nutritional fibrosis and steatohepatitis in mice." *Hepatology* **39**(5): 1286-1296.

Ip, E., Farrell, G. C., Robertson, G., Hall, P., Kirsch, R. and Leclercq, I. (2003). "Central role of PPARalpha-dependent hepatic lipid turnover in dietary steatohepatitis in mice." *Hepatology* **38**(1): 123-132.

Irvin, J. L. (1952). "The secretion and enterohepatic circulation of bile acids; replacement of bile acids in biliary insufficiency." *N. C. Med. J.* **13**(4): 206-212.

Ishibashi, S., Herz, J., Maeda, N., Goldstein, J. L. and Brown, M. S. (1994). "The two-receptor model of lipoprotein clearance: tests of the hypothesis in "knockout" mice lacking the low density lipoprotein receptor, apolipoprotein E, or both proteins." *Proc. Natl. Acad. Sci. U. S. A.* **91**(10): 4431-4435.

Istvan, E. (2003). "Statin inhibition of HMG-CoA reductase: a 3-dimensional view." *Atheroscler. Suppl.* **4**(1): 3-8.

Istvan, E. S. (2002). "Structural mechanism for statin inhibition of 3-hydroxy-3-methylglutaryl coenzyme A reductase." *Am. Heart J.* **144**(6 Suppl): S27-32.

Istvan, E. S. and Deisenhofer, J. (2001). "Structural mechanism for statin inhibition of HMG-CoA reductase." *Science* **292**(5519): 1160-1164.

Istvan, E. S., Palnitkar, M., Buchanan, S. K. and Deisenhofer, J. (2000). "Crystal structure of the catalytic portion of human HMG-CoA reductase: insights into regulation of activity and catalysis." *EMBO J.* **19**(5): 819-830.

Ito, M., Suzuki, J., Tsujioka, S., Sasaki, M., Gomori, A., Shirakura, T., Hirose, H., Ishihara, A., Iwaasa, H. and Kanatani, A. (2007). "Longitudinal analysis of murine steatohepatitis model induced by chronic exposure to high-fat diet." *Hepatol. Res.* **37**(1): 50-57.

Iturriaga, C., Pineda, M., Fernandez-Valero, E. M., Vanier, M. T. and Coll, M. J. (2006). "Niemann-Pick C disease in Spain: clinical spectrum and development of a disability scale." *J. Neurol. Sci.* **249**(1): 1-6.

Iuliano, L. (2011). "Pathways of cholesterol oxidation via non-enzymatic mechanisms." *Chem. Phys. Lipids.*

Ivanov, V. N., Deng, G., Podack, E. R. and Malek, T. R. (1995). "Pleiotropic effects of Bcl-2 on transcription factors in T cells: potential role of NF-kappa B p50-p50 for the anti-apoptotic function of Bcl-2." *Int. Immunol.* 7(11): 1709-1720.

Jackson, S. M., Ericsson, J., Osborne, T. F. and Edwards, P. A. (1995). "NF-Y has a novel role in sterol-dependent transcription of two cholesterogenic genes." *J. Biol. Chem.* **270**(37): 21445-21448.

Jacobs, M. D. and Harrison, S. C. (1998). "Structure of an IkappaBalpha/NF-kappaB complex." *Cell* **95**(6): 749-758.

Jagger, D., Collin, G., Kelly, J., Towers, E., Nevill, G., Longo-Guess, C., Benson, J., Halsey, K., Dolan, D., Marshall, J., Naggert, J. and Forge, A. (2011). "Alstrom Syndrome protein ALMS1 localizes to basal bodies of cochlear hair cells and regulates cilium-dependent planar cell polarity." *Hum. Mol. Genet.* **20**(3): 466-481.

Jander, S. and Stoll, G. (1998). "Differential induction of interleukin-12, interleukin-18, and interleukin-1beta converting enzyme mRNA in experimental autoimmune encephalomyelitis of the Lewis rat." *J. Neuroimmunol.* **91**(1-2): 93-99.

Jedlitschky, G., Leier, I., Buchholz, U., Hummel-Eisenbeiss, J., Burchell, B. and Keppler, D. (1997). "ATP-dependent transport of bilirubin glucuronides by the multidrug resistance protein MRP1 and its hepatocyte canalicular isoform MRP2." *Biochem. J.* **327 (Pt 1)**: 305-310.

Jeong, H. J., Lee, H. S., Kim, K. S., Kim, Y. K., Yoon, D. and Park, S. W. (2008). "Sterol-dependent regulation of proprotein convertase subtilisin/kexin type 9 expression by sterol-regulatory element binding protein-2." *J. Lipid Res.* **49**(2): 399-409.

Ji, C., Kaplowitz, N., Lau, M. Y., Kao, E., Petrovic, L. M. and Lee, A. S. (2011). "Liver-specific loss of glucose-regulated protein 78 perturbs the unfolded protein response and exacerbates a spectrum of liver diseases in mice." *Hepatology* **54**(1): 229-239.

Jia, E. Z., Yang, Z. J., Chen, S. W., Qi, G. Y., You, C. F., Ma, J. F., Zhang, J. X., Wang, Z. Z., Qian, W. C., Li, X. L., Wang, H. Y. and Ma, W. Z. (2005). "Significant association of insulin and proinsulin with clustering of cardiovascular risk factors." *World J. Gastroenterol.* **11**(1): 149-153.

Jia, L., Betters, J. L. and Yu, L. (2011). "Niemann-pick C1-like 1 (NPC1L1) protein in intestinal and hepatic cholesterol transport." *Annu. Rev. Physiol.* **73**: 239-259.

Jia, L., Ma, Y., Liu, G. and Yu, L. (2010). "Dietary cholesterol reverses resistance to diet-induced weight gain in mice lacking Niemann-Pick C1-Like 1." *J. Lipid Res.* **51**(10): 3024-3033.

Jiang, D., Liang, J., Fan, J., Yu, S., Chen, S., Luo, Y., Prestwich, G. D., Mascarenhas, M. M., Garg, H. G., Quinn, D. A., Homer, R. J., Goldstein, D. R., Bucala, R., Lee, P. J., Medzhitov, R. and Noble, P. W. (2005).

"Regulation of lung injury and repair by Toll-like receptors and hyaluronan." *Nat. Med.* **11**(11): 1173-1179.

Johnston, T. P., Baker, J. C., Hall, D., Jamal, S., Palmer, W. K. and Emeson, E. E. (2000). "Regression of poloxamer 407-induced atherosclerotic lesions in C57BL/6 mice using atorvastatin." *Atherosclerosis* **149**(2): 303-313.

Johs, A., Hammel, M., Waldner, I., May, R. P., Laggner, P. and Prassl, R. (2006). "Modular structure of solubilized human apolipoprotein B-100: low resolution model revealed by small angle neutron scattering." *J. Biol. Chem.* **281**: 19732-19739.

Jones, C. L. and Weiss, D. S. (2011). "TLR2 signaling contributes to rapid inflammasome activation during F. novicida infection." *PLoS ONE* **6**(6): e20609.

Kaemmer, D., Bozkurt, A., Otto, J., Junge, K., Klink, C., Weis, J., Sellhaus, B., O'Dey, D. M., Pallua, N., Jansen, M., Schumpelick, V. and Klinge, U. (2010). "Evaluation of tissue components in the peripheral nervous system using Sirius red staining and immunohistochemistry: a comparative study (human, pig, rat)." *J. Neurosci. Methods* **190**(1): 112-116.

Kaisho, T. and Akira, S. (2006). "Toll-like receptor function and signaling." *J. Allergy Clin. Immunol.* **117**(5): 979-987; quiz 988.

Kanagarajan, N., Nam, J. H., Noah, Z. A. and Murthy, S. (2008). "Disease modifying effect of statins in dextran sulfate sodium model of mouse colitis." *Inflamm. Res.* **57**(1): 34-38.

Kanayama, T., Arito, M., So, K., Hachimura, S., Inoue, J. and Sato, R. (2007). "Interaction between sterol regulatory element-binding proteins and liver receptor homolog-1 reciprocally suppresses their transcriptional activities." *J. Biol. Chem.* **282**(14): 10290-10298.

Kane, R. E., Tector, J., Brems, J. J., Li, A. and Kaminski, D. (1991). "Sulfation and glucuronidation of acetaminophen by cultured hepatocytes reproducing in vivo sex-differences in conjugation on Matrigel and type 1 collagen." *In Vitro Cell. Dev. Biol.* **27A**(12): 953-960.

Karin, M. and Ben-Neriah, Y. (2000). "Phosphorylation meets ubiquitination: the control of NF-[kappa]B activity." *Annu. Rev. Immunol.* **18**: 621-663.

Kawai, T. and Akira, S. (2007). "Signaling to NF-kappaB by Toll-like receptors." *Trends Mol. Med.* **13**(11): 460-469.

Keber, I. and Keber, D. (1992). "Increased plasminogen activator inhibitor activity in survivors of myocardial infarction is associated with metabolic risk factors of atherosclerosis." *Haemostasis* **22**(4): 187-194.

Kedi, X., Ming, Y., Yongping, W., Yi, Y. and Xiaoxiang, Z. (2009). "Free cholesterol overloading induced smooth muscle cells death and activated both ER- and mitochondrial-dependent death pathway." *Atherosclerosis* **207**(1): 123-130.

Kellner-Weibel, G., Geng, Y. J. and Rothblat, G. H. (1999a). "Cytotoxic cholesterol is generated by the hydrolysis of cytoplasmic cholesteryl ester and transported to the plasma membrane." *Atherosclerosis* **146**(2): 309-319.

Kellner-Weibel, G., Jerome, W. G., Small, D. M., Warner, G. J., Stoltenborg, J. K., Kearney, M. A., Corjay, M. H., Philips, M. C. and Rothblat, G. H. (1998). "Effects of intracellular free cholesterol accumulation on macrophage viability: a model for foam cell death." *Arterioscler. Thromb. Vasc. Biol.* **18**: 423-431.

Kellner-Weibel, G., Luke, S. J. and Rothblat, G. H. (2003). "Cytotoxic cellular cholesterol is selectively removed by apoA-I via ABCA1." *Atherosclerosis* **171**(2): 235-243.

Kellner-Weibel, G., Yancey, P. G., Jerome, W. G., Walser, T., Mason, R. P., Philips, M. C. and Rothblat, G. H. (1999b). "Crystallization of free cholesterol in model macrophage foam cells." *Arterioscler. Thromb. Vasc. Biol.* **19**: 1891-1898.

Kelly, D. A., Portmann, B., Mowat, A. P., Sherlock, S. and Lake, B. D. (1993). "Niemann-Pick disease type C: diagnosis and outcome in children, with particular reference to liver disease." *J. Pediatr.* **123**(2): 242-247.

Keppler, D. and Konig, J. (1997). "Hepatic canalicular membrane 5: Expression and localization of the conjugate export pump encoded by the MRP2 (cMRP/cMOAT) gene in liver." *FASEB J.* **11**(7): 509-516.

Keppler, D., Konig, J. and Buchler, M. (1997). "The canalicular multidrug resistance protein, cMRP/MRP2, a novel conjugate export pump expressed in the apical membrane of hepatocytes." *Adv. Enzyme Regul.* **37**: 321-333.

Kieser, A., Kaiser, C. and Hammerschmidt, W. (1999). "LMP1 signal transduction differs substantially from TNF receptor 1 signaling in the molecular functions of TRADD and TRAF2." *EMBO J.* **18**(9): 2511-2521.

Kim, C. H., Kallman, J. B., Bai, C., Pawloski, L., Gewa, C., Arsalla, A., Sabatella, M. E. and Younossi, Z. M. (2010). "Nutritional assessments of patients with non-alcoholic fatty liver disease." *Obes. Surg.* **20**(2): 154-160.

Kim, J. H., Lee, J. N. and Paik, Y. K. (2001). "Cholesterol biosynthesis from lanosterol. A concerted role for Sp1 and NF-Y-binding sites for sterol-mediated regulation of rat 7-dehydrocholesterol reductase gene expression." *J. Biol. Chem.* **276**(21): 18153-18160.

Kimura, Y., Morita, S. Y., Matsuo, M. and Ueda, K. (2007). "Mechanism of multidrug recognition by MDR1/ABCB1." *Cancer Sci.* **98**(9): 1303-1310.

Kischkel, F. C., Lawrence, D. A., Chuntharapai, A., Schow, P., Kim, K. J. and Ashkenazi, A. (2000). "Apo2L/TRAIL-dependent recruitment of endogenous FADD and caspase-8 to death receptors 4 and 5." *Immunity* **12**(6): 611-620.

Kiyak, J. H. (1997). "Cholesterol crystals, smooth muscle cells and new data on the genesis of atherosclerosis." *Pol. J. Pathol.* **48**(1): 49-55.

Kleiner, D. E., Brunt, E. M., Van Natta, M., Behling, C., Contos, M. J., Cummings, O. W., Ferrell, L. D., Liu, Y. C., Torbenson, M. S., Unalp-Arida, A., Yeh, M., McCullough, A. J. and Sanyal, A. J. (2005). "Design and validation of a histological scoring system for nonalcoholic fatty liver disease." *Hepatology* **41**(6): 1313-1321.

Klett, E. L., Lee, M. H., Adams, D. B., Chavin, K. D. and Patel, S. B. (2004). "Localization of ABCG5 and ABCG8 proteins in human liver, gall bladder and intestine." *BMC Gastroenterol.* **4**: 21-33.

Kluwe, J., Pradere, J. P., Gwak, G. Y., Mencin, A., De Minicis, S., Osterreicher, C. H., Colmenero, J., Bataller, R. and Schwabe, R. F. (2010). "Modulation of hepatic fibrosis by c-Jun-N-terminal kinase inhibition." *Gastroenterology* **138**(1): 347-359.

Koca, S. S., Bahcecioglu, I. H., Poyrazoglu, O. K., Ozercan, I. H., Sahin, K. and Ustundag, B. (2008). "The treatment with antibody of TNF-alpha reduces the inflammation, necrosis and fibrosis in the non-alcoholic steatohepatitis induced by methionine- and choline-deficient diet." *Inflammation* **31**(2): 91-98.

Kockx, M. M., De Meyer, G. R., Muhring, J., Bult, H., Bultinck, J. and Herman, A. G. (1996). "Distribution of cell replication and apoptosis in atherosclerotic plaques of cholesterol-fed rabbits." *Atherosclerosis* **120**(1-2): 115-124.

Kotzka, J., Lehr, S., Roth, G., Avci, H., Knebel, B. and Muller-Wieland, D. (2004). "Insulin-activated Erk-mitogen-activated protein kinases phosphorylate sterol

regulatory element-binding Protein-2 at serine residues 432 and 455 in vivo." *J. Biol. Chem.* **279**(21): 22404-22411.

Kotzka, J., Muller-Wieland, D., Roth, G., Kremer, L., Munck, M., Schurmann, S., Knebel, B. and Krone, W. (2000). "Sterol regulatory element binding proteins (SREBP)-1a and SREBP-2 are linked to the MAP-kinase cascade." *J. Lipid Res.* **41**(1): 99-108.

Koumenis, C., Naczki, C., Koritzinsky, M., Rastani, S., Diehl, A., Sonenberg, N., Koromilas, A. and Wouters, B. G. (2002). "Regulation of protein synthesis by hypoxia via activation of the endoplasmic reticulum kinase PERK and phosphorylation of the translation initiation factor eIF2alpha." *Mol. Cell. Biol.* **22**(21): 7405-7416.

Kouris-Blazos, A. and Wahlqvist, M. L. (2007). "Health economics of weight management: evidence and cost." *Asia Pac. J. Clin. Nutr.* **16 Suppl 1**: 329-338.

Kozuki, M., Kurata, T., Miyazaki, K., Morimoto, N., Ohta, Y., Ikeda, Y. and Abe, K. (2011). "Atorvastatin and pitavastatin protect cerebellar Purkinje cells in AD model mice and preserve the cytokines MCP-1 and TNF-alpha." *Brain Res.* **1388**: 32-38.

Krysiak, R. and Okopien, B. (2011). "The effect of ezetimibe and simvastatin on monocyte cytokine release in patients with isolated hypercholesterolemia." *J. Cardiovasc. Pharmacol.* **57**(4): 505-512.

Ktistaki, E. and Talianidis, I. (1997). "Modulation of hepatic gene expression by hepatocyte nuclear factor 1." *Science* **277**(5322): 109-112.

Kuipers, F., Nagelkerke, J. F., Bakkeren, H., Havinga, R., Van Berkel, T. J. and Vonk, R. J. (1989). "Processing of cholesteryl ester from low-density lipoproteins in the rat. Hepatic metabolism and biliary secretion after uptake by different hepatic cell types." *Biochem. J.* **257**(3): 699-704.

Kusminski, C. M., Shetty, S., Orci, L., Unger, R. H. and Scherer, P. E. (2009). "Diabetes and apoptosis: lipotoxicity." *Apoptosis* **14**(12): 1484-1495.

La Montagna, G., Cacciapuoti, F., Buono, R., Manzella, D., Mennillo, G. A., Arciello, A., Valentini, G. and Paolisso, G. (2007). "Insulin resistance is an independent risk factor for atherosclerosis in rheumatoid arthritis." *Diab. Vasc. Dis. Res.* **4**(2): 130-135.

Lalloyer, F., Wouters, K., Baron, M., Caron, S., Vallez, E., Vanhoutte, J., Bauge, E., Shiri-Sverdlov, R., Hofker, M., Staels, B. and Tailleux, A. (2011). "Peroxisome proliferator-activated receptor-alpha gene level differently affects lipid metabolism and inflammation in apolipoprotein E2 knock-in mice." *Arterioscler. Thromb. Vasc. Biol.* **31**(7): 1573-1579.

Lande, M. B., Donovan, J. M. and Zeidel, M. L. (1995). "The relationship between membrane fluidity and permeabilities to water, solutes, ammonia, and protons." *J. Gen. Physiol.* **106**(1): 67-84.

Larsson, D. A., Baird, S., Nyhalah, J. D., Yuan, X. M. and Li, W. (2006). "Oxysterol mixtures, in atheroma-relevant proportions, display synergistic and proapoptotic effects." *Free Radical Biol. Med.* **41**(6): 902-910.

Larter, C. Z., Chitturi, S., Heydet, D. and Farrell, G. C. (2010). "A fresh look at NASH pathogenesis. Part 1: the metabolic movers." *J. Gastroenterol. Hepatol.* **25**(4): 672-690.

Larter, C. Z. and Yeh, M. M. (2008). "Animal models of NASH: getting both pathology and metabolic context right." *J. Gastroenterol. Hepatol.* **23**(11): 1635-1648.

Larter, C. Z., Yeh, M. M., Haigh, W. G., Williams, J., Brown, S., Bell-Anderson, K. S., Lee, S. P. and Farrell, G. C. (2008a). "Hepatic free fatty acids

accumulate in experimental steatohepatitis: role of adaptive pathways." *J. Hepatol.* **48**(4): 638-647.

Larter, C. Z., Yeh, M. M., Van Rooyen, D. M., Brooling, J., Ghatora, K. and Farrell, G. C. (2011). "The PPAR-alpha agonist, Wy 14,643, improves metabolic indices, steatosis and ballooning in diabetic mice with NASH." *J. Gastroenterol. Hepatol.* **In press**.

Larter, C. Z., Yeh, M. M., Van Rooyen, D. M., Teoh, N. C., Brooling, J., Hou, J. Y., Williams, J., Clyne, M., Nolan, C. J. and Farrell, G. C. (2009). "Roles of adipose restriction and metabolic factors in progression of steatosis to steatohepatitis in obese, diabetic mice." *J. Gastroenterol. Hepatol.* **24**(10): 1658-1668.

Larter, C. Z., Yeh, M. M., Williams, J., Bell-Anderson, K. S. and Farrell, G. C. (2008b). "MCD-induced steatohepatitis is associated with hepatic adiponectin resistance and adipogenic transformation of hepatocytes." *J. Hepatol.* **49**(3): 407-416.

Lau, Y. Y., Okochi, H., Huang, Y. and Benet, L. Z. (2006). "Multiple transporters affect the disposition of atorvastatin and its two active hydroxy metabolites: application of in vitro and ex situ systems." *J. Pharmacol. Exp. Ther.* **316**(2): 762-771.

Lazo, M. and Clark, J. M. (2008). "The epidemiology of nonalcoholic fatty liver disease: a global perspective." *Semin. Liver Dis.* **28**(4): 339-350.

Leclercq, I. A., Farrell, G. C., Field, J., Bell, D. R., Gonzalez, F. J. and Robertson, G. R. (2000). "CYP2E1 and CYP4A as microsomal catalysts of lipid peroxides in murine nonalcoholic steatohepatitis." *J. Clin. Invest.* **105**(8): 1067-1075.

Leclercq, I. A., Lebrun, V. A., Starkel, P. and Horsmans, Y. J. (2007). "Intrahepatic insulin resistance in a murine model of steatohepatitis: effect of PPARgamma agonist pioglitazone." *Lab. Invest.* **87**(1): 56-65.

Lee, C. S., Park, W. J., Han, E. S. and Bang, H. (2007). "Differential modulation of 7-ketocholesterol toxicity against PC12 cells by calmodulin antagonists and Ca2+ channel blockers." *Neurochem. Res.* **32**(1): 87-98.

Lee, M. H., Lu, K., Hazard, S., Yu, H., Shulenin, S., Hidaka, H., Kojima, H., Allikmets, R., Sakuma, N., Pegoraro, R., Srivastava, A. K., Salen, G., Dean, M. and Patel, S. B. (2001). "Identification of a gene, ABCG5, important in the regulation of dietary cholesterol absorption." *Nat. Genet.* **27**: 79-83.

Lee, Y., Hirose, H., Ohneda, M., Johnson, J. H., McGarry, J. D. and Unger, R. H. (1994). "Beta-cell lipotoxicity in the pathogenesis of non-insulin-dependent diabetes mellitus of obese rats: impairment in adipocyte-beta-cell relationships." *Proc. Natl. Acad. Sci. U. S. A.* **91**(23): 10878-10882.

Lee, Y. K., Choi, Y. H., Chua, S., Park, Y. J. and Moore, D. D. (2006). "Phosphorylation of the hinge domain of the nuclear hormone receptor LRH-1 stimulates transactivation." *J. Biol. Chem.* **281**(12): 7850-7855.

Lee, Y. K., Dell, H., Dowhan, D. H., Hadzopoulou-Cladaras, M. and Moore, D. D. (2000). "The orphan nuclear receptor SHP inhibits hepatocyte nuclear factor 4 and retinoid X receptor transactivation: two mechanisms for repression." *Mol. Cell. Biol.* **20**(1): 187-195.

Lee, Y. K. and Moore, D. D. (2002). "Dual mechanisms for repression of the monomeric orphan receptor liver receptor homologous protein-1 by the orphan small heterodimer partner." *J. Biol. Chem.* **277**(4): 2463-2467.

Lee, Y. K., Schmidt, D. R., Cummins, C. L., Choi, M., Peng, L., Zhang, Y., Goodwin, B., Hammer, R. E., Mangelsdorf, D. J. and Kliewer, S. A. (2008). "Liver receptor homolog-1 regulates bile acid homeostasis but is not essential

for feedback regulation of bile acid synthesis." *Mol. Endocrinol.* **22**(6): 1345-1356.

Lehmann, J. M., Kliewer, S. A., Moore, L. B., Smith-Oliver, T. A., Oliver, B. B., Su, J. L., Sundseth, S. S., Winegar, D. A., Blanchard, D. E., Spencer, T. A. and Willson, T. M. (1997). "Activation of the nuclear receptor LXR by oxysterols defines a new hormone response pathway." *J. Biol. Chem.* **272**(6): 3137-3140.

Lei, K. and Davis, R. J. (2003). "JNK phosphorylation of Bim-related members of the Bcl2 family induces Bax-dependent apoptosis." *Proc. Natl. Acad. Sci. U. S. A.* **100**(5): 2432-2437.

Lei, K., Nimnual, A., Zong, W. X., Kennedy, N. J., Flavell, R. A., Thompson, C. B., Bar-Sagi, D. and Davis, R. J. (2002). "The Bax subfamily of Bcl2-related proteins is essential for apoptotic signal transduction by c-Jun NH(2)-terminal kinase." *Mol. Cell. Biol.* **22**(13): 4929-4942.

Lemaire-Ewing, S., Prunet, C., Montange, T., Vejux, A., Berthier, A., Bessede, G., Corcos, L., Gambert, P., Neel, D. and Lizard, G. (2005). "Comparison of the cytotoxic, pro-oxidant and pro-inflammatory characteristics of different oxysterols." *Cell Biol. Toxicol.* **21**(2): 97-114.

Leung, K. (2004). "[11C]Acetoacetate."

Li, F., Guo, Y., Sun, S., Jiang, X., Tang, B., Wang, Q. and Wang, L. (2008). "Free cholesterol-induced macrophage apoptosis is mediated by inositol-requiring enzyme 1 alpha-regulated activation of Jun N-terminal kinase." *Acta Biochim Biophys Sin (Shanghai)* **40**(3): 226-234.

Li, G., Vega, R., Nelms, K., Gekakis, N., Goodnow, C., McNamara, P., Wu, H., Hong, N. A. and Glynne, R. (2007). "A role for Alstrom syndrome protein, alms1, in kidney ciliogenesis and cellular quiescence." *PLoS Genet.* **3**(1): e8.

Li, H., Chen, F., Shang, Q., Pan, L., Shneider, B. L., Chiang, J. Y. L., Forman, B. M., Ananthanarayanan, M., Tint, G. S., Salen, G. and Xu, G. (2005). "FXR-activating ligands inhibit rabbit ASBT expression via FXR-SHP-FTF cascade." *Am. J. Physiol. Gastrointest. Liver Physiol.* **288**: G60-G66.

Li, J. and Holbrook, N. J. (2004). "Elevated gadd153/chop expression and enhanced c-Jun N-terminal protein kinase activation sensitizes aged cells to ER stress." *Exp. Gerontol.* **39**(5): 735-744.

Li, J., Volpe, D. A., Wang, Y., Zhang, W., Bode, C., Owen, A. and Hidalgo, I. J. (2011a). "Use of transporter knockdown Caco-2 cells to investigate the in vitro efflux of statin drugs." *Drug Metab. Dispos.* **39**(7): 1196-1202.

Li, L., Chen, L., Hu, L., Liu, Y., Sun, H. Y., Tang, J., Hou, Y. J., Chang, Y. X., Tu, Q. Q., Feng, G. S., Shen, F., Wu, M. C. and Wang, H. Y. (2011b). "Nuclear factor high-mobility group box1 mediating the activation of toll-like receptor 4 signaling in hepatocytes in the early stage of nonalcoholic fatty liver disease in mice." *Hepatology.*

Li, Q., Liu, Z., Guo, J., Chen, J., Yang, P., Tian, J., Sun, J., Zong, Y. and Qu, S. (2009). "Cholesterol overloading leads to hepatic L02 cell damage through activation of the unfolded protein response." *Int. J. Mol. Med.* **24**(4): 459-464.

Li, W., Dalen, H., Eaton, J. W. and Yuan, X. M. (2001). "Apoptotic death of inflammatory cells in human atheroma." *Arterioscler. Thromb. Vasc. Biol.* **21**(7): 1124-1130.

Lim, C., Sohn, H., Gwack, Y. and Choe, J. (2000). "Latency-associated nuclear antigen of Kaposi's sarcoma-associated herpesvirus (human herpesvirus-8) binds ATF4/CREB2 and inhibits its transcriptional activation activity." *J. Gen. Virol.* **81**(Pt 11): 2645-2652.

Lin, Y., Devin, A., Cook, A., Keane, M. M., Kelliher, M., Lipkowitz, S. and Liu, Z. G. (2000). "The death domain kinase RIP is essential for TRAIL (Apo2L)-induced activation of IkappaB kinase and c-Jun N-terminal kinase." *Mol. Cell. Biol.* **20**(18): 6638-6645.

Lioudaki, E., Ganotakis, E. S. and Mikhailidis, D. P. (2011). "Ezetimibe; more than a low density lipoprotein cholesterol lowering drug? An update after 4 years." *Curr. Vasc. Pharm.* **9**(1): 62-86.

Liscum, L., Luskey, K. L., Chin, D. J., Ho, Y. K., Goldstein, J. L. and Brown, M. S. (1983). "Regulation of 3-hydroxy-3-methylglutaryl coenzyme A reductase and its mRNA in rat liver as studied with a monoclonal antibody and a cDNA probe." *J. Biol. Chem.* **258**(13): 8450-8455.

Liu, H., Jones, B. E., Bradham, C. and Czaja, M. J. (2002a). "Increased cytochrome P-450 2E1 expression sensitizes hepatocytes to c-Jun-mediated cell death from TNF-alpha." *Am. J. Physiol. Gastrointest. Liver Physiol.* **282**(2): G257-266.

Liu, H., Lo, C. R. and Czaja, M. J. (2002b). "NF-kappaB inhibition sensitizes hepatocytes to TNF-induced apoptosis through a sustained activation of JNK and c-Jun." *Hepatology* **35**(4): 772-778.

Liu, X. Y., Nothias, J. M., Scavone, A., Garfinkel, M. and Millis, J. M. (2010). "Biocompatibility investigation of polyethylene glycol and alginate-poly-L-lysine for islet encapsulation." *ASAIO J.* **56**(3): 241-245.

Liu, Y., Binz, J., Numerick, M. J., Dennis, S., Luo, G., Desai, B., MacKenzie, K. I., Mansfield, T. A., Kliewer, S. A., Goodwin, B. and Jones, S. A. (2003). "Hepatoprotection by the farnesoid X receptor agonist GW4064 in rat models of intra- and extrahepatic cholestasis." *J. Clin. Invest.* **112**(11): 1678-1687.

Lordan, S., Mackrill, J. J. and O'Brien, N. M. (2008). "Involvement of Fas signalling in 7beta-hydroxycholesterol-and cholesterol-5beta,6beta-epoxide-induced apoptosis." *Int. J. Toxicol.* **27**(3): 279-285.

Lu, N., Li, Y., Qin, H., Zhang, Y. L. and Sun, C. H. (2008). "Gossypin up-regulates LDL receptor through activation of ERK pathway: a signaling mechanism for the hypocholesterolemic effect." *J. Agric. Food Chem.* **56**(23): 11526-11532.

Lu, S. C., Alvarez, L., Huang, Z. Z., Chen, L., An, W., Corrales, F. J., Avila, M. A., Kanel, G. and Mato, J. M. (2001). "Methionine adenosyltransferase 1A knockout mice are predisposed to liver injury and exhibit increased expression of genes involved in proliferation." *Proc. Natl. Acad. Sci. U. S. A.* **98**(10): 5560-5565.

Lu, S. C., Tsukamoto, H. and Mato, J. M. (2002). "Role of abnormal methionine metabolism in alcoholic liver injury." *Alcohol* **27**(3): 155-162.

Lu, X., Liu, J., Hou, F., Liu, Z., Cao, X., Seo, H. and Gao, B. (2011). "Cholesterol induces pancreatic beta cell apoptosis through oxidative stress pathway." *Cell Stress Chaperones* **16**(5): 539-548.

Lu, Y., Onda, M., Uchida, E., Yamamura, S., Yanagi, K., Matsushita, A., Kobayashi, T., Fukuhara, M., Aida, K. and Tajiri, T. (2000). "The cytotoxic effects of bile acids in crude bile on human pancreatic cancer cell lines." *Surg. Today* **30**(10): 903-909.

Luc, G., Douste-Blazy, P. and Fruchart, J. C. (1989). "[Cholesterol: from where does it come, how does it circulate, where does it go?]." *Rev. Prat.* **39**(12): 1011-1017.

Ludi, H. and Hasselbach, W. (1982). "Fluorescence studies on N-(3-pyrene)maleinimide-labeled sarcoplasmic reticulum ATPase in native and solubilized membranes." *Z Naturforsch C* **37**(11-12): 1170-1179.

Lund, E. G., Menke, J. G. and Sparrow, C. P. (2003). "Liver X receptor agonists as potential therapeutic agents for dyslipidemia and atherosclerosis." *Arterioscler. Thromb. Vasc. Biol.* **23**(7): 1169-1177.

Lunde, G. (1930). "The 1927 and 1928 Nobel chemistry prize winners, Wieland and Windaus." *J. Chem. Educ.* 7(8): 1763.

Ma, K. L., Ruan, X. Z., Powis, S. H., Chen, Y., Moorhead, J. F. and Varghese, Z. (2008). "Inflammatory stress exacerbates lipid accumulation in hepatic cells and fatty livers of apolipoprotein E knockout mice." *Hepatology* **48**(3): 770-781.

Madon, J., Eckhardt, U., Gerloff, T., Stieger, B. and Meier, P. J. (1997). "Functional expression of the rat liver canalicular isoform of the multidrug resistance-associated protein." *FEBS Lett.* **406**(1-2): 75-78.

Malerod, L., Juvet, L. K., Hanssen-Bauer, A., Eskild, W. and Berg, T. (2002). "Oxysterol-activated LXRalpha/RXR induces hSR-BI-promoter activity in hepatoma cells and preadipocytes." *Biochem. Biophys. Res. Commun.* **299**(5): 916-923.

Malerod, L., Sporstol, M., Juvet, L. K., Mousavi, S. A., Gjoen, T., Berg, T., Roos, N. and Eskild, W. (2005). "Bile acids reduce SR-BI expression in hepatocytes by a pathway involving FXR/RXR, SHP, and LRH-1." *Biochem. Biophys. Res. Commun.* **336**(4): 1096-1105.

Malhi, H., Bronk, S. F., Werneburg, N. W. and Gores, G. J. (2006). "Free fatty acids induce JNK-dependent hepatocyte lipoapoptosis." *J. Biol. Chem.* **281**(17): 12093-12101.

Malhi, H. and Gores, G. J. (2008). "Molecular mechanisms of lipotoxicity in nonalcoholic fatty liver disease." *Semin. Liver Dis.* **28**(4): 360-369.

Manchekar, M., Richardson, P. E., Forte, T. M., Datta, G., Segrest, J. P. and Dashti, N. (2004). "Apolipoprotein B-containing lipoprotein particle assembly." *J. Biol. Chem.* **279**: 39757-39766.

Marais, A. D., Firth, J. C., Bateman, M. E., Byrnes, P., Martens, C. and Mountney, J. (1997). "Atorvastatin: an effective lipid-modifying agent in familial hypercholesterolemia." *Arterioscler. Thromb. Vasc. Biol.* **17**(8): 1527-1531.

Marchant, C. E., Van der Veen, C., Law, N. S., Hardwick, S. J., Carpenter, K. L. and Mitchinson, M. J. (1996). "Oxidation of low-density lipoprotein by human monocyte-macrophages results in toxicity to the oxidising culture." *Free Radical Res.* **24**(5): 333-342.

Mari, M., Caballero, F., Colell, A., Morales, A., Caballeria, J., Fernandez, A., Enrich, C., Fernandez-Checa, J. C. and Garcia-Ruiz, C. (2006). "Mitochondrial free cholesterol loading sensitizes to TNF- and Fas-mediated steatohepatitis." *Cell Metab.* **4**(3): 185-198.

Mariathasan, S. and Monack, D. M. (2007). "Inflammasome adaptors and sensors: intracellular regulators of infection and inflammation." *Nat. Rev. Immunol.* **7**(1): 31-40.

Mariathasan, S., Weiss, D. S., Newton, K., McBride, J., O'Rourke, K., Roose-Girma, M., Lee, W. P., Weinrauch, Y., Monack, D. M. and Dixit, V. M. (2006). "Cryopyrin activates the inflammasome in response to toxins and ATP." *Nature* **440**(7081): 228-232.

Marra, F., Romanelli, R. G., Giannini, C., Failli, P., Pastacaldi, S., Arrighi, M. C., Pinzani, M., Laffi, G., Montalto, P. and Gentilini, P. (1999). "Monocyte chemotactic protein-1 as a chemoattractant for human hepatic stellate cells." *Hepatology* **29**(1): 140-148.

Martin, C. E. and Thompson, G. A., Jr. (1978). "Use of fluorescence polarization to monitor intracellular membrane changes during temperature acclimation.

Correlation with lipid compositional and ultrastructural changes." *Biochemistry* **17**(17): 3581-3586.

Martin, T., Cardarelli, P. M., Parry, G. C., Felts, K. A. and Cobb, R. R. (1997). "Cytokine induction of monocyte chemoattractant protein-1 gene expression in human endothelial cells depends on the cooperative action of NF-kappa B and AP-1." *Eur. J. Immunol.* **27**(5): 1091-1097.

Masters, S. L., Latz, E. and O'Neill, L. A. (2011). "The inflammasome in atherosclerosis and type 2 diabetes." *Sci Transl Med* **3**(81): 81ps17.

Mathews, C. K., van Holde, K. E. and Ahern, K. G. (2000). *Biochemistry. Third Edition.* New York, Addison Wesley Longman, Inc.

Mathur, A., Walker, J. J., Al-Azzawi, H. H., Lu, D., Swartz-Basile, D. A., Nakeeb, A. and Pitt, H. A. (2007). "Ezetimibe ameliorates cholecystosteatosis." *Surgery* **142**(2): 228-233.

Matteoni, C. A., Younossi, Z. M., Gramlich, T., Boparai, N., Liu, Y. C. and McCullough, A. J. (1999). "Nonalcoholic fatty liver disease: a spectrum of clinical and pathological severity." *Gastroenterology* **116**(6): 1413-1419.

Mattey, D. L. and Garrod, D. R. (1986). "Splitting and internalization of the desmosomes of cultured kidney epithelial cells by reduction in calcium concentration." *J. Cell Sci.* **85**: 113-124.

McCoy, A. J., Koizumi, Y., Higa, N. and Suzuki, T. (2010). "Differential regulation of caspase-1 activation via NLRP3/NLRC4 inflammasomes mediated by aerolysin and type III secretion system during Aeromonas veronii infection." *J. Immunol.* **185**(11): 7077-7084.

McCullough, A. J. (2006). "Pathophysiology of nonalcoholic steatohepatitis." *J. Clin. Gastroenterol.* **40 Suppl 1**: S17-29.

McKenna, N. J. and O'Malley, B. W. (2001). "Nuclear receptors, coregulators, ligands, and selective receptor modulators: making sense of the patchwork quilt." *Ann. N. Y. Acad. Sci.* **949**: 3-5.

McNamara, J. R., Warnick, G. R. and Cooper, G. R. (2006). "A brief history of lipid and lipoprotein measurements and their contribution to clinical chemistry." *Clin. Chim. Acta* **369**(2): 158-167.

McPherson, R. and Gauthier, A. (2004). "Molecular regulation of SREBP function: the Insig-SCAP connection and isoform-specific modulation of lipid synthesis." *Biochem. Cell Biol.* **82**: 201-211.

Meiner, V. L., Case, S., Myer, H. M., Sande, E. R., Bellosta, S., Schambelan, M., Pitas, R. E., McGuire, J., Herz, J. and Farese Jr., R. V. (1996). "Disruption of the acyl-CoA:cholesterol acyltransferase gene in mice: evidence suggesting multiple cholesterol esterification enzymes in mammals." *Proc. Natl. Acad. Sci. U. S. A.* **93**: 14041-14046.

Memon, R. A., Grunfeld, C. and Feingold, K. R. (2001). "TNF-alpha is not the cause of fatty liver disease in obese diabetic mice." *Nat. Med.* **7**(1): 2-3.

Mencacci, A., Bacci, A., Cenci, E., Montagnoli, C., Fiorucci, S., Casagrande, A., Flavell, R. A., Bistoni, F. and Romani, L. (2000). "Interleukin 18 restores defective Th1 immunity to Candida albicans in caspase 1-deficient mice." *Infect. Immun.* **68**(9): 5126-5131.

Mendler, M. H., Kanel, G. and Govindarajan, S. (2005). "Proposal for a histological scoring and grading system for non-alcoholic fatty liver disease." *Liver Int.* **25**(2): 294-304.

Mercer, S. W. and Trayhurn, P. (1987). "Effect of high fat diets on energy balance and thermogenesis in brown adipose tissue of lean and genetically obese ob/ob mice." *J. Nutr.* **117**(12): 2147-2153.

Meshkani, R. and Adeli, K. (2009). "Hepatic insulin resistance, metabolic syndrome and cardiovascular disease." *Clin. Biochem.* **42**(13-14): 1331-1346.

Miao, E. A., Mao, D. P., Yudkovsky, N., Bonneau, R., Lorang, C. G., Warren, S. E., Leaf, I. A. and Aderem, A. (2010). "Innate immune detection of the type III secretion apparatus through the NLRC4 inflammasome." *Proc. Natl. Acad. Sci. U. S. A.* **107**(7): 3076-3080.

Miao, J., Choi, S. E., Seok, S. M., Yang, L., Zuercher, W. J., Xu, Y., Willson, T. M., Xu, H. E. and Kemper, J. K. (2011). "Ligand-dependent regulation of the activity of the orphan nuclear receptor, small heterodimer partner (SHP), in the repression of bile acid biosynthetic CYP7A1 and CYP8B1 genes." *Mol. Endocrinol.* **25**(7): 1159-1169.

Mihalcea, C. and Pandele, G. I. (2010). "[Correlation between atherosclerosis--coronary disease and insulin resistance, regarded as the basis of metabolic syndrome]." *Rev. Med. Chir. Soc. Med. Nat. Iasi* **114**(1): 59-68.

Mihalik, S. J., Steinberg, S. J., Pei, Z., Park, J., Kim, D. G., Heinzer, A. K., Dacremont, G., Wanders, R. J. A., Cubas, D. A., Smith, K. D. and Watkins, P. A. (2002). "Participation of two members of the very long-chain acyl-CoA synthetase family in bile acid synthesis and recycling." *J. Biol. Chem.* **277**(27): 24771-24779.

Miller, S. J., Parker, R. A. and Gibson, D. M. (1989). "Phosphorylation and degradation of HMG-CoA reductase." *Adv. Enzyme Regul.* **28**: 65-77.

Miquilena-Colina, M. E., Lima-Cabello, E., Sanchez-Campos, S., Garcia-Mediavilla, M. V., Fernandez-Bermejo, M., Lozano-Rodriguez, T., Vargas-Castrillon, J., Buque, X., Ochoa, B., Aspichueta, P., Gonzalez-Gallego, J. and Garcia-Monzon, C. (2011). "Hepatic fatty acid translocase CD36 upregulation is associated with insulin resistance, hyperinsulinaemia and increased steatosis in non-alcoholic steatohepatitis and chronic hepatitis C." *Gut.*

Misawa, K., Horiba, T., Arimura, N., Hirano, Y., Inoue, J., Emoto, N., Shimano, H., Shimizu, M. and Sato, R. (2003). "Sterol regulatory element-binding protein-2 interacts with hepatocyte nuclear factor-4 to enhance sterol isomerase gene expression in hepatocytes." *J. Biol. Chem.* **278**(38): 36176-36182.

Miura, K., Kodama, Y., Inokuchi, S., Schnabl, B., Aoyama, T., Ohnishi, H., Olefsky, J. M., Brenner, D. A. and Seki, E. (2010). "Toll-like receptor 9 promotes steatohepatitis by induction of interleukin-1beta in mice." *Gastroenterology* **139**(1): 323-334 e327.

Morganroth, J., Levy, R. I. and Fredrickson, D. S. (1975). "The biochemical, clinical, and genetic features of type III hyperlipoproteinemia." *Ann. Intern. Med.* **82**(2): 158-174.

Mori, K., Kawahara, T., Yoshida, H., Yanagi, H. and Yura, T. (1996). "Signalling from endoplasmic reticulum to nucleus: transcription factor with a basic-leucine zipper motif is required for the unfolded protein-response pathway." *Genes Cells* **1**(9): 803-817.

Mori, S., Yamasaki, T., Sakaida, I., Takami, T., Sakaguchi, E., Kimura, T., Kurokawa, F., Maeyama, S. and Okita, K. (2004). "Hepatocellular carcinoma with nonalcoholic steatohepatitis." *J. Gastroenterol.* **39**(4): 391-396.

Mullick, A. E., Tobias, P. S. and Curtiss, L. K. (2005). "Modulation of atherosclerosis in mice by Toll-like receptor 2." *J. Clin. Invest.* **115**(11): 3149-3156.

Muraoka, T., Aoki, K., Iwasaki, T., Shinoda, K., Nakamura, A., Aburatani, H., Mori, S., Tokuyama, K., Kubota, N., Kadowaki, T. and Terauchi, Y. (2011).

"Ezetimibe decreases SREBP-1c expression in liver and reverses hepatic insulin resistance in mice fed a high-fat diet." *Metabolism.* **60**(5): 617-628.

Muroya, T., Ihara, Y., Ikeda, S., Yasuoka, C., Miyahara, Y., Urata, Y., Kondo, T. and Kohno, S. (2003). "Oxidative modulation of NF-kappaB signaling by oxidized low-density lipoprotein." *Biochem. Biophys. Res. Commun.* **309**(4): 900-905.

Murthy, S., Born, E., Mathur, S. N. and Field, F. J. (2002). "LXR/RXR activation enhances basolateral efflux of cholesterol in CaCo-2 cells." *J. Lipid Res.* **43**: 1054-1065.

Musanti, R., Giorgini, L., Lovisolo, P. P., Pirillo, A., Chiari, A. and Ghiselli, G. (1996). "Inhibition of acyl-CoA: cholesterol acyltransferase decreases apolipoprotein B-100-containing lipoprotein secretion from HepG2 cells." *J. Lipid Res.* **37**(1): 1-14.

Nagai, M., Sakakibara, J., Nakamura, Y., Gejyo, F. and Ono, T. (2002). "SREBP-2 and NF-Y are involved in the transcriptional regulation of squalene epoxidase." *Biochem. Biophys. Res. Commun.* **295**(1): 74-80.

Namazi, M. R. (2002). "Minor thalassemia as a protective factor against cerebrovascular accidents." *Med. Hypotheses* **59**(3): 361-362.

Nan, Y. M., Wu, W. J., Yao, X. X. and Wang, L. (2007). "[The role of apoptosis and the related genes in non-alcoholic steatohepatitis]." *Zhonghua Gan Zang Bing Za Zhi* **15**(1): 41-46.

Nanji, A. A., Jokelainen, K., Rahemtulla, A., Miao, L., Fogt, F., Matsumoto, H., Tahan, S. R. and Su, G. L. (1999). "Activation of nuclear factor kappa B and cytokine imbalance in experimental alcoholic liver disease in the rat." *Hepatology* **30**(4): 934-943.

Napolitano, L. M., Lopez, J., Saland, L., Sterzing, P. V. and Kelley, R. O. (1972). "Localization of cholesterol in peripheral nerve: use of (3 H) digitonin for electron microscopic autoradiography." *Anat. Rec.* **174**(2): 157-164.

Nassir, F., Wilson, B., Han, X., Gross, R. W. and Abumrad, N. A. (2007). "CD36 is important for fatty acid and cholesterol uptake by the proximal but not distal intestine." *J. Biol. Chem.* **282**(19493-19501).

Natarajan, R., Ghosh, S. and Grogan, W. M. (1999). "Regulation of the rat neutral cytosolic cholesteryl ester hydrolase promoter by hormones and sterols: a role for nuclear factor-Y in the sterol-mediated response." *J. Lipid Res.* **40**(11): 2091-2098.

Natoli, G., Costanzo, A., Ianni, A., Templeton, D. J., Woodgett, J. R., Balsano, C. and Levrero, M. (1997). "Activation of SAPK/JNK by TNF receptor 1 through a noncytotoxic TRAF2-dependent pathway." *Science* **275**(5297): 200-203.

Nemchausky, B. A., Layden, T. J. and Boyer, J. L. (1977). "Effects of chronic choleretic infusions of bile acids on the membrane of the bile canaliculus. A biochemical and morphologic study." *Lab. Invest.* **36**(3): 259-267.

Ness, G. C. (1983). "Regulation of 3-hydroxy-3-methylglutaryl coenzyme A reductase." *Mol. Cell. Biochem.* **53/54**: 299-306.

Netea, M. G., Kullberg, B. J., Verschueren, I. and Van Der Meer, J. W. (2000). "Interleukin-18 induces production of proinflammatory cytokines in mice: no intermediate role for the cytokines of the tumor necrosis factor family and interleukin-1beta." *Eur. J. Immunol.* **30**(10): 3057-3060.

Neuschwander-Tetri, B. A. (2010a). "Hepatic lipotoxicity and the pathogenesis of nonalcoholic steatohepatitis: the central role of nontriglyceride fatty acid metabolites." *Hepatology* **52**(2): 774-788.

Neuschwander-Tetri, B. A. (2010b). "Nontriglyceride hepatic lipotoxicity: the new paradigm for the pathogenesis of NASH." *Curr. Gastroenterol. Rep.* **12**(1): 49-56.

Nishikori, M. (2005). "Classical and alternative NF-κB activation pathways and their roles in lymphoid malignancies." *J. Clin. Exp. Hematop.* **45**(15-25).

Nomura, M., Ishii, H., Kawakami, A. and Yoshida, M. (2009). "Inhibition of Hepatic Neiman-Pick C1-Like 1 Improves Hepatic Insulin Resistance." *Am. J. Physiol. Endocrinol. Metab.*

Norata, G. D., Pirillo, A., Callegari, E., Hamsten, A., Catapano, A. L. and Eriksson, P. (2003). "Gene expression and intracellular pathways involved in endothelial dysfunction induced by VLDL and oxidised VLDL." *Cardiovasc. Res.* **59**(1): 169-180.

Norlin, M. and Chiang, J. Y. (2004). "Transcriptional regulation of human oxysterol 7alpha-hydroxylase by sterol response element binding protein." *Biochem. Biophys. Res. Commun.* **316**(1): 158-164.

Nouchi, T., Tanaka, Y., Tsukada, T., Sato, C. and Marumo, F. (1991). "Appearance of alpha-smooth-muscle-actin-positive cells in hepatic fibrosis." *Liver* **11**(2): 100-105.

Oakes, N. D., Cooney, G. J., Camilleri, S., Chisholm, D. J. and Kraegen, E. W. (1997). "Mechanisms of liver and muscle insulin resistance induced by chronic high-fat feeding." *Diabetes* **46**(11): 1768-1774.

Ohta, T., Miyajima, K. and Yamada, T. (2007). "A high-sucrose diet induces fatty liver, but not deterioration of diabetes mellitus in Zucker diabetic fatty rats." *Res. Commun. Mol. Pathol. Pharmacol.* **120-121**(1-6): 55-64.

Okada, T., Haze, K., Nadanaka, S., Yoshida, H., Seidah, N. G., Hirano, Y., Sato, R., Negishi, M. and Mori, K. (2003). "A serine protease inhibitor prevents endoplasmic reticulum stress-induced cleavage but not transport of the membrane-bound transcription factor ATF6." *J. Biol. Chem.* **278**(33): 31024-31032.

Okros, I. (1968). "Digitonin reaction in electron microscopy." *Histochemie* **13**(1): 91-96.

Olsen, A. L., Bloomer, S. A., Chan, E. P., Gaca, M. D., Georges, P. C., Sackey, B., Uemura, M., Janmey, P. A. and Wells, R. G. (2011). "Hepatic stellate cells require a stiff environment for myofibroblastic differentiation." *Am. J. Physiol. Gastrointest. Liver Physiol.* **301**(1): G110-118.

Olson, R. E. (1998). "Discovery of the lipoproteins, their role in fat transport and their significance as risk factors." *J. Nutr.* **128**: 439-443.

Omkumar, R. V., Darnay, B. G. and Rodwell, V. W. (1994). "Modulation of Syrian hamster 3-hydroxy-3-methylglutaryl-CoA reductase activity by phosphorylation. Role of serine 871." *J. Biol. Chem.* **269**(9): 6810-6814.

Ontko, J. A. and Zilversmit, D. B. (1967). "Metabolism of chylomicrons by the isolated rat liver." *J. Lipid Res.* **8**(2): 90-96.

Oram, J. F. (2003). "HDL apolipoproteins and ABCA1: partners in the removal of excess cellular cholesterol." *Arterioscler. Thromb. Vasc. Biol.* **23**: 720-727.

Oram, J. F. and Heinecke, J. W. (2005). "ATP-binding cassette transporter A1: A cell cholesterol exporter that protects against cardiovascular disease." *Physiol. Rev.* **85**: 1343-1372.

Oram, J. F. and Vaughan, A. M. (2000). "ABCA1-mediated transport of cellular cholesterol and phospholipids to HDL apolipoproteins." *Curr. Opin. Lipidol.* **11**(3): 253-260.

Ory, D. S. (2000). "Niemann-Pick type C: a disorder of cellular cholesterol trafficking." *Biochim. Biophys. Acta* **1529**(1-3): 331-339.

Osborne, T. F. (1991). "Single nucleotide resolution of sterol regulatory region in promoter for 3-hydroxy-3-methylglutaryl coenzyme A reductase." *J. Biol. Chem.* **266**(21): 13947-13951.

Oude Elferink, R. P. J., Meijer, D. K. F., Kuipers, F., Jansen, P. L. M., Groen, A. K. and Groothuis, G. M. M. (1995). "Hepatobiliary secretion of organic compounds; molecular mechanisms of membrane transport." *Biochim. Biophys. Acta* **1241**: 215-268.

Pai, J. T., Guryev, O., Brown, M. S. and Goldstein, J. L. (1998). "Differential stimulation of cholesterol and unsaturated fatty acid biosynthesis in cells expressing individual nuclear sterol regulatory element-binding proteins." *J. Biol. Chem.* **273**(40): 26138-26148.

Pak, Y. K. (1996). "Serum response element-like sequences of the human low density lipoprotein receptor promoter: possible regulation sites for sterol-independent transcriptional activation." *Biochem. Mol. Biol. Int.* **38**(1): 31-36.

Paolisso, G., Ferrannini, E., Sgambato, S., Varricchio, M. and D'Onofrio, F. (1992). "Hyperinsulinemia in patients with hypercholesterolemia." *J. Clin. Endocrinol. Metab.* **75**(6): 1409-1412.

Pape, M. E., Schultz, P. A., Rea, T. J., DeMattos, R. B., Kieft, K., Bisgaier, C. L., Newton, R. S. and Krause, B. R. (1995). "Tissue specific changes in acyl-CoA:cholesterol acyltransferase (ACAT) mRNA levels in rabbits." *J. Lipid Res.* **36**: 823-838.

Pare, J. F., Roy, S., Galarneau, L. and Belanger, L. (2001). "The mouse fetoprotein transcription factor (FTF) gene promoter is regulated by three GATA elements with tandem E box and Nkx motifs, and FTF in turn activates the Hnf3beta, Hnf4alpha, and Hnf1alpha gene promoters." *J. Biol. Chem.* **276**(16): 13136-13144.

Parini, P., Davis, M., Lada, A. T., Erickon, S. K., Wright, T. L., Gustafsson, U., Sahlin, S., Einarsson, C., Erickson, M., Angelin, B., Tomoda, H., Omura, S., Willingham, M. C. and Rudel, L. L. (2004). "ACAT2 is localized to hepatocytes and is the major cholesterol-esterifying enzyme in human liver." *Circulation* **110**: 2017-2023.

Park, H., Shima, T., Yamaguchi, K., Mitsuyoshi, H., Minami, M., Yasui, K., Itoh, Y., Yoshikawa, T., Fukui, M., Hasegawa, G., Nakamura, N., Ohta, M., Obayashi, H. and Okanoue, T. (2011). "Efficacy of long-term ezetimibe therapy in patients with nonalcoholic fatty liver disease." *J. Gastroenterol.* **46**(1): 101-107.

Park, H. Y., Kyeong, H., Park, D. S., Lee, H. S., Chang, H., Kim, Y. S. and Cho, K. H. (2008). "Correlation between insulin resistance and intracranial atherosclerosis in patients with ischemic stroke without diabetes." *J Stroke Cerebrovasc Dis* **17**(6): 401-405.

Park, K. J., Choi, S. H., Koh, M. S., Kim, D. J., Yie, S. W., Lee, S. Y. and Hwang, S. B. (2001). "Hepatitis C virus core protein potentiates c-Jun N-terminal kinase activation through a signaling complex involving TRADD and TRAF2." *Virus Res.* **74**(1-2): 89-98.

Parks, D. J., Blanchard, S. G., Bledsoe, R. K., Chandra, G., Consler, T. G., Kliewer, S. A., Stimmel, J. B., Willson, T. M., Zavacki, A. M., Moore, D. D. and Lehmann, J. M. (1999). "Bile acids: natural ligands for an orphan nuclear receptor." *Science* **284**(5418): 1365-1368.

Paszty, C., Maeda, N., Verstuyft, J. and Rubin, E. M. (1994). "Apolipoprotein AI transgene corrects apolipoprotein E deficiency-induced atherosclerosis in mice." *J. Clin. Invest.* **94**(2): 899-903.

Peet, D. J., D., T. S., Ma, W., Janowski, B. A., Lobaccaro, J.-M., A., Hammer, R. E. and Mangelsdorf, D. J. (1998a). "Cholesterol and bile acid metabolism are impaired in mice lacking the nuclear oxysterol receptor LXRα." *Cell* **93**: 693-704.

Peet, D. J., Turley, S. D., Ma, W., Janowski, B. A., Lobaccaro, J. M., Hammer, R. E. and Mangelsdorf, D. J. (1998b). "Cholesterol and bile acid metabolism are impaired in mice lacking the nuclear oxysterol receptor LXR alpha." *Cell* **93**(5): 693-704.

Perez-Aguilar, F. (2005). "[Etiopathogenesis of non-alcoholic steatohepatitis]." *Gastroenterol. Hepatol.* **28**(7): 396-406.

Perez, M. J. and Briz, O. (2009). "Bile-acid-induced cell injury and protection." *World J. Gastroenterol.* **15**(14): 1677-1689.

Persson, J., Nilsson, J. and Lindholm, M. W. (2006). "Cytokine response to lipoprotein lipid loading in human monocyte-derived macrophages." *Lipids Health Dis.* **5**: 17.

Petras, S. F., Lindsey, S. and Harwood, H. J., Jr. (1999). "HMG-CoA reductase regulation: use of structurally diverse first half-reaction squalene synthetase inhibitors to characterize the site of mevalonate-derived nonsterol regulator production in cultured IM-9 cells." *J. Lipid Res.* **40**(1): 24-38.

Petrilli, V., Papin, S., Dostert, C., Mayor, A., Martinon, F. and Tschopp, J. (2007). "Activation of the NALP3 inflammasome is triggered by low intracellular potassium concentration." *Cell Death Differ.* **14**(9): 1583-1589.

Pfaffenbach, K. T., Gentile, C. L., Nivala, A. M., Wang, D., Wei, Y. and Pagliassotti, M. J. (2010). "Linking endoplasmic reticulum stress to cell death in hepatocytes: roles of C/EBP homologous protein and chemical chaperones in palmitate-mediated cell death." *Am. J. Physiol. Endocrinol. Metab.* **298**(5): E1027-1035.

Phillips, M. C. (1990). "Cholesterol packing, crystallization and exchange properties in phosphatidylcholine vesicle systems." *Hepatology* **12**(3 Pt 2): 75S-80S; discussion 80S-82S.

Ping, D., Boekhoudt, G. H., Rogers, E. M. and Boss, J. M. (1999). "Nuclear factor-kappa B p65 mediates the assembly and activation of the TNF-responsive element of the murine monocyte chemoattractant-1 gene." *J. Immunol.* **162**(2): 727-734.

Pirhonen, J., Sareneva, T., Kurimoto, M., Julkunen, I. and Matikainen, S. (1999). "Virus infection activates IL-1 beta and IL-18 production in human macrophages by a caspase-1-dependent pathway." *J. Immunol.* **162**(12): 7322-7329.

Pramfalk, C., Angelin, B., Eriksson, M. and Parini, P. (2007). "Cholesterol regulates ACAT2 gene expression and enzyme activity in human hepatoma cells." *Biochem. Biophys. Res. Commun.* **364**(2): 402-409.

Pramfalk, C., Davis, M. A., Eriksson, M., Rudel, L. L. and Parini, P. (2005). "Control of ACAT2 liver expression by HNF1." *J. Lipid Res.* **46**(9): 1868-1876.

Pramfalk, C., Jiang, Z. Y., Cai, Q., Hu, H., Zhang, S. D., Han, T. Q., Eriksson, M. and Parini, P. (2010). "HNF1alpha and SREBP2 are important regulators of NPC1L1 in human liver." *J. Lipid Res.* **51**(6): 1354-1362.

Pramfalk, C., Karlsson, E., Groop, L., Rudel, L. L., Angelin, B., Eriksson, M. and Parini, P. (2009). "Control of ACAT2 liver expression by HNF4{alpha}: lesson from MODY1 patients." *Arterioscler. Thromb. Vasc. Biol.* **29**(8): 1235-1241.

Puri, P., Baillie, R. A., Wiest, M. M., Mirshahi, F., Choudhury, J., Cheung, O., Sargeant, C., Contos, M. J. and Sanyal, A. J. (2007). "A lipidomic analysis of nonalcoholic fatty liver disease." *Hepatology* **46**(4): 1081-1090.

Puri, P., Mirshahi, F., Cheung, O., Natarajan, R., Maher, J. W., Kellum, J. M. and Sanyal, A. J. (2008). "Activation and dysregulation of the unfolded protein response in nonalcoholic fatty liver disease." *Gastroenterology* **134**(2): 568-576.

Putcha, G. V., Le, S., Frank, S., Besirli, C. G., Clark, K., Chu, B., Alix, S., Youle, R. J., LaMarche, A., Maroney, A. C. and Johnson, E. M., Jr. (2003). "JNK-mediated BIM phosphorylation potentiates BAX-dependent apoptosis." *Neuron* **38**(6): 899-914.

Qu, Y., Franchi, L., Nunez, G. and Dubyak, G. R. (2007). "Nonclassical IL-1 beta secretion stimulated by P2X7 receptors is dependent on inflammasome activation and correlated with exosome release in murine macrophages." *J. Immunol.* **179**(3): 1913-1925.

Qu, Y., Ramachandra, L., Mohr, S., Franchi, L., Harding, C. V., Nunez, G. and Dubyak, G. R. (2009). "P2X7 receptor-stimulated secretion of MHC class II-containing exosomes requires the ASC/NLRP3 inflammasome but is independent of caspase-1." *J. Immunol.* **182**(8): 5052-5062.

Quack, M., Frank, C. and Carlberg, C. (2002). "Differential nuclear receptor signalling from DR4-type response elements." *J. Cell. Biochem.* **86**(3): 601-612.

Quinet, E. M., Savio, D. A., Halpern, A. R., Chen, L., Schuster, G. U., Gustafsson, J. A., Basso, M. D. and Nambi, P. (2006). "Liver X receptor (LXR)-beta regulation in LXRalpha-deficient mice: implications for therapeutic targeting." *Mol. Pharmacol.* **70**(4): 1340-1349.

Rabinowitz, S. S. and Gordon, S. (1991). "Macrosialin, a macrophage-restricted membrane sialoprotein differentially glycosylated in response to inflammatory stimuli." *J. Exp. Med.* **174**(4): 827-836.

Radhakrishnan, A., Goldstein, J. L., McDonald, J. G. and Brown, M. S. (2008). "Switch-like control of SREBP-2 transport triggered by small changes in ER cholesterol: a delicate balance." *Cell Metab.* **8**(6): 512-521.

Rajamaki, K., Lappalainen, J., Oorni, K., Valimaki, E., Matikainen, S., Kovanen, P. T. and Eklund, K. K. (2010). "Cholesterol crystals activate the NLRP3 inflammasome in human macrophages: a novel link between cholesterol metabolism and inflammation." *PLoS ONE* **5**(7): e11765.

Ramalho, R. M., Cortez-Pinto, H., Castro, R. E., Sola, S., Costa, A., Moura, M. C., Camilo, M. E. and Rodrigues, C. M. (2006). "Apoptosis and Bcl-2 expression in the livers of patients with steatohepatitis." *Eur. J. Gastroenterol. Hepatol.* **18**(1): 21-29.

Ramm, G. A., Shepherd, R. W., Hoskins, A. C., Greco, S. A., Ney, A. D., Pereira, T. N., Bridle, K. R., Doecke, J. D., Meikle, P. J., Turlin, B. and Lewindon, P. J. (2009). "Fibrogenesis in pediatric cholestatic liver disease: role of taurocholate and hepatocyte-derived monocyte chemotaxis protein-1 in hepatic stellate cell recruitment." *Hepatology* **49**(2): 533-544.

Ramprasad, M. P., Terpstra, V., Kondratenko, N., Quehenberger, O. and Steinberg, D. (1996). "Cell surface expression of mouse macrosialin and human CD68 and their role as macrophage receptors for oxidized low density lipoprotein." *Proc. Natl. Acad. Sci. U. S. A.* **93**(25): 14833-14838.

Rausa, F. M., Galarneau, L., Belanger, L. and Costa, R. H. (1999). "The nuclear receptor fetoprotein transcription factor is coexpressed with its target gene HNF-3beta in the developing murine liver, intestine and pancreas." *Mech. Dev.* **89**(1-2): 185-188.

Rector, R. S., Thyfault, J. P., Uptergrove, G. M., Morris, E. M., Naples, S. P., Borengasser, S. J., Mikus, C. R., Laye, M. J., Laughlin, M. H., Booth, F. W. and Ibdah, J. A. (2010). "Mitochondrial dysfunction precedes insulin resistance and hepatic steatosis and contributes to the natural history of non-alcoholic fatty liver disease in an obese rodent model." *J. Hepatol.* **52**(5): 727-736.

Reid, V. C. and Mitchinson, M. J. (1993). "Toxicity of oxidised low density lipoprotein towards mouse peritoneal macrophages in vitro." *Atherosclerosis* **98**(1): 17-24.

Reinhard, C., Shamoon, B., Shyamala, V. and Williams, L. T. (1997). "Tumor necrosis factor alpha-induced activation of c-jun N-terminal kinase is mediated by TRAF2." *EMBO J.* **16**(5): 1080-1092.

Ren, S., Hylemon, P. B., Marques, D., Gurley, E., Bodhan, P., Hall, E., Redford, K., Gil, G. and Pandak, W. M. (2004). "Overexpression of cholesterol transporter StAR increases in vivo rates of bile acid synthesis in the rat and mouse." *Hepatology* **40**(4): 910-917.

Renart, J., Reiser, J. and Stark, G. R. (1979). "Transfer of proteins from gels to diazobenzyloxymethyl-paper and detection with antisera: a method for studying antibody specificity and antigen structure." *Proc. Natl. Acad. Sci. U. S. A.* **76**(7): 3116-3120.

Repa, J. J., Berge, K. E., Pomajzl, C., Richardson, J. A., Hobbs, H. and Mangelsdorf, D. J. (2002). "Regulation of ATP-binding cassette sterol transporters ABCG5 and ABCG8 by the liver X receptors alpha and beta." *J. Biol. Chem.* **277**(21): 18793-18800.

Repa, J. J. and Mangelsdorf, D. J. (2002). "The liver X receptor gene team: potential new players in atherosclerosis." *Nat. Med.* **8**(11): 1243-1248.

Ribeiro, P. S., Cortez-Pinto, H., Sola, S., Castro, R. E., Ramalho, R. M., Baptista, A., Moura, M. C., Camilo, M. E. and Rodrigues, C. M. (2004). "Hepatocyte apoptosis, expression of death receptors, and activation of NF-kappaB in the liver of nonalcoholic and alcoholic steatohepatitis patients." *Am. J. Gastroenterol.* **99**(9): 1708-1717.

Rilling, H. C. and Chayet, L. T. (1985). Biosynthesis of cholesterol. *Sterols and bile acids*. Danielsson, H. and Sjövall, J., Elsevier: 1-40.

Rinella, M. E., Elias, M. S., Smolak, R. R., Fu, T., Borensztajn, J. and Green, R. M. (2008). "Mechanisms of hepatic steatosis in mice fed a lipogenic methionine choline-deficient diet." *J. Lipid Res.* **49**(5): 1068-1076.

Rinella, M. E. and Green, R. M. (2004). "The methionine-choline deficient dietary model of steatohepatitis does not exhibit insulin resistance." *J. Hepatol.* **40**(1): 47-51.

Rinella, M. E., Siddiqui, M. S., Gardikiotes, K., Gottstein, J., Elias, M. and Green, R. M. (2011). "Dysregulation of the unfolded protein response in db/db mice with diet induced steatohepatitis." *Hepatology*.

Rivera, C. A., Gaskin, L., Allman, M., Pang, J., Brady, K., Adegboyega, P. and Pruitt, K. (2010). "Toll-like receptor-2 deficiency enhances non-alcoholic steatohepatitis." *BMC Gastroenterol.* **10**: 52.

Robertson, G., Leclercq, I. and Farrell, G. C. (2001). "Nonalcoholic steatosis and steatohepatitis. II. Cytochrome P-450 enzymes and oxidative stress." *Am. J. Physiol. Gastrointest. Liver Physiol.* **281**(5): G1135-1139.

Roitelman, J. and Shechter, I. (1984). "Regulation of rat liver 3-hydroxy-3-methylglutaryl coenzyme A reductase." *J. Biol. Chem.* **259**: 870-877.

Roth, G., Kotzka, J., Kremer, L., Lehr, S., Lohaus, C., Meyer, H. E., Krone, W. and Muller-Wieland, D. (2000). "MAP kinases Erk1/2 phosphorylate sterol regulatory element-binding protein (SREBP)-1a at serine 117 in vitro." *J. Biol. Chem.* **275**(43): 33302-33307.

Roth, W. and Reed, J. C. (2004). "FLIP protein and TRAIL-induced apoptosis." *Vitam. Horm.* **67**: 189-206.

Roulston, A., Reinhard, C., Amiri, P. and Williams, L. T. (1998). "Early activation of c-Jun N-terminal kinase and p38 kinase regulate cell survival in response to tumor necrosis factor alpha." *J. Biol. Chem.* **273**(17): 10232-10239.

Ruan, X. Z., Varghese, Z. and Moorhead, J. F. (2009). "An update on the lipid nephrotoxicity hypothesis." *Nat Rev Nephrol* **5**(12): 713-721.

Ruetz, S. and Gros, P. (1994). "A mechanism for P-glycoprotein action in multidrug resistance: are we there yet?" *Trends Pharmacol. Sci.* **15**(7): 260-263.

Ruiz, A. G., Casafont, F., Crespo, J., Cayon, A., Mayorga, M., Estebanez, A., Fernadez-Escalante, J. C. and Pons-Romero, F. (2007). "Lipopolysaccharide-binding protein plasma levels and liver TNF-alpha gene expression in obese patients: evidence for the potential role of endotoxin in the pathogenesis of non-alcoholic steatohepatitis." *Obes. Surg.* **17**(10): 1374-1380.

Rull, A., Rodriguez, F., Aragones, G., Marsillach, J., Beltran, R., Alonso-Villaverde, C., Camps, J. and Joven, J. (2009). "Hepatic monocyte chemoattractant protein-1 is upregulated by dietary cholesterol and contributes to liver steatosis." *Cytokine* **48**(3): 273-279.

Russell, D. W. (2003). "The enzymes, regulation, and genetics of bile acid synthesis." *Annu. Rev. Biochem.* **72**: 137-174.

Ryabinin, A. E., Wang, Y. M. and Finn, D. A. (1999). "Different levels of Fos immunoreactivity after repeated handling and injection stress in two inbred strains of mice." *Pharmacol. Biochem. Behav.* **63**(1): 143-151.

Ryan, L., O'Callaghan, Y. C. and O'Brien, N. M. (2005). "The role of the mitochondria in apoptosis induced by 7beta-hydroxycholesterol and cholesterol-5beta,6beta-epoxide." *Br. J. Nutr.* **94**(4): 519-525.

Rytomaa, M., Martins, L. M. and Downward, J. (1999). "Involvement of FADD and caspase-8 signalling in detachment-induced apoptosis." *Curr. Biol.* **9**(18): 1043-1046.

Ryu, M. H. and Cha, Y. S. (2003). "The effects of a high-fat or high-sucrose diet on serum lipid profiles, hepatic acyl-CoA synthetase, carnitine palmitoyltransferase-I, and the acetyl-CoA carboxylase mRNA levels in rats." *J. Biochem. Mol. Biol.* **36**(3): 312-318.

Rzouq, F. S., Volk, M. L., Hatoum, H. H., Talluri, S. K., Mummadi, R. R. and Sood, G. K. (2010). "Hepatotoxicity fears contribute to underutilization of statin medications by primary care physicians." *Am. J. Med. Sci.* **340**(2): 89-93.

Sabesin, S. M. and Frase, S. (1977). "Electron microscopic studies of the assembly, intracellular transport, and secretion of chylomicrons by rat intestine." *J. Lipid Res.* **18**(4): 496-511.

Sabroe, I., Dower, S. K. and Whyte, M. K. (2005). "The role of Toll-like receptors in the regulation of neutrophil migration, activation, and apoptosis." *Clin. Infect. Dis.* **41 Suppl 7**: S421-426.

Sahoo, D., Trischuk, T. C., Chan, T., Drover, V. A. B., JHo, S., Chimini, G., Agellon, L. B., Agnihotri, R., Francis, G. A. and Lehner, R. (2004). "ABCA1-dependent lipid efflux to apolipoprotein A-I mediates HDL particle

formation and decreases VLDL secretion from murine hepatocytes." *J. Lipid Res.* **45**: 1122-1131.

Sakakura, Y., Shimano, H., Sone, H., Takahashi, A., Inoue, N., Toyoshima, H., Suzuki, S. and Yamada, N. (2001). "Sterol regulatory element-binding proteins induce an entire pathway of cholesterol synthesis." *Biochem. Biophys. Res. Commun.* **286**(1): 176-183.

Sansonetti, P. J., Phalipon, A., Arondel, J., Thirumalai, K., Banerjee, S., Akira, S., Takeda, K. and Zychlinsky, A. (2000). "Caspase-1 activation of IL-1beta and IL-18 are essential for Shigella flexneri-induced inflammation." *Immunity* **12**(5): 581-590.

Sanyal, A. J., Banas, C., Sargeant, C., Luketic, V. A., Sterling, R. K., Stravitz, R. T., Shiffman, M. L., Heuman, D., Coterrell, A., Fisher, R. A., Contos, M. J. and Mills, A. S. (2006). "Similarities and differences in outcomes of cirrhosis due to nonalcoholic steatohepatitis and hepatitis C." *Hepatology* **43**(4): 682-689.

Sanyal, A. J., Campbell-Sargent, C., Mirshahi, F., Rizzo, W. B., Contos, M. J., Sterling, R. K., Luketic, V. A., Shiffman, M. L. and Clore, J. N. (2001). "Nonalcoholic steatohepatitis: association of insulin resistance and mitochondrial abnormalities." *Gastroenterology* **120**(5): 1183-1192.

Sathiaraj, E., Chutke, M., Reddy, M. Y., Pratap, N., Rao, P. N., Reddy, D. N. and Raghunath, M. (2011). "A case-control study on nutritional risk factors in non-alcoholic fatty liver disease in Indian population." *Eur. J. Clin. Nutr.* **65**(4): 533-537.

Sato, R., Goldstein, J. L. and Brown, M. S. (1993). "Replacement of serine-871 of hamster 3-hydroxy-3-methylglutaryl-CoA reductase prevents phosphorylation by AMP-activated kinase and blocks inhibition of sterol synthesis induced by ATP depletion." *Proc. Natl. Acad. Sci. U. S. A.* **90**: 9261-9265.

Sato, R., Miyamoto, W., Inoue, J., Terada, T., Imanaka, T. and Maeda, M. (1999). "Sterol regulatory element-binding protein negatively regulates microsomal triglyceride transfer protein gene transcription." *J. Biol. Chem.* **274**(35): 24714-24720.

Schattenberg, J. M., Singh, R., Wang, Y., Lefkowitch, J. H., Rigoli, R. M., Scherer, P. E. and Czaja, M. J. (2006). "JNK1 but not JNK2 promotes the development of steatohepatitis in mice." *Hepatology* **43**(1): 163-172.

Scheen, A. J. and Luyckx, F. H. (2003). "Nonalcoholic steatohepatitis and insulin resistance: interface between gastroenterologists and endocrinologists." *Acta Clin. Belg.* **58**(2): 81-91.

Scheidereit, C. (2006). "IkappaB kinase complexes: gateways to NF-kappaB activation and transcription." *Oncogene* **25**(51): 6685-6705.

Schmitz, F. J. and McDonald, F. J. (1974). "Determination of hepatic cholesterol 7alpha-hydroxylase activity in man." *J. Lipid Res.* **15**(2): 146-151.

Schoonjans, K., Annicotte, J. S., Huby, T., Botrugno, O. A., Fayard, E., Udea, Y., Chapman, J. and Auwerx, J. (2002). "Liver receptor homolog 1 controls the expression of the scavenger receptor class B type I." *EMBO Rep.* **3**(12): 1181-1187.

Schrauwen, P., Schrauwen-Hinderling, V., Hoeks, J. and Hesselink, M. K. (2010). "Mitochondrial dysfunction and lipotoxicity." *Biochim. Biophys. Acta* **1801**(3): 266-271.

Schroder, M. and Kaufman, R. J. (2005). "The mammalian unfolded protein response." *Annu. Rev. Biochem.* **74**: 739-789.

Schroepfer, G. J., Jr. (2000). "Oxysterols: modulators of cholesterol metabolism and other processes." *Physiol. Rev.* **80**(1): 361-554.

Schuetz, E. G., Li, D., Omiecinski, C. J., Muller-Eberhard, U., Kleinman, H. K., Elswick, B. and Guzelian, P. S. (1988). "Regulation of gene expression in adult rat hepatocytes cultured on a basement membrane matrix." *J. Cell. Physiol.* **134**(3): 309-323.

Schuetz, E. G., Schuetz, J. D., May, B. and Guzelian, P. S. (1990). "Regulation of cytochrome P-450b/e and P-450p gene expression by growth hormone in adult rat hepatocytes cultured on a reconstituted basement membrane." *J. Biol. Chem.* **265**(2): 1188-1192.

Schuster, G. U., Parini, P., Wang, L., Alberti, S., Steffensen, K. R., Hansson, G. K., Angelin, B. and Gustafsson, J. A. (2002). "Accumulation of foam cells in liver X receptor-deficient mice." *Circulation* **106**(9): 1147-1153.

Schwabe, R. F., Uchinami, H., Qian, T., Bennett, B. L., Lemasters, J. J. and Brenner, D. A. (2004). "Differential requirement for c-Jun NH2-terminal kinase in TNFalpha- and Fas-mediated apoptosis in hepatocytes." *FASEB J.* **18**(6): 720-722.

Seedorf, U., Engel, T., Lueken, A., Bode, G., Lorkowski, S. and Assmann, G. (2004). "Cholesterol absorption inhibitor Ezetimibe blocks uptake of oxidized LDL in human macrophages." *Biochem. Biophys. Res. Commun.* **320**(4): 1337-1341.

Seeley, E. S. and Nachury, M. V. (2010). "The perennial organelle: assembly and disassembly of the primary cilium." *J. Cell Sci.* **123**(Pt 4): 511-518.

Seki, E. and Brenner, D. A. (2008). "Toll-like receptors and adaptor molecules in liver disease: update." *Hepatology* **48**(1): 322-335.

Senokuchi, T., Liang, C. P., Seimon, T. A., Han, S., Matsumoto, M., Banks, A. S., Paik, J. H., DePinho, R. A., Accili, D., Tabas, I. and Tall, A. R. (2008). "Forkhead transcription factors (FoxOs) promote apoptosis of insulin-resistant macrophages during cholesterol-induced endoplasmic reticulum stress." *Diabetes* **57**(11): 2967-2976.

Sever, N., Song, B.-L., Yabe, D., Goldstein, J. L., Brown, M. S. and DeBose-Boyd, R. A. (2003a). "Insig-dependent ubiquitination and degradation of mammalian 3-hydroxy-3-methylglutaryl-CoA reductase stimulated by sterols and geranylgeraniol." *J. Biol. Chem.* **278**(52): 52479-52490.

Sever, N., Yang, T., Brown, M. S., Goldstein, J. L. and DeBose-Boyd, R. A. (2003b). "Accelerated degradation of HMG-CoA reductase mediated by binding of Insig-1 to its sterol-sensing domain." *Mol. Cell* **11**: 25-33.

Sevin, M., Lesca, G., Baumann, N., Millat, G., Lyon-Caen, O., Vanier, M. T. and Sedel, F. (2007). "The adult form of Niemann-Pick disease type C." *Brain* **130**(Pt 1): 120-133.

Shanab, A. A., Scully, P., Crosbie, O., Buckley, M., O'Mahony, L., Shanahan, F., Gazareen, S., Murphy, E. and Quigley, E. M. (2011). "Small intestinal bacterial overgrowth in nonalcoholic steatohepatitis: association with toll-like receptor 4 expression and plasma levels of interleukin 8." *Dig. Dis. Sci.* **56**(5): 1524-1534.

Sharawy, M., Dirksen, T. and Chaffin, J. (1979). "Increase in free cholesterol content of the adrenal cortex after stress: radioautographic and biochemical study." *Am. J. Anat.* **156**(4): 567-575.

Sharma, M., Urano, F. and Jaeschke, A. (2011). "Cdc42 and Rac1 are major contributors to the saturated fatty acid-stimulated JNK pathway in hepatocytes." *J. Hepatol.*

Shefer, S., Cheng, F. W., Batta, A. K., Dayal, B., Tint, S., Salen, G. and Mosback, E. H. (1978). "Stereospecific side chain hydroxylations in the biosynthesis of chenodeoxycholic acid." *J. Biol. Chem.* **253**(18): 6386-6392.

Shen, J. and Prywes, R. (2004). "Dependence of site-2 protease cleavage of ATF6 on prior site-1 protease digestion is determined by the size of the luminal domain of ATF6." *J. Biol. Chem.* **279**(41): 43046-43051.

Shen, J. and Prywes, R. (2005). "ER stress signaling by regulated proteolysis of ATF6." *Methods* **35**(4): 382-389.

Shen, Q., Bai, Y., Chang, K. C., Wang, Y., Burris, T. P., Freedman, L. P., Thompson, C. C. and Nagpal, S. (2011). "Liver X receptor-retinoid X receptor (LXR-RXR) heterodimer cistrome reveals coordination of LXR and AP1 signaling in keratinocytes." *J. Biol. Chem.* **286**(16): 14554-14563.

Shibata, N. and Glass, C. K. (2010). "Macrophages, oxysterols and atherosclerosis." *Circ. J.* **74**(10): 2045-2051.

Shibata, S., Hayakawa, K., Egashira, Y. and Sanada, H. (2007). "Roles of nuclear receptors in the up-regulation of hepatic cholesterol 7α-hydroxylase by cholestyramine in rats." *Life Sci.* **80**: 546-553.

Shimabukuro, M., Zhou, Y. T., Levi, M. and Unger, R. H. (1998). "Fatty acid-induced beta cell apoptosis: a link between obesity and diabetes." *Proc. Natl. Acad. Sci. U. S. A.* **95**(5): 2498-2502.

Shiri-Sverdlov, R., Wouters, K., van Gorp, P. J., Gijbels, M. J., Noel, B., Buffat, L., Staels, B., Maeda, N., van Bilsen, M. and Hofker, M. H. (2006). "Early diet-induced non-alcoholic steatohepatitis in APOE2 knock-in mice and its prevention by fibrates." *J. Hepatol.* **44**(4): 732-741.

Shu, H. B., Agranoff, A. B., Nabel, E. G., Leung, K., Duckett, C. S., Neish, A. S., Collins, T. and Nabel, G. J. (1993). "Differential regulation of vascular cell adhesion molecule 1 gene expression by specific NF-kappa B subunits in endothelial and epithelial cells." *Mol. Cell. Biol.* **13**(10): 6283-6289.

Shu, H. B., Takeuchi, M. and Goeddel, D. V. (1996). "The tumor necrosis factor receptor 2 signal transducers TRAF2 and c-IAP1 are components of the tumor necrosis factor receptor 1 signaling complex." *Proc. Natl. Acad. Sci. U. S. A.* **93**(24): 13973-13978.

Siddiqi, S. A. (2008). "VLDL exits from the endoplasmic reticulum in a specialized vesicle, the VLDL transport vesicle, in rat primary hepatocytes." *Biochem. J.* **413**: 333-342.

Silversand, C. and Haux, C. (1997). "Improved high-preformance liquid chromatographic method for the separation and quantification of lipid classes: application to fish lipids." *J. Chromatogr. B* **703**: 7-14.

Simons, J. (2003). "The $10 billion pill." *Fortune* **147**(1): 58-62, 66, 68.

Singh, R., Bullard, J., Kalra, M., Assefa, S., Kaul, A. K., Vonfeldt, K., Strom, S. C., Conrad, R. S., Sharp, H. L. and Kaul, R. (2011). "Status of bacterial colonization, Toll-like receptor expression and nuclear factor-kappa B activation in normal and diseased human livers." *Clin. Immunol.* **138**(1): 41-49.

Sinha-Hikim, I., Sinha-Hikim, A. P., Shen, R., Kim, H., French, S. W., Vaziri, N. D., Crum, A., Rajavashisth, T. B. and Norris, K. C. (2011). "A novel cystine based antioxidant attenuates oxidative stress and hepatic steatosis in diet-induced obese mice." *Exp. Mol. Pathol.* **91**(1): 419-428.

Siperstein, M. D. and Murray, A. W. (1955). "Cholesterol metabolism in man." *J. Clin. Invest.* **34**(9): 1449-1453.

Sirard, J. C., Vignal, C., Dessein, R. and Chamaillard, M. (2007). "Nod-like receptors: cytosolic watchdogs for immunity against pathogens." *PLoS Pathog.* **3**(12): e152.

Smit, J. J., Schinkel, A. H., Oude Elferink, R. P., Groen, A. K., Wagenaar, E., van Deemter, L., Mol, C. A., Ottenhoff, R., van der Lugt, N. M., van Roon, M. A. and et al. (1993). "Homozygous disruption of the murine mdr2 P-glycoprotein gene leads to a complete absence of phospholipid from bile and to liver disease." *Cell* **75**(3): 451-462.

Song, B.-L., Sever, N. and DeBose-Boyd, R. A. (2005). "Gp78, a membrane-anchored ubiquitin ligase, associates with Insig-1 and couples sterol-regulated ubiquitination to degradation of HMG-CoA reductase." *Mol. Cell* **19**: 829-840.

Song, K. H., Li, T., Owsley, E. and Chiang, J. Y. (2010). "A putative role of micro RNA in regulation of cholesterol 7alpha-hydroxylase expression in human hepatocytes." *J. Lipid Res.* **51**(8): 2223-2233.

Song, K. H., Li, T., Owsley, E., Strom, S. and Chiang, J. Y. (2009). "Bile acids activate fibroblast growth factor 19 signaling in human hepatocytes to inhibit cholesterol 7alpha-hydroxylase gene expression." *Hepatology* **49**(1): 297-305.

Song, X., Kaimal, R., Yan, B. and Deng, R. (2008). "Liver receptor homolog 1 transcriptionally regulates human bile salt export pump expression." *J. Lipid Res.* **49**(5): 973-984.

Soon, R. K., Jr., Yan, J. S., Grenert, J. P. and Maher, J. J. (2010). "Stress signaling in the methionine-choline-deficient model of murine fatty liver disease." *Gastroenterology* **139**(5): 1730-1739, 1739 e1731.

Sparrow, C. P., Baffic, J., Lam, M. H., Lund, E. G., Adams, A. D., Fu, X., Hayes, N., Jones, A. B., Macnaul, K. L., Ondeyka, J., Singh, S., Wang, J., Zhou, G., Moller, D. E., Wright, S. D. and Menke, J. G. (2002). "A potent synthetic LXR agonist is more effective than cholesterol loading at inducing ABCA1 mRNA and stimulating cholesterol efflux." *J. Biol. Chem.* **277**(12): 10021-10027.

Spencer, A. F. and Lowenstein, J. M. (1966). "Citrate and the conversion of carbohydrate into fat. Citrate cleavage in obesity and lactation." *Biochem. J.* **99**(3): 760-765.

Srinivasula, S. M., Ahmad, M., Ottilie, S., Bullrich, F., Banks, S., Wang, Y., Fernandes-Alnemri, T., Croce, C. M., Litwack, G., Tomaselli, K. J., Armstrong, R. C. and Alnemri, E. S. (1997). "FLAME-1, a novel FADD-like anti-apoptotic molecule that regulates Fas/TNFR1-induced apoptosis." *J. Biol. Chem.* **272**(30): 18542-18545.

Stöckel, B., König, J., Nies, A. T., Cui, Y., Brom, M. and Keppler, D. (2000). "Characterization of the 5'-flanking region of the human multidrug resistance protein 2 (MRP2) gene and its regulation in comparison with multidrug resistance protein 3 (MRP3) gene." *Eur. J. Biochem.* **267**: 1347-1358.

Stone, B. G., Evans, D., Prigge, W. F., Duane, W. C. and Gebhard, R. L. (1989). "Lovastatin treatment inhibits sterol synthesis and induces HMG-CoA reductase activity in mononuclear leukocytes of normal subjects." *J. Lipid Res.* **30**: 1943-1952.

Strautnieks, S. S., Byrne, J. A., Pawlikowska, L., Cebecauerová, D., Rayner, A., Dutton, L., Meier, Y., Antoniou, A., Stieger, B., Arnell, H., Özçay, F., Al–Hussaini, H. F., Bassas, A. F., Verkade, H. J., Fischler, B., Németh, A., Kotalová, R., Shneider, B. L., Cielecka–Kuszyk, J., McClean, P., Whitington, P. F., Sokal, E., Jirsa, M., Wali, S. H., Jankowska, I., Pawłowska, J., Mieli–Vergani, G., Knisely, A. S., Bull, L. N. and Thompson,

R. J. (2008). "Severe bile salt export pump deficiency: 82 different ABCB11 mutations in 109 families." *Gastroenterology* **134**: 1203-1214.

Subramanian, S., Goodspeed, L., Wang, S., Kim, J., Zeng, L., Ioannou, G. N., Haigh, W. G., Yeh, M. M., Kowdley, K. V., O'Brien, K. D., Pennathur, S. and Chait, A. (2011). "Dietary cholesterol exacerbates hepatic steatosis and inflammation in obese LDL receptor-deficient mice." *J. Lipid Res.* **52**(9): 1626-1635.

Sudhop, T., Lutjohann, D., Kodal, A., Igel, M., Tribble, D. L., Shah, S., Perevozskaya, I. and von Bergmann, K. (2002). "Inhibition of intestinal cholesterol absorption by ezetimibe in humans." *Circulation* **106**(15): 1943-1948.

Sutterwala, F. S., Ogura, Y., Szczepanik, M., Lara-Tejero, M., Lichtenberger, G. S., Grant, E. P., Bertin, J., Coyle, A. J., Galan, J. E., Askenase, P. W. and Flavell, R. A. (2006). "Critical role for NALP3/CIAS1/Cryopyrin in innate and adaptive immunity through its regulation of caspase-1." *Immunity* **24**(3): 317-327.

Suzuki, H. and Sugiyama, Y. (1998). "Excretion of GSSG and glutathione conjugates mediated by MRP1 and cMOAT/MRP2." *Semin. Liver Dis.* **18**(4): 359-376.

Sweat, F., Puchtler, H. and Rosenthal, S. I. (1964). "Sirius Red F3ba as a Stain for Connective Tissue." *Arch. Pathol.* **78**: 69-72.

Szabo, G., Velayudham, A., Romics, L., Jr. and Mandrekar, P. (2005). "Modulation of non-alcoholic steatohepatitis by pattern recognition receptors in mice: the role of toll-like receptors 2 and 4." *Alcohol. Clin. Exp. Res.* **29**(11 Suppl): 140S-145S.

Tabas, I. (2002). "Consequences of cellular cholesterol accumulation: basic concepts and physiological implications." *J. Clin. Invest.* **110**(7): 905-911.

Takeuchi, O., Takeda, K., Hoshino, K., Adachi, O., Ogawa, T. and Akira, S. (2000). "Cellular responses to bacterial cell wall components are mediated through MyD88-dependent signaling cascades." *Int. Immunol.* **12**(1): 113-117.

Tamimi, T. I., Elgouhari, H. M., Alkhouri, N., Yerian, L. M., Berk, M. P., Lopez, R., Schauer, P. R., Zein, N. N. and Feldstein, A. E. (2011). "An apoptosis panel for nonalcoholic steatohepatitis diagnosis." *J. Hepatol.* **54**(6): 1224-1229.

Tanaka, T., Uchiumi, T., Hinoshita, E., Inokuchi, A., Toh, S., Wada, M., Takano, H., Kohno, K. and Kuwano, M. (1999). "The human multidrug resistance protein 2 gene: functional characterization of the 5'-flanking region and expression in hepatic cells." *Hepatology* **30**(6): 1507-1512.

Tandra, S., Yeh, M. M., Brunt, E. M., Vuppalanchi, R., Cummings, O. W., Unalp-Arida, A., Wilson, L. A. and Chalasani, N. (2010). "Presence and significance of microvesicular steatosis in nonalcoholic fatty liver disease." *J. Hepatol.*

Temel, R. E., Tang, W., Ma, Y., Rudel, L. L., Willingham, M. C., Ioannou, Y. A., Davies, J. P., Nilsson, L.-M. and Yu, L. (2007). "Hepatic Niemann-Pick C1-like 1 regulates biliart cholesterol concentration and is a target of ezetimibe." *J. Clin. Invest.* **117**(7): 1968-1978.

Teoh, N. C., Williams, J., Hartley, J., Yu, J., McCuskey, R. S. and Farrell, G. C. (2010). "Short-term therapy with peroxisome proliferation-activator receptor-alpha agonist Wy-14,643 protects murine fatty liver against ischemia-reperfusion injury." *Hepatology* **51**(3): 996-1006.

Tessari, P., Coracina, A., Cosma, A. and Tiengo, A. (2009). "Hepatic lipid metabolism and non-alcoholic fatty liver disease." *Nutr. Metab. Cardiovasc. Dis.* **19**(4): 291-302.

Thomas, L. R., Henson, A., Reed, J. C., Salsbury, F. R. and Thorburn, A. (2004). "Direct binding of Fas-associated death domain (FADD) to the tumor necrosis factor-related apoptosis-inducing ligand receptor DR5 is regulated by the death effector domain of FADD." *J. Biol. Chem.* **279**(31): 32780-32785.

Thomson, A. B. and Keelan, M. (1989). "Rechallenge following an early life exposure to a high-cholesterol diet enhances diet-associated alterations in intestinal permeability." *J. Pediatr. Gastroenterol. Nutr.* **9**(1): 98-104.

Thomson, A. B., Keelan, M. and Tavernini, M. (1987). "Early feeding of a high-cholesterol diet enhances intestinal permeability to lipids in rabbits." *Pediatr. Res.* **21**(4): 347-351.

Thorburn, A. W. (2005). "Prevalence of obesity in Australia." *Obes. Rev.* **6**(3): 187-189.

Tokushige, K., Hashimoto, E., Yatsuji, S., Tobari, M., Taniai, M., Torii, N. and Shiratori, K. (2010). "Prospective study of hepatocellular carcinoma in nonalcoholic steatohepatitis in comparison with hepatocellular carcinoma caused by chronic hepatitis C." *J. Gastroenterol.* **45**(9): 960-967.

Tomkins, G. M. and Chaikoff, I. L. (1952). "Cholesterol synthesis by liver. I. Influence of fasting and of diet." *J. Biol. Chem.* **196**(2): 569-573.

Toshimitsu, K., Matsuura, B., Ohkubo, I., Niiya, T., Furukawa, S., Hiasa, Y., Kawamura, M., Ebihara, K. and Onji, M. (2007). "Dietary habits and nutrient intake in non-alcoholic steatohepatitis." *Nutrition* **23**(1): 46-52.

Tournier, C., Hess, P., Yang, D. D., Xu, J., Turner, T. K., Nimnual, A., Bar-Sagi, D., Jones, S. N., Flavell, R. A. and Davis, R. J. (2000). "Requirement of JNK for stress-induced activation of the cytochrome c-mediated death pathway." *Science* **288**(5467): 870-874.

Tous, M., Ferre, N., Camps, J., Riu, F. and Joven, J. (2005). "Feeding apolipoprotein E-knockout mice with cholesterol and fat enriched diets may be a model of non-alcoholic steatohepatitis." *Mol. Cell. Biochem.* **268**(1-2): 53-58.

Towbin, H., Staehelin, T. and Gordon, J. (1979). "Electrophoretic transfer of proteins from polyacrylamide gels to nitrocellulose sheets: procedure and some applications." *Proc. Natl. Acad. Sci. U. S. A.* **76**(9): 4350-4354.

Trauner, M., Arrese, M. and Wagner, M. (2010). "Fatty liver and lipotoxicity." *Biochim. Biophys. Acta* **1801**(3): 299-310.

Trayhurn, P. and Jennings, G. (1988). "Nonshivering thermogenesis and the thermogenic capacity of brown fat in fasted and/or refed mice." *Am. J. Physiol.* **254**(1 Pt 2): R11-16.

Tremblay, A. J., Lamarche, B., Lemelin, V., Hoos, L., Benjannet, S., Seidah, N. G., Davis, H. R., Jr. and Couture, P. (2011). "Atorvastatin increases intestinal expression of NPC1L1 in hyperlipidemic men." *J. Lipid Res.* **52**(3): 558-565.

Tso, P. and Balint, J. A. (1986). "Formation and transport of chylomicrons by enterocytes to the lymphatics." *Am. J. Physiol. Gastrointest. Liver Physiol.* **13**: 715-726.

Uematsu, S., Sato, S., Yamamoto, M., Hirotani, T., Kato, H., Takeshita, F., Matsuda, M., Coban, C., Ishii, K. J., Kawai, T., Takeuchi, O. and Akira, S. (2005). "Interleukin-1 receptor-associated kinase-1 plays an essential role for Toll-like receptor (TLR)7- and TLR9-mediated interferon-{alpha} induction." *J. Exp. Med.* **201**(6): 915-923.

Unger, R. H. and Zhou, Y. T. (2001). "Lipotoxicity of beta-cells in obesity and in other causes of fatty acid spillover." *Diabetes* **50 Suppl 1**: S118-121.

Uppal, H., Zhai, Y., Gangopadhyay, A., Khadem, S., Ren, S., Moser, J. A. and Xie, W. (2008). "Activation of liver X receptor sensitizes mice to gallbladder cholesterol crystallization." *Hepatology* **47**(4): 1331-1342.

Urano, F., Wang, X., Bertolotti, A., Zhang, Y., Chung, P., Harding, H. P. and Ron, D. (2000). "Coupling of stress in the ER to activation of JNK protein kinases by transmembrane protein kinase IRE1." *Science* **287**(5453): 664-666.

Urizar, N. L., Liverman, A. B., Dodds, D. T., Silva, F. V., Ordentlich, P., Yan, Y., Gonzalez, F. J., Heyman, R. A., Mangelsdorf, D. J. and Moore, D. D. (2002). "A natural product that lowers cholesterol as an antagonist ligand for FXR." *Science* **296**(5573): 1703-1706.

van Greevenbroek, M. M. J. and de Bruin, T. W. A. (1998). "Chylomicron synthesis by intestinal cells in vitro and in vivo." *Atheroscler. Suppl.* **141**(1): S9-S16.

Van Rooyen, D. M. and Farrell, G. C. (2011). "SREBP-2: a link between insulin resistance, hepatic cholesterol, and inflammation in NASH." *J. Gastroenterol. Hepatol.* **26**(5): 789-792.

Vance, D. E. and Van den Bosch, H. (2000). "Cholesterol in the year 2000." *Biochim. Biophys. Acta* **1529**: 1-8.

Vaziri, N. D. (2006). "Dyslipidemia of chronic renal failure: the nature, mechanisms, and potential consequences." *Am. J. Physiol. Renal Physiol.* **290**(2): F262-272.

Vedhachalam, C., Duong, P. T., Nickel, M., Nguyen, D., Dhanasekaran, P., Saito, H., Rothblat, G. H., Lund-Katz, S. and Phillips, M. C. (2007). "Mechanism of ATP-binding cassette transporter A1-mediated cellular lipid efflux to apolipoprotein A-I and formation of high density lipoprotein particles." *J. Biol. Chem.* **282**(34): 25123-25130.

Verhoef, P. A., Kertesy, S. B., Estacion, M., Schilling, W. P. and Dubyak, G. R. (2004). "Maitotoxin induces biphasic interleukin-1beta secretion and membrane blebbing in murine macrophages." *Mol. Pharmacol.* **66**(4): 909-920.

Videla, L. A., Tapia, G., Rodrigo, R., Pettinelli, P., Haim, D., Santibanez, C., Araya, A. V., Smok, G., Csendes, A., Gutierrez, L., Rojas, J., Castillo, J., Korn, O., Maluenda, F., Diaz, J. C., Rencoret, G. and Poniachik, J. (2009). "Liver NF-kappaB and AP-1 DNA binding in obese patients." *Obesity (Silver Spring, Md* **17**(5): 973-979.

Vine, D. F., Glimm, D. R. and Proctor, S. D. (2008). "Intestinal lipid transport and chylomicron production: possible links to exacerbated atherogenesis in a rodent model of the metabolic syndrome." *Atheroscler. Suppl.* **9**: 69-76.

Voet, D. and Voet, J. G. (1999). Lipid metabolism. *Biochemistry*. New York, John Wiley and Sons, Inc.: 662-726.

von Jagow, R., Kampffmeyer, H. and Kiese, M. (1965). "The preparation of microsomes." *Naunyn. Schmiedebergs Arch. Exp. Pathol. Pharmakol.* **251**: 73-87.

Vuoristo, M. and Miettinen, T. A. (1982). "Cholesterol absorption, elimination and synthesis in coeliac disease." *Eur. J. Clin. Investig.* **12**(4): 285-291.

Vuppalanchi, R., Cummings, O. W., Saxena, R., Ulbright, T. M., Martis, N., Jones, D. R., Bansal, N. and Chalasani, N. (2007). "Relationship among histologic, radiologic, and biochemical assessments of hepatic steatosis: a study of human liver samples." *J. Clin. Gastroenterol.* **41**(2): 206-210.

Walls, H. L., Magliano, D. J., Stevenson, C. E., Backholer, K., Mannan, H. R., Shaw, J. E. and Peeters, A. (2011). "Projected Progression of the Prevalence of Obesity in Australia." *Obesity (Silver Spring, Md.*

Wang, L., Han, Y., Kim, C. S., Lee, Y. K. and Moore, D. D. (2003). "Resistance of SHP-null mice to bile acid-induced liver damage." *J. Biol. Chem.* **278**(45): 44475-44481.

Wang, P., Xiao, X. and Chou, K. C. (2011a). "NR-2L: a two-level predictor for identifying nuclear receptor subfamilies based on sequence-derived features." *PLoS ONE* **6**(8): e23505.

Wang, Y., Wang, X., Sun, M., Zhang, Z., Cao, H. and Chen, X. (2011b). "NF-kB activity-dependent P-selectin involved in ox-LDL-induced foam cell formation in U937 cell." *Biochem. Biophys. Res. Commun.* **411**(3): 543-548.

Watari, H., Blanchette-Mackie, E. J., Dwyer, N. K., Glick, J. M., Patel, S., Neufeld, E. B., Brady, R. O., Pentchev, P. G. and Strauss, J. F., 3rd (1999). "Niemann-Pick C1 protein: obligatory roles for N-terminal domains and lysosomal targeting in cholesterol mobilization." *Proc. Natl. Acad. Sci. U. S. A.* **96**(3): 805-810.

Watari, H., Blanchette-Mackie, E. J., Dwyer, N. K., Sun, G., Glick, J. M., Patel, S., Neufeld, E. B., Pentchev, P. G. and Strauss, J. F., 3rd (2000). "NPC1-containing compartment of human granulosa-lutein cells: a role in the intracellular trafficking of cholesterol supporting steroidogenesis." *Exp. Cell Res.* **255**(1): 56-66.

Welihinda, A. A., Tirasophon, W. and Kaufman, R. J. (1999). "The cellular response to protein misfolding in the endoplasmic reticulum." *Gene Expr.* **7**(4-6): 293-300.

Whitby, R. J., Stec, J., Blind, R. D., Dixon, S., Leesnitzer, L. M., Orband-Miller, L. A., Williams, S. P., Willson, T. M., Xu, R., Zuercher, W. J., Cai, F. and Ingraham, H. A. (2011). "Small molecule agonists of the orphan nuclear receptors steroidogenic factor-1 (SF-1, NR5A1) and liver receptor homologue-1 (LRH-1, NR5A2)." *J. Med. Chem.* **54**(7): 2266-2281.

Whiteside, C. H., Harkins, R. W., Fluckiger, H. B. and Sarett, H. P. (1965). "Utilization of Fat-Soluble Vitamins by Rats and Chicks Fed Cholestyramine, a Bile Acid Sequestrant." *Am. J. Clin. Nutr.* **16**: 309-314.

Wieckowska, A., Zein, N. N., Yerian, L. M., Lopez, A. R., McCullough, A. J. and Feldstein, A. E. (2006). "In vivo assessment of liver cell apoptosis as a novel biomarker of disease severity in nonalcoholic fatty liver disease." *Hepatology* **44**(1): 27-33.

Wietek, C., Miggin, S. M., Jefferies, C. A. and O'Neill, L. A. (2003). "Interferon regulatory factor-3-mediated activation of the interferon-sensitive response element by Toll-like receptor (TLR) 4 but not TLR3 requires the p65 subunit of NF-kappa." *J. Biol. Chem.* **278**(51): 50923-50931.

Williams, C. D., Stengel, J., Asike, M. I., Torres, D. M., Shaw, J., Contreras, M., Landt, C. L. and Harrison, S. A. (2011). "Prevalence of nonalcoholic fatty liver disease and nonalcoholic steatohepatitis among a largely middle-aged population utilizing ultrasound and liver biopsy: a prospective study." *Gastroenterology* **140**(1): 124-131.

Willingham, S. B., Bergstralh, D. T., O'Connor, W., Morrison, A. C., Taxman, D. J., Duncan, J. A., Barnoy, S., Venkatesan, M. M., Flavell, R. A., Deshmukh, M., Hoffman, H. M. and Ting, J. P. (2007). "Microbial pathogen-induced necrotic cell death mediated by the inflammasome components CIAS1/cryopyrin/NLRP3 and ASC." *Cell Host Microbe* **2**(3): 147-159.

Willy, P. J. and Mangelsdorf, D. J. (1997). "Unique requirements for retinoid-dependent transcriptional activation by the orphan receptor LXR." *Genes Dev.* **11**(3): 289-298.

Willy, P. J., Umesono, K., Ong, E. S., Evans, R. M., Heyman, R. A. and Mangelsdorf, D. J. (1995). "LXR, a nuclear receptor that defines a distinct retinoid response pathway." *Genes Dev.* **9**(9): 1033-1045.

Wisse, E., De Zanger, R. B., Charels, K., Van Der Smissen, P. and McCuskey, R. S. (1985). "The liver sieve: considerations concerning the structure and function of endothelial fenestrae, the sinusoidal wall and the space of Disse." *Hepatology* **5**: 683-692.

Wong, J., Quinn, C. M. and Brown, A. J. (2006). "SREBP-2 positively regulates transcription of the cholesterol efflux gene, ABCA1, by generating oxysterol ligands for LXR." *Biochem. J.* **400**(3): 485-491.

Wong, V. W., Chu, W. C., Wong, G. L., Chan, R. S., Chim, A. M., Ong, A., Yeung, D. K., Yiu, K. K., Chu, S. H., Woo, J., Chan, F. K. and Chan, H. L. (2011). "Prevalence of non-alcoholic fatty liver disease and advanced fibrosis in Hong Kong Chinese: a population study using proton-magnetic resonance spectroscopy and transient elastography." *Gut*.

Wouters, K., Shiri-Sverdlov, R., van Gorp, P. J., van Bilsen, M. and Hofker, M. H. (2005). "Understanding hyperlipidemia and atherosclerosis: lessons from genetically modified apoe and ldlr mice." *Clin. Chem. Lab. Med.* **43**(5): 470-479.

Wouters, K., van Bilsen, M., van Gorp, P. J., Bieghs, V., Lutjohann, D., Kerksiek, A., Staels, B., Hofker, M. H. and Shiri-Sverdlov, R. (2010). "Intrahepatic cholesterol influences progression, inhibition and reversal of non-alcoholic steatohepatitis in hyperlipidemic mice." *FEBS Lett.* **584**(5): 1001-1005.

Wouters, K., van Gorp, P. J., Bieghs, V., Gijbels, M. J., Duimel, H., Lutjohann, D., Kerksiek, A., van Kruchten, R., Maeda, N., Staels, B., van Bilsen, M., Shiri-Sverdlov, R. and Hofker, M. H. (2008). "Dietary cholesterol, rather than liver steatosis, leads to hepatic inflammation in hyperlipidemic mouse models of nonalcoholic steatohepatitis." *Hepatology* **48**(2): 474-486.

Wree, A., Kahraman, A., Gerken, G. and Canbay, A. (2011). "Obesity affects the liver - the link between adipocytes and hepatocytes." *Digestion* **83**(1-2): 124-133.

Xie, X., Liao, H., Dang, H., Pang, W., Guan, Y., Wang, X., Shyy, J. Y., Zhu, Y. and Sladek, F. M. (2009). "Down-regulation of hepatic HNF4alpha gene expression during hyperinsulinemia via SREBPs." *Mol. Endocrinol.* **23**(4): 434-443.

Xu, F., Rychnovsky, S. D., Belani, J. D., Hobbs, H. H., Cohen, J. C. and Rawson, R. B. (2005). "Dual roles for cholesterol in mammalian cells." *Proc. Natl. Acad. Sci. U. S. A.* **102**(41): 14551-14556.

Xu, H., He, J. H., Xiao, Z. D., Zhang, Q. Q., Chen, Y. Q., Zhou, H. and Qu, L. H. (2010). "Liver-enriched transcription factors regulate microRNA-122 that targets CUTL1 during liver development." *Hepatology* **52**(4): 1431-1442.

Yamagishi, S., Nakamura, K., Matsui, T., Sato, T. and Takeuchi, M. (2006). "Inhibition of intestinal cholesterol absorption by ezetimibe is a novel therapeutic target for fatty liver." *Med. Hypotheses* **66**(4): 844-846.

Yamaoka, K., Nouchi, T., Marumo, F. and Sato, C. (1993). "Alpha-smooth-muscle actin expression in normal and fibrotic human livers." *Dig. Dis. Sci.* **38**(8): 1473-1479.

Yamaoka, S., Courtois, G., Bessia, C., Whiteside, S. T., Weil, R., Agou, F., Kirk, H. E., Kay, R. J. and Israel, A. (1998). "Complementation cloning of NEMO, a component of the IkappaB kinase complex essential for NF-kappaB activation." *Cell* **93**(7): 1231-1240.

Yan, D., Mayranpaa, M. I., Wong, J., Perttila, J., Lehto, M., Jauhiainen, M., Kovanen, P. T., Ehnholm, C., Brown, A. J. and Olkkonen, V. M. (2008). "OSBP-related protein 8 (ORP8) suppresses ABCA1 expression and cholesterol efflux from macrophages." *J. Biol. Chem.* **283**(1): 332-340.

Yang, J., Huang, C., Jiang, H. and Ding, J. (2010). "Statins attenuate high mobility group box-1 protein induced vascular endothelial activation : a key role for TLR4/NF-kappaB signaling pathway." *Mol. Cell. Biochem.* **345**(1-2): 189-195.

Yang, S. Q., Lin, H. Z., Mandal, A. K., Huang, J. and Diehl, A. M. (2001). "Disrupted signaling and inhibited regeneration in obese mice with fatty livers: implications for nonalcoholic fatty liver disease pathophysiology." *Hepatology* **34**(4 Pt 1): 694-706.

Yao, P. M. and Tabas, I. (2000). "Free cholesterol loading of macrophages induces apoptosis involving the fas pathway." *J. Biol. Chem.* **275**(31): 23807-23813.

Yasui, K., Hashimoto, E., Komorizono, Y., Koike, K., Arii, S., Imai, Y., Shima, T., Kanbara, Y., Saibara, T., Mori, T., Kawata, S., Uto, H., Takami, S., Sumida, Y., Takamura, T., Kawanaka, M. and Okanoue, T. (2011). "Characteristics of patients with nonalcoholic steatohepatitis who develop hepatocellular carcinoma." *Clin. Gastroenterol. Hepatol.* **9**(5): 428-433; quiz e450.

Yasumiba, S., Tazuma, S., Ochi, H., Kajiyama, G. and Mdt (2001). "Modifying hepatic phospholipid synthesis associates with biliary phospholipid secretion rate in a transporter-independent manner in rats: relation to canalicular membrane fluidity." *Dig. Dis. Sci.* **46**(6): 1290-1298.

Yasutake, K., Nakamuta, M., Shima, Y., Ohyama, A., Masuda, K., Haruta, N., Fujino, T., Aoyagi, Y., Fukuizumi, K., Yoshimoto, T., Takemoto, R., Miyahara, T., Harada, N., Hayata, F., Nakashima, M. and Enjoji, M. (2009). "Nutritional investigation of non-obese patients with non-alcoholic fatty liver disease: the significance of dietary cholesterol." *Scand. J. Gastroenterol.* **44**(4): 471-477.

Yeagle, P. L. (1991). "Modulation of membrane function by cholesterol." *Biochimie* **73**: 1303-1310.

Yeh, M. M. and Brunt, E. M. (2007). "Pathology of nonalcoholic fatty liver disease." *Am. J. Clin. Pathol.* **128**(5): 837-847.

Yokota, N., O'Donnell, M., Daniels, F., Burne-Taney, M., Keane, W., Kasiske, B. and Rabb, H. (2003). "Protective effect of HMG-CoA reductase inhibitor on experimental renal ischemia-reperfusion injury." *Am. J. Nephrol.* **23**(1): 13-17.

Yoneda, M., Fujita, K., Nozaki, Y., Endo, H., Takahashi, H., Hosono, K., Suzuki, K., Mawatari, H., Kirikoshi, H., Inamori, M., Saito, S., Iwasaki, T., Terauchi, Y., Kubota, K., Maeyama, S. and Nakajima, A. (2010). "Efficacy of ezetimibe for the treatment of non-alcoholic steatohepatitis: An open-label, pilot study." *Hepatol. Res.* **40**(6): 613-621.

Yoshida, H., Oku, M., Suzuki, M. and Mori, K. (2006). "pXBP1(U) encoded in XBP1 pre-mRNA negatively regulates unfolded protein response activator pXBP1(S) in mammalian ER stress response." *J. Cell Biol.* **172**(4): 565-575.

Yoshioka, Y., Hashimoto, E., Yatsuji, S., Kaneda, H., Taniai, M., Tokushige, K. and Shiratori, K. (2004). "Nonalcoholic steatohepatitis: cirrhosis, hepatocellular carcinoma, and burnt-out NASH." *J. Gastroenterol.* **39**(12): 1215-1218.

Yu, C., Chen, J., Lin, S., Liu, J., Chang, C. C. Y. and Chang, T. Y. (1999). "Human acyl-CoA:cholesterol acyltransferase-1 is a homotetrameric enzyme in intact cells and *in vitro*." *J. Biol. Chem.* **274**: 36139-36145.

Yu, L. (2008). "The structure and function of Niemann-Pick C1-like 1 protein." *Curr. Opin. Lipidol.* **19**(3): 263-269.

Yu, Q., Gao, F. and Ma, X. L. (2011). "Insulin says NO to cardiovascular disease." *Cardiovasc. Res.* **89**(3): 516-524.

Zanke, B. W., Lee, C., Arab, S. and Tannock, I. F. (1998). "Death of tumor cells after intracellular acidification is dependent on stress-activated protein kinases (SAPK/JNK) pathway activation and cannot be inhibited by Bcl-2 expression or interleukin 1beta-converting enzyme inhibition." *Cancer Res.* **58**(13): 2801-2808.

Zarubica, A., Trompier, D. and Chimini, G. (2007). "ABCA1, from pathology to membrane function." *Pflueg. Arch. Eur. J. Physiol.* **453**: 569-579.

Zatta, P., Taylor, A., Zambenedetti, P. and Milacic, R. d. A., P. (2000). "Aluminum inhibits the lysosomal proton pump from rat liver." *Life Sci.* **66**(23): 2261-2266.

Zelcer, N. and Tontonoz, P. (2006). "Liver X receptors as integrators of metabolic and inflammatory signaling." *J. Clin. Invest.* **116**(3): 607-614.

Zen, Y., Katayanagi, K., Tsuneyama, K., Harada, K., Araki, I. and Nakanuma, Y. (2001). "Hepatocellular carcinoma arising in non-alcoholic steatohepatitis." *Pathol. Int.* **51**(2): 127-131.

Zeng, L., Liao, H., Liu, Y., Lee, T. S., Zhu, M., Wang, X., Stemerman, M. B., Zhu, Y. and Shyy, J. Y. (2004). "Sterol-responsive element-binding protein (SREBP) 2 down-regulates ATP-binding cassette transporter A1 in vascular endothelial cells: a novel role of SREBP in regulating cholesterol metabolism." *J. Biol. Chem.* **279**(47): 48801-48807.

Zhang, C., Cai, Y., Adachi, M. T., Oshiro, S., Aso, T., Kaufman, R. J. and Kitajima, S. (2001a). "Homocysteine induces programmed cell death in human vascular endothelial cells through activation of the unfolded protein response." *J. Biol. Chem.* **276**(38): 35867-35874.

Zhang, C. K., Lin, W., Cai, Y. N., Xu, P. L., Dong, H., Li, M., Kong, Y. Y., Fu, G., Xie, Y. H., Huang, G. M. and Wang, Y. (2001b). "Characterization of the genomic structure and tissue-specific promoter of the human nuclear receptor NR5A2 (hB1F) gene." *Gene* **273**(2): 239-249.

Zhang, D. W., Lagace, T. A., Garuti, R., Zhao, Z., McDonald, M., Horton, J. D., Cohen, J. C. and Hobbs, H. H. (2007). "Binding of proprotein convertase subtilisin/kexin type 9 to epidermal growth factor-like repeat A of low density lipoprotein receptor decreases receptor recycling and increases degradation." *J. Biol. Chem.* **282**(25): 18602-18612.

Zhang, F., Yu, W., Hargrove, J. L., Greenspan, P., Dean, R. G., Taylor, E. W. and Hartle, D. K. (2002). "Inhibition of TNF-alpha induced ICAM-1, VCAM-1 and E-selectin expression by selenium." *Atherosclerosis* **161**(2): 381-386.

Zhang, G., Li, Q., Wang, L., Chen, Y. and Zhang, W. (2011). "Interleukin-1beta enhances the intracellular accumulation of cholesterol by up-regulating the expression of low-density lipoprotein receptor and 3-hydroxy-3-methylglutaryl coenzyme A reductase in podocytes." *Mol. Cell. Biochem.* **346**(1-2): 197-204.

Zhang, K., Wong, H. N., Song, B., Miller, C. N., Scheuner, D. and Kaufman, R. J. (2005). "The unfolded protein response sensor IRE1alpha is required at 2 distinct steps in B cell lymphopoiesis." *J. Clin. Invest.* **115**(2): 268-281.

Zhang, M. and Chiang, J. Y. (2001). "Transcriptional regulation of the human sterol 12alpha-hydroxylase gene (CYP8B1): roles of heaptocyte nuclear factor 4alpha in mediating bile acid repression." *J. Biol. Chem.* **276**(45): 41690-41699.

Zhang, N., Huan, Y., Huang, H., Song, G. M., Sun, S. J. and Shen, Z. F. (2010). "Atorvastatin improves insulin sensitivity in mice with obesity induced by monosodium glutamate." *Acta Pharmacol. Sin.* **31**(1): 35-42.

Zhang, X., Fitzsimmons, R. L., Cleland, L. G., Ey, P. L., Zannettino, A. C. W., Farmer, E. A., Sincock, P. and Mayrhofer, G. (2003). "CD36/Fatty acid translocase in rats: distribution, isolation from hepatocytes, and comparison with the scavenger receptor SR-B1." *Lab. Invest.* **83**(5): 317-332.

Zhang, Z., Burch, P. E., Cooney, A. J., Lanz, R. B., Pereira, F. A., Wu, J., Gibbs, R. A., Weinstock, G. and Wheeler, D. A. (2004). "Genomic analysis of the nuclear receptor family: new insights into structure, regulation, and evolution from the rat genome." *Genome Res.* **14**(4): 580-590.

Zhao, L., Chen, Y., Tang, R., Chen, Y., Li, Q., Gong, J., Huang, A., Varghese, Z., Moorhead, J. F. and Ruan, X. Z. (2011). "Inflammatory stress exacerbates hepatic cholesterol accumulation via increasing cholesterol uptake and de novo synthesis." *J. Gastroenterol. Hepatol.* **In press**.

Zheng, S., Hoos, L., Cook, J., Tetzloff, G., Davis Jr, H., van Heek, M. and Hwa, J. J. (2008). "Ezetimibe improves high fat and cholesterol diet-induced non-alcoholic fatty liver disease in mice." *Eur. J. Pharmacol.* **584**: 118-124.

Zhou, C., King, N., Chen, K. Y. and Breslow, J. L. (2009). "Activation of PXR induces hypercholesterolemia in wild-type and accelerates atherosclerosis in apoE deficient mice." *J. Lipid Res.* **50**(10): 2004-2013.

Zhou, G. X., Meier, K. E. and Buse, M. G. (1993a). "Sequential activation of two mitogen activated protein (MAP) kinase isoforms in rat skeletal muscle following insulin injection." *Biochem. Biophys. Res. Commun.* **197**(2): 578-584.

Zhou, Q., Smith, T. L. and Kummerow, F. A. (1993b). "Cytotoxicity of oxysterols on cultured smooth muscle cells from human umbilical arteries." *Proc. Soc. Exp. Biol. Med.* **202**(1): 75-80.

Zhu, X., Lee, J. Y., Timmins, J. M., Brown, J. M., Boudyguina, E., Mulya, A., Gebre, A. K., Willingham, M. C., Hiltbold, E. M., Mishra, N., Maeda, N. and Parks, J. S. (2008). "Increased cellular free cholesterol in macrophage-specific Abca1 knock-out mice enhances pro-inflammatory response of macrophages." *J. Biol. Chem.* **283**(34): 22930-22941.

Zinchuk, V. S., Okada, T., Akimaru, K. and Seguchi, H. (2002). "Asynchronous expression and colocalization of Bsep and Mrp2 during development of rat liver." *Am. J. Physiol. Gastrointest. Liver Physiol.* **282**: G540-G548.

Zou, Y., Li, J., Lu, C., Wang, J., Ge, J., Huang, Y., Zhang, L. and Wang, Y. (2006). "High-fat emulsion-induced rat model of nonalcoholic steatohepatitis." *Life Sci.* **79**(11): 1100-1107.